



Bridge Design to Eurocodes Worked examples

Worked examples presented at the Workshop “Bridge Design to Eurocodes”, Vienna, 4-6 October 2010

Support to the implementation, harmonization and further development of the Eurocodes

**Y. Bouassida, E. Bouchon, P. Crespo, P. Croce, L. Davaine, S. Denton, M. Feldmann, R. Frank,
G. Hanswille, W. Hensen, B. Kolias, N. Malakatas, G. Mancini, M. Ortega, J. Raoul, G. Sedlacek, G. Tsionis**



Editors
A. Athanasopoulou, M. Poljansek, A. Pinto
G. Tsionis, S. Denton

EUR 25193 EN - 2012

The mission of the JRC is to provide customer-driven scientific and technical support for the conception, development, implementation and monitoring of EU policies. As a service of the European Commission, the JRC functions as a reference centre of science and technology for the Union. Close to the policy-making process, it serves the common interest of the Member States, while being independent of special interests, whether private or national.

European Commission
Joint Research Centre

Contact information

Address: JRC, ELSA Unit, TP 480, I-21027, Ispra (VA), Italy
E-mail: eurocodes@jrc.ec.europa.eu
Tel.: +39-0332-789989
Fax: +39-0332-789049

<http://www.jrc.ec.europa.eu/>

Legal Notice

Neither the European Commission nor any person acting on behalf of the Commission is responsible for the use which might be made of this publication.

***Europe Direct is a service to help you find answers
to your questions about the European Union***

Freephone number (*):

00 800 6 7 8 9 10 11

(*) Certain mobile telephone operators do not allow access to 00 800 numbers or these calls may be billed.

A great deal of additional information on the European Union is available on the Internet. It can be accessed through the Europa server <http://europa.eu/>

JRC 68415

EUR 25193 EN
ISBN 978-92-79-22823-0
ISSN 1831-9424
doi: 10.2788/82360

Luxembourg: Publications Office of the European Union, 2012

© European Union, 2012

Reproduction is authorised provided the source is acknowledged

Printed in Italy

Acknowledgements

The work presented in this report is a deliverable within the framework of the Administrative Arrangement SI2.558935 under the Memorandum of Understanding between the Directorate-General for Enterprise and Industry of the European Commission (DG ENTR) and the Joint Research Centre (JRC) on the support to the implementation, harmonisation and further development of the Eurocodes.

Table of Contents

Acknowledgements	i
Table of contents	iii
List of authors and editors	xi
Foreword	xiii
Introduction	xv
Chapter 1	
Introduction to the design example	
1.1 Introduction	3
1.2 Geometry of the deck	3
1.2.1 LONGITUDINAL ELEVATION	3
1.2.2 TRANSVERSE CROSS-SECTION	3
1.2.3 ALTERNATIVE DECKS	4
1.3 Geometry of the substructure	5
1.3.1 PIERS	5
1.3.2 ABUTMENTS	7
1.3.3 BEARINGS	7
1.4 Design specifications	8
1.4.1 DESIGN WORKING LIFE	8
1.4.2 NON-STRUCTURAL ELEMENTS	8
1.4.3 TRAFFIC DATA	9
1.4.4. ENVIRONMENTAL CONDITIONS	10
1.4.5 SOIL CONDITIONS	11
1.4.6 SEISMIC DATA	11
1.4.7 OTHER SPECIFICATIONS	11
1.5 Materials	11
1.6 Details on structural steel and slab reinforcement	12
1.6.1 STRUCTURAL STEEL DISTRIBUTION	12
1.6.2 DESCRIPTION OF THE SLAB REINFORCEMENT	15

1.7 Construction process	16
1.7.1 LAUNCHING OF THE STEEL GIRDERS	16
1.7.2 SLAB CONCRETING	16
Chapter 2	
Basis of design (EN 1990)	
2.1 Introduction	21
2.2 EN 1990 Section 1 – General	21
2.3 EN 1990 Section 2 - Requirements	21
2.4 EN 1990 Section 3 – Principles of limit state design	22
2.4.1 DESIGN SITUATIONS	22
2.4.2 ULTIMATE LIMIT STATES	23
2.4.3 SERVICEABILITY LIMIT STATES	23
2.5 EN 1990 Section 4 – Basic variables	24
2.5.1 ACTIONS	24
2.5.2 MATERIAL AND PRODUCTS PROPERTIES	25
2.6 EN 1990 Section 5 – Structural analysis and design assisted by testing	26
2.7 EN 1990 Section 6 – Limit states design and Annex A2 – Application for bridges	26
2.7.1 DESIGN VALUES	26
2.7.2 ULTIMATE LIMIT STATES	27
2.7.3 SINGLE SOURCE PRINCIPLE	27
2.7.4 SPECIAL CASES IN THE APPLICATION OF EQU	28
2.7.5 COMBINATIONS OF ACTIONS	29
2.7.6 LIMIT STATE VERIFICATIONS	31
2.8 Conclusions	32
2.9 Summary of key concepts	33
CHAPTER 3	
Actions on bridge deck and piers (EN 1991)	
<i>Part A: Wind and thermal action on bridge deck and piers</i>	
3.1 Introduction	37
3.2 Brief description of the procedure	37

3.3 Wind actions on the deck	40
3.3.1 BRIDGE DECK DURING ITS SERVICE LIFE, WITHOUT TRAFFIC	40
3.3.2 BRIDGE DURING ITS SERVICE LIFE, WITH TRAFFIC	43
3.3.3 BRIDGE UNDER CONSTRUCTION (MOST CRITICAL CASE AND TERMINATION OF PUSHING)	43
3.3.4 VERTICAL WIND FORCES ON THE BRIDGE DECK (Z- DIRECTION)	45
3.3.5 WIND FORCES ALONG THE BRIDGE DECK (Y-DIRECTION)	46
3.4 Wind actions on the piers	46
3.4.1 SQUAT RECTANGULAR PIER 2.50x5.00x10.00	46
3.4.2 'HIGH' CIRCULAR CYLINDRICAL PIER Ø4.00x 40.00	47
3.5 Thermal actions	48
<i>Part B: Action during execution, accidental actions and traffic loads</i>	
3.6 Introduction	50
3.7 Actions during execution	50
3.7.1 LAUNCHING PHASE	52
3.8 Accidental actions	55
3.8.1 IMPACT OF VEHICLES ON THE BRIDGE SUBSTRUCTURE	56
3.8.2 IMPACT OF VEHICLES ON THE BRIDGE SUPERSTRUCTURE	56
3.9 Traffic loads	57
3.9.1 STATIC LOAD MODELS	58
3.9.2 GROUPS OF TRAFFIC LOADS ON ROAD BRIDGES	60
3.9.3 LOAD COMBINATIONS FOR THE CASE STUDY	61
3.9.4 FATIGUE LOAD MODELS	65
3.9.5 FATIGUE ASSESSMENT OF THE COMPOSITE BRIDGE	67
CHAPTER 4	
Bridge deck modelling and structural analysis	
4.1 Introduction	79
4.2 Shear lag effect	79
4.2.1 GLOBAL ANALYSIS	79
4.2.2. SECTION ANALYSIS	80

4.3 Concrete creep effect (modular ratios)	81
4.3.1 SHORT TERM MODULA RATIO	81
4.3.2 LONG TERM MODULAR RATIO	81
4.4 Elastic mechanical properties of the cross sections	83
4.4.1 UN-CRACKED COMPOSITE BEHAVIOR	83
4.4.2 CKRACKED COMPOSITE BEHAVIOR	84
4.5 Actions modelling	85
4.5.1 SELF-WEIGHT	85
4.5.2 NON-STRUCTURAL EQUIPMENTS	85
4.5.3 CONCRETE SHRINKAGE IN THE COMPOSITE DECK	86
4.5.4 ROAD TRAFFIC	87
4.6 Global analysis	90
4.7 Main results	91
4.7.1 VERTICAL SUPPORT REACTIONS	92
4.7.2 INTERNAL FORCES AND MOMENTS	92
4.7.3 STRESSES AT ULS	92
CHAPTER 5	93
Concrete bridge design (EN 1992-2)	
5.1 Introduction	97
5.2 Local verifications in the concrete slab	97
5.2.1 DURABILITY – CPVER TO REINFORCEMENT	97
5.2.2 TRANSVERSE REINFORCEMENT VERIFICATIONS	99
5.2.3 LONGITUDINAL REINFORCEMENT VERIFICATIONS	116
5.2.4 PUNCHING SHEAR (ULS)	118
5.3 Second order effects in the high piers	121
5.3.1 MAIN FEATURES OF THE PIERS5.2.3 FORCES AND MOMENTS ON TOP OF THE PIERS	121
5.3.2 FORCES AND MOMENTS ON TOP OF THE PIERS	122
5.3.3 SECOND ORDER EFFECTS	122

CHAPTER 6

Composite bridge design (EN 1994-2)

6.1 Verification of cross-section at mid-span P1-P2	127
6.1.1. GEOMETRY AND STRESSES	127
6.1.2 DETERMINING THE CROSS-SECTION CLASS (ACCORDING TO EN1994-2, 5.5.2)	127
6.1.3 PLASTIC SECTION ANALYSIS	130
6.2 Verification of cross-section at internal support P1	132
6.2.1 GEOMETRY AND STRESSES	132
6.2.2 DETERMINING THE CROSS-SECTION CLASS (ACCORDING TO EN1994-2, 5.5.2)	132
6.2.3 SECTION ANALYSIS	134
6.3 Alternative double composite cross-section at internal support P-1	139
6.3.1 DETERMINING THE CROSS-SECTION CLASS (ACCORDING TO EN1994-2, 5.5.2)	142
6.3.2 PLASTIC SECTION ANALYSIS. BENDING AND RESISTANCE CHECK	144
6.3.3 SOME COMMENTS ABOUT EVENTUAL CRUSHING OF THE EXTREME FIBRE OF THE BOTTOM CONCRETE	144
6.4 Verification of the Serviceability Limit States (SLS)	145
6.5 Stresses control at Serviceability Limit States	145
6.5.1 CONTROL OF COMPRESSIVE STRESS IN CONCRETE	145
6.5.2 CONTROL OF STRESS IN REINFORCEMENT STEEL BARS	146
6.5.3 STRESS LIMITATION IN STRUCTURAL STEEL	147
6.5.4 ADDITIONAL VERIFICATION OF FATIGUE UNDER A LOW NUMBER OF CYCLES	150
6.5.5 LIMITATION OF WEB BREATHING	151
6.6 Control of cracking for longitudinal global bending	151
6.6.1 MAXIMUM VALUE OF CRACK WIDTH	151
6.6.2 CRACKING OF CONCRETE. MINIMUM REINFORCEMENT AREA	152
6.6.3 CONTROL OF CRACKING UNDER DIRECT LOADING	153
6.6.4 CONTROL OF CRACKING UNDER INDIRECT LOADING	155
6.7 Shear connection at steel-concrete interface	156
6.7.1 RESISTANCE OF HEADED STUDS	156
6.7.2 DETAILING OF SHEAR CONNECTION	157

6.7.3 CONNECTION DESIGN FOR THE CHARACTERISTIC SLS COMBINATION OF ACTIONS	160
6.7.4 CONNECTION DESIGN FOR THE ULS COMBINATION OF ACTIONS OTHER THAN FATIGUE	163
6.7.5 SYNOPSIS OF THE DESIGN EXAMPLE	165
6.7.6 DESIGN OF THE SHEAR CONNECTION FOR THE FATIGUE ULS COMBINATION OF ACTIONS	166
6.7.7 INFLUENCE OF SHRINKAGE AND THERMAL ACTION ON THE CONNECTION DESIGN AT BOTH DECK ENDS	171
CHAPTER 7	
Geotechnical aspects of bridge design (EN 1997)	
7.1 Introduction	177
7.2 Geotechnical data	177
7.3 Ultimate limit states	183
7.3.1 SUPPORT REACTIONS	183
7.3.2 GENERAL: THE 3 DESIGN APPROACHES OF EUROCODE 7	185
7.4 Abutment C0	189
7.4.1 BEARING CAPACITY (ULS)	189
7.4.2 SLIDING (ULS)	192
7.5 Pier P1 (Squat Pier)	193
7.5.1 BEARING CAPACITY (ULS)	193
7.5.2 SETTLEMENT (SLS)	195
7.6 Seismic design situations	196
CHAPTER 8	
Overview of seismic issues for bridge design (EN 1998-1, EN 1998-2)	
8.1 Introduction	201
8.2 Example of ductile pier	201
8.2.1 BRIDGE CONFIGURATION – DESIGN CONCEPT	201
8.2.2 SEISMIC STRUCTURAL SYSTEM	203
8.2.3 FUNDAMENTAL MODE ANALYSIS IN THE LONGITUDINAL DIRECTION	205
8.2.4 MULTIMODE RESPONSE ANALYSIS	206
8.2.5 DESIGN ACTION EFFECTS AND VERIFICATION	209
8.2.6 BEARINGS AND ROADWAY JOINTS	219

8.2.7 CONCLUSION FOR DESIGN CONCEPT	224
8.3 Example of limited ductile piers	224
8.3.1 BRIDGE CONFIGURATION – DESIGN CONCEPT	224
8.3.2 DESIGN SEISMIC ACTION	225
8.3.3 SEISIC ANALYSIS	226
8.3.4 VERIFICATIONS OF PIERS	237
8.3.5 BEARINGS AND JOINTS	239
8.4 Example of seismic isolation	241
8.4.1 BRIDGE CONFIGURATION – DESIGN CONCEPT	241
8.4.2 DESIGN FOR HORIZONTAL NON-SEISMIC ACTIONS	247
8.4.3 DESIGN SEISMI ACTION	249
8.4.4 SEISMIC STRUCTURAL SYSTEM	253
8.4.5 FUNDAMENTAL MODE METHOD	257
8.4.6 NON-LINERTIME HISTORY ANALYSIS	262
8.4.7 VERIFICATION OF THE ISOLATION SYSTEM	269
8.4.8 VERIFICATION OF SUBSTRUCTURE	271
8.4.9 DESIGN ACTION EFFECTS FOR THE FOUNDATION	278
8.4.10 COMPARISON WITH FUNDAMENTAL MODE METHOD	279
APPENDICES	283
APPENDIX A	A-1
Design of steel bridges. Overview of key contents of EN 1993.	
APPENDIX B	B-1
A sample analytical method for bearing resistance calculation	
APPENDIX C	C-1
Examples of a method to calculate settlements for spread foundations	
APPENDIX D	D-1
Generation of semi-artificial accelerograms for time-history analysis through modification of natural records	

List of authors and editors

Authors

Introduction

Steve Denton, *Parsons Brinckerhoff, Chairman of CEN/TC250 Horizontal Group Bridges*

Georgios Tsionis, *University of Patras, Secretary of CEN/TC250 Horizontal Group Bridges*

Chapter 1 – Introduction to the design example

Pilar Crespo, *Ministry of Public Works (Spain)*

Laurence Davaine, *French Railway Bridge Engineering Department (SNCF, IGOA)*

Chapter 2 – Basis of design (EN 1990)

Steve Denton, *Parsons Brinckerhoff, Chairman of CEN/TC250 Horizontal Group Bridges*

Chapter 3 – Actions on bridge decks and piers (EN 1991)

Nikolaos Malakatas, *Ministry of Infrastructures, Transports and Networks (Greece)*

Pietro Croce, *Department of Civil Engineering, University of Pisa, Italy*

Chapter 4 – Bridge deck modeling and design

Laurence Davaine, *French Railway Bridge Engineering Department (SNCF, IGOA)*

Chapter 5 – Concrete bridge design (EN 1992)

Emmanuel Bouchon, *Large Bridge Division, Setra/CTOA, Paris, France*

Giuseppe Mancini, *Politecnico di Torino, Italy*

Chapter 6 – Composite bridge design (EN 1994-2)

Miguel Ortega Cornejo, *IDEAM S.A., University “Europea de Madrid”, Spain*

Joel Raoul, *Large Bridge Division, Setra/CTOA, Ecole Nationale de Ponts et Chausses, Paris, France*

Chapter 7 – Geotechnical aspects of bridge design (EN 1997)

Roger Frank, *University Paris-Est, Ecole des Ponts ParisTech, Navier-CERMES*

Yosra Bouassida, *University Paris-Est, Ecole des Ponts ParisTech, Navier-CERMES*

Chapter 8 – Overview of seismic issues for bridge design (EN 1998-1, EN 1998-2)

Basil Kolias, *DENCO S.A., Athens*

Appendix A – Design of steel bridges. Overview of key content of EN 1993.

Gerhard Hanswille, *Bergische Universitat*

Wolfgang Hensen, *PSP - Consulting Engineers*

Markus Feldmann, *RWTH Aachen University*
Gerhard Sedlacek, *RWTH Aachen University*

Editors

Adamantia Athanasopoulou, Martin Poljansek, Artur Pinto

*European Laboratory for Structural Assessment
Institute for the Protection and Security of the Citizen
Joint Research Centre, European Commission*

Georgios Tsionis, Steve Denton

CEN/TC250 Horizontal Group Bridges

Foreword

The **construction sector** is of strategic importance to the EU as it delivers the buildings and infrastructure needed by the rest of the economy and society. It represents more than **10% of EU GDP and more than 50% of fixed capital formation**. It is the largest single economic activity and the biggest industrial employer in Europe. The sector employs directly almost 20 million people. In addition, construction is a key element for the implementation of the **Single Market** and other construction relevant EU Policies, e.g.: **Environment and Energy**.

In line with the EU's strategy for smart, sustainable and inclusive growth (EU2020), **Standardization** will play an important part in supporting the strategy. The **EN Eurocodes** are a set of **European standards** which provide common rules for the design of construction works, to check their strength and stability against live and extreme loads such as earthquakes and fire.

With the publication of all the 58 Eurocodes parts in 2007, the implementation of the Eurocodes is extending to all European countries and there are firm steps towards their adoption internationally. The Commission Recommendation of 11 December 2003 stresses the importance of **training in the use of the Eurocodes**, especially in engineering schools and as part of continuous professional development courses for engineers and technicians, noting that they should be promoted both at national and international level.

In light of the Recommendation, DG JRC is collaborating with DG ENTR and CEN/TC250 "Structural Eurocodes" and is publishing the Report Series '**Support to the implementation, harmonization and further development of the Eurocodes**' as JRC Scientific and Technical Reports. This Report Series include, at present, the following types of reports:

1. Policy support documents – Resulting from the work of the JRC and cooperation with partners and stakeholders on 'Support to the implementation, promotion and further development of the Eurocodes and other standards for the building sector.
2. Technical documents – Facilitating the implementation and use of the Eurocodes and containing information and practical examples (Worked Examples) on the use of the Eurocodes and covering the design of structures or their parts (e.g. the technical reports containing the practical examples presented in the workshops on the Eurocodes with worked examples organized by the JRC).
3. Pre-normative documents – Resulting from the works of the CEN/TC250 Working Groups and containing background information and/or first draft of proposed normative parts. These documents can be then converted to CEN technical specifications.
4. Background documents – Providing approved background information on current Eurocode part. The publication of the document is at the request of the relevant CEN/TC250 Sub-Committee.
5. Scientific/Technical information documents – Containing additional, non-contradictory information on current Eurocodes parts which may facilitate implementation and use, preliminary results from pre-normative work and other studies, which may be used in future revisions and further development of the standards. The authors are various stakeholders involved in Eurocodes process and the publication of these documents is authorized by the relevant CEN/TC250 Sub-Committee or Working Group.

Editorial work for this Report Series is **assured by the JRC** together with partners and stakeholders, when appropriate. The publication of the reports type 3, 4 and 5 is made after approval for publication from the CEN/TC250 Co-ordination Group.

The publication of these reports by the JRC serves the purpose of implementation, further harmonization and development of the Eurocodes. However, it is noted that neither the Commission nor CEN are obliged to follow or endorse any recommendation or result included in these reports in the European legislation or standardization processes.

This report is part of the so-called Technical documents (Type 2 above) and contains a comprehensive description of the practical examples presented at the workshop “Bridge Design to the Eurocodes” with emphasis on worked examples of bridge design. The workshop was held on 4-6 October 2010 in Vienna, Austria and was co-organized with CEN/TC250/Horizontal Group Bridges, the Austrian Federal Ministry for Transport, Innovation and Technology and the Austrian Standards Institute, with the support of CEN and the Member States. The workshop addressed representatives of public authorities, national standardisation bodies, research institutions, academia, industry and technical associations involved in training on the Eurocodes. The main objective was to facilitate training on Eurocode Parts related to Bridge Design through the transfer of knowledge and training information from the Eurocode Bridge Parts writers (CEN/TC250 Horizontal Group Bridges) to key trainers at national level and Eurocode users.

The workshop was a unique occasion to compile a state-of-the-art training kit comprising the slide presentations and technical papers with the worked example for a bridge structure designed following the Eurocodes. The present JRC Report compiles all the technical papers prepared by the workshop lecturers resulting in the presentation of a bridge structure analyzed from the point of view of each Eurocode.

The editors and authors have sought to present useful and consistent information in this report. However, it must be noted that **the report is not a complete design example and that the reader may identify some discrepancies between chapters.** Users of information contained in this report must satisfy themselves of its suitability for the purpose for which they intend to use it. It is also noted that the chapters presented in the report have been prepared by different authors, and reflecting the different practices in the EU Member States both ‘.’ and ‘,’ are used as decimal separators.

We would like to gratefully acknowledge the workshop lecturers and the members of CEN/TC250 Horizontal Group Bridges for their contribution in the organization of the workshop and development of the training material comprising the slide presentations and technical papers with the worked examples. We would also like to thank the Austrian Federal Ministry for Transport, Innovation and Technology, especially Dr. Eva M. Eichinger-Vill, and the Austrian Standards Institute for their help and support in the local organization of the workshop.

All the material prepared for the workshop (slides presentations and JRC Report) is available to download from the “Eurocodes: Building the future” website (<http://eurocodes.jrc.ec.europa.eu>).

Ispra, November 2011

Adamantia Athanasopoulou, Martin Poljansek, Artur Pinto

European Laboratory for Structural Assessment (ELSA)

Institute for the Protection and Security of the Citizen (IPSC)

Joint Research Centre (JRC)

Steve Denton, George Tsionis

CEN/TC250 Horizontal Group Bridges

Introduction

The Eurocodes are currently in the process of national implementation towards becoming the Europe-wide means for structural design of civil engineering works.

As part of the strategy and general programme for promotion and training on the Eurocodes, a workshop on bridge design to Eurocodes was organised in Vienna in October 2010. The main objective of this workshop was to transfer background knowledge and expertise. The workshop aimed to provide state-of-the-art training material and background information on Eurocodes, with an emphasis on practical worked examples.

This report collects together the material that was prepared and presented at the workshop by a group of experts who have been actively involved in the development of the Eurocodes. It summarises important points of the Eurocodes for the design of concrete, steel and composite road bridges, including foundations and seismic design. The worked examples utilise a common bridge project as a basis, although inevitably, they are not exhaustive.

THE EUROCODES FOR THE DESIGN OF BRIDGES

The Eurocodes

The Eurocodes, listed in the Table I, constitute a set of 10 European standards (EN) for the design of civil engineering works and construction products. They were produced by the European Committee for Standardization (CEN) and embody national experience and research output together with the expertise of international technical and scientific organisations. The Eurocodes suite covers all principal construction materials, all major fields of structural engineering and a wide range of types of structures and products.

Table I: Eurocode parts

EN 1990	Eurocode: Basis of structural design
EN 1991	Eurocode 1: Actions on structures
EN 1992	Eurocode 2: Design of concrete structures
EN 1993	Eurocode 3: Design of steel structures
EN 1994	Eurocode 4: Design of composite steel and concrete structures
EN 1995	Eurocode 5: Design of timber structures
EN 1996	Eurocode 6: Design of masonry structures
EN 1997	Eurocode 7: Geotechnical design
EN 1998	Eurocode 8: Design of structures for earthquake resistance
EN 1999	Eurocode 9: Design of aluminium structures

From March 2010, the Eurocodes were intended to be the only Standards for the design of structures in the countries of the European Union (EU) and the European Free Trade Association (EFTA). The Member States of the EU and EFTA recognise that the Eurocodes serve as:

- a means to prove compliance of buildings and civil engineering works with the essential requirements of the Construction Products Directive (Directive 89/106/EEC), particularly Essential Requirement 1 "Mechanical resistance and stability" and Essential Requirement 2 "Safety in case of fire";
- a basis for specifying contracts for construction works and related engineering services;

- a framework for drawing up harmonised technical specifications for construction products (ENs and ETAs).

The Eurocodes were developed under the guidance and co-ordination of CEN/TC250 “Structural Eurocodes”. The role of CEN/TC250 and its subcommittees is to manage all the work for the Eurocodes and to oversee their implementation. The Horizontal Group Bridges was established within CEN/TC250 with the purpose of facilitating technical liaison on matters related to bridges and to support the wider strategy of CEN/TC250. In this context, the strategy for the Horizontal Group Bridges embraces the following work streams: maintenance and evolution of Eurocodes, development of National Annexes and harmonisation, promotion (training/guidance and international), future developments and promotion of research needs.

Bridge Parts of the Eurocodes

Each Eurocode, except EN 1990, is divided into a number of parts that cover specific aspects. The Eurocodes for concrete, steel, composite and timber structures and for seismic design comprise a Part 2 which covers explicitly the design of road and railway bridges. These parts are intended to be used for the design of new bridges, including piers, abutments, upstand walls, wing walls and flank walls etc., and their foundations. The materials covered are i) plain, reinforced and prestressed concrete made with normal and light-weight aggregates, ii) steel, iii) steel-concrete composites and iv) timber or other wood-based materials, either singly or compositely with concrete, steel or other materials. Cable-stayed and arch bridges are not fully covered. Suspension bridges, timber and masonry bridges, moveable bridges and floating bridges are excluded from the scope of Part 2 of Eurocode 8.

A bridge designer should use EN 1990 for the basis of design, together with EN 1991 for actions, EN 1992 to EN 1995 (depending on the material) for the structural design and detailing, EN 1997 for geotechnical aspects and EN 1998 for design against earthquakes. The main Eurocode parts used for the design of concrete, steel and composite bridges are given in Table II.

The ten Eurocodes are part of the broader family of European standards, which also include material, product and execution standards. The Eurocodes are intended to be used together with such normative documents and, through reference to them, adopt some of their provisions. Fig. 1 schematically illustrates the use of Eurocodes together with material (e.g. concrete and steel), product (e.g. bearings, barriers and parapets) and execution standards for the design and construction of a bridge.

Table II: Overview of principal Eurocode parts used for the design of concrete, steel and composite bridges and bridge elements

EN Part	Scope	Concrete	Steel	Composite
EN 1990	Basis of design	√	√	√
EN 1990/A1	Bridges	√	√	√
EN 1991-1-1	Self-weight	√	√	√
EN 1991-1-3	Snow loads	√	√	√
EN 1991-1-4	Wind actions	√	√	√
EN 1991-1-5	Thermal actions	√	√	√
EN 1991-1-6	Actions during execution	√	√	√
EN 1991-1-7	Accidental actions	√	√	√
EN 1991-2	Traffic loads	√	√	√
EN 1992-1-1	General rules	√		√
EN 1992-2	Bridges	√		√
EN 1993-1-1	General rules		√	√
EN 1993-1-5	Plated elements		√	√
EN 1993-1-7	Out-of-plane loading		√	√
EN 1993-1-8	Joints		√	√
EN 1993-1-9	Fatigue		√	√
EN 1993-1-10	Material toughness		√	√
EN 1993-1-11	Tension components		√	√
EN 1993-1-12	Transversely loaded plated structures		√	√
EN 1993-2	Bridges		√	√
EN 1993-5	Piling		√	√
EN 1994-1-1	General rules			√
EN 1994-2	Bridges			√
EN 1997-1	General rules	√	√	√
EN 1997-2	Testing	√	√	√
EN 1998-1	General rules, seismic actions	√	√	√
EN 1998-2	Bridges	√	√	√
EN 1998-5	Foundations	√	√	√

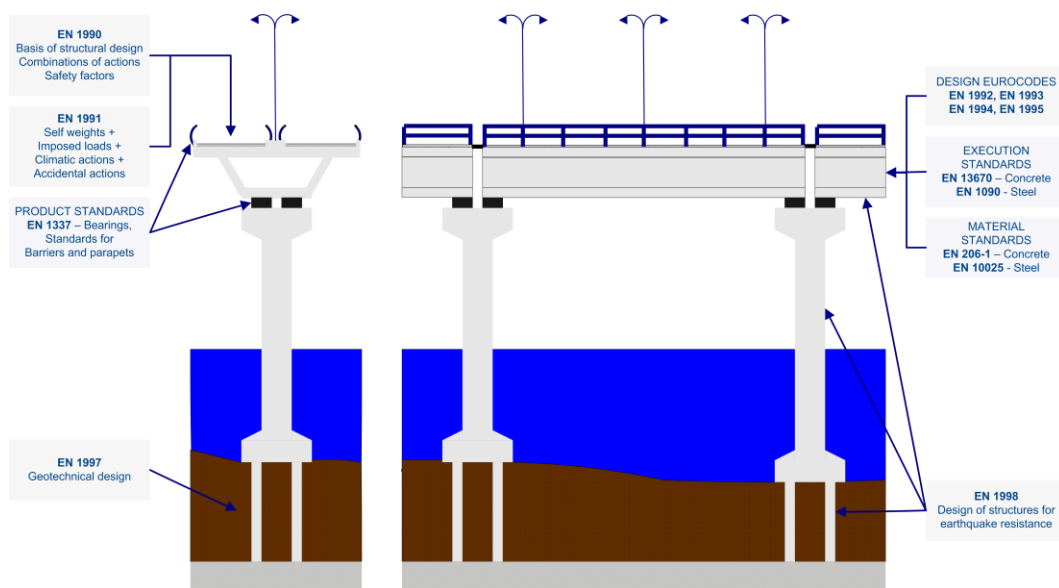


Figure I: Use of Eurocodes with product, material and execution standards for a bridge

THE DESIGN EXAMPLE

The worked examples in this report refer to the same structure. However some modifications and/or extensions are introduced to cover some specific issues that would not otherwise be addressed; details are given in the pertinent chapters. Timber bridges are not treated in this report, although their design is covered by the Eurocodes.

The following assumptions have been made:

- the bridge is not spanning a river and therefore no hydraulic actions are considered;
- the climatic conditions are such that snow actions are not considered;
- the soil properties allow for the use of shallow foundations;
- the recommended values for the Nationally Determined Parameters are used throughout.

The example structure, shown in Fig. II, is a road bridge with three spans (60.0 m + 80.0 m + 60.0 m). The continuous composite deck is made up of two steel girders with I cross-section and a concrete slab with total width 12.0 m. Alternative configurations, namely transverse connection at the bottom of the steel girders and use of external tendons, are also studied. Two solutions are considered for the piers: squat and slender piers with a height 10.0 m and 40.0 m, respectively. The squat piers have a 5.0x2.5 m rectangular cross-section while the slender piers have a circular cross-section with external diameter 4.0 m and internal diameter 3.2 m. For the case of slender piers, the deck is fixed on the piers and free to move on the abutments. For the case of squat piers, the deck is connected to each pier and abutment through triple friction pendulum isolators. The piers rest on rectangular shallow footings. The abutments are made up of gravity walls that rest on rectangular footings.

The configuration of the example bridge was chosen for the purpose of this workshop. It is not proposed as the optimum solution and it is understood that other possibilities exist. It is also noted that the example is not fully comprehensive and there are aspects that are not covered.

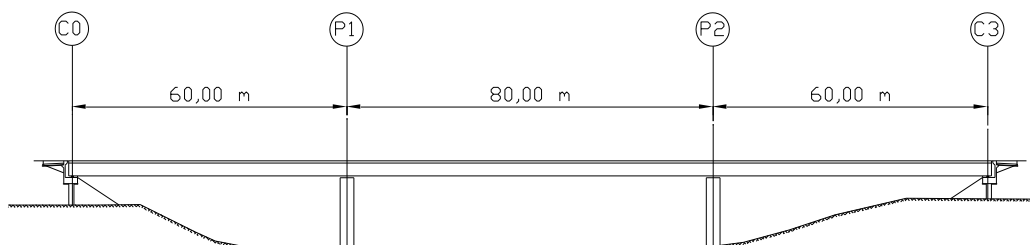


Figure II: Geometry of the example bridge

OUTLINE OF THE REPORT

Following the introduction, Chapter 1 describes the geometry and materials of the example bridge as well as the main assumptions and the detailed structural calculations. Each of the subsequent chapters presents the main principles and rules of a specific Eurocode and their application on the example bridge. The key concepts of basis of design, namely design situations, limit states, the single source principle and the combinations of actions, are discussed in Chapter 2. Chapter 3 deals with the permanent, wind, thermal, traffic and fatigue actions and their combinations. The use of FEM analysis and the design of the deck and the piers for the ULS and the SLS, including the second-order effects are presented in Chapters 4 and 5, respectively. Chapter 6 handles the classification of

composite cross-sections, the ULS, SLS and fatigue verifications and the detailed design for creep and shrinkage. Chapter 7 presents the settlement and resistance calculations for the pier, three design approaches for the abutment and the verification of the foundation for the seismic design situation. Finally, Chapter 8 is concerned with the conceptual design for earthquake resistance considering the alternative solutions of slender or squat piers; the latter case involves seismic isolation and design for ductile behaviour.

Steve Denton, Chairman of Horizontal Group Bridges

Georgios Tsionis, University of Patras, Secretary of Horizontal Group Bridges

CHAPTER 1

Introduction to the design example

Pilar CRESPO

Ministry of Public Works (Spain)

Laurence DAVAINÉ

French Railway Bridge Engineering Department (SNCF, IGOA)

1.1 Introduction

The main characteristics of the bridge worked out in the following chapters are presented here. The dimensions of the deck and the substructure, the constituent materials, the construction process and the relevant design assumptions are summarized in this chapter.

There is a main example which is analysed from the point of view of each Eurocode all along this Report. However, where an author has considered of interest to highlight some specific aspect, a partial alternative example has been developed to explain the relevant issue. These alternative examples, like different cross-sections of the deck, different pier heights or bearing configurations are presented here as well.

1.2 Geometry of the deck

1.2.1 LONGITUDINAL ELEVATION

As shown in Fig. 1.1, the bridge, with a continuous three-span deck: 60 m - 80 m - 60 m, has a total length of 200 m. The deck has a constant depth along the whole length and its longitudinal axis is straight and horizontal.

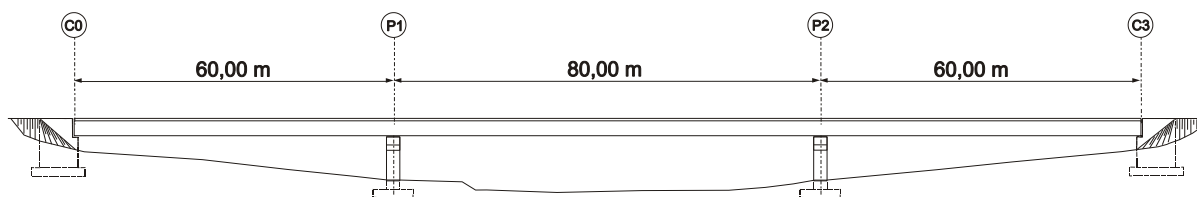


Fig. 1.1 Longitudinal elevation

1.2.2 TRANSVERSE CROSS-SECTION

The deck is made up of a symmetrical two-girder composite cross-section. The depth of the main steel girders is 2800 mm.

The slab depth, with a 2.5% symmetrical superelevation, varies from 0.4 m over the girders to 0.25 m at its free edges and 0.3075 m at the central point.

The total slab width is 12 m. The centre-to-centre spacing between main girders is 7 m and the slab cantilever either side is 2.5 m long.

In Fig. 1.2, it is represented a typical cross-section of the deck.

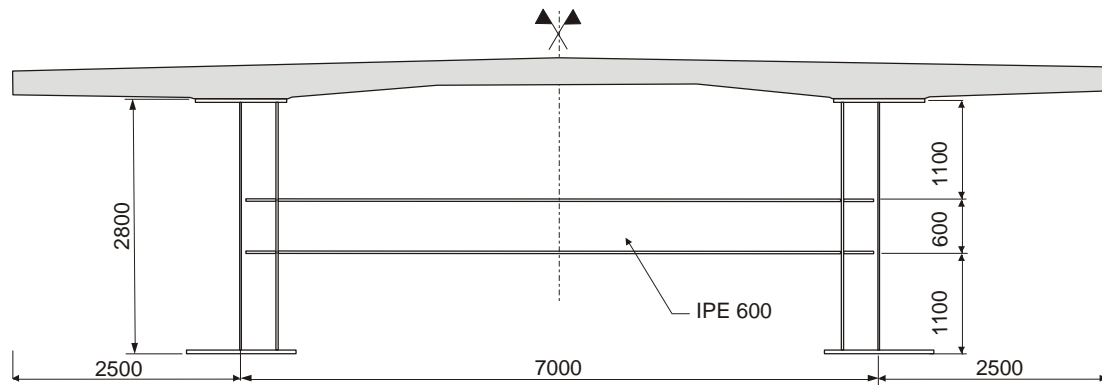


Fig. 1.2 Typical in-span cross-section

1.2.3 ALTERNATIVE DECKS

1.2.3.1 Double composite action

As an alternative to the simple composite action, a double composite cross-section, located at the hogging areas, will be presented and analysed in Chapter 6- *Composite bridge design*.

The bottom reinforced concrete slab, with a constant thickness of 0.5 m, is placed between the two steel girders and connected to them (Fig. 1.3). Notice that the lower steel flange has been reduced in comparison to the main example (see Fig. 1.13).

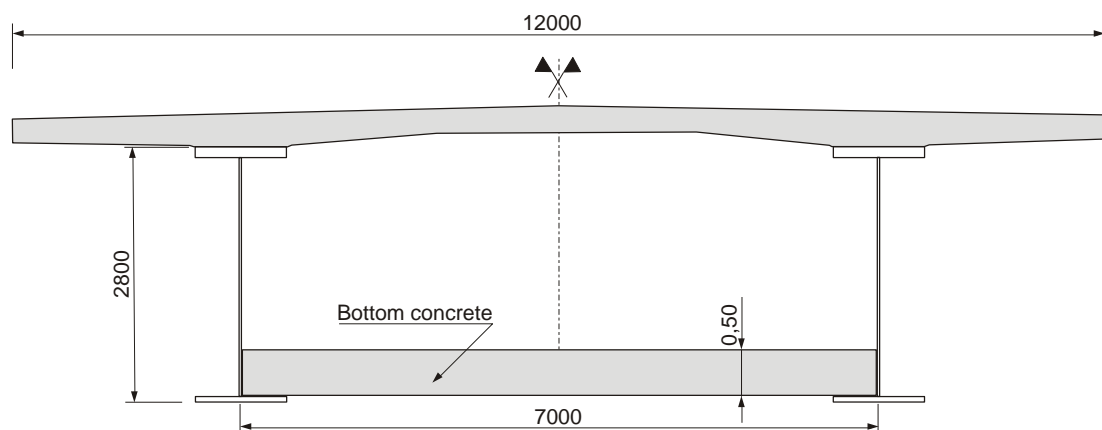


Fig. 1.3 Alternative deck: Double composite cross-section at hogging areas

1.2.3.2 Prestressed composite deck

In Chapter 5 - *Concrete bridge design*, the effects of the external prestressing are analysed.

Four different solutions are considered for the external prestressing of the main example composite deck: two different layouts of the tendons and two ways of applying the prestress forces (to the steel girders or to the composite section).

In Fig. 1.4, one of the prestressing layouts is shown.

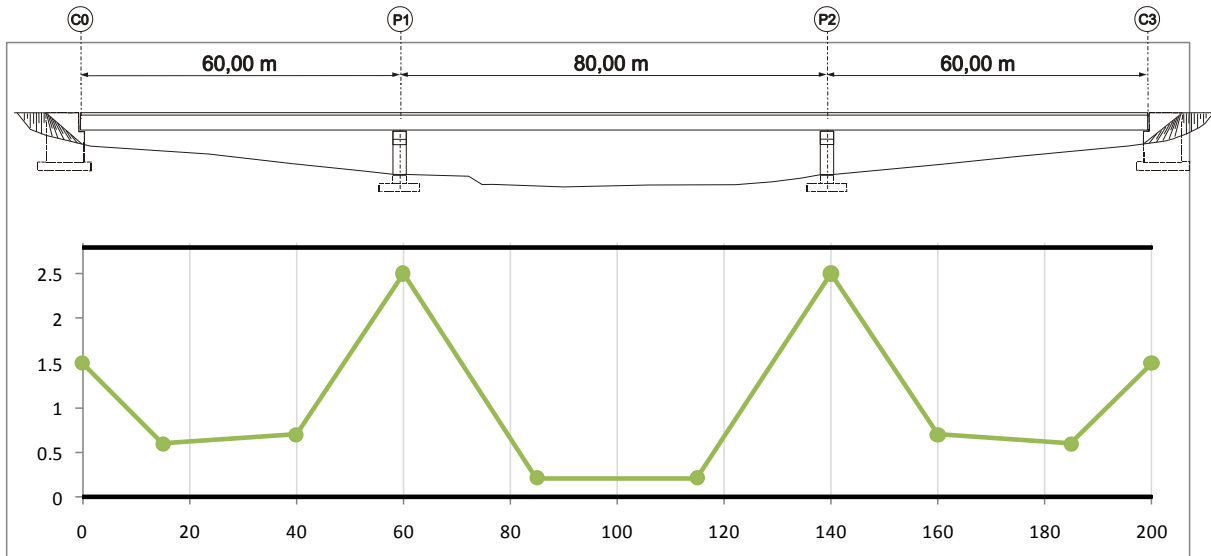


Fig. 1.4 Alternative deck: Longitudinal prestressing layout

1.3 Geometry of the substructure

1.3.1 PIERS

Two alternatives are analysed according to EN 1992 and EN 1998 in the relevant Chapters.

1.3.1.1 Squat piers

The piers are 10 m high with a solid rectangular cross-section of 5.0 m x 2.5 m. They have a pier head to receive the deck, 9.0 m x 2.5 m in plan (see Fig. 1.5). The bridge elevation with squat piers is shown in Fig. 1.1.

The dimensions of the pier with its foundation pad are represented in Fig. 1.5.

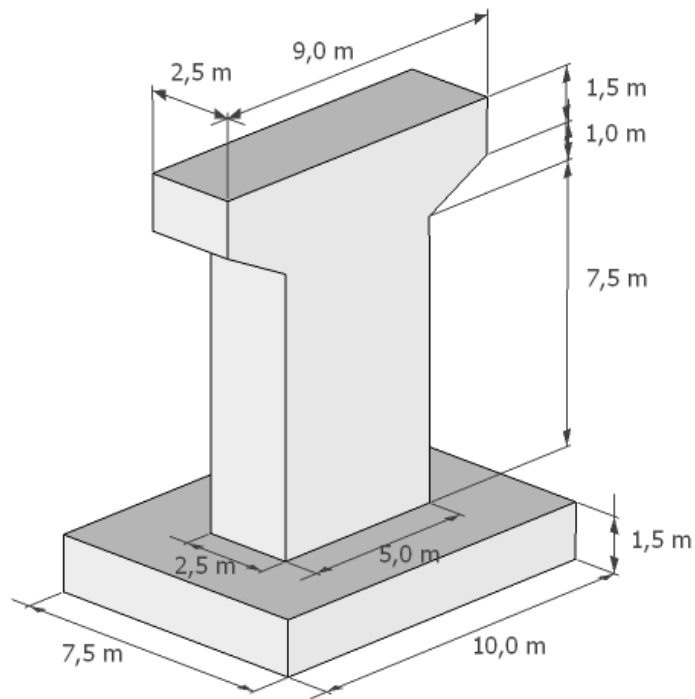


Fig. 1.5 Pier elevation, $H = 10$ m

1.3.1.2 High piers

The height of the piers is 40 m. They have a circular hollow section with an external diameter of 4.0 m and walls 0.40 m thick. A pier head is designed at the top to receive the deck.

The foundation pad is 10.0 m x 10.0 m x 2.5 m.

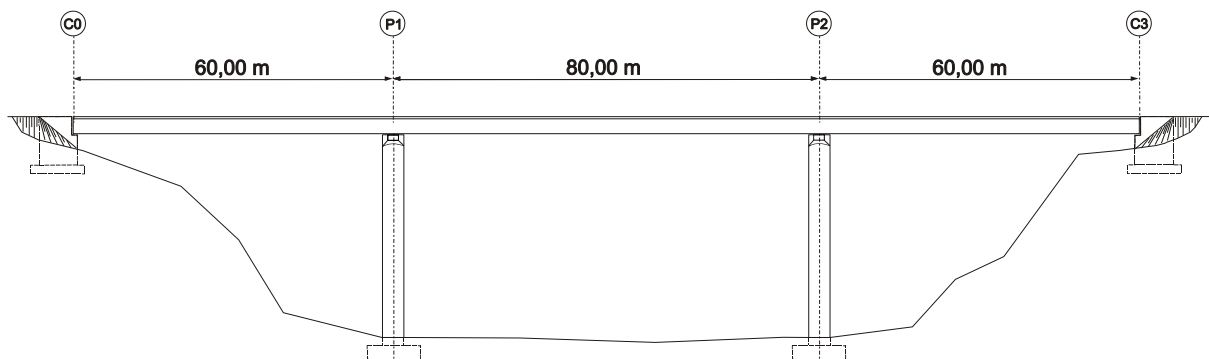


Fig. 1.6 Bridge elevation with piers $H = 40$ m

1.3.2 ABUTMENTS

The abutments geometry is represented in Fig. 1.7.

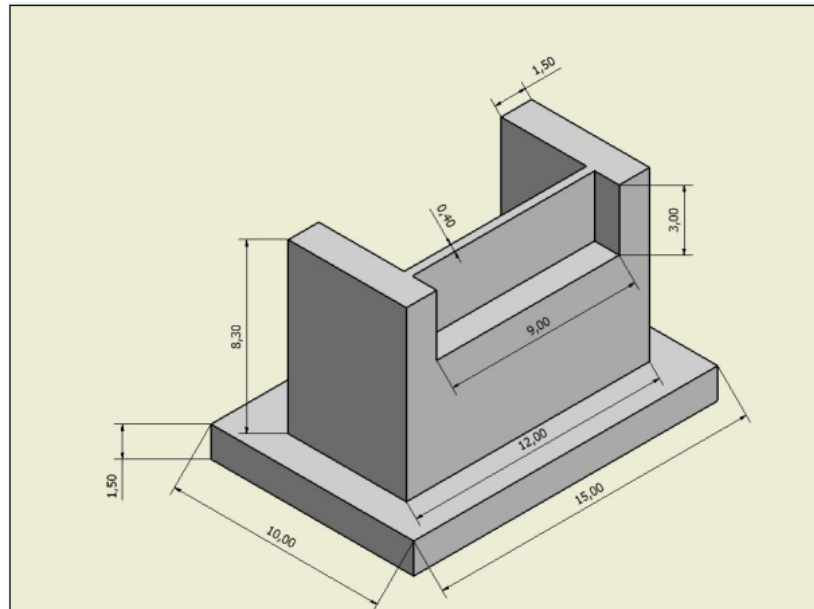


Fig. 1.7 Abutment geometry

1.3.3 BEARINGS

1.3.3.1 For the squat piers case

There are two bearings at each abutment and pier with non-linear friction behaviour in both, longitudinal and transverse direction (Triple Friction Pendulum System, FPS).

The bearing dimensions are:

- 1.20 m x 1.20 m, $h = 0.40$ m at piers
- 0.90 m x 0.90 m, $h = 0.40$ m at abutments

The configuration of the bearings is as shown in Fig. 1.8.

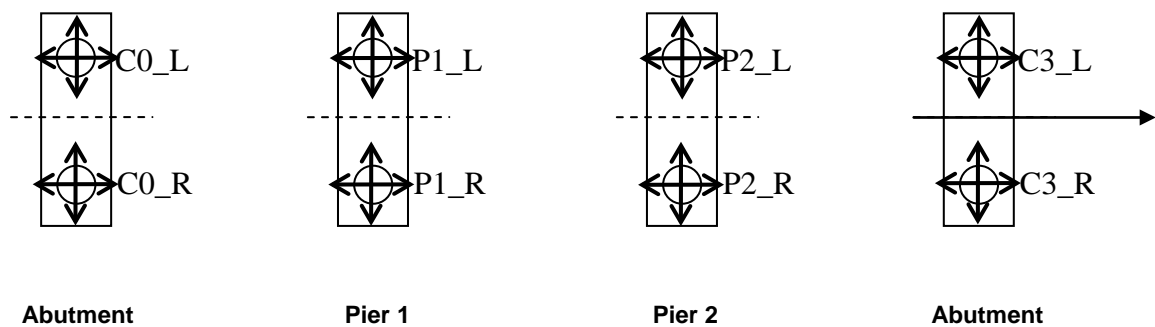


Fig. 1.8 Bearings layout for the squat pier case

1.3.3.2 For the high piers case

For this case (Fig. 1.6), the configuration of the bearings is as follows (see Fig. 1.9):

- At piers: a fixed articulated connection on the right side and an articulated connection on the left side, fixed in the longitudinal direction and free in the transverse.
- At abutments: a displacement-free bearing in both directions on the left side and transversally restraint on the right side.

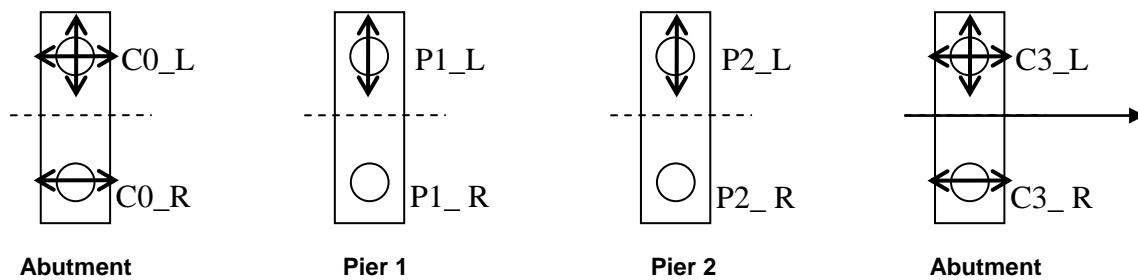


Fig. 1.9 Bearings layout for the high pier case

1.3.3.3 Special case for seismic design

There is a third configuration of the bearings dealt with at the Chapter 8 - *Overview of seismic design issues for bridge design*. It is not a partial alternative to the main example. In this case, the whole bridge is a special example to show the design of ductile piers rigidly connected to the deck. There are bearings just at abutments.

1.4 Design specifications

1.4.1 DESIGN WORKING LIFE

The bridge will be designed for 100 year working life.

1.4.2 NON-STRUCTURAL ELEMENTS

For the assessment of dead loads, the following elements are considered: two parapets, two cornices, a waterproofing layer 3 cm thick and an asphalt layer 8 cm thick.

These elements are according to the generic detail shown in Fig. 1.10.

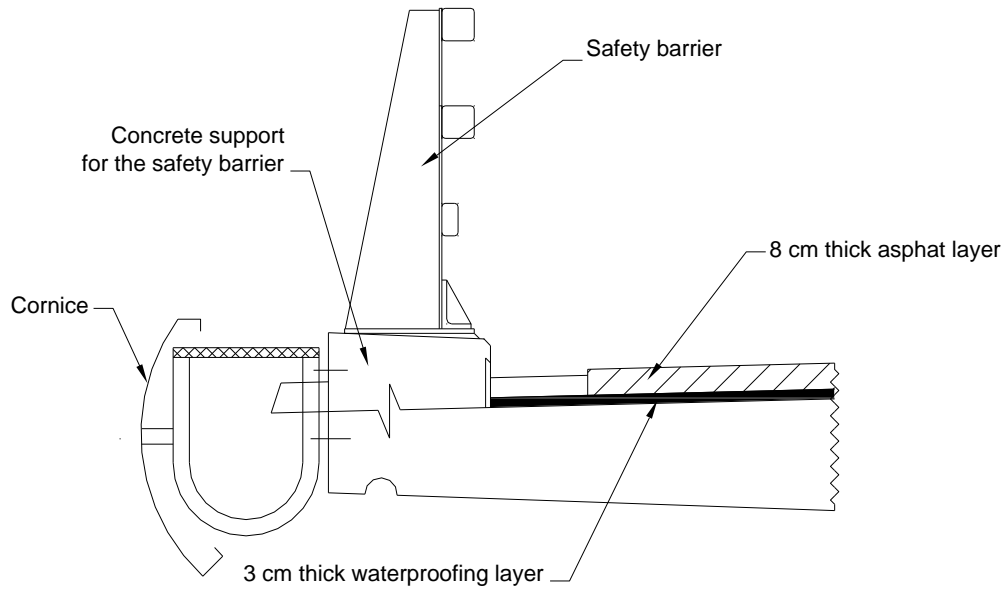


Fig. 1.10 Non-structural elements

1.4.3 TRAFFIC DATA

1.4.3.1 Traffic lines arrangement

The road has two traffic lanes 3.5 m wide and a hard strip 2.0 m wide each side. It makes a total width of 11 m for the carriageway. See Fig. 1.11.

Considering 0.5 m for the vehicle parapet of each side, we get the total width of the concrete slab equal to 12 m.

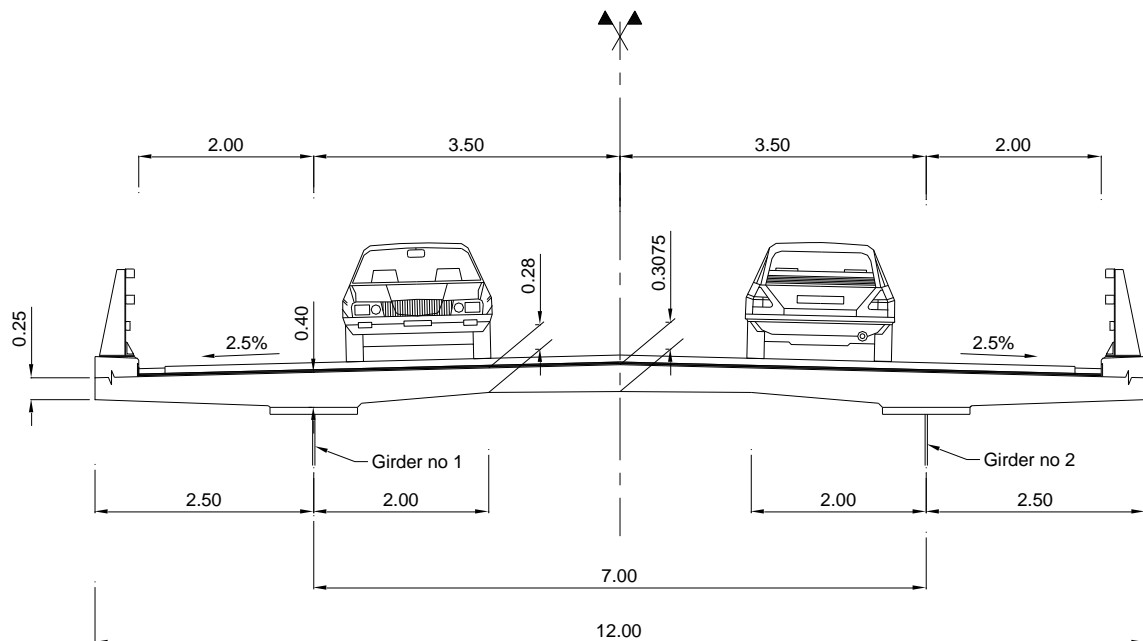


Fig. 1.11 Traffic lanes

1.4.3.2 Traffic composition

Traffic loads will be represented by Load Model 1. According to EN 1991-2, LM1, which is formed by a uniform distributed load (UDL) and the concentrated loads of the tandem system (TS), can be adjusted by means of some α -coefficients. The values of these α -coefficients can be given by the National Annexes based on different traffic classes. For this example, the values $\alpha_{Q1} = \alpha_{q1} = \alpha_{qr} = 1.0$ will be adopted (these values are recommended by EN 1991-2, 4.3.2, in the absence of specification about the composition of the traffic).

No abnormal vehicles will be considered.

1.4.3.3 Assumptions for fatigue

For this example, two slow traffic lanes in opposite directions will be considered, at the same position as the actual traffic lanes.

For this example, the following simplification will be accepted: the model vehicle used to calculate the longitudinal internal forces and moments in the deck will be placed centrally in the actual slow lane width.

The road is supposed to have “medium flow rate of lorries” with an average gross weight of the lorries equal to 445 kN.

1.4.4 ENVIRONMENTAL CONDITIONS

1.4.4.1 Temperature

The minimum shade air temperature at the bridge location to be considered for the selection of the steel quality is -20°C . It corresponds to a return period of 50 years.

The maximum shade air temperature at the bridge location to be considered in the calculations, if relevant, is $+40^{\circ}\text{C}$.

The vertical difference component will be considered as a difference of $\pm 10^{\circ}\text{C}$ between the concrete slab temperature and the steel part temperature.

1.4.4.2 Humidity

The ambient relative humidity (RH) is assumed to be equal to 80%.

1.4.4.3 Wind

The bridge is spanning a flat valley with little and isolated obstacles like some tree or house.

It is located at an area where the fundamental value of the basic wind velocity is $v_{b,0} = 26 \text{ m/s}$.

It is assumed that no pushing operation of the steel beams will be performed if wind velocity is over 50 km/h.

1.4.4.4 Exposure Class

The bridge is located in a moderate freezing zone where de-icing agents are frequently used.

To determine the concrete cover, the following exposure classes, according to Table 4.1 of EN 1992-1-1, will be taken into account:

- XC3 for the top face of the concrete slab (under the waterproofing layer)
- XC4 for the bottom face of the concrete slab

1.4.5 SOIL CONDITIONS

Soil conditions are such that no deep foundation is needed. Both piers and abutments have shallow foundations.

A settlement of 30 mm at Pier 1 will take place for the quasi-permanent combination of actions. It can be assumed that this displacement occurs at the end of the construction stage.

1.4.6 SEISMIC DATA

Two alternative configurations are analysed in the Chapter 8 - *Overview of seismic design issues for bridge design*:

- Squat piers ($H=10$ m) with seismic isolation
- High piers ($H=40$ m) with longitudinal fixed connection between piers and deck

For the seismic analysis, the ground under the bridge is considered to be formed by deposits of very dense sand (it can be identified as ground type B, according to EN 1998-1, Table 3.1).

The bridge has a medium importance for the communications system after an earthquake, so the importance factor γ_I will be taken equal to 1.0.

No special regional seismic situation is considered.

For the squat piers case, the reference peak ground acceleration will be $a_{gR} = 0.40g$.

For the high piers case, the reference peak ground acceleration will be $a_{gR} = 0.30g$. In this case, a limited elastic behavior is selected and, according to Table 4.1 of EN 1998-2, the behaviour factor is taken $q = 1.5$ (reinforced concrete piers).

1.4.7 OTHER SPECIFICATIONS

The action of snow is considered to be negligible.

Hydraulic actions are not relevant.

Accidental design situations will not be analysed in the example.

1.5 Materials

a) Structural steel

For the structural steel of the deck, grade S355 is used with the subgrades indicated in Table 1.1, depending on the plate thickness.

Table 1.1 Structural steel subgrades

Thickness	Subgrade
$t \leq 30$ mm	S 355 K2
$30 \leq t \leq 80$ mm	S 355 N
$80 \leq t \leq 135$ mm	S 355 NL

b) Concrete

Concrete class C35/45 is used for all the concrete elements in the example (deck slab, piers, abutments and foundations).

c) Reinforcing steel

The reinforcing bars used in the example are class B high bond bars with a yield strength $f_{sk} = 500$ MPa.

d) Shear connectors

Stud shear connectors in S235J2G3 steel grade are adopted. Their ultimate strength is $f_u = 450$ MPa.

1.6 Details on structural steel and slab reinforcement

1.6.1 STRUCTURAL STEEL DISTRIBUTION

The structural steel distribution for a main girder is presented in Fig. 1.12.

Every main girder has a constant depth of 2800 mm and the variations in thickness of the upper and lower flanges are found towards the inside of the girder. The lower flange is 1200 mm wide whereas the upper flange is 1000 mm wide.

The two main girders have transverse bracing at abutments and at internal supports, as well as every 7.5 m in side spans (C0-P1 and P2-C3) and every 8 m in central span (P1-P2). Fig. 1.13 and Fig. 1.14 illustrate the geometry and dimensions adopted for this transverse cross-bracing.

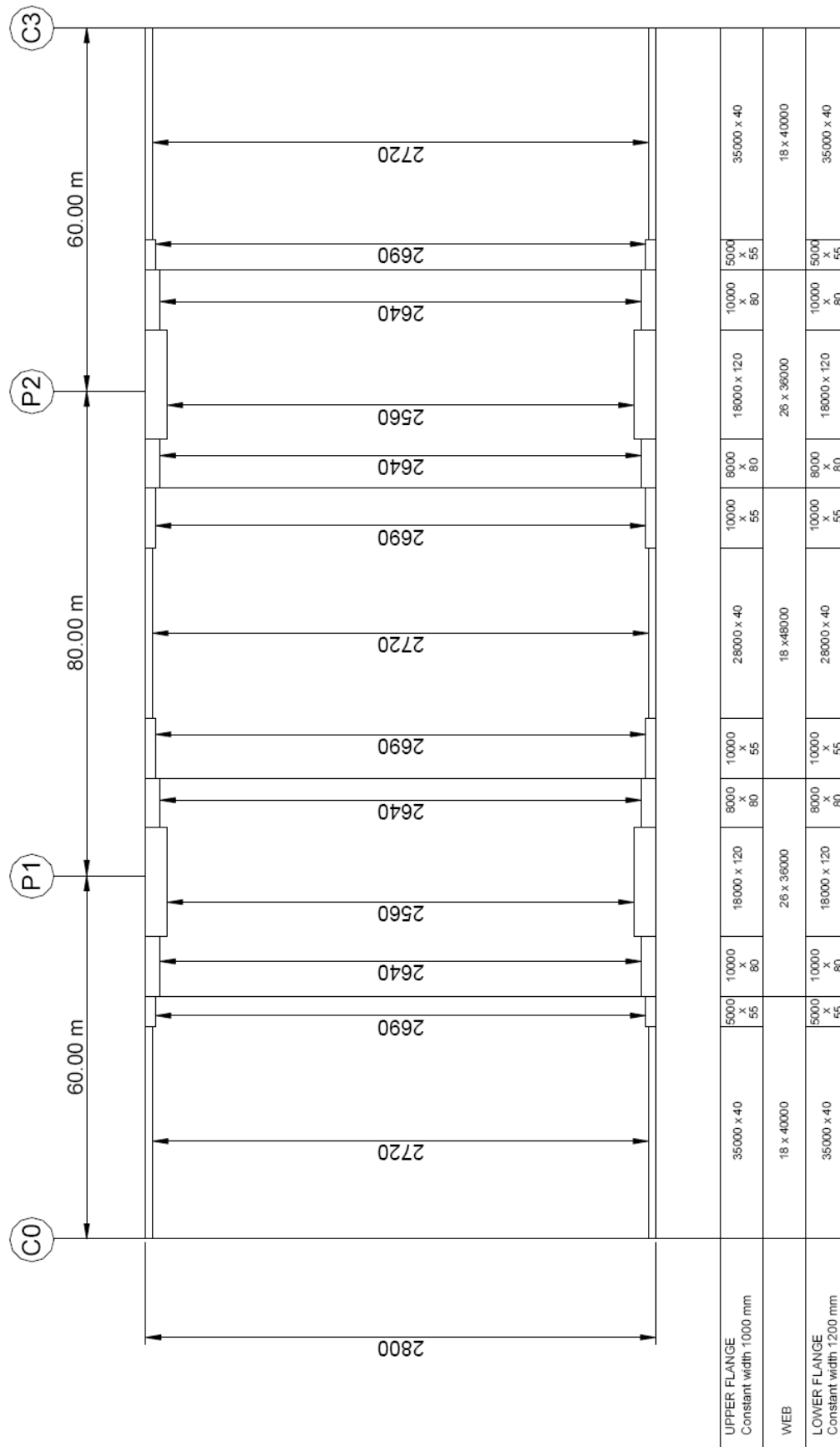
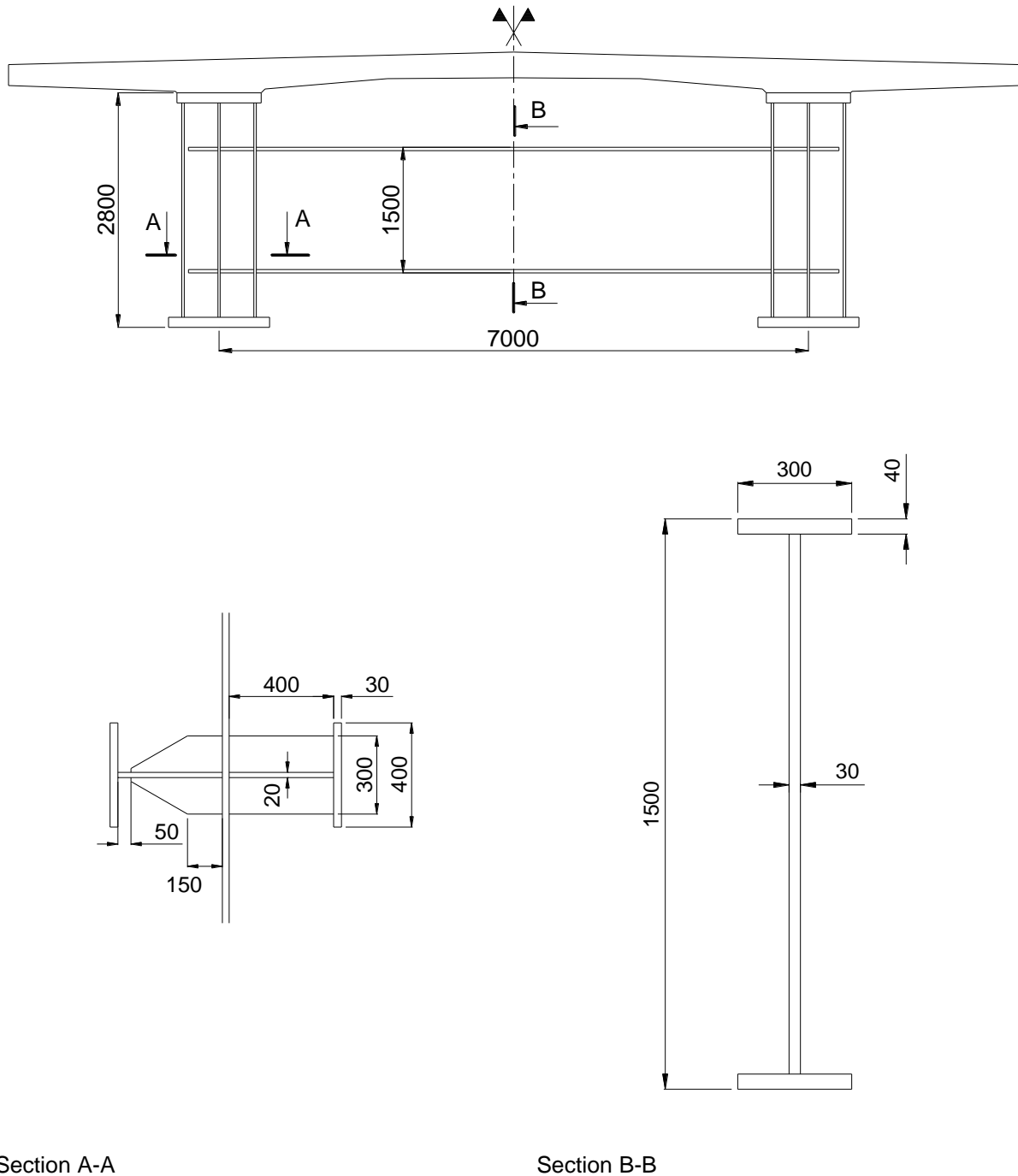


Fig. 1.12 Structural steel distribution (main girder)

The transverse girders in span are made of IPE600 rolled sections whereas the transverse girders at internal supports and abutments are built-up welded sections. The vertical T-shaped stiffeners are duplicated and welded on the lower flange at supports whereas the flange of the vertical T-shaped stiffeners in span has a V-shaped cut-out for fatigue reasons.



Section A-A

Section B-B

Fig. 1.13 Detailing of transverse cross-bracing at supports

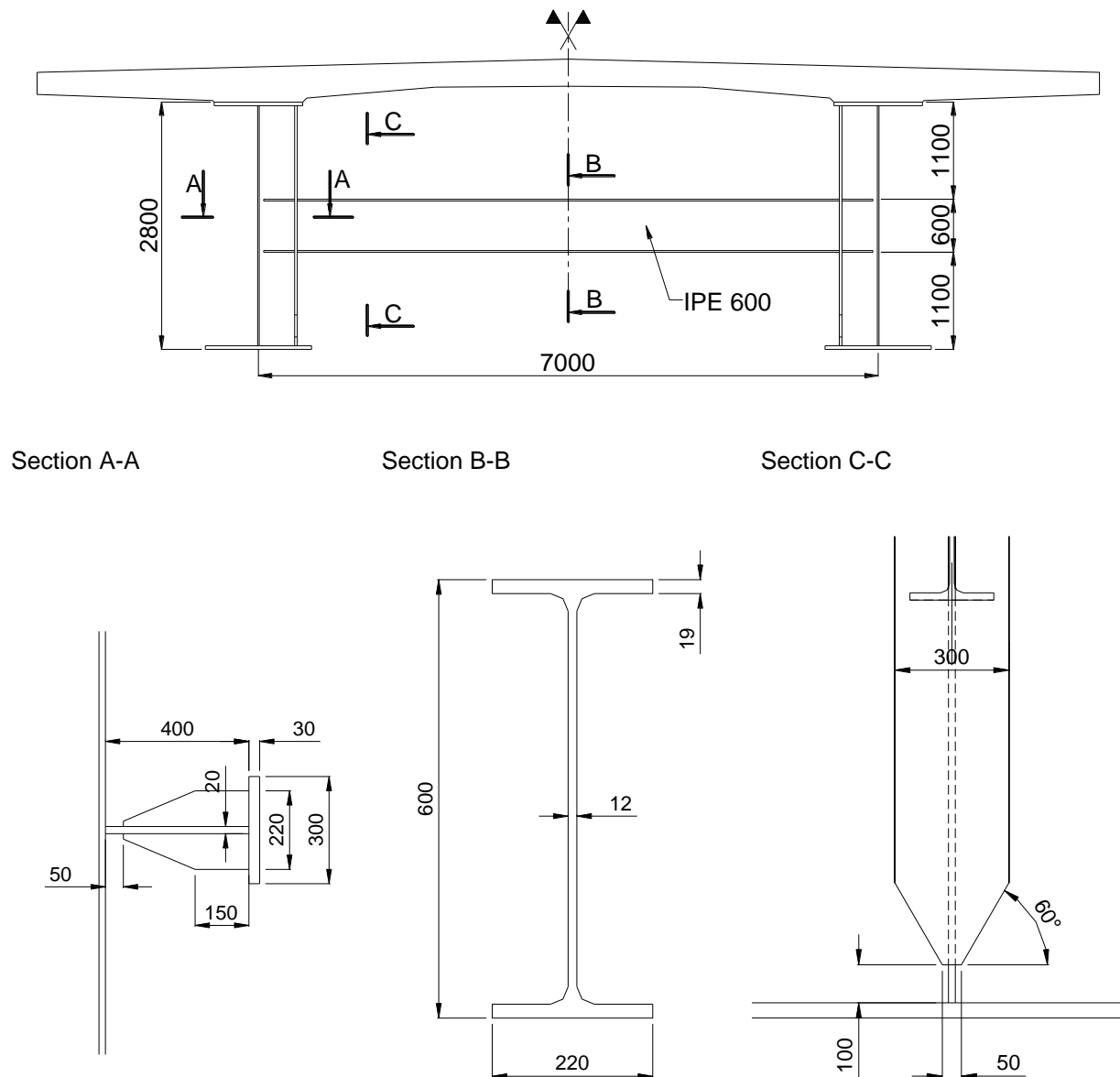


Fig. 1.14 Detailing of in-span transverse cross-bracing

1.6.2 DESCRIPTION OF THE SLAB REINFORCEMENT

For both steel reinforcing layers, the transverse bars are placed outside the longitudinal ones, on the side of the slab free surface (Fig. 1.15). High bond bars are used.

a) Longitudinal reinforcing steel

- In span regions: $\Phi = 16$ mm every 130 mm in upper and lower layers
(i.e. in total $\rho_s = 0.92\%$ of the concrete section)
- In intermediate support regions: $\Phi = 20$ mm every 130 mm in upper layer
 $\Phi = 16$ mm every 130 mm in lower layer

b) Transverse reinforcing steel

- At mid-span of the slab (between the main steel girders):

$\Phi = 20$ mm every 170 mm in upper layer

$\Phi = 25$ mm every 170 mm in lower layer

- Over the main steel girders: $\Phi = 20$ mm every 170 mm in upper layer

$\Phi = 16$ mm every 170 mm in lower layer

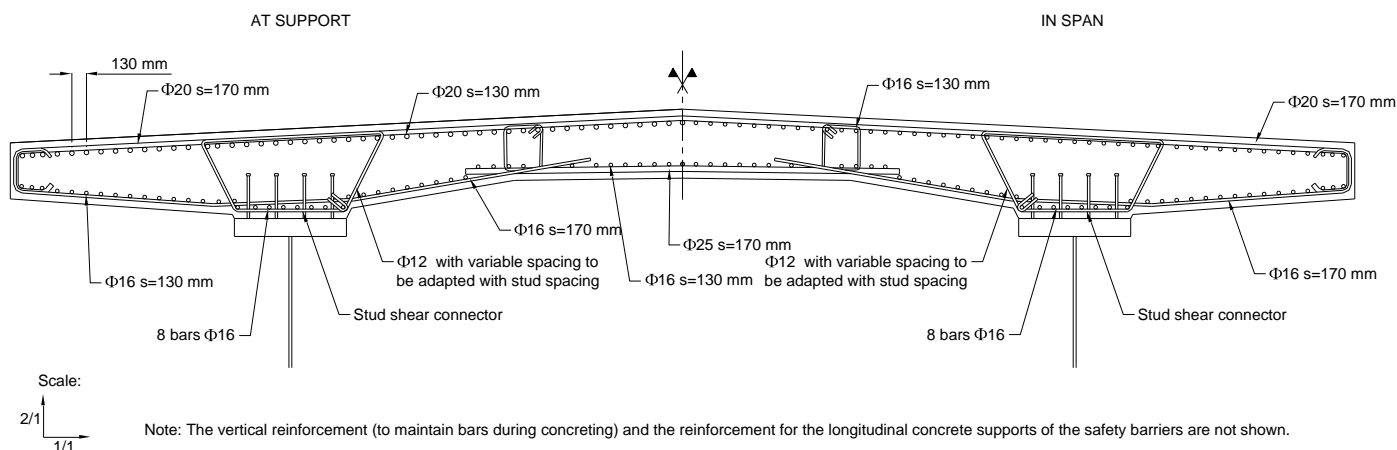


Fig. 1.15 Steel reinforcement in a slab cross-section

1.7 Construction process

1.7.1 LAUNCHING OF THE STEEL GIRDERS

It is assumed that the steel structure is launched and it is pushed from the left abutment (C0) to the right one (C3) without the addition of any nose-girder.

1.7.2 SLAB CONCRETING

After the installation of the steel structure, concrete is poured on site casting the slab elements in a selected order: the total length of 200 m is split into 16 identical 12.5-m-long concreting segments. They are poured in the order indicated in Fig. 1.16.

The start of pouring the first slab segment is the time origin ($t = 0$). Its definition is necessary to determine the respective ages of the concrete slab segments during the construction phases. The time taken to pour each slab segment is assessed as 3 working days. The first day is devoted to the concreting, the second day to its hardening and the third to moving the formwork. This sequence respects a minimum concrete strength of 20 MPa before removal of the formwork. The slab is thus completed within 66 days (including the non-working days over the weekend).

It is assumed that the installation of non-structural bridge equipments is completed within 44 days, so that the deck is fully constructed at the date $t = 66 + 44 = 110$ days.

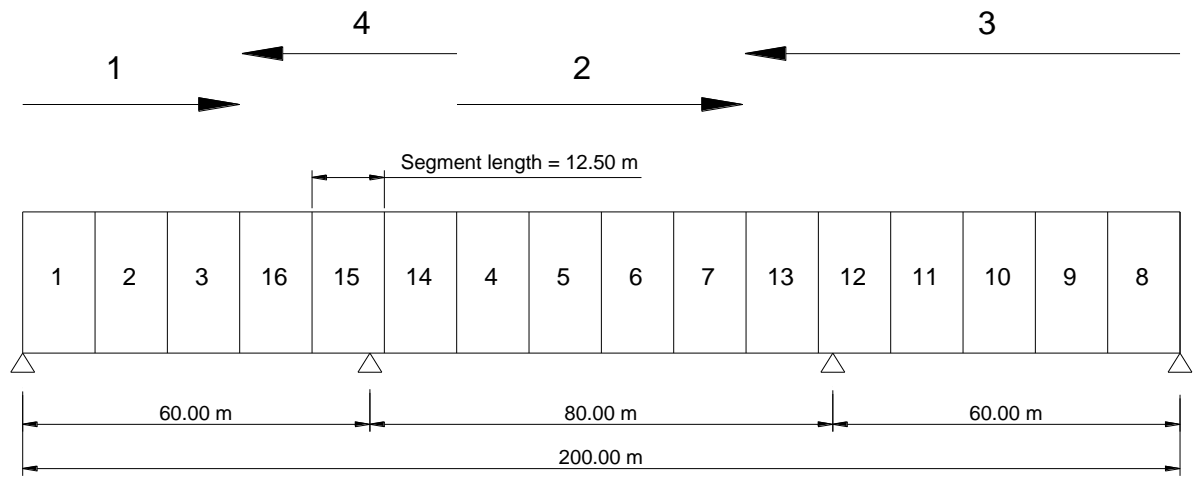


Fig. 1.16 Order for concreting the slab segments

CHAPTER 2

Basis of design (EN 1990)

Steve DENTON

*Engineering Director, Parsons Brinckerhoff
Visiting Professor, University of Bath, U.K.*

2.1 Introduction

EN 1990:2002 was the first of the Eurocodes published, and it is frequently referred to as the ‘head’ Eurocode. This is because EN 1990:2002 essentially serves a dual role, and understanding this fact is very helpful in understanding the Standard.

As would be expected, EN 1990:2002 sets out principles and requirements to be applied by designers. In addition, it also establishes the overall framework of tools and principles used by the drafters of the other Eurocode parts.

As a result, EN 1990:2002 includes some very general statements, such as clause **2.1(2)P** which states that a structure ‘shall be designed to have adequate structural resistance, serviceability, and durability’. Whilst this is clearly an entirely sensible statement, EN 1990:2002 gives little guidance on how this should actually be done. Once designers are familiar with the full Eurocode suite this is not a problem, because the means of fulfilling such general principles are given in the other Eurocode parts.

It is sometimes helpful to think of EN 1990:2002 as a toolbox – providing the tools that are then used by the other Eurocode parts. This can make reading EN 1990 in isolation rather tricky as it is not always immediately clear how the tools it creates are to be deployed. This chapter aims to help with that challenge, and serve as a general introduction to the principles, terminology and notation used throughout this report.

It does so by providing an overview of EN 1990:2002 following its structure and drawing out important issues. In doing so, six key concepts are identified that bridge designers should understand. These are: design situations; reversible and irreversible serviceability limit states; representative values of variable actions; the six different ultimate limit states; the single source principle; and the five general expressions for the combination of actions. A summary of each of these concepts is provided in Section 2.9.

2.2 EN1990 Section 1 – General

Section 1 of EN 1990:2002 sets out its scope and assumptions. It also contains definitions and notation. It is noteworthy that the scope of EN 1990:2002 includes ‘structural design of civil engineering works, including execution and temporary structures’, i.e. temporary works (clause **1.1(2)**), and also that it includes ‘the structural appraisal of existing construction, in developing the design of repairs and alterations or in assessing changes of use’ (clause **1.1(4)**). However, there is an important note below this latter clause that explains that ‘additional or amended provisions’ may be required for this purpose, which enables countries to maintain the use of any existing assessment standards for bridges.

It is also worth noting that the assumptions given in clause **1.3(2)** are quite onerous and impact the designer, contractor and client. They include requirements for competency and quality control.

2.3 EN1990 Section 2 – Requirements

Section 2 of EN 1990:2002 sets out basic requirements, and also general requirements for reliability management, design working life, durability and quality management.

The basic requirements include the three stated in clause **2.1(2)P**. These are that the structure should be designed to have adequate structural resistance, serviceability, and durability. There is, however, effectively a fourth basic requirement embodied in clause **2.1(4)P** which states that a structure 'shall be designed and executed in such a way that it will not be damaged by events...to an extent disproportionate to the original cause'. This clause requires structures to be *robust*, and designers should be very mindful of this fundamental requirement, particularly when designing structures with complicated structural forms, when using brittle (or quasi-brittle) materials, components or connections, and in structures with limited redundancy (*i.e.* without alternative load paths).

2.4 EN1990 Section 3 – Principles of limit state design

Section 3 of EN 1990:2002 sets of general principles of limit state design, addressing both ultimate and serviceability limit states.

2.4.1 DESIGN SITUATIONS

EN 1990:2002, **3.2**, introduces the concept of design situations. This is the first of the six key concepts summarised in Section 2.9. Design situations are circumstances (sets of physical conditions) that the structure might experience during its life. As explained in clause **3.2(3)P**, the design situations taken into account in the design, 'shall be sufficiently severe and varied so as to encompass all conditions that can reasonably be foreseen to occur during the execution and use of the structure'. Although it is important that the designer satisfies him or herself that this principle has been followed, in general, the design situations that need to be considered in bridge design are addressed through the requirements for actions in the various parts of EN 1991, and in the requirements given in the other relevant Eurocode parts, depending on the materials used and form of construction.

The real usefulness of the concept of design situations, however, lies in the way in which they are classified. Design situations are drawn together into families that share common characteristics. These categories or families are called persistent, transient, accidental and seismic design situations.

The value of these categorisations is that they recognise that the design requirements for the different families may be different. In practice, the distinction between persistent and transient design situations is rather subtle, but the treatment of accidental and seismic design situations is quite different.

Persistent design situations refer to conditions of 'normal use' (clause **3.2(2)P**). The word 'persistent' is used because the structure will be in this configuration with the potential to experience one of this family of design situations for an extended period of time, in fact, typically for most of its design working life.

Transient design situations refer to temporary conditions when a structure is itself in some special configuration for a period of time, such as during execution or maintenance. An important distinction between persistent and transient design situations therefore stems from the different duration of exposure, so that for example, for transient design situations it can be reasonable to use reduced wind and thermal actions because of the shorter duration of the design situation.

Accidental design situations refer to exceptional conditions in which there is typically some extreme accidental event, such as a vehicle impact with a bridge pier or superstructure. An important distinction with accidental design situations is that, because they are so unlikely to occur in practice, some degree of damage to a structure can typically be accepted.

Seismic design situations refer to conditions applicable to the structure when subject to seismic events.

In bridge design identifying whether a design situation is accidental, seismic, transient or persistent is usually straightforward. If the situation involves an accidental action then it is an accidental design situation. If the situation involves an earthquake then it is a seismic design situation. If not, and the structure is itself in some special configuration for a short period of time, then it is a transient design situation. And if it is not a transient design situation, it will be a persistent design situation.

2.4.2 ULTIMATE LIMIT STATES

Ultimate limit states are defined in EN 1990:2002 as limit states that concern the safety of people, and/or the safety of the structure (see clause **3.3(1)P**). As discussed later, a distinction is made between six different specific ultimate limits.

2.4.3 SERVICEABILITY LIMIT STATES

Ultimate limit states are defined in EN 1990:2002 as limit states that concern the functioning of the structure or structural members under normal use; the comfort of people; or the appearance of the construction works (see clause **3.4(1)P**).

However, EN 1990:2002 then introduces a concept that may be new in some countries, when in clause **3.4(2)P** it states that a distinction shall be made between reversible and irreversible serviceability limit states. This is the second of the six key concepts. Of the six, it is the one that perhaps has the least direct impact on bridge design, but it plays an important role in understanding the different combinations of actions defined for serviceability limit state verifications as discussed later (as the sixth key concept).

The concept of reversible and irreversible serviceability limit states is perhaps best understood considering the case of a simply supported reinforced concrete beam with a point load at mid-span. As the load applied to the beam is increased its deflection will also increase. At some point this deflection may exceed a serviceability criterion. Whilst this is not an event that the designer would wish to occur (too frequently), provided the beam remains elastic the beam will return to an acceptable deflection when the load is reduced *i.e.* it is *reversible* condition. The situation is rather different if the steel reinforcement yields when the load is further increased. Yielding of the reinforcement is another serviceability criterion and if it occurs it will mean that some permanent damage will be done to the beam; it will not return to its original position when it is unloaded and cracks will remain *i.e.* it is *irreversible* condition. Clearly, this is a more serious situation than the reversible condition.

Thus, it can be seen that not all serviceability limit states are of equal concern. Those which are reversible are of less concern than irreversible once. Differentiating between reversible and irreversible serviceability limit states is useful because it enables a different probability of exceedence to be applied to each. As will be seen later, this can be done by using different combinations of actions for reversible and irreversible serviceability limit states.

2.5 EN 1990 Section 4 – Basic variables

Section 4 of EN 1990 covers the three sets of basic variables considered in structural design, *viz.* actions, material properties and geometry. Here the treatment of actions and material properties will be discussed.

2.5.1 ACTIONS

It is appropriate first to note the use of the term actions in this context. In the past the term loads has traditionally been used, and in fact it remains an entirely valid term in a Eurocode context. However, in the Eurocodes the term loads is used to refer to a set of forces applied to a structure or the ground (*i.e.* direct actions). The term action is used more generically to mean both loads and also imposed deformations or accelerations, such as those due to thermal movements or earthquakes (*i.e.* indirect actions). In many ways, the use of the term actions addresses an ambiguity in the way the term load has been used in the past.

Actions are classified by their variation in time as either (see clause **4.1.1(1)P**):

- *permanent actions* (denoted G), *e.g.* self-weight of structures, road surfacing and indirect actions such as uneven settlements;
- *variable actions* (denoted Q), *e.g.* traffic load, wind and thermal actions; or,
- *accidental actions* (denoted A), *e.g.* impact from vehicles.

It will be sensible for designers to become familiar with this terminology, rather than using the terms dead and live load that may have been used in the past. Likewise, it will be advisable to reserve the words persistent and transient for design situations. Referring to a transient load in a Eurocode context is potentially rather confusing since it mixes the terminology for actions and design situations.

For permanent actions, EN 1990:2002, **4.1.2(2)P** explains that their characteristic value should either be taken as a single value, G_k , or if the variability of G cannot be considered as small, as the worst case of an upper value, $G_{k,sup}$, or a lower value, $G_{k,inf}$. Further guidance is provided on where the variability can be considered to be small and specifically, EN 1990:2002, **4.1.2(5)** states that the self weight of the structure may be represented by a single value G_k based on mean density and nominal dimensions.

In bridge design, important cases where the variability of G cannot be considered as small are loads due to surfacing and ballast (see EN 1991-1-1:2002, **5.2.3**). When the variability in G cannot be considered as small, it is helpful to note that **4.1.2(2)P** does not require upper and lower values of G to be applied to the adverse and relieving areas of the influence surface. Rather, whichever single value gives the worst case is taken throughout.

For variable actions, EN 1990:2002, **4.1.3** introduces another new concept for many bridge designers. This is the concept of the four *representative values* of a variable action, and it is the third key concept, as summarised in Section 2.9. As discussed later, these representative values are used in the different combinations of actions.

The four representative values have different probabilities of occurrence. They are called the characteristic, combination, frequent and quasi-permanent values. The characteristic value is the main representative value, and is the value generally specified in the various parts of EN 1991. It is a statistically extreme value: in the calibration of the basic highway traffic loading model, LM1, it is a 1000-year return period value (see EN 1991-2: 2003, **Table 2.1**); for wind and thermal actions it is generally a 50-year return period value.

The combination value is established by EN 1990:2002 to address the reduced likelihood that extreme values of more than one variable action will occur simultaneously. The frequent value of a variable action can be understood as the value that is exceeded 'occasionally, but not too often' – perhaps weekly or monthly. The calibration of the frequent value of LM1 is based on a one week return period. The use of the word frequent here sometimes causes some confusion, since it is essentially a relative term; here it is frequent in relation to the characteristic value. The quasi-permanent value is generally the value that is exceeded most of the time. For traffic loads on bridges and wind actions, the recommended quasi-permanent value is therefore zero.

The four representative values of a variable action are illustrated in Fig. 2.1. The combination, frequent and quasi-permanent values of a variable action are found by multiplying the characteristic value by ψ_0 , ψ_1 , and ψ_2 respectively. For bridge design, recommended ψ -factors are given in EN 1990:2002, **A2.2**. The UK National Annex modifies the values for road bridges and footbridges.

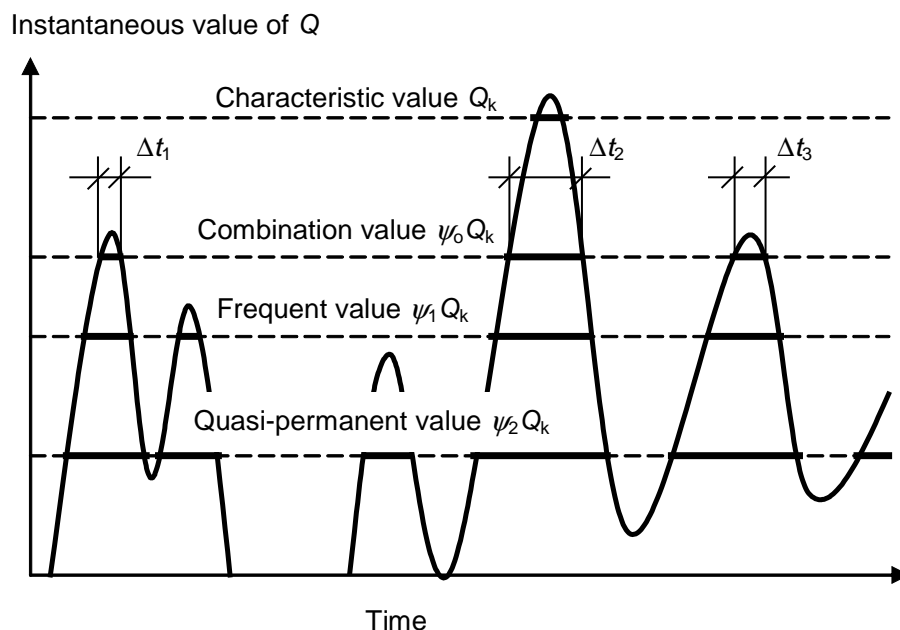


Fig. 2.1. Illustration of four representative values of a variable action

2.5.2 MATERIAL AND PRODUCT PROPERTIES

EN 1990:2002, **4.2(1)** explains that properties of materials (including soil and rock) should be represented by characteristic values. It also states that when a limit state verification is sensitive to the variability of a material property, upper and lower characteristic values of the material property should be taken into account (clause **4.2(2)**). Although it is rare that an upper characteristic material property will govern a design, rather than the lower value that is generally used, there are some important cases in bridge design when it can do so. These include earth pressures applied to integral bridges and other buried structures, where an upper characteristic angle of shearing resistance of the soil can govern.

2.6 EN1990 Section 5 – Structural analysis and design assisted by testing

Section 5 of EN 1990:2002 gives general principles and requirements for structural modelling and analysis. These provide the framework for the more detailed treatment included in the various Eurocode material parts.

2.7 EN1990 Section 6 – Limit state design and Annex A2 – Application for bridges

Section 6 of EN 1990:2002 describes how the partial factor method is applied in limit state verifications. It provides the overall framework for the applications of the partial factor method, including the way in which actions are combined and partial factors are applied. It is best considered, however, in conjunction with EN 1990:2002, **Annex A2** which gives supplementary bridge-specific requirements for establishing combinations of actions (except for fatigue verifications which are typically addressed in the relevant material part), provides ψ -factors and material-independent partial factors, and also gives methods and rules for some material-independent serviceability limit states (e.g. vibrations and deformations of rail bridges).

2.7.1 DESIGN VALUES

The design values of action effects are determined accounting for uncertainties in the actions themselves and also uncertainties in the evaluation of effects of actions. Similarly, design values of resistances are determined accounting for uncertainties in material properties and also uncertainties in resistances models.

Strictly this is done by using two partial factors in determining action effects (with one applied to the action and the other to the effect of the action) and two partial factors in determining resistances (with one applied to material properties and the other applied to resistances). These factors are:

Action effects:	γ_f	partial factor for the action which takes account of the possibility of unfavourable deviations of the action values from the representative values
	γ_{fd}	partial (model) factor taking account of uncertainties in modelling the effects of actions
Resistances:	γ_m	partial factor for the material property which takes account of the possible unfavourable deviations of a material from its characteristic value
	γ_{Rd}	partial (model) factor covering uncertainty in the resistance model

The model factors γ_{fd} and γ_{Rd} are illustrated in Fig. 2.3.

Whilst it is quite rational to recognise these four different sources of uncertainty, in practice the application of partial factors is generally simplified in the Eurocodes by combining:

- i. γ_f and γ_{fd} into a single partial factor denoted γ_f (or more specifically γ_Q for variable actions and γ_G for permanent actions), and,
- ii. γ_m and γ_{Rd} into a single partial factor denoted γ_M

Values of γ_f and γ_M are given in the relevant Eurocode parts, and their National Annexes, with material-behaviour independent factors (i.e. almost all partial factors on actions) given in EN 1990:2002, **Annex A2**. Clearly for linear analyses combining the partial factors in this way will not affect the overall result. For non-linear analyses some careful thought is always required concerning the correct application of partial factors (see e.g. EN 1992-2, 5.7).

2.7.2 ULTIMATE LIMIT STATES

EN 1990:2002 and EN 1997-1:2004 require *six ultimate limit states* to be explicitly verified where relevant. Although all of these would typically have been considered in past bridge design practice, their explicit identification and treatment is the fourth key concept, as summarised in Section 2.9.

The six ultimate limit states are referred to as EQU, STR, GEO, FAT, UPL and HYD. Three of these (EQU, UPL and HYD) are principally concerned with stability, and three (STR, GEO and FAT) are principally concerned with resistances. Two (Uplift and Hydraulic heave) are only dealt with in EN 1997-1:2004 and are rarely relevant in bridge design so will not be considered further here.

The three ultimate limit states principally concerned with resistances, STR, GEO and FAT, cover failure of structural members, failure of the ground and fatigue failure respectively. The EQU ultimate limit state covers the loss of static equilibrium of a structure, although as discussed further below, it has a very important relationship with the single source principle.

The usefulness of explicitly identifying six different ultimate limit states lies in the opportunity it provides to use different criteria and different partial factors in their verification. For example, in EQU verifications the recommended partial factors on actions given in EN 1990:2002, **Table A2.4(A)** are used; for STR verifications not involving geotechnical actions of resistances, the partial factor in **Table A2.4(B)** are used; and, for STR and GEO verifications involving geotechnical actions or resistances the partial factors in both **Table A2.4(B)** and **Table A2.4(C)** can be required, depending upon the Design Approach adopted (see EN 1990:2002, **A2.3.1(5)**).

2.7.3 SINGLE SOURCE PRINCIPLE

Tables A2.4(A)-(C) give two partial factors for each permanent action: a higher value, denoted, $\gamma_{G,sup}$, to be used when the action is unfavourable; and, a lower value, denoted $\gamma_{G,inf}$, to be used when the action is favourable.

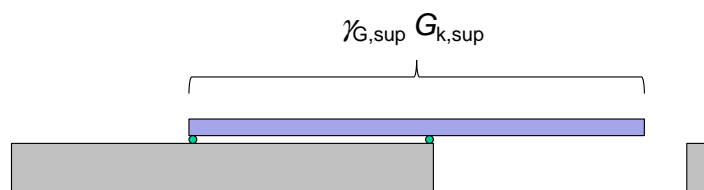
There is, however, a very important Note 3 in **Table A2.4(B)**. This note states that the characteristic values of all permanent actions from one source may be multiplied by $\gamma_{G,sup}$ if the total resulting action effect from this source is unfavourable, and by $\gamma_{G,inf}$ if the total resulting action from this source is favourable. This note is a statement of the *single source principle*, which is the fifth key concept in Section 2.9.

The single source principle is very convenient for designers as it means that it is not necessary to apply different partial factors to the favourable and unfavourable parts of a permanent action arising from a single source such as a continuous bridge deck (*i.e.* to the adverse and relieving areas of the influence surface). Because the note is included in **Table A2.4(B)** it means that the single source principle may be used in STR verifications.

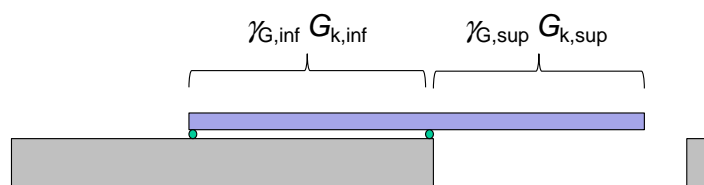
There is, however, a risk in applying the single source principle, particularly in conjunction with the single characteristic value for a permanent action allowed by EN 1990:2002, **4.1.2(2)P**. This risk arises because the sensitivity of the structure to minor variations in the magnitude or spatial distribution of a permanent action from a single source is not examined. Where such minor variations could lead to collapse it is critical that this is done. The EQU ultimate limit state fulfils this purpose. The single source principle is not (and in fact, must not) be applied at EQU.

In reality, cases where minor variations in the magnitude or spatial distribution of a permanent action from a single source could potentially lead to collapse are rare. They should certainly be very rare in persistent design situation, since if not, it would clearly be questionable whether sufficient robustness is being achieved in designs. Typically, the collapse load of statically indeterminate structures with even very modest ductility will be insensitive to variations in the magnitude or spatial distribution of a

permanent action. Cases can, however, be unavoidable in transient design situations, such as during bridge launches or in balanced cantilever construction, see Fig. 2.2.



Case A. Bridge launch, STR Verification, Moment over central support¹.



Case B. Bridge launch, EQU Verification².

NOTES:

1. In Case A, STR verification, single-source principle can be applied. EN1990 Set B partial factors used.
2. In Case B, EQU verification, single source principle not applied. EN1990 Set A partial factors used.

Fig. 2.2. Illustration of partial factors used for STR and EQU verifications

2.7.4 SPECIAL CASES IN THE APPLICATION OF EQU

There is a recognised issue with the current drafting of the definition of EQU in EN 1990:2002, **6.4.1(1)P**. EQU is defined as, 'loss of static equilibrium of the structure or any part of it considered as a rigid body, where (i) minor variations in the value or the spatial distribution of actions from a single source are significant, and (ii) the strengths of construction materials or ground are generally not governing'.

The first part of this definition explains that EQU is concerned with a loss of static equilibrium of the structure or any part of it considered as a rigid body, *i.e.* the formation of a collapse mechanism. It is perhaps questionable whether it needs to be explicitly stated that the structure or any part of it needs to be considered as a 'rigid body', but otherwise the intention is clear. The second part of the definition aligns with the key role of EQU to account for the implication of possible minor variations in the value or the spatial distribution of actions from a single source. A query may arise, however, with the third part of the definition, particularly since it is given as an additional requirement (*i.e.* the word 'and' used) rather than an alternative one.

The issue is that there are cases where minor variations in the value or the spatial distribution of actions from a single source could lead to collapse, but the strengths of construction materials or the

ground are governing. An example would be the design of a prop to prevent overturning of the deck during balanced cantilever construction. EN 1990:2002 effectively acknowledges this issue in **Table A2.4(A)** Note 2, as discussed below.

Although such cases are rather rare, being effectively a special case of a special case, it is valuable to provide some advice on how they should be treated. Firstly, it is clearly crucial (and a necessary part of the EQU limit state) that the single source principle is not applied, *i.e.* that the favourable and unfavourable parts of permanent actions from a single source are modelled and factored separately.

Secondly, applying either the partial factors for permanent actions in **Tables A2.4(A) or (B)** alone will be not appropriate. The partial factors for permanent actions in **Table A2.4(A)** account for relative uncertainty in their value and spatial distribution; whereas those partial factors for permanent actions in **Tables A2.4(B)** reflect overall uncertainty in the magnitude of the action effect.

Generally, it will be appropriate to adopt an approach such as the following where minor variations in the value or the spatial distribution of permanent actions from a single source are significant *and* the strengths of *construction materials* are governing:

- i. model the favourable and unfavourable parts of permanent actions from a single source separately
- ii. factor the (effects of) unfavourable parts of permanent actions by the product of γ_G^* and $\gamma_{G,sup}$ as given in **Table A2.4(A)**
- iii. factor the (effects of) favourable parts of permanent actions by the product of γ_G^* and $\gamma_{G,inf}$ as given in **Table A2.4(A)**

where γ_G^* is either $\gamma_{G,sup}$ or $\gamma_{G,inf}$ as given in **Table A2.4(B)**, whichever is more onerous for the particular verification.

The approach given in Note 2 in **Table A2.4(A)** is essentially similar to this approach, except that γ_G^* is taken as approximately 1.3, rather than $\gamma_{G,sup}$ from Table A2.4(B), and no adjustment is made to the value of $\gamma_{G,inf}$ from Table A2.4(B).

Where minor variations in the value or the spatial distribution of permanent actions from a single source are significant *and* the strength of the *ground* is governing, it is likely to be appropriate to use a similar approach to that suggested above and adjust the **Table A2.4(B)** and **Table A2.4(C)** partial factors in a similar fashion, applying them in conjunction with the partial factors on materials and resistances defined in EN 1997-1:2004, depending upon the Design Approach applied.

2.7.5 COMBINATIONS OF ACTIONS

EN 1990:2002 identifies six general expressions for the *combination of actions* that are used for bridge design.

'Combinations of actions' is the sixth key concept summarised in Section 2.9. They are summarised in Table 2.1. Each combination of actions has a different statistical likelihood of occurring and they are used for different limit state verifications.

EN 1990:2002 expresses the requirement that all actions that can occur simultaneously should be considered together in these combinations of actions (see clause **A2.2.1(1)**). There are, of course, cases where for functional or physical reasons actions cannot occur simultaneously and examples are given in EN 1990:2002, **A2.2**. In the case of bridge design, the way in which actions are combined is further simplified by forming traffic loads into groups which are then treated as a single (multi-component) variable action (see EN 1991-2).

Three combinations of actions are used for ultimate limit state verifications: one is used for persistent and transient design situations, one for accidental design situations and one for seismic design situations.

Three combinations of actions are used for serviceability limit state verifications. These are called the characteristic combination, the frequent combination and the quasi-permanent combination. The quasi-permanent combination is also used for calculating long-term effects, such as creep. Although not always wholly honoured by the other Eurocode parts, it was the intention of EN 1990:2002 that the characteristic combination would generally be used for irreversible serviceability limit state verifications and the less onerous frequent combination would be used for reversible serviceability limit state verifications.

Table 2.1. Combinations of actions

		EN 1990 Equ ⁿ	Permanent actions, G_k	Prestress, P	Accidental action	Leading variable action, $Q_{k,1}$		Accompanying variable actions, $Q_{k,j}$ ($j > 1$)	
			$\gamma^{(1)}$	$\gamma^{(1)}$		$\gamma^{(1)}$	$\psi^{(2)}$	$\gamma^{(1)}$	$\psi^{(2)}$
Ultimate limit states	Persistent or transient design situations	6.10 ⁽³⁾	γ_G	γ_P	n/a	γ_Q	1.0	γ_Q	ψ_0
	Accidental design situations	6.11	1.0	1.0	A_d	1.0	ψ_1 or $\psi_2^{(4)}$	1.0	ψ_2
	Seismic design situations	6.12	1.0	1.0	A_{Ed}	1.0	ψ_2	1.0	ψ_2
Serviceability limit states ⁽⁶⁾	Characteristic combination	6.14	1.0	1.0	n/a	1.0	1.0	1.0	ψ_0
	Frequent combination	6.15	1.0	1.0	n/a	1.0	ψ_1	1.0	ψ_2
	Quasi-permanent combination ⁽⁵⁾	6.16	1.0	1.0	n/a	1.0	ψ_2	1.0	ψ_2

Notes:

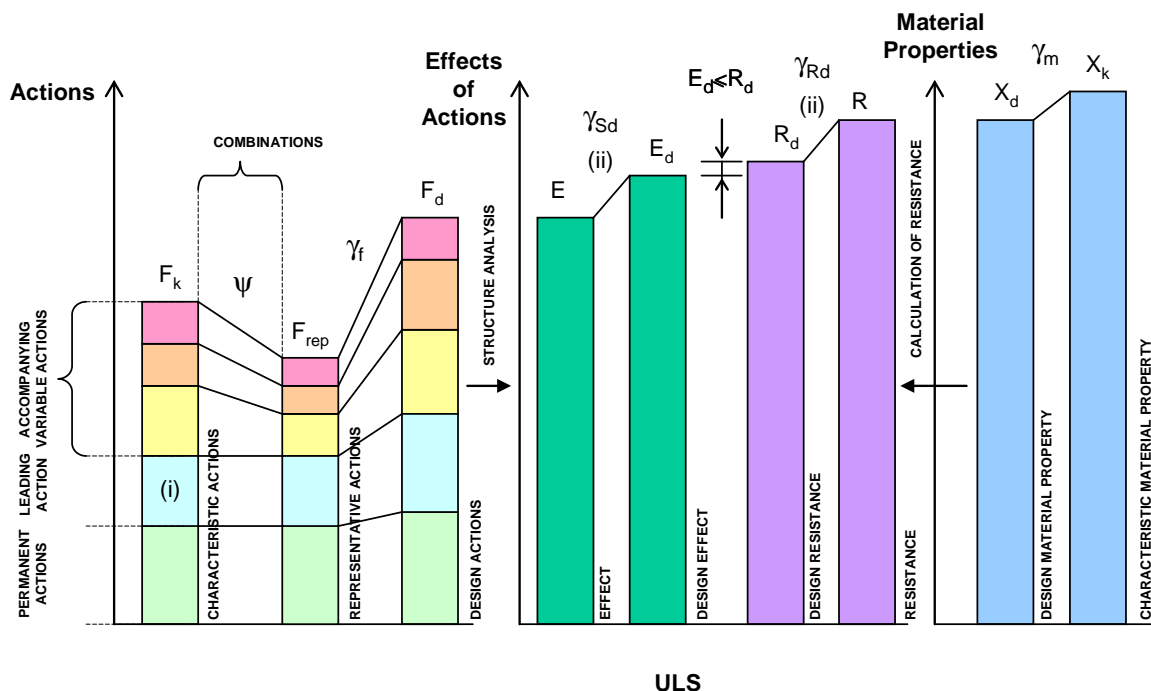
- (1) Values of γ are obtained from **Tables A2.4(A)-(C)**
- (2) Values of ψ are obtained from **Tables A2.1, Table A2.2, Table A2.3** for road bridges, footbridges and rail bridges respectively
- (3) Either expressions 6.10 or the more onerous of 6.10a and 6.10b may be used (the decision is a Nationally Determined Parameter). **Expression 6.10 is used in this example.**
- (4) Expression 6.11 allows the use of either or ψ_1 or ψ_2 . The decision is a Nationally Determined Parameter, see **Table A2.5**. However, see also EN 1990:2002, **A2.2.5(3)**.
- (5) Also used for long term effects.
- (6) Guidance on which combination should be used for specific serviceability limit state verifications is given in the relevant parts of EN 1992 to EN 1999.

2.7.6 LIMIT STATE VERIFICATION

The approach to limit state verification is dependent on the limit state being considered but in all cases is based on ensuring that the relevant effect does not exceed a relevant design value, which

may be a resistance, a stabilising action or some serviceability criterion (see EN 1990:2002, **6.4.2(1)P**, **6.4.2(3)P** and **6.5.1(1)P**).

As an illustration, the overall approach to the verification of STR ultimate limit state for a persistent or transient design situation is shown in Figure 2.3. This figure highlights the way in which partial factors and ψ -factors are applied, including the way in which γ_f , γ_{Sd} , γ_m and γ_{Rd} may be used, although as discussed above and indicated in note (ii) they are more generally combined into two partial factors γ_F and γ_M .



- (i) Where the action is a traffic load group, ψ factors will have been pre-applied to the non-leading actions within that group
- (ii) In many cases, γ_{Sd} may be combined with γ_f and applied as a single factor γ_F to the actions, and γ_{Rd} is combined with γ_m and applied as a single factor γ_M to the material properties.

Figure 2.3. Verification of STR limit state for persistent or transient design situation

2.8 Conclusions

An overview of the key aspects of EN 1990:2002 relevant to bridge design has been presented. Six key concepts have been identified that bridge designers should understand, viz:

- i. design situations;
- ii. reversible and irreversible serviceability limit states;
- iii. representative values of variable actions;
- iv. six ultimate limit states;
- v. single source principle; and,
- vi. combinations of actions.

The first five concepts all play a key role in understanding the sixth concept. The category of design situation dictates the combination of actions used for ultimate limit state verifications. The distinction between reversible and irreversible serviceability limit states explains why both the characteristic and frequent combinations of actions are used for serviceability limit state verifications. The four representative values of variable actions play a key role in accounting for the reduced likelihood that extreme values of several variable actions will occur at the same time and in the various combinations of actions having different statistical likelihoods of occurring. The six ultimate limit states and the single source principle dictate how partial factors are applied and the values used for persistent and transient design situations.

2.9 Summary of key concepts

Key concept summary 1: Design situations

Design situations are categorised as persistent, transient, accidental or seismic. These categorisations draw together families of circumstances or conditions that the structure might experience during its life. Persistent design situations refer to conditions of normal use. As such, for a highway bridge, they will include the passage of heavy vehicles since the ability to carry heavy vehicles is a key functional requirement. Transient design situations refer to circumstances when the structure is itself in some temporary configuration, such as during execution or maintenance. Accidental design situations refer to exceptional circumstances when a structure is experiencing an extreme accidental event.

Key concept summary 2: Reversible and irreversible serviceability limit states

The Eurocodes differentiate between reversible and irreversible serviceability limit states. Irreversible serviceability limit states are of greater concern than reversible serviceability limit states. The acceptable probability of an irreversible serviceability limit state being exceeded is lower than that for a reversible serviceability limit state. A more onerous combination of actions is used for irreversible serviceability limit states than reversible serviceability limit states.

Key concept summary 3: Representative values of a variable action

There are four different representative values of a Variable Action. The characteristic value is a statistically extreme value. It is the main representative value, and the value generally defined in EN1991. The other representative values are called the combination value, frequent value and quasi-permanent value. They are determined by multiplying the characteristic value by ψ_0 , ψ_1 and ψ_2 respectively. The combination, frequent and quasi-permanent values are less statistically extreme than the characteristic value, so ψ_0 , ψ_1 and ψ_2 are always less than 1.

Key concept summary 4: Ultimate limit states

The Eurocodes explicitly establish six different ultimate limit states. Two of these, UPL and HYD, are specific to EN1997. Two are concerned with resistances: STR when verifying structural resistance and GEO when verifying the resistance of the ground. FAT is concerned with fatigue. EQU is principally concerned with ultimate limit states involving a loss of overall equilibrium. However, it has an important relationship with the single source principle (see key concept summary 5). Different partial factors on actions and geotechnical material properties are used for different ultimate limit states

Key concept summary 5: Single source principle

Application of the single source principle allows a single partial factor to be applied to the whole of an action arising from a single source. The value of the partial factor used depends on whether the resulting action effect is favourable or unfavourable. EN1990 allows the single source principle to be used for STR and GEO verifications. EQU addresses cases when minor variations in the magnitude or spatial distribution of a permanent action from a single source are significant

Key concept summary 6: Combinations of actions

EN1990 establishes six different combinations of actions relevant to bridge design. Different combinations of actions are used for verifying different limit states. They have different statistical likelihoods of occurring. The quasi-permanent combination is also used when analysing long-term effects. The differences between the combinations of actions concern: whether partial factors are applied; which representative values of variable actions are used; and, whether there is an accidental or seismic action included. The different combinations of actions are used in conjunction with the Eurocode 'material parts'. The Eurocode part generally states explicitly which combination is to be used in each SLS verification.

CHAPTER 3

Actions on bridge decks and piers (EN 1991)

Part A: Wind and thermal actions on bridge deck and piers

Nikolaos MALAKATAS

Director, Min. of Infrastructures, Transports and Networks (Greece)

Chairman, CEN/TC250/SC1

Part B: Actions during execution, accidental actions and traffic loads

Pietro CROCE

Department of Civil Engineering, Structural Division

University of Pisa

Part A: Wind and thermal actions on bridge deck and piers

3.1 Introduction

The scope of the following example is to present the wind actions and effects usually applied on a bridge, to both deck and piers.

The following cases will be handled:

- Bridge during its service life, without traffic
- Bridge during its service life, with traffic
- Bridge under construction (most critical case)

The aforementioned cases will be considered for two alternative pier dimensions:

- Squat piers of 10 m height and rectangular cross section 2.5 m x 5.0 m
- “High” piers of 40 m height and circular cross section of 4 m diameter

Essentially, a wind action transversal to the deck (normal to its longitudinal axis) will be considered. Additional indications will be given for wind action along the bridge deck and in the vertical direction.

Through the presentation of the example reference to the relevant EN Eurocodes Parts (essentially EN 1991-1-4) will be given as appropriate and some comments, where necessary. In the following all references to clauses of EN 1991-1-4 will be given within brackets in italics [...]. If the reference concerns another EN Eurocode Part, then it will be noted, as well.

The wind actions on bridges are described in Section [8], with some cross references to other clauses, where necessary. In [8.2] it is noted that an assessment should be made, whether a dynamic response procedure is needed. This matter is left open for the NAs. It is also stated that “normal” bridges with spans less than 40 m generally do not need dynamic calculations; some Member States (MS) have adopted as limit span for this purpose 100 m.

In this example it is considered that there is no need for a dynamic response procedure.

3.2 Brief description of the procedure

The general expression of a wind force F_w acting on a structure or structural member is given by the following formula [5.3]:

$$F_w = c_s \times c_d \times c_f \times q_p(z_e) \times A_{ref}$$

Where:

$c_s c_d$ is the structural factor [6]

c_f is the force coefficient [8.3.1, 7.6 and 7.13, 7.9.2, respectively, for the deck, the rectangular and the cylindrical pier]

$q_p(z_e)$ is the peak velocity pressure [4.5] at reference height z_e , which is usually taken as the height z above the ground of the C.G. of the structure subjected to the wind action

A_{ref} is the reference area of the structure [8.3.1, 7.6, 7.9.1, respectively, for the deck, the rectangular and the cylindrical pier]

In the example considered, as no dynamic response procedure will be used, it may be assumed that $c_s, c_d = 1.0$ [8.2(1)]. Otherwise [6.3] together with [Annex B or C] should be used to determine the structural factor.

The peak velocity pressure $q_p(z)$ at height z , includes the mean and the short-term (turbulent) fluctuations and is expressed by the formula [4.8]:

$$q_p(z) = \left[1 + 7 \times I_v(z)\right] \times \frac{1}{2} \times \rho \times v_m^2(z) = c_e(z) \times q_b = c_e(z) \times \frac{1}{2} \times \rho \times v_b^2$$

where:

ρ is the air density (which depends on the altitude, temperature and barometric pressure to be expected in the region during wind storms; the recommended value, used in this example, is 1.25 kg/m^3)

$v_m(z)$ is the mean wind velocity at a height z above the ground [4.3]

$I_v(z)$ is the turbulence intensity at height z , defined [4.4(1)] as the ratio of the standard deviation of the turbulence divided by the mean velocity, and is expressed by the following formula [4.7]

$$I_v(z) = \frac{\sigma_v}{v_m(z)} = \frac{k_I}{c_o(z) \times \ln(z/z_0)} \quad \text{for } z_{\min} \leq z \leq z_{\max}$$

$$I_v(z) = I_v(z_{\min}) \quad \text{for } z < z_{\min}$$

where:

k_I is the turbulence factor (NDP value). The recommended value, used in the example, is 1.0

$c_o(z)$ is the orography factor [4.3.3]

z_0 is the roughness length [Table 4.1]

The peak velocity pressure may also be expressed as a product of the exposure factor $c_e(z)$ and the basic velocity pressure q_b [Eq. 4.10]. Charts of $c_e(z)$ may be drawn as a function of the terrain category and the orography, such as [Fig. 4.2] for $c_o = 1.0$ (flat terrain, [4.3.3]).

The mean wind velocity is expressed by the formula [4.3]:

$$v_m(z) = c_r(z) c_o(z) v_b$$

where:

$c_r(z)$ is the roughness factor, which may be an NDP, and is recommended to be determined according to the following formulas [4.3.2]:

$$c_r(z) = k_r \times \ln\left(\frac{z}{z_0}\right) \quad \text{for } z_{\min} \leq z \leq z_{\max}$$

$$c_r(z) = c_r(z_{\min}) \quad \text{for } z_{\min} \leq z \leq z_{\max}$$

where:

z_0 is the roughness length [Table 4.1]

k_r terrain factor depending on the roughness length and evaluated according the following formula [4.5]:

$$k_r = 0.19 \times \left(\frac{z_0}{z_{0,II}} \right)^{0.07}$$

with:

$z_{0,II}$ = 0.05 m (terrain category II, [Table 4.1])

z_{min} is the minimum height defined in [Table 4.1]

z_{max} is to be taken as 200 m

z_0 , z_{min} depend on the terrain category; recommended values are given in [Table 4.1]

It is to note, by comparing the formulas [4.8] and [4.3], that the following expression may be deduced for $c_e(z)$:

$$c_e(z) = [1 + 7 \cdot I_v(z)] c_r^2(z) c_o^2(z)$$

Finally, the basic wind velocity v_b is expressed by the formula [4.1]:

$$v_b = (c_{prob}) c_{dir} c_{season} v_{b,0}$$

Where:

v_b is the basic wind velocity, defined at 10 m above ground of terrain category II

$v_{b,0}$ is the fundamental value of the basic wind velocity, defined as the characteristic 10 minutes mean wind velocity (irrespective of wind direction and season of the year) at 10 m above ground level in open country with low vegetation and few isolated obstacles (distant at least 20 obstacle heights)

c_{dir} is the directional factor, which may be an NDP; the recommended value is 1.0

c_{season} is the season factor, which may be an NDP; the recommended value is 1.0

In addition to that a probability factor c_{prob} should be used, in cases where the return period for the design differs from $T = 50$ years. This is usually the case, when the construction phase is considered. Quite often also for bridges $T = 100$ is considered as the duration of the design life, which should lead to $c_{prob} > 1.0$. The expression of c_{prob} is given in the following formula [4.2], in which the values of K and n are NDPs; the recommended values are 0.2 and 0.5, respectively:

$$c_{prob} = \left(\frac{1 - K \times \ln(-\ln(1 - p))}{1 - K \times \ln(-\ln(0.98))} \right)^n$$

To resume:

To determine the wind actions on bridge decks and piers, it seems convenient to follow successively the following steps:

- Determine v_b (by choosing $v_{b,0}$, c_{dir} , c_{season} and c_{prob} , if relevant); q_b may also be determined at this stage.
- Determine $v_m(z)$ (by choosing terrain category and reference height z to evaluate $c_r(z)$ and $c_o(z)$).
- Determine $q_p(z)$ (either by choosing directly $c_e(z)$, where possible, either by evaluating $I_v(z)$, after choosing $c_o(z)$).
- Determine F_w (after evaluating A_{ref} and by choosing c_f and $c_s c_d$, if relevant).

3.3 Wind actions on the deck

3.3.1 BRIDGE DECK DURING ITS SERVICE LIFE, WITHOUT TRAFFIC

The fundamental wind velocity $v_{b,0}$ is an NDP to be determined by each Member State (given in the form of zone/iso-curves maps, tables etc.). For the purpose of this example the value $v_{b,0} = 26$ m/s (see Chapter 1, 1.4.4.3) has been considered. It is also considered that $c_{dir} = 1.0$ and $c_{season} = 1.0$.

In the case of bridges it is usually considered that $T = 100$ years (see Chapter 1, 1.4.1) Such design working life is reflected by a (mean) probability of occurrence of the extreme event $p = 0.01$. Therefore one gets :

$$c_{prob} = \left(\frac{1 - 0.2 \times \ln(-\ln(1 - 0.01))}{1 - 0.2 \times \ln(-\ln(0.98))} \right)^{0.5} = (1.92 / 1.78)^{0.5} \approx 1.08^{0.5} \approx 1.04$$

This value ($c_{prob} = 1.04$) will be further used in this example. (Note : The relevant presentation during the Workshop has been based on $c_{prob} = 1.0$). Thus :

$$v_b = (c_{prob}) c_{dir} c_{season} v_{b,0} = 1.04 \times 1.0 \times 1.0 \times 26 = 27 \text{ m/s}$$

The corresponding (basic velocity) pressure may also be computed, according to [Eq. 4.10]:

$$q_b = \frac{1}{2} \times 1.25 \times 27^2 = 455.6 \text{ N/m}^2 \text{ (Pa)}$$

Concerning the reference height of the deck z_e , this may be considered more or less equal to the mean distance z between the centre of the bridge deck and the soil surface [8.3.1(6)]. In the general case of a sloppy valley it is more conservative to use a lower (deeper) point of the soil surface (or the water) beneath the bridge deck. In the present example a very flat valley will be considered with a roughness category II. It is also to note that in practice the upper part of the foundation is covered by a soil layer of some thickness. Following these considerations it has been considered, for simplicity, that $z_e = z$.

The two cases of pier heights will, of course, be considered separately.

Squat pier, $z = 10$ m

For terrain category II, $z_0 = 0.05$ and $z_{min} = 2 \text{ m} < 10 \text{ m} = z$ [Table 4.1], thus: $k_r = 0.19 \times \left(\frac{0.05}{0.05} \right)^{0.07} = 0.19$

and

$$c_r(10) = 0.19 \times \ln \left(\frac{10.00}{0.05} \right) = 0.19 \times \ln 200 = 0.19 \times 5.298 = 1.0066 \approx 1.0$$

As far as the orography factor $c_o(z)$ is concerned, due to the flat valley it is considered that $c_o(10) = 1.0$. In fact, in the general case where the ground level beneath the bridge is lower than the surrounding ground the $c_o < 1.0$. Therefore the peak wind velocity is:

$$v_m(10) = 1.0 \times 1.0 \times 27 = 27 \text{ m/s}$$

The turbulence intensity is:

$$I_v(10) = \frac{1.0}{1.0 \times \ln(10 / 0.05)} = \frac{1}{5.298} = 0.189$$

and

$$q_p(10) = [(1 + 7 \times 0.189)] \times \frac{1}{2} \times 1.25 \times 27^2 = 2.32 \times 455.6 = 1057 = c_e(10) \times 455.6 \text{ in N/m}^2$$

Hence

$$c_e(10) = 2.32$$

In this specific case the same result could be obtained by making use of [Fig. 4.2], because $c_o(10) = 1.0$.

Further calculations are needed to determine the wind force on the deck [5.3].

Both the force coefficient c_f and the reference area A_{ref} of the bridge deck [8.3.1] depend on the width to (total) depth ratio b/d_{tot} of the deck, where d_{tot} represents the depth of the parts of the deck which are considered to be subjected to the wind pressure.

In the case of the bridge in service, without consideration of the traffic, according to [8.3.1(4) and Table 8.1], d_{tot} is the sum of the projected (windward) depth of the structure, including the projecting solid parts, such as footway or safety barrier base, plus 0.3m for the open safety barrier used in the present example, in each side of the deck (see also Fig. 1.10 and drawings (Fig.1.11) of the cross section). Consequently:

$$\begin{aligned} d_{tot} &= 2.800 + 0.400 - 0.025 \times 2.500 + 0.200 + 2 \times 0.300 = 3.1375 + 0.200 + 0.600 = \\ &= 3.9375 \approx 4.00 \text{ m} \end{aligned}$$

The depth (height) of the concrete support of the safety barrier has been taken into account, since $0.200 > 0.025 \times 3.500 + 0.030 + 0.080 = 0.0875 + 0.110 = 0.1975 \text{ m}$ (projection of the remaining slope of the deck to the center line, waterproofing layer, asphalt layer).

Hence:

$$b/d_{tot} = 12.00 / 4.00 = 3 \text{ (} 12.00 / 3.94 \approx 3.05 \text{)}$$

$$A_{ref} = d_{tot} \cdot L = 4.00 \times 200.00 = 800.00 \text{ m}^2$$

$$c_{fx,0} \approx 1.55 \text{ [Fig. 8.3]}$$

$$c_{fx} = c_{fx,0} \approx 1.55 \text{ [Eq. 8.1]}$$

If the bridge is sloped transversally (e.g. a curved bridge) $c_{fx,0}$ should be increased by 3% per degree of inclination, but no more than 25% [8.3.1(3)]

Finally:

$$F_w = 1.0 \times 1.55 \times 1057 \times 800.00 = 1638.35 \times 800.00 = 1310680 \text{ N} \approx 1310 \text{ kN}$$

Or "wind load" in the transverse (x-direction): $w = 1310/200 \approx 6.55 \text{ kN/m}$

It is also to note that in [8.3.2] a simplified method is proposed for the evaluation of the wind force in x-direction. In fact formula [5.3] is slightly modified and becomes the following formula [8.2]:

$$F_w = 1 / 2 \times \rho \times v_b^2 \times C \times A_{ref,x}$$

Where $C = c_e \cdot c_{f,x}$ is given in [Tab. 8.2] depending on b/d_{tot} and z_e . In our case one would get (by interpolation) the value: $(3.0-0.5) / (4.0-0.5) = (6.7-C)/(6.7-3.6) \rightarrow 2.5/3.5 = (6.7-C)/3.1 \rightarrow C = 6.7 - 3.1 \times 2.5/3.5 = 4.4857 \approx 4.49 \approx 4.5$, to be compared with the "exact" value $C = c_e \cdot c_{f,x} = 2.32 \times 1.55 = 3.596 \approx 3.6$. Using the interpolated value of C one gets:

$$F_w = 0.5 \times 1.25 \times 27^2 \times 3.6 \times 800.00 = 1640.25 \times 800.00 = 1312200 \text{ N} = 1312 \text{ kN}$$

Which, in this case, is practically equal with the “exact” value.

“High” pier, $z = 40 \text{ m}$

For terrain category II, $z_0 = 0.05$ and $z_{min} = 2 \text{ m} < 40 \text{ m} = z$ [Table 4.1], thus: $k_r = 0.19 \times \left(\frac{0.05}{0.05} \right)^{0.07} = 0.19$

and

$$c_r(40) = 0.19 \times \ln \left(\frac{40.00}{0.05} \right) = 0.19 \cdot \ln 800 = 0.19 \times 6.6846 = 1.27$$

$$c_o(40) = 1.0$$

Hence:

$$v_m(40) = 1.27 \times 1.0 \times 27 = 34.3 \text{ m/s}$$

The turbulence intensity is:

$$I_v(40) = \frac{1.0}{1.0 \times \ln(40 / 0.05)} = \frac{1}{6.6846} = 0.15$$

And

$$q_p(40) = [(1 + 7 \times 0.15)] \times \frac{1}{2} \times 1.25 \times 34.3^2 = 2.05 \times 734.9 = 1506.5 \text{ in N/m}^2$$

Hence

$$c_e(40) = 2.05 \times 1.27^2 \times 1.0^2 = 2.05 \times 1.61 \times 1.0 = 3.30$$

All other magnitudes for the deck are not differentiated, compared to the case of the squat pier. Namely:

$$d_{tot} \approx 4.00 \text{ m}, b/d_{tot} = 3, A_{ref} = 800.00 \text{ m}^2, c_{fx} = c_{fx,0} \approx 1.55.$$

Hence:

$$F_w = 1.0 \times 1.55 \times 1506.5 \times 800.00 = 2335 \times 800.00 = 1868060 \text{ N} \approx 1868 \text{ kN}$$

Or “wind load” in the transverse (x-direction): $w = 9.34 \text{ kN/m}$

The comparison with the simplified method of [8.3.2] requires double interpolations, as follows:

- For $z_e \leq 20 \text{ m}$, $(3.0-0.5) / (4.0-0.5) = (6.7-C)/(6.7-3.6) \rightarrow 2.5/3.5 = (6.7-C)/3.1 \rightarrow C = 6.7 - 3.1 \times 2.5/3.5 = 4.4857 \approx 4.49 \approx 4.5$
- For $z_e = 50 \text{ m}$, $(3.0-0.5) / (4.0-0.5) = (8.3-C)/(8.3-4.5) \rightarrow 2.5/3.5 = (8.3-C)/3.8 \rightarrow C = 6.3 - 3.8 \times 2.5/3.5 = 5.5857 \approx 5.59 \approx 5.6$
- Finally: $(50-40) / (50-20) = (5.6-C)/(5.6-4.5) \rightarrow 10/30 = (5.6-C)/1.1 \rightarrow C = 5.6 - 1.1 \times 1/3 \approx 5.23$

Using the interpolated value of C one gets:

$$F_w = 0.5 \times 1.25 \times 27^2 \times 5.23 \times 800.00 = 2382.92 \times 800.00 = 1906335 \text{ N} \approx 1906 \text{ kN}$$

which is almost identical to (2% greater than) the “exact” value.

3.3.2 BRIDGE DURING ITS SERVICE LIFE, WITH TRAFFIC

Squat pier, $z = 10$ m

The magnitude which is differentiated, compared to the case without traffic, is the reference depth d_{tot} of exposure on wind action transversally to the deck. In that case:

$$d_{tot} = 3.1375 + 0.200 + 2.0 = 5.3375 \approx 5.34 \text{ m}$$

and

$$b/d_{tot} = 12.00/5.34 = 2.25, c_{fx} = c_{fx,0} \approx 1.83 \text{ and } A_{ref} = 5.34 \times 200.00 = 1068 \text{ m}^2$$

Hence:

$$F_w = 1.0 \times 1.83 \times 1057 \times 1068.00 = 1934.31 \times 1068.00 = 2065843 \text{ N} \approx 2066 \text{ kN}$$

Or “wind load” in the transverse (x-direction): $w \approx 10.33 \text{ kN/m}$

“High” pier, $z = 40$ m

Again, the magnitude which is differentiated, compared to the case without traffic, is d_{tot} which has the value previously computed, i.e. $d_{tot} \approx 5.34 \text{ m}$

and hence:

$$b/d_{tot} = 2.25, c_{fx} = c_{fx,0} \approx 1.83 \text{ and } A_{ref} = 1068 \text{ m}^2$$

Finally:

$$F_w = 1.0 \times 1.83 \times 1506.5 \times 1068.00 = 2756.9 \times 1068.00 = 2944364 \text{ N} \approx 2944 \text{ kN}$$

Or “wind load” in the transverse (x-direction): $w \approx 14.72 \text{ kN/m}$

3.3.3 BRIDGE UNDER CONSTRUCTION (MOST CRITICAL CASE AND TERMINATION OF PUSHING)

In practice the construction of the deck of a bridge similar to the bridge used in the present example has a duration of few months. In particular the launching phase is planned to last some hours, not even days, and is not getting started in case adverse weather conditions (wind etc.) are foreseen. This explains the relevant assumption made for the wind velocity (see Chapter 1, 1.4.4.3). So, it has been agreed to use for the present example the value of $v_b = 50 \text{ km/h}$, i.e. in m/s $v_b = 50/3.6 = 13.89 \approx 14 \text{ m/s}$.

More generally, given that the construction phase has a limited duration and subsequently the associated return period of the actions considered is lesser than the service design life of the structure, c_{prob} may be modified accordingly. In several cases this might also be the case for c_{season} for a time period up to 3 months [EN 1991-1-6, Table 3.1]. In the same table the return periods for (up to) 3 months and (up to) 1 year are given, respectively $T = 5$ and 10 years. Therefore, the corresponding probabilities for the exceedance of the extreme event once, are $p = 1/5 = 0.20$ and $1/10 = 0.10$, respectively. In the specific case of this example one might reasonably assume 3 months for the

duration of the construction, before casting the concrete slab, leading to $c_{prob} = 0.85$. Nevertheless, a more conservative approach would be to assume virtual delays, thus leading to a value of $c_{prob} = 0.9$, as it may be seen below:

$$c_{prob} = \left(\frac{1 - 0.2 \times \ln(-\ln(1 - 0.10))}{1 - 0.2 \times \ln(-\ln(0.98))} \right)^{0.5} = (1.45/1.78)^{0.5} = 0.8146^{0.5} = 0.902 \approx 0.9$$

It is rather evident that the termination of the construction phases, following the casting of the concrete slab and its hardening, is not a critical design situation by itself. Still, it will be included in the example, so that it can be combined with other relevant actions, after termination of the pushing of the steel structure and before starting the concrete casting. During detailed design the various construction phases should be considered and verified individually. In this example the situation, where the steel structure launched (without addition of a nose-girder) from one side (abutment C0) is about to reach as cantilever the pier P2, will be considered as representative of design situations critical for the dimensioning of key steel structural elements. In that specific the length of the bridge to be taken into account is $L = 60.00 + 80.00 = 140.00$ m and $d_{tot} = 2 \cdot d_{main\ beam} = 2 \times 2.80 = 5.60$ m.

Hence:

$$A_{ref} = 5.60 \times 140.00 = 784.00 \text{ m}^2$$

And

$$b/d_{tot} = 12.00/5.60 = 2.14, \quad c_{fx} = c_{fx,0} \approx 1.9$$

Squat pier, $z = 10$ m

$$v_m(10) = 1.0 \times 1.0 \times 14 = 14 \text{ m/s}$$

$$q_p(10) = [1 + 7 \times 0.189] \times \frac{1}{2} \times 1.25 \times 14^2 = 2.32 \times 122.5 = 284.2 \text{ in N/m}^2$$

Finally:

$$F_w = 1.0 \times 1.9 \times 284.2 \times 784.00 = 539.98 \times 784.00 = 423360 \text{ N} \approx 423.5 \text{ kN}$$

Or “wind load” in the transverse (x-direction): $w \approx 423.5 / 140 \approx 3 \text{ kN/m}$

The results corresponding to the end of pushing are:

$$A_{ref} = 5.60 \times 200.00 = 1120.00 \text{ m}^2$$

$$F_w = 1.0 \times 1.9 \times 284.2 \times 1120.00 = 539.98 \times 1120.00 = 604777.6 \text{ N} \approx 605 \text{ kN}$$

Or “wind load” in the transverse (x-direction) remains, of course, unchanged:

$$w \approx 605 / 200 \approx 3 \text{ kN/m}$$

“High” pier, $z = 40$ m

$$v_m(40) = 1.27 \times 1.0 \times 14 = 17.78 \approx 18 \text{ m/s}$$

$$q_p(40) = [(1 + 7 \times 0.15)] \times \frac{1}{2} \times 1.25 \times 18^2 = 2.05 \times 202.5 = 415.125 \approx 415 \text{ in N/m}^2$$

Finally:

$$F_w = 1.0 \times 1.9 \times 415 \times 784.00 = 788.5 \times 784.00 = 618184 \text{ N} \approx 618 \text{ kN}$$

Or “wind load” in the transverse (x-direction): $w \approx 4.4 \text{ kN/m}$

The results corresponding to the end of pushing are:

$$F_w = 1.0 \times 1.9 \times 415 \times 1120.00 = 788.5 \times 1120.00 = 883120 \text{ N} \approx 883 \text{ kN}$$

Or “wind load” in the transverse (x-direction) remains, of course, unchanged:

$$w \approx 883 / 200 \approx 4.4 \text{ kN/m}$$

The main results may be summarized in Table 3.1 as follows:

Table 3.1 Summary of results

	Service life without traffic		Service life with traffic		Construction phase (steel alone – end of pushing)		Construction phase (steel alone - cantilever at P2)	
$z = z_e \text{ (m)}$	10	40	10	40	10	40	10	40
$v_{b,0} \text{ (m/s)}$	26	26	26	26	-	-	-	-
$v_b \text{ (m/s)}$	27	27	27	27	14	14	14	14
$v_m \text{ (m/s)}$	27	34.3	27	34.3	14	18	14	18
$q_b \text{ (N/m}^2\text{)}$	455.6	455.6	455.6	455.6	122.5	122.5	122.5	122.5
$q_m \text{ (N/m}^2\text{)}$	455.6	734.9	455.6	734.9	122.5	202.5	122.5	202.5
$q_p \text{ (N/m}^2\text{)}$	1057	1506.5	1057	1506.5	284.2	415	284.2	415
c_e	2.32	3.30	2.32	3.30	2.32	3.30	2.32	3.30
$d_{tot} \text{ (m)}$	4.00	4.00	5.34	5.34	5.60	5.60	5.60	5.60
$L \text{ (m)}$	200	200	200	200	140	140	140	140
$A_{ref,x} \text{ (m}^2\text{)}$	800	800	1068	1068	1120	1120	784	784
b/d_{tot}	3.00	3.00	2.25	2.25	2.14	2.14	2.14	2.14
$c_{f,x}$	1.55	1.55	1.83	1.83	1.9	1.9	1.9	1.9
$F_w \text{ (kN)}$	1312	1868	2066	2944	605	883	423	618
$w \text{ (kN/m)}$	6.55	9.34	10.33	14.72	3	4.4	3	4.4

Using the values of $w \text{ (kN/m)}$ summarized in the table one can get the resulting wind forces acting on the supports of the deck. The deck may be considered as a three span continuous “beam” at service life (without and with traffic) and a single span one-sided cantilevered beam during construction (one case examined).

3.3.4 VERTICAL WIND FORCES ON THE BRIDGE DECK (Z-DIRECTION)

[8.3.3] refers to the wind action on bridge decks in the vertical direction. The associated force coefficients $c_{f,z}$ are left as NDPs, but it is recommended that a value ± 0.9 could be used, in the absence of appropriate experimental evidence (wind tunnel tests). There is also the possibility to use [Fig. 8.6] for this purpose. An excentricity of the force in the transverse (x) direction of $e=b/4$ should also be taken into account. Still, it should be pointed out that generally for several common types of

bridges vertical wind forces are almost an order of magnitude less than the self weight and the permanent loads.

3.3.5 WIND FORCES ALONG THE BRIDGE DECK (Y-DIRECTION)

[8.3.4] refers to the wind action on bridge decks in the longitudinal direction, to be taken into account, where relevant. The values are also left as NDPs, but it is recommended that a 25% percentage of the wind forces in x-direction is considered, in the case of plated bridges, and a 50% in the case of truss bridges.

These two additional cases (wind action in y- and z-direction) are not treated in this example of application.

3.4 Wind actions on the piers

3.4.1 SQUAT RECTANGULAR PIER 2.50X5.00X10.00

According to [8.4.2] simplified rules for the evaluation of wind effects on piers may be given in the National Annexes. Otherwise the procedures described in [7.6], [7.8] and [7.9], should be applied, respectively for rectangular, regular polygonal and circular cross sections.

The general formula [5.3] already used for the deck is also valid for structural elements like free standing piers. The main task consists to compute the appropriate magnitudes $(c_s c_d), c_f, q_p(z_e), A_{ref}$.

In this case $c_s c_d = 1.0$ and c_f are given by the following formula [7.9]:

$$c_f = c_{f,0} \psi_r \psi_\lambda$$

Where:

$c_{f,0}$ is the force coefficient of rectangular sections with sharp corners and without free-end flow [Fig. 7.23]

ψ_r is the reduction factor for square sections with rounded corners

ψ_λ is the end-effect factor (for elements with free-end flow [7.13])

In this case $d/b = 5.00/2.50 = 2$ and hence $c_{f,0} = 1.65$ [Fig. 7.23]

Also $\psi_r = 1.0$ [Fig. 7.24], since $r/b = 0$ (corners not rounded)

From [Tab. 7.16] of [7.13] and for $l (= z = 10 \text{ m}) < 15 \text{ m}$ the effective slenderness λ is given as follows:
 $\lambda = \min \{ 2 l/b ; 70 \} = \min \{ 2 \times 10.00/2.50 ; 70 \} = 8$

Formula [7.28] defines the solidity ratio $\phi = A / A_c$, the ration between the sum of the projected area(s) A to the overall envelope area $A_c = l \cdot b$. In this case $A = A_c$ and $\phi = 1.0$.

By using [Fig. 7.36] one gets $\psi_\lambda \approx 0.69$

And: $c_f = 1.65 \times 1.0 \times 0.69 = 1.1385 \approx 1.14$

$A_{ref} = l \cdot b = 10.00 \times 2.50 = 25.00 \text{ m}^2$

$q_p(10) = 1057 \text{ N/m}^2$ (284.2 N/m² for the construction phase)

According to [Fig 7.4] of [7.2.2] applied for the squat pier considered, $h = 10 \text{ m} > 2 \cdot b = 2 \times 2.50 = 5.00$

one should use the following values of q_p along the height of the pier:

- $q_p(2.5)$ for the zone $0 < z \leq 2.5$ m
- $q_p(10.0)$ for the zone $7.5 \text{ m} < z \leq 10.0$ m
- $q_p(2.5) < q_p(z) \leq q_p(10.0)$ for the zone $2.5 \text{ m} < z \leq 7.5$ m

Due to the limited influence of the wind action for a squat not very high pier, a unique value will be considered, $q_p(10) = 1057 \text{ N/m}^2$

Finally: $F_w = 1.0 \times 1.14 \times 1057 \times 25.00 = 1205 \times 25.00 = 30125 \text{ N} \approx 30 \text{ kN}$

3.4.2 “HIGH” CIRCULAR CYLINDRICAL PIER Ø 4.00 X 40.00

The force coefficient in the case of a (finite) circular cylinder is given by formula [7.19] of [7.9.2]:

$$C_f = C_{f,0} \psi_\lambda$$

Where:

$C_{f,0}$ is the force coefficient of circular sections (finite cylinders) without free-end flow [Fig. 7.28]

ψ_λ is the end-effect factor (for elements with free-end flow [7.13])

For the use of [Fig. 7.28] the Reynolds number [Eq. 7.15] based on the peak wind velocity according to [4.5, Eq. 4.8] and the equivalent surface roughness k [Tab. 7.13] need first to be computed.

The combination of formulas [7.15] and [4.8] leads to the following expression:

$$v(z_e) = v_m(z_e) \{1 + 7 I_V(z_e)\}^{0.5}$$

For $z_e = 40$ m one gets:

$$v(40) = 34.3 \times \{1 + 7 \times 0.15\}^{0.5} = 34.3 \times 2.05^{0.5} = 34.3 \times 1.432 = 49.1 \text{ m/s}$$

$$Re = b \cdot v(z_e) / \nu = 4.00 \times 49.1 / (15 \times 10^{-6}) = 13 \times 10^6 = 1.3 \times 10^7$$

This value is a bit further than the limiting value of [Fig. 7.28].

The equivalent roughness is 0.2 mm for smooth and 1.0 mm for rough concrete. Smooth concrete surface will be assumed. This leads to $k/b = 0.2/4000 = 5 \times 10^{-5}$. From Fig 7.28 a value greater than 0.7 is expected. By using the relevant formula one gets:

$$\begin{aligned} c_{f,0} &= 1.2 + \{0.18 \times \log(10 k/b)\} / \{1 + 0.4 \log(Re/10^6)\} = \\ &= 1.2 + \{0.18 \times \log(10 \times 5 \times 10^{-5})\} / \{1 + 0.4 \log(13 \times 10^6/10^6)\} = \\ &= 1.2 - 0.594 / 1.445 = 1.2 - 0.411 = 0.788 \approx 0.79 \end{aligned}$$

In the case of rough concrete one would get: $c_{f,0} = 0.876$

Concerning the evaluation of ψ_λ one should use interpolation, while using [Tab. 7.16] and [Fig. 7.36] since $15 \text{ m} < l = 40 \text{ m} < 50 \text{ m}$.

For $l = 15$ m the effective slenderness λ is given as follows: $\lambda = \min \{ l/b ; 70 \} = \min \{ 40.00/4.00 ; 70 \} = 10$

For $l = 50$ m the effective slenderness λ is given as follows: $\lambda = \min \{ 0.7 l/b ; 70 \} = \min \{ 0.7 \times 40.00/4.00 ; 70 \} = 7$

Interpolation gives $\lambda = 0.786 l/b = 0.786 \times 40.00 / 4.00 = 7.86$

By using [Fig. 7.36] with $\phi = 1.0$ one gets $\psi_\lambda \approx 0.685$

And: $c_f = 0.79 \times 1.0 \times 0.685 \approx 0.54$

$$A_{ref} = l \times b = 40.00 \times 4.00 = 160.00 \text{ m}^2$$

$$q_p(40) = 1506.5 \text{ N/m}^2 \text{ (415 N/m}^2 \text{ for the construction phase)}$$

According to [7.9.2(5)] the reference height z_e is equal to the maximum height above the ground of the section being considered. As a conservative approach the value for $z_e = 40 \text{ m}$ may be considered, given that [Fig. 7.4] is not directly applicable. Nevertheless, a splitting of the pier in adjacent strips with various z_e and the associated values for v , q_p etc. might be considered, as a more realistic and less conservative approach

$$\text{Finally: } F_w = 1.0 \times 0.54 \times 1506.5 \times 160.00 = 813.51 \times 160.00 = 130161 \text{ N} \approx \mathbf{130.2 \text{ kN}}$$

3.5 Thermal actions

Thermal actions are defined in [EN 1991-1-6]. In particular thermal actions concerning bridges are described in [6]. In general, the temperature profile at each cross section of the bridge may be represented by four components (uniform ΔT_u , linear about the z-z axis (following the vertical axis) of the deck ΔT_{My} , linear about the y-y axis (following the transversal axis) of the deck ΔT_{Mz} and non-linear self-equilibrated ΔT_E). In the case of bridge decks, at least as far as the present example is considered, only the second one is of practical importance (temperature gradient in the vertical direction), given that bearings and joints are not dealt with. Would it be the case, the uniform temperature component ΔT_u should be considered, as it induces a variation in length of the bridge (when the longitudinal displacements are free on supports).

Distinction is made in [6.1.1] among three different bridge deck types, essentially steel (type 1), steel-concrete composite (type 2) and concrete (type 3), resulting in different values of upper and lower temperature difference and different distributions.

As far as temperature difference component following the vertical axis of the deck ΔT_{My} is concerned, the choice is left open for the National Annexes between the two following approaches (definitions) for this thermal component in a bridge:

Approach 1: (Vertical) linear thermal gradient over the entire depth of the bridge deck

In that case “heating” and “cooling” of the upper surface of the deck (in practice, respectively, the upper surface warmer or cooler than the bottom) are considered separately.

Recommended values are given in [Tab. 6.1]. The influence of the surfacing may be considered, as an NDP. Recommended values are given in [Tab. 6.2].

Approach 2: Non-linear thermal gradient which can be defined by two methods, continuous (defined as “normal procedure”) or discontinuous (defined as “simplified” procedure, sometimes called Approach 2*). The associated diagrams are shown in the following figure (Fig.3.1). The values ΔT_1 and ΔT_2 shown in the figure are defined according to the type of deck surfacing in [Annex B]. Recommended values are given in [Tab. B.2] The relevant choice is left open for NDPs.

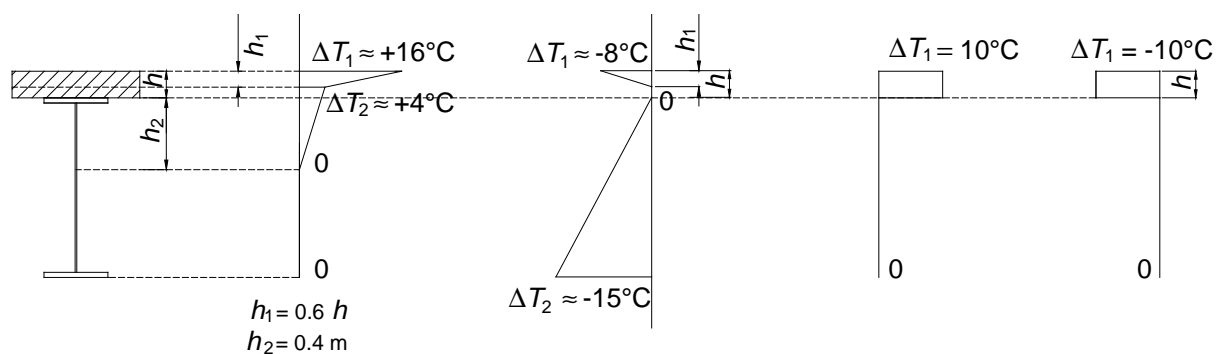


Fig. 3.1 Non-linear thermal gradient approach

The option adopted in this example is the non-linear discontinuous thermal gradient with a temperature difference of $\pm 10^\circ\text{C}$ between the slab concrete and the structural steel. The linear temperature difference components are noted $\Delta T_{M,\text{heat}}$ (heating) and $\Delta T_{M,\text{cool}}$ (cooling).

This thermal gradient is classified as a variable action (like traffic load) and is applied to composite cross-sections which are described with the short-term modular ratio.

Where appropriate, the simultaneity of uniform and temperature difference components, should be considered [6.1.5].

In that case the characteristic value of thermal action T_k is defined as an envelope of eight combinations of actions written with the two fundamental thermal actions described previously, and noting that $\Delta T_{N,\text{con}}$ (or $\Delta T_{N,\text{exp}}$) are used for contraction and expansion, respectively:

$$0.35 \Delta T_{N,\text{con}} \text{ (or } \Delta T_{N,\text{exp}}) + \Delta T_{M,\text{heat}} \text{ (or } \Delta T_{M,\text{cool}})$$

$$\Delta T_{N,\text{con}} \text{ (or } \Delta T_{N,\text{exp}}) + 0.75 \Delta T_{M,\text{heat}} \text{ (or } \Delta T_{M,\text{cool}})$$

To note also that in [6.1.6] and [6.2] differences of the uniform temperature components between structural members and thermal actions on bridge piers, respectively, are defined.

Part B: Actions during execution, accidental actions and traffic loads

3.6 Introduction

Aim of the present note is to illustrate the application of Eurocode Parts concerning Actions during execution (EN1991-1-6), Accidental actions (EN1991-1-7) and Traffic loads on bridges (EN1991-2), with special reference to the design of a three span continuous steel-concrete composite two girders bridge, which has been chosen as relevant reference case study (see Chapter 1 – Crespo and Davaine).

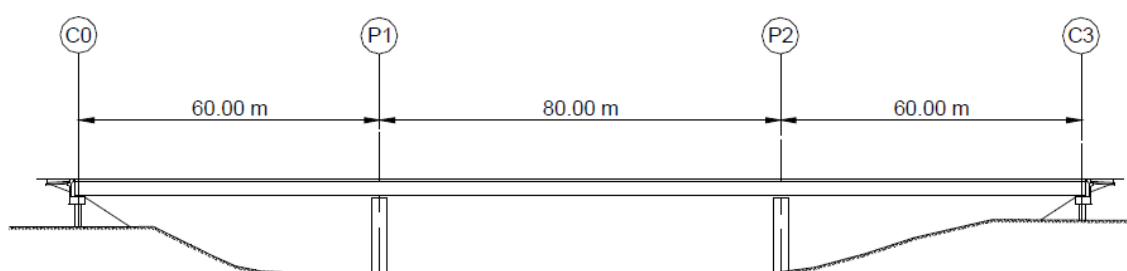


Fig. 3.2 Example of a three-span steel-concrete composite bridge

The attention will be devoted only to the most significant aspects of the design, so that the discussion will focus mainly on

- launching phase;
- lane numbering for static and fatigue verifications;
- braking and acceleration forces;
- fatigue verifications of steel details;

referring, when necessary, to other pertinent EN parts.

3.7 Actions during execution

In EN 1991-1-6, actions during execution are separated, according to their origin and in conformity with EN 1990, in Construction loads and Non construction loads. Here, only construction loads Q_c are treated.

Construction loads Q_c are direct, variable actions coming from six different sources, Q_{ca} , Q_{cb} , ..., Q_{cf} according to Table 3.2 (see table 4.1 of EN 1991-1-6). Usually, they are modelled as free actions.

Construction load Q_{ca} is a uniformly distributed load; the recommended value is $q_{ca,k}=1.0 \text{ kN/m}^2$.

Table 3.2 Construction loads

Q_{ca}	<i>Personnel and hand tools</i> (working personnel, staff and visitors with hand tools or other small site equipment)
Q_{cb}	<i>Storage of movable items</i> (building and construction materials, precast elements, equipment)
Q_{cc}	<i>Non-permanent equipment in position for use during execution</i> (formwork panels, scaffolding, falsework, machinery, containers) <i>or during movement</i> (travelling forms, launching girders and nose, counterweights)
Q_{cd}	<i>Movable heavy machinery and equipment</i> (cranes, lifts, vehicles, power installations, jacks, heavy lifting devices and trucks)
Q_{ce}	<i>Accumulation of waste materials</i> (surplus of construction materials or excavated soil, demolition materials)
Q_{cf}	<i>Loads from part of structure in a temporary state or loads from lifting operations</i>

Construction load Q_{cb} is represented by a uniformly distributed load q_{cb} and a concentrated load F_{cb} . For bridges, the minimum recommended values are $q_{cb,k}=0.2 \text{ kN/m}^2$ and $F_{cb,k}=100 \text{ kN}$.

Unless more accurately specified, construction loads Q_{cc} are represented by a uniformly distributed load q_{cc} ; the minimum recommended value is $q_{cc,k}=0.5 \text{ kN/m}^2$.

When loads Q_{cd} are not defined in project specification, information about their definition may be found in the relevant ENs: for example, in EN1991-2 for vehicles or in EN1991-3 for cranes and machinery.

Loads Q_{ce} due to accumulation of waste materials may vary significantly, and over short time periods, depending on types of materials, climatic conditions, build-up and clearance rates, and they can also induce possible mass effects on horizontal, inclined and vertical elements (such as walls).

Finally, loads Q_{cf} should be taken into account and modeled according to the planned execution sequences and their consequences, like load reversals and/or variation of the static scheme.

Construction loads Q_c may be represented in the appropriate design situations (see EN 1990), either, as one single variable action, or where relevant by a group of different types of construction loads, which is applied as a single variable action. Single and/or a grouping of construction loads should be considered to act simultaneously with *Non construction loads* as appropriate.

During the casting of the concrete slab, working personnel (Q_{ca}), formwork and load-bearing members (Q_{cc}) and weight of the fresh concrete, which is classified as Q_{cf} , should be considered acting simultaneously. According to EN 1991-1-7 recommendations, during the concrete casting of the deck, in the actual area it can be identified two parts, the working area, which is a square whose side is the minimum between 3.0 m and the span length, and the remaining (outside the working area).

The actual area is loaded by the self-weight of the formwork and load bearing element Q_{cc} and by the weight of the fresh concrete Q_{cf} (about 7.5 kN/m^2 in the example), the working area by $0.10 Q_{cf}$, with the restriction $0.75 \text{ kN/m}^2 \leq 0.10 Q_{cf} \leq 1.5 \text{ kN/m}^2$ (0.75 kN/m^2), and the area outside the working area by 0.75 kN/m^2 , covering Q_{ca} .

In the example, two different load cases could be envisaged in principle, as shown in Fig. 3.3 and 3.4, to maximize effects on the slab cross sections on the support and on the midspan, respectively; in

effect they are coincident, as loads inside and outside the working area are, in the current case, exactly the same.

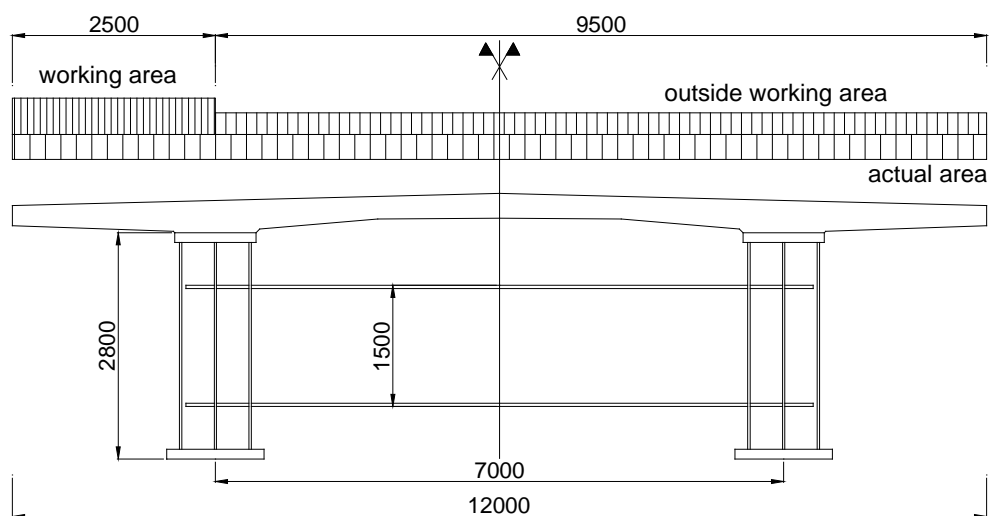


Fig. 3.3 Load arrangement maximizing effects on the support cross section of the slab

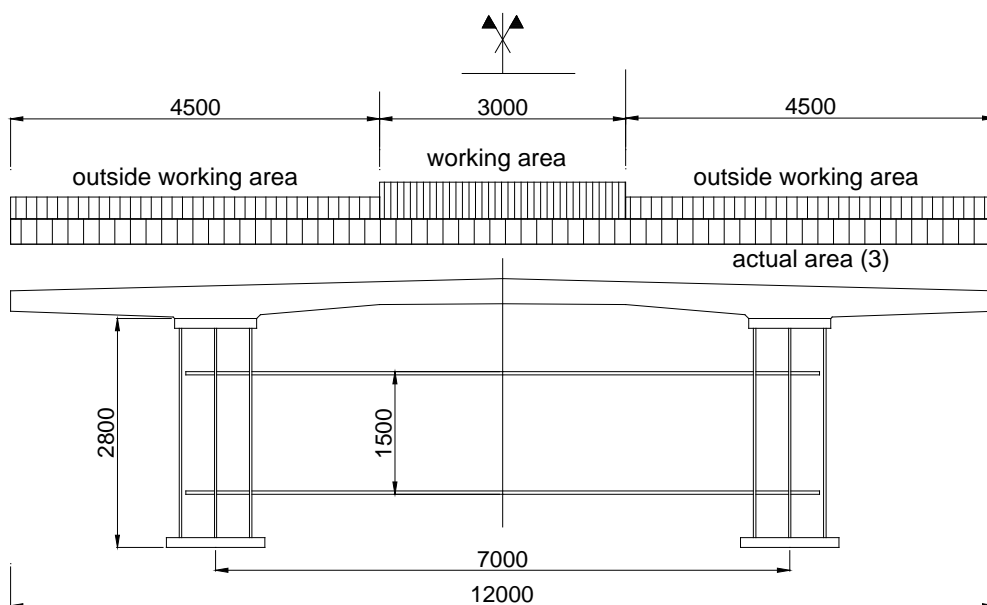


Fig. 3.4 Load arrangement maximizing effects on the midspan of the slab

3.7.1 LAUNCHING PHASE

An incremental launching of the steel part of the bridge is foreseen. The first launch takes place when two spans are assembled, for a total length of 150.5 m about (see Fig. 3.5).

In this phase it is necessary to assess if a counterweight is necessary or not.

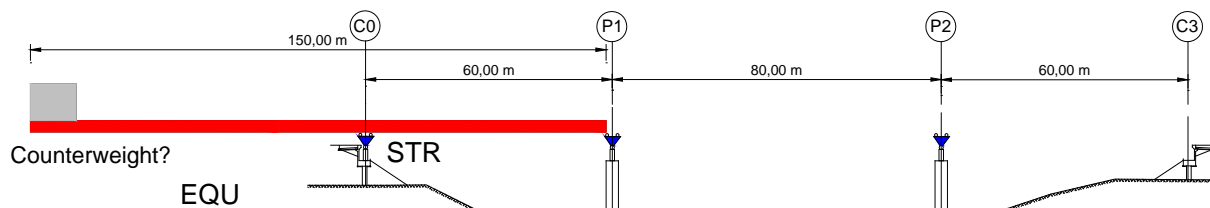


Fig. 3.5 First launching phase

Considering that the steel distribution is the one given in Fig. 3.6 (Davaine, 2010) and according to table A2.4(A) (EQU) of EN1990, the design value of the destabilizing loads is given by

$$\gamma_{G,sup} G_{k,sup} + \gamma_Q Q_{ck}$$

where

$G_{k,sup}$ is the upper fractile of the permanent loads,

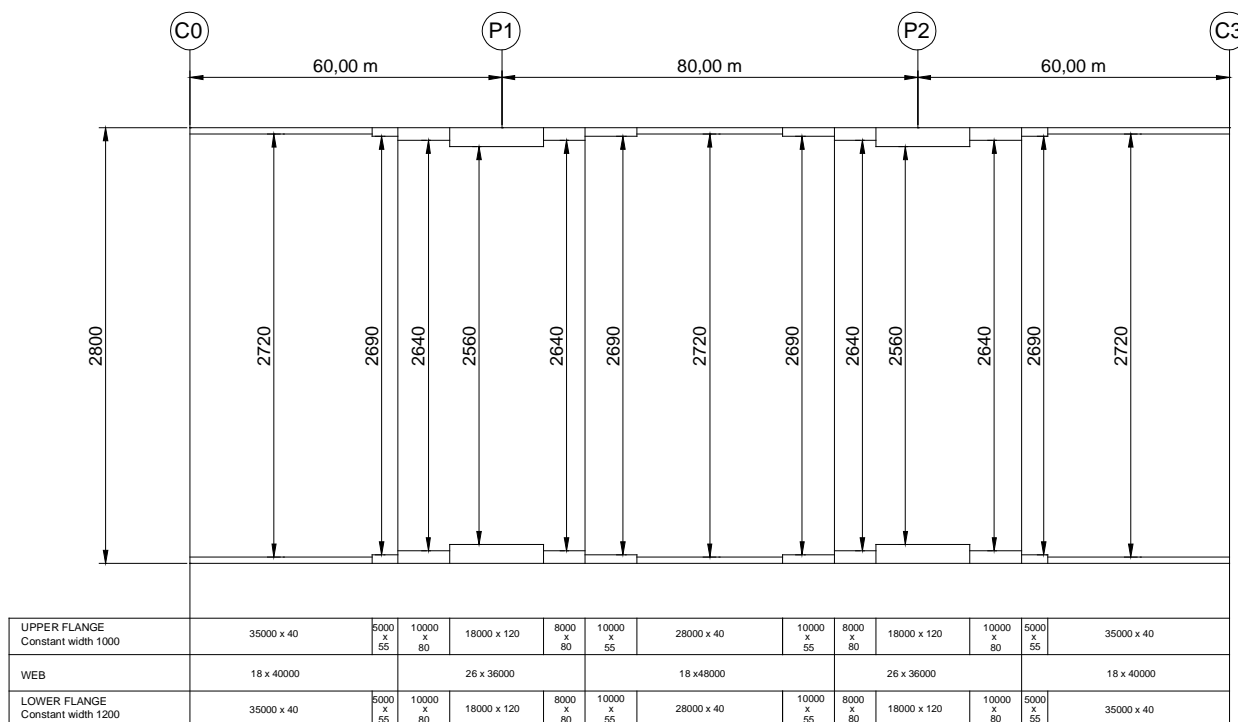


Fig. 3.6 Steel distribution

$Q_{k,sup}$ is the construction load during the launching phase, which can be set to 4.0 kN/m, including also the vertical wind load which can occur during the launch;

$\gamma_{G,suo}=1.05$ and

$\gamma_Q=1.35$, as the construction phase is a transient design situation;

the design value of the stabilizing loads is

$$\gamma_{G,inf} G_{k,inf} ,$$

being $\gamma_{G,inf}=0.95$.

The destabilizing design effect is then given by

$$E_{d,dsb} = 1.05 \times 4311.05 + 1.35 \times 7200 = 14246.6 \text{ kNm}$$

and the stabilizing effect by

$$E_{d,sb} = 0.95 \times 15603.8 = 14823.6 \text{ kNm}$$

so that $E_{d,dsb} < E_{d,sb}$ and the counterweight is not necessary.

It must be noted that, when a counterweight is used, the variability of its characteristics and/or its position should be taken into account: for instance, adopting a reduced value of the partial factor $\gamma_{G,inf}=0.80$, when the weight is not well defined, or considering unfavourable variations of the given design position, when the position is not fixed. The range of variation commonly accepted for steel bridge design is ± 1.0 m.

In the launching phase, also STR verification should be performed for the steel sections. According to of EN1990, table A2.4(B) (STR) and equation (6.10), design values should be determined considering

$$\gamma_{G,sup} G_{k,sup} + \gamma_Q Q_{ck}$$

where

$\gamma_{G,sup}=1.35$ and $\gamma_Q=1.50$. For example, the design bending moment at the support P1 is

$$M_d = -(1.35 \times 4311.05 + 1.5 \times 7200) = -16619.9 \text{ kNm}$$

According to §A2.5 of Annex A2 of EN1991-1-6, during the launch also horizontal forces due to friction must be considered. The minimum recommended value of the total friction forces is 10% of the vertical load.

For low friction surfaces, individual friction force effects on each pier can be assessed adopting the following recommended values: $\mu_{min}=0$ and $\mu_{min}=0.04$. In the present case study, at the end of the first launching phase the design values of the friction forces on the top of the pier P1 result

$$F_{fr,d,min} = 0 \text{ and } F_{fr,d,max} = 0.04 (1.35 \times 377.3 + 1.5 \times 490.4) = 49.8 \text{ kN}$$

Once reached the pier P1, the launch can go on (Fig. 3.7) for maximum 60.0 m more and afterward, the remaining part of the beam can be joined and the final phase of the launch can be take place. During this final phase, when the free end of the beam is near the pier P2, the span of the cantilevered part is maximum (see Fig. 3.7) and the design bending moment at the support P1 is:

$$M_d = -(1.35 \times 8892.0 + 1.5 \times 12800) = -31204.3 \text{ kNm}$$

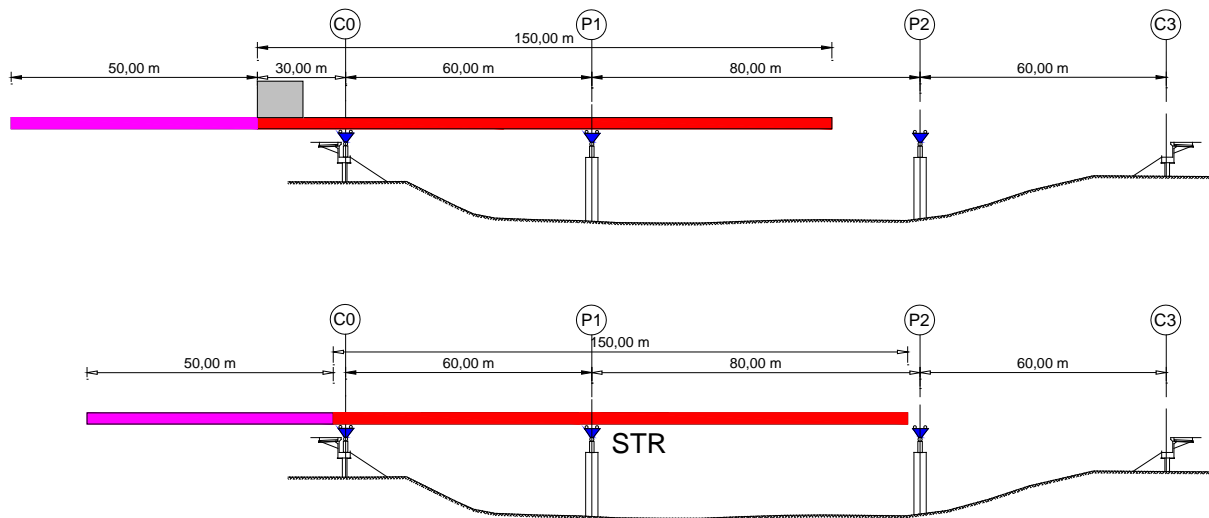


Fig. 3.7 Intermediate and final launching phase

Beside the afore mentioned actions, in the launching phase also the following actions should be taken into account, considering the most unfavourable scenario

- wind, which is described in Malakatas (2010);
- vertical temperature difference between bottom and upper part of the beam;
- horizontal temperature difference;
- differential deflection between the supports in longitudinal direction (± 10 mm);
- differential deflection between the supports in transverse direction (± 2.5 mm).

3.8 Accidental actions

General principles for classification of accidental actions and their modelling in structural verifications are introduced in EN 1990 Basis of Design, where partial factors and combination rules to be used in the design calculations are given.

Accidental loads usually never occur during the lifetime of a structure. But if they are present, it takes only a short time and their duration depends on the load itself. Typical accidental loads for bridges are impact loads.

Detailed description of individual actions and guidance for their application in design calculations is given in EN 1991-1-7, which covers the following topics:

- impact loads due to road traffic;
- impact loads due to train traffic;
- impact loads due to ships,

also giving information about the control of accidental loads, since in many cases structural measures alone cannot be considered as sufficient.

The load models given in the main text of EN1991-1-7 are rather conventional, while more advanced models are presented in Annex C of EN1991-1-7 itself.

In the following short reference will be made to collisions due to trucks on road bridges, being the other topics outside of the scope of the present note.

3.8.1 IMPACT OF VEHICLES ON THE BRIDGE SUBSTRUCTURE

Road vehicles can impact on the bridge substructure or the bridge superstructure.

Impacts on the substructure of bridges by road vehicles are relatively frequent. In case of soft impact, when the impacting body consumes most of the available kinetic energy, recommended minimum design values for the equivalent horizontal actions due to impact on vertical structural elements (columns, walls, piers) can be derived from table 4.1 of EN1991-1-7 (see Table 3.3), depending on the road classification.

In the table, forces in the driving direction and perpendicular to it are denoted as F_{dx} and F_{dy} , respectively. These collision forces are supposed to act at 1.25 m above the level of the driving surface (0.5 m for cars). The force application area may be taken as 0.25 m (height) by 1.50 m (width) or the member width, whichever is the smallest. Generally, F_{dx} and F_{dy} can be considered not acting simultaneously.

Table 3.3 Static equivalent impact design forces on substructures over roadways

<i>Type of road</i>	<i>Type of vehicle</i>	<i>Force F_{dx} [kN]</i>	<i>Force F_{dy} [kN]</i>
Motorway	Truck	1000	500
Country road	Truck	750	375
Urban area	Truck	500	250
Courtyards/garages	Passengers cars only	50	25
Courtyards/garages	Trucks	150	75

More advanced probabilistic models as well as more refined models for dynamic and non-linear analyses are provided in informative Annexes of EN1991-1-7.

3.8.2 IMPACT OF VEHICLES ON THE BRIDGE SUPERSTRUCTURE

Impact of vehicles on the bridges superstructure can happen in two different scenarios, according to whether the lorries are travelling on or under the bridge.

The impact on restraint system of the superstructure belongs to the first scenario: in this case actions depend on the road restraint system mechanical characteristics, i.e. the restraint system class, that govern the maximum loads transmitted by the road restraint system itself to the main structure. Recommended classes and recommended impact forces are indicated in table 4.9 of EN1991-2.

Concerning the impact on vehicles on main structural elements, indicative recommended equivalent static design forces are given in EN1991-1-7, as reported in Table 3.4. These forces should be applied perpendicularly to the direction of normal travel.

The second scenario must be considered when a roadway underpasses the bridge, unless adequate clearances or suitable protection measures to avoid impact are provided.

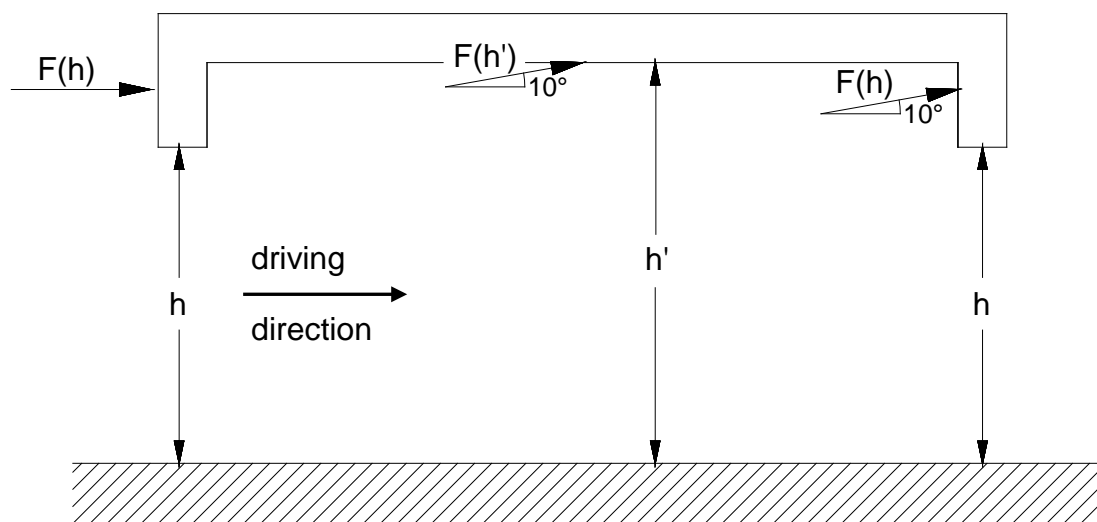
Table 3.4 Indicative equivalent static design forces due to impact on superstructures.

<i>Category of traffic</i>	<i>Equivalent static design force F_{dx} [kN]*</i>
Motorways and country national and main roads	500
Country roads in rural area	375
Roads in urban area	250
Courtyards and parking garages	75

* x = direction of normal travel.

Excluding future re-surfacing of the roadway under the bridge, the recommended value for adequate clearance h to avoid impact is in the range 5.0 m to 6.0 m (Fig. 3.8). When the clearance is $h \leq 5.0$ m, impact forces can be derived again from Table 3.4, when the clearance is $h \geq 6.0$ m, impact forces can be set to zero, resorting to linear interpolation when h ranges between 5.0 m and 6.0 m.

The same impact forces as given in Table 3.4 are also considered on the underside surfaces of bridge decks with an upward inclination angle of 10° (see Fig. 3.8).

**Fig. 3.8 Impact forces on underside surfaces of superstructure**

3.9 Traffic loads

Static and fatigue traffic load models for bridges are given in EN 1991-2, while bases for combinations of traffic loads with non-traffic loads are given in EN 1990.

Traffic models for road bridges have been derived and calibrated starting from the real traffic data recorded in Auxerre (F) on the motorway Paris- Lyon in May 1986.

In effect, on the basis of the analysis of real European traffic data recorded in two large experimental campaigns between 1980 and 1994, the Auxerre traffic was identified as the most representative European continental traffic in terms of composition and severity, also taking into account the expected traffic trends.

3.9.1 STATIC LOAD MODELS

3.9.1.1 Division of the carriageway and numbering of notional lanes

For the application of the load models, in the EN 1991-2 the carriageway is divided in notional lanes, generally 3 m wide, and in the remaining area, according to Table 3.5.

Table 3.5 Subdivision of the carriageway in notional lanes

<i>Carriageway width w</i>	<i>Number of notional lanes n_l</i>	<i>Width of a notional lane</i>	<i>Width of the remaining area</i>
$w < 5.4 \text{ m}$	1	3 m	$w - 3 \text{ m}$
$5.4 \text{ m} \leq w < 6 \text{ m}$	2	$0.5 w$	0
$6 \text{ m} \leq w$	$\text{int}(w/3)$	3 m	$w - 3 \times n_l$

The carriageway is defined as the part of the roadway surface sustained by a single structure (deck, pier etc.).

The carriageway includes all the physical lanes (marked on the roadway surface), the hard shoulders, the hard strips and the marker strips. The carriageway width w should be measured between the kerbs, if their height is greater than 100 mm (recommend value), or between the inner limits of the safety barriers, in all other cases.

The number and the positions of the notional lanes depend on the element under consideration and should be chosen each time in order to maximize the considered effect. In general, the notional lane that gives the most severe effect is numbered lane n. 1 and so on, in decreasing order of severity. For this reason, the locations of the notional lanes are not linked with their numbering, nor with the position of physical lanes (see Fig. 3.9, for example).

In particular cases, for example for some serviceability limit states or for fatigue verifications, it is possible to derogate from this rule and to consider less severe locations of the notional lanes, as it will be shown in the following.

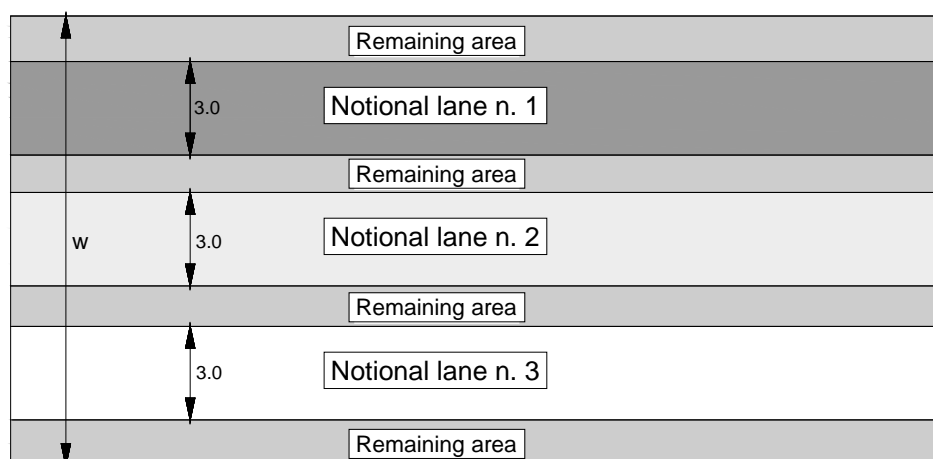


Fig. 3.9 Example of lane numbering

3.9.1.2 Static load models for vertical loads

For the evaluation of road traffic effects associated with ULS verifications and with particular serviceability verifications, four different load models, LM1 to LM4, are considered in EN1991-2:

- Load model n. 1 (LM1) generally reproduces traffic effects to be taken into account for global and local verifications; it is composed by concentrated and uniformly distributed loads: a system of two concentrated axle loads, one per notional lane i , representing a tandem system weighing $2 \cdot \alpha Q_i \cdot Q_{ki}$ (see Table 3.6), whose geometry is shown diagrammatically in Fig. 3.10, and by a system of uniformly distributed loads having a weight density per square meter of $\alpha q_i \cdot q_{ki}$. The adjustment factors αQ_i and αq_i depend on the class of the route and on the expected traffic type: in absence of specific indications, they are assumed equal to 1, as in the present example.

Table 3.6 Load model n. 1 – characteristic values

<i>Position</i>	<i>Tandem system – Axle load Q_{ik} [kN]</i>	<i>Uniformly distributed load q_{ik} [kN/m²]</i>
Notional lane n. 1	300	9.0
Notional lane n. 2	200	2.5
Notional lane n. 3	100	2.5
Other notional lanes	0	2.5
Remaining area	0	2.5

- Load model n. 2 (LM2) reproduces traffic effects on short structural members. The local load model n. 2, LM2 (Fig. 3.11), consists of a single axle load $\beta Q \cdot Q_{ak}$ on specific rectangular tire contact areas, 0.35×0.6 m, being $Q_{ak} = 400$ kN, dynamic amplification included. Unless otherwise specified $\beta Q = \alpha Q_1$. LM2, which is intended only for local verifications, should be considered alone on the bridge, travelling in the direction of the longitudinal axis of the bridge, in the most unfavourable position. When unfavourable, only one wheel should be considered.

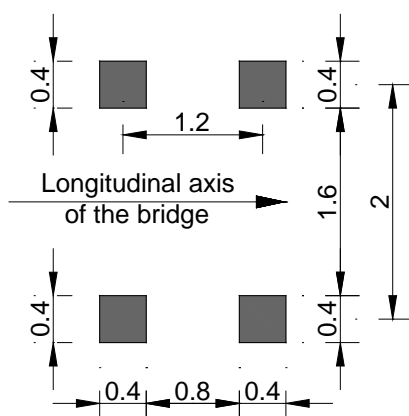


Fig. 3.10 Tandem system of LM1

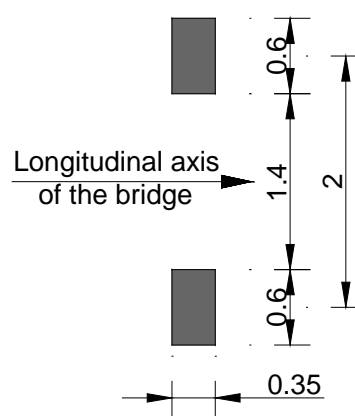


Fig. 3.11 LM2 – Single axle

- Load model n. 3 (LM3), special vehicles, should be considered only when requested, in a transient design situation. It represents abnormal vehicles not complying with national regulations on weight and dimension of vehicles. The geometry and the axle loads of the special vehicles to be considered in the bridge design should be assigned by the bridge owner. Additional information can be found in Annex A of EN 1991-2.
- Load model n. 4 (LM4), a crowd loading, is particularly significant for bridges situated in urban areas. It should be applied on all the relevant parts of the length and width of the bridge deck, including the central reservation, if necessary. Anyhow, it should be considered only when expressly required. The nominal value of the load, including dynamic amplification, is equal to 5.0 kN/m², while the combination value is reduced to 3.0 kN/m².

3.9.1.3 Horizontal forces

The braking or acceleration force, denoted by Q_{lk} , should be taken as longitudinal force acting at finished carriageway level.

The characteristic values of Q_{lk} depend on the total maximum vertical load induced by LM1 on notional lane n. 1, as follows

$$180 \times \alpha_{Q_1} \text{ kN} \leq Q_{lk} = 0.6 \times \alpha_{Q_1} \times (2 \times Q_{1k}) + 0.10 \times \alpha_{q_1} \times q_{1k} \times w_1 \times L \leq 900 \text{ kN}$$

where w_1 is the width of the notional lane n. 1 and L the length of the loaded area. The force Q_{lk} , that includes dynamic magnification, should be applied along the axis of any lane.

The centrifugal force Q_{tk} is acting at the finished carriageway level, perpendicularly to the axis of the carriageway. EN1991-2 states that, unless otherwise specified, Q_{tk} should be considered as a point load at any deck cross section.

The characteristic value of Q_{tk} , including dynamic magnification, depends on the horizontal radius r [m] of the carriageway centreline and on the total maximum weight of the vertical concentrated loads of the tandem systems of the main loading system Q_v , $Q_v = \sum_i \alpha_{Q_i} \times (2 \times Q_{ik})$, and it is given

by $Q_{tk} = 0.2 \times Q_v$ [kN], if $r < 200$ m; $Q_{tk} = 40 \times \frac{Q_v}{r}$ [kN], if $200 \text{ m} \leq r \leq 1500$ m; $Q_{tk} = 0$, if $r > 1500$ m.

3.9.2 GROUPS OF TRAFFIC LOADS ON ROAD BRIDGES

According to table 4.4.a of EN1991-2, the characteristic values of the traffic actions acting simultaneously with non-traffic actions can be determined considering the five different, and mutually exclusive, groups of loads reported in Table 3.7, where the dominant action is highlighted. Each group of loads should be considered as defining a characteristic action for combination with non-traffic loads, but it can be also used to evaluate infrequent and frequent values.

To obtain infrequent combination values it is sufficient to replace characteristic values with the infrequent ones, leaving unchanged the others, while frequent combination values are obtained replacing characteristic values with the frequent ones and setting to zero all the others. The recommended values of ψ -factors for traffic loads on road bridges, as indicated in table A2.1 of EN1990 are reported in Table 3.8.

The values of ψ_0 , ψ_1 , ψ_2 for gr1a, referring to load model n.1 are assigned for routes with traffic corresponding to adjusting factors α_{Q_1} , α_{q_1} , α_{qr} and β_Q equal to 1, while those relating to UDL correspond to the most common traffic scenarios, in which accumulations of lorries is not frequent. In different scenarios, for example, in situations characterised by severe presence of continuous traffic,

like for bridges in urban or industrial areas, a value of ψ_2 other than zero may be envisaged for the UDL system of LM1 only.

Table 3.7 Characteristic values of multicomponent actions for traffic loads on road bridges

Carriageway						Footways and cycle tracks
Vertical loads				Horizontal loads		Vertical loads only
Group of loads	Main load model	Special vehicles	Crowd loading	Braking force	Centrifugal force	Uniformly distributed
1	Characteristic values					Combination value
2	Frequent values			Characteristic values	Characteristic values	
3						Characteristic values
4			Characteristic values			Characteristic values
5	see Annex A of EN1991-2	Characteristic values				

Table 3.8 Recommended values of ψ - factors for traffic loads on road bridges

Action	Symbol		ψ_0	ψ_{1inf}	ψ_1	ψ_2
Traffic loads (see table 6)	gr1a (LM1)	Tandem System	0.75	0.80	0.75	0
		UDL	0.40	0.80	0.40	0
	gr1b (single axle)		0	0.80	0.75	0
	gr2 (Horizontal Forces)		0	0	0	0
	gr3 (Pedestrian loads)		0	0.80	0	0
	gr4 (LM4 – Crowd loading))		0	0.80	0.75	0
	gr5 (LM3 – Special vehicles))		0	1.0	0	0

3.9.3 LOAD COMBINATIONS FOR THE CASE STUDY

Load combinations to be considered for ULS and SLS verifications of the bridge considered in the case study are summarized in the following.

3.9.3.1 Fundamental combinations of actions

The fundamental load combinations to be considered for structural (STR) ULS verifications, determined according to §4.2 and table A.2.4(B) of EN1990, applying equation (6.10) of EN1990 are synthesized below,

$$\sum_{j \geq 1} (1,35 G_{kj, \text{sup}} \text{ or } 1,00 G_{kj, \text{inf}}) "+" (1,00 \text{ or } 0) \times S "+" \left\{ \begin{array}{l} \text{Leading action, } \mathbf{gr1a} \\ \text{accompanying} \\ 1,35 \times (TS + UDL + q_{fk}^*) + 1,5 \times \left\{ \begin{array}{l} \min(0,6 F_{Wk}, F_w^*) \\ \text{or } 0,6 T_k \end{array} \right. \\ 1,35 \text{ gr1b} \\ 1,35 \text{ gr2} + 1,5 \times 0,6 T_k \\ 1,35 (\text{gr3 or gr4}) + 1,5 \times 0,6 T_k \\ 1,35 \text{ gr5} \\ 1,5 T_k + 1,35 \times (0,75 TS + 0,4 UDL + 0,4 q_{fk}^*) \\ 1,5 F_{Wk} \\ 1,5 Q_{Sn,k} \end{array} \right. \underbrace{\hspace{10em}}_{\mathbf{\psi_0 gr1a}}$$

where S represents the settlements, TS and UDL indicate the tandem system and the uniformly distributed load of the LM1, respectively, q_{fk}^* the combination value of the crowd loading, $Q_{Sn,k}$ the snow load, $F_{W,k}$ the wind force, F_w^* the upper limit of the wind force compatible with normal traffic, and T_k the thermal action.

It is important to recall that partial factor γ_Q for unfavourable effects of traffic actions on road bridges is 1.35.

3.9.3.2 Characteristic, frequent and quasi-permanent combinations of traffic actions

With the same meaning of the symbols, the combinations of actions to be considered for SLS verifications can be easily written. So the characteristic combinations of actions become

$$\sum_{j \geq 1} (G_{kj, \text{sup}} \text{ or } G_{kj, \text{inf}}) "+" (1,00 \text{ or } 0) \times S "+" \left\{ \begin{array}{l} \text{Leading action, } \mathbf{gr1a} \\ \text{accompanying} \\ (TS + UDL + q_{fk}^*) + \left\{ \begin{array}{l} \min(0,6 F_{Wk}, F_w^*) \\ \text{or } 0,6 T_k \end{array} \right. \\ \text{gr1b} \\ \text{gr2} + 0,6 T_k \\ (\text{gr3 or gr4}) + 0,6 T_k \\ \text{gr5} \\ T_k + (0,75 TS + 0,4 UDL + 0,4 q_{fk}^*) \\ F_{Wk} \\ Q_{Sn,k} \end{array} \right. \underbrace{\hspace{10em}}_{\mathbf{\psi_0 gr1a}}$$

the frequent combinations of actions become

$$\sum_{j \geq 1} (G_{kj, \text{sup}} \text{ or } G_{kj, \text{inf}}) "+" (1,00 \text{ or } 0) \times S "+" \left\{ \begin{array}{l} \text{Leading action, } \psi_1 \text{gr1a} \\ \text{accompanying} \\ (0,75TS + 0,4UDL) + 0,5 T_k \\ 0,75 \text{ gr1b} \\ 0,4 \text{ gr3} + 0,5 T_k \\ 0,75 \text{ gr4} + 0,5 T_k \\ 0,2 F_{Wk} \\ 0,6 T_k \end{array} \right.$$

and, finally, the unique quasi-permanent combination is

$$\sum_{j \geq 1} (G_{kj, \text{sup}} \text{ or } G_{kj, \text{inf}}) "+" (1,00 \text{ or } 0) \times S "+" 0,5 T_k$$

Leading action (no accompanying)

3.9.3.3 Subdivision of the carriageway in notional lanes for global verifications

As said before, the division of the carriageway width in notional lanes should aim to determine the most severe effects in the element under consideration.

Considering that the carriageway carries a road section composed by two physical lanes 3.50 m wide, and by two hard shoulders, 2.0 m wide, for a total carriageway width of 11.0 m (see Fig. 3.12), three notional lanes can be considered maximum, so that the maximum width of the remaining area results 2.0 m, as shown for example in Fig. 3.13.

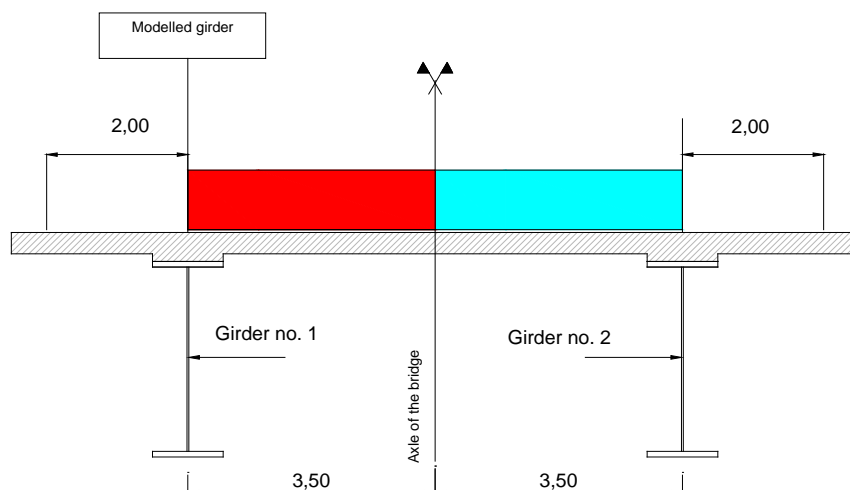


Fig. 3.12 Location of physical lanes and hard shoulders on the carriageway

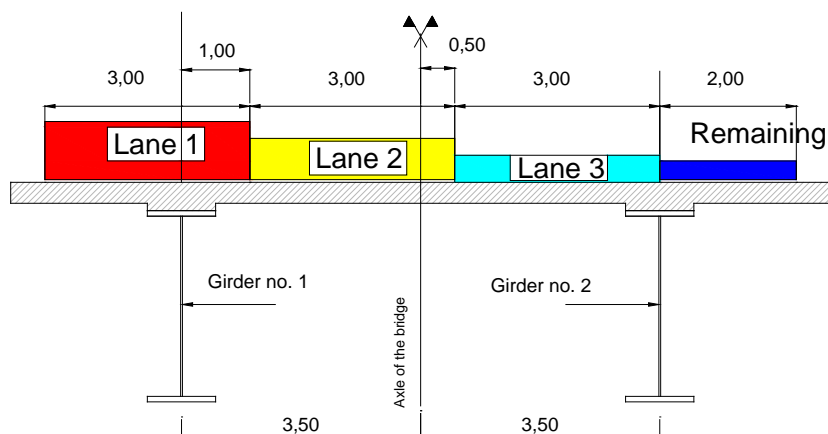


Fig. 3.13 An example of subdivision of the carriageway in notional lanes

Of course, the number and the position of the notional lanes and the width of the remaining area depend on the particular member under consideration.

Adopting a linear transverse influence line, the notional lanes arrangement to be adopted for global verification of the main girder is the one reported in Fig. 3.14, where the pertinent influence coefficients are reported on the axis of each notional lane. Obviously, remaining area should not be considered, since it stands on the negative part of the influence surface.

For static assessments see Chapter 4 (Davaine) and Chapter 6 (Ortega Cornejo and Raoul)

3.9.3.4 Braking and acceleration forces

As just said, the characteristic values of braking and acceleration forces, which appear in traffic load group gr2, depend on the loaded length L .

Since in the present example $\alpha_{Q1} = \alpha_{q1} = 1.0$, the characteristic values are given by

$$180 \text{ kN} \leq Q_{lk} = 0.6 \times (2 \times Q_{1k}) + 0.10 \times q_{1k} \times w_1 \times L \leq 900 \text{ kN}.$$

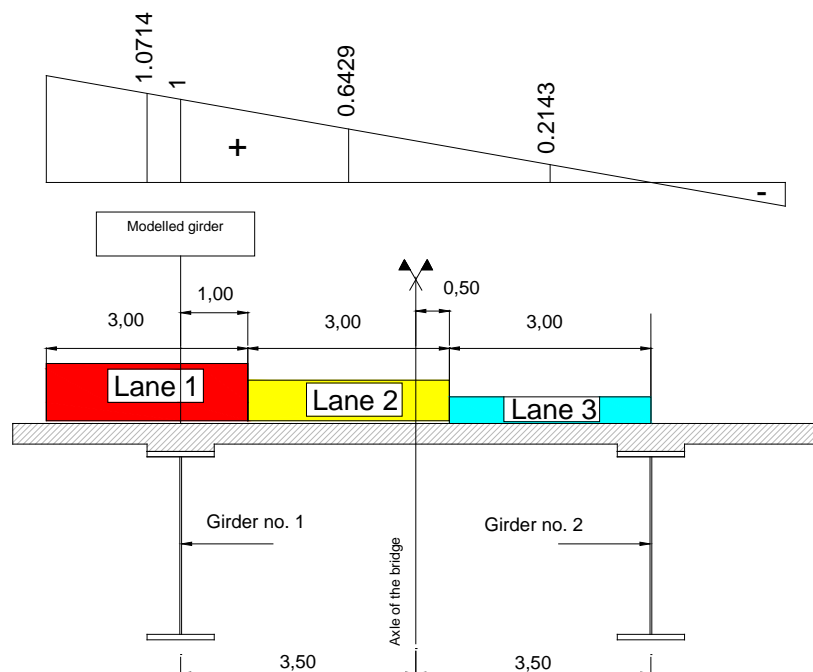


Fig. 3.14 Notional lanes arrangement for global verifications of the main girders

The values of braking and acceleration forces for the most significant longitudinal traffic load arrangements are reported in Figure 3.15.

3.9.4 FATIGUE LOAD MODELS

As known, fatigue resistance of structural details is commonly described by the so-called *S-N* (or Wöhler) curves. In the logarithmic *S-N* plane, *S-N* curves for steel details, characterised by constant amplitude fatigue limit (endurance limit), are usually represented by a bilinear curve, characterised by a sloping branch of constant slope, $m=3$ and a horizontal branch, or by a trilinear curve, characterised by two sloping branches, $m=3$ and $m=5$, and a horizontal branch, according as boundless fatigue life or fatigue damage is to be assessed. In other cases, like for example prestressing tendons and reinforcing bars in concrete, endurance limit cannot be detected and the *S-N* curves are bi-linear.

Since the fatigue traffic models should reproduce the real traffic effects, from the above-mentioned considerations, it derives that at least two conventional fatigue load models must be given: the one to be used for boundless fatigue life assessments, the other for fatigue damage calculations. Besides, since an adequate fitting of the effects induced by the real traffic requires very sophisticated load models, whose application is often difficult, the introduction of simplified and safe-sided models, to be used when sophisticated checks are unnecessary, could be very helpful in common design practice.

For this reason in EN 1991-2 two fatigue load models are foreseen for each kind of fatigue verification: the former is essential, safe-sided and easy to use, the latter is more refined and accurate, but also more complicated. In conclusion, in EN 1991-2 four conventional models are given:

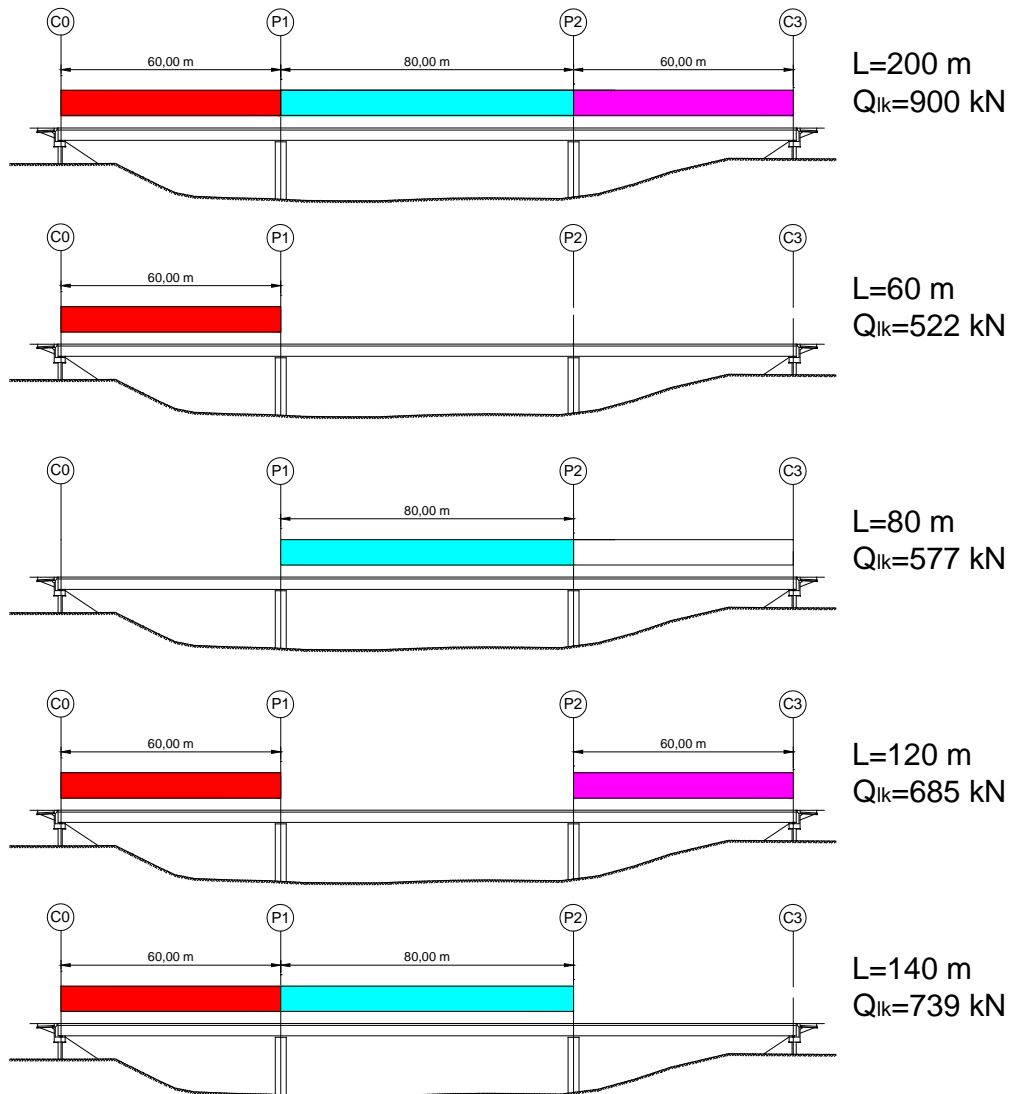


Fig. 3.15 Calculation of braking and acceleration forces in various load cases

- models 1 and 2 for boundless fatigue checks;
- models 3 and 4 for damage calculations.

Detailed discussion of the fatigue load models is outside the scope of the present note and only fatigue load model n. 3 will be considered in the following §3.9.4.1.

It is only necessary to stress that fatigue load models n. 2 and n. 4 are the most refined ones and they are load spectra constituted by five standardised vehicles, representative of the most common European lorries, while fatigue load 1 is extremely simple and very safe-sided.

Fatigue load model n. 2, is a set of lorries with frequent values of axle loads, and fatigue model n. 4 is a set of lorries with equivalent values of the axle loads, are illustrated in Tables 3.2 and 3.3, respectively. They allow to perform very precise and sophisticated verifications, provided that the interactions amongst vehicles simultaneously crossing the bridge are negligible or opportunely considered.

Fatigue load model n. 2 derives from the main load model used for assessing static resistance: the load values are simply reduced to frequent ones, multiplying the axle loads Q_{ik} of the tandem system by 0.7 and the weight density of the uniformly distributed loads q_{ik} by 0.3.

Obviously, beside the conventional models, EN 1991-2 allows also the use of real traffic data (fatigue load model n. 5, which is the most accurate one), provided that the recorded traffic is representative of the expected traffic on the bridge.

In conclusion, from the above consideration, the number of fatigue load models provided in §4.6 of EN1991-2 it is not surprising, as they answer to different design demands.

3.9.4.1 Fatigue load model n. 3

The simplified fatigue load model n. 3, conceived for damage computations, is constituted by a symmetrical conventional four axle vehicle, also said fatigue vehicle (Fig. 3.16). The equivalent load of each axle is 120 kN. This model is accurate enough for spans bigger than 10 m, while for smaller spans it results generally safe-sided.

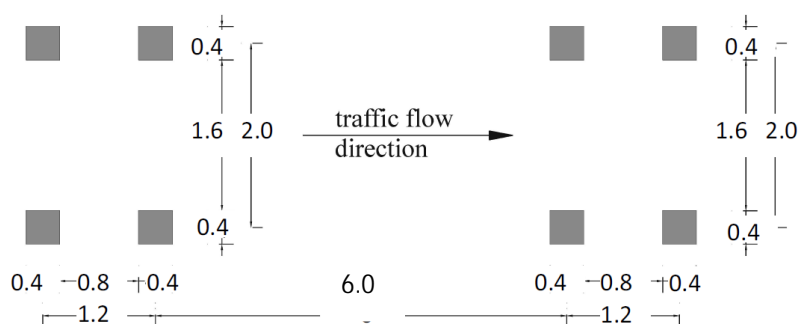


Fig. 3.16 Fatigue load model n. 3

The use of the model is two-fold. In effect it can be used both directly to evaluate the cumulative fatigue damage according to the Palmgren-Miner rule, as it will be made below, and indirectly to determine the equivalent stress range to be used in the λ -coefficient method.

The λ -coefficient method, proposed originally for railway bridges, aims to bring back fatigue verifications to conventional resistance checks, comparing a conventional equivalent stress range, $\Delta\sigma_{eq}$, depending on appropriate λ -coefficients, with the fatigue detail category, provided that appropriate and reliable λ -coefficients are available.

Usually, λ -coefficients depend on the shape and on the base length of the influence surface, on the detail material, on the annual lorry flow, on the fatigue life of bridge and on the vehicle interaction. Additional information are given in relevant EN parts, EN1992-2, EN1993-1-9, EN1993-2, EN1994-2.

3.9.5 FATIGUE ASSESSMENT OF THE COMPOSITE BRIDGE

The fatigue assessment of the main details of the composite bridge has been performed considering the four cross sections highlighted in Fig. 3.17, under the following assumptions:

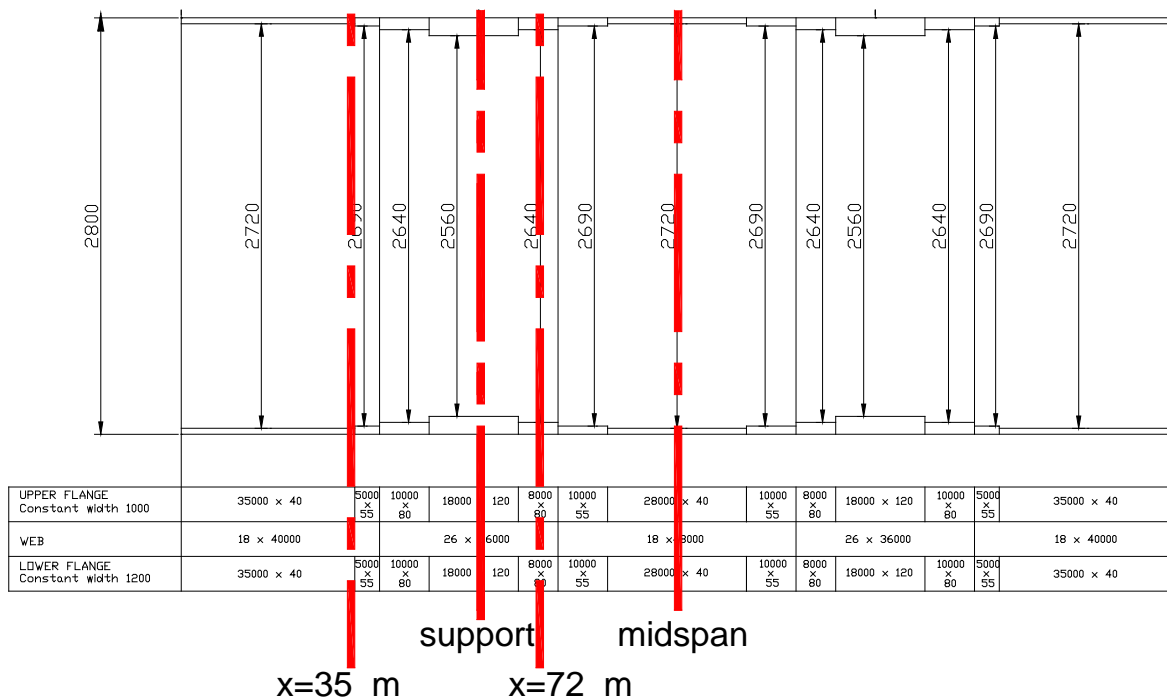


Fig. 3.17 Cross sections considered for fatigue assessment

- annual traffic flow of lorries per slow lane set to $0.5 \cdot 10^6$, considering a road with medium flow of lorries according to EN1991-2 (table 4.5);
- fatigue life equal to 100 years, consequently
- the total lorry flow per lane resulted $5.0 \cdot 10^7$;
- according to table 3.1 of EN1993-1-9, a partial factor for fatigue strength $\gamma_{MF}=1.15$ has been adopted, considering damage tolerant details and high consequences of fatigue failure;
- stress cycles have been identified using the reservoir counting method, or, equivalently, the rainflow method;
- fatigue damage has been assessed using the Palmgren-Miner rule $D = \sum_i \frac{n_i}{N_i} \leq 1$, where n_i

is the actual number of cycles at the stress range $\gamma_{MF} \Delta \sigma_i$ and N_i the characteristic fatigue strength at $\gamma_{MF} \Delta \sigma_i$.

3.9.5.1 Classification of steel fatigue details

Steel details have been classified according to tables 8.1 to 8.4 of EN 1993-1-9, as follows.

In the cross section x=35, full penetration transverse butt welds of upper and lower flange have been identified as class 11 details of table 8.3 of EN1993-1-9 (see Fig. 3.18.a), considering the tapered zone far from the weld. The basic classification of this detail is 80 MPa, but, as the plate thickness is 40 mm, the effective detail class results

$$\Delta\sigma_{c,ef} = k_s \Delta\sigma_c = \left(\frac{25}{40}\right)^{0.2} 80 = 0.91 \times 80 = 72.8 \text{ MPa}.$$

The basic upper flange detail of the other three cross sections can be classified as 80 MPa, due to the presence of welded studs, according to detail 9 of table 8.4 of EN1993-1-9 (see Fig. 3.18.b).

Finally, the basic lower flange detail of the other three cross sections can be classified as 100 MPa, according to detail 7 of table 8.2 of EN1993-1-9 (see Fig. 3.18.c).

The characteristic $S-N$ curves of the above mentioned details are finally illustrated in Fig. 3.19.

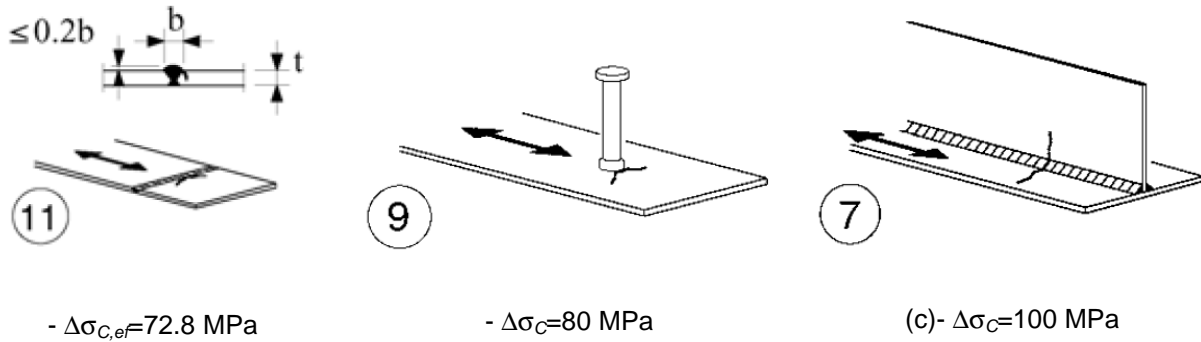


Fig. 3.18 Fatigue classification of steel details

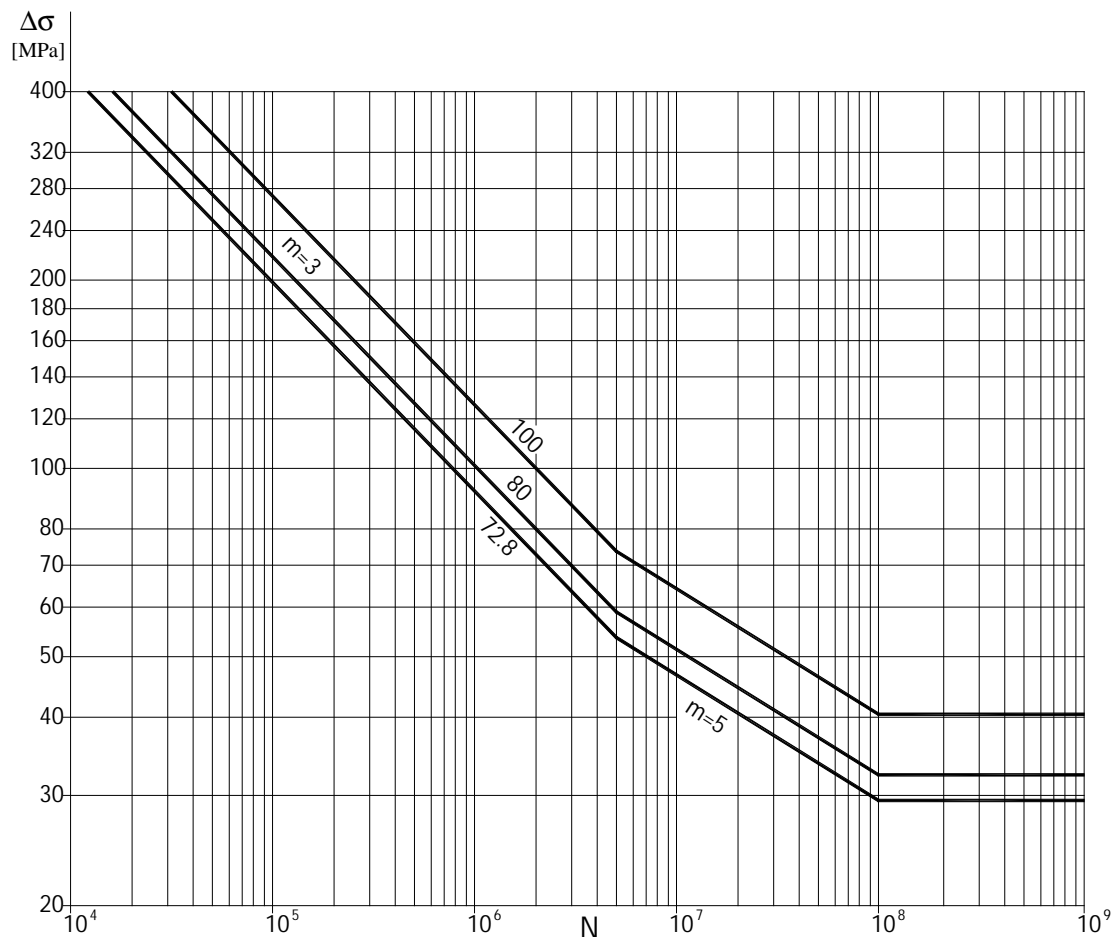


Fig. 3.19 S-N curves of steel details

3.9.5.2 Classification of reinforcing steel details

Fatigue classification for steel reinforcement details and for prestressing steel is reported in EN1992-1-1, tables 6.3N and 6.4N, and it is summarized in Table 3.9. In the present example only straight bars are concerned and the pertinent $S-N$ curve is indicated with A in Fig. 3.20. To enlarge the analysis, it has been also considered the case where the reinforcing bars are welded, characterised by the $S-N$ curve indicated with B in Fig. 3.20.

Table 3.9 Fatigue classification of steel reinforcement and prestressing steel

<i>Steel reinforcement</i>	<i>S-N curve n.</i>	N^*	k_1	k_2	$\Delta\sigma(N^*)$ [MPa]
Straight bars	2	10^6	5	9	162.5
Welded bars and meshes	4	10^7	3	5	58.5
Jointing devices	7	10^7	3	5	35
<i>Prestressing steel</i>					
Pre-tensioning	1	10^6	5	9	185
Post tensioning					
single strands in plastic ducts	1	10^6	5	9	185
straight tendons or curved tendons in plastic ducts	3	10^6	5	10	150
curved tendons in plastic ducts	5	10^6	5	7	120
Jointing devices	6	10^6	3	5	80

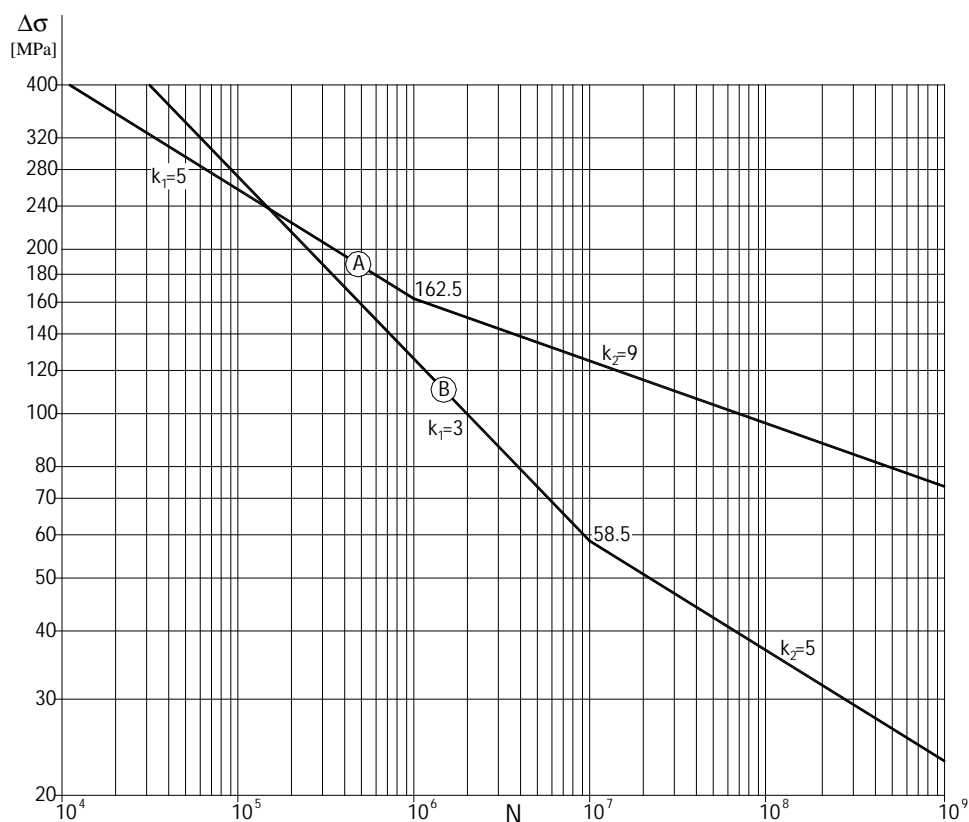


Fig. 3.20 S-N curves of reinforcing steel details

3.9.5.3 Bending moment histories and reference stress spectra

The bending moment histories induced by fatigue load model n. 3 in the four cross sections can be easily determined, once the influence lines are known. The influence lines, in [m], and the bending moment histories obtained considering a unit influence coefficient η , are reported in Figs. 3.21, 3.22, 3.23 and 3.24 for the cross sections $x=35$ m, $x=60$ m (second support), $x=72$ m and at midspan ($x=100$ m), respectively.

In the bending moment histories the stress cycles are indicated too.

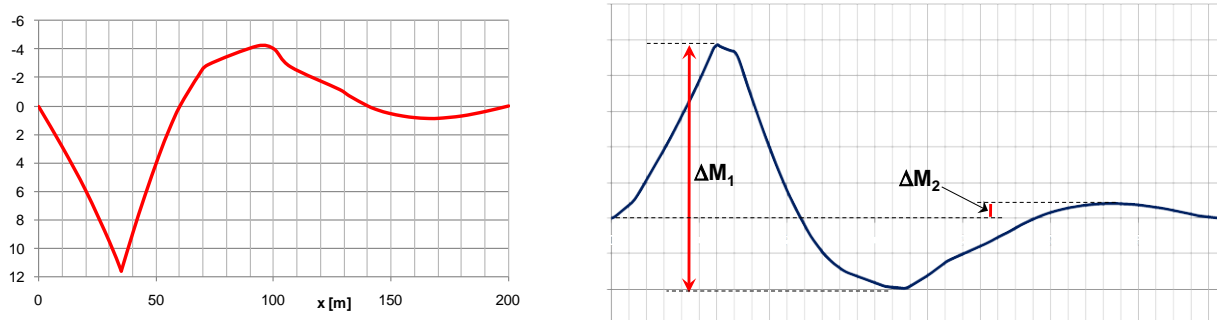


Fig. 3.21 Influence line and stress history induced by LM3 (cross section $x=35$ m, $\eta=1$)



Fig. 3.22 Influence line and stress history induced by LM3 (cross section $x=60$ m, $\eta=1$)

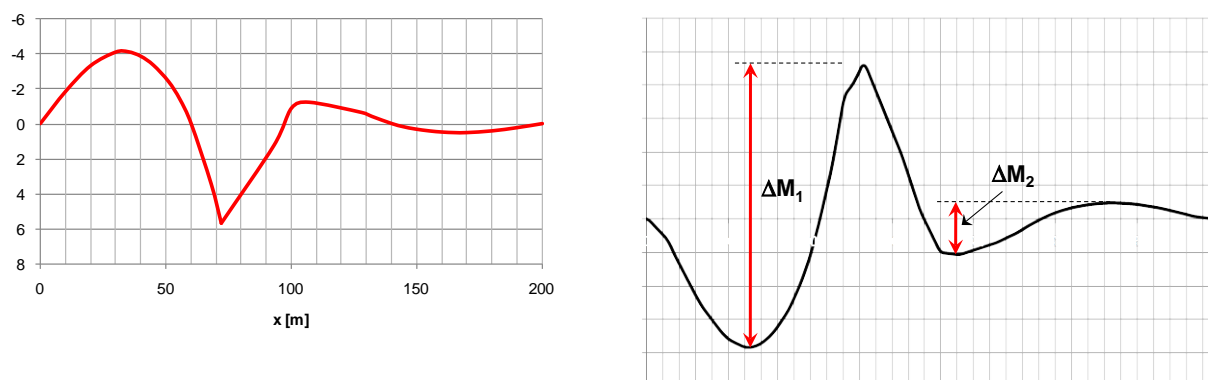


Fig. 3.23 Influence line and stress history induced by LM3 (cross section $x=72$ m, $\eta=1$)

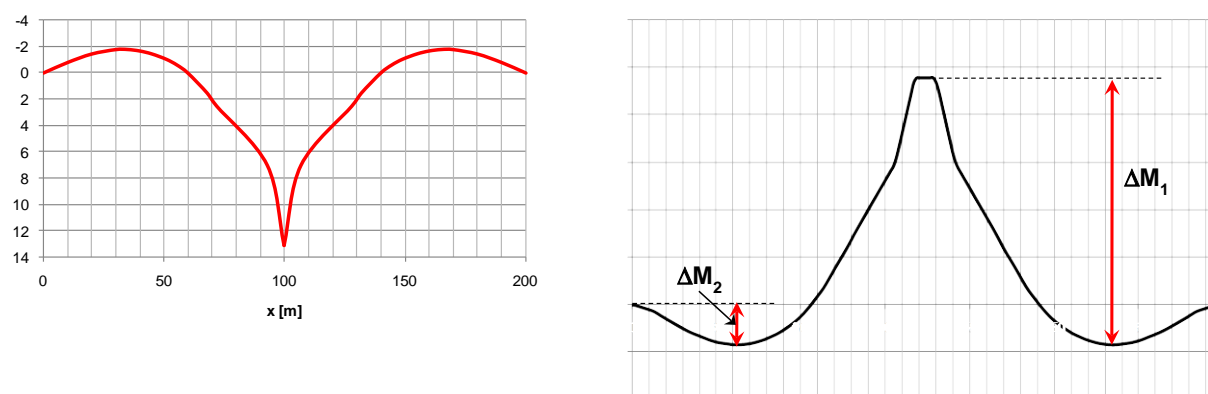


Fig. 3.24 Influence line and stress history induced by LM3 (cross section $x=100$ m, $\eta=1$)

3.9.5.4 Notional lanes arrangements for fatigue assessment

Strictly speaking, the notional lanes arrangement for fatigue assessment should be determined using the same criteria just indicated for static verifications, but this methodology could result too much safe-sided, as it will be shown below, so that more realistic assumption are to be adopted. This is not contradictory with EN1991-2, as it states that, in some cases, it is possible to consider less severe lane arrangements for fatigue or SLS verifications.

In the present example, influence coefficients $\eta_1=1.0714$ for the first lane and $\eta_2=0.6429$ for the second lane correspond to the most severe notional lanes arrangement (see Fig. 3.25), which will be indicated as case 1 in the following. Nevertheless, this lane arrangement appears clearly unrealistic for fatigue assessment purposes.

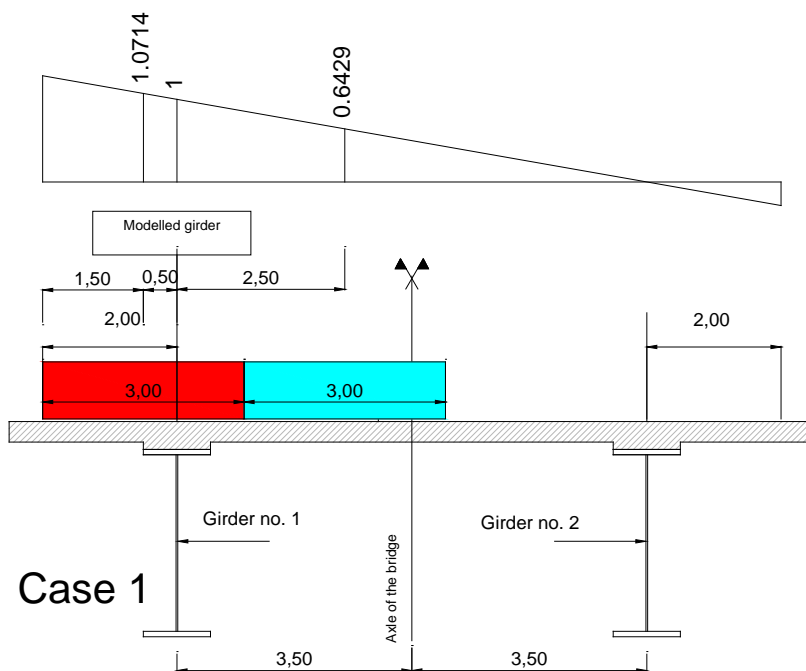


Fig. 3.25 Most severe notional lanes arrangement for fatigue (unrealistic)

Consequently, more realistic notional lanes arrangements can be envisaged, like the one shown in Fig. 3.26, where the borders of the notional lanes corresponds to the borders of the physical lanes. In this case, case 2, influence coefficients become $\eta_1=0.7857$ and $\eta_2=0.2857$, for the first and the second lane, respectively

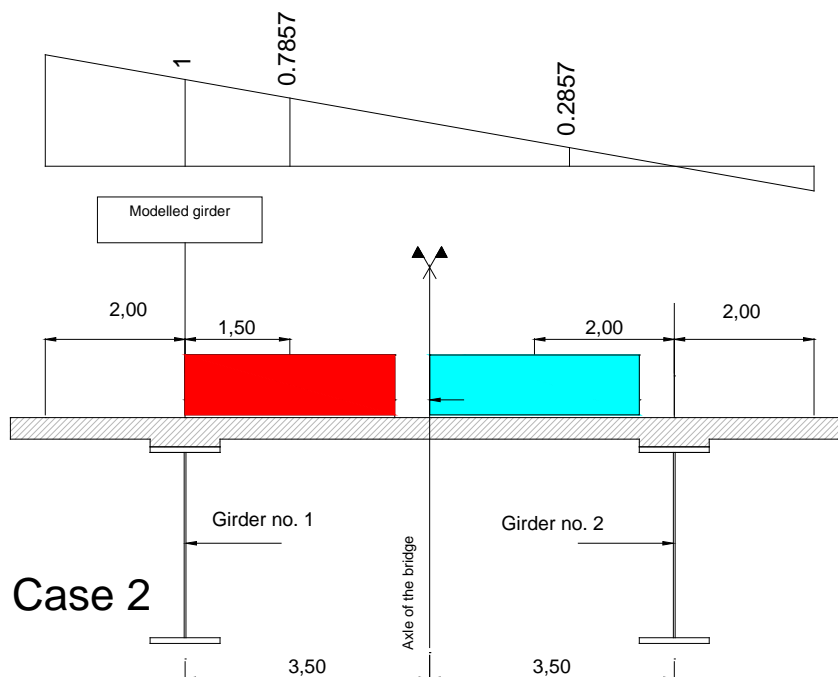


Fig. 3.26 Realistic notional lanes arrangement for fatigue (unrealistic)

3.9.5.5 Fatigue assessments

Under the above mentioned hypotheses, fatigue assessments have been performed considering that sections $x=35$ m and $x=100$ m (midspan) are un-cracked and that sections $x=60$ m and $x=72$ m are cracked. Mechanical properties of the cross sections have been derived by Davaine (2010) (see Chapter 4).

The results, in terms of bending moment design cycles are summarized in Tables 3.10 to 3.13, where case 1 and case 2 are compared also in terms of fatigue damages.

Table 3.10 Summary of fatigue assessments of cross section $x=35$ m

	Case 1	Case 2
$\gamma_{Mf} \Delta M_1$ [kNm]	8400.5	6160.4
$\gamma_{Mf} \Delta M_2$ [kNm]	5040.3	2240.1
$\gamma_{Mf} \Delta M_3$ [kNm]	507.9	372.5
$\gamma_{Mf} \Delta M_4$ [kNm]	304.7	135.4
D (upper flange)	0.00E+00	0.00E+00
D (lower flange)	3.52E+00	7.47E-01
D (straight rebar)	1.06E-09	6.44E-11
D (welded rebar)	1.04E-03	2.06E-04

Table 3.11 Summary of fatigue assessments of cross section $x=60$ m (support)

	Case 1	Case 2
$\gamma_{Mf} \Delta M_1$ [kNm]	5030.3	3688.9
$\gamma_{Mf} \Delta M_2$ [kNm]	3018.2	1341.4
$\gamma_{Mf} \Delta M_3$ [kNm]	2166.9	1589.0
$\gamma_{Mf} \Delta M_4$ [kNm]	1300.1	577.8
D (upper flange)	0.00E+00	0.00E+00
D (lower flange)	0.00E+00	0.00E+00
D (straight rebar)	2.90E-08	1.76E-09
D (welded rebar)	6.64E-03	1.32E-03

Table 3.12 Summary of fatigue assessments of cross section $x=72$ m

	Case 1	Case 2
$\gamma_{Mf} \Delta M_1$ [kNm]	5207.7	3819.0
$\gamma_{Mf} \Delta M_2$ [kNm]	3124.6	1388.7
$\gamma_{Mf} \Delta M_3$ [kNm]	953.8	699.5
$\gamma_{Mf} \Delta M_4$ [kNm]	572.3	254.4
D (upper flange)	0.00E+00	0.00E+00
D (lower flange)	0.00E+00	0.00E+00
D (straight rebar)	2.96E-12	1.80E-13
D (welded rebar)	3.97E-05	7.87E-06

Table 3.13 Summary of fatigue assessments of cross section x=100 m (midspan)

	<i>Case 1</i>	<i>Case 2</i>
$\gamma_{Mf} \Delta M_1$ [kNm]	6936.0	5086.4
$\gamma_{Mf} \Delta M_2$ [kNm]	4161.6	1849.6
$\gamma_{Mf} \Delta M_3$ [kNm]	1037.8	761.1
$\gamma_{Mf} \Delta M_4$ [kNm]	622.7	276.7
D (upper flange)	0.00E+00	0.00E+00
D (lower flange)	0.00E+00	0.00E+00
D (straight rebar)	1.89E-10	1.15E-11
D (welded rebar)	4.00E-04	7.92E-05

As anticipated, it must be stressed that notional lanes arrangement considered in case 1 is much more severe than notional lane arrangement considered in case 2. For example, in the cross section x=35 m the fatigue check of lower flange detail fails considering case 1 and the fatigue damage results about five times higher than those obtained considering case 2.

Finally, it is necessary to recall that, in principle, the achievement of a fatigue damage $D=0$ for structural steel details it is not sufficient by itself to conclude that fatigue check is satisfactory, if equivalent fatigue load models are used, as in the current case.

In fact, by definition, *equivalent* fatigue models are not able to reproduce the maximum stress ranges which are significant for fatigue, which should be compared with the constant amplitude fatigue limit. For the latter purpose, it is necessary to use *frequent* fatigue load models.

REFERENCES

- CEN 2002. *Eurocode: Basis of structural design*. EN 1990: 2002. European Committee for Standardization (CEN): Brussels.
- CEN 2005. *Eurocode 1 - Actions on structures. Part 1-6: General actions. Actions during execution*. EN 1991-1-6: 2005. European Committee for Standardization (CEN): Brussels.
- CEN 2006. *Eurocode 1 - Actions on structures. Part 1-7: General actions. Accidental actions*. EN 1991-1-7: 2006. European Committee for Standardization (CEN): Brussels.
- CEN 2003. *Eurocode 1 - Actions on structures. Part 2: Traffic loads on bridges*. EN 1991-2: 2003. European Committee for Standardization (CEN): Brussels.
- CEN 2006. *Eurocode 1 - Actions on structures. Part 3: Actions induced by cranes and machinery*. EN 1991-3: 2006. European Committee for Standardization (CEN): Brussels.
- CEN 2004. *Eurocode 2 – Design of concrete structures. Part 1-1: General rules and rules for buildings*. EN 1992-1-1: 2004. European Committee for Standardization (CEN): Brussels.
- CEN 2005. *Eurocode 2 – Design of concrete structures. Part 2: Concrete bridges. Design and detailing rules*. EN 1992-2: 2005. European Committee for Standardization (CEN): Brussels.
- CEN 2005. *Eurocode 3 – Design of steel structures. Part 1-1: General rules and rules for buildings*. EN 1993-1-1: 2005. European Committee for Standardization (CEN): Brussels.
- CEN 2005. *Eurocode 3 – Design of steel structures. Part 1-9: Fatigue*. EN 1993-1-9: 2005. European Committee for Standardization (CEN): Brussels.
- CEN 2006. *Eurocode 3 – Design of steel structures. Part 2: Steel bridges*. EN 1993-2: 2006. European Committee for Standardization (CEN): Brussels.
- CEN 2004. *Eurocode 4 – Design of composite steel and concrete structures. Part 1-1: General rules and rules for buildings*. EN 1994-1-1: 2004. European Committee for Standardization (CEN): Brussels.
- CEN 2005. *Eurocode 4 – Design of composite steel and concrete structures. Part 2: General rules and rules for bridges*. EN 1994-2: 2005. European Committee for Standardization (CEN): Brussels.
- Davaine L. 2010. *Global analysis of a steel-concrete composite two-girder bridge according to Eurocode 4*, Note for Workshop “Bridge design to Eurocodes” to be held in Vienna, 4-6 October 2010.
- Malakatas N. 2010. *Example of application for wind actions on bridge deck and piers*, Note for Workshop “Bridge design to Eurocodes” to be held in Vienna, 4-6 October 2010.
- Ortega Cornejo, M., Raoul, J. 2010. *Composite bridge design (EN1994-2). Illustration of basic element design*, Note for Workshop “Bridge design to Eurocodes” to be held in Vienna, 4-6 October 2010.

CHAPTER 4

Bridge deck modelling and structural analysis

Laurence DAVAINÉ

French Railway Bridge Engineering Department (SNCF, IGOA)

4.1 Introduction

The global structural analysis of the composite twin girder bridge given in introduction is presented here. The first step of this analysis is the bridge modelling. For the longitudinal global bending behaviour only one structural steel girder with half of the reinforced concrete slab is modelled. The structural analysis is a first order elastic linear one. The calculation of the elastic mechanical properties for each cross section requires:

- the effective width of the flanges (shear lag effect)
- the different modular ratios between concrete and steel (creep effect)

The second step of the global analysis is the calculation of the internal forces and moments distribution along the whole girder. The analysis should respect the construction phases and takes into account the concrete cracking on internal supports by a simplified method. The cracked global analysis is performed according to EN 1994-2 rules.

The results of this global analysis in terms of internal forces and moments, stresses and deformations, will be linearly combined following the combinations of actions defined in EN 1990 for the Serviceability Limit State (SLS) and the Ultimate Limit State (ULS). More detailed information about the load cases definition and the combination rules are also given in another chapter of this Report.

The further chapters are devoted to the section analysis and other design verifications based on the outcome of this global analysis.

4.2 Shear lag effect

In the Eurocodes the shear lag effect is taken into account by the calculation of an effective width for each flange of the structure. For a composite twin-girder bridge it mainly affects the concrete slab (composite upper flange) where the actual width to span ratio is not negligible. The shear lag effect should theoretically also be checked for the bottom steel flange but usually no reduction occurs (the verification is performed below).

In the Eurocodes the reduction is not the same for the global analysis (calculation of internal forces and moments) and the section analysis (calculation of the elastic mechanical properties for obtaining the stress distribution). The value calculated at mid-span could be used for the whole span in the global analysis but not for the section analysis.

4.2.1 GLOBAL ANALYSIS

4.2.1.1 Bottom steel flange

$b_f = 1200$ mm for the bottom flange width so $b_0 = \frac{b_f - t_w}{2} = \frac{1200 - 18}{2} = 591$ mm with the EN1993-1-5 notations.

As $b_0 \leq L/8 = 7500$ mm for the side spans (60 m long) and $b_0 \leq L/8 = 10000$ mm for the inner span (80 m long) of the bridge, the bottom flange width is not reduced to an effective width for the global analysis (see EN 1993-1-5, 2.2).

4.2.1.2 Upper concrete slab

According to EN 1994-2, 5.4.1.2, the effective width of the concrete slab for the global analysis (calculation of the internal forces and moments) is equal to the value calculated at mid-span for the section analysis. These calculations are explained in the next paragraph of this report devoted to the section analysis and show that no reduction of the concrete slab width is needed for the global analysis as the mid-span width is not reduced.

4.2.2 SECTION ANALYSIS

4.2.2.1 Bottom steel flange

The equivalent span lengths of the bridge are $L_{e1} = 0.85L_1 = 51$ m for the side spans and the abutments, $L_{e2} = 0.7L_2 = 56$ m for the inner span, and for the support regions around the piers P1 and P2, the effective length is equal to $L_{e3} = 0.25 \cdot 60 + 80 = 35$ m.

For each case, $\frac{b_0}{L_e} \leq 0.02$ and according to EN 1993-1-5, 3.1, no effective reduction of the bottom flange width is needed for the section analysis.

4.2.2.2 Upper concrete slab

In a given cross-section of one of the main girder, the effective width of the concrete slab is the sum of 3 terms $b_{eff} = b_0 + \beta_1 b_{e1} + \beta_2 b_{e2}$ with:

- $b_0 = 750$ mm for the centre-to-centre distance between the outside stud rows
- $b_{ei} = \min\left(\frac{L_e}{8}; b_i\right)$ where L_e is the equivalent span length for the considered cross-section and b_i is the actual geometric width of the slab associated to the main girder
- $b_1 = \frac{7.0 \text{ m}}{2} - \frac{b_0}{2} = 3.125$ m between the main steel girders
- $b_2 = \frac{2.5 \text{ m}}{2} - \frac{b_0}{2} = 2.125$ m for the cantilever slab outside the main steel girder
- $\beta_1 = \beta_2 = 1$ except for the cross-sections at end supports C0 and C3 where $\beta_i = 0.55 + 0.025 \frac{L_e}{b_{ei}} \leq 1$ with b_{ei} equal to the effective width at mid-end span.

As $\frac{L_e}{8}$ is always greater than b_i for the example it is deduced that the effective width is equal to the actual width except for the cross-sections at end supports C0 and C3 where the factor β_i influences:

- $\beta_1 = 0.55 + 0.025 \frac{L_{e1}}{b_{e1}} = 0.55 + 0.025 \frac{51}{3.125} = 0.958 \leq 1.0$
- $\beta_2 = 0.55 + 0.025 \frac{L_{e1}}{b_{e2}} = 0.55 + 0.025 \frac{51}{2.125} = 1.15$ but should be ≤ 1.0 so $\beta_2 = 1$

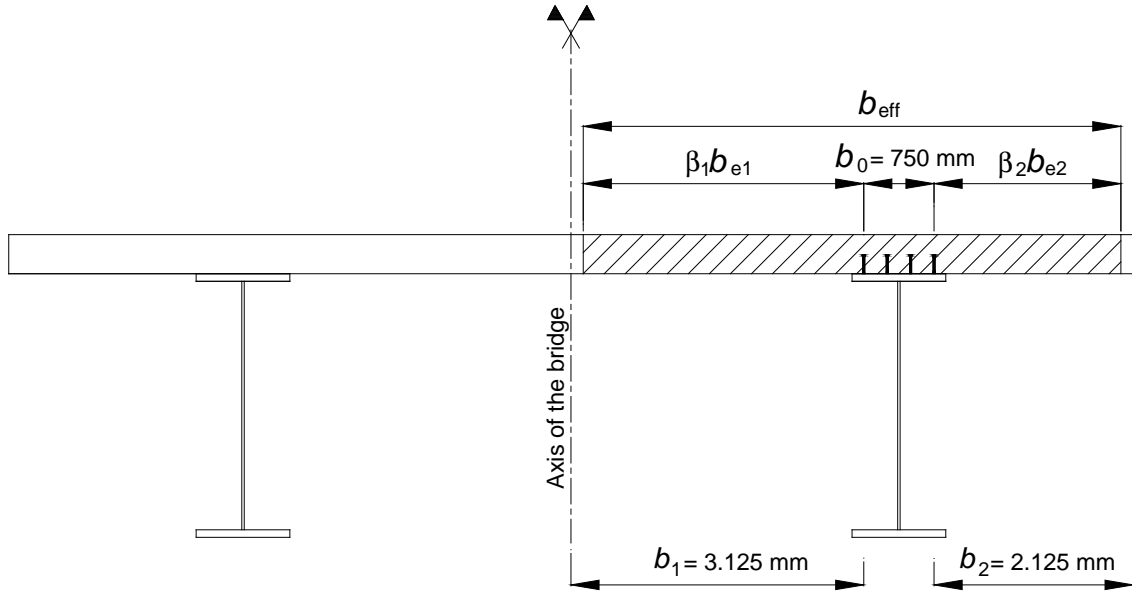


Fig. 4.1 Effective width in the concrete slab for the section analysis

Finally the slab width will linearly vary from $0.750 \text{ m} + 0.958 \cdot 3.125 \text{ m} + 1.0 \cdot 2.125 \text{ m} = 5.869 \text{ m}$ at end support C0 to 6.0 m for the abscissa $0.25 \cdot L_1 = 15 \text{ m}$ in the span C0-P1. Afterwards it will be constant and equal to 6.0 m up to the abscissa $2L_1 + L_2 - 0.25L_1 = 185 \text{ m}$ and then it will vary linearly from 6.0 m to 5.869 m at end support C3.

This variable effective width is always taken into account to calculate the longitudinal stress distribution.

4.3 Concrete creep effect (modular ratios)

4.3.1 SHORT TERM MODULAR RATIO

The short term modular ratio is calculated directly by the following formula:

$$n_0 = \frac{E_a}{E_{cm}} = \frac{210000}{22000 \left(\frac{f_{cm}}{10} \right)^{0.3}} = \frac{210000}{22000 \left(\frac{35+8}{10} \right)^{0.3}} = 6.16$$

where E_a and E_{cm} are respectively the modulus of elasticity for the structural steel and the concrete.

4.3.2 LONG TERM MODULAR RATIO

The long term modular ratio n_L depends on the type of loading on the girder (through the coefficient ψ_L) and on the creep level at the time considered (through the creep coefficient $\varphi(t, t_0)$):

$$n_L = n_0 \cdot [1 + \psi_L \cdot \varphi(t, t_0)]$$

ψ_L conveys the dependence of the modular ratio on the type of applied loading :

- permanent load (self-weight of the slab segments, non-structural bridge equipments): $\psi_L = 1.1$
- concrete shrinkage: $\psi_L = 0.55$
- settlement : $\psi_L = 1.5$

$$\varphi_{t,t_0} = \varphi_0 \cdot \beta_{ct,t_0} = \varphi_0 \cdot \left(\frac{t-t_0}{\beta_H + t - t_0} \right)^{0.3} = \varphi_0 \text{ when } t \text{ tends towards the infinite (long term calculations).}$$

$$\varphi_0 = \varphi_{RH} \cdot \beta_{f_{cm}} \cdot \beta_{t_0} = \left[1 + \frac{1 - \frac{RH}{100}}{0.10 \cdot \sqrt[3]{h_0}} \cdot \alpha_1 \right] \cdot \alpha_2 \cdot \left[\frac{16.8}{\sqrt{f_{cm}}} \right] \cdot \left[\frac{1}{0.1 + t_0^{0.2}} \right]$$

The coefficients α_1 and α_2 take account of the influence of the concrete strength when $f_{cm} \geq 35 \text{ MPa}$ (otherwise $\alpha_1 = \alpha_2 = 1$). In this example, $f_{cm} = 43 \text{ MPa}$ resulting in:

$$\alpha_1 = \left(\frac{35}{f_{cm}} \right)^{0.7} = 0.87 \text{ and } \alpha_2 = \left(\frac{35}{f_{cm}} \right)^{0.2} = 0.96$$

$h_0 = \frac{2A_c}{u}$ is the notional size of the slab, with $A_c = 3.9 \text{ m}^2$ the area of the concrete slab and u the slab perimeter exposed to drying. The asphalt layer width (11 m) and the upper steel flange widths (2 x 1.0 m) should be extracted from the actual perimeter is $p = 24.6 \text{ m}$ to get $u = p - 11 - 2 \cdot 1.0 = 11.6 \text{ m}$. Finally $h_0 = 672 \text{ mm}$.

The relative humidity is 80%.

The time parameter t_0 is the mean value of the concrete age (in days) when the considered load case is applied to the structure (see 7.2 in the Introduction Chapter of this Report).

- Self-weight of the concrete slab:

As a simplification EN1994-2 allows to use only one mean value for t_0 when applying the load cases corresponding to all the slab concreting phases. Regarding the very low influence of the choice of t_0 on the final distribution of internal forces and moments, and the difficulties to get the final concreting sequence during the project design, a reasonable approach consists in taking t_0 equal to half the concreting time of the entire slab, $t_0 = 66/2 = 33 \text{ days}$ for the example.

- Non-structural bridge equipments: $t_0 = 66 + 44/2 = 88 \text{ days}$
- Concrete shrinkage:

Shrinkage is assumed to begin as soon as the concrete is poured and extends through its lifetime. EN1994-2 imposes a value of $t_0 = 1 \text{ day}$ for evaluating the corresponding modular ratio.

- Settlement:

The 3 cm settlement is assumed to occur at $t_0 = 50 \text{ days}$ when the self-weight of the bridge deck is entirely applied to the structure. This hypothesis can be discussed for an actual bridge design.

Load case	ψ_L	t_0 (days)	φ_{∞, t_0}	$n_L = n_0 \cdot [1 + \psi_L \cdot \varphi_{\infty, t_0}]$
Concreting	1.10	33	1.4	15.6
Shrinkage	0.55	1	2.7	15.2
Bridge equipments	1.10	88	1.2	14.1
Settlement	1.50	50	1.3	18.1

4.4 Elastic mechanical properties of the cross sections

After the determination of the effective width of the concrete slab and the modular ratios for the different elementary load cases, it becomes possible to calculate the elastic mechanical properties of each composite cross-section along the bridge girder. Following the construction phases these properties have to be given to the bar elements modelling the bridge for getting the internal forces and moments and the stress distribution by applying the general rules of the Strength of Materials. Notations are as follows:

A_a area of the structural steel part of the composite cross-section

A_s area of the reinforcing steel of the composite cross-section (within the effective width for shear lag)

A_b area of the concrete part of the composite cross-section (within the effective width for shear lag)

n modular ratio

I_a second moment of area of the structural steel part of the composite cross-section

I_b second moment of area of the concrete part of the composite cross-section

According to EN 1994-2, 6.2.1.1(4), the concrete in tension ($\sigma_{Ed} \leq 0$) is cracked and should always be neglected in the composite cross-section resistance.

4.4.1 UN-CRACKED COMPOSITE BEHAVIOUR

It occurs in the mid-span regions where the bending moment acting on the composite section is positive (concrete in compression). The reinforcing steel in compression could be neglected.

$$A = A_a + \frac{A_b}{n}$$

$$Ay_G = A_a y_{Ga} + \frac{A_b}{n} y_{Gb}$$

$$I = I_a + A_a y_G - y_{Ga}^2 + \frac{1}{n} I_b + \frac{A_b}{n} y_G - y_{Gb}^2$$

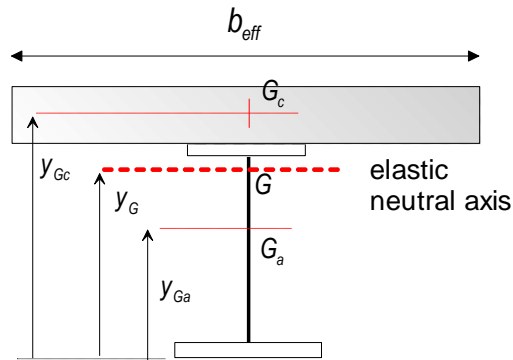


Fig. 4.2 Un cracked composite behaviour

4.4.2 CRACKED COMPOSITE BEHAVIOUR

It occurs in the regions surrounding the internal supports where the bending moment acting on the composite section is negative (concrete in tension). Any part of the concrete in tension should be neglected in the calculation of the elastic mechanical properties. EN 1994-2 considers that the modular ratio between structural steel and reinforcing steel is equal to 1 ($E_a = E_s = 210000 \text{ MPa}$).

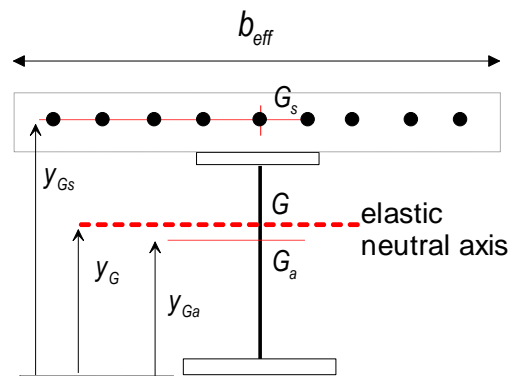


Fig. 4.3 Cracked composite behaviour

Figure 4.3 above is a simplified example where only one reinforcement layer is used.

$$A = A_a + A_s$$

$$Ay_G = A_a y_{Ga} + A_s y_{Gs}$$

$$I = I_a + A_a y_G - y_{Ga}^2 + A_s y_G - y_{Gs}^2 \text{ neglecting the inertia of the reinforcing bars } (I_s = 0)$$

4.5 Actions modelling

4.5.1 SELF-WEIGHT

Density of the structural steel: 77 kN/m^3

For the longitudinal bending global analysis, the self-weight of the in-span located transverse cross-girders is modelled by a vertical uniformly distributed load of 1500 N/m applied to each main girder (about 10% of the weight of this main girder).

Density of the reinforced concrete: 25 kN/m^3

The self-weight of the structural steel is resisted by the steel structure alone whereas the self-weight of the poured concrete (segment by segment) is resisted by a main girder which is partially concreted according to the construction sequence.

4.5.2 NON STRUCTURAL EQUIPMENTS

They are described in Chapter 1 – *Introduction to the design example* of this Report.

Item	Characteristics	Maximum multiplier	Minimum multiplier
Concrete support of the safety barrier	Area $0.5 \times 0.2 \text{ m}^2$	1.0	1.0
Safety barrier	65 kg/ml	1.0	1.0
Cornice	25 kg/ml	1.0	1.0
Waterproofing layer	3 cm thick	1.2	0.8
Asphalt layer	8 cm thick	1.4	0.8

The multiplier coefficients are defined in EN 1991-1-1. For the waterproofing and asphalt layers, they take into account the uncertainty on the thickness and a further retrofitting of the asphalt layer during the bridge lifetime.

Density of the waterproofing material and of the asphalt: 25 kN/m^3

The table below gives the uniformly distributed loads to apply to one of the bridge composite girder to get the envelope of the internal forces and moments distribution for the non-structural bridge equipments.

Item	q_{nom} (kN/ml)	q_{min} (kN/ml)	q_{max} (kN/ml)
Concrete support of the safety barrier	2.5	2.5	2.5
Safety barrier	0.638	0.638	0.638
Cornice	0.245	0.245	0.245
Waterproofing layer	4.2	5.04	3.36
Asphalt layer	11	15.4	8.8
Total	18.6 kN/ml	23.8 kN/ml	15.5 kN/ml

4.5.3 CONCRETE SHRINKAGE IN THE COMPOSITE DECK

The concrete shrinkage is modelled by an imposed deformation ε_r applied to the concrete area in compression. The three physical origins are the thermal shrinkage ε_{th} , the autogenous shrinkage ε_{ca} and the drying shrinkage ε_{cd} . Taking place over the bridge life, the drying shrinkage starts as soon as the concrete is poured. EN1992-1-1 (to which EN1994-2 refers) therefore deals with ε_{ca} and ε_{cd} simultaneously. A total shrinkage $\varepsilon_{cs} = \varepsilon_{ca} + \varepsilon_{cd}$ will then be calculated for a bridge state corresponding to the first opening to traffic loads (persistent design situation for $t_{ini} = 110$ days) and at infinite time (persistent design situation for $t_{fin} = 100$ years). Thermal shrinkage is dealt with in EN1994-2 as it is a peculiarity of a composite structure.

4.5.3.1 Shrinkage deformation at traffic opening

The calculation of ε_{cs} requires the age t of the concrete at the considered date t_{ini} . At this date each slab segment has a different age. To simplify, the mean value of the ages of all slab segments is considered taking account of the construction phases: $t = 66/2 + 44 = 77$ days. The formulae from Annex B and 3.1.4 in EN1992-1-1 are used.

$\varepsilon_{ca}(t) = \beta_{as}(t) \varepsilon_{ca}(\infty)$ with $\varepsilon_{ca}(\infty) = 2.5(f_{ck} - 10)10^{-6} = 6.25 \cdot 10^{-5}$ and $\beta_{as}(t) = 1 - \exp(-0.2\sqrt{t}) = 0.83$ for $t = 77$ days. Finally $\varepsilon_{ca}(t) = 5.2 \cdot 10^{-5}$

$$\varepsilon_{cd}(t) = \beta_{ds}(t, t_s) \cdot k_h \varepsilon_{cd,0} \text{ with } \varepsilon_{cd,0} = 0.85 \cdot \left[(220 + 110 \cdot \alpha_{ds1}) \cdot \exp\left(-\alpha_{ds2} \frac{f_{cm}}{f_{cm0}}\right) \right] \cdot 10^{-6} \cdot \beta_{RH}$$

$$\beta_{RH} = 1.55 \cdot \left[1 - \left(\frac{RH}{100} \right)^3 \right] = 0.76 \text{ with } RH = 80\%$$

$$f_{cm0} = 10 \text{ MPa}$$

$$\alpha_{ds1} = 4 \text{ and } \alpha_{ds2} = 0.12 \text{ for the hardening speed of a normal type of cement (class N)}$$

$$\text{Finally } \varepsilon_{cd,0} = 2.53 \cdot 10^{-4}$$

$$k_h = 0.7 \text{ because } h_0 = 672 \text{ mm} \geq 500 \text{ mm}$$

Drying shrinkage begins at the age $t_s = 1$ day (hypothesis).

$$\beta_{ds}(t, t_s) = \frac{t - t_s}{t - t_s + 0.04 \cdot \sqrt{h_0^3}} = 0.10 \text{ for } t = 77 \text{ days, and finally } \varepsilon_{cd}(t) = 1.8 \cdot 10^{-5}$$

$\varepsilon_{cs}(t) = \varepsilon_{ca}(t) + \varepsilon_{cd}(t) = 7 \cdot 10^{-5}$ is applied to each slab segment as soon as the corresponding concrete is put in place. A possible simplified hypothesis consists in applying this early age shrinkage deformation in a single phase at the end of the slab concreting. It is incorporated (phase by phase or all at once) for the structure justifications at traffic opening in the load combinations for the persistent design situation.

4.5.3.2 Shrinkage deformation at infinite time

Making t tends towards the infinite in the equations from the previous paragraph gives $\beta_{as}(\infty) = 1$ and $\beta_{ds}(\infty, t_s) = 1$. Subsequently $\varepsilon_{cs}(\infty) = \varepsilon_{cd}(\infty) + \varepsilon_{ca}(\infty)$ with $\varepsilon_{ca}(\infty) = 6.25 \cdot 10^{-5}$ and $\varepsilon_{cd}(\infty) = k_h \varepsilon_{cd,0} = 1.77 \cdot 10^{-4}$.

Finally $\varepsilon_{cs}(\infty) = 2.4 \cdot 10^{-4}$ is applied to the complete concrete slab (in a single phase). This action is incorporated for the bridge verifications in the load combinations for the persistent design situation at infinite time.

4.5.3.3 Thermal shrinkage

EN1994-2 7.4.1(6) takes account of the thermal shrinkage produced by the difference in temperature ΔT between structural steel and concrete when concreting. The recommended value is $\Delta T = 20^\circ\text{C}$ thus giving a strain $\varepsilon_{th} = \alpha_{th} \Delta T = 10^{-5} \cdot 20\text{K} = 2 \cdot 10^{-4}$ which is relatively high.

In fact, on-site measurements show that this temperature difference seems correct but a part of the corresponding thermal shrinkage applies to a structure which has not yet a composite behaviour. For this reason a half value ($\varepsilon_{th} = 1 \cdot 10^{-4}$) has been used in this bridge design example.

The thermal shrinkage applies to the composite structure with the early age shrinkage $\varepsilon_{cs} = 7 \cdot 10^{-5}$. It should normally be used only to determine the cracked zones of the global analysis and to control the crack width in the concrete slab.

4.5.4 ROAD TRAFFIC

4.5.4.1 Transverse positioning of the traffic lanes

UDL and TS from load model LM1 defined in EN1991-2 are longitudinally and transversally positioned on the deck so as to achieve the most unfavourable effect for the studied main girder. A linear transverse influence line is used with the assumption that a vertical load introduced in the web plane of a main girder goes entirely in this girder. The unfavourable parts of each longitudinal influence line are then loaded according to the transverse distribution of the traffic vertical loads UDL and TS between the two main girders.

The free pavement width between the concrete longitudinal supports of the safety barriers is equal to $w = 11$ m. Three traffic lanes each 3 m wide and a 2 m wide remaining area can be placed within this width. Given the transverse symmetry of the deck, only girder no. 1 is studied. The traffic lanes are thus arranged in the most unfavourable way according to the Fig. 4.4 below.

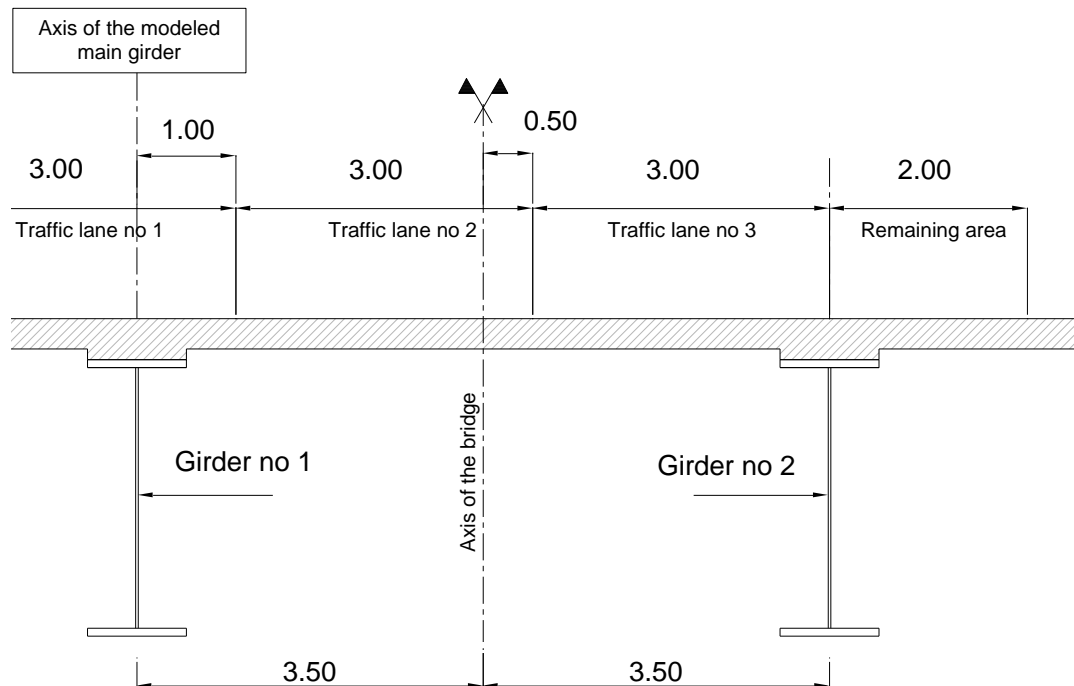


Figure 4.4 Transverse positioning of the traffic lanes

4.5.4.2 Tandem system TS

For simplifying the longitudinal global bending calculations, EN1991-2 4.3.2(1) allows that each tandem TS axle may be centred in its traffic lane. The vertical load magnitudes per axle are given in EN1991-2 Table 4.2. Fig. 4.5 below indicates the transverse position of the three tandems considered with respect to the main structural steel girders.

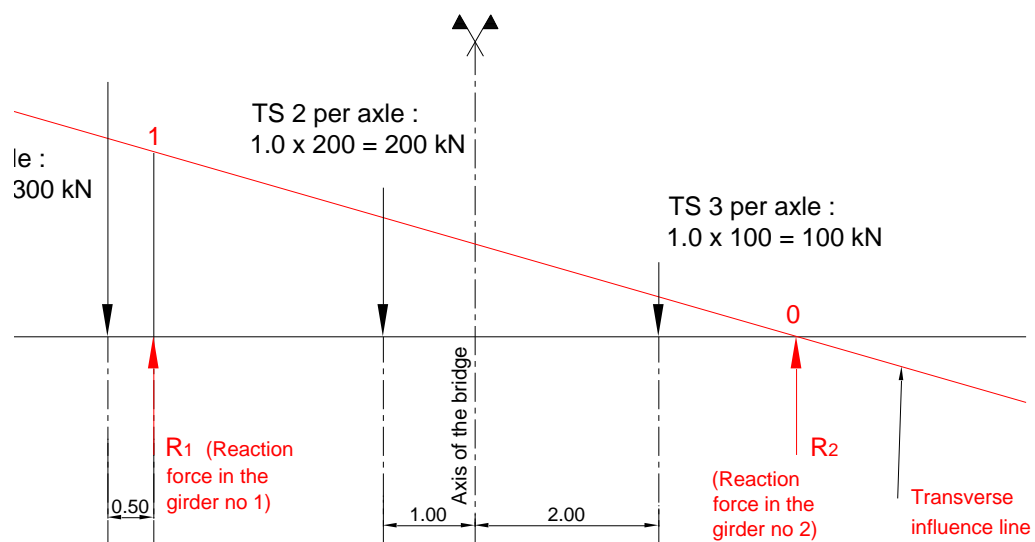


Figure 4.5 Tandem TS loading on the deck

The structural system in Figure 4.6 is statically determined and the reaction forces on each main girder are therefore $R_1 = 471.4$ kN for an axle (two per tandem) and $R_2 = 128.6$ kN.

$$300 \text{ kN} \cdot 7\text{m} + 0.5\text{m} + 200 \text{ kN} \cdot \left(\frac{7\text{m}}{2} + 1\text{m}\right) + 100 \text{ kN} \cdot \left(\frac{7\text{m}}{2} - 2\text{m}\right) = R_1 \cdot 7\text{m}$$

$$300 \text{ kN} + 200 \text{ kN} + 100 \text{ kN} = R_1 + R_2$$

Each traffic lane can only support a single tandem TS in the longitudinal direction. The three used tandem TS (one per lane) could not be necessarily located in the same transverse cross-section.

4.5.4.3 Uniformly distributed load UDL

Given the transverse influence line, the traffic lanes are loaded with UDL up to the axis of girder no. 2 (see Figure 5.1) which is the positive zone of the influence line. The vertical load magnitudes of UDL are given in EN1991-2 Table 4.2.

In the longitudinal direction, each traffic lane is loaded over a length corresponding to the unfavourable parts of the longitudinal influence line corresponding to the studied internal forces or moments and the location of the studied cross-section.

As for TS loading, the structural system in Fig. 4.6 below is statically determined and the reaction forces per unit length on each main girder are therefore $R_1 = 35.357 \text{ kN/m}$ and $R_2 = 6.643 \text{ kN/m}$. Note that if lane no. 3 extended beyond the axis of main girder no. 2 it would only be partly loaded in the positive zone of the transverse influence line.

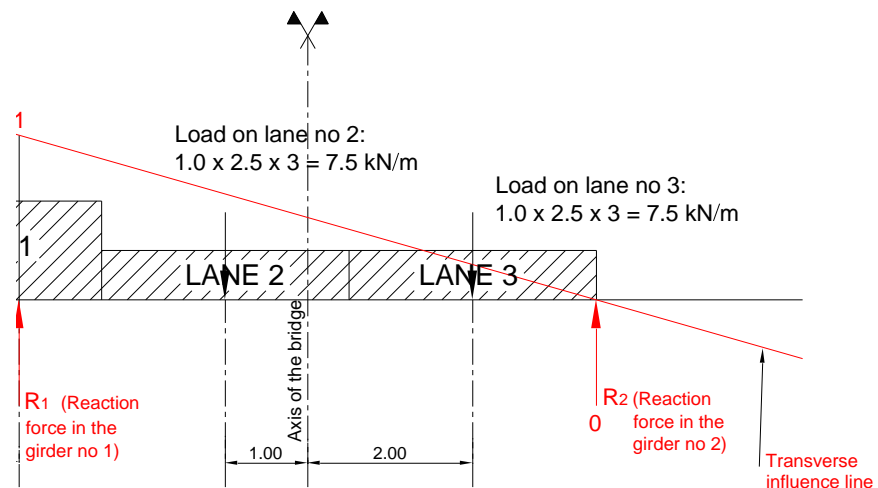


Figure 4.6 UDL transverse distribution on the bridge deck

4.5.4.4 Braking and acceleration (EN1991-2, 4.4.1)

$$Q_{ik} = 0.6\alpha_{Q1} 2Q_{1k} + 0.1\alpha_{q1}q_{1k}wL = 360 \text{ kN} + 540 \text{ kN} = 900 \text{ kN}$$

$$180\alpha_{Q1} \leq Q_{ik} \leq 900 \text{ kN}$$

4.5.4.5 Conclusions for the traffic load modelling

The two-dimensional bar model corresponding to the bridge half-deck is therefore loaded with an uniformly distributed load of 35.357 kN/m and a system of two concentrated loads of 471.4 kN (per load) which are longitudinally 1.2 m spaced. The curves for internal forces and moments are

calculated by loading systematically all the longitudinal influence lines and two envelopes are finally obtained for the two traffic load types.

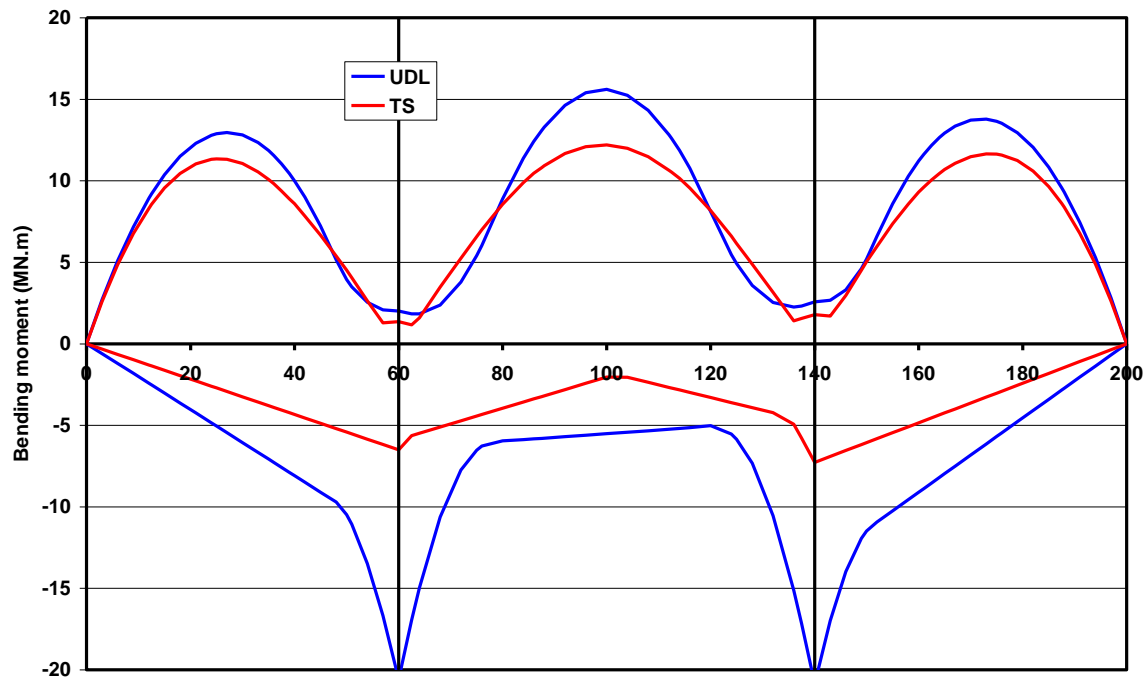


Figure 4.7 Bending moments due to UDL and TS in the bridge deck

4.6 Global analysis

4.6.1 GENERAL

The global analysis is performed by respecting the construction phases and by considering two peculiar dates in the bridge life – at traffic opening (short term situation) and at infinite time (long term situation or 100 years old). Excluding accidental loads, the analysis is a first order linear elastic one. However the concrete cracking near the internal support regions is taken into account by a simplified method based on a two-steps calculation as explained in the following paragraph.

This global analysis refers to the combinations of actions (SLS and ULS) that are given in another Chapter of this Report.

4.6.2 CRACKED ZONES SURROUNDING INTERNAL SUPPORTS

The first step of the global cracked analysis is to calculate the maximum stresses on the extreme fibres of the concrete slab for the characteristic SLS combination of actions. In this first step, the concrete strength is always considered for calculating the mechanical properties of all the cross-sections in the modelled main girder. The figure below gives the corresponding stress distribution.

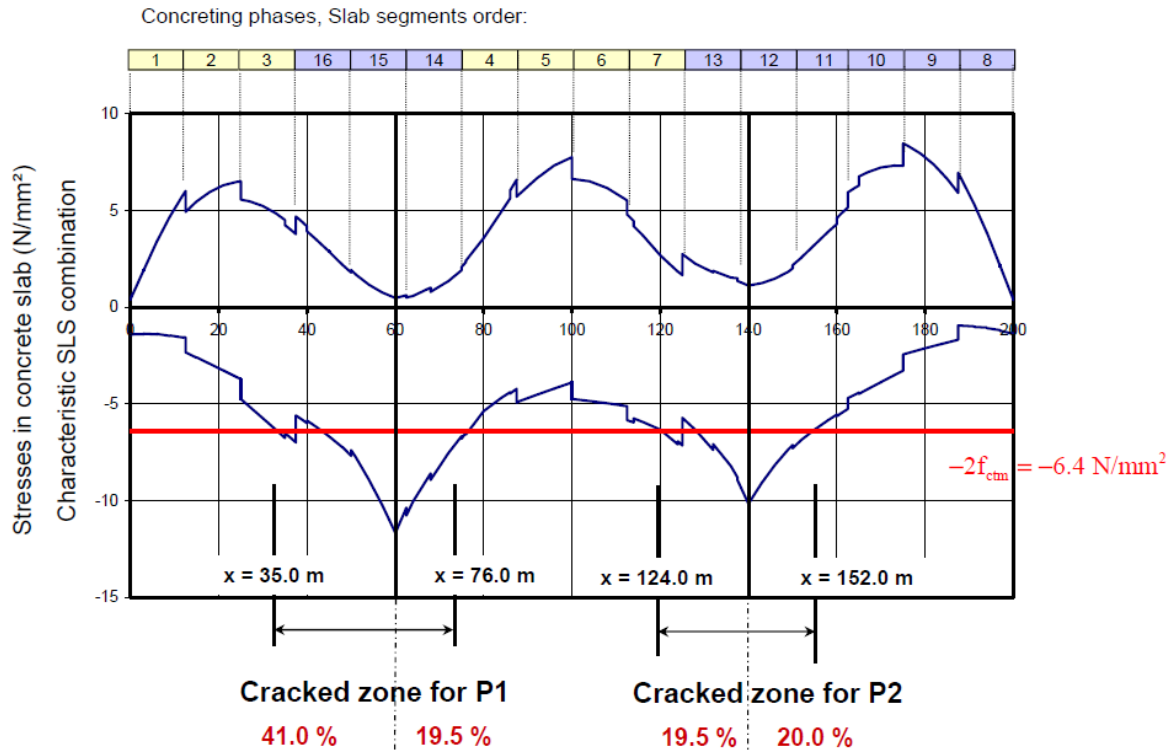


Figure 4.8 Cracked zones for each internal support

If the longitudinal tensile stress σ_c in the concrete slab is lower than $-2f_{ctm}$ ($= -6.4 \text{ MPa}$ in the example) then the concrete in this cross-section should be considered as cracked for the second step of the cracked global analysis. This criterion thus defines cracked zones on both sides of the intermediate supports on shown in Fig. 4.8.

For the second step of the global analysis, the concrete slab stiffness in the cracked zones is reduced to the stiffness of its reinforcing steel in tension. The calculations from the first step are then reproduced with this new longitudinal stiffness distribution. The concrete shrinkage should not be applied to the cross sections located in the cracked zones. Finally the internal forces and moments - as well as the corresponding stress distributions - at the end of this second step of analysis are used in the following chapters of this Report to justify all the transverse cross-sections of the bridge deck.

It should be noticed that the symmetry and the length of the cracked zones are very much influenced by the concreting sequence of the slab.

4.7 Main results

All the results coming from the global analysis can not be given extensively in this Report. Choices have been made to illustrate the main results of the global analysis.

4.7.1 VERTICAL SUPPORT REACTIONS

The vertical support reactions will be used for the verification of the piers, the abutments and the bearings. They are given on abutment C0 and on internal support P1 for the elementary load cases in the following table.

Load cases	Designation	C0 (MN)	P1 (MN)
Self weight (structural steel + concrete)	G_{k1}	1.1683	5.2867
Nominal non structural equipments	G_{k2}	0.39769	1.4665
3 cm settlement on support P1	S_k	0.060	-0.137
Traffic UDL	UDL	0.97612	2.693
Traffic TS	TS	0.92718	0.94458

To get the maximum (resp. minimum) value of the vertical support reaction for the non structural equipments, the nominal value should be multiplied by the coefficient 1.28 (resp. 0.83). Moreover these values should be combined according to the SLS and ULS combinations of actions from EN 1990.

4.7.2 INTERNAL FORCES AND MOMENTS

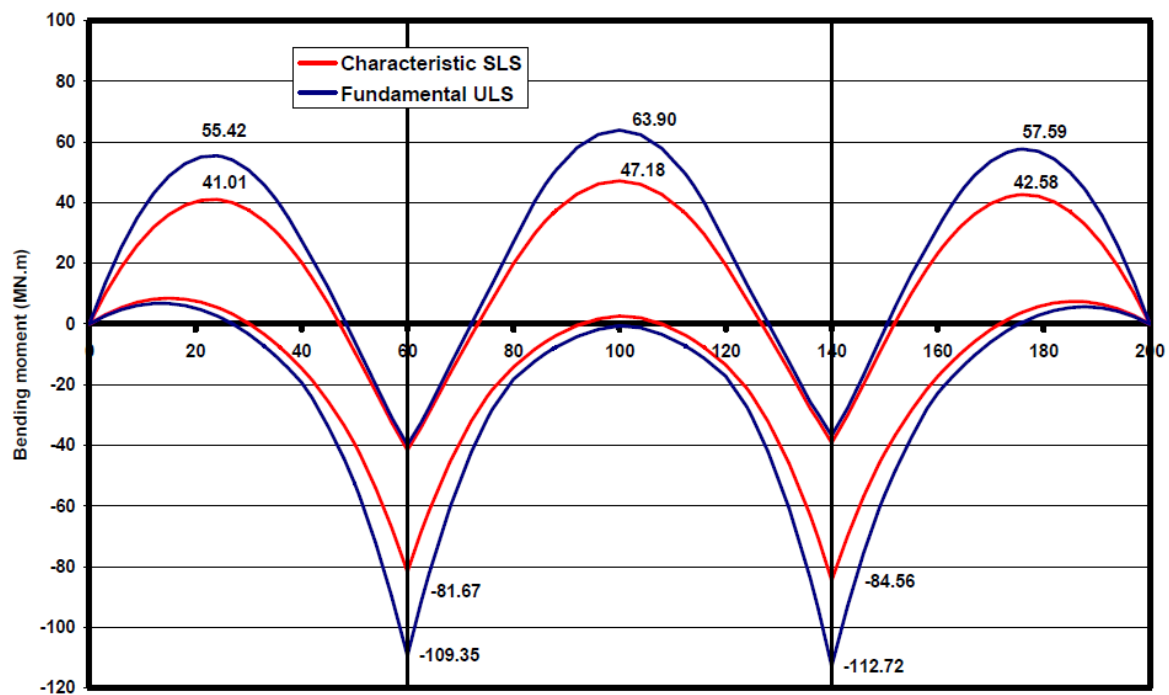


Figure 4.9 Bending moments (MN.m) in the bridge deck

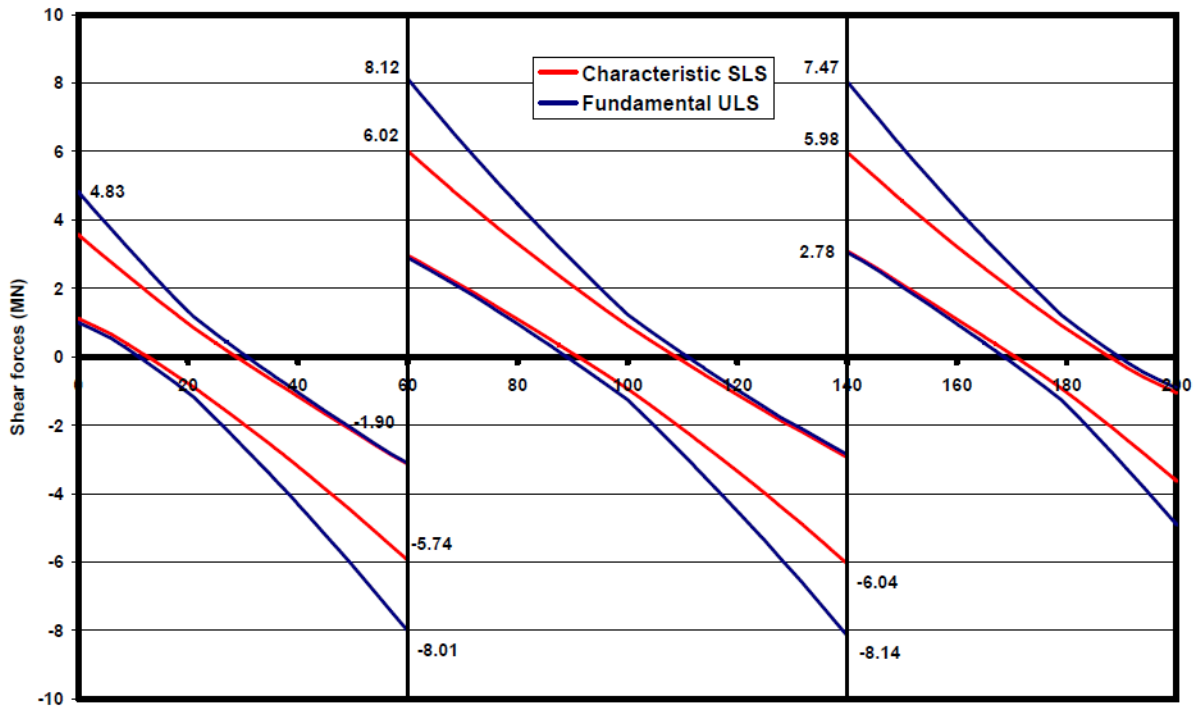


Figure 4.10 Shear force (MN) in the bridge deck

4.7.3 STRESSES AT ULS

The figure below gives a result example for the stress distribution at ULS in the steel flanges calculated with a cracked concrete. This hypothesis is valid for the verification of the cross-sections on internal support (see the relevant chapter in this Report).

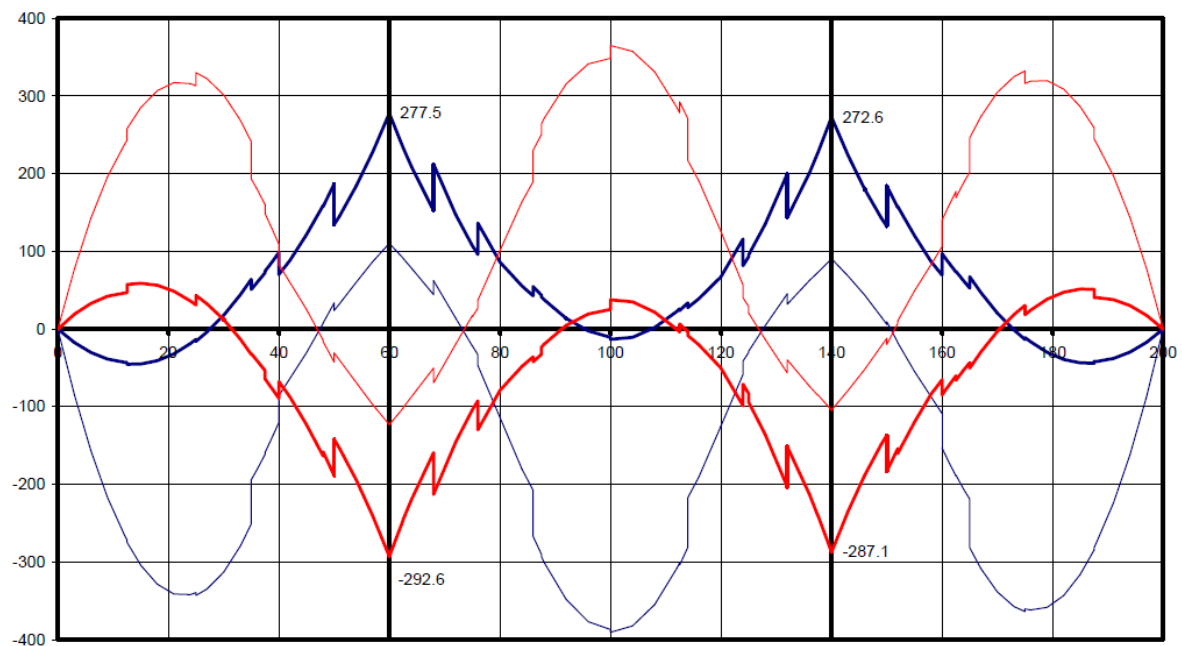


Figure 4.11 Stresses in the steel flanges (MPa) at ULS

References

- [1] “Eurocode 3 and 4, Application to steel-concrete composite road bridges”, Setra’s guidance book published in July 2007. This book can be downloaded at the following web address: <http://www.setra.equipement.gouv.fr/Technical-guides.html>
- [2] Eurocode 4 : Design of composite steel and concrete structures, Part 2 : General rules and rules for bridges, February 2006
- [3] Eurocode 3 : Design of steel structures, Part 1-5 : Plated structural elements, March 2007
- [4] Eurocode 1 : Actions on structures, Part 2 : Traffic loads on bridges, March 2004

CHAPTER 5

Concrete bridge design (EN1992-2)

Emmanuel Bouchon

Large bridge division. Sétra/CTOA. Paris, France

Giuseppe Mancini

Politecnico di Torino

5.1 Introduction

This chapter presents the practical application of some main issues of Eurocode 2. It does not deal with advanced methods of analysis and design. It mainly focuses on standard or simplified methods.

On the example of the concrete slab of the composite deck, will be illustrated the application of section 4 (durability), section 6 (ultimate limit states) and section 7 (serviceability limit states) of EN1992-1-1 and EN1992-2. Then, the analysis of second order effects by a simplified method is presented on the high pier case. This is an issue of section 5 of EN1992-1-1.

5.2 Local verifications in the concrete slab

The first verification to perform concerns the minimum cover, which governs the lever arm of the reinforcement.

Then, the concrete slab should undergo the following verifications:

- minimum reinforcement ratio in transverse direction,
- transverse bending resistance for the ULS combination of actions,
- limitations of the stresses for the characteristic SLS combination of actions,
- control of cracking at SLS,
- vertical shear resistance for the ULS combination of actions,
- longitudinal shear resistance for the ULS combination of actions,
- fatigue,
- shear resistance of the joints between adjacent slab concreting segments,
- rules for combining global and local effects,
- punching shear.

The verifications in this chapter are presented for two specific longitudinal sections of the concrete slab – above the main steel girder and at mid-span between the main steel girders – under transverse bending moment. The emphasis is on the peculiar topics for a composite bridge concrete slab, particularly the fact that it is in tension longitudinally around the internal supports.

5.2.1 DURABILITY – COVER TO REINFORCEMENT

Minimum cover, c_{min} (EN1992-1-1, 4.4.1.2)

The minimum cover must satisfy two criteria, bond and durability:

$$c_{min} = \max \{c_{min,b}; c_{min,dur}; 10 \text{ mm}\}$$

- $c_{min,b}$ (bond) is given in table 4.2 of EN 1992-1-1
 - $c_{min,b}$ = diameter of bar (max aggregate size ≤ 32 mm)
 - $c_{min,b}$ = 20 mm on top face of the slab
 - $c_{min,b}$ = 25 mm on bottom face at mid span between the steel main girders

- $c_{\min, \text{dur}}$ (durability) is given in table 4.4N, it depends on :
the exposure class (table 4.1)
the structural class (table 4.3N)

The procedure to determine $c_{\min, \text{dur}}$ is given hereafter.

Structural class (table 4.3N)

The basic structural class is 4. Table 4.3 gives the correction to apply following different criteria. For instance, for the top face of the slab, which exposure class is XC3, the structural class is increased by 2 because the design working life is 100 years, then reduced by 1 because of the strength class of concrete (closely related to its compaction), and by 1 because of slab geometry, and again by 1 for special control of concrete production, which is normally the case for bridges.

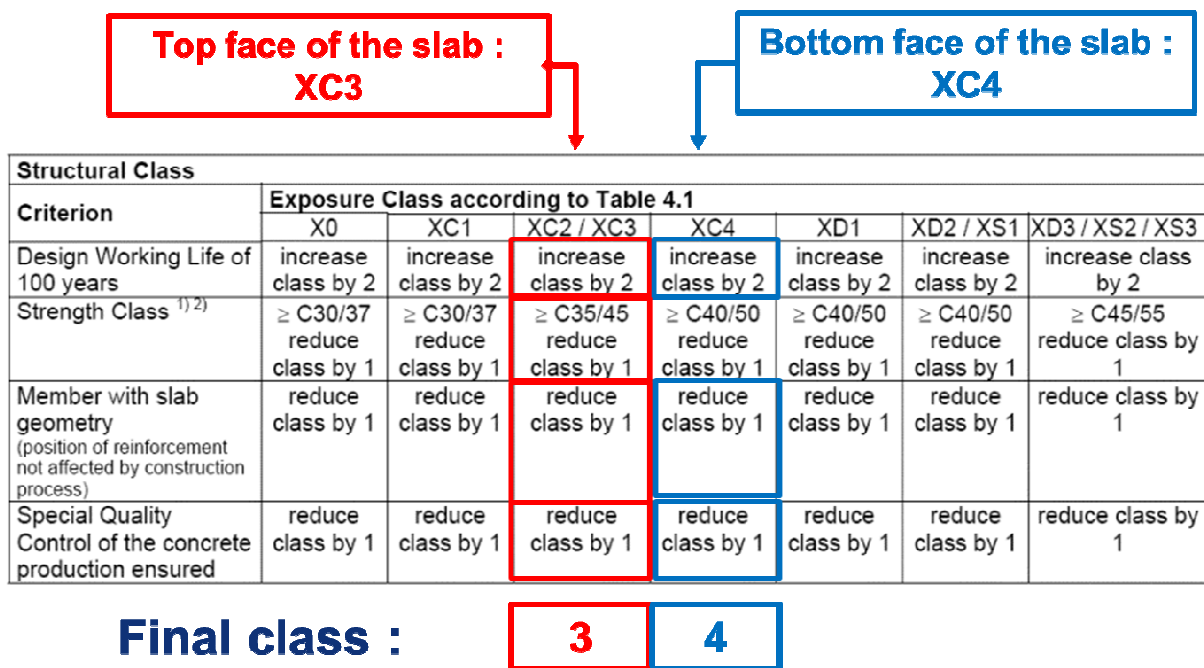


Fig. 5.1 Determination of the structural class

Then, the minimum cover is read in table 4.4N:

**Top face of the slab :
XC3 – str. class S3**

**Bottom face of the slab :
XC4 – str. class S4**

Table 4.4N: Values of minimum cover $c_{min,dur}$ requirements with regard to durability for reinforcement steel in accordance with EN 10080.

Environmental Requirement for $c_{min,dur}$ (mm)								
Structural Class	Exposure Class according to Table 4.1							
	X0	XC1	XC2	XC3	XC4	XD1 / XS1	XD2 / XS2	XD3 / XS3
S1	10	10	10	15	20	25	30	35
S2	10	10	15	20	25	30	35	40
S3	10	10	20	25	30	35	40	45
S4	10	15	25	30	35	40	45	50
S5	15	20	30	35	40	45	50	55
S6	20	25	35	40	45	50	55	60

Fig. 5.2 Minimum cover on the slab

The nominal cover – which is on the drawings and which is used for the calculations – is finally obtained by adding the allowance for deviation to the minimum cover, in order to be sure that the minimum cover is achieved on the structure.

$$c_{nom} = c_{min} + \Delta c_{dev} \quad (\text{allowance for deviation, expression 4.1})$$

$$\Delta c_{dev} = 10 \text{ mm (recommended value 4.4.1.3 (1)P)}$$

Δc_{dev} may be reduced in certain situations (4.4.1.3 (3))

- in case of quality assurance system with measurements of the concrete cover, the recommended value is:

$$10 \text{ mm} \geq \Delta c_{dev} \geq 5 \text{ mm}$$

Table 5.1 Nominal cover

Cover (mm)	$c_{min,b}$	$c_{min,dur}$	Δc_{dev}	c_{nom}
Top face of the slab	20	20	10	30
Bottom face of the slab	25	30	10	40

Of course, durability is not only a matter of concrete compaction and minimum cover. It must be one of the main concerns at all the stages of conceptual design.

5.2.2 TRANSVERSE REINFORCEMENT VERIFICATIONS

5.2.2.1 Internal forces and moments from transverse global analysis

For the verification, we use an equivalent beam model. But for the analysis, it is necessary to take into account the 2-dimensional behaviour of the slab, at least for traffic loads, which are not uniformly distributed.

a) Permanent loads

The internal forces and moments under permanent loads are pure bending and may be calculated from a truss element model. A transverse slab strip – which is 1-m-wide in the bridge longitudinal direction – is modelled as an isostatic girder lying on two vertical point supports representing the boundaries with the main steel girders. This hypothesis is unfavourable regarding the partially blocked boundary conditions that are applied to the concrete slab in relation with the width b_f of the upper steel flange. This isostatic model is subjected to the variable distributed loads – concrete self-weight and non-structural bridge equipments – according to Fig. 5.3.

After performing all calculations, the transverse bending moments in Fig. 5.4 are obtained.

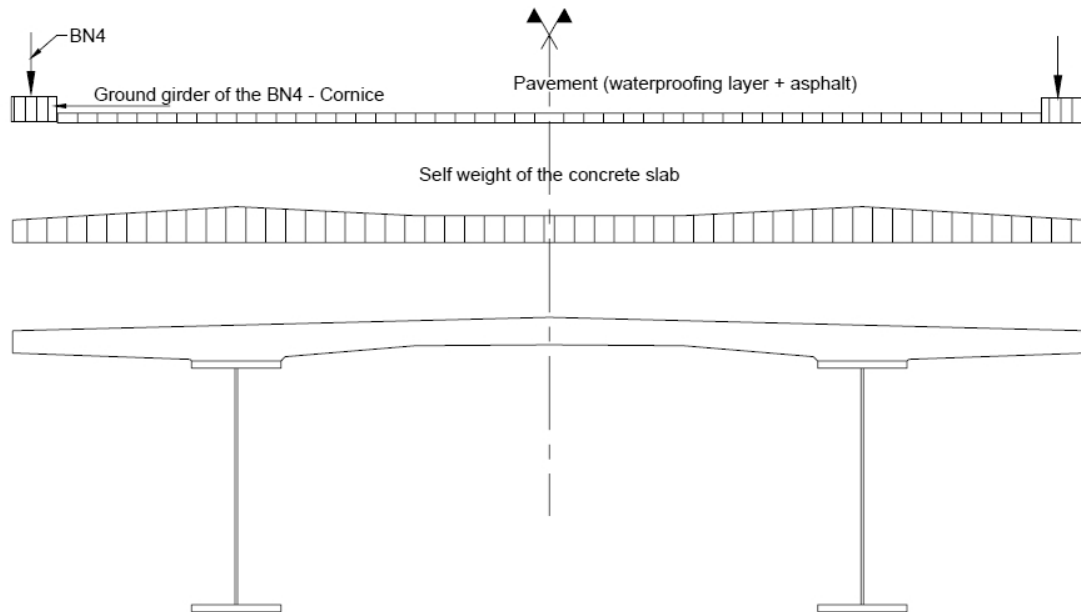


Fig. 5.3 Transverse distribution of permanent loads

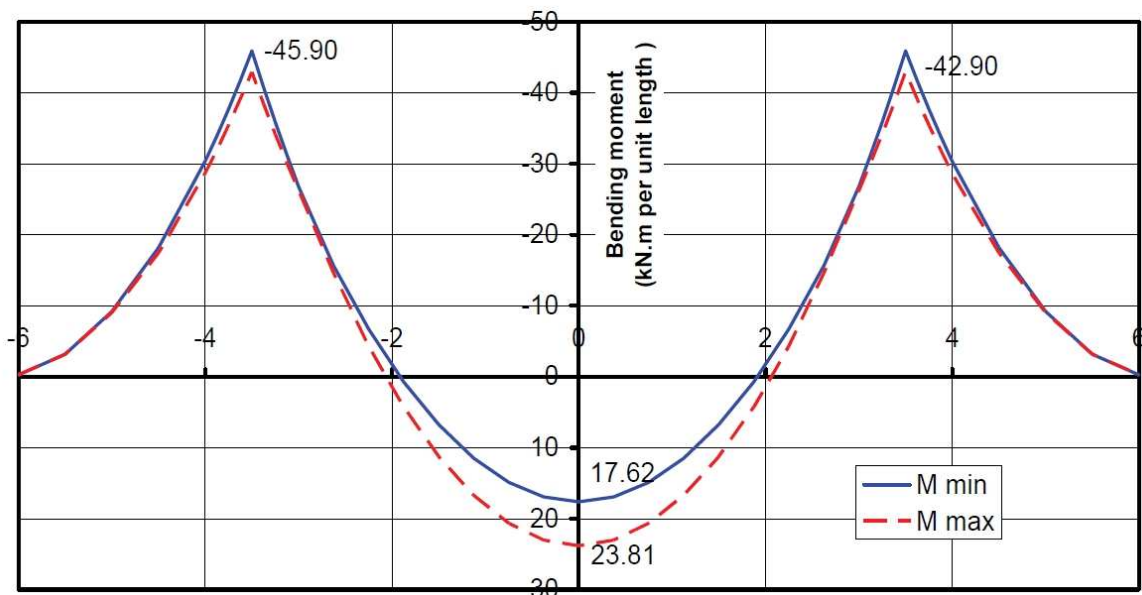


Fig. 5.4 Transverse bending moment envelope due to permanent loads

b) Traffic loads

The internal forces and moments are obtained reading charts which have been established by SETRA for the local bending of the slab in two-girder bridge with transverse girders. These charts are derived from the calculation of influence surfaces on a finite element model of a typical composite deck slab. The traffic load model LM1 is always governing the design.

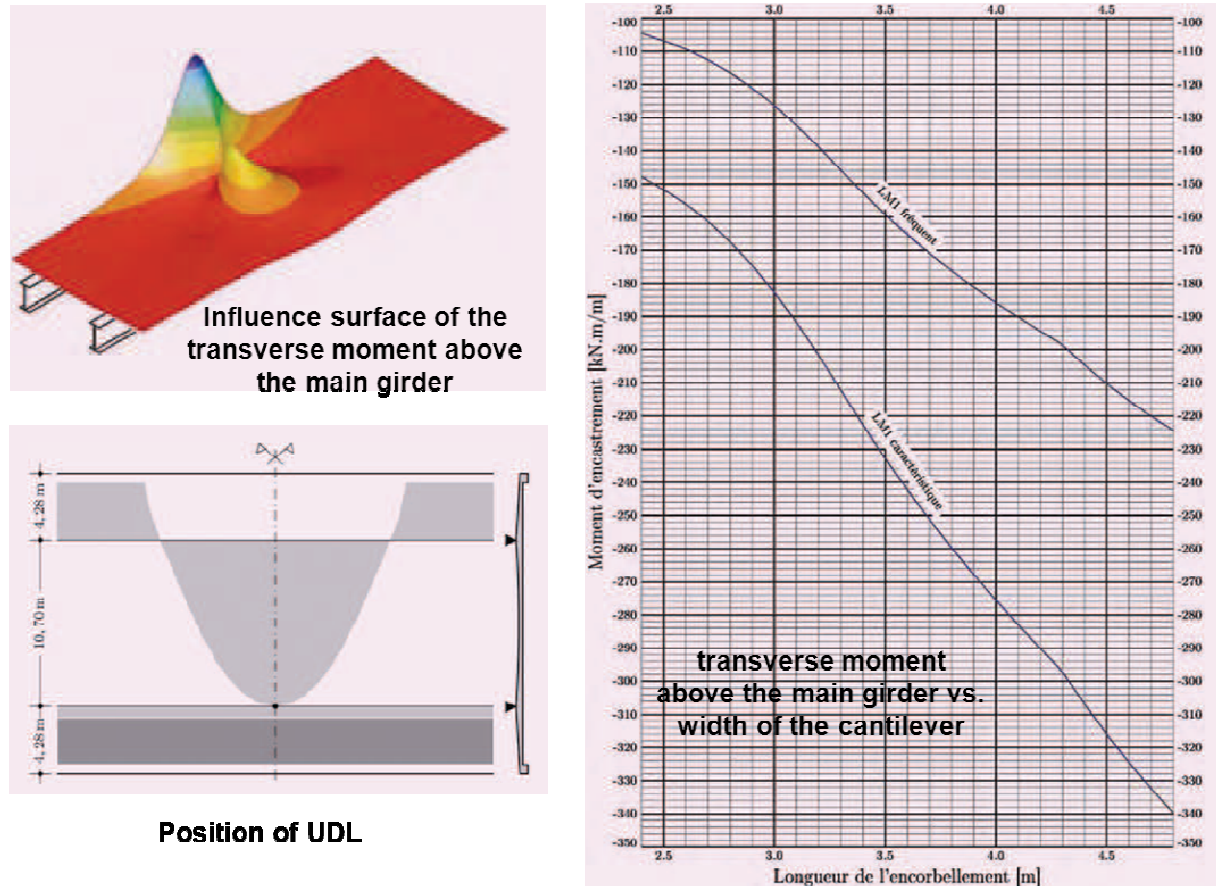


Fig. 5.5 Analysis – Maximum effect of traffic loads

For the studied slab section located above the steel main girder, the characteristic value of the transverse bending moment is equal to $M_{LM1} = -158$ kN.m and the frequent value is equal to $M_{LM1} = -110$ kN.m.

For the studied slab section at mid-span between the steel main girders, the characteristic value of the transverse bending moment is equal to $M_{LM1} = 160$ kN.m and the frequent value is equal to $M_{LM1} = 108$ kN.m.

c) Combinations of actions

Using the combinations of actions defined in this chapter finally gives the bending moment values in Table 5.2 below (for a 1-m-wide slab strip):

Table 5.2 Transverse bending moment

M (kNm/m)	Quasi permanent SLS	Frequent SLS	Characteristic SLS	ULS
Section above the main girder	-46	-156	-204	-275
Section at mid-span	24	132	184	248

5.2.2.2 Minimum reinforcement area

EN1992-1-1 (clauses 9.3.1 and 9.2.1(1)) requires a minimum bending reinforcement area to be set in the concrete slab. The recommended value (which can be modified by the National Annex of each European country) is:

$$A_{s,min} = 0.26 \frac{f_{ctm}}{f_{yk}} b_t d \geq 0.0013 b_t d$$

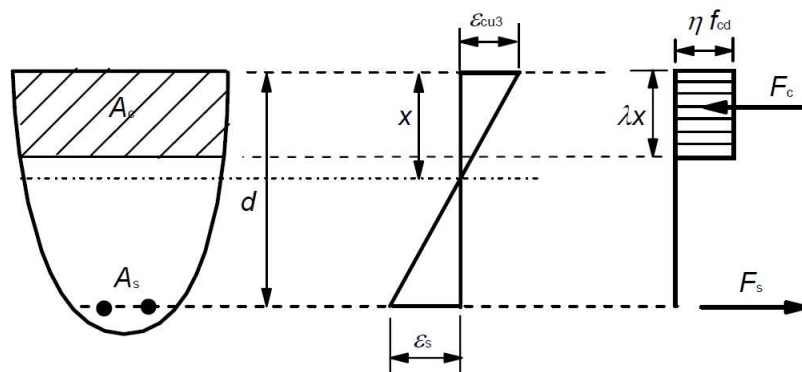
where b_t is the slab width (reasoning here is based on a 1-m-wide slab strip therefore $b_t = 1$ m) and d is the effective depth of the cross-section (i.e. the distance between the centre of gravity of the considered reinforcement layer and the extreme compressed fibre of the concrete).

For the design example, the reinforcement area which has been used in the design is clearly greater than the minimum reinforcement area: $A_{s,min} = 6.0 \text{ cm}^2/\text{m}$ above the main girder and $4.3 \text{ cm}^2/\text{m}$ at mid-span.

5.2.2.3 ULS bending resistance

The design value of the bending moment M_{Ed} at ULS should be less than the design value of the resistance bending moment M_{Rd} which is calculated according to the following stress-strain relationships:

- for the concrete, a simplified rectangular stress distribution:
 $\lambda = 0.80$ and $\eta = 1.00$ as $f_{ck} = 35 \text{ MPa} \leq 50 \text{ MPa}$
 $f_{cd} = 19.8 \text{ MPa}$ (with $\alpha_{cc} = 0.85$ – recommended value)
 $\varepsilon_{cu3} = 3.5 \text{ mm/m}$

**Fig. 5.6 Simplified rectangular stress distribution in concrete**

- for the reinforcement, a bi-linear stress-strain relationship with strain hardening (Class B steel bars according to Annex C to EN1992-1-1):

$$f_{yd} = 435 \text{ MPa}$$

$$k = 1.08$$

$$\varepsilon_{ud} = 0.9 \cdot \varepsilon_{uk} = 45 \text{ mm/m (recommended value)}$$

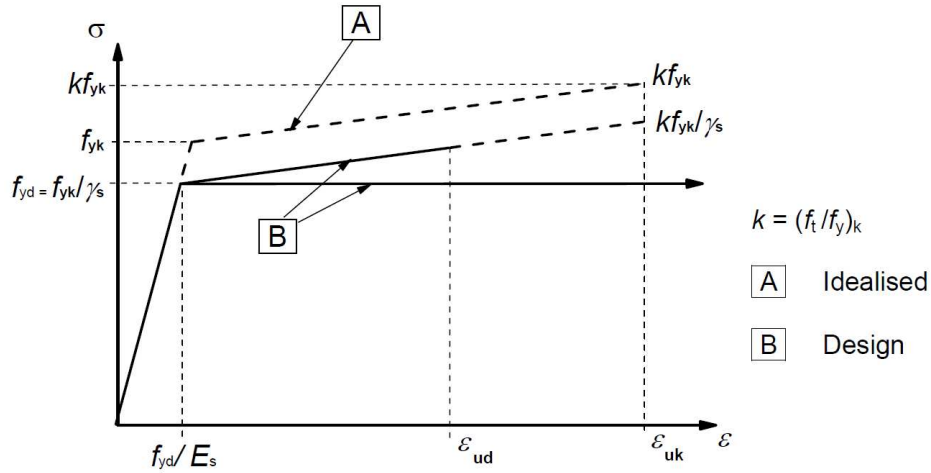


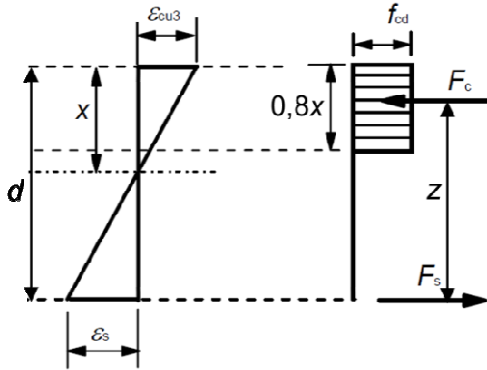
Fig. 5.7 Stress-strain relationship for reinforcement

$$\text{for } \varepsilon_s \leq f_{yd} / E_s \quad \sigma_s = E_s \varepsilon_s$$

$$\text{for } \varepsilon_s \geq f_{yd} / E_s \quad \sigma_s = f_{yd} + (k - 1) f_{yd} (\varepsilon_s - f_{yd} / E_s) / (\varepsilon_{uk} - f_{yd} / E_s)$$

Reinforcement in compression is neglected.

- $\varepsilon_s = \varepsilon_{cu3} (d - x) / x$
- $\sigma_s = f_{yd} + (k - 1) f_{yd} (\varepsilon_s - f_{yd} / E_s) / (\varepsilon_{uk} - f_{yd} / E_s)$ (inclined top branch)
- Equilibrium : $N_{Ed} = 0 \Leftrightarrow A_s \sigma_s = 0.8 b \cdot x \cdot f_{cd}$ where $b = 1 \text{ m}$



- Then, x is the solution of a quadratic equation
- The resistant bending moment is given by:

$$M_{Rd} = 0.8 b \cdot x \cdot f_{cd} (d - 0.4x)$$

$$= A_s \sigma_s (d - 0.4x)$$

The calculation of M_{Rd} in the design example gives:

- Section above the main steel girder (absolute values of moments):

with $d = 0.36 \text{ m}$ and $A_s = 18.48 \text{ cm}^2$ ($\phi 20$ every 0.17 m):

$x = 0.052 \text{ m}$, $\varepsilon_s = 20.6 \text{ mm/m}$ ($< \varepsilon_{ud}$) and $\sigma_s = 448 \text{ MPa}$

Therefore $M_{Rd} = 0.281 \text{ MN.m} > M_{Ed} = 0.275 \text{ MN.m}$

- Section at mid-span between the main steel girders:

with $d = 0.26 \text{ m}$ and $A_s = 28.87 \text{ cm}^2$ ($\phi 25$ every 0.17 m):

$x = 0.08 \text{ m}$, $\varepsilon_s = 7.9 \text{ mm/m}$ ($< \varepsilon_{ud}$) and $\sigma_s = 439 \text{ MPa}$

Therefore $M_{Rd} = 0.289 \text{ MN.m} > M_{Ed} = 0.248 \text{ MN.m}$

The transverse reinforcement is well designed regarding the local transverse bending at ULS. $M_{Rd} = M_{ULS}$ would be reached in the section above the steel main girder for $A_s = 18.04 \text{ cm}^2/\text{m}$ only. It is useful to know this value to justify the interaction between the transverse bending moment and the longitudinal shear stress (see paragraph 5.2.2.9).

5.2.2.4 Calculation of normal stresses at serviceability limit state

Normal stresses have to be calculated under the assumption of either uncracked cross-sections or cracked cross-sections. According to EN 1992-1-1, 7.1(2):

- (2) In the calculation of stresses and deflections, cross-sections should be assumed to be uncracked provided that the flexural tensile stress does not exceed $f_{ct,eff}$. The value of $f_{ct,eff}$ maybe taken as f_{ctm} or $f_{ctm,fl}$ provided that the calculation for minimum tension reinforcement is also based on the same value. For the purposes of calculating crack widths and tension stiffening f_{ctm} should be used.

That means that, if the tensile stresses, calculated in the uncracked cross-section, are not greater than f_{ctm} , then there is no need to perform a calculation of normal stresses under the assumption of cracked cross-section.

5.2.2.5 Stress limitation for characteristic SLS combination of actions

Stress limitations under characteristic combination are checked to avoid inelastic deformation of the reinforcement and longitudinal cracks in concrete. It is an irreversible limit state. The following limitations should be checked (EN1992-1-1, 7.2(5) and 7.2(2)):

$$\sigma_s \leq k_3 f_{yk} = 0.8 \times 500 = 400 \text{ MPa}$$

$$\sigma_c \leq k_1 f_{ck} = 0.6 \times 35 = 21 \text{ MPa}$$

where k_1 and k_3 are defined by the National Annex to EN1992-1-1. The recommended values are $k_1 = 0.6$ and $k_3 = 0.8$.

Stresses are calculated in the cracked section, assuming linear elastic behaviour of the materials and neglecting the contribution of concrete in tension. The results depend on the modular ratio n (reinforcement/concrete), which lies between the short term value (E_s/E_{cm}) and the long term value, approximately equal to 15. The value to take into account depends on the ratio between the moments under characteristic combination and quasi-permanent combination. To be rigorous, two calculations should be performed: a short-term calculation – with the short term value of n – and a long term calculation taking into account the long-term effects of permanent loads and the short-term effects of traffic loads.

The most unfavourable compressive stresses σ_c in the concrete are generally provided by the short-term calculations, performed with a modular ratio $n = E_s/E_{cm} = 5.9$ ($E_s = 200 \text{ GPa}$ for reinforcing steel and $E_{cm} = 34 \text{ GPa}$ for concrete C35/45). The most unfavourable tensile stresses σ_s in the reinforcement are generally provided by the long-term calculations, performed with $n = 15$.

The design example in the section above the steel main girder gives $d = 0.36 \text{ m}$, $A_s = 18.48 \text{ cm}^2$ and $M = 0.204 \text{ MN.m}$.

Using $n = 15$, $\sigma_s = 344 \text{ MPa} < 400 \text{ MPa}$ is obtained.

Using $n = 5.9$, $\sigma_c = 15.6 \text{ MPa} < 21 \text{ MPa}$ is obtained.

The design example in the section at mid-span between the steel main girders gives $d = 0.26 \text{ m}$, $A_s = 28.87 \text{ cm}^2$ and $M = 0.184 \text{ MN.m}$.

Using $n = 15$, $\sigma_s = 287 \text{ MPa} < 400 \text{ MPa}$ is obtained.

Using $n = 5.9$, $\sigma_c = 20.0 \text{ MPa} < 21 \text{ MPa}$ is obtained.

The above calculations show that, for the design example, under the most unfavourable value of the modular ratio, the stress limits are not exceeded. However, it is not necessary to consider such a wide range of modular ratio. The modular ratio for long-term might have been determined by linear interpolation between $E_s/E_{cm} = 5.9$ and 15:

$n = (15M_{qp} + 5.9M_{LM1}) / (M_{qp} + M_{LM1})$ where M_{qp} is the moment under quasi-permanent combination and M_{LM1} is the moment under the characteristic value of the traffic loads.

This expression gives $n = 8$ above the main girder and $n = 7.1$ at mid-span. As the stress limit in steel is satisfied with $n = 15$, there is no need to go further

5.2.2.6 Control of cracking

According to EN1992-2, 7.3.1(105), Table 7.101N, the calculated crack width should not be greater than 0,3 mm under quasi-permanent combination of actions, for reinforced concrete, whatever the exposure class. It is important to notice that the limitation apply to calculated crack width, which can differ notably from measured crack width in the real structure.

In the design example, transverse bending is mainly caused by live loads, the bending moment under quasi-permanent combination is far lesser than the moment under characteristic combinations. It is the same for the tension in reinforcing steel. Therefore, there is no problem with the control of cracking, as can be seen hereafter.

The concrete stresses due to transverse bending under quasi permanent combination, are as follows:

- above the steel main girder: $M = -46 \text{ kNm/m}$ $\sigma_c = \pm 1.7 \text{ MPa}$
- at mid-span between the main girders: $M = 24 \text{ kNm/m}$ $\sigma_c = \pm 1.5 \text{ MPa}$

Since $\sigma_c > -f_{ctm}$, the sections are assumed to be uncracked (EN1992-1-1, 7.1(2)) and there is no need to check the crack openings. A minimum amount of bonded reinforcement is required in areas where tension is expected (EN1992-1-1 and EN1992-2, 7.3.2). The minimum area of tensile reinforcement is given by expression (7.1), which is obtained from equilibrium between the tensile force in concrete just before cracking and tensile force in reinforcement just after cracking:

$$A_{s,min}\sigma_s = k_c k f_{ct,eff} A_{ct}$$

where

- A_{ct} is the area of concrete within the tensile zone just before the formation of the first crack
- k takes account of size effects
- k_c takes account of the stress distribution and of the change of lever arm when cracking occurs.

In the design example:

- $A_{ct} = bh/2$ ($b = 1 \text{ m}$; $h = 0.40 \text{ m}$ above main girder and 0.32 m at mid-span)
- $\sigma_s = f_{yk}$ (a lower value needs be taken only when control of cracking is ensured limiting bar size or spacing according to 7.3.3).
- $f_{ct,eff} = f_{ctm} = 3.2 \text{ MPa}$
- $k = 0.65$ (flanges with width $\geq 800 \text{ mm}$)
- $k_c = 0.4$ (expression 7.2 with $\sigma_c = \text{mean stress in the concrete} = 0$)

The following areas of reinforcement are obtained:

- $A_{s,min} = 3.33 \text{ cm}^2/\text{m}$ on top face of the slab above the main girders
- $A_{s,min} = 2.67 \text{ cm}^2/\text{m}$ on bottom face of the slab at mid-span.

The result is about 0.17 % of the area of the concrete in tension.

Note

The French national annex asks for checking crack width under frequent combination of actions. For this combination, the tensile stresses of concrete are:

- above the main girder: $M = -156 \text{ kN.m/m}$ $\sigma_c = 5.9 \text{ MPa}$
- at mid-span $M = 132 \text{ kN.m/m}$ $\sigma_c = 8.2 \text{ MPa}$

Both sections are cracked under frequent combination. Normal stresses in concrete and steel must be calculated in the cracked cross-section. Control of crack width can then be done by the direct method (EN1992-1-1, 7.3.4). The crack width is given by:

$$w_k = s_{r,max} (\epsilon_{sm} - \epsilon_{cm})$$

where

- $s_{r,max}$ is the maximum crack spacing
- $\epsilon_{sm} - \epsilon_{cm}$ is the difference of mean tensile strains between reinforcement and concrete

$\epsilon_{sm} - \epsilon_{cm}$ may be calculated from the expression (7.9):

$$\epsilon_{sm} - \epsilon_{cm} = \frac{\sigma_s - k_t \frac{f_{ct,eff}}{\rho_{p,eff}} (1 + \alpha_e \rho_{p,eff})}{E_s}$$

where

- $\alpha_e = E_s/E_{cm}$
- $\rho = A_s/A_{c,eff}$ (according to EN1992-1-1, 7.3.2, $A_{c,eff} = b h_{c,ef}$, where $h_{c,ef}$ is the lesser of $2.5(h - d)$, $(h - x)/3$, or $h/2$)
- $k_t = 0.6$ for short term loading and 0.4 for long term loading.

If the spacing of reinforcement is less than $5(c + \phi/2)$, $s_{r,max}$ may be given by:

$$s_{r,max} = k_3 c + k_1 k_2 k_4 \phi / \rho_{p,eff}$$

where $k_1 = 0.8$ (high bond bars), $k_2 = 0.5$ (bending), $k_3 = 3.4$ and $k_4 = 0.425$.

Design example

For a rectangular section without axial force, the depth of the neutral axis x is equal to:

$$x = \frac{n A_s}{b} \left(\sqrt{1 + \frac{2 b d}{n A_s}} - 1 \right) \text{ where } n \text{ is the modular ratio. The tensile stress in the reinforcement is then}$$

calculated from: $\sigma_s = M / [(d - x/3) A_s]$

For a 1-m-wide slab strip:

- above the main girder: $n = 8.6$ $M = 156 \text{ kNm}$ $h = 0.40 \text{ m}$
 $d = 0.36 \text{ m}$ $A_s = 18.48 \text{ cm}^2$ $c = 0.03 \text{ m}$ $\phi = 0.02 \text{ m}$
- Then $x = 0.092 \text{ m}$ $\sigma_s = 256 \text{ MPa}$ $h_{c,ef} = 0.10 \text{ m}$
 $A_{c,eff} = 0.10 \text{ m}^2$ $\rho_{p,eff} = 0.0185$ $k_t = 0.6$
 $\epsilon_{sm} - \epsilon_{cm} = 0.70 \times 10^{-3}$ $s_{r,max} = 0.29 \text{ m}$

Finally $w_k = 0.20 \text{ mm}$

- at mid-span $n = 7.6$ $M = 132 \text{ kNm}$ $h = 0.318 \text{ m}$ $d = 0.26 \text{ m}$
 $A_s = 28.87 \text{ cm}^2$ $c = 0.04 \text{ m}$ $\phi = 0.025 \text{ m}$
- Then $x = 0.077 \text{ m}$ $\sigma_s = 198 \text{ MPa}$ $h_{c,ef} = 0.077 \text{ m}$
 $A_{c,eff} = 0.077 \text{ m}^2$ $\rho_{p,eff} = 0.0375$ $k_t = 0.6$
 $\varepsilon_{sm} - \varepsilon_{cm} = 0.68 \cdot 10^{-3}$ $s_{r,max} = 0.25 \text{ m}$
- Finally $w_k = 0.17 \text{ mm}$

5.2.2.7 Resistance to vertical shear force

The shear force calculations are not detailed. The maximum shear force at ULS is obtained in the section located above the steel main girder by applying the traffic load model LM1 between the two steel main girders. This gives $V_{Ed} = 235 \text{ kN}$ to be resisted by a 1-m-wide slab strip.

The concrete slab is not in tension in the transverse direction of the bridge. It behaves as a reinforced concrete element and its resistance to vertical shear – without specific shear reinforcement – is thus obtained directly by using the formula (6.2a) in EN1992-2:

$$V_{Rd,c} = b_w d \{ k_1 \sigma_{cp} + \max [C_{Rd,c} k (100 \rho_l f_{ck})^{1/3} ; v_{\min}] \}$$

where:

- f_{ck} is given in MPa
- $k = 1 + \sqrt{\frac{200}{d}} \leq 2.0$ with d in mm
- $\rho_l = \frac{A_{sl}}{b_w d} \leq 0.02$

A_{sl} is the area of reinforcement in tension (see Figure 6.3 in EN1992-2 for the provisions that have to be fulfilled by this reinforcement). For the design example, A_{sl} represents the transverse reinforcing steel bars of the upper layer in the studied section above the steel main girder. b_w is the smallest width of the studied section in the tensile area. In the studied slab $b_w = 1000 \text{ mm}$ in order to obtain a resistance $V_{Rd,c}$ to vertical shear for a 1-m-wide slab strip (rectangular section).

- $\sigma_{cp} = \frac{N_{Ed}}{A_c} \leq 0.2 f_{cd}$ in MPa. This stress is equal to zero where there is no normal force (which is the case in the transverse slab direction in the example).
- The values of $C_{Rd,c}$ and k_1 can be given by the National Annex to EN1992-2. The recommended ones are used:
 $C_{Rd,c} = \frac{0.18}{\gamma_c} = 0.12$
 $k_1 = 0.15$
- $v_{\min} = 0.035 k^{3/2} f_{ck}^{1/2}$

Design example

The design example in the studied slab section above the steel main girder gives successively:

$$\begin{aligned} f_{ck} &= 35 \text{ MPa} \\ C_{Rd,c} &= 0.12 \\ d &= 360 \text{ mm} \end{aligned}$$

$$k = 1 + \sqrt{\frac{200}{360}} = 1.75$$

$A_{sl} = 1848 \text{ mm}^2$ (high bond bars with diameter of 20 mm and spacing of 170 mm).

$$b_w = 1000 \text{ mm}$$

$$\rho = \frac{1848}{1000 \times 360} = 0.51\%$$

$$C_{Rd,c} k (100 \rho f_{ck})^{1/3} = 0.55 \text{ MPa}$$

$$\sigma_{cp} = 0$$

$$v_{min} = 0.035 \times 1.75^{3/2} \times 35^{1/2} = 0.48 \text{ MPa} < 0.55 \text{ MPa}$$

The shear resistance without shear reinforcement is:

$$V_{Rd,c} = C_{Rd,c} k (100 \rho f_{ck})^{1/3} b_w d = 198 \text{ kN / m} < V_{Ed} = 235 \text{ kN / m}.$$

According to EN1992-1-1, shear reinforcement is needed in the slab, near the main girders. With vertical shear reinforcement, the shear design is based on a truss model (EN1992-1-1 and EN1992-2, 6.2.3, fig. 6.5) where α is the inclination of the shear reinforcement and θ the inclination of the struts:

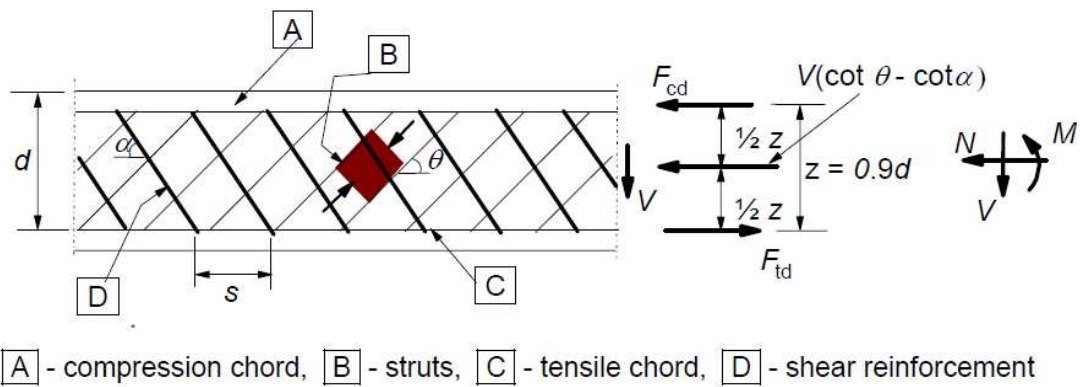


Fig. 5.8 Truss model (fig. 6.5 of EN1992-1-1)

With vertical shear reinforcement ($\alpha = \pi/2$), the shear resistance V_{Rd} is the smaller value of:

$$V_{Rd,s} = (A_{sw}/s) z f_{ywd} \cot \theta \text{ and}$$

$$V_{Rd,max} = \alpha_{cw} b_w z \nu_1 f_{cd} / (\cot \theta + \tan \theta)$$

where:

- z is the inner lever arm ($z = 0.9d$ may normally be used for members without axial force)
- θ is the angle of the compression strut with the horizontal, must be chosen such as $1 \leq \cot \theta \leq 2.5$
- A_{sw} is the cross-sectional area of the shear reinforcement
- s is the spacing of the stirrups
- f_{ywd} is the design yield strength of the shear reinforcement
- ν_1 is a strength reduction factor for concrete cracked in shear, the recommended value of ν_1 is $\nu = 0.6(1 - f_{ck}/250)$

- α_{cw} is a coefficient taking account of the interaction of the stress in the compression chord and any applied axial compressive stress; the recommended value of α_{cw} is 1 for non prestressed members.

In the design example, choosing $\cot\theta = 2.5$, with a shear reinforcement area $A_{sw}/s = 6.8 \text{ cm}^2/\text{m}$ for a 1-m-wide slab strip:

$$V_{Rd,s} = 0.00068 \times (0.9 \times 0.36) \times 435 \times 2.5 = 240 \text{ kN/m} > V_{Ed}$$

$$V_{Rd,max} = 1.0 \times 1.0 \times (0.9 \times 0.36) \times 0.6 \times (1 - 35/250) \times 35 / (2.5 + 0.4) = 2.02 \text{ MN/m} > V_{Ed}$$

Note

In EN1992-1-1, the shear resistance without shear reinforcement is the same for beams and for slabs. This does not take account of the 2-dimensional behaviour of slabs and of the possibility of transverse redistribution. The calibration of the expression of v_{min} is based on tests made on beam elements only. For these reasons, v_{min} has been modified by the French National Annex to EN1992-1-1 :

$$v_{min} = 0.035 k^{3/2} f_{ck}^{1/2} \text{ for beam elements (it is the recommended value)}$$

$v_{min} = (0.34/\gamma_c) f_{ck}^{1/2}$ for slab elements where transverse redistribution of loads is possible. This is based on French experience. Such a difference already existed in former French code. With this expression: $v_{min} = (0.34/1.5) \cdot 35^{1/2} = 1.34 \text{ MPa} > 0.55 \text{ MPa}$ and there is no need to add shear reinforcement in the slab.

5.2.2.8 Resistance to longitudinal shear stress

The longitudinal shear force per unit length at the steel/concrete interface is determined by an elastic analysis at characteristic SLS and at ULS. The number of shear connectors is designed thereof, to resist to this shear force per unit length and thus to ensure the longitudinal composite behaviour of the deck.

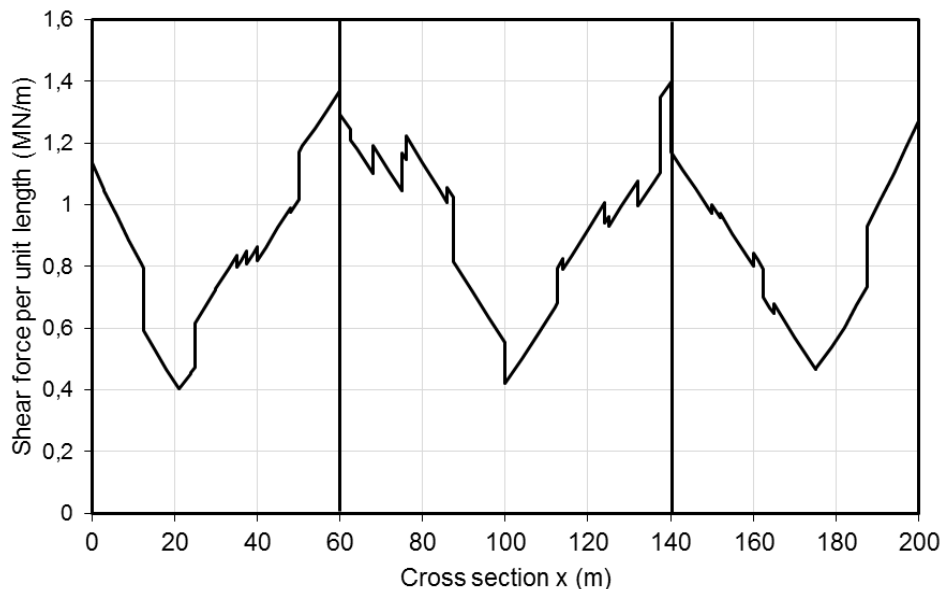


Fig. 5.9 Shear force per unit length resisted by the studs (MN/m)

At ULS this longitudinal shear stress should also be resisted to for any potential surface of longitudinal shear failure within the slab. This means that the reinforcing steel bars holding such kind of surface

should be designed to prevent any shear failure of the concrete or any longitudinal splitting within the slab.

Two potential surfaces of shear failure are defined in EN1994-2, 6.6.6.1 (see Fig. 5.10(a)):

- surface a-a holding only once by the two transverse reinforcement layers, $A_s = A_{sup} + A_{inf}$
- surface b-b holding twice by the lower transverse reinforcement layer, $A_s = 2.A_{inf}$

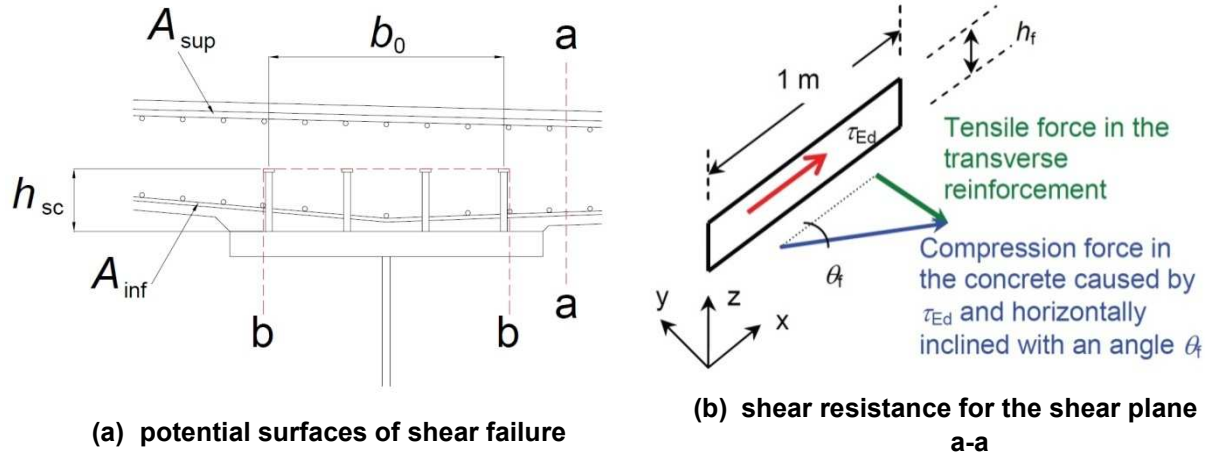


Fig. 5.10 Potential surfaces of shear failure in the concrete slab

According to Fig. 5.9, the maximum longitudinal shear force per unit length resisted to by the shear connectors is equal to 1.4 MN/m. This value is used here for verifying shear failure within the slab. The shear force on each potential failure surface is proportional to the first moment of area, about the centre of gravity of the composite section, of the part of the slab outside the failure surface. For a nearly horizontal concrete slab, it can then be considered that the shear force applied on a potential failure surface is proportional to the area of the part of the concrete section situated outside this surface. The shear force on each potential failure surface (see fig. 5.10(a)) is as follows:

- surface a-a, on the cantilever side : 0.59 MN/m
- surface a-a, on the central slab side : 0.81 MN/m
- surface b-b : 1.4 MN/m

Failure in shear planes a-a

The shear resistance is determined according to EN1994-2, 6.6.6.2(2), which refers to EN1992-1-1, 6.2.4, fig. 6.7 (see Fig. 5.11 below), the resulting shear stress is:

$$v_{Ed} = \Delta F_d / (h_f \cdot \Delta x)$$

where:

- h_f is the thickness of flange at the junctions
- Δx is the length under consideration, see fig. 6.7
- ΔF_d is the change of the normal force in the flange over the length Δx .

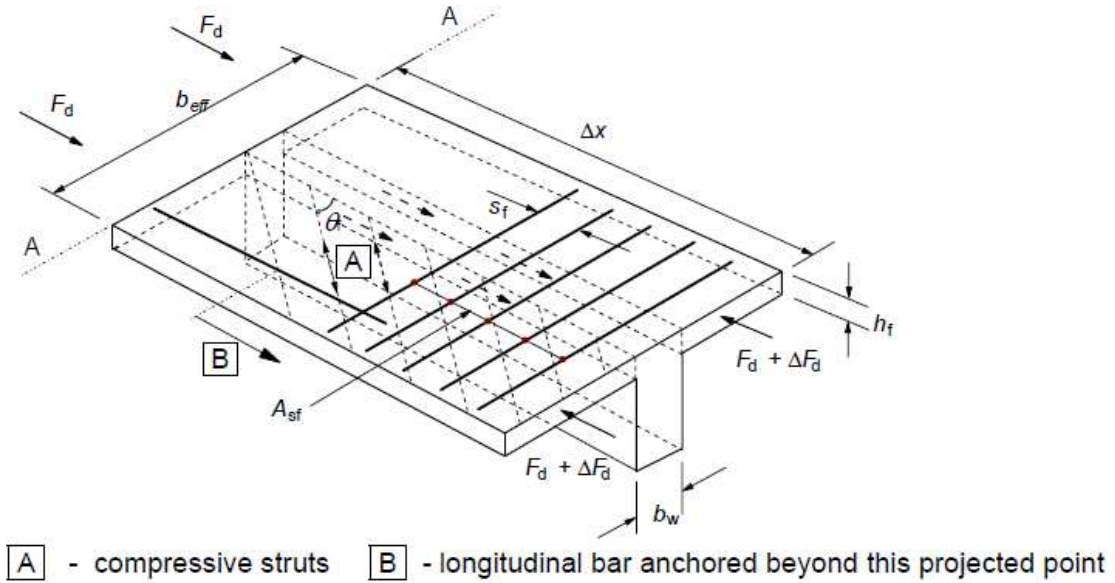


Fig. 5.11 Shear between web and flanges (fig. 6.7 of EN1992-1-1)

The longitudinal shear stress causes horizontal compressive struts in the concrete slab. They are inclined with an angle θ_f with regards to the longitudinal axis of the deck (see Fig. 5.10(b) and Fig. 5.11).

The calculation is made only for the surface a-a on the central slab side, where the longitudinal shear is higher than on cantilever side.

Shear stress: $v_{Ed} = \Delta F_d / (h_f \cdot \Delta x) = 0.81 / 0.40 = 2.03 \text{ MPa}$ ($h_f = 0.40 \text{ m}$)

Two different verifications should be carried out:

- the transverse reinforcement should be designed to resist to the tensile force:

$$v_{Ed} h_f \tan \theta_f \leq \frac{A_s}{s} f_{yd}$$

where s is the spacing between the transverse reinforcing steel bars and A_s is the corresponding area within the 1-m-wide slab strip.

- the crushing should be prevented in the concrete compressive struts:

$$v_{Ed} \leq \nu f_{cd} \sin \theta_f \cos \theta_f$$

with $\nu = 0.6 \left(1 - \frac{f_{ck}}{250} \right)$ and f_{ck} in MPa (strength reduction factor for the concrete cracked in shear).

As the concrete slab is in tension in the longitudinal direction of the deck, the angle θ_f for the concrete compressive strut should be limited to $\cotan \theta_f = 1.25$ i.e. $\theta_f = 38.65^\circ$.

For the design example, above the steel main girder, the transverse reinforcement is made of high bond bars with a 20 mm diameter for the upper layer, and of high bond bars with a 16 mm diameter for the lower layer with a spacing $s = 170 \text{ mm}$, i.e. $A_s/s = 30.3 \text{ cm}^2/\text{m}$. The previous criterion is thus verified:

$$A_s/s \geq \frac{v_{Ed} h_f}{f_{yd} \cotan \theta_f} = 0.81 / (435 \times 1.25) = 14.9 \text{ cm}^2/\text{m}$$

The second criterion is also verified for the shear plane a-a:

$$v_{Ed} = 2.03 \text{ MPa} \leq v \cdot f_{cd} \cdot \sin \theta_f \cdot \cos \theta_f = 6.02 \text{ MPa}.$$

A minimum reinforcement area of 14.9 cm²/m should be put in the concrete slab in order to prevent the longitudinal shear failure for the surface a-a.

Failure in shear plane b-b

The verification is made in the same way as for shear plane a-a, taking for h_f the total developed length of b-b. The longitudinal shear force per unit length applied in the shear plane b-b is equal to 1.4 MN/m. The length of this shear surface is calculated by encompassing the studs as closely as possible within 3 straight lines (see Fig. 5.10(a)):

$$h_f = 2h_{sc} + b_0 + \phi_{head} = 2 \times 0.200 + 0.75 + 0.035 = 1.185 \text{ m}.$$

The shear stress for the surface b-b of shear failure is equal to:

$$v_{Ed} = 1.4/1.185 = 1.18 \text{ MPa}$$

For the design example, only the second criterion is satisfied:

$$A_s/s \geq \frac{v_{Ed} h_f}{f_{yd} \cot \theta_f} = 1.4/(435 \times 1.25) = 25.75 \text{ cm}^2/\text{m}$$

$$v_{Ed} = 1.18 \text{ MPa} \leq v \cdot f_{cd} \cdot \sin \theta_f \cdot \cos \theta_f = 6.02 \text{ MPa}$$

$A_s/s = 23.65 \text{ cm}^2/\text{m}$ (two layers of high bond bars with a 16 mm diameter and a spacing $s = 170 \text{ mm}$) does not satisfy the first criterion. Additional reinforcement is needed in areas close to the piers where the shear force per unit length is greater than 1.29 MN/m.

5.2.2.9 Interaction between longitudinal shear stress and transverse bending moment

The traffic load models are such that they can be arranged on the pavement to provide a maximum longitudinal shear flow and a maximum transverse bending moment simultaneously. EN1992-2, 6.2.4(105), sets the following rules to take account of this concomitance:

- the criterion for preventing the crushing in the compressive struts (see paragraph 5.2.2.8) is verified with a height h_f reduced by the depth of the compressive zone considered in the transverse bending assessment (as this concrete is worn out under compression, it cannot simultaneously take up the shear stress);
- the total reinforcement area should be not less than $A_{flex} + A_{shear}/2$ where A_{flex} is the reinforcement area needed for the pure bending assessment and A_{shear} is the reinforcement area needed for the pure longitudinal shear flow. Eurocode 2 does not specify how to distribute the final total reinforcement area between the two layers.

Crushing of the compressive struts

Paragraph 5.2.2.8 above notes that the compression in the struts is much lower than the limit. The reduction in h_f is not a problem therefore.

- shear plane a-a:

$$h_{f,red} = h_f - x_{ULS} = 0.40 - 0.05 = 0.35 \text{ m}$$

$$v_{Ed,red} = v_{Ed} \cdot h_f/h_{f,red} = 0.57/0.35 = 1.63 \text{ MPa} \leq 6.02 \text{ MPa}$$

- shear plane b-b:

$$h_{f,red} = h_f - 2x_{ULS} = 1.185 - 2 \times 0.05 = 1.085 \text{ m}$$

$$v_{Ed,red} = v_{Ed} \cdot h_f / h_{f,red} = 1.4 / 1.085 = 1.29 \text{ MPa} \leq 6.02 \text{ MPa}$$

Total reinforcement area

The question of adding reinforcement areas is only raised for the shear plane a-a where the upper transverse reinforcement layer is provided for both the transverse bending moment and the longitudinal shear flow.

For the longitudinal slab section above the steel main girder, the minimum reinforcement area $A_{flex,sup}$ required by the transverse bending assessment at ULS is equal to 18,1 cm²/m (see paragraph 5.2.2.3). The minimum reinforcement area A_{shear} required by the longitudinal shear flow is equal to 14.9 cm²/m.

In general terms, it should be verified that:

$$A_{sup} \geq A_{flex,sup}$$

$$A_{inf} \geq A_{flex,inf}$$

$$A_{inf} + A_{sup} \geq \max \{ A_{shear} ; A_{shear}/2 + A_{flex,sup} ; A_{shear}/2 + A_{flex,inf} \}$$

For the design example, the criterion is satisfied:

$$A_{flex,sup} = 18.1 \text{ cm}^2/\text{m} ; A_{flex,inf} = 0 ; A_{shear} = 14.9 \text{ cm}^2/\text{m}$$

$$A_{shear}/2 + A_{flex,sup} = 14.9/2 + 18.1 = 25.6 \leq A_{inf} + A_{sup} = 30.3 \text{ cm}^2/\text{m}$$

$$A_{shear}/2 + A_{flex,inf} = 14.9/2 = 7.5 \leq A_{inf} + A_{sup} = 30.3 \text{ cm}^2/\text{m}$$

$$A_{shear} = 14.9 \leq A_{inf} + A_{sup} = 30.3 \text{ cm}^2/\text{m}$$

If these conditions are not satisfied, a more refined method given in annex MM may be used.

5.2.2.10 ULS of fatigue under transverse bending

For this verification, the slow lane is assumed to be close to the parapet and the fatigue load is centred on this lane.

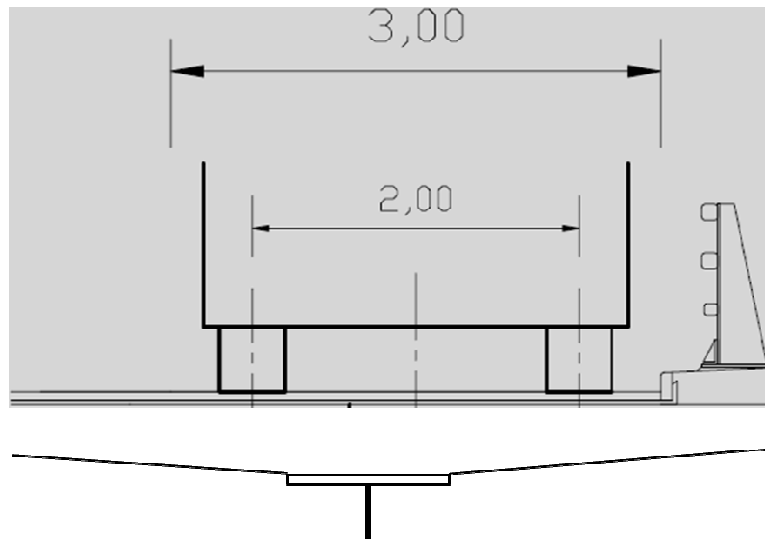


Fig. 5.12 Position of the slow lane

Fatigue load model FLM3 is used. Verifications are performed by the damage equivalent stress range method (EN1992-1-1, 6.8.5 and EN1992-2, Annex NN).

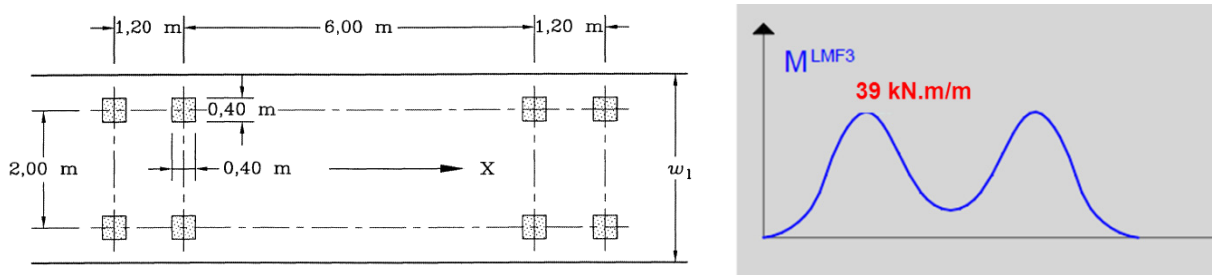


Fig. 5.13 Load model FLM3 (axle loads 120 kN) – Variation of bending moment.

The variation of the transverse bending moment in the section above the main steel girder during the passage of FLM3 is calculated using a finite element model of the slab. The moment variation is equal to 39 kNm/m. The corresponding stress range in the reinforcement is calculated assuming a cracked cross section (even if under permanent loads, the section may be considered as uncracked):

$$\Delta\sigma_s(\text{FLM3}) = 63 \text{ MPa}$$

The damage equivalent stress range method is defined in EN1992-1-1, 6.8.5 and the procedure for road traffic load on bridges is detailed in EN1992-2, Annex NN.

Adequate fatigue resistance of the reinforcing (or prestressing) steel should be assumed if the following expression is satisfied:

$$\gamma_{F,\text{fat}} = \Delta\sigma_{S,\text{eq}}(N^*) \leq \frac{\Delta\sigma_{Rsk}(N^*)}{\gamma_{F,\text{fat}}}$$

where:

$\Delta\sigma_{Rsk}(N^*)$ is the stress range at N^* cycles from the appropriate S-N curve in Figure 6.30. For reinforcement made of straight or bent bars, $\Delta\sigma_{Rsk}(N^*) = 162.5 \text{ MPa}$ (EN1992-1-1, table 6.3N)

$\Delta\sigma_{S,\text{eq}}(N^*)$ is the damage equivalent stress range for the reinforcement and considering the number of loading cycles N^* .

$\gamma_{F,\text{fat}}$ is the partial factor for fatigue load (EN1992-1-1, 2.4.2.3). The recommended value is 1.0

$\gamma_{s,\text{fat}}$ is the partial factor for reinforcing steel (EN1992-1-1, 2.4.2.4). The recommended value is 1.15.

The equivalent damage stress range is calculated according to EN1992, Annex NN, NN.2.1:

$$\Delta\sigma_{s,\text{equ}} = \Delta\sigma_{s,\text{Ec}} \cdot \lambda_s$$

where

○ $\Delta\sigma_{s,\text{Ec}} = \Delta\sigma_s(1.4 \text{ FLM3})$ is the stress range due to 1.4 times FLM3. In the case of pure bending, it is equal to $1.4\Delta\sigma_s(\text{FLM3})$. For a verification of fatigue on intermediate supports of continuous bridges, the axle loads of FLM3 are multiplied by 1.75.

○ λ_s is the damage coefficient.

$$\lambda_s = \phi_{\text{fat}} \cdot \lambda_{s,1} \cdot \lambda_{s,2} \cdot \lambda_{s,3} \cdot \lambda_{s,4}$$

where

○ ϕ_{fat} is a dynamic magnification factor

- $\lambda_{s,1}$ takes account of the type of member and the length of the influence line or surface
- $\lambda_{s,2}$ takes account of the volume of traffic
- $\lambda_{s,3}$ takes account of the design working life
- $\lambda_{s,4}$ takes account of the number of loaded lanes.

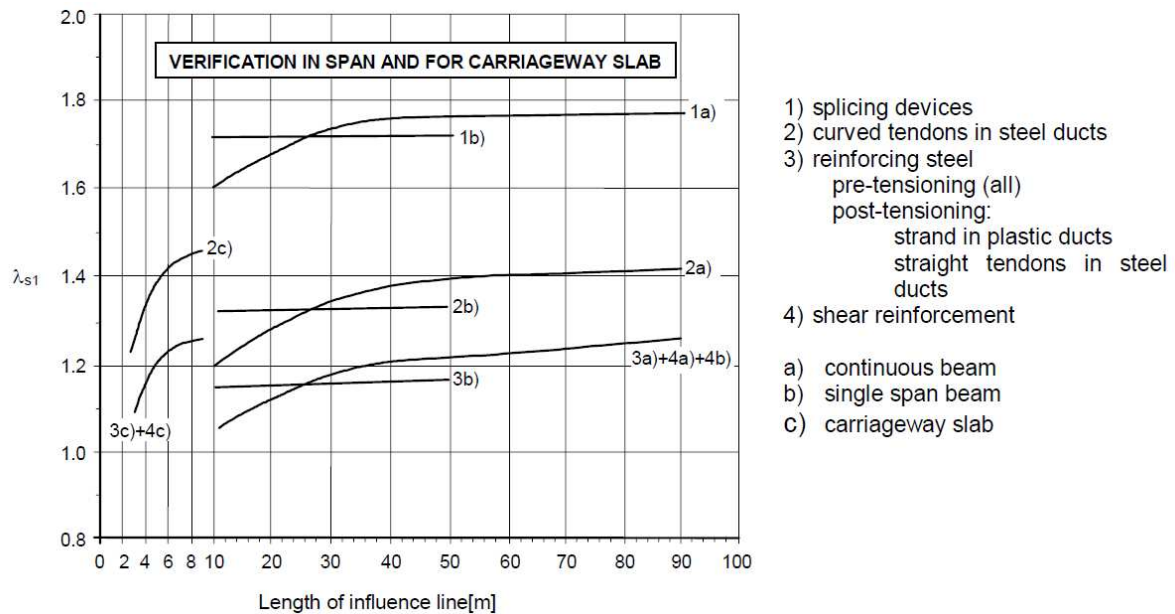


Fig. 5.14 $\lambda_{s,1}$ value for fatigue verification (EN1992-2, Figure NN.2)

$\lambda_{s,1}$ is given by figure NN.2, curve 3c). In the design example, the length of the influence line is 2,5 m. Therefore, $\lambda_{s,1} \approx 1.1$

$$\lambda_{s,2} = \bar{Q}^{k_2} \sqrt{\frac{N_{obs}}{2.0}} \quad (\text{expression NN.103})$$

where

- N_{obs} is the number of lorries per year according to EN1991-2, Table 4.5
- k_2 is the slope of the appropriate S-N line to be taken from Tables 6.3N and 6.4N of EN1992-1-1
- \bar{Q} is a factor for traffic type according to Table NN.1 of EN1992-2

\bar{Q} - factor for	Traffic type (see EN 1991-2 Table 4.7)		
	Long distance	Medium distance	Local traffic
$k_2 = 5$	1.0	0.90	0.73
$k_2 = 7$	1.0	0.92	0.78
$k_2 = 9$	1.0	0.94	0.82

Fig. 5.15 Factors for traffic types (Table NN.1 of EN1992-2)

For the design example: $k_2 = 9$ (Table 6.3N); $N_{obs} = 0.5 \times 10^6$ (EN1991-2, Table 4.5), assuming medium distance traffic: $\bar{Q} = 0.94$

Finally: $\lambda_{s,2} = 0.81$

$\lambda_{s,3} = 1$ (design working life = 100 years)

$\lambda_{s,4} = 1$ (different from 1 if more than one lane are loaded)

$\varphi_{fat} = 1.0$ except for the areas close to the expansion joints where $\varphi_{fat} = 1.3$

It comes:

$$\lambda_s = 0.89 \quad (1.16 \text{ near the expansion joints})$$

$$\Delta\sigma_{s,Ec} = 1.4 \times 63 = 88 \text{ MPa}$$

Then:

$$\Delta\sigma_{s,eq} = 78 \text{ MPa (102 MPa near the expansion joints)}$$

$$\Delta\sigma_{Rsk}/\gamma_{s,fat} = 162.5/1.15 = 141 \text{ MPa} > 102 \text{ MPa}$$

The resistance of reinforcement to fatigue under transverse bending is verified. Generally, for transverse bending of road bridge slabs, ULS of resistance is more unfavourable than ULS of fatigue.

Note

In addition, EN1992-2, 6.8.7, requires fatigue verification for concrete under compression. The verification should be made using traffic data (6.8.7(101)) or by a simplified method (6.8.7(2)). In this case, the condition to satisfy is:

$\sigma_{c,max}/f_{cd,fat} \leq 0.5 + 0.45 \sigma_{c,min}/f_{cd,fat}$ (Expression 6.77) where $\sigma_{c,max}$ and $\sigma_{c,min}$ are the maximum and minimum compressive stresses in a fibre under frequent combination of actions. $f_{cd,fat}$ is the design fatigue strength of concrete, given by Expression 6.76:

$f_{cd,fat} = k_1 \beta_{cc}(t_0) f_{cd} (1 - f_{ck}/250)$ where $k_1 = 0.85$ (recommended value) and t_0 is the time at the beginning of the cyclic loading.

For the design example, depending on t_0 , $\beta_{cc}(t_0)$ is lying between 1,1 and 1,2 and $f_{cd,fat}$ is between 16 and 17.5 MPa. The maximum and minimum compressive stresses on the lower fibre – calculated in the cracked section with a modular ratio equal to 5.9 – are 11.9 MPa and 3.5 MPa. The condition is not satisfied. However, this condition is very conservative and does not represent the effects of cyclic traffic load: the effects of the frequent traffic loads are much more aggressive than those of fatigue traffic loads. Moreover, the design fatigue strength is based on f_{cd} , calculated with the recommended value of α_{cc} , equal to 0.85 in EN1992-2. It seems to be no reason to take this value – relevant for long term loading – for fatigue verifications (with $\alpha_{cc} = 1$ and $\beta_{cc}(t_0) = 1,2$ the condition given by Expr.6.77 is satisfied).

For concrete fatigue verification, there is no method of damage equivalent stress range as for reinforcement. Such a method, intermediate between the rough and conservative condition of Expr.6.77 and a more sophisticated method using traffic data, would be useful.

5.2.3 LONGITUDINAL REINFORCEMENT VERIFICATIONS

5.2.3.1 Resistance for local bending – Adding local and global bending effect

The local longitudinal bending moment at ULS in the middle of the concrete slab – halfway between the structural steel main girders – is equal to $M_{loc} = 90 \text{ kN.m/m}$. It causes compression in the upper longitudinal reinforcement layer (just below the contact surface of a wheel, for example).

The internal forces and moments from the longitudinal global analysis at ULS cause tensile stresses in the reinforcement for the composite cross-section at support P1 which are equal to $\sigma_{s,sup} = 190$

MPa in the upper layer and to $\sigma_{s,inf} = 166$ MPa in the lower layer (see Figure 6.6 in the chapter “Composite bridge design”). The corresponding values for the internal forces and moments in the concrete slab are:

$$\begin{aligned}
 N_{glob} &= A_{s,sup}\sigma_{s,sup} + A_{s,inf}\sigma_{s,inf} \\
 &= 24.2 \text{ cm}^2/\text{m} \times 190 \text{ MPa} + 15.5 \text{ cm}^2/\text{m} \times 166 \text{ MPa} = 715 \text{ kN/m} \\
 M_{glob} &= -A_{s,sup}\sigma_{s,sup}(h/2 - d_{sup}) + A_{s,inf}\sigma_{s,inf}(d_{inf} - h/2) \\
 &= -24.2 \text{ cm}^2/\text{m} \times 171 \text{ MPa} \times (308/2 - 60) \text{ mm} + 15.5 \text{ cm}^2/\text{m} \times 149 \text{ MPa} \times (240 - 308/2) \text{ mm} \\
 &= -21 \text{ kNm/m} \\
 &(\text{d}_{sup} \text{ and } \text{d}_{inf} \text{ are the distance of the upper layer – resp. lower layer – to the top face of the slab})
 \end{aligned}$$

The longitudinal reinforcement around support P1 should be designed for these local and global effects. The local (M_{loc}) and global (N_{glob} and M_{glob}) effects should be combined according to Annex E to EN1993-2. The following combinations should be taken into account:

$$(N_{glob} + M_{glob}) + \psi M_{loc} \text{ and } M_{loc} + \psi (N_{glob} + M_{glob})$$

where ψ is a combination factor equal to 0.7 for spans longer than 40 m.

First combination: $(N_{glob} + M_{glob}) + \psi M_{loc}$

$$N = N_{glob} = 715 \text{ kN/m}$$

$$M = M_{glob} + \psi M_{loc} = -21 + 0.7 \times 90 = 42 \text{ kN.m/m}$$

The slab is fully in tension for this first combination and the tensile stresses in the upper and lower reinforcement layers (resp. 190 MPa and 166 MPa for N_{glob} alone) become:

$$\sigma_{s,sup} = 45 \text{ MPa}$$

$$\sigma_{s,inf} = 392 \text{ MPa}$$

which remain less than $f_{sd} = 435$ MPa.

Second combination: $M_{loc} + \psi (N_{glob} + M_{glob})$

$$N = \psi N_{glob} = 0.7 \times 715 = 501 \text{ kN/m}$$

$$M = M_{loc} + \psi M_{glob} = 90 + 0.7 \times (-21) = 75 \text{ kNm/m}$$

The top fibre of the slab is in compression for this second combination and the tensile stress in the lower reinforcement layer is equal to:

$$\sigma_{s,inf} = 386 \text{ MPa}$$

which remains less than $f_{yd} = 435$ MPa.

Note that this verification governs the design of the longitudinal reinforcement at internal support. For this reason, there are advantages in designing a strong longitudinal reinforcement lower layer at support (nearly half the total area) in case of a two-girder bridge with cross-girders.

5.2.3.2 Shear stress for the transverse joint surfaces between slab concreting segments

As the slab is concreted in several steps, it should be verified that the shear stress can be transferred through the joint interface between the slab concreting segments, according to EN1992-1-1, 6.2.5(1), it should be verified that:

$$v_{Ed,i} \leq v_{Rd,i} = \min \{ c f_{ctd} + \mu \sigma_n + \mu \rho f_{yd} ; 0.5 v_{fcd} \}$$

where

- $v_{Ed,i}$ is the design value of the shear stress at the joint interface,
- σ_n is the normal stress at the interface (negative for tension),
- ρ is the reinforcement ratio of longitudinal high bond bars holding the interface (assumed to be perpendicular to the interface plane),
- μ , c are parameters depending on the roughness quality for the interface. In case of interface in tension $c = 0$.
- $v = 0.6(1 - f_{ck}/250)$ with f_{ck} in MPa (strength reduction factor for the concrete cracked in shear).

The shear stresses at the interface are small (in the order of 0.2 MPa). But applying the formula directly can cause problems as it gives $v_{Rd,i} < 0$ as soon as $\sigma_n + \rho f_{yd} < 0$ i.e. $\sigma_n < -1.19\% \times 435 \text{ MPa} = -5.18 \text{ MPa}$ in the design example. The ULS stress calculation assuming an uncracked behaviour of the composite cross-sections shows that this tensile stress is exceeded on piers.

In fact, as the slab is cracked at ULS, $A_c \sigma_n$ should be taken as equal to the tensile force in the longitudinal reinforcement of the cracked cross-section, i.e.:

$$\sigma_n = - (A_{s,sup} \sigma_{s,sup} + A_{s,inf} \sigma_{s,inf}) / A_c$$

(as this involves ULS calculations, the tension stiffening effects are not taken into account)

In the design example, the following is obtained for the joint interface closest to the cross-section at support P1:

$$\sigma_n = - 0.73\% \times 190 \text{ MPa} - 0.46\% \times 166 \text{ MPa} = - 2.15 \text{ MPa}$$

The shear resistance $v_{Rd,i}$ is deduced:

$$v_{Rd,i} = \mu(\sigma_n + \rho f_{yd}) = \mu(-2.15 + 5.18) = \mu 3.24 \text{ MPa}$$

$\mu = 0.7$ if a good roughness quality is assumed at the interface. Hence $v_{Rd,i} = 2.27 \text{ MPa}$. The resistance to shear at the joint interface is thus verified.

5.2.4 PUNCHING SHEAR (ULS)

5.2.4.1 Rules for a composite bridge slab

The punching shear verification is carried out at ULS. It involves verifying that the shear stress caused by a concentrated vertical load applied on the deck remains acceptable for the concrete slab. If appropriate, it could be necessary to add shear reinforcement in the concrete slab.

This verification is carried out by using the single wheel of the traffic load model LM2 which represents a much localized vertical load.

Control perimeter around loaded areas

The diffusion of the vertical load through the concrete slab depth induces a distribution of the load on a larger surface. To take account of this favourable effect, EN1992-1-1 defines reference control perimeters. It is thus assumed that the load is uniformly distributed in the area within this perimeter u_1 (see Fig. 5.16).

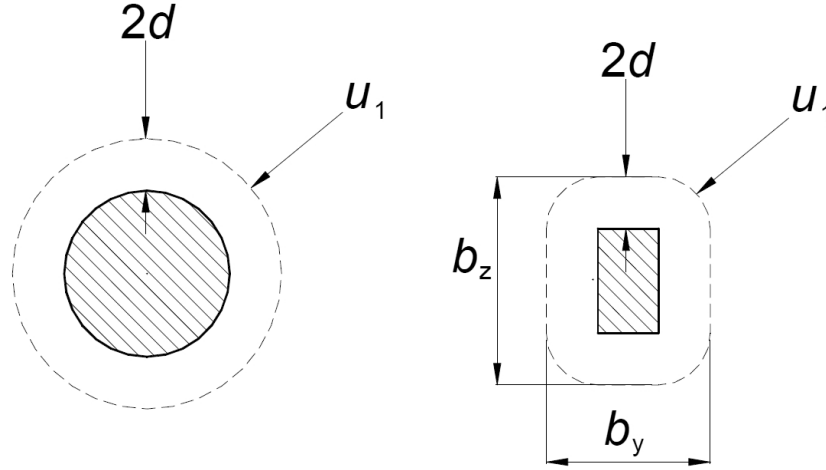


Fig. 5.16 Reference control perimeters

d is the mean value of the effective depths of the reinforcement in longitudinal and transverse directions of the slab – vertical distance between the lower reinforcement layer in tension and the contact surface of the wheel – noted respectively d_y and d_z : $d = (d_y + d_z)/2$

Note that the load diffusion is considered not only over the whole depth of the concrete slab, but also at 45° through the thickness of the asphalt and the waterproofing layers. Thus, the reference control perimeter should take account of these additional depths (i.e. $8+3 = 11$ cm).

Design value of the shear stress v_{Ed} around the control perimeter

The vertical load is applied on a shear surface $u_1 d$ in the concrete slab. The shear stress is then given by:

$$v_{Ed} = \beta \frac{V_{Ed}}{u_1 d}$$

where:

- V_{Ed} is the punching shear force
- β is a factor representing the influence of an eventual load eccentricity on the pavement (boundary effects); $\beta = 1$ is taken in case of a centered load.

Shear resistance $v_{Rd,c}$ of the concrete

The shear resistance of the slab without shear reinforcement is given by EN1992-1-1, 6.4.4(1) and is equal to:

$$v_{Rd,c} = \max \{ (C_{Rd,c} k (100 \rho f_{ck})^{1/3} + k_1 \sigma_{cp}) ; v_{min} + k_1 \sigma_{cp} \}$$

where:

- f_{ck} is in MPa
- $k = 1 + \sqrt{\frac{200}{d}} \leq 2.0$ with d in mm
- $\rho = \sqrt{\rho_{ly} \rho_{lz}} \leq 0.02$ is the ratio of reinforcement in tension (lower layer) in the two orthogonal directions y and z

$$\sigma_{cp} = \frac{\sigma_{cy} + \sigma_{cz}}{2} \text{ with a minimum value of } -1.85 \text{ MPa (EN1994-2, 6.2.2.5(3))}$$

In the concrete slab of a composite bridge, around an internal support, there is no tension in the transverse direction but the tensile stress is very high in the longitudinal direction (about -9 MPa for the design example). This gives thus:

$$\sigma_{cp} = \max(\sigma_{c,long}/2; -1.85) = -1.85 \text{ MPa}$$

The values for $C_{Rd,c}$ and k_1 can be provided by the National Annex to EN1994-2. The recommended values are (EN1994-2, 6.2.2.5(3), note):

$$\begin{aligned} \circ \quad C_{Rd,c} &= 0.15/\gamma_c = 0.10 \\ \circ \quad k_1 &= 0.12 \end{aligned}$$

These values are different from those recommended by EN1992-1-1 ($0.18/\gamma_c$ and 0.1). It will be seen that the note in EN1994-2, 6.2.2.5(3), only relates to concrete flanges in tension ($\sigma_{cp} < 0$) as part of a steel/concrete composite structural beam, which is the case here in the longitudinal direction. In case of a concrete slab under bending moment or compression, the values for $C_{Rd,c}$ and k_1 would have been provided by the National Annex to EN1992-1-1. See also paragraph 5.2.2.7.

$$\circ \quad v_{min} = 0.035 k^{3/2} f_{ck}^{1/2}$$

5.2.4.2 Design example

The vertical load induced by the single wheel of the traffic load model LM2 is equal to:

$$V_{Ed} = \gamma_Q \beta_Q Q_{ak}/2 = 1.35 \times 1.00 \times 400/2 = 270 \text{ kN}$$

Its contact surface is a rectangular area of $0.35 \times 0.6 \text{ m}^2$.

To calculate the depth d , the wheel of LM2 is put along the outside edge of the pavement on the cantilever part of the slab. The centre of gravity of the load surface is therefore at $0.5 + 0.6/2 = 0.8 \text{ m}$ from the free edge of the slab. At this location, the slab thickness to consider is equal to 0.30 m . Hence:

$$d = 0.5 \cdot [(0.30 - 0.035 - 0.016/2) + (0.30 - 0.035 - 0.016 - 0.016/2)] = 0.249 \text{ m}$$

The reference control perimeter is defined following the contact surface dimensions.

$$u_1 = 2(0.35 + 0.6 \times 4 \times 0.11) + 4\pi d = 5.91 \text{ m is obtained.}$$

The shear stress along this control perimeter is then equal to:

$$v_{Ed} = \beta \frac{V_{Ed}}{u_1 d} = 0.18 \text{ MPa (with } \beta = 1)$$

The design value of the resistance to punching shear is as follows:

$$\rho_1 = \sqrt{\rho_y \rho_z} = \sqrt{0.394\% \cdot 0.52\%} = 0.45\%$$

$$k = 1 + \sqrt{\frac{200}{249}} = 1.90 \leq 2.0$$

$$\sigma_{cp} = -1.85 \text{ MPa}$$

$$C_{Rd,c} = 0.10$$

$$k_1 = 0.12$$

$$C_{Rd,c} k (100 \rho_1 f_{ck})^{1/3} = 0.48 \text{ MPa}$$

$$v_{min} = 0.035 \times 1.90^{3/2} \times 35^{1/2} = 0.54 \text{ MPa} > 0.48 \text{ MPa}$$

$$v_{Rd,c} = v_{min} + k_1 \sigma_{cp} = 0.32 \text{ MPa}$$

The punching shear is thus verified:

$$v_{Ed} = 0.18 \text{ MPa} \leq v_{Rd,c} = 0.32 \text{ MPa}.$$

There is no need to add shear reinforcement in the concrete slab.

5.3 Second order effects in the high piers

5.3.1 MAIN FEATURES OF THE PIERS

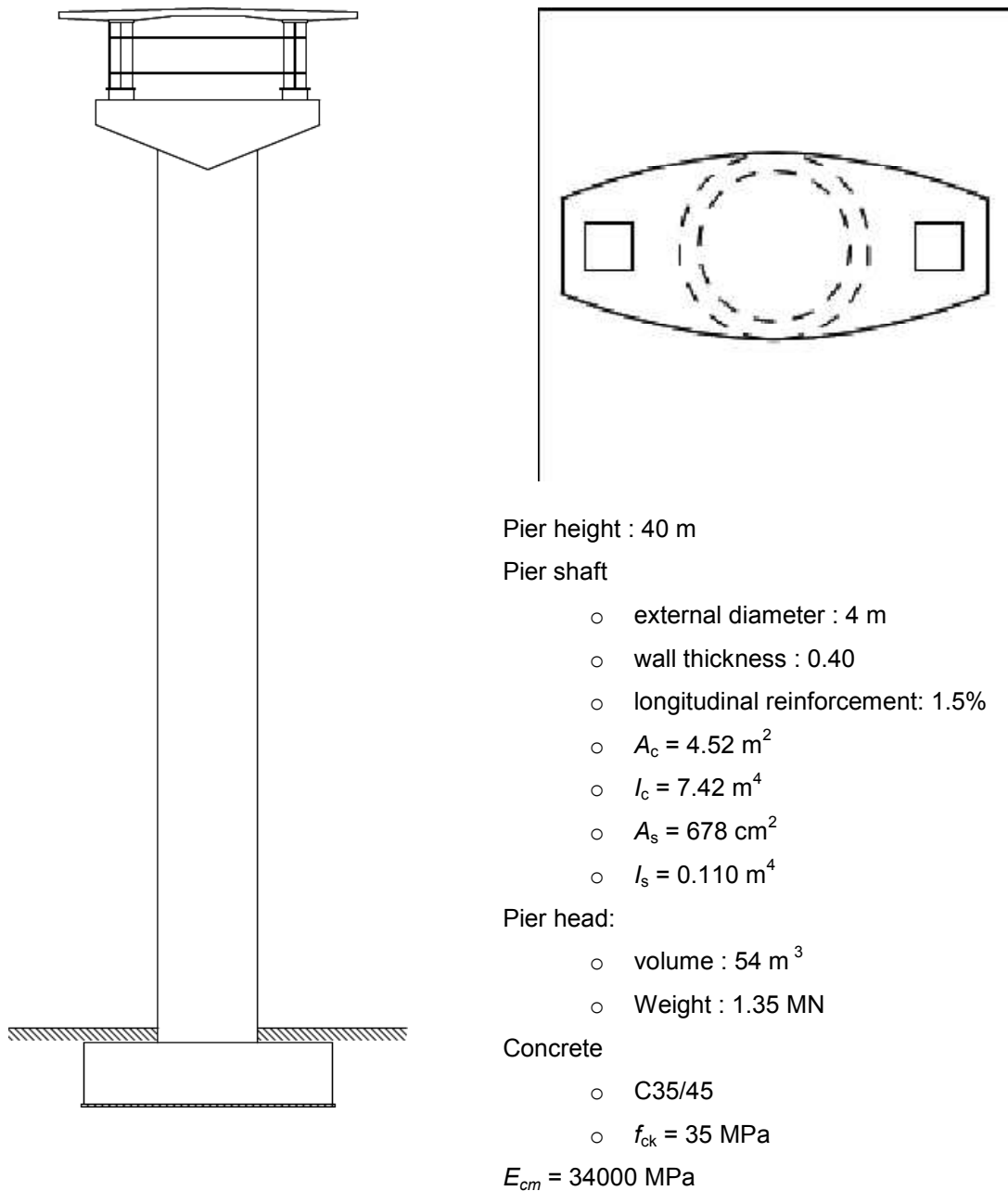


Fig.5.17 Main features of the high piers

I_c is the uncracked inertia of the pier shaft, I_s is the second moment of area of the reinforcement about the centre of area of the concrete cross-section.

5.3.2 FORCES AND MOMENTS ON TOP OF THE PIERS

Forces and moments on top of the piers are calculated assuming that the inertia of the piers is equal to 1/3 of the uncracked inertia.

Two ULS combinations are taken into account:

- Comb 1: $1.35G + 1.35(UDL + TS) + 1.5(0.6F_{wkT})$ (transverse direction)
- Comb 2: $1.35G + 1.35(0.4UDL + 0.75TS + \text{braking}) + 1.5(0.6T_k)$ (longitudinal direction)

Table 5.3 Forces and moments on top of piers

	F_z (vertical)	F_y (trans.)	F_x (long.)	M_x (trans.)
G	14.12 MN	0	0	0
UDL	3.51 MN	0	0	8.44 MN.m
TS	1.21 MN	0	0	2.42 MN.m
Braking	0	0	0.45 MN	0
F_{wkT} (wind on traffic)	0	0.036 MN	0	0.11 MN.m
T_k	0	0	0.06 MN	0
Comb 1	25.43 MN	0.032 MN	0	14.76 MN.m
Comb 2	22.18 MN	0	0.66 MN	7.01 MN.m

5.3.3 SECOND ORDER EFFECTS

The second order effects are analysed by a simplified method: EN1992-1-1, 5.8.7 - method based on nominal stiffness. For the design example, the analysis is performed only in longitudinal direction.

Geometric imperfection (EN1992-2, 5.2(105)):

- $\vartheta_l = \vartheta_0 \alpha_h$

where

$\vartheta_0 = 1/200$ (recommended value)

$\alpha_h = 2/l^{1/2}$; $\alpha_h \leq 1$

l is the height of the pier = 40 m

- $\vartheta_l = 0.0016$ resulting in a moment under permanent combination
 $M_{0Eqp} = 1.12 \text{ MNm}$ at the base of the pier

First order moment at the base of the pier:

- $M_{0Ed} = 1.35 M_{0Eqp} + 1.35 F_z (0.4UDL + 0.75TS) / \vartheta_l + 1.35 F_x(\text{braking}) / + 1.5(0.6F_x(T_k)) /$

$M_{0Ed} = 28.2 \text{ MNm}$

- Effective creep ratio (EN 1992-1-1, 5.8.4 (2)):

$$\varphi_{\text{ef}} = \varphi_{(\infty, t_0)} \cdot M_{0\text{Eqp}} / M_{0\text{Ed}}$$

where:

$\varphi_{(\infty, t_0)}$ is the final creep coefficient according to 3.1.4

$M_{0\text{Eqp}}$ is the first order bending moment in quasi-permanent load combination (SLS)

$M_{0\text{Ed}}$ is the first order bending moment in design load combination (ULS)

$$\varphi_{\text{ef}} = 2 (1.12/28.2) = 0.08$$

Nominal stiffness (EN1992-1-1, 5.8.7.2 (1))

$$EI = K_c E_{\text{cd}} I_c + K_s E_s I_s \quad (\text{Expression 5.21})$$

where:

E_{cd} is the design value of the modulus of elasticity of concrete, see 5.8.6 (3)

I_c is the moment of inertia of concrete cross section

E_s is the design value of the modulus of elasticity of reinforcement, 5.8.6 (3)

I_s is the second moment of area of reinforcement, about the centre of area of the concrete

K_c is a factor for effects of cracking, creep etc, see 5.8.7.2 (2) or (3)

K_s is a factor for contribution of reinforcement, see 5.8.7.2 (2) or (3)

The expression (5.21) is the sum of the full stiffness of the reinforcement ($K_s = 1$) and of the reduced stiffness of the concrete, function of the axial force and of the slenderness of the pier.

In the design example:

$$E_{\text{cd}} = E_{\text{cm}} / \gamma_{\text{cE}} = 34000 / 1.2 = 28300 \text{ MPa}$$

$$I_c = 7.42 \text{ m}^4$$

$$E_s = 200000 \text{ MPa}$$

$$I_s = 0.110 \text{ m}^4$$

$$K_s = 1$$

K_c is given by the following expression

$$K_c = k_1 k_2 / (1 + \varphi_{\text{ef}})$$

where:

ρ is the geometric reinforcement ratio, A_s/A_c

A_s is the total area of reinforcement

A_c is the area of concrete section

φ_{ef} is the effective creep ratio, see 5.8.4

k_1 is a factor which depends on concrete strength class, Expression (5.23)

k_2 is a factor which depends on axial force and slenderness, Expression (5.24)

$$k_1 = \sqrt{f_{\text{ck}}/20} \text{ (MPa)}$$

$$k_2 = n \cdot \frac{\lambda}{170} \leq 0.20$$

where:

n is the relative axial force $N_{\text{Ed}}/(A_c f_{\text{cd}})$

λ is the slenderness ratio, see 5.8.3

In the design example:

$$\rho = 0.015$$

$$k_1 = 1.32$$

$$N_{Ed} = 22.18 \text{ MN}$$

$$n = 22.18 / (4.52 \cdot 19.8) = 0.25$$

$$\lambda = l_0 / i; \quad l_0 = 1.43 \cdot l = 57.20 \text{ m (taking into account the rigidity of the second pier)}; \quad i = (I_c / A_c)^{0.5} = 1.28 \text{ m}$$

l_0 is the effective length of the elastic buckling mode. It is calculated taking into account the restraints at the end of the column. Here, the pier is assumed to have a full restraint at the bottom. Due to the presence of the other pier, there is an elastic restraint for the horizontal displacement at the top. This can be modeled by a spring which stiffness is equal to $3EI/l^3$ (taking the same EI for both piers). In the longitudinal direction, the rotation is free at the top of the pier.

$$\lambda = 45$$

$$k_2 = 0.25 \cdot (45/170) = 0.066$$

$$K_c = 1.32 \times 0.066 / 1.08 = 0.081$$

$$EI = 39200 \text{ MN.m}^2 \quad (\approx EI_{\text{uncracked}}/6)$$

Moment magnification factor (EN 1992-1-1, 5.8.7.3)

(1) The total design moment, including second order moment, may be expressed as a magnification of the bending moments resulting from a linear analysis, namely:

$$M_{Ed} = M_{0Ed} \left[1 + \frac{\beta}{(N_B / N_{Ed}) - 1} \right] \quad (5.28)$$

where:

- M_{0Ed} is the first order moment; see also 5.8.8.2 (2)
- β is a factor which depends on distribution of 1st and 2nd order moments, see 5.8.7.3 (2)-(3)
- N_{Ed} is the design value of axial load
- N_B is the buckling load based on nominal stiffness

(2) For isolated members with constant cross section and axial load, the second order moment may normally be assumed having a sine-shaped distribution. Then

$$\beta = \pi^2 / c_0 \quad (5.29)$$

In the design example, $c_0 = 12$, assuming a triangular distribution of the first order moment. Then:

$$M_{0Ed} = 28.2 \text{ MN.m}$$

$$\beta = 0.85 \quad (c_0 = 12)$$

$$N_B = \pi^2 EI / l_0^2 = 118 \text{ MN}$$

$$N_{Ed} = 26 \text{ MN (mean value on the height of the pier)}$$

Finally, the moment magnification factor is equal to 1.23, and:

$$M_{Ed} = 1.23 M_{0Ed} = 33.3 \text{ MN.m}$$

This method gives a safe design of the piers, but it is possible that the longitudinal displacements are overestimated. For a better assessment of the displacements, a general method, based on moment-curvature relationship is necessary.

CHAPTER 6

Composite bridge design (EN1994-2)

Miguel ORTEGA CORNEJO

Project Manager. IDEAM S.A.

Prof. at University “Europea de Madrid”. Spain.

Joël RAOUL

Assistant to the Director of Large Bridge Division. Sétra/CTOA

Prof. at “Ecole Nationale de Ponts et Chaussées”. Paris. France.

Convenor EN-1994-2

6.1 Verification of cross-section at mid-span P1-P2

6.1.1 GEOMETRY AND STRESSES

At mid-span P1-P2 in ULS the concrete slab is in compression across its whole thickness. Its contribution is therefore taken into account in the cross-section resistance. The stresses in Fig. 6.1 are subsequently calculated with the composite mechanical properties and obtained by summing the various steps whilst respecting the construction phases.

The internal forces and moments in this cross-section are: $M_{Ed} = 63.89 \text{ MN}\cdot\text{m}$, $V_{Ed} = 1.25 \text{ MN}$

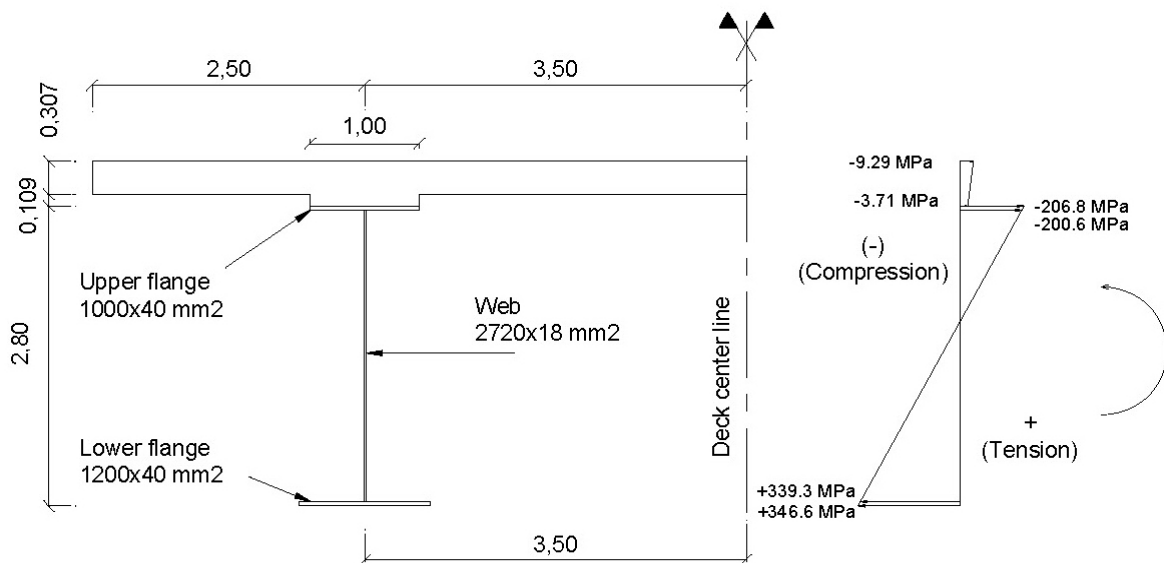


Fig. 6.1 Stresses at ULS in cross-section at mid-span P1-P2

Note: The sign criteria for stresses are according to EN-1994-2 (+) tension and (-) compression.

6.1.2 DETERMINING THE CROSS-SECTION CLASS (ACCORDING TO EN1994-2, 5.5.2)

Lower flange is in tension therefore it is Class 1. The upper flange is composite and connected following the recommendations of EN1994-2, 6.6, therefore it is Class 1.

To classify the steel web, the position of the Plastic Neutral Axis (PNA) is determined as follows:

- Design plastic resistance of the concrete in compression:

$$F_c = A_c \frac{0.85f_{ck}}{\gamma_c} = 1.9484 \times \frac{0.85 \cdot 35}{1.50} = 38.643 \text{ MN (force of } \frac{1}{2} \text{ slab)}$$

Note that the design compressive strength of concrete is $f_{cd} = \frac{f_{ck}}{\gamma_c}$ (EN-1994-2, 2.4.1.2).

EN-1994 differs from EN-1992-1-1, 3.1.6 (1), in which an additional coefficient α_{cc} is

applied: $f_{cd} = \frac{\alpha_{cc} \cdot f_{ck}}{\gamma_c}$. α_{cc} takes account of the long term effects on the compressive strength and of unfavourable effects resulting from the way the loads are applied.

The value for α_{cc} is to be given in each National annex. EN-1994-2 used the value 1.00, without permitting national choice for several reasons¹:

- The plastic stress block for use in resistance of composite sections, defined in EN-1994, 6.2.1.2 (figure 6.2) consist of a stress $0.85f_{cd}$ extending to the neutral axis, as shown in Figs. 6.2 and 6.3.

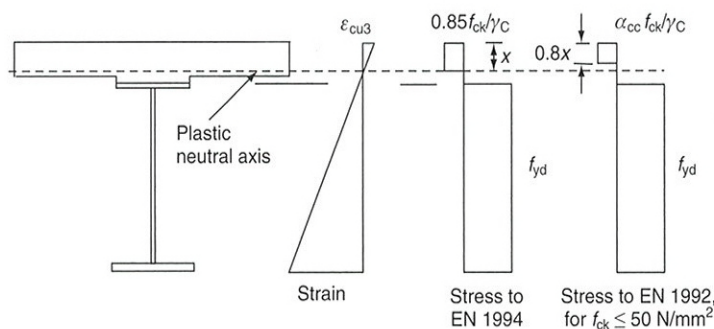


Fig. 6.2 Rectangular stress blocks for concrete in compression at ULS (figure 2.1 of¹)

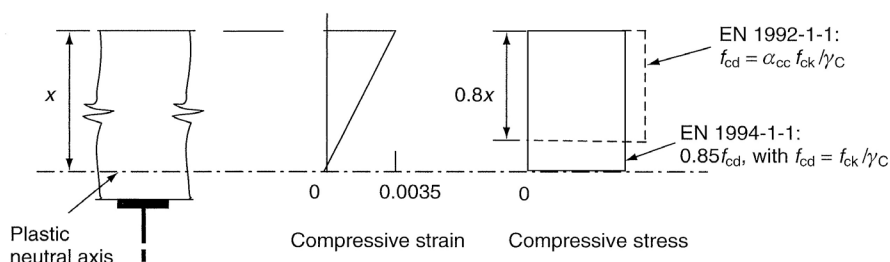


Fig 6.3 Detail of the stress block for concrete al ULS (figure 6.1 of¹)

- Predictions using the stress block of EN-1994 have been verified against the results for composite members conducted independently from the verifications for concrete bridges.
- The EN-1994 block is easier to apply. The Eurocode 2 rule for rectangular block (EN-1992-1-1, 3.1.7 (3)) was not used in Eurocode 4 because resistance formulae became complex where the neutral axis is close to or within the steel flange adjacent to concrete slab.
- Resistance formulae for composite elements given in EN-1994 are based on calibrations using stress block, with $\alpha_{cc}=1.00$.
 - o The reinforcing steel bars in compression are neglected.
 - o Design plastic resistance of the structural steel upper flange (1 flange):

¹ See "Designers' Guide to EN-1994-2. Eurocode 4: Design of composite steel and concrete structures. Part 2: General rules and rules for bridges", C.R. Hendy and R.P. Johnson

$$F_{s,uf} = A_{s,uf} \frac{f_{y,uf}}{\gamma_{M0}} = (1.0 \times 0.04) \times \frac{345}{1.0} = 13.80 \text{ MN}$$

Note that for the thickness $16 < t \leq 40 \text{ mm}$ $f_y = 345 \text{ MPa}$.

- Design plastic resistance of the structural steel web (1 web):

$$F_{s,w} = A_{s,w} \frac{f_{y,w}}{\gamma_{M0}} = (2.72 \times 0.018) \times \frac{345}{1.0} = 16.891 \text{ MN}$$

- Design plastic resistance of the structural steel lower flange (1 flange):

$$F_{s,lf} = A_{s,lf} \frac{f_{y,lf}}{\gamma_{M0}} = (1.20 \times 0.04) \times \frac{345}{1.0} = 16.56 \text{ MN}$$

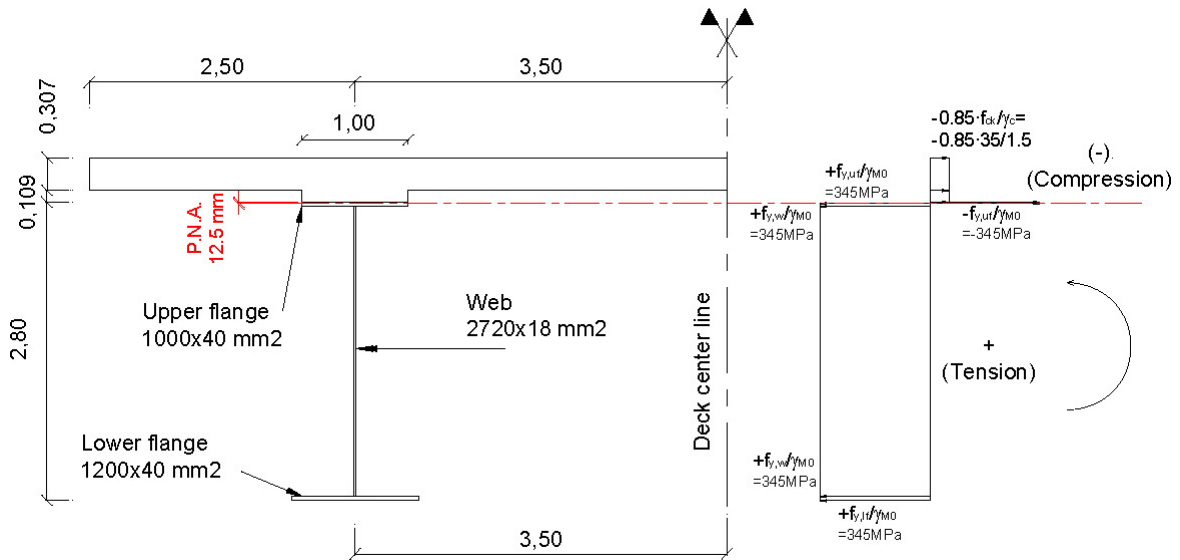


Fig. 6.4 Plastic neutral axis and design of plastic resistance moment at mid span P1-P2

As $|F_c| \leq |F_{s,uf}| + |F_{s,w}| + |F_{s,lf}|$ ($38.643 \leq 47.25$) and $|F_c| + |F_{s,uf}| \geq |F_{s,w}| + |F_{s,lf}|$ ($52.44 \geq 33.451$) it is concluded that the PNA is located in the structural steel upper flange at a distance x from the upper extreme fibre of this flange.

The internal axial forces equilibrium of the cross section leads to the location of the PNA:

$$-F_c - F_{s,uf} \cdot x + F_{s,uf} \cdot \frac{(0.04 - x)}{0.04} + F_{s,w} + F_{s,lf} = 0$$

$$-38.643 - 345 \cdot x + 13.8 - 345 \cdot x + 16.891 + 16.56 = 0 ; X = 0.0125 \text{ m} = 12.5 \text{ mm}$$

As the PNA is located in the upper steel flange (Fig. 6.4) the whole web and the bottom flange are in tension and therefore in Class 1 (EN-1993-1-1, 5.5.2)

Conclusion: The cross-section at mid-span P1-P2 is in Class 1 and is checked by a plastic section analysis.

This is what usually happens in composite bridges in sagging areas, with cross sections in class 1, with the PNA near or in the upper concrete slab, or at least in class 2, with only a small upper part of the compressed web.

6.1.3 PLASTIC SECTION ANALYSIS

6.1.3.1 Bending resistance check

The design plastic resistance moment is calculated from the position of the PNA according to EN1994-2, 6.2.1.2(1) (see Fig. 6.3):

$$M_{pl,Rd} = 38.643 \times (0.2505 + 0.0125) + (0.0125 \times 1.0) \times 345/1.0 \times (0.0125/2) + (0.0275 \times 1.0) \times (345/1.0) \times (0.0275/2) + 16.891 \times (0.0275 + 2.72/2) + 16.56 \times (0.0275 + 2.72 + 0.04/2)$$

$$M_{pl,Rd} = 79.59 \text{ MN}\cdot\text{m}$$

$M_{Ed} = 63.89 \text{ MN}\cdot\text{m} \leq M_{pl,Rd} = 79.59 \text{ MN}\cdot\text{m}$ is then verified.

The cross-section at adjacent support P1 is in Class 3 but there is no need to reduce $M_{pl,Rd}$ by a factor 0.9 because the ratio of lengths of the spans adjacent to P1 is 0.75 which is not less than 0.6 (EN1994-2, 6.2.1.3(2)).

6.1.3.2 Shear resistance check

As $\frac{h_w}{t_w} = \frac{2.72}{0.018} = 151.11 \geq \frac{31\varepsilon}{\eta} \sqrt{k_\tau} = 51.36$, the web (stiffened by the vertical stiffeners) should be

checked in terms of shear buckling, according to EN-1993-1-5, 5.1.

The maximum design shear resistance is given by $V_{Rd} = \min(V_{bw,Rd}; V_{pl,a,Rd})$, where $V_{bw,Rd}$ is the shear buckling resistance according to EN-1993-1-5, 5 and $V_{pl,a,Rd}$ is the resistance to vertical shear according to EN-1993-1-1, 6.2.6.

$$V_{b,Rd} = V_{bw,Rd} + V_{bf,Rd} \leq \frac{\eta f_{yw} h_w t}{\sqrt{3} \gamma_{M1}} = \frac{1.2 \times 345 \times 2720 \cdot 18}{\sqrt{3} \times 1.10} \times 10^{-6} = 10.63 \text{ MN} \quad (\text{EN 1993-1-5, 5.2})$$

Given the distribution of the transverse bracing frames in the span P1-P2 (spacing $a = 8 \text{ m}$), a vertical frame post is located in the studied cross-section (as for the cross-section at support P1). The shear buckling check is therefore performed in the adjacent web panel with the highest shear force. The maximum shear force registered in this panel is $V_{Ed} = 2.21 \text{ MN}$.

As the vertical frame posts are assumed to be rigid:

$$k_\tau = 5.34 + 4 \left(\frac{h_w}{a} \right)^2 = 5.34 + 4 \times \left(\frac{2.72}{8} \right)^2 = 5.802 \quad \text{is the shear buckling coefficient according to EN-1993-1-5 Annex A.3}$$

$$\sigma_E = \frac{\pi^2 \times E t_w^2}{12(1-\nu^2) h_w^2} = \frac{\pi^2 \times 2.1 \times 10^5 \times 18^2}{12 \times (1-0.3^2) \times 2720^2} = 8.312 \text{ MPa} \quad (\text{EN-1993-1-5 Annex A.1})$$

$$\tau_{cr} = k_\tau \sigma_E = 5.802 \times 8.312 = 48.22 \text{ MPa} \quad (\text{EN-1993-1-5, 5.3})$$

$$\bar{\lambda}_w = \sqrt{\frac{f_{y,w}}{\tau_{cr} \cdot \sqrt{3}}} = 0.76 \sqrt{\frac{f_{y,w}}{\tau_{cr}}} = 0.76 \sqrt{\frac{345}{48.22}} = 2.032 \quad \text{is the slenderness of the panel according to EN-1993-1-5, 5.3. As } \bar{\lambda}_w \text{ is } \geq 1.08 \text{ then:}$$

The factor for the contribution of the web to the shear buckling resistance χ_w is:

$$\chi_w = \frac{1.37}{(0.7 + \bar{\lambda}_w)} = \frac{1.37}{(0.7 + 2.032)} = 0.501 \text{ (Table 5.1. of EN-1993-1-5, 5.3)}$$

Finally the contribution of the web to the shear buckling resistance is:

$$V_{bw,Rd} = \frac{\chi_w f_{y,w} h_w t}{\sqrt{3} \gamma_{M1}} = \frac{0.501 \times 345 \times 2720 \times 18}{\sqrt{3} \cdot 1 \times 10} \times 10^{-6} = 4.441 \text{ MN}$$

If we neglect the contribution of the flanges to the shear buckling resistance $V_{bf,Rd} \approx 0$ then:

$$V_{b,Rd} = V_{bw,Rd} + V_{bf,Rd} = 4.44 + 0 \leq 10.63 \text{ MN} ; V_{b,Rd} = 4.44 \text{ MN}$$

$$\text{And } V_{pl,a,Rd} = \frac{\eta f_{y,w} h_w t}{\sqrt{3} \gamma_{M0}} = \frac{1.2 \times 345 \times 2720 \times 18}{\sqrt{3} \times 1.0} E^{-6} = 11.70 \text{ MN (EN 1993-1-1, 6.2.6)}$$

So, as $V_{Ed} = 2.21 \text{ MN} \leq V_{Rd} = \min(V_{bw,Rd} ; V_{pl,a,Rd}) = \min(4.44 ; 11.70) = 4.44$, then is verified.

6.1.3.3 Bending and vertical shear interaction

According to EN-1994-2, 6.2.2.4 if the vertical shear force V_{Ed} does not exceed half the shear resistance V_{Rd} , obtained before, there is no need to check the interaction M, V (Fig. 6.5)

In our case $V_{Ed} = 2.21 < 0.5 \cdot 4.44 = 2.22 \text{ MN}$ then there is no need to check the interaction $M-V$.

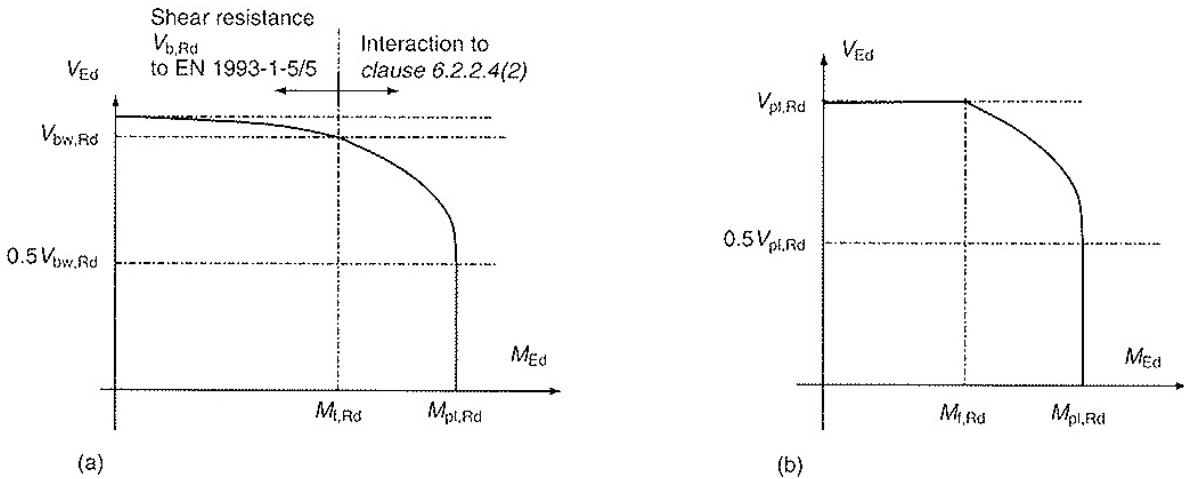


Fig. 6.5 Shear-Moment interaction for class 1 and 2 cross-sections (a) with shear buckling and without shear buckling (b). (Figure 6.6 of ¹)

6.2 Verification of cross-section at internal support P1

6.2.1 GEOMETRY AND STRESSES

At internal support P1 in ULS the concrete slab is in tension across its whole thickness. Its contribution is therefore neglected in the cross-section resistance. The stresses in Fig. 6.6 are subsequently calculated and obtained by summing the various steps whilst respecting the construction phases.

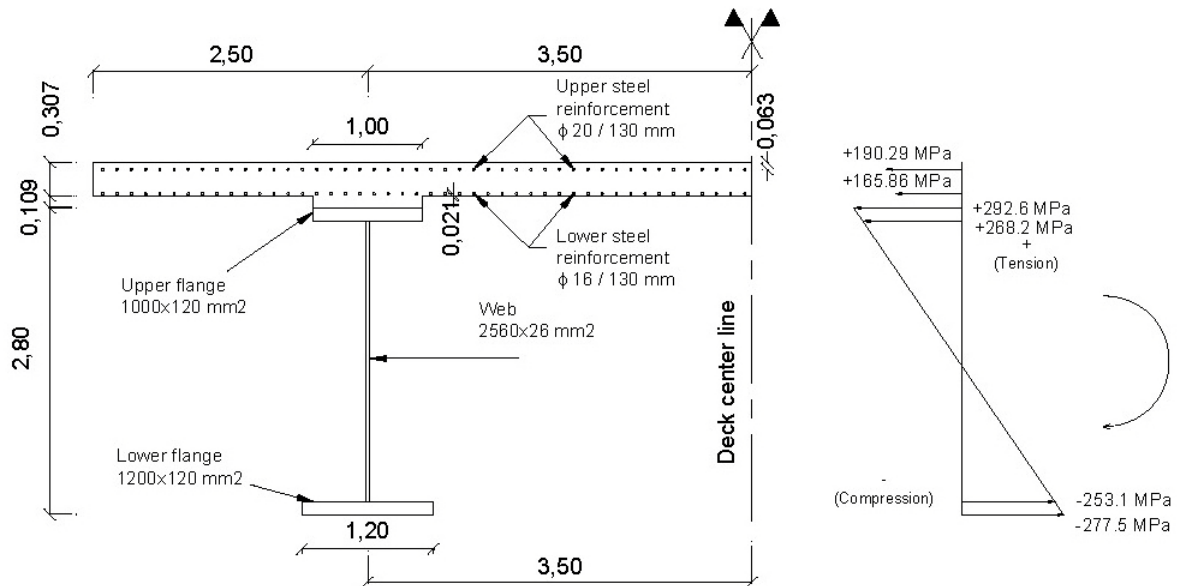


Fig. 6.6 Stresses at ULS in cross-section at internal support P1

Note: The sign criteria for stresses are according to EN-1994-2 + tension and – compression.

The internal forces and moments in this cross-section are:

$$M_{Ed} = -109.35 \text{ MN}\cdot\text{m}$$

$$V_{Ed} = 8.12 \text{ MN}$$

6.2.2 DETERMINING THE CROSS-SECTION CLASS (ACCORDING TO EN1994-2, 5.5.2)

The upper flange is in tension, therefore is in Class 1 (EN 1993-1-1, 5.5.2).

The lower flange is in compression and then must be classified according to (EN 1993-1-1, Table 5.2):

$$c = \frac{b_{ff} - t_w}{2} = \frac{1200 - 26}{2} = 587 \text{ mm}$$

$$\frac{c}{t_{ff}} = \frac{587}{120} = 4.891 \leq 9\epsilon = 9 \times \sqrt{\frac{235}{295}} = 8.033$$

(Lower flange t_{ff}=120 mm, f_{y,lf}=295 MPa)

Then the lower flange is in Class 1.

The web is in tension in its upper part and in compression in its lower part. The position of the Plastic Neutral Axis (PNA) is determined as follows:

- The slab is cracked and its contribution is neglected.
- Ultimate force of the tensioned upper reinforcing steel bars (ϕ 20/130 mm) (located in the slab):

$$F_{s,1} = A_{s,1} \frac{f_{sk}}{\gamma_s} = 144.996 \times 10^{-4} m^2 \times \frac{500}{1.15} = 6.304 MN \quad (\text{force of } \frac{1}{2} \text{ slab})$$

- Ultimate force of the tensioned lower reinforcing steel bars (ϕ 16/130 mm) (located in the slab):

$$F_{s,2} = A_{s,2} \frac{f_{sk}}{\gamma_s} = 92.797 \times 10^{-4} m^2 \times \frac{500}{1.15} = 4.034 MN \quad (\text{force of } \frac{1}{2} \text{ slab})$$

- Design plastic resistance of the structural steel upper flange (1 flange):

$$F_{s,uf} = A_{s,uf} \frac{f_{y,uf}}{\gamma_{M0}} = (1.2 \times 0.12) \times \frac{295}{1.0} = 35.4 MN$$

- Design plastic resistance of the total structural steel web (1 web):

$$F_{s,w} = A_{s,w} \frac{f_{y,w}}{\gamma_{M0}} = (2.56 \times 0.026) \times \frac{345}{1.0} = 22.963 MN$$

- Design plastic resistance of the structural steel lower flange (1 lower flange):

$$F_{s,lf} = A_{s,lf} \frac{f_{y,lf}}{\gamma_{M0}} = (1.20 \times 0.12) \times \frac{295}{1.0} = 42.48 MN$$

As $|F_{s,1}| + |F_{s,2}| + |F_{s,uf}| \leq |F_{s,w}| + |F_{s,lf}|$ ($45.73 \leq 65.44$) and $|F_{s,1}| + |F_{s,2}| + |F_{s,uf}| + |F_{s,w}| \geq |F_{s,lf}|$ ($68.70 \leq 42.48$) the PNA is deduced to be located in the steel web.

If we consider that the P.N.A. is located at a distance x from the upper extreme fibre of the web, then the internal axial forces equilibrium of the cross-section leads to the location of the PNA:

$$F_{s,1} + F_{s,2} + F_{s,uf} + F_{s,w} \frac{x}{2.56} - F_{s,w} \frac{(2.56 - x)}{2.56} F_{s,w} - F_{s,lf} = 0$$

$$6.304 + 4.034 + 35.4 + 8.97 \cdot x - 22.963 + 8.97 \cdot x - 42.48 = 0 ; \quad \mathbf{x = 1.098 \text{ m}}$$

Over half of the steel web is in compression (the lower part): $2.56 - 1.098 = \mathbf{1.462 \text{ m}}$.

$$\alpha = \frac{h_w - x}{h_w} = \frac{2.56 - 1.098}{2.56} = 0.571 > 0.50$$

Then, according to EN-1993-1-1, 5.5 and table 5.2 (sheet 1 of 3), if $\alpha > 0.50$ then:

The limiting slenderness between Class 2 and Class 3 is given by:

$$\frac{c}{t} = \frac{2.56}{0.026} = 98.46 >> \frac{456\varepsilon}{13\alpha - 1} = \frac{456 \cdot \sqrt{\frac{235}{345}}}{13 \cdot 0.571 - 1} = 58.59$$

The steel web is at least in Class 3 and reasoning is now based on the elastic stress distribution at ULS given in Fig. 6.6: $\psi = -(268.2 / 253.1) = -1.059 \leq -1$ therefore the limiting slenderness between Class 3 and Class 4 is given by (EN-1993-1-1, 5.5 and table 5.2):

$$\frac{c}{t} = \frac{2.56}{0.026} = 98.46 \leq 62 \times \varepsilon (1 - \psi) \sqrt{-\psi} = 62 \times \sqrt{\frac{235}{345}} \times (1 + 1.059) \times \sqrt{1.059} = 108.49$$

It is concluded that the steel web is in Class 3.

Conclusion: The cross-section at support P1 is in Class 3 and is checked by an elastic section analysis.

6.2.3 SECTION ANALYSIS

6.2.3.1 Elastic bending verification

In the elastic bending verification, the maximum stresses in the structural steel must be below the yield strength $|\sigma_s| \leq \frac{f_y}{\gamma_{M0}}$.

As we have 292.63 MPa in the upper steel flange and -277.54 MPa in the lower steel flange, which are below the limit of $f_y/\gamma_{M0}=295\text{MPa}$ admitted in an elastic analysis for the thickness of 120 mm, the bending resistance is verified.

This verification could be made, not with the extreme fibre stresses, but with the stresses of the center of gravity of the flanges (EN-1993-1-1, 6.2.1(9)).

6.2.3.2 Alternative: Plastic bending verification (Effective Class 2 cross-section)

EN-1994-2, 5.5.2(3) establishes that a cross-section with webs in Class 3 and flanges in Classes 1 or 2 may be treated as an effective cross-section in Class 2 with an effective web in accordance to EN-1993-1-1, 6.2.2.4.

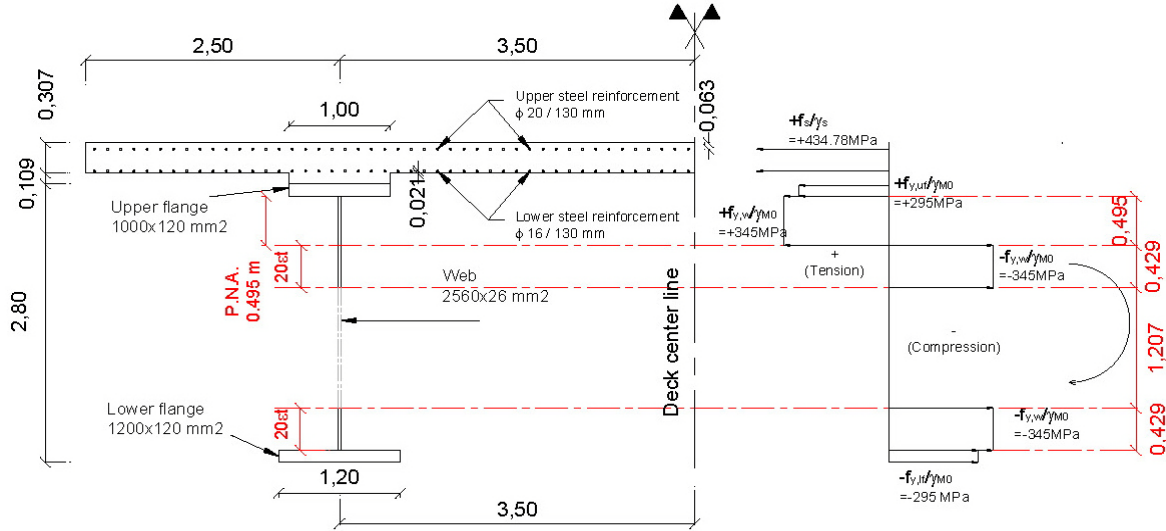


Fig. 6.7 Effective class 2 cross-section at support P-1. Design plastic bending resistance

If we consider that the PNA is located at a distance x from the extreme upper fibre of the upper part of the web, then the internal axial forces equilibrium of the cross section leads to the location of the PNA:

$$F_{s,1} + F_{s,2} + F_{s,uf} + X \times t_w \frac{f_{y,w}}{\gamma_{M0}} - 2 \times \left(20 \times \varepsilon \times t_w \times \frac{f_{y,w}}{\gamma_{M0}} \right) - F_{s,lf} = 0$$

$6.304 + 4.034 + 35.4 + 8.97 \cdot X - 2 \cdot 3.848 - 42.48 = 0$, then $X = 0.495$ m

And the hogging bending moment resistance of the effective class 2 cross-section is:

$$M_{pl,Rd} = -(6.304 \cdot (0.353 + 0.12 + 0.495) + 4.034 \cdot (0.13 + 0.12 + 0.495) + 35.4 \cdot (0.06 + 0.495) + 4.44 \cdot (0.495/2) + 3.848 \cdot (2.56 - 0.495 - 0.429/2) + 42.48 \cdot (2.56 - 0.495 - 0.06)) = -122.97 \text{ MN}\cdot\text{m}$$

As $|M_{Ed}| = 109.35 < |M_{pl,Rd}| = 122.53$ the bending resistance is verified.

6.2.3.3 Shear resistance check

As $\frac{h_w}{t_w} = \frac{2.56}{0.026} = 98.46 \geq \frac{31\varepsilon}{\eta} \sqrt{k_\tau} = 51.36$, the web (stiffened by the vertical stiffeners) should be checked in terms of shear buckling, according to EN-1993-1-5, 5.1.

The maximum design shear resistance is given by $V_{Rd} = \min(V_{bw,Rd}; V_{pl,a,Rd})$, where $V_{bw,Rd}$ is the shear buckling resistance according to EN-1993-1-5, 5 and $V_{pl,a,Rd}$ is the resistance to vertical shear according to EN-1993-1-1, 6.2.6.

$$V_{b,Rd} = V_{bw,Rd} + V_{bf,Rd} \leq \frac{\eta f_{y,w} h_w t}{\sqrt{3} \gamma_{M1}} = \frac{1.2 \times 345 \times 2560 \times 26}{\sqrt{3} \cdot 1 \times 10} \times 10^{-6} = 14.46 \text{ MN} \quad (\text{EN 1993-1-5, 5.2})$$

Given the distribution of the bracing transverse frames (spacing $a = 8$ m), a vertical frame post is located in the cross-section at support P1. The shear buckling check is therefore performed in the adjacent web panel with the highest shear force. The maximum shear force registered in this panel is $V_{Ed} = 8.12$ MN.

The vertical frame posts are assumed to be rigid. This yields:

$k_\tau = 5.34 + 4 \left(\frac{h_w}{a} \right)^2 = 5.34 + 4 \left(\frac{2.56}{8} \right)^2 = 5.75$ is the shear buckling coefficient according to EN-1993-1-5 Annex A.3

$$\sigma_E = \frac{\pi^2 E t_w^2}{12(1-\nu^2) h_w^2} = \frac{\pi^2 \times 2.1 \times 10^5 \times 26^2}{12 \times (1-0.3^2) \times 2560^2} = 19.58 \text{ MPa (EN-1993-1-5 Annex A.1)}$$

$$\tau_{cr} = k_\tau \cdot \sigma_E = 5.75 \times 19.58 = 112.58 \text{ MPa (EN-1993-1-5, 5.3)}$$

$$\bar{\lambda}_w = \sqrt{\frac{f_{y,w}}{\tau_{cr} \cdot \sqrt{3}}} = 0.76 \sqrt{\frac{f_{y,w}}{\tau_{cr}}} = 0.76 \sqrt{\frac{345}{112.58}} = 1.33 \text{ is the slenderness of the panel according to EN-1993-1-5, 5.3. As } \bar{\lambda}_w \text{ is } \geq 1.08 \text{ then:}$$

The factor for the contribution of the web to the shear buckling resistance χ_w is:

$$\chi_w = \frac{1.37}{(0.7 + \bar{\lambda}_w)} = \frac{1.37}{(0.7 + 1.33)} = 0.675 \text{ (Table 5.1. of EN-1993-1-5, 5.3)}$$

Finally the contribution of the web to the shear buckling resistance is:

$$V_{bw,Rd} = \frac{\chi_w f_{y,w} h_w t}{\sqrt{3} \gamma_{M1}} = \frac{0.675 \times 345 \times 2560 \times 26}{\sqrt{3} \times 1.10} \times 10^{-6} = 8.14 \text{ MN}$$

If we neglect the contribution of the flanges to the shear buckling resistance $V_{bf,Rd} \approx 0$ then:

$$V_{b,Rd} = V_{bw,Rd} + V_{bf,Rd} = 8.14 + 0 \leq 14.46 \text{ MN} ; V_{b,Rd} = 8.14 \text{ MN}$$

$$\text{And } V_{pl,a,Rd} = \frac{\eta f_{y,w} h_w t}{\sqrt{3} \gamma_{M0}} = \frac{1.2 \times 345 \times 2560 \times 26}{\sqrt{3} \times 1.0} \times 10^{-6} = 15.91 \text{ MN (EN 1993-1-1, 6.2.6)}$$

As $V_{Ed} = 8.12 \text{ MN} \leq V_{Rd} = \min(V_{bw,Rd} ; V_{pl,a,Rd}) = \min(8.14 ; 15.91) = 8.14$, the shear design force is lower than the shear buckling resistance.

6.2.3.4 Flange contribution to the shear buckling resistance

When the flange resistance is not fully used to resist the design bending moment, and therefore $M_{Ed} < M_{f,Rd}$ the contribution from the flanges could be evaluated according to EN-1993-1-5, 5.4.

$$V_{bf,Rd} = \frac{b_f t_f^2 f_{yf}}{c \gamma_{M1}} \left(1 - \left(\frac{M_{Ed}}{M_{f,Rd}} \right)^2 \right)$$

Note that in our case it is not strictly necessary the use of the shear buckling resistance of the flanges, as seen in the previous paragraph, but we will develop the calculation in an academic way.

Where b_f and t_f must be taken for the flange which provides the smallest axial resistance, with the condition that b_f must be not larger than $15t_f$ on each side of the web.

$M_{f,Rd}$ is the plastic bending resistance of the cross-section neglecting the web area.

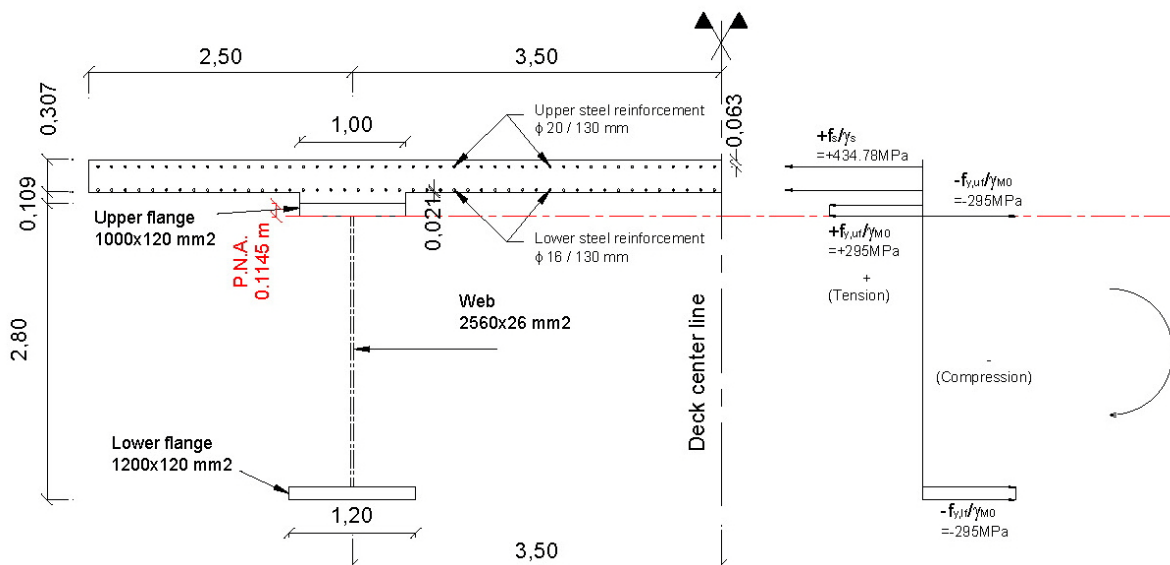


Fig. 6.8 Design plastic bending resistance neglecting the web area

If we consider that the PNA is located at a distance x from the extreme upper fibre of the upper flange, then the internal axial forces equilibrium of the cross section leads to the location of the PNA:

$$F_{s,1} + F_{s,2} + F_{s,uf} \frac{x}{0.12} - F_{s,uf} \frac{(0.12 - x)}{0.12} - F_{s,lf} = 0$$

$$6.304 + 4.034 + 35.4 \cdot \frac{x}{0.12} - 35.4 \cdot \frac{(0.12 - x)}{0.12} - 42.48 = 0$$

Then $x = 0.1145$ m

And the hogging bending moment resistance of the effective cross-section neglecting the web area is:

$$M_{f,Rd} = -2 \cdot (6.304 \cdot (0.353 + 0.1145) + 4.034 \cdot (0.13 + 0.1145) + 33.777 \cdot (0.1145/2) + 1.628 \cdot (0.12 - 0.1145)/2 + 42.48 \cdot (2.8 - 0.06 - 0.1145)) = -117.40 \text{ MN}\cdot\text{m}.$$

As $|M_{Ed}| = 109.35 < |M_{f,Rd}| = 117.40$, the bending resistance is verified without considering the influence of the web, and the shear resistance is already verified neglecting the contribution of the flanges, there's no need to verify the interaction M-V. However we will check the interaction M-V for the example.

Once the bending resistance of the cross-section neglecting the web $M_{f,Rd}$ is obtained, the contribution of the flanges to the shear buckling resistance can be evaluated as:

$$V_{bf,Rd} = \frac{b_f t_f^2 f_{yf}}{c \gamma_{M1}} \left(1 - \left(\frac{M_{Ed}}{M_{f,Rd}} \right)^2 \right)$$

As the upper flange is a composite flange, made of the steel reinforcement and the steel upper flange itself, we will take the lower steel flange (1200x120 mm²) to evaluate the contribution of the flanges to the shear buckling resistance

According to EN-1993-1-5, 5.4 (1):

$$c = a \left(0.25 + \frac{1.6 b_f t_f^2 f_{yf}}{t_w^2 f_{yw}} \right) = 8 \left(0.25 + \frac{1.6 \times 1200 \times 120^2 \times 295}{26 \times 2.56^2 \times 345} \right) = 3.110 \text{ m}$$

$$\text{Then: } V_{bf,Rd} = \frac{1200 \times 120^2 \times 295}{3110 \times 1.1} \left(1 - \left(\frac{109.35}{117.40} \right)^2 \right) 10^{-6} = 0.197 \text{ MN}$$

The shear buckling resistance is the sum of the contribution of the web, $V_{bw,Rd} = 8.14 \text{ MN}$, obtained before, and the contribution of the flanges $V_{bf,Rd} = 0.197 \text{ MN}$, so the total shear buckling resistance in this case is

$$V_{b,Rd} = V_{bw,Rd} + V_{bf,Rd} = 8.14 + 0.197 \leq 14.46 \text{ MN}; V_{b,Rd} = 8.337 \text{ MN}$$

The contribution of the flanges to shear buckling resistance represents in this case less than 2.5%, which could be considered negligible as supposed before.

According to EN-1993-1-5, 5.5, the shear verification is:

$$\eta_3 = \frac{V_{Ed}}{V_{b,Rd}} \leq 1.0; \text{ and in this case } \eta_3 = \frac{8.12}{8.14} = 0.9975 \text{ without considering the contribution of the flanges to the shear buckling resistance.}$$

6.2.3.5 Bending and shear interaction

The interaction M - V should be considered according to EN-1993-1-5, 7.1 (1). As the design shear force is higher than 50% of the shear buckling resistance then it has to be verified:

$$\bar{\eta}_1 + \left[1 - \frac{M_{f,Rd}}{M_{pl,Rd}} \right] \left[2\bar{\eta}_3 - 1 \right]^2 \leq 1.0$$

Where:

$$\bar{\eta}_1 = \frac{M_{Ed}}{M_{pl,Rd}}, \text{ and } \bar{\eta}_3 = \frac{V_{Ed}}{V_{bw,Rd}}$$

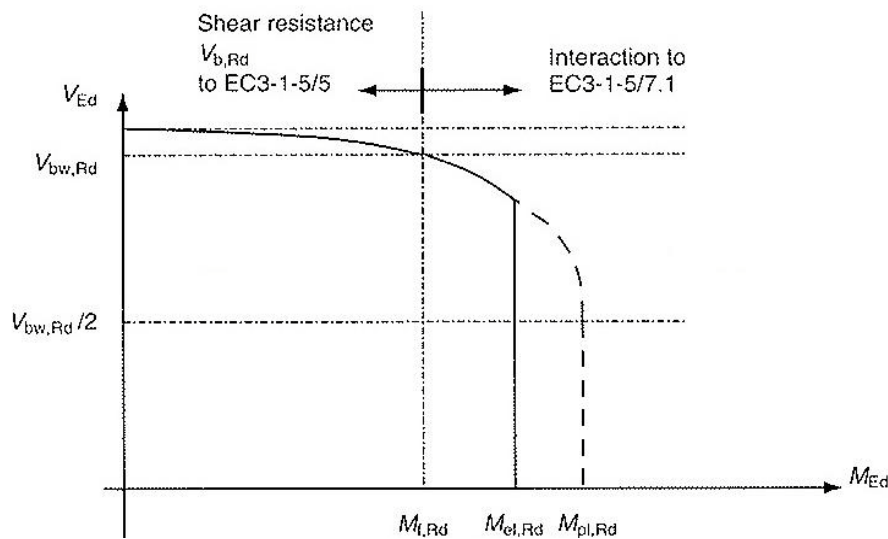


Fig. 6.9 Shear-Moment interaction for Class 3 and 4 cross-sections according to clause 7.1 of EN-1993-1-5. (Figure 6.7 of¹)

This criterion should be verified, according to EN-1993-1-5. 7.1 (2) at all sections other than those located at a distance less than $h_w/2$ from a support with vertical stiffener.

If we consider the internal shear forces and moments of the section located over P-1 ($x=60\text{m}$): $V_{Ed}=8.124\text{MN}$, $M_{Ed}=-109.35\text{mMN}$, and the section located at $X=62.5\text{ m}$: $V_{Ed}=7.646\text{MN}$, $M_{Ed}=-91.86\text{mMN}$, we could obtain the values of the design shear force and bending moment of the section located at $X=61.25\text{ m}$, which approximately is at $h_w/2$ from the support, as an average of both values, on the safe side:

Then, we will verify the interaction for the design internal forces and moments:

$$V_{Ed}=(8.124+7.646)/2=7.885\text{ MN}, \text{ and } M_{Ed}=(-109.35-91.86)/2=-100.605\text{ mMN}$$

That leads to: $\bar{\eta}_1 = \frac{100.605}{122.97} = 0.818$; $\bar{\eta}_3 = \frac{7.885}{8.14} = 0.9686$, and:

$$\bar{\eta}_1 + \left[1 - \frac{M_{f,Rd}}{M_{pl,Rd}} \right] \left[2\bar{\eta}_3 - 1 \right]^2 = 0.818 + \left[1 - \frac{117.40}{122.97} \right] \left[2 \times 0.9686 - 1 \right]^2 = 0.858 \leq 1$$

So the interaction M - V is verified.

Note that we have considered that $M_{pl,Rd}$ is the value obtained before for the effective class 2 cross-section.

6.3 Alternative double composite cross-section at internal support P-1

As an alternative to the simple composite cross-section located at the hogging bending moments area, it is possible to design a double composite cross-section, with a bottom concrete slab located between the two steel girders, connected to them.

The double composite action in hogging areas is an economical alternative to reduce the steel weight of the compressed bottom flange.

Compression stresses from negative bending usually keep the bottom slab uncracked, so bending and torsional stiffness in these areas are noticeably higher than those classically obtained with steel sections. Double composite action greatly improves the deformational and dynamic response both to bending and torsion.

The main structural advantage of the double composite action is related to the bridge response at ultimate limit state. Cross-sections along the whole bridge are in Class 1 or Class 2, not only in sagging areas, but also usually in hogging areas. Thus instability problems at ultimate limit state are avoided: not only at the bottom flange because of its connection to the concrete, but also in webs, due to the low position of the neutral axis in an ultimate limit state.

As a result, a safe and economical design is possible using a global elastic analysis with cross-section elastoplastic resistances, both in sagging and hogging areas. There is even enough capacity for almost reaching global plasticity in ULS by means of adequate control of elastoplastic rotations with no risk of brittle instabilities. This constitutes a structural advantage of the cross sections with double composite action solution when compared to the more classical twin girder alternatives.

Fig. 6,10 shows two examples of road bridges, bridge over river Mijares (main span 64 m) in Betxi-Borriol (Castellón, Spain), and bridge over river Jarama (main span 75 m) in Madrid, Spain, with double composite action in hogging areas.



Fig. 6.10 Two examples of road composite bridges with double composite action in hogging areas

Fig. 6.11 shows a view of Viaduct “Arroyo las Piedras” in the Spanish High Speed Railway Line Córdoba-Málaga. This is the first composite steel-concrete Viaduct of the Spanish railway lines, with a main span of 63.5 m.

In High Speed bridges the typical twin girder solution for road bridges must improve their torsional stiffness in order to respond to the high speed railway requirements. In this case, in hogging areas the double composite action is materialized not only for bending but also for torsion.

The double composite action was extended to the whole length of the deck to allow the torsion circuit to be closed. A strict box cross section is obtained in sagging areas with the use of discontinuous precast slabs only connected to the steel girders for torsion and not for bending.



Fig. 6.11 Example of a High Speed Railway Viaduct with double composite action

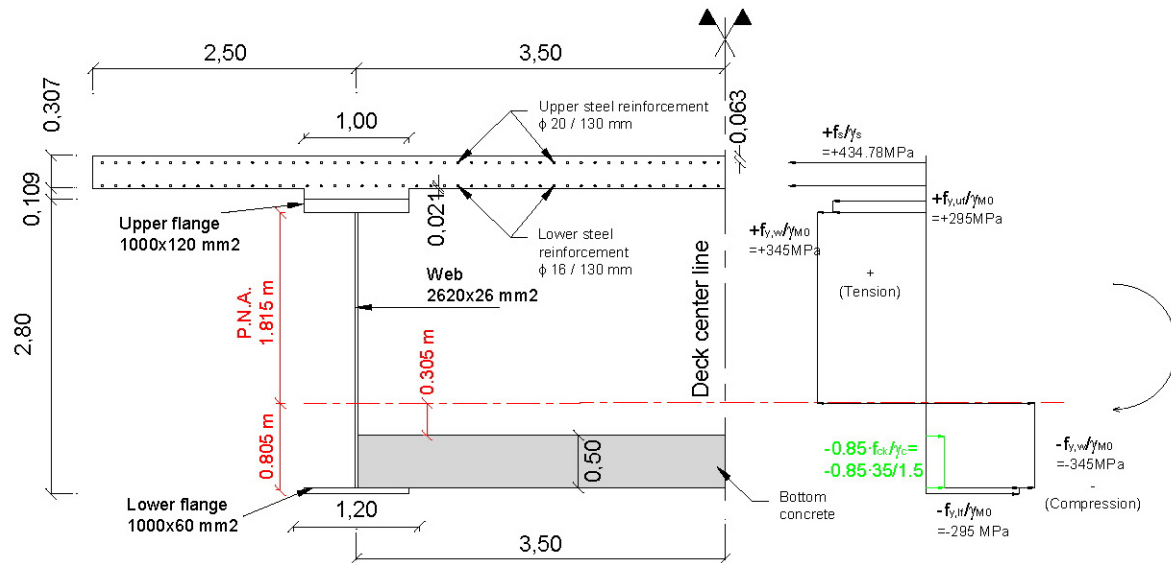


Fig. 6.12 Cross-section at support P-1 with double composite action. Design plastic bending resistance

Back to our case study, if we change the lower steel flange from 1200x120 mm² to a smaller one, of 1000x60 mm² plus a 0.50 m thick bottom slab of concrete C35/45 (Fig. 6.12), we could verify the bending resistance to compare both cross sections. We could also resize the upper steel flange or even the upper slab reinforcement, but for this example, we will keep the original ones and only change the lower steel flange.

Fig. 6.13 shows a classical solution for composite road bridges with double composite action. The bottom concrete slab, in hogging areas, is extended to a length of 20 or 25% of the main span. The maximum thickness at support cross section is 0.50 m and the minimum thickness at the end of the slab is 0.25 m. Fig. 6.13 defines in red line the thickness distribution of the bottom concrete slab, and in green the lower steel flange reduction.

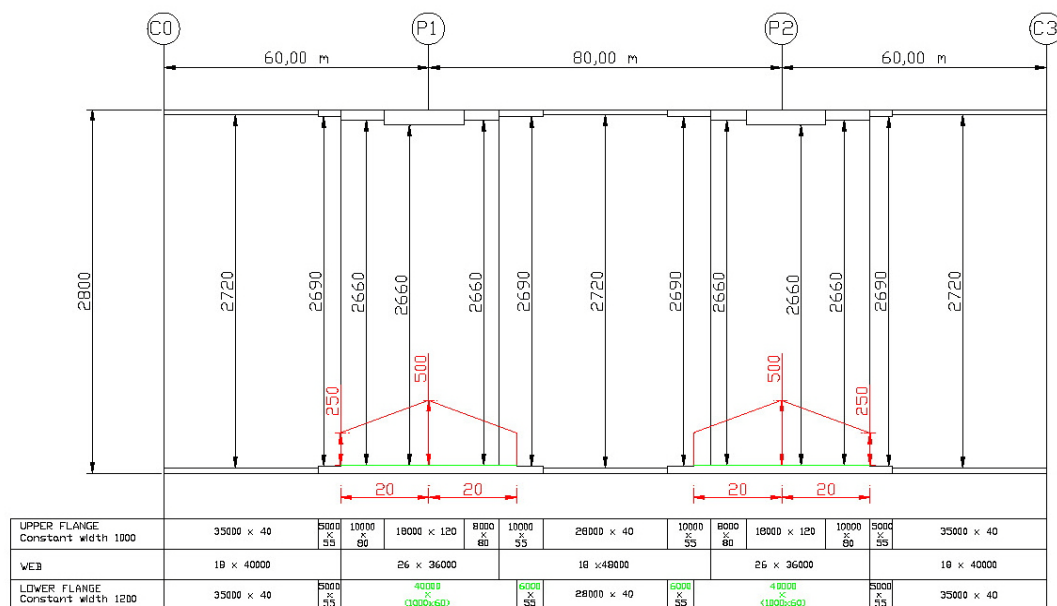


Fig. 6.13 Alternative steel distribution of the double composite main girder and bottom concrete slab thickness

For the example we are only calculating the ultimate bending resistance of the double composite cross section at support P-1, but it is necessary to clarify some aspects treated by EN-1994-2 related to the double composite action.

EN 1994-2, establishes in 5.4.2.2 (2) the modular ratio simplified method for considering the creep and shrinkage of concrete in a simple composite cross-section. For double composite cross sections this simplified method is not fully applicable.

EN-1994-2, 5.4.2.2 (10) requires that for double composite cross section with both slabs un-cracked (e.g. in the case of pre-stressing) the effects of creep and shrinkage should be determined by more accurate methods.

Strictly speaking, in our case, we do not have double composite action with both slabs un-cracked, because the upper slab will be cracked, and we will neglect its contribution and only consider the upper reinforcement, so what we have in hogging areas is a simple composite cross-section with the reinforcement of the upper slab and bottom concrete in compression.

6.3.1 DETERMINING THE CROSS-SECTION CLASS (ACCORDING TO EN1994-2, 5.5.2)

The upper flange is in tension therefore it is in Class 1 (EN 1993-1-1, 5.5.2).

The lower flange is in compression, and then must be classified according to (EN 1993-1-1, Table 5.2):

$$c = \frac{b_{ff} - t_w}{2} = \frac{1000 - 26}{2} = 487 \text{ mm}$$

$$\frac{c}{t_{ff}} = \frac{487}{60} = 8.116 \leq 10 \cdot \varepsilon = 10 \cdot \sqrt{\frac{235}{335}} = 8.375$$

(Lower flange $t_{ff}=60$ mm, $f_{y,ff}=335$ MPa)

Then the lower flange is in Class 2.

The upper part of the web is in tension and the lower part is in compression. The position of the Plastic Neutral Axis (PNA) is determined as follows:

- The tensioned upper slab is cracked and we neglect its contribution.
- Ultimate force of the tensioned upper reinforcing steel bars (ϕ 20/130 mm) (located in the slab):

$$F_{s,1} = A_{s,1} \frac{f_{sk}}{\gamma_s} = 144.996 \times 10^{-4} \text{ m}^2 \times \frac{500}{1.15} = 6.304 \text{ MN} \quad (\text{force of } \frac{1}{2} \text{ slab})$$

- Ultimate force of the tensioned lower reinforcing steel bars (ϕ 16/130 mm) (located in the slab):

$$F_{s,2} = A_{s,2} \frac{f_{sk}}{\gamma_s} = 92.797 \times 10^{-4} \text{ m}^2 \times \frac{500}{1.15} = 4.034 \text{ MN} \quad (\text{force of } \frac{1}{2} \text{ slab})$$

- Design plastic resistance of the structural steel upper flange (1 flange):

$$F_{s,uf} = A_{s,uf} \frac{f_{y,uf}}{\gamma_{M0}} = (1.2 \times 0.12) \times \frac{295}{1.0} = 35.4 \text{ MN}$$

- Design plastic resistance of the total structural steel web (1 web):

$$F_{s,w} = A_{s,w} \frac{f_{y,w}}{\gamma_{M0}} = (2.62 \times 0.026) \times \frac{345}{1.0} = 23.50 \text{ MN}$$

- Design plastic resistance of the structural steel lower flange (1 lower flange):

$$F_{s,lf} = A_{s,lf} \frac{f_{y,lf}}{\gamma_{M0}} = (1.00 \times 0.06) \times \frac{335}{1.0} = 20.1 \text{ MN}$$

- Design plastic resistance of the bottom concrete slab in compression:

$$F_{c,inf} = A_c \frac{0.85 f_{ck}}{\gamma_c} = 3.5 \times 0.5 \times \frac{0.85 \times 35}{1.50} = 34.7 \text{ MN}$$

As $|F_{s,1}| + |F_{s,2}| + |F_{s,uf}| \leq |F_{s,w}| + |F_{s,lf}| + |F_{c,inf}|$ (45.73 ≤ 78.3) and

$|F_{s,1}| + |F_{s,2}| + |F_{s,uf}| + |F_{s,w}| \geq |F_{s,lf}| + |F_{c,inf}|$ (69.23 ≤ 54.8) the PNA is located in the steel web.

If we consider that the P.N.A. is located at a distance x from the upper extreme fibre of the web, then the internal axial forces equilibrium of the cross-section gives the location of the PNA:

$$F_{s,1} + F_{s,2} + F_{s,uf} + F_{s,w} \frac{x}{2.62} - F_{s,w} \frac{(2.62 - x)}{2.62} - F_{s,lf} - F_{c,inf} = 0$$

$$6.304 + 4.034 + 35.4 + 8.97 \cdot X - 23.5 + 8.97 \cdot X - 54.8 = 0; \mathbf{X = 1.815 \text{ m}}$$

Only around 30% of the steel web is in compression (the lower part): $2.62 - 1.815 = \mathbf{0.805 \text{ m}}$.

$$\alpha = \frac{h_w - x}{h_w} = \frac{2.62 - 1.815}{2.62} = 0.307 \leq 0.50$$

Then according to EN-1993-1-1, 5.5 and table 5.2 (sheet 1 of 3), if $\alpha < 0.50$ then:

Therefore the limiting slenderness between Class 2 and Class 3 is given by:

$$\frac{c}{t} = \frac{2.62}{0.026} = 100.76 < \frac{41.5 \varepsilon}{\alpha} = \frac{41.5 \times \sqrt{\frac{235}{345}}}{0.307} = 111.56$$

According to this, the steel web is in Class 2.

However, the part of the web in touch with the bottom concrete slab, is laterally connected to it, so only 0.305 m of the total length under compression (0.805 m) could have buckling problems. If we take this into consideration, the actual depth of the web considered for the classification of the compressed panel, is $1.815 + 0.305 = 2.12 \text{ m}$ instead of 2.62 m, considered before.

$$\text{With this new values, } \alpha = \frac{h_w^* - x}{h_w^*} = \frac{2.12 - 1.815}{2.12} = 0.144 \leq 0.50$$

Then according to EN-1993-1-1, 5.5 and table 5.2 (sheet 1 of 3), if $\alpha < 0.50$ then:

Therefore the limiting slenderness between Class 1 and Class 2 is given by:

$$\frac{c}{t} = \frac{2.12}{0.026} = 81.54 < \frac{36\varepsilon}{\alpha} = \frac{36 \times \sqrt{\frac{235}{345}}}{0.144} = 206.33$$

The steel web could be in fact classified as Class 1.

Conclusion: The cross-section at support P1 with double composite action is in Class 2 (due to the lower steel flange), and can be checked by plastic section analysis, as we said at the beginning of this section.

6.3.2 PLASTIC SECTION ANALYSIS. BENDING RESISTANCE CHECK

If we consider that the PNA is located at a distance $x=1.815$ m from the upper extreme fibre of the upper part of the web, then the hogging bending moment resistance of the Class 2 cross-section is:

$$M_{pl,Rd} = -(6.304 \cdot (0.353 + 0.12 + 1.815) + 4.034 \cdot (0.13 + 0.12 + 1.815) + 35.4 \cdot (0.06 + 1.815) + 16.28 \cdot (1.185/2) + 7.22 \cdot (0.805/2) + 34.72 \cdot (0.805 - 0.25) + 20.1 \cdot (0.805 + 0.06/2)) = -142.85 \text{ MN}\cdot\text{m}$$

In comparison with the simple composite action cross-section we have significantly increased the bending moment resistance, locally reducing the amount of structural steel just by adding the bottom concrete slab connected to the steel girders.

For the final verification M_{Ed} should be lower than the ultimate bending resistance $M_{pl,Rd}$. For the example we haven't recalculated the new design bending moment M_{Ed} , increased by the self weight of the bottom concrete, something that of course should had been done in a real case.

6.3.3 SOME COMMENTS ABOUT AN EVENTUAL CRUSHING OF THE EXTREME FIBRE OF THE BOTTOM CONCRETE

EN-1994-2, 6.2.1.2 (2) establishes that for a composite cross-section with structural steel grade S420 or S460, if the distance between the PNA (x_{pl}) and the extreme fiber of the concrete slab in compression exceeds 15% of the overall depth of the cross section (h), the design resistance moment M_{Rd} should be taken as $\beta \cdot M_{Rd}$, reduced by the β factor defined on figure 6.3 of EN-1994-2. This figure limits this ratio to a maximum value of 40%.

Although this paragraph applies to the steel grade, we could consider limiting the maximum ratio x_{pl}/h to avoid an eventual crushing of the concrete.

In standard composite bridges, in sagging bending moment areas, the ratio x_{pl}/h is usually below the limit of 0.15. This value generally varies from 0.10 to 0.15, so there is not a practical incidence of the reduction of the bending moment resistance.

Meanwhile in composite cross-sections with double composite action, in hogging bending moment areas, the ratio x_{pl}/h is usually around 25-30%. The incidence of the β factor, in a real case of double composite action, has not a very big influence, barely reducing the plastic bending moment resistance of the composite cross-section from 94 to 91% of its total plastic bending resistance.

In our case study, for the alternative double composite cross-section, this ratio is $x_{pl}/h = 0.865/3.216 = 0.269$. This value leads to a β factor of 0.93, so the reduced bending moment resistance would be $\beta \cdot M_{Rd} = 0.93 \cdot (-142.85) = -132.85 \text{ MN}\cdot\text{m}$.

In our case study we have considered the resistance of the bottom concrete, equal to the upper concrete C35/45, but in practice it is not unusual to use higher resistance in the bottom concrete: C40/50, C45/55, or even C50/60.

6.4 Verification of the Serviceability Limit States (SLS)

EN-1994-2, 7.1 (1) establishes that a composite bridge shall be designed such that all the relevant SLS are satisfied according to the principles of EN-1990, 3.4. The limit states that concern are:

- The functioning of the structure or structural members under normal use.
- The comfort of people.
- The “appearance” of the construction work. This is related with such criteria as high deflections and extensive cracking, rather than aesthetics.

At SLS under global longitudinal bending the following should be verified:

- Stress limitation and web breathing, according to EN-1994, 7.2.
- Deformations: deflections and vibrations, according to EN-1994, 7.3.
- Cracking of concrete, according to EN-1994, 7.4

In this case study we are only analyzing the stress limitation and the cracking of concrete. And we will not carry out a deflection or vibration control, that should be done according to EN-1994, 7.3.

6.5 Stresses control at Serviceability Limit States

6.5.1 CONTROL OF COMPRESSIVE STRESS IN CONCRETE

EN-1994-2, 7.2.2 (1) establishes that the excessive creep and microcracking of concrete shall be avoided by limiting the compressive stress in concrete. EN-1994-2, 7.2.2 (2) refers to EN-1992-1-1 and EN-1992-2, 7.2 for that limitation.

EN-1992-1-1, 7.2 (2) recommends to limit the compressive stress in concrete under the characteristic combination to a value of $k_1 \cdot f_{ck}$ (k_1 is a nationally determined parameter, and the recommended value is 0.60) so as to control the longitudinal cracking of concrete, and also recommends to limit compressive stress in concrete under the quasi-permanent loads to $k_2 \cdot f_{ck}$ (k_2 is a national parameter, and the recommended value is 0.45) in order to admit linear creep assumption.

Fig. 6.14 shows the maximum and minimum normal stresses of the upper concrete slab calculated in two different hypotheses, upper slab cracked or uncracked under the characteristic SLS combination. The results for all cross-sections of the bridge are very far from both compression limits, $0.6 \cdot f_{ck} = -21$ MPa or $0.45 \cdot f_{ck} = -15.75$ MPa.

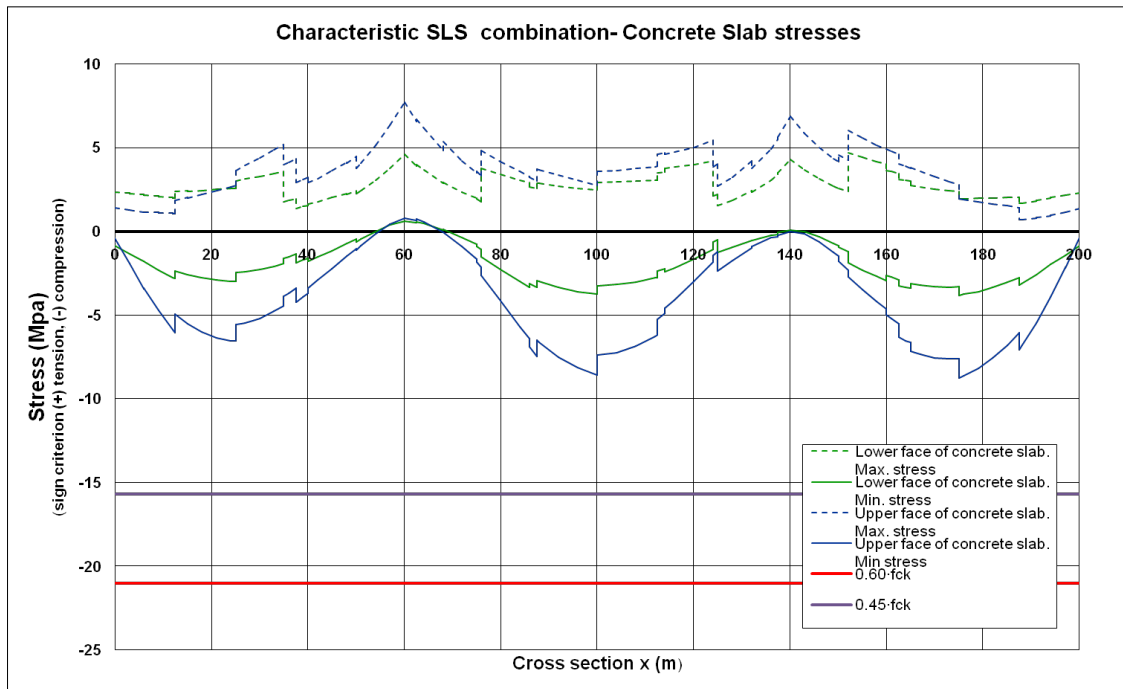


Fig. 6.14 Concrete slab stress under the characteristic SLS combination

6.5.2 CONTROL OF STRESS IN REINFORCEMENT STEEL BARS

Tensile stresses in the reinforcement shall be limited in order to avoid inelastic strain, unacceptable cracking or deformation according to EN-1992-1-1, 7.2(4).

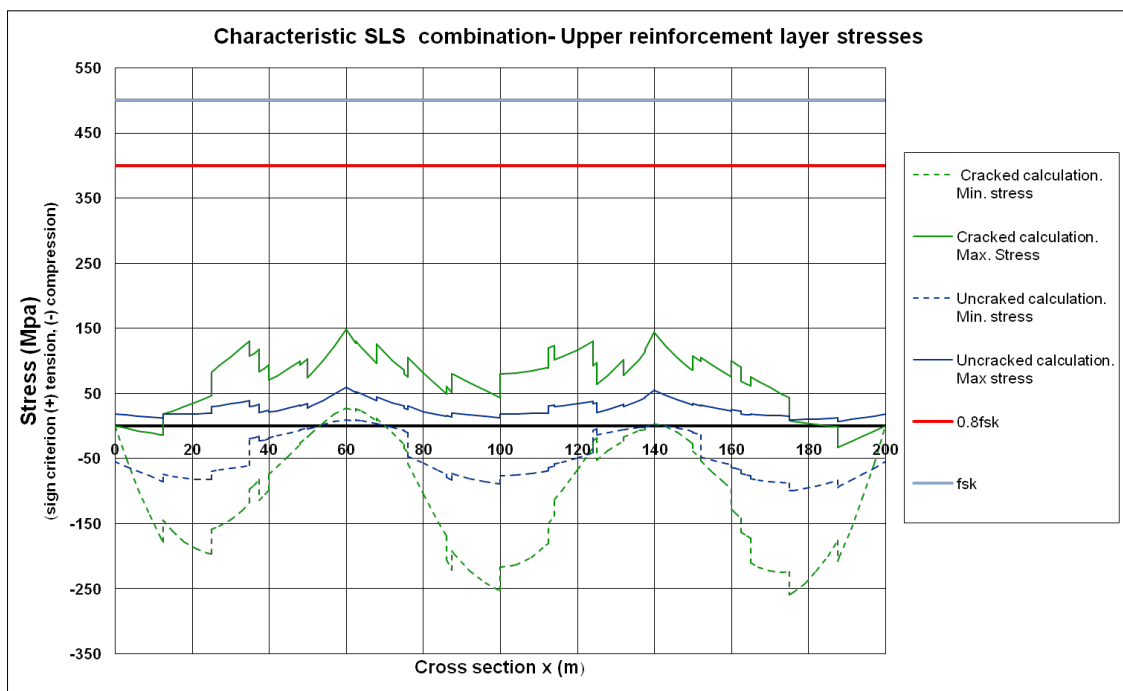


Fig. 6.15 Upper reinforcement layer stress under the characteristic SLS combination

Unacceptable cracking or deformation may be assumed to be avoided if, under the characteristic combination of loads, the tensile stress in the reinforcement does not exceed $k_3 \cdot f_{sk}$, and where the stress is caused by an imposed deformation, the tensile stress should not exceed $k_4 \cdot f_{sk}$. k_3 and k_4 are nationally determined parameters, and the recommended values are $k_3 = 0.8$ and $k_4 = 1.0$.

Fig. 6.15 shows the maximum and minimum normal stresses of the upper reinforcement layer of the slab, calculated in two different hypotheses, upper slab cracked or uncracked under the characteristic SLS combination. The stress results for all cross-sections of the bridge are widely verified for the example, very far from both tensile limits $0.8 \cdot f_{sk} = 400$ MPa or $1.0 \cdot f_{sk} = 500$ MPa.

Note that the stresses calculated with a contributing concrete strength are not equal to zero at the deck ends because of the shrinkage self-balanced stresses (isostatic or primary effects of shrinkage).

When $M_{c,Ed}$ is negative, the tension stiffening term $\Delta\sigma_s$ should be added to the stress values in Fig. 5.2 calculated without taking the concrete strength into account. This term $\Delta\sigma_s$ is in the order of 100 MPa (see paragraph 6.6.3).

6.5.3 STRESS LIMITATION IN STRUCTURAL STEEL

EN-1994-2, 7.2.2 (5) refers to EN-1993-2, 7.3 for the stress limitation in structural steel under SLS.

For the characteristic SLS combination of actions, considering the effect of shear lag in flanges and the secondary effects caused by deflections (if applicable), the following criteria for the normal and shear stresses in the structural steel should be verified (EN-1993-2, 7.3 equations 7.1, 7.2 and 7.3).

$$\sigma_{Ed,ser} \leq \frac{f_y}{\gamma_{M,ser}}$$

$$\tau_{Ed,ser} \leq \frac{f_y}{\sqrt{3} \cdot \gamma_{M,ser}}$$

$$\sqrt{\sigma_{Ed,ser}^2 + 3 \cdot \tau_{Ed,ser}^2} \leq \frac{f_y}{\gamma_{M,ser}}$$

The partial factor $\gamma_{M,ser}$ is a national parameter, and the recommended value is 1.0 according to EN-1993-2, 7.2 (note 2).

Strictly speaking the Von Mises criterion of the third equation only makes sense if it is calculated with concomitant stress values.

For the verification of the stresses control at SLS, the stresses should be considered on the external faces of the steel flanges, and not in the flange midplane (EN-1993-1-1, 6.2.1 (9)).

Figs. 6.16 and 6.17 show the maximum and minimum normal stresses of the upper and lower steel flanges calculated in two different hypotheses, upper slab cracked or uncracked.

The normal stresses for all cross-sections of the bridge are far from the limit of the yield strength, which depends on the steel plate thickness (Figs. 6.16 and 6.17):

$$\sigma_{Ed,ser} \leq \frac{f_y}{\gamma_{M,ser}}$$

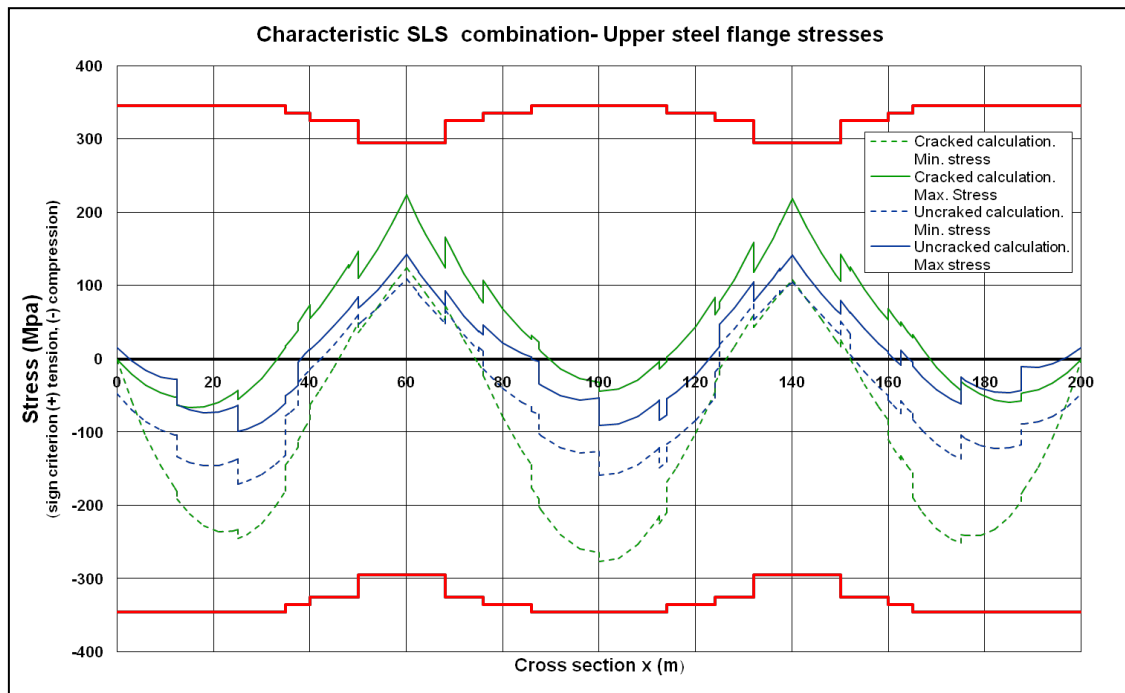


Fig. 6.16 Upper steel flange stress under the characteristic SLS combination

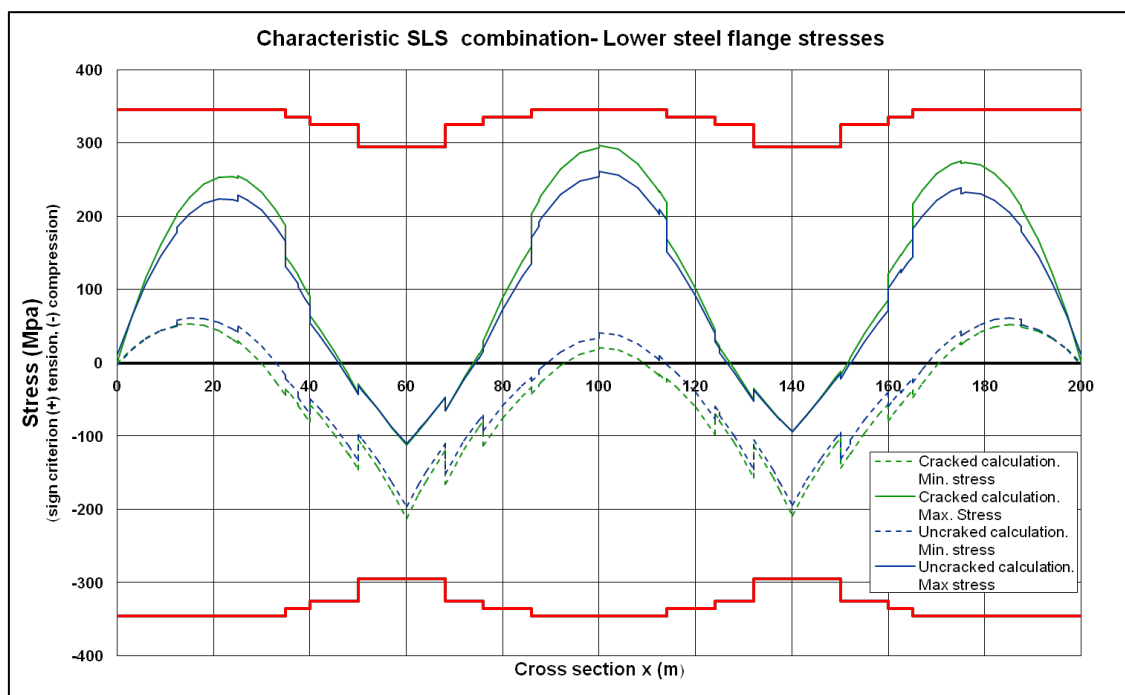


Fig. 6.17 Lower steel flange stress under the characteristic SLS combination

These figures make it clear that the normal stress calculated in the steel flanges without taking the concrete strength into account are logically equal to zero at both deck ends. However this is not true for the stresses calculated by taking the concrete strength into account as the self-balanced stresses from shrinkage (still called isostatic effects or primary effects of shrinkage in EN1994-2) were then taken into account.

Fig. 6.18 shows the maximum and minimum shear stresses in the centroid of the cross section calculated in two different hypotheses, upper slab cracked or uncracked. The shear stress results for all cross-sections of the bridge are very far from the limit:

$$\tau_{Ed,ser} \leq \frac{f_y}{\sqrt{3}\gamma_{M,ser}} = \frac{355}{\sqrt{3} \times 1.0} = 204.96 \text{ MPa}$$

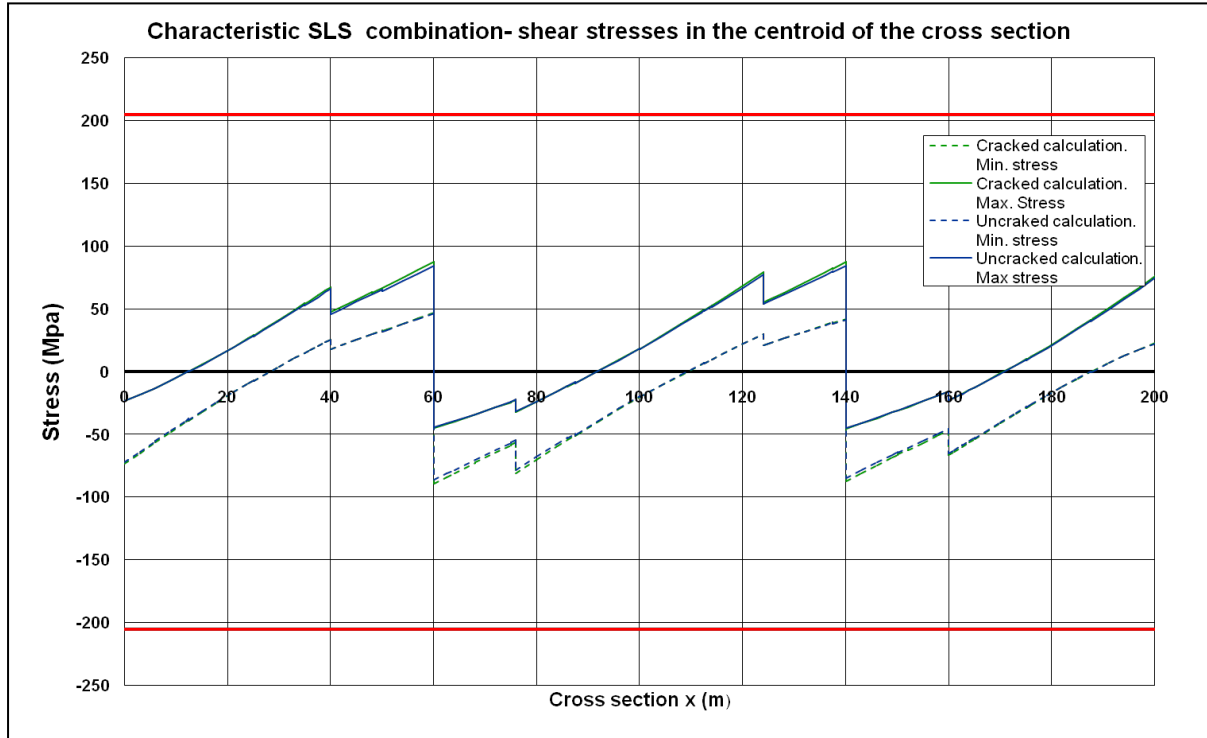


Fig. 6.18 Shear stress in the centre of gravity of the cross-section under the characteristic SLS combination

To be safe without increasing the number of stress calculations (and because this criterion is widely verified for the example, see Figs. 6.19 and 6.20), the Von Mises criterion has been assessed for each steel flange by considering the maximum normal stress in this flange and the maximum shear stress in the web (i.e. non-concomitant stresses and hypotheses on the safe side).

Figs. 6.19 and 6.20 show the maximum and minimum stresses applying the Von Mises safety criterion described in both steel flanges. All cross-sections of the bridge are very far from the limit:

$$\sqrt{\sigma_{Ed,ser}^2 + 3\tau_{Ed,ser}^2} \leq \frac{f_y}{\gamma_{M,ser}}$$

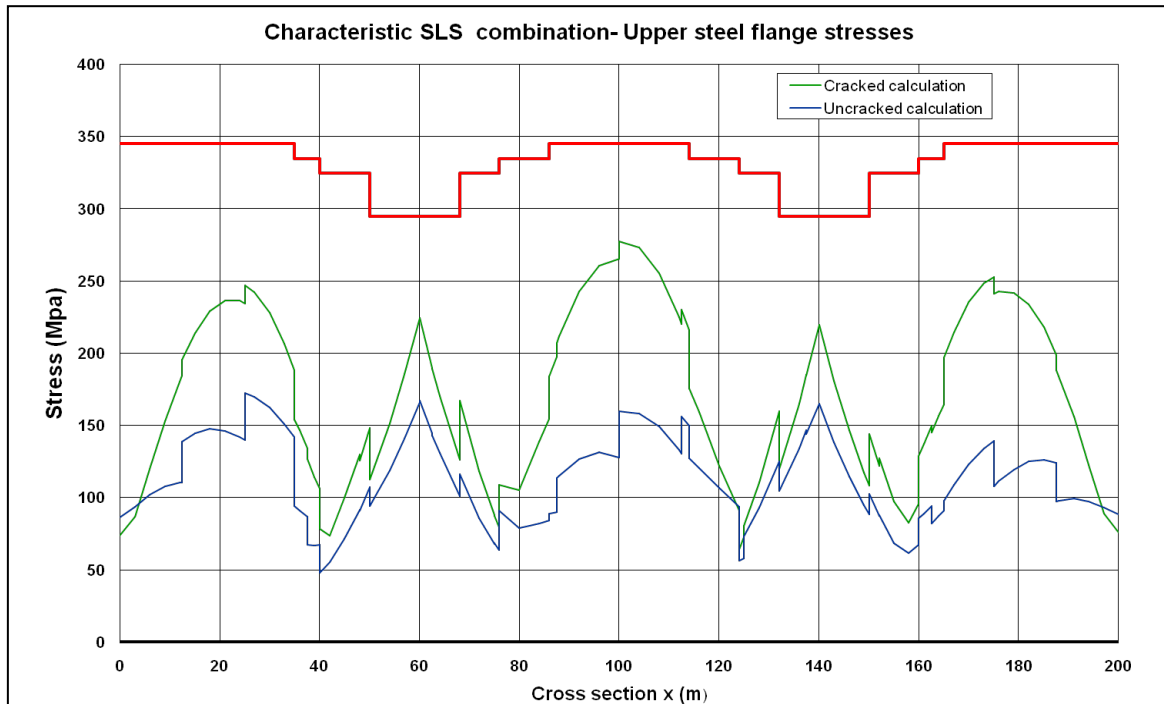


Fig. 6.19 Von Mises criterion in the upper flange under the characteristic SLS combination

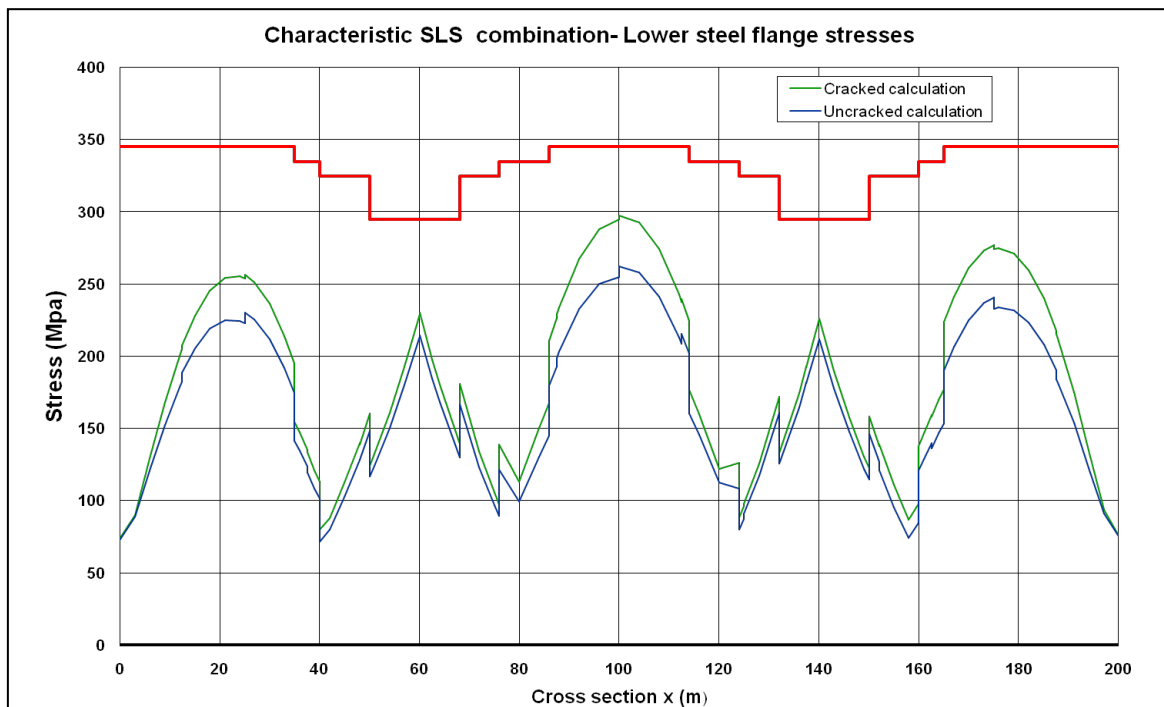


Fig. 6.20 Von Mises criterion in the lower flange under the characteristic SLS combination

6.5.4 ADDITIONAL VERIFICATION OF FATIGUE UNDER A LOW NUMBER OF CYCLES

According to EN-1993-2, 7.3 (2), it is assumed that the nominal stress range in the structural steel framework due to the SLS frequent load combination is limited to:

$$\Delta\sigma_{fre} \leq \frac{1.5f_y}{\gamma_{M,ser}}$$

This criterion is used to ensure that the "frequent" variations remain confined in the strictly linear part (+/- 0.75 f_y) of the structural steel stress-strain relationship. With this, any fatigue problems for a low number of cycles are avoided.

6.5.5 LIMITATION OF WEB BREATHING

Every time a vehicle crosses the bridge, the web gets slightly deformed out of its plane according to the deformed shape of the first buckling mode and then returns to its initial shape. This repeated deformation called web breathing is likely to generate fatigue cracks at the weld joint between web and flange or between web and vertical stiffener.

According to EN-1993-2, 7.4 (2), for webs without longitudinal stiffeners (or for a sub-panel in a stiffened web), the web breathing occurrence can be avoided for road bridges if:

$$\frac{h_w}{t_w} \leq 30 + 4.0L \leq 300$$

Where L is the span length in m, but not less than 20 m.

For the design example:

- in end-span: $h_w/t_w = 151.1 \leq 30 + 4 \cdot 60 = 270$
- in central span: $h_w/t_w = 151.1 \leq 300$

Generally speaking this criterion is widely verified for road bridges. Otherwise EN1993-2 defines a more accurate criterion (EN-1993, 7.4 (3)), if EN-1993-2, 7.4 (2) is not satisfied, based on:

- the critical plate buckling stresses of the unstiffened web (or of the sub-panel):
 $\sigma_{cr} = k_\sigma \cdot \sigma_E$ and $\tau_{cr} = k_\tau \cdot \sigma_E$,
- the stresses $\sigma_{x,Ed,ser}$ and $\tau_{x,Ed,ser}$ for frequent SLS combination of actions (calculated at a particular point where fatigue crack initiation could occur):

$$\sqrt{\left(\frac{\sigma_{x,Ed,ser}}{\sigma_{cr}}\right)^2 + \left(\frac{1.1\tau_{x,Ed,ser}}{\tau_{cr}}\right)^2} \leq 1.1$$

6.6 Control of cracking for longitudinal global bending

6.6.1 MAXIMUM VALUE OF CRACK WIDTH

The maximum values of the crack width are defined in EN-1992-1-1, 7.31 table 7.1N, depending on the exposure class (EN-1992-1-1, 4 table 4.1).

For the example we assume that the upper reinforcement of the slab, located under the waterproofing layer is XC3 exposure class, and the lower reinforcement of the slab is XC4.

According to EN-1992-1-1, 7.31 table 7.1N, for exposure classes XC3 and XC4 the recommended value of the maximum crack width w_{max} is 0.3 mm under the quasi-permanent load combination.

We will also verify the crack width, limited to $w_{max}=0.3$ mm, under indirect non-calculated actions (restrained shrinkage), in the tensile zone for the characteristic SLS combination of actions.

6.6.2 CRACKING OF CONCRETE. MINIMUM REINFORCEMENT AREA

The simplified procedure of EN-1994-2, 7.4.2 (1) requires a minimum reinforcement area for the composite beams given by:

$$A_s = k_s k_c k f_{ct,eff} A_{ct} / \sigma_s$$

Where:

$f_{ct,eff}$ is the mean value of the tensile strength of the concrete effective at the time when the cracks may first be expected to occur. $f_{ct,eff}$ may be taken as $f_{ctm}=3.2$ MPa for a concrete C35/45 (according to EN-1992-1-1 table 3.1).

k is a coefficient which accounts for the effect of non-uniform self balanced stresses. It may be taken equal to 0.80 (EN-1994-2, 7.4.2 (1)).

k_s is a coefficient which accounts for the effect of the reduction of the normal force of the concrete slab due to initial cracking and local slip of the shear connection, which may be taken equal to 0.90 (EN-1994-2, 7.4.2 (1)).

k_c is a coefficient which takes into account the stress distribution within the section immediately prior to cracking, and is given by:

$$k_c = \frac{1}{1 + h_c / (2z_0)} + 0.3 \leq 1.0$$

h_c is the thickness of the concrete slab, excluding any haunch or ribs. In our case $h_c=0.307$ m

z_0 is the vertical distance between the centroid of the uncracked concrete flange, and the uncracked composite section, calculated using the modular ratio n_0 for short term loading. In our case, for P-1 cross section, $z_0=1.02677-(0.109+0.307/2)= 0.764$ m, and for the P1/P2 mid-span cross-section, $z_0=0.66854-(0.109+0.307/2)= 0.406$ m.

σ_s is the maximum stress permitted in the reinforcement immediately after cracking. This may be taken as its characteristic yield strength f_{sk} (according to EN-1994-2, 7.4.2). In our case $f_{sk}=500$ MPa.

A_{ct} is the area of the tensile zone, caused by direct loading and primary effect of shrinkage, immediately prior to cracking of the cross section. For simplicity the area of the concrete section within the effective width may be used. In our case $A_{ct}=1.95$ m².

Then:

$$k_c = \frac{1}{1 + 0.307 / (2 \times 0.764)} + 0.3 = 1.13 \leq 1.0 \text{ for the support P-1 cross-section, hence } k_c=1.0$$

$$k_c = \frac{1}{1 + 0.307 / (2 \times 0.406)} + 0.3 = 1.02 \leq 1.0 \text{ for the mid-span P-1-P-2 cross-section, hence } k_c=1.0$$

$$A_{s,min} = 0.9 \times 1.0 \times 0.8 \times 3.2 \times 1.950 \times 10^6 / 500 = 8985.6 \text{ mm}^2 = 89.85 \text{ cm}^2 \text{ for half of slab (6 m).}$$

As we have ϕ 20/130 in the upper reinforcement level and ϕ 16/130 in the lower reinforcement level, the reinforcement area is $(24.166+15.466) \text{ cm}^2/\text{m} \cdot 6.0\text{m} = 237.79 \text{ cm}^2 \gg A_{smin}$, so the minimum reinforcement of the slab is verified.

6.6.3 CONTROL OF CRACKING UNDER DIRECT LOADING

According to EN-1994-2, 7.4.3 (1), when the minimum reinforcement calculated before (according to EN-1994-2, 7.4.2) is provided, the limitation of crack widths may generally be achieved by limiting the maximum bar diameter (according to EN-1994-2 table 7.1), and limiting the maximum bar spacing (according to table 7.2 of EN-1994-2, 7.4.3). Both limits depend on the stress in the reinforcement and the crack width.

Table 6.1 Maximum bar diameter for high bond bars (EN-1994-2, 7.4.3 table 7.2)

Steel Stresses $\sigma_s (\text{N/mm}^2)$	Maximum bar diameter ϕ^* (mm) for design crack width w_k		
	$w_k=0.4 \text{ mm}$	$w_k=0.3 \text{ mm}$	$w_k=0.2 \text{ mm}$
160	40	32	25
200	32	25	16
240	20	16	12
280	16	12	8
320	12	10	6
360	10	8	5
400	8	6	4
450	6	5	-

The maximum bar diameter ϕ for the minimum reinforcement may be obtained according to EN-1994-2, 7.4.2 (2):

$$\phi = \phi^* \frac{f_{ct,eff}}{f_{ct,0}}$$

Where ϕ^* is obtained of table 7.1 of EN-1994, and $f_{ct,0}$ is a reference strength of 2.9 MPa.

Table 6.2 Maximum bar spacing for high bond bars (EN-1994-2, 7.4.3 table 7.2)

Steel Stresses $\sigma_s (\text{N/mm}^2)$	Maximum bar spacing (mm) for design crack width w_k		
	$w_k=0.4 \text{ mm}$	$w_k=0.3 \text{ mm}$	$w_k=0.2 \text{ mm}$
160	300	300	200
200	300	250	150
240	250	200	100
280	200	150	50
320	150	100	-
360	100	50	-

The stresses in the reinforcement should be determined taking into account the effect of tension stiffening of concrete between cracks. In EN-1994-2, 7.4.3 (3) there is a simplified procedure for calculating this.

In a composite beam where the concrete slab is assumed to be cracked, stresses in reinforcement increase due to the effect of tension stiffening of concrete between cracks compared with the stresses based on a composite section neglecting concrete.

The direct tensile stress in the reinforcement σ_s due to direct loading may be calculated according to EN-1994-2, 7.4.3 (3)

$$\sigma_s = \sigma_{s,0} + \Delta\sigma_s$$

$$\text{With } \Delta\sigma_s = \frac{0.4f_{ctm}}{\alpha_{st}\rho_s} \text{ and } \alpha_{st} = \frac{A/I}{A_a I_a}$$

Where:

$\sigma_{s,0}$ is the stress in the reinforcement caused by the internal forces acting on the composite section, calculated neglecting concrete in tension.

f_{ctm} is the mean tensile strength of the concrete. For a concrete C35/45 (according to EN-1992-1-1 table 3.1) $f_{ctm}=3.2$ MPa.

ρ_s is the reinforcement ratio, given by $\rho_s = \frac{A_s}{A_{ct}}$

A_{ct} is the area of the tensile zone. For simplicity the area of the concrete section within the effective width may be used. In our case $A_{ct}=1.95$ m².

A_s is the area of all layers of longitudinal reinforcement within the effective concrete area.

A, I are area and second moment of area, respectively, of the effective composite section neglecting concrete in tension.

A_a, I_a are area and second moment of area, respectively, of the structural steel section.

Although there could be another section of the bridge with higher tensile stresses in the reinforcement, due to the sequence of the concreting phase, we will check for the application example only two cross sections, over the support P-1, which normally would be the worst section, and mid span P-1/P-2.

At the P-1 cross-section: $A_s=237.79$ cm² (ϕ 20/130 + ϕ 16/130 in 6 m), hence

$$\rho_s = \frac{237.79 \times 10^{-4}}{1.95} = 0.01219, \text{ and the mid-span P-1/P-2 cross-section } A_s=185.59 \text{ cm}^2 (\phi 16/130 + \phi$$

$$16/130 \text{ in 6 m), hence } \rho_s = \frac{185.59 \times 10^{-4}}{1.95} = 0.00952.$$

The value of α_{st} at the P-1 cross-section is $\alpha_{st} = \frac{0.3543 \times 0.5832}{0.3305 \times 0.5076} = 1.232$, while in the mid-span P-1/P-2

$$\text{cross-section } \alpha_{st} = \frac{0.1555 \times 0.2456}{0.1369 \times 0.1969} = 1.416.$$

Then, the effect of tension-stiffening at the P-1 cross-section is:

$$\Delta\sigma_s = \frac{0.4 \times 3.2}{1.232 \times 0.01219} = 85.23 \text{ MPa}$$

Meanwhile in the mid span P-1/P-2: $\Delta\sigma_s = \frac{0.4 \times 3.2}{1.416 \times 0.0} = 94.95 \text{ MPa}$

As the tensile stresses in the reinforcement caused by the internal forces acting on the composite section, calculated neglecting concrete in tension are:

- Support P-1 cross section: $\sigma_{s,0} = 65.94 \text{ MPa}$
- Mid span P-1/P-2 cross section: $\sigma_{s,0} = 27.45 \text{ MPa}$

Then the direct tensile stresses in reinforcement σ_s due to direct loading (according to EN-1994-2, 7.4.3) are:

- Support P-1 cross section: $\sigma_s = \sigma_{s,0} + \Delta\sigma_s = 65.94 + 85.23 = 151.17 \text{ MPa}$
- Mid span P-1/P-2 cross section: $\sigma_s = \sigma_{s,0} + \Delta\sigma_s = 27.45 + 94.95 = 122.4 \text{ MPa}$

As both values are below 160 MPa, according to table 6.2, the maximum bar spacing for the design crack width $w_k = 0.3 \text{ mm}$ is 300 mm. As we have 130 mm, the maximum bar spacing is verified.

According to table 6.1, the maximum bar diameter ϕ^* for the minimum reinforcement should be 32 mm, and

$$\phi = 32 \frac{3.2}{2.9} = 35.31 \text{ mm}$$

As the example verifies the minimum reinforcement established by EN-1994-2, 7.4.2 (1), the actual maximum diameter used in the longitudinal steel reinforcement is $\phi 20$, lower than the limit established by EN-1994-2, 7.4.2 (2), and the bar spacing also verifies the limits established by EN-1994-2, 7.4.2 (3), then the crack width is controlled.

6.6.4 CONTROL OF CRACKING UNDER INDIRECT LOADING

It has to be verified that the crack widths remain below 0.3 mm using the indirect method in the tensile zones of the slab for characteristic SLS combination of actions. This method assumes that the stress in the reinforcement is known. But that is not true under the effect of shrinkages (drying, endogenous and thermal shrinkage). The following conventional calculation is then suggested:

From the expression of the minimum reinforcement area for the composite beams given by EN-1994-2, 7.4.2 (1) $A_s = k_s k_c k_{ct,eff} A_{ct} / \sigma_s$ we can get:

$$\sigma_s = k_s k_c k_{ct,eff} A_{ct} / A_s$$

Let's consider that this is the stress in the reinforcement due to shrinkage at the cracking instant.

In our case, for the P-1 cross-section: $A_s = 237.79 \text{ cm}^2$ ($\phi 20/130 + \phi 16/130$ in 6 m), and the mid span P-1/P-2 cross section $A_s = 185.59 \text{ cm}^2$.

This gives:

- Support P-1 cross section: $\sigma_s = 0.9 \times 1.0 \times 0.8 \times 3.2 \times 1.95 / (237.79 \times 10^{-4}) = 188.94 \text{ MPa}$
- Mid-span P-1/P-2 cross section: $\sigma_s = 0.9 \times 1.0 \times 0.8 \times 3.2 \times 1.95 / (185.59 \times 10^{-4}) = 242.08 \text{ MPa}$

High bond bars with diameter $\phi = 20 \text{ mm}$ have been chosen in the upper reinforcement layer of the slab at the support cross-section, and $\phi = 16 \text{ mm}$ at the mid-span P-1/P-2 cross section. This gives:

- Support P-1 cross-section: $\phi^* = \phi \cdot 2.9/3.2 = 18.125 \text{ mm}$

- Mid-span P-1/P-2 cross-section: $\phi^* = \phi 2.9/3.2 = 14.5$ mm

The maximum reinforcement stress is obtained by linear interpolation in Table 7.1 in EN1994-2:

- Support P-1 cross-section: 230.18 MPa > 188.94 MPa
- Mid-span P-1/P-2 cross-section: 255.00 MPa > 242.08 MPa

Hence both sections are verified.

6.7 Shear connection at steel-concrete interface

6.7.1 RESISTANCE OF HEADED STUDS

The design shear resistance of a headed stud (Fig. 6.22) (P_{Rd}) automatically welded in accordance with EN-14555 is defined in EN-1994-2, 6.6.3:

$$P_{Rd} = \min(P_{Rd}^{(1)}; P_{Rd}^{(2)})$$

$P_{Rd}^{(1)}$ is the design resistance when the failure is due to the shear of the steel shank toe of the stud:

$$P_{Rd}^{(1)} = \frac{0.8 f_u \frac{\pi d^2}{4}}{\gamma_v}$$

$P_{Rd}^{(2)}$ is the design resistance when the failure is due to the concrete crushing around the shank of the stud:

$$P_{Rd}^{(2)} = \frac{0.29 \alpha d^2 \sqrt{f_{ck} E_{cm}}}{\gamma_v}$$

With:

$$\alpha = 0.2 \left(\frac{h_{sc}}{d} + 1 \right) \text{ for } 3 \leq \frac{h_{sc}}{d} \leq 4$$

$$\alpha = 1.0 \text{ for } \frac{h_{sc}}{d} > 4$$

Where:

γ_v is the partial factor. The recommended value is $\gamma_v = 1.25$.

d is the diameter of the shank of the headed stud ($16 \leq d \leq 25$ mm).

f_u is the specified ultimate tensile strength of the material of the stud ($f_u \leq 500$ MPa).

f_{ck} is the characteristic cylinder compressive strength of the concrete. In our case $f_{ck} = 35$ MPa.

E_{cm} is the secant modulus of elasticity of concrete (EN-1992-1-1, 3.1.2 table 3.1). In our case $E_{cm} = 22000 (f_{cm}/10)^{0.3} = 34077.14$ MPa. ($f_{cm} = f_{ck} + 8$ MPa)

h_{sc} is the overall nominal height of the stud.

In our case, if we consider headed studs of steel S-235-J2G3 of diameter $d=22$ mm, height $h_{sc}=200$ mm, and $f_{tU}=450$ MPa, then:

$$P_{Rd}^{(1)} = \frac{0.8 \times 450 \times \frac{\pi \times 22^2}{4}}{1.25} = 0.1095 \times 10^6 \text{ N} = 0.1095 \text{ MN}$$

$$\frac{h_{sc}}{d} = \frac{200}{22} = 9.09 \gg 4, \alpha = 1.0 \text{ and } P_{Rd}^{(2)} = \frac{0.29 \times 1 \cdot 22^2 \times \sqrt{35 \times 34077.14}}{1.25} = 0.1226 \text{ MN}$$

Then: $P_{Rd} = 0.1095$ MN. Each row of 4 headed studs (Fig. 6.21) resist at ULS: $4 \cdot P_{Rd} = 0.438$ MN

For Serviceability State Limit, EN-1994, 7.2.2 (6) refers to 6.8.1 (3). Under the characteristic combination of actions the maximum longitudinal shear force per connector should not exceed $k_s \cdot P_{Rd}$ (the recommended value for $k_s=0.75$).

Then: $k_s \cdot P_{Rd} = 0.75 \times 0.1095 \text{ MN} = 0.0766 \text{ MN}$. Each row of 4 headed studs (Fig. 6.21) resist at SLS:
 $4 \cdot k_s \cdot P_{Rd} = 0.3064 \text{ MN}$

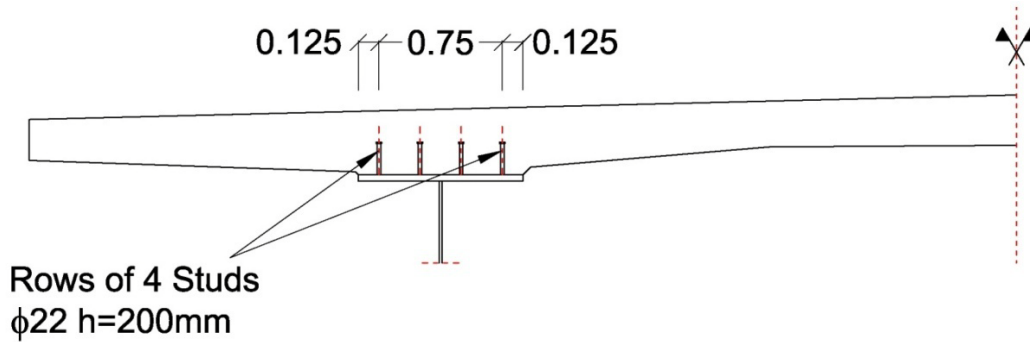


Fig. 6.21 Detail of headed studs connection

6.7.2 DETAILING OF SHEAR CONNECTION

The following construction detailing applies for in-situ poured concrete slabs (EN-1994-2, 6.6.5). When the slab is precast, these provisions may be reviewed paying particular attention to the various instability problems (buckling in the composite upper flange between two groups of shear connectors, for example) and to the lack of uniformity of the longitudinal shear flow at the steel-concrete interface (EN-1994-2, 6.6.5.5 (4))

Maximum longitudinal spacing between rows of connectors

According to EN-1994-2, 6.6.5.5 (3), to ensure a composite behaviour of the main girder, the maximum longitudinal center to center spacing (s) between two successive rows of connectors is limited to: $s_{max} \leq \min(800 \text{ mm} ; 4 h_c)$, with h_c the concrete slab thickness.

When verifying the mid-span P1/P2 cross-section (see paragraph 6.1.2), it was considered that the upper structural steel flange in compression was a Class 1 element as it was connected to the concrete slab.

However if we consider the upper flange non-connected to the upper concrete slab, according to EN-1993-1-1 table 5.2 sheet 2 of 3, $c/t_f = ((1000-18)/2)/40=12.275$ and that would result a Class 4 flange as $c/t_f=12.275 > 14 \cdot \sqrt{235/345} = 11.55$

In order to classify a compressed upper flange connected to the slab as a Class 1 or 2 because of the restraint from shear connectors, the headed studs rows should be sufficiently close to each other to prevent buckling between two successive rows (EN-1994-2, 6.6.5.5(2)). This gives an additional criterion in s_{max} :

$$s_{max} \leq 22t_f \sqrt{235/f_y} \text{ if the concrete slab is solid and there is contact over the full length.}$$

$s_{max} \leq 15t_f \sqrt{235/f_y}$ if the concrete slab is not in contact over the full length (e.g. slab with transverse ribs). This is not our case.

Where t_f is the thickness of the upper flange, and f_y the yield strength of the steel flange.

Table 6.3 summarizes the results of applying both conditions to our case.

Table 6.3 Maximum longitudinal spacing for rows of studs

Upper Steel flange t_f (mm)	f_y (N/mm ²)	s_{max}	e_D
40	345	726	297
55	335	800	414
80	325	800	*
120	295	800	*

* Only applies for flanges in compression (not in tension)

This criterion is supplemented by EN-1994-2, 6.6.5.5(2) defining a maximum distance between the longitudinal row of shear connectors closest to the free edge of the upper flange in compression – to which they are welded – and the free edge itself (Fig. 6.22):

$$e_D \leq 9 \times t_f \sqrt{235/f_y}$$

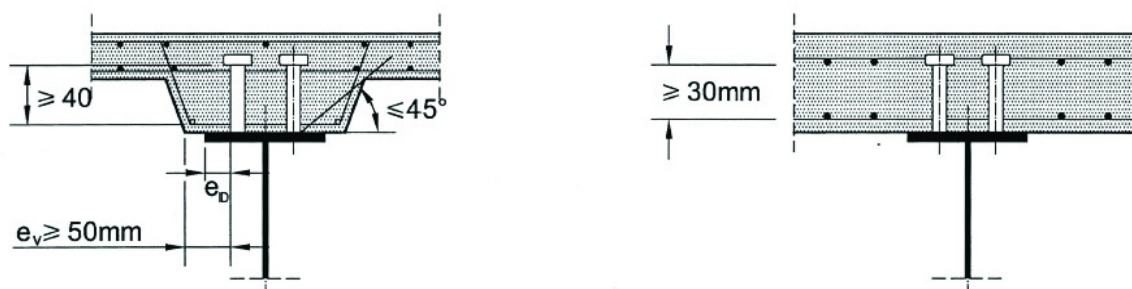


Fig. 6.22 Detailing

Minimum distance between the edge of a connector and the edge of a plate

According to EN-1994-2, 6-6-5-6 (2), the distance e_D between the edge of a headed stud and the edge of a steel plate must not be less than 25 mm, in order to ensure the correct stud welding.

In this example (Fig. 6.21), $e_d = \frac{b_f - b_0}{2} - \frac{d}{2} = \frac{1000 - 750}{2} - \frac{22}{2} = 114 > 25$

Minimum dimensions of the headed studs

According to EN-1994-2 6.6.5.7 (1) and (2) the height of a stud should not be less than $3 \cdot d$, where d is the diameter of the shank, and the head of the stud should have a diameter not less than $1.5 \cdot d$, and a depth of at least $0.4 \cdot d$ (Fig. 6.23).

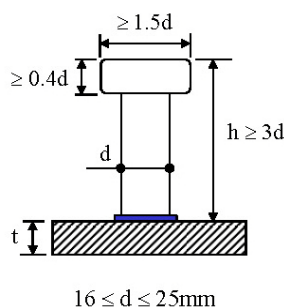


Fig. 6.23 Minimum dimensions of a headed stud

As we have studs of $d=22$ mm, the head should have a diameter over 33 mm, and a depth of at least 8.8 mm. With a total height of the studs of 200 mm, we are far from the limit of $3 \cdot d=66$ mm.

EN-1994-2 also establishes a condition between the diameter of the connector and the thickness of the steel plate (EN-1994-2, 6.6.5.7 (3)). For studs welded to steel plates in tension subjected to fatigue loading, the diameter of the stud should be:

$$d \leq 1.5 \cdot t_f$$

This is widely satisfied in the example, with $t_{fmin}=55\text{mm}$ in the tensile area, and $d=22\text{mm}$.

This limitation also applies to steel webs. This verification allows the use of the detail category $\Delta\tau_c = 90$ MPa.

Clause 6.6.5.7 (5) establishes that the limit for other elements than plates in tension or webs is $d \leq 2.5 \cdot t_f$

Minimum spacing between rows of connectors

According to EN-1994-2 6.6.5.6 (4) the longitudinal spacing of studs in the direction of the shear force should be not less than $5d=110$ mm in our case, while the spacing in the transverse direction to the shear force should be not less than $2.5d$ in solid slabs, or $4d$ in other cases. In our example $2.5d=55$ mm. Both limits are widely fulfilled in the example, with $s_{trans}=250$ mm

Criteria related to the stud anchorage in the slab

Where a concrete haunch is used between the upper structural steel flange and the soffit of the concrete slab, the sides of the haunch should lie outside a line drawn 45° from the outside edge of the connector (Fig. 6.22) (EN-1994-2, 6.6.5.4 (1)).

Clause 6.6.5.4 (2) establishes that the nominal concrete lateral cover from the side of the haunch to the connector should be not less than 50 mm, and the clear distance between the lower face of the stud head and the lower reinforcement layer should be not less than 40 mm, according to clause

6.6.5.4 (2). This value could be reduced to 30 mm if no concrete haunch is used (EN-1994-2 6.6.5.1 (1)) (see Fig. 6.22).

Figs. 6.24 and 6.25 show a general view and a detail of the connection with headed studs of the upper flange of a composite bridge, and Fig. 6.26 shows the connection of the lower flange of the main steel girders in a double composite cross-section.



Figs. 6.24 & 6.25 View and detail of an upper flange connection



Fig. 6.26 View of the lower flange connection of a steel girder

6.7.3 CONNECTION DESIGN FOR THE CHARACTERISTIC SLS COMBINATION OF ACTIONS

When the structure behaviour remains elastic in a given cross-section, each load case from the global longitudinal bending analysis produces a longitudinal shear force per unit length $v_{L,k}$ at the interface between the concrete slab and the steel main girder. For a girder with uniform moment of area (S) subjected to a continuous bending moment, this shear force per unit length is easily deduced from the cross-section properties and the internal forces and moments the girder is subjected to:

$$v_{L,k} = \frac{S_c V_k}{I}$$

Where:

$v_{L,k}$ is the longitudinal shear force per unit length at the interface concrete-steel

S_c is the moment of area of the concrete slab with respect to the centre of gravity of the composite cross-section

I is the second moment of area of the composite cross-section

V_k is the shear force for the considered load case and coming from the elastic global cracked analysis

According to EN-1994-2, 6.6.2.1 (2), to calculate normal stresses, when the composite cross-section is ultimately (characteristic SLS combination of actions in this paragraph) subjected to a negative bending moment $M_{c,Ed}$, the concrete is taken as cracked and does not contribute to the cross-section strength. But to calculate the shear force per unit length at the interface, even if $M_{c,Ed}$ is negative, the characteristic cross-section properties S_c and I are calculated by taking the concrete strength into account (uncracked composite behaviour of the cross-section).

The final shear force per unit length is obtained by adding algebraically the contributions of each single load case and considering the construction phases. As for the normal stresses calculated with an uncracked composite behaviour of the cross-section, the modular ratio used in S_c and I is the same as the one used to calculate the corresponding shear force contribution for each single load case.

For SLS combination of actions, the structure behaviour remains entirely elastic and the longitudinal global bending calculation is performed as an envelope. Thus the value of the shear force per unit length is determined in each cross-section at abscissa x by:

$$v_{L,k}(x) = \max \left[|v_{\min,k}(x)|; |v_{\max,k}(x)| \right]$$

Fig. 6.27 shows the variations in this longitudinal shear force per unit length for the characteristic SLS combination of actions, for the case of the example.

In each cross-section of the deck there should be enough studs to resist all the shear force per unit length.

The following should be therefore verified at all abscissa x :

$$v_{L,k}(x) \leq \frac{N_i}{L_i} \cdot (k_s \cdot P_{Rd}) , \text{ with } k_s \cdot P_{RD} = 4 \cdot k_s \cdot P_{RD, \text{ of 1 stud}}$$

Where:

$v_{L,k}$ is the shear force per unit length in the connection under the characteristic SLS combination

N_i is the number of rows of 4 headed studs $\phi 22\text{mm}$ and $h=200\text{ mm}$ located at the length L_i

L_i is the length of a segment with constant row spacing

$k_s \cdot P_{Rd} = 4 \cdot k_s \cdot P_{Rd, \text{ of 1 stud}} = 0.3064 \text{ MN}$ is the SLS resistance of a row of 4 headed studs, calculated in 7.1

For the example we have divided the total length of the bridge into segments delimited by the following abscissa x in (m), corresponding with nodes of the design model:

0.0	6.0	12.5	25.0	35.0	42.0	50.0	62.5
80.0	87.5	100.0	108.0	112.5	120.0	132.0	140.0
150.0	162.5	170.0	176.0	187.5	194.0	200.0	

For example, for the segment [50.0 m ; 62.5 m] around the support P1, the shear force per unit length obtained in absolute value for characteristic SLS combination of actions is as follows (in MN/m):

Table 6.4 Shear force per unit length at SLS at segment 50-62.5 m

x (m)	50 ⁺	54 ⁻	54 ⁺	60 ⁻	60 ⁺	62.5 ⁻
$v_{L,k}$ (MN/m)	0.842	0.900	0.900	0.989	0.943	0.906

The maximum SLS shear force per unit length to be considered is therefore 0.989 MN/m, which is guaranteed providing the stud rows are placed at the maximum spacing of (4 studs per row):

$$\frac{(4 \cdot k_s \cdot P_{Rd})}{\max(v_{L,k}(x))} = \frac{0.3064 \text{ MN}}{0.989 \text{ MN/m}} = 0.31 \text{ m} ; \text{ on a safe side } 0.30 \text{ m}.$$

Fig. 6.27 illustrates this elastic design of the connection for characteristic SLS combination of actions. The curve representing the shear force per unit length that the shear connectors are able to take up thus encompasses fully the curve of the SLS design shear force per unit length.

The corresponding values of row spacing, obtained for the design of the connection in SLS are summarized in paragraph 6.7.5 of this chapter. Note that we have considered regular spacing jumps from 50 to 50 mm.

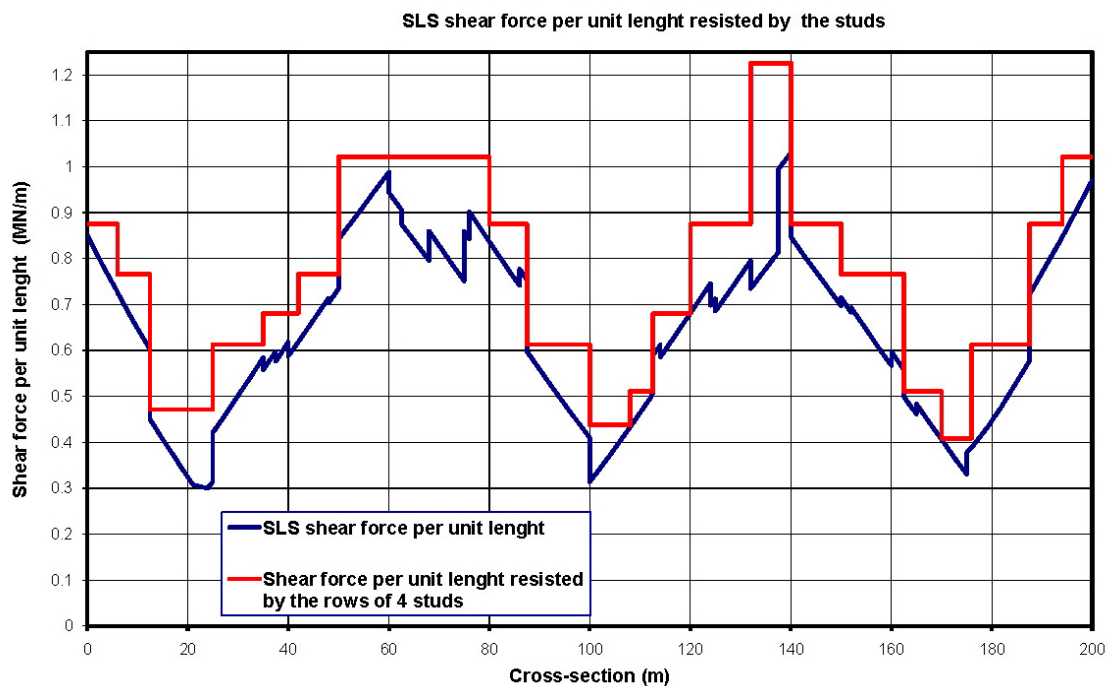


Fig. 6.27 SLS shear force per unit length resisted by the headed studs

6.7.4 CONNECTION DESIGN FOR THE ULS COMBINATION OF ACTIONS OTHER THAN FATIGUE

6.7.4.1 Elastic design

Whatever the behaviour of the bridge at ULS – elastic in all cross-sections or elasto-plastic in some cross-sections – the design of the connection at ULS starts by an elastic calculation of the shear force per unit length at the interface steel-concrete, by elastic analysis with the cross-sections properties of the uncracked section taking into account the effects of construction (EN-1994, 6.6.2.2 (4)), following the same procedure as made for SLS in the previous paragraph.

In each cross-section, the shear force per unit length at ULS is therefore given by:

$$v_{L,Ed}(x) = \max \left[|v_{\min,Ed}(x)|; |v_{\max,Ed}(x)| \right]$$

With:

$$v_{L,Ed} = \frac{S_c V_{Ed}}{I}$$

Where:

$v_{L,Ed}$ is the design longitudinal shear force per unit length at the concrete-steel interface.

S_c is the moment of area of the concrete slab with respect to the centre of gravity of the composite cross-section.

I is the second moment of area of the composite cross-section.

V_{Ed} is the design shear force for the considered load case and coming from the elastic global cracked analysis considering the constructive procedure.

Fig. 6.28 shows the variations in this design longitudinal shear force per unit length for the ULS combination of actions, for the case of the example.

According to EN-1994-2, 6.6.1.2 (1) the number of shear connectors (headed studs) per unit length, constant per segment, should verify the following two criteria:

- locally in each segment “ i ”, the shear force per unit length should not exceed by more than 10% what the number of shear connectors per unit length can resist:

$$v_{L,Ed}(x) \leq 1.1 \cdot \frac{N_i}{L_i} \cdot P_{RD}, \text{ with } P_{RD} = 4 \cdot P_{RD, \text{ of 1 stud}}$$

Where:

N_i is the number of rows of 4 headed studs $\phi 22$ mm and $h=200$ mm located at the length L_i

L_i is the length of a segment with constant row spacing

$P_{RD}=4 \cdot P_{RD, \text{ of 1 stud}}=0.438$ MN is the ULS resistance of a row of 4 headed studs, calculated in 7.1.

- over every segment length (L_i), the number of shear connectors should be sufficient so that the total design shear force does not exceed the total design shear resistance:

$$\int_{x_i}^{x_{i+1}} v_{L,Ed}(x) dx \leq N_i(P_{RD}) , \text{ with } P_{RD} = 4 \cdot P_{RD, \text{ of } 1 \text{ stud}}$$

Where x_i and x_{i+1} designates the abscissa at the border of the segment L_i .

For the design of the connection at ULS we have considered the same segment division as used for the SLS verification.

In the example, for the segment [50.0 m ; 62.5 m] around the support P1, the design shear force per unit length obtained in absolute value for ULS combination of actions is as follows (in MN/m):

Table 6.5 Design shear force per unit length at ULS at segment 50-62.5 m

x (m)	50 ⁺	54 ⁻	54 ⁺	60 ⁻	60 ⁺	62.5 ⁻
$v_{L,Ed}$(MN/m)	1.124	1.203	1.203	1.323	1.264	1.213

The maximum ULS design shear force per unit length to be resisted is therefore 1.323 MN/m, which is guaranteed providing the stud rows are placed at the maximum spacing of (4 studs per row):

$$\frac{1.10 \times (4 \cdot P_{Rd, 1 \text{ stud}})}{\max(v_{L,Ed}(x))} = \frac{1.1 \times 0.438 \text{ MN}}{1.323 \text{ MN/m}} = 0.365 \text{ m}$$

And the second condition:

$$\int_{x_i}^{x_{i+1}} v_{L,Ed}(x) dx = 15.407 \text{ MN (in 12.5 m)} = 1.232 \text{ MN/m} \leq \frac{(4 \cdot P_{Rd, 1 \text{ stud}})}{s}$$

Then $s \geq (4 \cdot P_{Rd, \text{ of } 1 \text{ stud}}) / 1.232 = 0.438 / 1.232 = 0.355 \text{ m}$, then on the safe side the spacing for this segment would be $s = 0.35 \text{ m}$.

Fig. 6.28 illustrates the elastic design of the connection for the Ultimate Limit State (ULS) combination of actions.

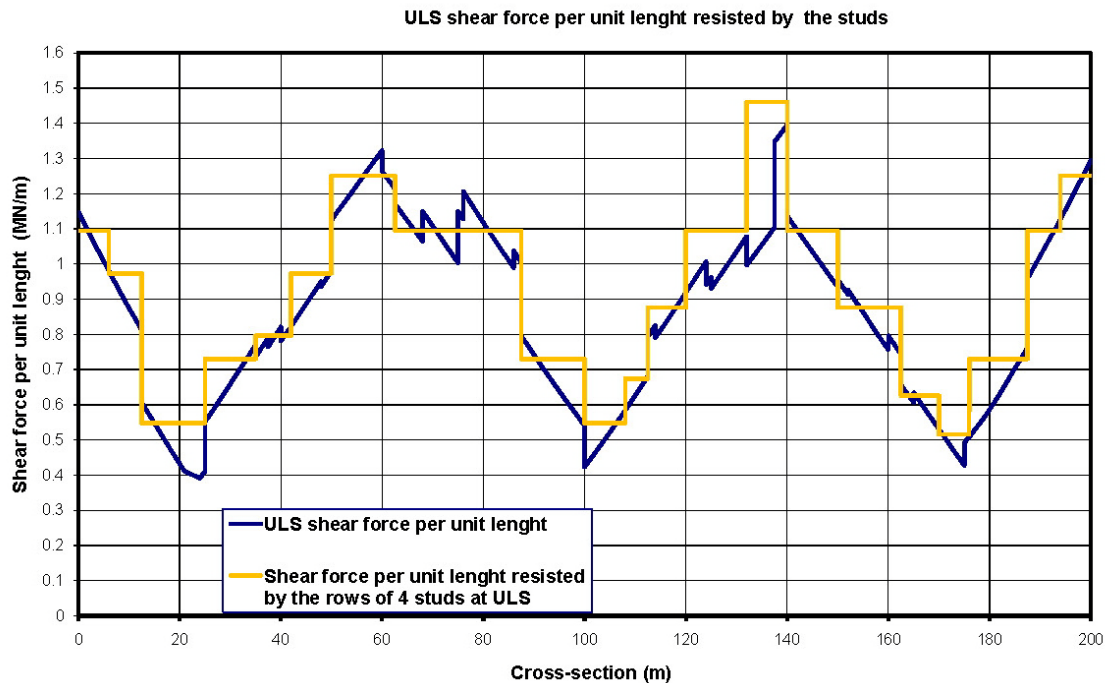


Fig. 6.28 ULS shear force per unit length resisted by the headed studs

6.7.4.2 Design with plastic zones in sagging bending areas

If, a cross-section with a positive bending moment at ULS has partially yielded, the previous elastic calculation, made for the ULS combination of actions, should be supplemented (EN-1994-2, 6.6.2.2 (1)).

As far as the structure behaviour is no longer elastic, the relationship between the shear force per unit length and the global internal forces and moments is no longer linear. Therefore the previous elastic calculation becomes inaccurate. In a plastic zone, the shear connection is normally heavily loaded and a significant bending moment redistribution occurs between close cross-sections.

In our case, although the mid-span cross-sections are Class 1 sections, no yielding occurs, as we can see on Fig. 6.1, with a medium tensile value for the lower flange of $342.9\text{MPa} < f_y = 345\text{MPa}$. There is therefore no need to perform the more complex calculations established by EN-1994-2 in clauses 6.6.2.2 (2) and (3).

6.7.5 SYNOPSIS OF THE DESIGN EXAMPLE

Paragraphs 6.7.3 and 6.7.4 summarize, respectively, the connection design at SLS and ULS. Fig. 6.29 shows the results of the spacing of rows of 4 headed stud connectors resulting from the design at SLS (red solid line), the design at ULS (orange solid line), and the results of applying the maximum spacing requirements (green solid line) defined in paragraph 6.7.1, according to EN-1994-2.

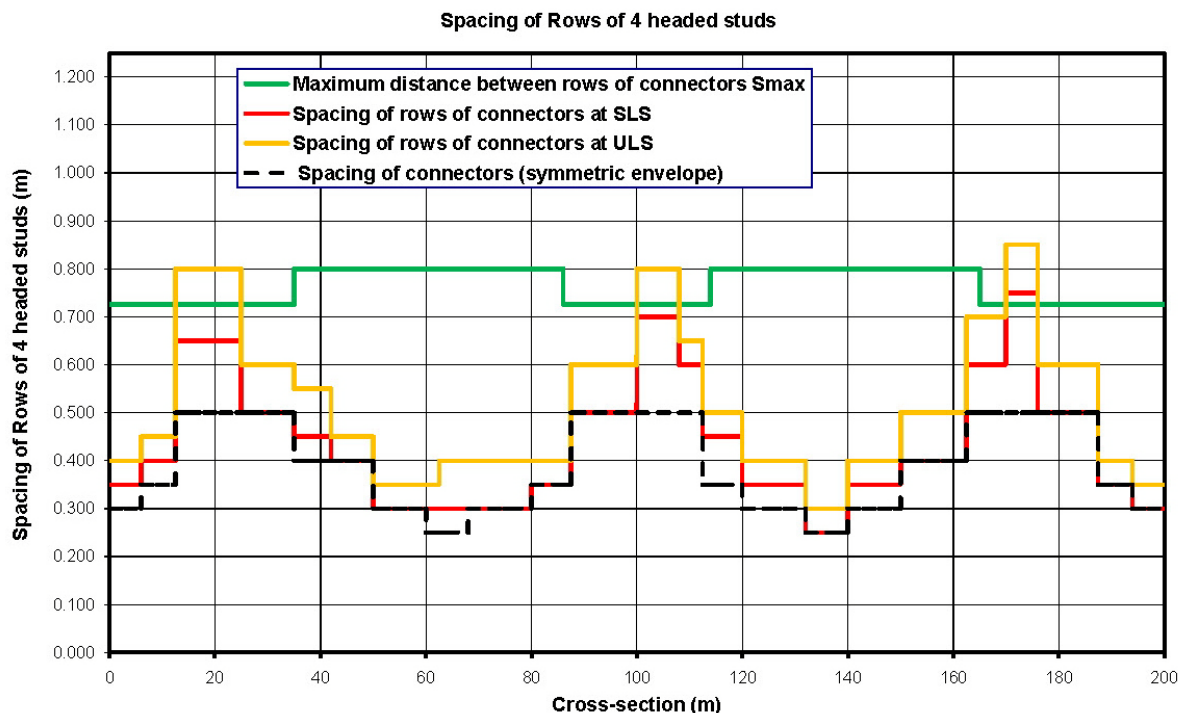


Fig. 6.29 Envelope of spacing of rows of 4 connectors after connection dimensioning

As described before, we have used an engineering criterion of dimensioning the spacing of rows of connectors, with 50 mm steps. This figure also shows the final envelope (in black dotted line) resulting from the three mentioned conditions, and with the provision of symmetrical spacing design of the connection in the total length of the bridge. Although that could not be theoretically necessary, constructively thinking it is absolutely convenient.

Note that, in general, the SLS criteria nearly always govern the design over the ULS requirements, except for the sections around the mid-span. In these zones, the spacing just necessary to resist the SLS shear flow becomes too large to avoid buckling in the steel flange between two successive stud rows. And then the governing criterion becomes the construction detailing.

6.7.6 DESIGN OF THE SHEAR CONNECTION FOR THE FATIGUE ULS COMBINATION OF ACTIONS

In this paragraph we summarize the fatigue verification that has to be performed to confirm the design of the connection already performed in previous paragraphs under SLS and ULS combination of actions.

Once the connection is designed, and decided the final spacing of rows of connectors, fatigue ULS of the connectors has to be verified according to EN-1994-2, section 6.8.

The fatigue load model FLM3 induces the following stress ranges:

- $\Delta\tau$, shear stress range in the stud shank, calculated at the level of its weld on the upper structural steel flange.

Unlike normal stress range, the shear stresses at the steel-concrete interface are calculated using the uncracked cross-section mechanical properties. The shear stress for the basic combination of non-cyclic loads (EN1992-1-1, 6.8.3) has therefore no influence. $\Delta\tau$ is thus deduced from variations in the shear force per unit length under the FLM3 crossing only – noted $\Delta V_{L,FLM3}$ – by taking account of its transverse location on the

pavement and using the short term modular ratio n_0 . $\Delta\tau$ also depends on the local shear connector density and the nominal value of the stud shank area:

$$\Delta\tau = \frac{\Delta v_{L,FLM3}}{\left(\frac{\pi d^2}{4}\right) \frac{N_i}{L_i}}$$

Where:

N_i is the number of rows of 4 headed studs ϕ 22mm and $h=200$ mm located at the length L_i .

L_i is the length of a segment with constant row spacing.

d is the diameter of the shank of the headed stud.

$\Delta v_{L,FLM3}$ is the variations in the shear force per unit length under the FLM3 crossing.

- $\Delta\sigma_p$, normal stress range in the upper steel flange to which the studs are welded.

6.7.6.1 Equivalent constant amplitude stress range

For verification of stud shear connectors based on nominal stress ranges, the equivalent constant range of shear stress $\Delta\tau_{E,2}$ for two million cycles is given by (EN-1994-2, 6.8.6.2(1)):

$$\Delta\tau_{E,2} = \lambda_v \cdot \Delta\tau$$

Where:

$\Delta\tau$ is the range of shear stress due to fatigue loading, related to the cross-sectional area of the shank of the stud $\pi d^2/4$ with d the diameter of the shank.

λ_v is the damage equivalent factor depending on the spectra and the slope m of the fatigue curve.

For bridges, the damage equivalent factor λ_v for headed studs in shear should be determined from $\lambda_v = \lambda_{v1} \cdot \lambda_{v2} \cdot \lambda_{v3} \cdot \lambda_{v4}$ (EN-1994-2, 6.8.6.2 (3))

Factors λ_{v2} to λ_{v4} should be determined in accordance with EN-1993-2, 9.5.2 (3) to (6) but using exponents 8 and 1/8 instead of 5 and 1/5, to allow for the relevant slope $m=8$ of the fatigue strength curve for headed studs given in EN-1994-2, 6.8.3 (3).

- λ_{v1} is the factor for damage effect of traffic. According to EN-1994-2, 6.8.6.2 (4) $\lambda_{v1}=1.55$ for road bridges up to 100 m span.
- λ_{v2} is the factor for the traffic volume

$$\lambda_{v2} = \frac{Q_{m1}}{Q_0} \left(\frac{N_{obs}}{N_0} \right)^{1/8}$$

Where:

$$Q_{m1} = \left[\frac{\sum n_i Q_i^8}{\sum n_i} \right]^{1/8} \quad (\text{EN-1993-2, 9.5.2 (3)})$$

is the average gross weight (kN) of the lorries in the slow lane.

$$Q_0 = 480 \text{ kN}$$

$$N_0 = 0.5 \times 10^6$$

N_{obs} is the total number of lorries per year in the slow lane. In this example we have $N_{obs} = 0.5 \times 10^6$, equivalent to a road or motorway with medium rates of lorries (EN-1991-2, table 4.5 (n))

Q_i is the gross weight in kN of the lorry i in the slow lane.

n_i is the number of lorries of gross weight Q_i in the slow lane.

Table 6.6 Traffic assumption for obtaining λ_{v2}

Lorry	Q (kN)	Long. distance
1	200	20%
2	310	5%
3	490	50%
4	390	15%
5	450	10%

If we substitute table 6.6 values into the previous equations, then we obtain:

$$Q_{m1} = 457.37 \text{ kN}$$

$$\lambda_{v2} = \frac{457.37}{480} = 0.952$$

- λ_{v3} is the factor for the design life of the bridge. For 100 years of design life, then $\lambda_{v3} = 1.0$ according to EN-1993-2, 9.5.2 (5)
- λ_{v4} takes into account the effects of the heavy traffic on the other additional slow lane defined in the example. In the case of a single slow lane, $\lambda_{v4} = 1.0$.

In the present case, the factor depends on the transverse influence of each slow lane on the internal forces and moments in the main girders:

$$\lambda_{v4} = \left[1 + \frac{N_2}{N_1} \left(\frac{\eta_2 Q_{m2}}{\eta_1 Q_{m1}} \right)^8 \right]^{1/8}$$

$$\eta = \frac{1}{2} - \frac{e}{b}$$

With

e is the eccentricity of the FLM3 load with respect to the bridge deck axis (in the example +/- 1.75 m);

b is the distance between the main girders (in the example 7.0 m).

$$\eta_1 = \frac{1}{2} + \frac{1.75}{7.0} = 0.75 \text{ and } \eta_2 = \frac{1}{2} - \frac{1.75}{7.0} = 0.25$$

The factor η_I represents the maximum influence of the transverse location of the traffic slow lanes on the fatigue-verified main girder. $N_I=N_2$ (same number of heavy vehicles in each slow lane) and $Q_{m1}=Q_{m2}$ (same type of lorry in each slow lane) will be considered for the example.

This gives finally $\lambda_{v4}=1.0$.

Then $\lambda_v=1.55 \cdot 0.952 \cdot 1.0 \cdot 1.0=1.477$

For the upper steel plate, a stress range $\Delta\sigma_E$ is defined according to EN-1994-2, 6.8.6.1 (2):

$$\Delta\sigma_E = \lambda\phi \left| \sigma_{\max,f} - \sigma_{\min,f} \right|$$

Where:

$\sigma_{\max,f}$ and $\sigma_{\min,f}$ are the maximum and minimum stresses due to the maximum and minimum internal bending moments resulting from the combination of actions defined in EN-1992-1-1, 6.8.3 (3):

$$\left(\sum_{j \geq 1} G_{k,j} + P + \psi_{1,1} Q_{k,1} + \sum_{i > 1} \psi_{2,i} Q_{k,i} \right) + Q_{fat}$$

λ is the damage equivalent factor, calculated according to EN-1993-2, 9.5.2., for road bridges, with the relevant slope of the fatigue strength curve $m=5$.

ϕ is a damage equivalent impact factor. For road bridges $\phi = 1.0$ (EN-1994-2, 6.8.6.1 (7)), however ϕ is increased when crossing an expansion joint, according to EN-1991-2, 4.6.1(6), $\phi = 1.3[1-D/26] \geq 1.0$, where D (in m) is the distance between the detail verified for fatigue and the expansion joint (with $D \leq 6m$).

6.7.6.2 Fatigue verifications

For stud connectors welded to a steel flange that is always in compression under the relevant combination of actions (see paragraph 7.6.1), the fatigue assessment should be made by checking the criterion, which corresponds to a crack propagation in the stud shank:

$$\gamma_{Ff} \Delta\tau_{E-2} \leq \Delta\tau_c / \gamma_{Mf,s}$$

Where:

$\Delta\tau_{E,2}$ is the equivalent constant range of shear stress for two millions cycles

$$\Delta\tau_{E,2} = \lambda_v \cdot \Delta\tau \text{ (see paragraph 7.6.1)}$$

$\Delta\tau_c$ is the reference value of fatigue strength at 2 million cycles. $\Delta\tau_c=90$ MPa

γ_{Ff} is the fatigue partial factor. According to EN-1993-2, 9.3 the recommended value is $\gamma_{Ff}=1.0$

$\gamma_{Mf,s}$ is the partial factor for verification of headed studs in bridges. According to EN-1994-2, 2.4.1.2 (6), the recommended value is $\gamma_{Mf,s}=1.0$.

Meanwhile, where the maximum stress in the steel flange to which studs connectors are welded is tensile under the relevant combination, the interaction at any cross-section between shear stress range $\Delta\tau_E$ in the weld of the stud connector and the normal stress range $\Delta\sigma_E$ in the steel flange should be verified according to EN-1994-2, 6.8.7.2 (2):

$$\frac{\gamma_{Ff}\Delta\sigma_{E,2}}{\Delta\sigma_c/\gamma_{Mf}} \leq 1.0 ; \quad \frac{\gamma_{Ff}\Delta\tau_{E,2}}{\Delta\tau_c/\gamma_{Mf,s}} \leq 1.0 \quad \text{and} \quad \frac{\gamma_{Ff}\Delta\sigma_{E,2}}{\Delta\sigma_c/\gamma_{Mf}} + \frac{\gamma_{Ff}\Delta\tau_{E,2}}{\Delta\tau_c/\gamma_{Mf,s}} \leq 1.3$$

Where:

$\Delta\sigma_E$ is the stress range in the flange connected (see paragraph 7.6.1)

$\Delta\sigma_c$ is the reference value of fatigue strength at 2 million cycles. $\Delta\sigma_c=80$ MPa

γ_{Mf} is the partial factor defined by EN-1993-1-9 table 3.1. For safe life assessment method with high consequences of the upper steel flange failure of the bridge, $\gamma_{Mf}=1.35$.

In general, once the connection at the steel-concrete interface is designed under the SLS and ULS combination of actions, and the final spacing of connectors is decided fulfilling the maximum spacing limits established by EN-1994-2 (see paragraphs 6.7.2 to 6.7.5), the fatigue ULS verification does not influence the design of the connection.

Figure 6.30 shows the verification of the connection under the fatigue ULS, for the case of the example, and Figure 6.31 shows the spacing of the rows of 4 studs under the fatigue ULS.

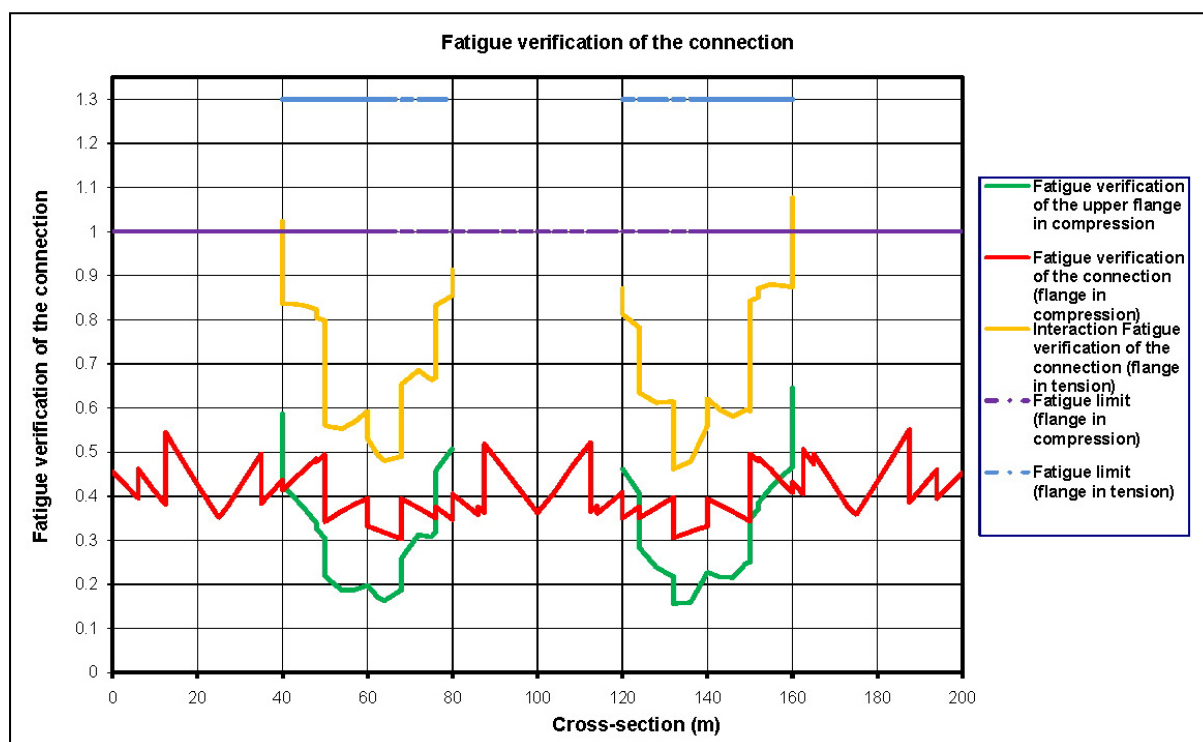


Fig. 6.30 Fatigue verification of the connection

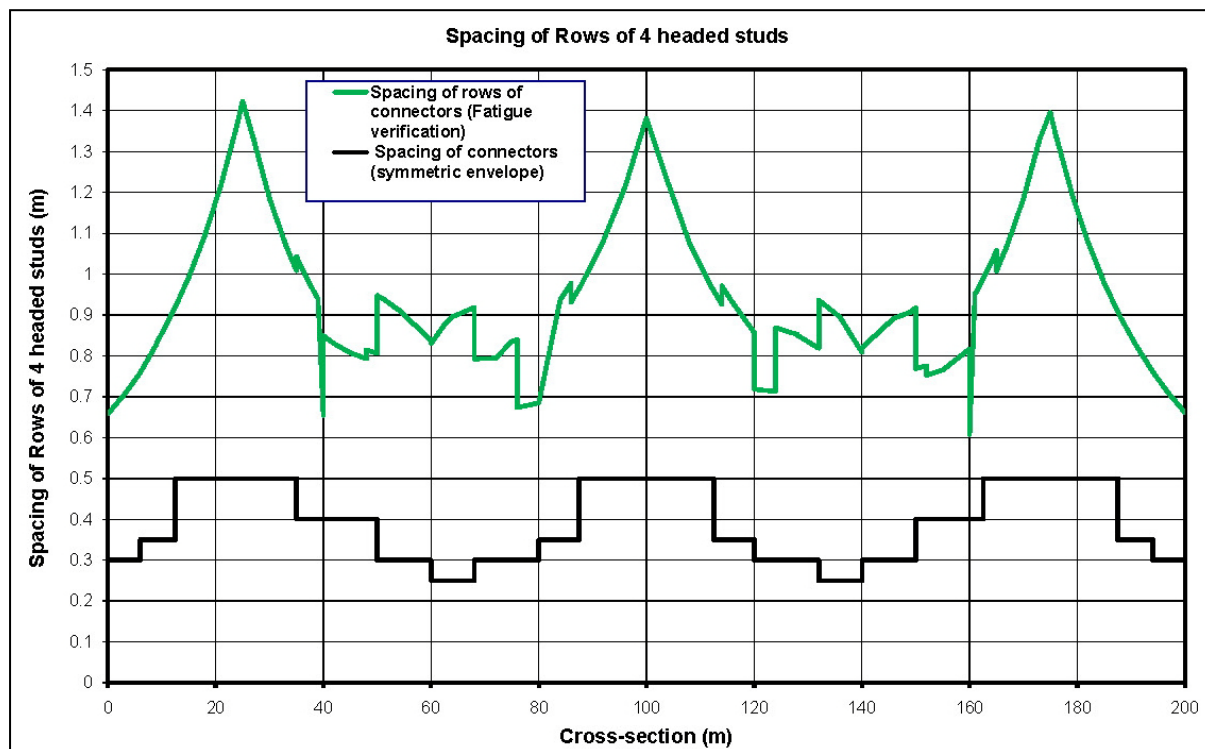


Fig. 6.31 Spacing of the rows of connectors under the fatigue ULS

6.7.7 INFLUENCE OF SHRINKAGE AND THERMAL ACTION ON THE CONNECTION DESIGN AT BOTH DECK ENDS

The shear force per unit length at the steel/concrete interface, used in the previous calculations, only takes account of hyperstatic (or secondary) effects of shrinkage and thermal actions. It is therefore necessary to also verify, according to EN-1994-2 6.6.2.4 (1), that sufficient shear connectors have been put in place at both free deck ends, to anchor the shear force per unit length coming from the isostatic (or primary) effects of shrinkage and thermal actions.

The first step is to calculate – in the cross-section at a distance L_v from the free deck end (anchorage length) – the normal stresses due to the isostatic effects of the shrinkage (envelope of short-term and long-term calculations) and thermal actions.

Integrating these stresses over the slab area gives the longitudinal shear force at the steel/concrete interface for the two considered load cases.

The second step is to determine the maximum longitudinal spacing between stud rows over the length L_v which is necessary to resist the corresponding shear force per unit length. The calculation is performed for ULS combination of actions only. In this case, EN1994-2, 6.6.2.4 (3) considers that the studs are ductile enough for the shear force per unit length $v_{L,Ed}$ to be assumed constant over the anchorage length L_v . This length is taken as equal to b_{eff} , which is the effective slab width in the global analysis at mid-end span (6 m for this example).

All calculations performed for the design example, a maximum longitudinal shear force of 2.15 MN is obtained at the steel/concrete interface under shrinkage action (obtained with the long-term calculation) and 1.14 MN under thermal actions.

This therefore gives $V_{L,Ed} = 1.0 \times 2.15 + 1.5 \times 1.14 = 3.86$ MN for ULS combination of actions.

Notice that according to EN-1992-1-1, 2.4.2.1 (1) the recommended partial factor for shrinkage action is $\gamma_{SH}=1.0$.

The design value of the shear flow $v_{L,Ed}$ (at ULS) and then the maximum spacing s_{max} over the anchorage length $L_v = b_{eff}$ between the stud rows are as follows:

$$v_{L,Ed} = \frac{V_{L,Ed}}{b_{eff}} = 0.643 \text{ MN/m} \quad (\text{rectangular shear stress block})$$

$$s_{max} = \frac{4P_{Rd, 1 \text{ stud}}}{v_{L,Ed}} = \frac{0.438}{0.643} = 0.681 \text{ m}$$

This spacing is significantly higher than the one already obtained through previous verifications (see Fig. 7.9). As it is generally the case, the anchorage of the shrinkage and thermal actions at the free deck ends does not govern the connection design.

Notes:

- To simplify the design example, the favourable effects of the permanent loads are not taken into account (self-weight and non-structural bridge equipments). Anyway they cause a shear flow which is in the opposite direction to the shear flow caused by shrinkage and thermal actions. So the suggested calculation is on the safe side.

Note that it is not always true. For instance, for a cross-girder in a cantilever outside the main steel girder and connected to the concrete slab, the shear flow coming from external load cases should be added to the shear flow coming from shrinkage and thermal actions. Finally the shear flow for ULS combination of these actions should be anchored at the free end of the cross-girder.

- EN1994-2, 6.6.2.4(3) suggests that the same verification could be performed by using the shear flow for SLS combination of actions and a triangular variation between the end cross-section and the one at the distance L_v . However, this will never govern the connection design and it is not explicitly required by section 7 of EN1994-2 dealing with the SLS justifications.

References

- EN-1992-1-1: Eurocode 2: Design of concrete structures. Part 1-1: General rules and rules for buildings.
- EN-1992-2: Eurocode 2: Design of concrete structures. Part 2: Concrete bridges- Design and detailing rules.
- EN-1993-1-1: Eurocode 3: Design of steel structures. Part 1-1: General rules and rules for buildings.
- EN-1993-1-5: Eurocode 3: Design of steel structures. Part 1-5: Plated steel structures.
- EN-1993-2: Eurocode 3: Design of steel structures. Part 2: Steel bridges.
- EN-1994-1-1: Eurocode 4: Design of composite steel and concrete structures. Part 1-1: General rules and rules for buildings.
- EN-1994-2: Eurocode 4: Design of composite steel and concrete structures. Part 2: General rules and rules for bridges.
- L.Davaine, F. Imbert, J. Raoul. 2007. *"Guidance book. Eurocodes 3 and 4. Application to steel-concrete composite road bridges"*. Sétra.
- C.R. Hendy and R.P. Johnson. 2006. *"Designers' Guide to EN-1994-2. Eurocode 4: Design of composite steel and concrete structures. Part 2: General rules and rules for bridges"*. Great Britain: Thomas Telford.

CHAPTER 7

Geotechnical aspects of bridge design (EN 1997)

Roger FRANK

Université Paris-Est, Ecole des Ponts ParisTech

Navier-CERMES

Yosra BOUASSIDA

Université Paris-Est, Ecole des Ponts ParisTech

Navier-CERMES

7.1 Introduction

Eurocode 7 deals with all the geotechnical aspects needed for the design of structures (buildings and civil engineering works). Eurocode 7 should be used for all the problems of interaction of structures with the ground (soils and rocks), through foundations or retaining structures. It addresses not only buildings but also bridges and other civil engineering works. It allows the calculation of the geotechnical actions on the structures, as well the resistances of the ground submitted to the actions from the structures. It also gives all the prescriptions and rules for good practice required for properly conducting the geotechnical aspects of a structural project or, more generally speaking, a purely geotechnical project.

Eurocode 7 consists of two parts:

EN 1997-1 Geotechnical design - Part 1: General rules (CEN, 2004)

EN 1997-2 Geotechnical design - Part 2: Ground investigation and testing (CEN, 2007).

In the following, it is applied to the geotechnical design of the supports for the steel-concrete composite two-girder bridge, shown in Fig. 7.1 (Davaine, 2010a). Only abutment C0 and pier P1 are considered, because of the symmetry of the bridge.

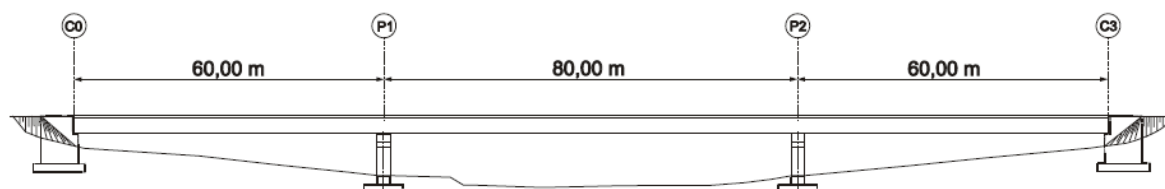


Fig. 7.1 Example of a steel-concrete composite two-girder bridge (Davaine, 2010a)

Both abutment C0 and pier P1 (only the squat pier is considered here) can be founded on spread foundations (see below): C0 is founded on a gravity wall and pier P1 is founded on a shallow foundation.

After some considerations about the geotechnical data, the following calculations will be presented:

- for abutment C0: bearing capacity and sliding resistance of the spread foundations (ULS verifications), taking account of the active earth pressures on the gravity wall; no SLS criterion is considered hereafter;
- for pier P1: bearing capacity (ULS verification) and settlement (SLS verification) of the spread foundation; pier P1 is a squat pier of height 10 m and a rectangular cross-section 5.00 m x 2.50 m
- some comments on verifications for the seismic design situation.

7.2 Geotechnical data

The soil investigation consisted of core sampling, laboratory tests (identification and triaxial compression tests), field tests (pressuremeter tests MPM and cone penetration CPT tests). (see EN 1997-2 for the use of these tests in geotechnical design)

Typical examples of these test results are given in Figs. 7.2 and 7.3.

The selection of appropriate values of soil properties for foundations (or other geotechnical structures) is probably the most difficult and challenging phase of the whole geotechnical design process and cannot be extensively described here.

In the Eurocodes procedures, in particular the Eurocode 7 one, characteristic values of these properties should be determined before applying any partial factor of safety. Fig. 7.4 shows the link between the two parts of Eurocode 7 and, more importantly, gives the main steps leading to characteristic values.

The present 'philosophy' with regard to the definition of characteristic values of geotechnical parameters is contained in the following clauses of Eurocode 7 – Part 1 (clause 2.4.5.2 in EN1997-1):

'(2)P The characteristic value of a geotechnical parameter shall be selected as a cautious estimate of the value affecting the occurrence of the limit state.'

'(7) [...]the governing parameter is often the mean of a range of values covering a large surface or volume of the ground. The characteristic value should be a cautious estimate of this mean value.'

These paragraphs in Eurocode 7 – Part 1 reflect the concern that one should be able to keep using the values of the geotechnical parameters that were traditionally used (the determination of which is not standardised, i.e. they often depend on the individual judgment of the geotechnical engineer, one should confess). However two remarks should be made at this point: on the one hand, the concept of 'derived value' of a geotechnical parameter (preceding the determination of the characteristic value), has been introduced (see Fig. 7.4) and, on the other hand, there is now a clear reference to the limit state involved (which may look evident, but is, in any case, a way of linking traditional geotechnical engineering and the new limit state approach) and to the assessment of the mean value (and not a local value; this might appear to be a specific feature of geotechnical design which, indeed, involves 'large' areas or 'large' ground masses).

Statistical methods are mentioned only as a possibility:

'(10) If statistical methods are employed [...], such methods should differentiate between local and regional sampling [...].'

'(11) If statistical methods are used, the characteristic value should be derived such that the calculated probability of a worse value governing the occurrence of the limit state under consideration is not greater than 5%.'

NOTE In this respect, a cautious estimate of the mean value is a selection of the mean value of the limited set of geotechnical parameter values, with a confidence level of 95%; where local failure is concerned, a cautious estimate of the low value is a 5% fractile.'

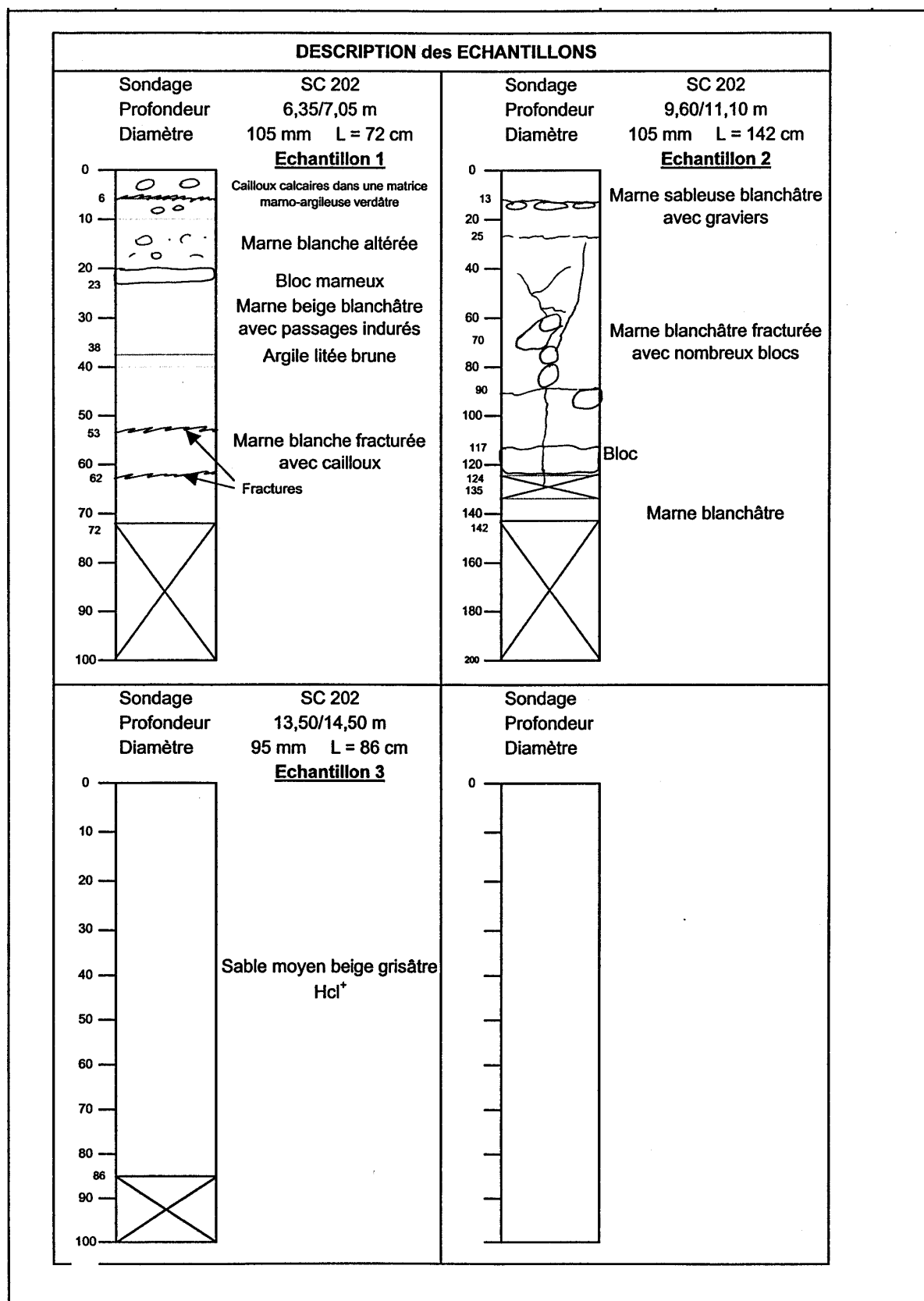


Fig. 7.2 Identification of soils : core sampling results between abutment C0 and pier P1

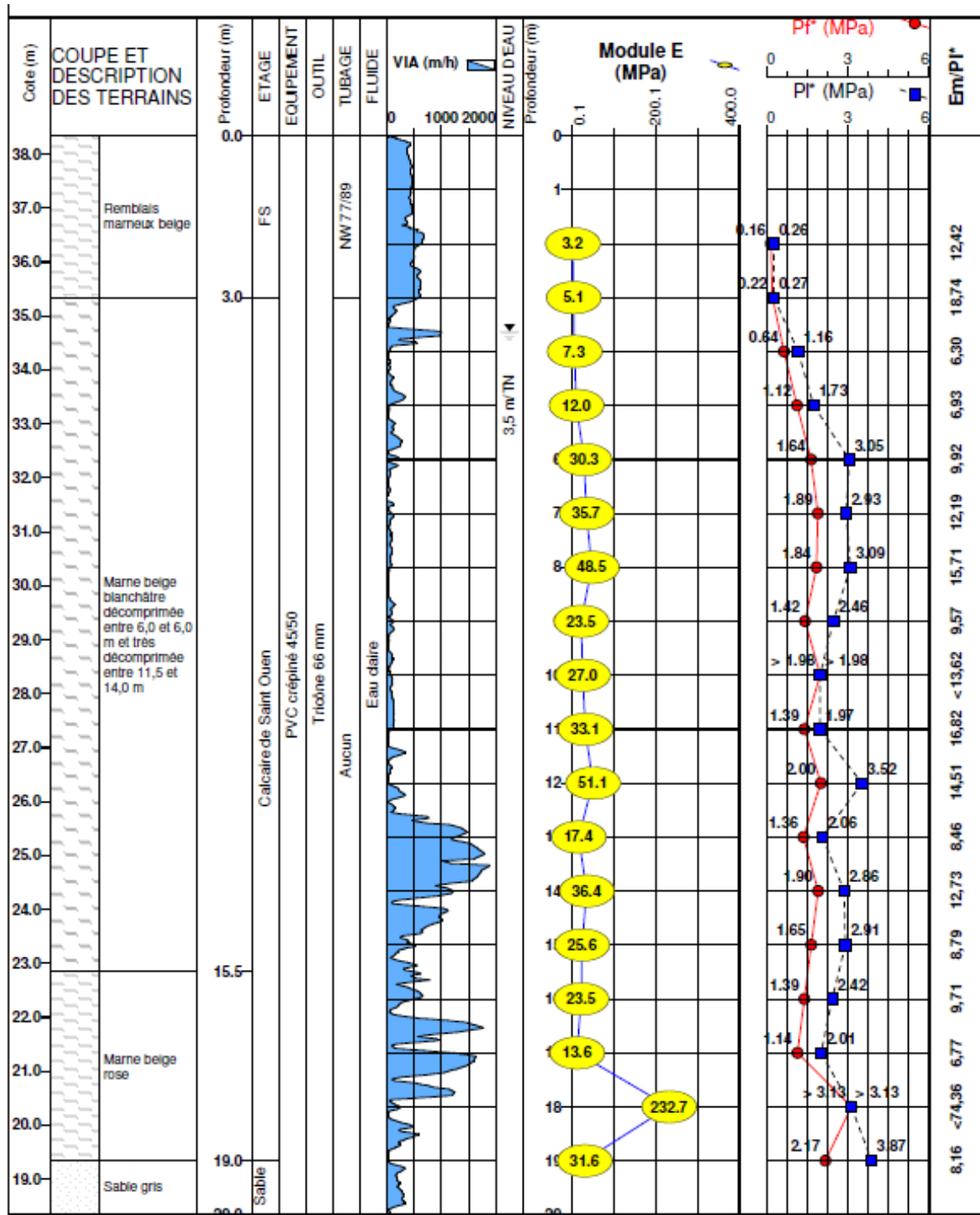


Fig. 7.3 Results of pressuremeter tests between abutment C0 and pier P1

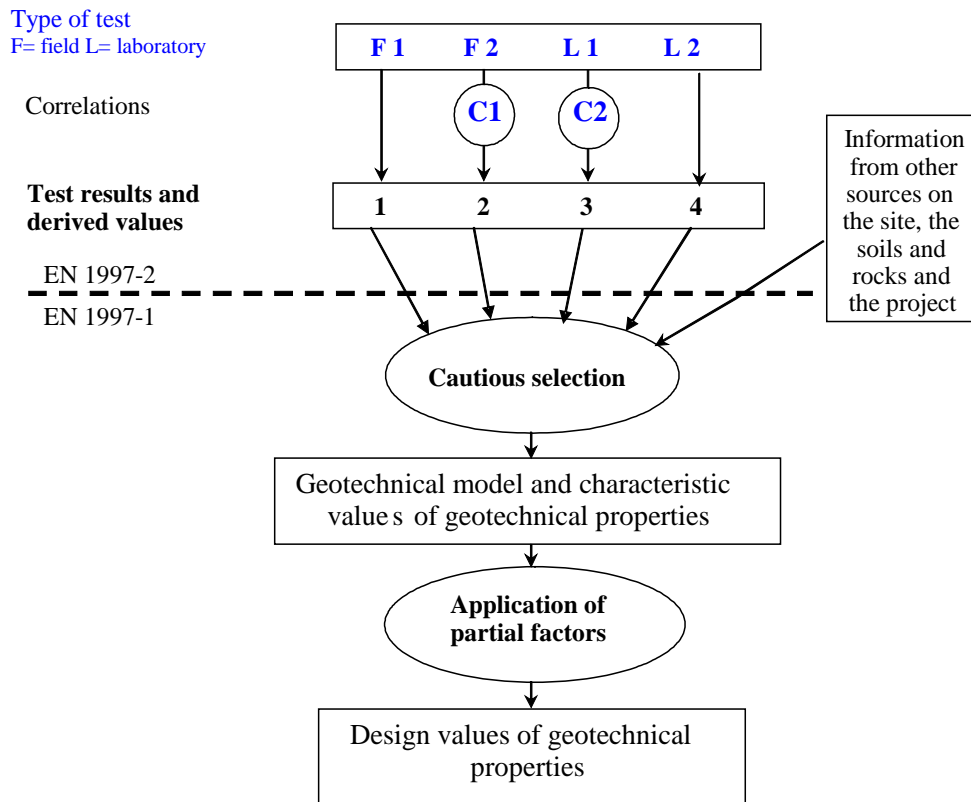


Fig. 7.4 General framework for the selection of derived values, characteristic values and design values of geotechnical properties (CEN, 2007)

At the start, it is assumed that both abutment C0 and pier P1 (only the squat pier is considered here) can be founded on spread foundations : C0 is founded on a gravity wall and P1 is founded on a shallow foundation, as shown in Figs. 7.5 and 7.6. For the sake of simplicity, in the present study, it is assumed that both the gravity wall (C0) and the shallow foundation (P1) rest on a normally fractured calcareous marl with the following characteristic values (respectively at 2.5 m depth and 3 m depth with regard to ground level):

- cohesion intercept in terms of effective stress : $c'_{kg} = 0$
- angle of shearing resistance in terms of effective stress: $\varphi'_{kg} = 30^\circ$
- total unit weight $\gamma_{kg} = 20 \text{ kN/m}^3$

The layer from ground level to the base of the foundation is assumed to have :

- unit weight $\gamma = 20 \text{ kN/m}^3$.

Water level is assumed to be one metre below the foundation level in both cases.

Finally, behind the gravity wall, the fill material is assumed to be a sand of good quality, well compacted :

- cohesion intercept in terms of effective stress : $c'_{kf} = 0$
- angle of shearing resistance in terms of effective stress: $\varphi'_{kf} = 30^\circ$
- total unit weight $\gamma_{kf} = 20 \text{ kN/m}^3$

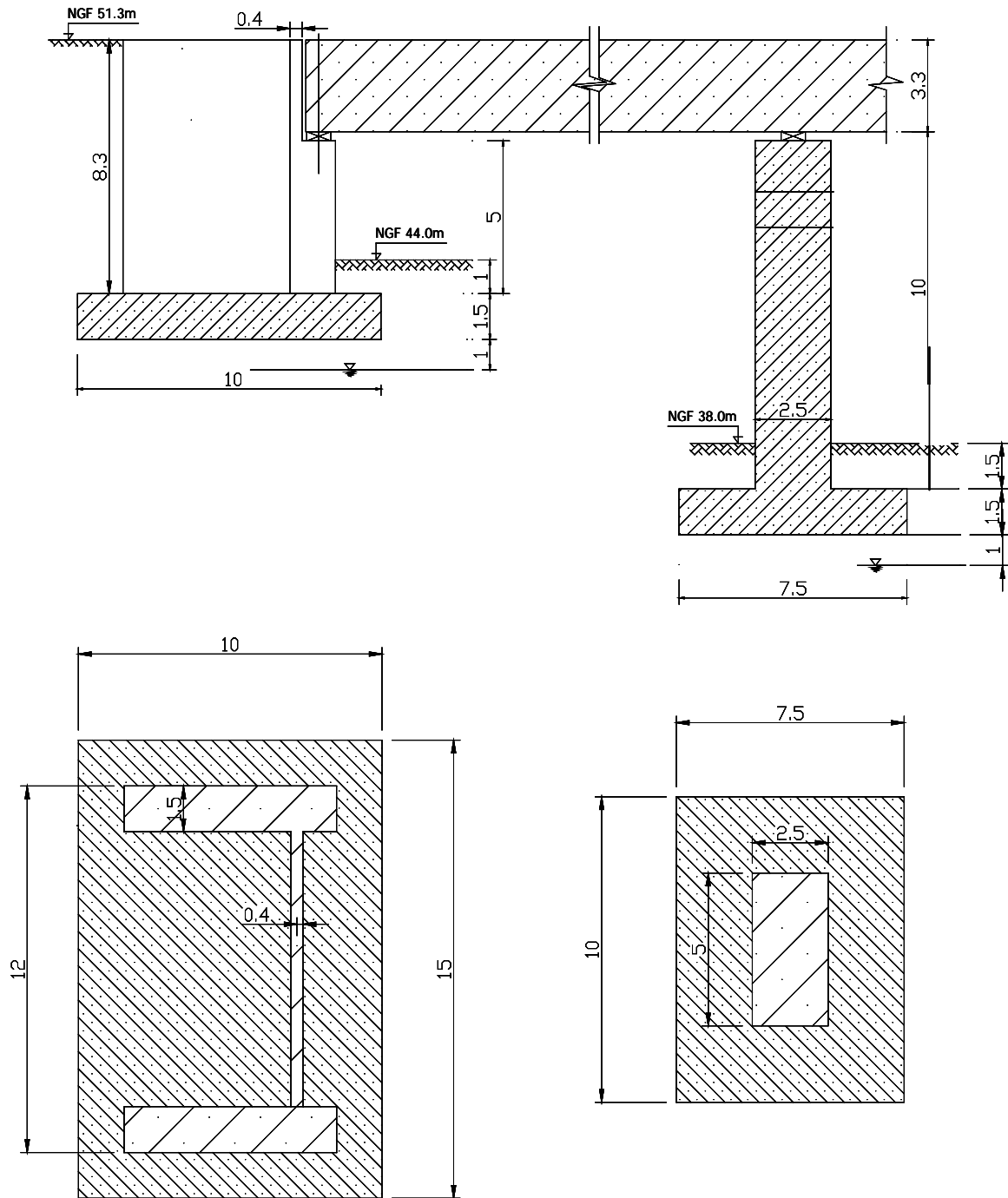


**Fig. 7.5 Gravity wall for abutment CO and shallow foundation for squat pier P1
(all dimensions in metres)**

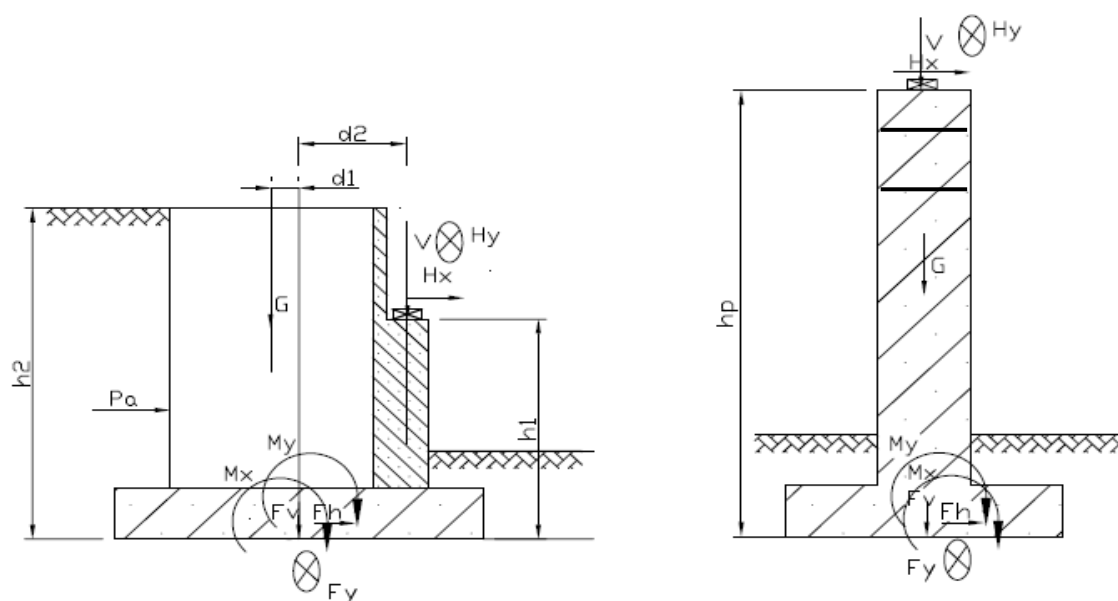


**Fig. 7.6 Gravity wall for abutment C0 and shallow foundation for squat pier P1.
Forces and notations**

7.3 Ultimate limit states

7.3.1 SUPPORT REACTIONS

The 'structural' actions to be considered on the foundations ('support reactions') and the most severe combinations are taken from the tables of the global analysis for half of the bridge deck (Davaine, 2010a and 2010c) and from the analysis of wind actions Malakatas (2010) and Davaine (2010c).

7.3.1.1 Vertical reaction on supports (Davaine, 2010a and 2010c)

The vertical reaction on abutment C0 and on internal support P1 is a combination of different elementary load cases as indicated in Table 7.1.

Table 7.1 Vertical 'structural' actions for half of the bridge deck (Davaine, 2010b and c)

Load cases	Designation	C0 (MN)	P1 (MN)
Self weight (structural steel + concrete)	$G_{k,1}$	1.1683	5.2867
Nominal non structural equipments	$G_{k,2}$	0.39769	1.4665
3 cm settlement on support P1	S_k	0.060	-0.137
Traffic UDL	$Q_{vk,1}$ max/min	0.97612/-0.21869	2.693/-0.15637
Traffic TS	$Q_{vk,2}$ max/min	0.92718/-0.11741	0.94458/-0.1057

To get the maximum value of the vertical support reaction, the nominal value of the support reaction for the non structural equipments should be multiplied by the coefficient 1.282. The minimum value is obtained with the coefficient 0.8364.

The ULS value of the **unfavourable** vertical reaction with traffic loads on support is then given by (for half bridge deck):

$$V_{d,max} = 1.35 (G_{k,1} + 1.282 G_{k,2}) + 1.0 S_k + 1.35 (Q_{vk,1} + Q_{vk,2})$$

This leads to 4.89 MN for C0 and 14.45 MN for P1.

The ULS value of the **favourable** vertical reaction with traffic loads on support is then given by (for half bridge deck):

$$\text{- for abutment C0 : } V_{d,min} = G_{k,1} + 0.8364 G_{k,2} + 1.35 (Q_{vk,1} + Q_{vk,2}) = 1.047 \text{ MN}$$

$$\text{- for pier P1 : } V_{d,min} = G_{k,1} + 0.8364 G_{k,2} + 1.0 S_k + 1.35 (Q_{vk,1} + Q_{vk,2}) = 6.022 \text{ MN}$$

7.3.1.2 Horizontal traffic action effects

The horizontal longitudinal reactions $Q_{xk,1} + Q_{xk,2}$ on abutments and piers due to traffic loads UDL and TS are, for half of the bridge deck (Davaine, 2010b) :

	min	max	
Braking :	-0.90658	0	MN
Acceleration :	0	0.90658	MN

7.3.1.3 Horizontal wind action effects (Malakatas, 2010 and Davaine 2010c)

The following values are extracted from Malakatas (2010)

$F_{wk,1} = 1310 \text{ kN}$ (or $q_{wk,1} = 1310\text{kN} / 200\text{m} = 6.55 \text{ kN/m}$) transversally and horizontally applied to the bridge deck without traffic loads

$F_{wk,2} = 2066 \text{ kN}$ (or $q_{wk,2} = 10.33 \text{ kN/m}$) with traffic loads

230 kN applied to the 10-m-high piers

For simplifications, the wind effects on piers are neglected in the foundation calculations.

According to Fig. 7.7, the transverse displacements of the bridge are prevented. The transverse horizontal wind is then applied to a continuous 3 span girder. For simplifications, this girder is assumed having a constant second moment of area.

Thus the transverse horizontal variable actions H_{ykw} due to wind are given in Table 7.2 (Davaine, 2010c).

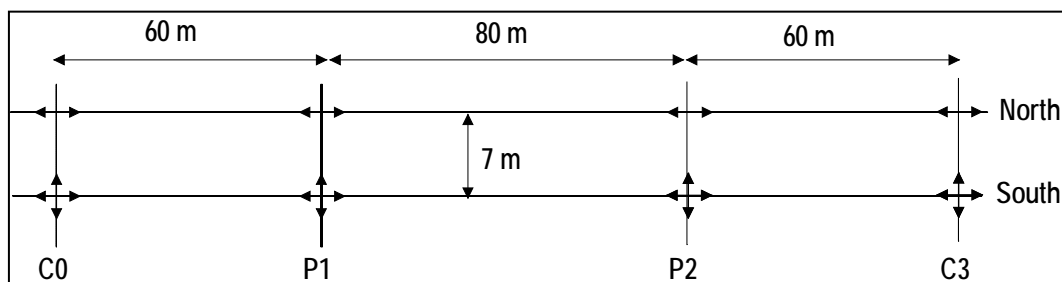


Fig. 7.7 Displacement conditions of the bridge (Davaine, 2010b and 2010c)

Table 7.2 Transverse horizontal variable actions H_{ykw} due to wind (Davaine, 2010c)

Transverse horizontal force H_y due to:	C0	P1
$F_{wk,1}$ without traffic load	141 kN	514 kN
$F_{wk,2}$ with traffic load	223 kN	810 kN

7.3.1.4 Fundamental combinations (persistent and transient design situations)

Including the wind effect gives the following ULS combinations governing the behaviour of the foundations (Davaine, 2010c) (“+” means “to be combined with”) :

- without traffic loads :

$$1.35 (G_{k,1} + 1.282 G_{k,2}) \text{ “+” } 1.0 S_k \text{ “+” } 1.5 F_{wk,1}$$

- with traffic loads

$$1.35 (G_{k,1} + 1.282 G_{k,2}) \text{ “+” } 1.0 S_k \text{ “+” } 1.35 (Q_{k,1} + Q_{k,2}) \text{ “+” } 1.5 \times 0.6 F_{wk,2}$$

In the following:

- the vertical components **V** come from $G_{k,1}$, $G_{k,2}$, S_k and $Q_{vk,1} + Q_{vk,2}$ (given above for half of the bridge deck);

- the horizontal longitudinal components **H_x** come from $Q_{xk,1} + Q_{xk,2}$ (given above for half of the bridge deck);

- and the horizontal transversal components **H_y** come from $F_{wk,1}$ and $F_{wk,2}$.

7.3 2 GENERAL: THE 3 DESIGN APPROACHES OF EUROCODE 7

When checking STR/GEO Ultimate Limit States for permanent and transient design situations (fundamental combinations), 3 Design Approaches (DA) are offered by Eurocode EN 1990 and Eurocode EN 1997-1 (Eurocode 7 – Part 1; CEN, 2004). The choice, for each geotechnical structure, is left to National determination.

For the bearing capacity of spread foundations and for retaining structures, these approaches can be summarised as follows.

7.3.2.1 Design Approach 1 (DA1)

Two combinations (DA1-1 and DA1-2) should be used. It should be checked that an ULS is not reached with either of the two combinations.

Combination 1 (DA1-1) is called the 'structural combination' because safety is applied on the actions (i.e. partial load factors γ_F larger or equal to 1.0) and the design value of the geotechnical resistance R_d is equal to the value of the characteristic resistance.

Combination 2 (DA1-2) is called the 'geotechnical combination' because the safety is applied on the geotechnical resistance R_d , through partial material factors γ_M larger than 1.0, applied at the 'source' to the ground parameters themselves. No safety is applied on unfavourable permanent ('structural' or 'geotechnical') actions. Note that for the resistance of piles and anchors resistances factors γ_R are used instead of material factors γ_M .

Thus, for DA1-1 (with the recommended values given in Note 2 of Table A2.4 (B) of EN 1990, for Eq. 6.10) :

$$E_d \{ \gamma_F F_{rep} \} \leq R_d \{ X_k \}$$

with $\gamma_{G,sup} = 1.35$; $\gamma_{G,inf} = 1.00$; $\gamma_{G,set} = 1.35$; 1.20 or 0; and $\gamma_Q = 1.20$ to 1.50 or 0

and for DA1-2 (with the recommended values given in the Note of Table A2.4 (C) of EN 1990 for Eq. 6.10):

$$E_d \{ \gamma_F F_{rep} \} \leq R_d \{ X_k / \gamma_M \}$$

with $\gamma_{G,sup} = 1.00$; $\gamma_{G,inf} = 1.00$; $\gamma_{G,set} = 1.00$ or 0; and $\gamma_Q = 1.15$ to 1.30 or 0

Table 7.3 summarises the recommended values of load factors used for DA1-1 (set A1) and DA1-2 (set A2).

Table 7.3 Partial factors on actions (γ_F) or the effects of actions (γ_E)
(table A.3 in EN 1997-1)

Action		Symbol	Set	
			A1	A2
Permanent	Unfavourable	γ_G	1.35	1.0
	Favourable		1.0	1.0
Variable	Unfavourable	γ_Q	1.5	1.3
	Favourable		0	0

For DA1-2, the recommended values for the partial factors γ_M both for 'geotechnical' actions and resistances are those of set M2 given in Table 7.4 (except for resistances of piles and anchors).

Table 7.4 Partial factors for soil parameters (γ_M) (table A.4 in EN 1997-1)

Soil parameter	Symbol	Set	
		<i>M1</i>	<i>M2</i>
Angle of shearing resistance ^a	$\gamma_{\phi'}$	1.0	1.5
Effective cohesion	$\gamma_{c'}$	1.0	1.25
Undrained shear strength	γ_{cu}	1.0	1.4
Unconfined strength	γ_{qu}	1.0	1.4
Weight density	γ_{γ}	1.0	1.0
^a This factor is applied to $\tan \phi'$			

7.3.2.2 Design Approach 2 (DA2 and DA2*)

Only one combination should be used to check that the ULS is not reached. Safety is applied on both the actions and the resistances. On the action side, the factors can be applied on the actions themselves (DA2, factors γ_F) or on the effect of the actions (DA2*, factors γ_E). Thus,

- for DA2:

$$E_d \{ \gamma_F F_{rep} \} \leq R_d \{ X_k \} / \gamma_R$$

- for DA2*:

$$\gamma_E E_d \{ F_{rep} \} \leq R_d \{ X_k \} / \gamma_R$$

The recommended values for γ_F or γ_E are those given in Note 2 of Table A2.4 (B) of EN 1990, for Eq. 6.10:

$\gamma_{G,sup} = 1.35$; $\gamma_{G,inf} = 1.00$; $\gamma_{G,set} = 1.35$; 1.20 or 0; and $\gamma_Q = 1.20$ to 1.50 or 0

The recommended values of the resistance factors for spread foundations and retaining structures are those for set R2 given in Table 7.5 and 7.6, respectively.

Table 7.5 Partial resistance factors (γ_R) for spread foundations (table A.5 in EN 1997-1)

Resistance	Symbol	Set		
		<i>R1</i>	<i>R2</i>	<i>R3</i>
Bearing	$\gamma_{R,v}$	1.0	1.4	1.0
Sliding	$\gamma_{R,h}$	1.0	1.1	1.0

Table 7.6 Partial resistance factors (γ_R) for retaining structures (table A.13 in EN 1997-1)

Resistance	Symbol	Set		
		<i>R1</i>	<i>R2</i>	<i>R3</i>
Bearing capacity	$\gamma_{R,v}$	1.0	1.4	1.0
Sliding resistance	$\gamma_{R,h}$	1.0	1.1	1.0
Earth resistance	$\gamma_{R,e}$	1.0	1.4	1.0

7.3.2.3 Design Approach 3

Only one combination should be used to check that the ULS is not reached. Safety is applied on both the actions (factors γ_F) and on the geotechnical resistance R_d , through partial material factors γ_M larger than 1.0, applied at the ‘source’ to the ground parameters themselves.

This writes:

$$E_d \{ \gamma_F F_{rep}; X_k / \gamma_M \} \leq R_d \{ X_k / \gamma_M \}$$

The recommended values for the actions are given:

- for ‘structural’ actions, in Note 2 of Table A2.4 (B) of EN 1990, for Eq. 6.10:

$$\gamma_{G,sup} = 1.35; \gamma_{G,inf} = 1.00 \text{ and } \gamma_Q = 1.20 \text{ to } 1.50 \text{ or } 0$$

and

- for ‘geotechnical’ actions, in the Note of Table A2.4 (C) of EN 1990 for Eq. 6.10:

$$\gamma_{G,sup} = 1.00; \gamma_{G,inf} = 1.00; \gamma_{G,set} = 1.00 \text{ or } 0; \text{ and } \gamma_Q = 1.15 \text{ to } 1.30 \text{ or } 0.$$

The recommended values of partial material factors γ_M for ground parameters are those of set M2 of Table 7.4.

7.3.2.4 Summary for DA1, DA2 and DA3 (for “fundamental” combinations)

For **spread foundations and retaining structures**, the 3 Design Approaches, for ULS in permanent and transient design situations, can be summarised in a symbolic manner, with sets A, M and R of Tables 7.3, 7.4, 7.5 and 7.6, as follows (“+” means “to be combined with”):

Design Approach 1 (DA1)

Combination 1: A1 “+” M1 “+” R1

Combination 2: A2 “+” M2 “+” R1

Design Approach 2 (DA2)

Combination: A1 “+” M1 “+” R2

Design Approach 3 (DA3)

Combination: (A1* or A2[†]) “+” M2 “+” R3

*on structural actions, [†]on geotechnical actions

For the **design of axially loaded piles and anchors**, see EN 1997-1 (CEN, 2004).

7.4 Abutment C0

7.4.1 BEARING CAPACITY (ULS)

The ULS condition is (Eq. 6.1 in EN 1997-1):

$$F_{vd} \leq R_d \quad (1)$$

where

- F_{vd} is the design value of the vertical component acting on the base of the foundation, coming from structural and geotechnical actions on the abutment;
- R_d is the design value of the resistance of the ground (bearing capacity) below the base of the foundation.

Structural actions

From the governing 'structural' loads given above, the following design loads are derived for each Design Approach in permanent and transient design situations.

Vertical:

$$\begin{aligned} \text{- for DA1-1 and DA2 and DA3 : } V_d &= 1.35 (G_{k,1} + 1.282 G_{k,2}) + 1.0 S_k + 1.35 (Q_{vk,1} + Q_{vk,2}) \\ &= 4.89 \times 2 = 9.88 \text{ MN} \end{aligned}$$

$$\begin{aligned} \text{- for DA1-2 : } V_d &= G_{k,1} + 1.282 G_{k,2} + 1.0 S_k + 1.15 (Q_{vk,1} + Q_{vk,2}) \\ &= 3.93 \times 2 = 7.86 \text{ MN} \end{aligned}$$

Horizontal X :

$$\text{- for DA1-1, DA2 and DA3 : } H_{xd} = 1.35 (Q_{xk,1} + Q_{xk,2}) = 1.35 \times 0.9 \times 2 = 2.43 \text{ MN}$$

$$\text{- for DA1-2 : } H_{xd} = 1.15 (Q_{xk,1} + Q_{xk,2}) = 1.15 \times 0.9 \times 2 = 2.07 \text{ MN}$$

Horizontal Y :

$$\text{- for DA1-1, DA2 and DA3 : } H_{yd} = 1.5 \times 0.6 F_{wk,2} = 1.5 \times 0.6 \times 0.22 = 0.20 \text{ MN}$$

$$\text{- for DA1-2 : } H_{yd} = 1.30 \times 0.6 F_{wk,2} = 1.30 \times 0.6 \times 0.22 = 0.17 \text{ MN}$$

Geotechnical actions

The additional and 'geotechnical actions' to be taken into account are :

- the weight of the gravity wall and its foundation, which is derived from geometrical data shown in Figs. 7.5, 7.6 and 7.8, with 1 m of ground above all the surface of the spread foundation, a sloping ground on its lateral walls and filled up inside the lateral walls, using $\gamma = 25 \text{ kN/m}^3$ for the concrete and $\gamma = 20 \text{ kN/m}^3$ for the ground:

$$G_{wall,k} = 26.4 \text{ MN}$$

$$\text{Thus, for DA1-1 and DA2 and DA3 : } G_{wall,d} = 1.35 \times 26.4 = 35.64 \text{ MN}$$

(note that for DA3, G_{wall} is considered as a 'structural' action, as it is a weight composed of ground and concrete above the base of the foundation)

$$\text{and for DA1-2 : } G_{wall,d} = 26.4 \text{ MN}$$

- resulting active earth pressures on the 'virtual' back of the wall, and as there is no water:

$$P_{ad} = \gamma_{G,sup} \times 0.5 K_{ad} \gamma_{kf} h_2^2 L_a \quad (2)$$

where K_{ad} is the design active earth pressure coefficient, assuming sufficient wall displacement; for a horizontal pressure (no inclination δ is assumed):

$$K_{ad} = \tan(\pi/4 - \varphi_{df}/2)^2 \quad (3)$$

(theory of Rankine; see also Fig. C.1.1 in Annex C for EN 1997-1 for a horizontal retained surface and making $\delta = 0$) and $h_2 = 9.8$ m and $L_a = 12$ m are the height and length (in the perpendicular plane) over which the active earth pressure applies, respectively – see Figs. 7.5 and 7.6. In this calculation it is assumed that the movement of the ground (at the level of the virtual back) is large enough to mobilise the active pressure (Annex C.3 of EN 1997-1 give some guidance).

Thus,

- for DA1-1 and DA2 : $\varphi_{df} = \varphi_{kf} = 30^\circ$; $K_{ad} = 0.333$ $\gamma_{kd} = \gamma_{kf} = 20$ kN/m³ and $P_{ad} = 1.35 \times 3.84 = 5.18$ MN

- for DA1-2 and DA3, considering $\gamma_{\varphi'} = 1$, 25 in Table 4: $\tan \varphi_{df} = (\tan \varphi_{kf})/1.25 = \tan 30^\circ/1.25$ and $\varphi_{df} = 24.8^\circ$; $K_{ad} = 0.409$ and

$$P_{ad} = 1.00 \times 4.71 = 4.71 \text{ MN}$$

Resultant actions

At the centre of the base of the foundation, the resultant actions are :

$$F_v = V + G_{wall}$$

$$F_x = H_x + P_a$$

$$F_y = H_y$$

$$M_y = P_a(h_2/3) + H_x h_1 - G_{wall} d_1 + V d_2$$

$$M_x = H_y h_1$$

with $h_1 = 6.5$ m ; $d_1 = 0.4$ m and $d_2 = 2.95$ m - see Figs 7.5 and 7.6.

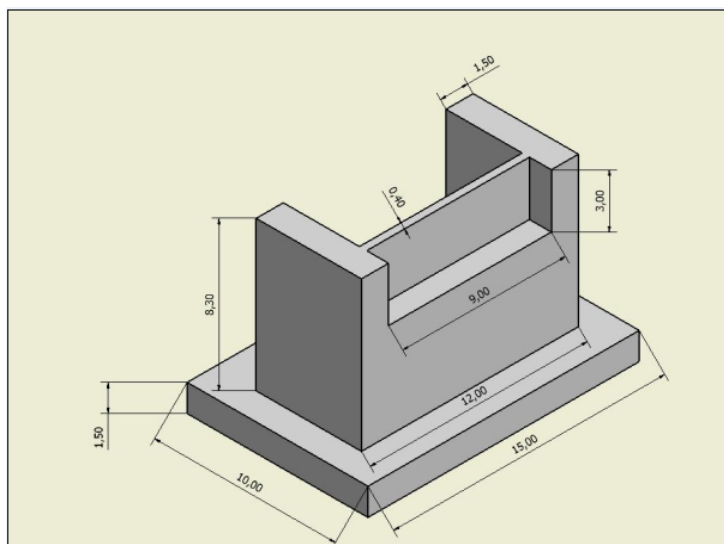


Fig. 7.8 Abutment C0. 3D view

Eccentricity, is calculated by:

- in the longitudinal (B) direction : $e_B = M_y/F_v$

- in the transversal (L) direction : $e_L = M_x/F_v$

Geotechnical resistance (bearing capacity)

The resistance R (bearing capacity) is calculated with the sample method of Annex D of EN 1997-1 (CEN, 2004) – see Appendix B below. In the present case, R takes the form (drained conditions are assumed, and $c'_{kd} = c'_{kg} = 0$):

$$R = (B-2e_B) \cdot (L-2e_L) \{q'N_q(\varphi')s_qi_q + 0.5\gamma'(B-2e_B)N_\gamma(\varphi')s_\gamma i_\gamma\} \quad (4)$$

and $R_d = R / \gamma_{R,v}$ (5)

with $B = 10$ m, $L = 15$ m, $q' = 50$ kPa, $\gamma' = 10$ kN/m³ (in order to be on the safe side, it is assumed that the water can reach the level of the base of the foundation), and $\varphi' = \varphi'_{dg}$, the design value of the angle of friction of the bearing stratum (calcareous marl). For the calculations of e_B , e_L , i_q , s_γ and i_γ , the design loads F_{vd} , F_{xd} and F_{yd} which depend on the Design Approach under consideration are also needed, as well as $h_1 = 6.5$ m, $d_1 = 0.4$ m and $d_2 = 2.95$ m. Partial factors γ_M and $\gamma_{R,v}$ are taken from the recommended values in Tables 4 and 6 respectively, for each Design Approach.

For DA1-1 : $\varphi'_{dg} = \varphi'_{kg} = 30^\circ$

$$F_{vd} = 9.88 + 35.64 = 45.52 \text{ MN}$$

$$F_{xd} = 2.43 + 5.18 = 7.61 \text{ MN}$$

$$F_{yd} = 0.20 \text{ MN}$$

$$\gamma_{R,v} = 1.0$$

Thus, $e_B = 1.05$ m, $e_L = 0.03$ m and $R_d = 150.2/1.0 = 150.2$ MN

For DA1-2 : $\tan \varphi'_{dg} = (\tan \varphi'_{kg}) / 1.25$, thus $\varphi'_{dg} = 24.8^\circ$

$$F_{vd} = 7.86 + 26.4 = 34.26 \text{ MN}$$

$$F_{xd} = 2.07 + 4.71 = 6.78 \text{ MN}$$

$$F_{yd} = 0.17 \text{ MN}$$

$$\gamma_{R,v} = 1.0$$

Thus, $e_B = 1.21$ m, $e_L = 0.03$ m and $R_d = 67.3/1.0 = 67.3$ MN

For DA2 : $\varphi'_{dg} = \varphi'_{kg} = 30^\circ$

$$F_{vd} = 9.88 + 35.64 = 45.52 \text{ MN}$$

$$F_{xd} = 2.43 + 5.18 = 7.61 \text{ MN}$$

$$F_{yd} = 0.20 \text{ MN}$$

$$\gamma_{R,v} = 1.4$$

Thus, $e_B = 1.05$ m, $e_L = 0.03$ m and $R_d = 150.2/1.4 = 107.3$ MN

For DA3 : $\tan \varphi'_{dg} = (\tan \varphi'_{kg}) / 1.25$, thus $\varphi'_{dg} = 24.8^\circ$

$$F_{vd} = 9.88 + 35.64 = 45.52 \text{ MN}$$

$$F_{xd} = 2.43 + 4.71 = 7.14 \text{ MN}$$

$$F_{yd} = 0.20 \text{ MN}$$

$$\gamma_{R,v} = 1.0$$

Thus, $e_B = 1.01$ m, $e_L = 0.03$ m and $R_d = 79.6/1.0 = 79.6$ MN

ULS conditions

The ULS-bearing capacity condition is :

$$F_{vd} \leq R_d \quad (1)$$

This condition is fulfilled for all Design Approaches (for permanent and transient design situations) with a large overdesign factor. For DA1, it can be seen that combination 2 (DA1-2) is governing. DA3 is the most conservative approach, with regard to the ULS of bearing capacity.

Furthermore, it can be noted that all eccentricities are small: the maximum is $e_B = 1.21$ m (DA 1-2) for width $B = 10$ m. Thus, there are no special precautions to be taken, as required by clause 6.5.4 of EN 1997-1 in case $e > (B \text{ or } L) / 3$. The eccentricities in L direction are negligible, and it appears that the transverse wind loads have nearly no influence on the bearing capacity of abutment C0.

7.4.2 SLIDING (ULS)

Only sliding in the longitudinal direction needs to be considered here.

The basic equation is (Eq. 6.2) in EN 1997-1 :

$$F_{xd} \leq R_d + R_{p;d} \quad (6)$$

where

- F_{xd} is the design value of the horizontal component of the load acting in the longitudinal direction on the base of the foundation, coming from structural and geotechnical actions on the abutment – see above for values in persistent transient design situations;

- R_d is the sliding resistance and $R_{p;d}$ is the passive earth force in front of the spread foundation.

For drained conditions the sliding resistance R_d is (Eqs. 6.3a and 6.3b in EN 1997-1) :

$$R_d = \{F'_{vd} (\tan \delta_k) / \gamma_M\} / \gamma_{R;h} \quad (7)$$

where

- F'_{vd} is the design value of the favourable effective vertical force. In the present case, it is equal to the total one $F_{inf;vd}$, as the water table is at the level of the foundation; hence the pore pressure $u = 0$ at the level of the base of the foundation);

- δ_k is the concrete-ground interface friction angle; it is usually assumed that $\delta_k = 2/3 \varphi_{kg}$, i.e. $\delta_k = 20^\circ$ and $\tan \delta_k = 0.364$;

- γ_M and $\gamma_{R;h}$ are taken from the recommended values in Tables 7.4 and 7.6 respectively, for each Design Approach in persistent and transient design situations.

Actions

$$F'_{vd} = V_{d,min} + G_{wall,d}$$

- for DA1-1, DA2 and DA3 : $V_{d,min} = G_{k,1} + 0.8364 G_{k,2} + 1.35(Q_{vk,1} + Q_{vk,2}) = 1.047 \times 2 = 2.09$ MN

- for DA1-2 : $V_{d,min} = G_{k,1} + 0.8364 G_{k,2} + 1.15 (Q_{vk,1} + Q_{vk,2}) = 1.114 \times 2 = 2.23$ MN

- and for all DAs : $G_{wall,d} = 1.0 G_{wall,k} = 26.4$ MN

DA1-1 : $F_{xd} = 7.61$ MN and $F'_{vd} = 2.09 + 26.4 = 28.49$ MN

DA1-2 : $F_{xd} = 6.78$ MN and $F'_{vd} = 2.23 + 26.4 = 28.63$ MN

$$\text{DA2} : F_{xd} = 7.61 \text{ MN and } F'_{vd} = 2.09 + 26.4 = 28.49 \text{ MN}$$

$$\text{DA3} : F_{xd} = 7.14 \text{ MN and } F'_{vd} = 2.09 + 26.4 = 28.49 \text{ MN}$$

Sliding resistances

$$\text{DA1-1} : \gamma_M = 1.0 \text{ and } \gamma_{R,h} = 1.0, \text{ thus } R_d = \{28.49 \times 0.364 / 1.0\} / 1.0 = 10.37 \text{ MN}$$

$$\text{DA1-2} : \gamma_M = 1.25 \text{ and } \gamma_{R,h} = 1.0, \text{ thus } R_d = \{28.63 \times 0.364 / 1.25\} / 1.0 = 8.33 \text{ MN}$$

$$\text{DA2} : \gamma_M = 1.0 \text{ and } \gamma_{R,h} = 1.1, \text{ thus } R_d = \{28.49 \times 0.364 / 1.0\} / 1.1 = 9.42 \text{ MN}$$

$$\text{DA3} : \gamma_M = 1.25 \text{ and } \gamma_{R,h} = 1.0, \text{ thus } R_d = \{28.49 \times 0.364 / 1.25\} / 1.0 = 8.29 \text{ MN}$$

ULS-sliding condition

Thus the ULS sliding condition (Eq. 6) is verified, without recourse to the passive force in front of the spread foundation $R_{p,d}$ for all Design Approaches for persistent and transient design situations.

7.5 PIER P1 (Squat Pier)

7.5.1 BEARING CAPACITY (ULS)

For conciseness, only Design Approach 2 for persistent and transient design situations is considered here.

The governing 'structural' design loads are (Davaine, 2010c) :

Vertical:

$$\begin{aligned} - \text{DA2} : V_d &= 1.35 (G_{k,1} + 1.282 G_{k,2}) + 1.0 S_k + 1.35 (Q_{vk,1} + Q_{vk,2}) \\ &= 14.45 \times 2 = 28.9 \text{ MN} \end{aligned}$$

Horizontal X :

$$- \text{DA2} : H_{xd} = 1.35 (Q_{xk,1} + Q_{xk,2}) = 1.35 \times 0.91 \times 2 = 2.45 \text{ MN}$$

Horizontal Y :

$$- \text{DA2} : H_{yd} = 1.5 \times 0.6 F_{wk,2} = 1.5 \times 0.6 \times 0.81 = 0.73 \text{ MN}$$

The additional action to be taken into account is the weight of the pier, spread foundation and ground above the foundation. From the geometrical data shown in Fig. 7.5, 7.6 and 7.9 and using $\gamma = 25 \text{ kN/m}^3$ for the concrete and $\gamma = 20 \text{ kN/m}^3$ for the ground:

$$G_{\text{pier},k} = 8.3 \text{ MN}$$

$$\text{Thus, for DA2 : } G_{\text{pier},d} = 1.35 \times 8.3 = 11.2 \text{ MN}$$

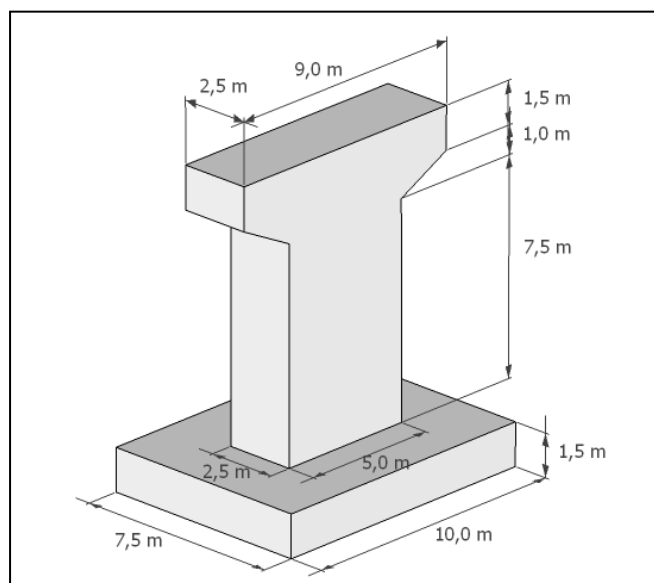


Fig. 7.9 Pier P1 (Squat pier). 3D view

At the centre of the spread foundation, the resultant actions are :

$$F_v = V + G_{\text{pier}}$$

$$F_x = H_x$$

$$F_y = H_y$$

$$M_y = H_x h_p$$

$$M_x = H_y h_p$$

with $h_p = 11.5$ m - see Figs. 7.5 and 7.6.

Eccentricity, is calculated by :

- in the longitudinal (B) direction : $e_B = M_y / F_v$

- in the transversal (L) direction : $e_L = M_x / F_v$

For DA2 : $F_{vd} = 28.9 + 11.2 = 40.1$ MN

$$F_{xd} = 2.45$$
 MN

$$F_{yd} = 0.73$$
 MN

The resistance R (bearing capacity) is calculated with the sample method of Annex D of EN 1997-1 (CEN, 2004) – see Appendix C below. In the present case, R takes the same form as above, for the abutment C0 (drained conditions are assumed, and $c'_{kg} = 0$).

For Design Approach DA 2,

$$R_d = R / \gamma_{R,v} \quad (8)$$

with $\gamma_{R,v} = 1.4$ recommended (see Table 7.5).

In DA 2, R_k is calculated with the characteristic values of soil parameters ($R = R_k$), e_B and e_L and the load inclination are determined using the design values of the actions.

In DA2*, R_k is also calculated with the characteristic values of soil parameters ($R = R_k$), but e_B and e_L and the load inclination are determined using the characteristic values of the actions.

Inserting into the calculation of R :

- $B = 7.5 \text{ m}$; $L = 10 \text{ m}$; $q' = 60 \text{ kPa}$; $\gamma = 10 \text{ kN/m}^3$ (in order to be on the safe side, it is assumed that the water can reach the level of the base of the foundation);

- $\varphi' = \varphi'_{dg} = 30^\circ$, the design value of the angle of friction of the bearing stratum (calcareous marl) (for DA2 : $\varphi'_{dg} = \varphi'_{kg} = 30^\circ$);

- the design loads F_{vd} , F_{xd} and F_{yd} , as well as $h_p = 11.5 \text{ m}$, for the calculations of e_B , e_L , i_q , s_γ and i_γ ; one obtains, for DA 2 : $e_B = 0.70 \text{ m}$, $e_L = 0.21 \text{ m}$

and $R_k = 100.9 \text{ MN}$ and $R_d = R_k/\gamma_{R;\gamma} = 100.9/1.4 = 72.1 \text{ MN}$

The ULS condition in permanent and transient design situation $F_{vd} \leq R_d$ is fulfilled, as

$40.1 \text{ MN} < 72.1 \text{ MN}$.

When comparing R_k to F_{vk} ($10.66 \times 2 + 8.3 = 29.62 \text{ MN}$) the overall factor of safety is equal to $F = 3.41$; it can be said that the usual capacity SLS criterion is also met ($F = 2.5$ to 3).

7.5.2 SETTLEMENT (SLS)

Settlements are usually checked under the vertical load Q obtained with quasi-permanent SLS combinations

From Table 7.1 : $Q = G_{k,1} + G_{k,2} = (5.2867 + 1.4665) \times 2 = 6.75 \times 2 = 13.5 \text{ MN}$

which correspond to the applied pressure on the ground :

$$q = Q/(BL) = 13.5/(7.5 \times 10) = 0.18 \text{ MPa}$$

Eurocode 7 – Part 2 (EN1997-2) provides, in informative Annexes, several sample methods for determining the settlement of spread foundations.

In the following the Ménard pressuremeter (MPM) method is used with the results of the MPM tests of Fig. 7.3. This method is the subject of Annex D2 of EN 1997-2 (CEN, 2002) – see Appendix C below.

.

The settlement is expressed as :

$$s = (q - \sigma_{v0}) \times \left[\frac{2B_0}{9E_d} \times \left(\frac{\lambda_d B}{B_0} \right)^\alpha + \frac{\alpha \lambda_c B}{9E_c} \right] \quad (9)$$

Here:

- $q = 0.18 \text{ MPa}$

- $\sigma_{v0} = q' = 60 \text{ kPa}$

- $B = 7.5 \text{ m}$

- $L/B = 1.33$, thus $\lambda_d = 1.26$ and $\lambda_c = 1.13$

- normally fractured rock : $\alpha = 0.5$

The Ménard pressuremeter moduli are the following (from Fig. 7.3; D is the depth of the base of the foundation) :

- from D to $D+B/2$: $E_1 = 7.3 \text{ MPa}$

- from $D+B/2$ to $D+B$: $E_2 = 27.0 \text{ MPa}$

- from $D+B$ to $D+3B/2$: $E_3 = 33.0 \text{ MPa}$

- from $D+3B/2$ to $D+2B$: $E_4 = 20.0 \text{ MPa}$

- from D+2B to D+5B/2 : $E_5 = 30.0 \text{ MPa}$
- from D+5B/2 to D+8B : $E_6 \text{ to } E_{16} \geq 30.0 \text{ MPa}$

Thus,

$$E_c = E_1 = 7.3 \text{ MPa}$$

and E_d is determined by the harmonic mean of E_i (I from 1 to 16), taking account of the distribution of the vertical stress from depth $D + B/2$ to $D + 8B$ (see MELT, 1993); when $E_6 \text{ to } E_{16} \geq E_5$, an approximation is :

$$3.2/E_d = 1/E_1 + 1/0.85 E_2 + 1/E_{3,5} \quad (10)$$

$$\text{with } 1/E_{3,5} = (1/E_3 + 1/E_4 + 1/E_5)/3 \quad (11)$$

Thus, in the present case : $E_d = 14,65 \text{ MPa}$

Finally,

$$\begin{aligned} s &= (0.18 - 0.06) [1.2 (1.26 \times 7.5 / 0.6)^{0.5} / (9 \times 14.65) + 0.5 \times 1.13 \times 7.5 / 9 \times 7.3] \\ &= 0.12 [0.036 + 0.065] = 0.012 \text{ m} = 12 \text{ mm}, \end{aligned}$$

which is largely acceptable for the bridge.

Note : a preliminary rough estimation can be done by assuming an homogeneous soil with $E_c = E_d = 6 \text{ MPa}$, for instance, with $\sigma_{vo} = 0$, which will obviously overestimate severely the settlement. In this case,

$$\begin{aligned} s &= 0.18 [1.2 (1.26 \times 7.5 / 0.6)^{0.5} / (9 \times 6) + 0.5 \times 1.13 \times 7.5 / 9 \times 6] \\ &= 0.18 [0.088 + 0.078] = 0.030 \text{ m} = 3 \text{ cm}, \end{aligned}$$

which is still acceptable for the bridge.

7.6 Seismic design situations

For the resistance to earthquakes, the rules of Eurocode 7 have to be complemented by those of Eurocode 8 - Part 5, devoted to the design of foundations and retaining structures in seismic areas (EN 1998-5, CEN, 2005).

Great attention should first be made to the liquefaction susceptibility of the various ground layers. In the present case, there is no liquefiable layer – see Figs. 7.2 and 7.3.

The two following Annexes in Eurocode 8 – Part 5 are particularly relevant to the design of the abutments retaining walls and piers of the bridge :

- Annex E (Normative) ‘Simplified analysis for retaining structures’, which allows the calculation of the earth pressures (static + dynamic) on the abutments;
- Annex F (Informative) ‘Seismic bearing capacity of shallow foundations’, which is a model for a shallow strip footing taking account of the soil strength, the design action effects (N_{Ed} , V_{Ed} , M_{Ed}) at the foundation level, and the inertia forces in the soil.

The seismic design action effects come from the capacity design of the superstructure, in general (see Koliass 2010a and 2010b, for the present case).

Specifically for limited ductile superstructures, the design action effects are calculated from the seismic analysis multiplied by the behaviour factor q .

The values of the partial factors (γ_M) for material properties c_u (undrained shear strength), $t_{cy,u}$ (cyclic undrained shear strength), q_u (unconfined compressive strength), and $\tan \phi'$ recommended by EN

1998-5 are $\gamma_{cu} = 1.4$, $\gamma_{tcy} = 1.25$, $\gamma_{qu} = 1.4$, and $\gamma_{\phi} = 1.25$. They correspond to the ones recommended by EN 1997-1 for persistent and transient design situations (see set M2 in Table 7.4). Some countries (Greece, for instance) have judged that these values are much too severe, given the safety already included in the calculations of the seismic design values of the action effects. Their National Annex have thus set them all equal to 1.0 (as well as alternative resistance factors γ_R).

REFERENCES

- CEN 2002. *Eurocode: Basis of structural design*. EN 1990 : 2002. European Committee for Standardization (CEN): Brussels.
- CEN 2004. *Eurocode 7: Geotechnical design - Part 1: General rules*. EN 1997-1:2004 (E), November 2004, European Committee for Standardization: Brussels.
- CEN 2005. *Eurocode 8: Design of structures for earthquake resistance - Part 5: Foundations, retaining structures and geotechnical aspects*. EN1998-5:2004 (E), May 2005, European Committee for Standardization: Brussels.
- CEN 2007. *Eurocode 7: Geotechnical design - Part 2: Ground investigation and testing*. EN1997-2:2007 (E), March 2007, European Committee for Standardization: Brussels.
- Davaine L. 2010a. *Global analysis of a steel-concrete composite two-girder bridge according to Eurocode 4*, Note for Workshop "Bridge design to Eurocodes" to be held in Vienna, 4-6 October 2010, June 2010, 39 pages.
- Davaine L. 2010b. *Excel sheet with a synthesis of the reactions and supports*, e-mail to TC 250/HGB : June 09, 2010 6:24 pm.
- Davaine L. 2010c. *Supplement for support reactions*, Private written communication, Workshop "Bridge design to Eurocodes", Vienna, 4-6 October 2010, June 2010, 16 August 2010, 2 pages.
- Kolias B. 2010a. *Squat piers with seismic isolation. Summary of seismic design results*. Note for Workshop "Bridge design to Eurocodes" to be held in Vienna, 4-6 October 2010, June 2010, 25 pages.
- Kolias B. 2010b. *Flexible piers with limited ductile behaviour. Summary of seismic design results*. Note for Workshop "Bridge design to Eurocodes", Vienna, 4-6 October 2010, July 2010, 14 pages.
- Malakatas N. 2010. *Example of application for Wind actions on bridge deck and piers*, Report for Workshop "Bridge design to Eurocodes", Vienna, 4-6 October 2010, January 2011, 20 pages.
- MELT-Ministère de l'Équipement, du logement et des transports 1993. *Règles Techniques de Conception et de Calcul des Fondations des Ouvrages de Génie Civil (in French: Technical Rules for the Design of Foundations of Civil Engineering Structures)*. Cahier des clauses techniques générales applicables aux marchés publics de travaux, FASCICULE N°62 -Titre V, Textes Officiels N° 93-3 T.O., 182 pages.

CHAPTER 8

Overview of seismic issues for bridge design (EN 1998-1, EN 1998-2)

Basil KOLIAS

DENCO S.A., Athens

8.1 Introduction

This chapter covers an overview of seismic issues for bridge design, in accordance with EN 1998-2:2005 and EN 1998-1:2004, developed along the lines of a general example, common for the application of Eurocodes 0, 1, 2, 3, 4, 7 and 8.

The general example is a bridge having composite steel and concrete continuous deck, with spans of 60 + 80 + 60 m. Two cases are assumed for the piers namely, 40 m high hollow cylindrical piers and 10 m high, solid rectangular piers. Regarding the seismic design situation, neither of these bridge configurations offers itself for a seismic load resisting system consisting of piers rigidly fixed to the deck, with ductile seismic behaviour. However a large part of EN 1998-2 deals with exactly this kind of seismic load resisting systems, as it is usually cost effective for bridges of relatively shorter spans and medium total length. To cover the main seismic issues of this important category of bridges, a special example of such a bridge is also included in this chapter.

Consequently this chapter contains following examples:

- **Section 8.2 - Example of ductile piers:** Special example of seismic design of a bridge with concrete deck rigidly connected to piers designed for ductile behavior.
- **Section 8.3 - Example of limited ductile piers:** Seismic design of the general example: Bridge on high piers designed for limited ductile behavior.
- **Section 8.4 - Example of seismic isolation:** Seismic design of the general example: Bridge on squat piers designed with seismic isolation.

It should be noted that the contents of the examples, although selected to illustrate the main seismic issues regulated by EN 1998-2, do not exhaust all relevant requirements of the standard, and do not cover of course all issues to be dealt by a real structural design.

8.2 Example of ductile piers

8.2.1 BRIDGE CONFIGURATION – DESIGN CONCEPT

The bridge is a 3 span overpass, with spans 23.0 + 35.0 + 23.0m and total length of 82.50m. The deck is a post tensioned cast in situ concrete voided slab. The piers consist of single cylindrical columns with diameter $D=1.20\text{m}$, rigidly connected to the deck. Pier heights are 8.0m for M1 and 8.5m for M2. The bridge is simply supported on the abutments through a pair of bearings allowing free sliding and rotation in and about both horizontal axes. The piers and abutments are founded on piles.

The detailed configuration of the bridge is shown in Fig. 8.1, Fig. 8.2 and Fig. 8.3.

The selection of single cylindrical column piers makes possible an orthogonal arrangement of the supports despite the slightly skew crossing in plan. For the given geometry of the bridge, the monolithic connection between piers and deck minimizes the use of expensive bearings or isolators (and their maintenance), without subjecting the bridge elements to excessive restraints, due to imposed deck deformations. Some comments on the cost efficiency of the seismic resistant system are given, as conclusions, in 8.2.7.

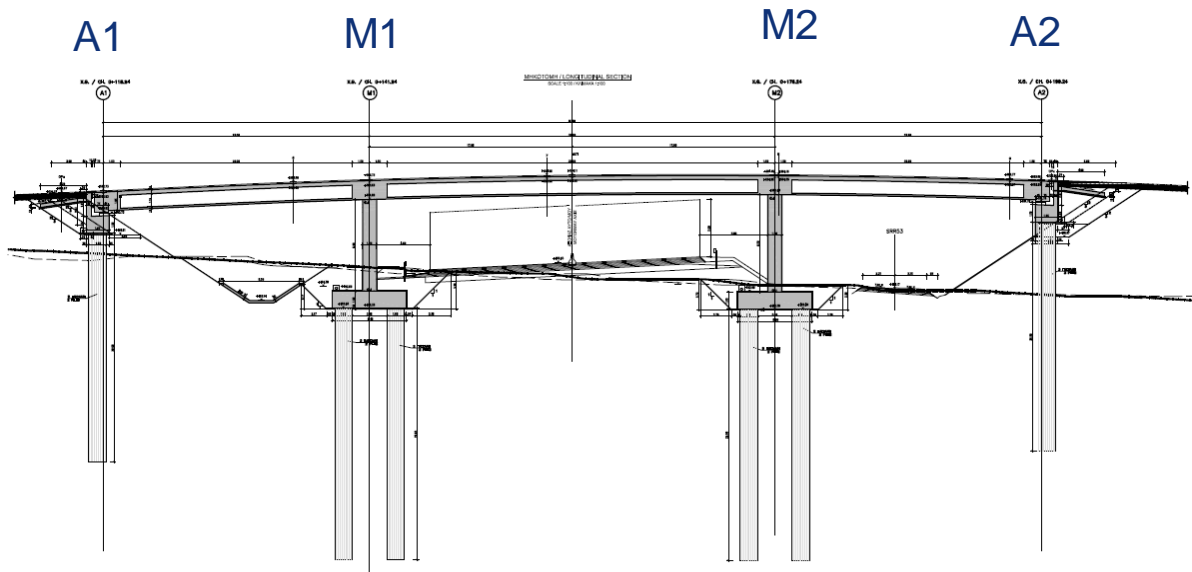


Fig. 8.1 Longitudinal section

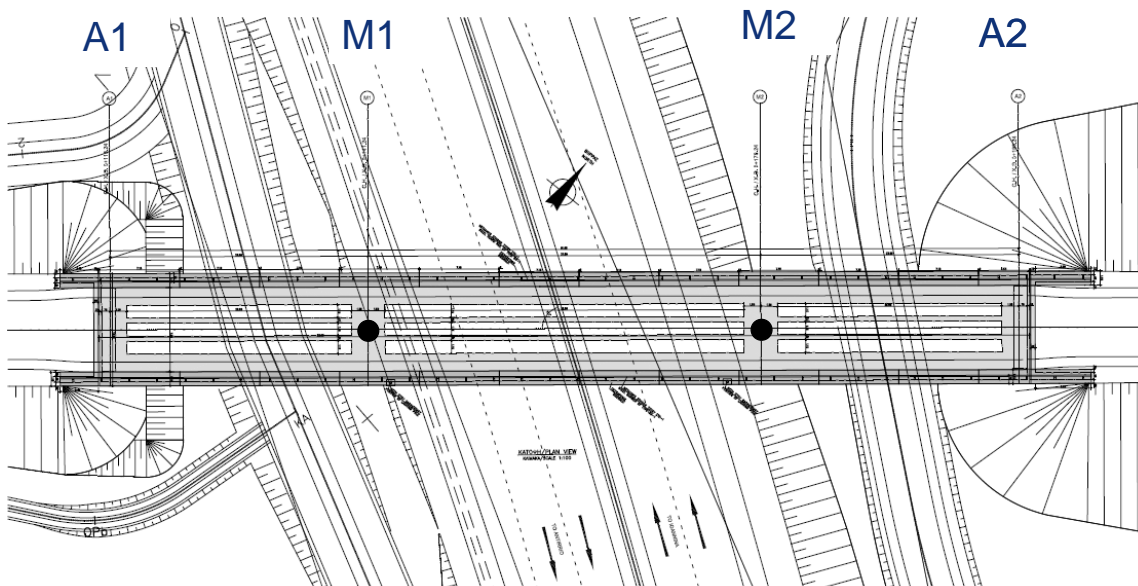


Fig. 8.2 Plan view



8.2.2.1 Structural system and ductility class

8.2.2.2. Stiffness of elements

The value of piers effective stiffness for seismic analysis is estimated initially and is checked after the selection of the required reinforcement for the piers.

Deck

8.2.2.3 Design seismic action

The seismic action in horizontal directions is:

203

The behaviour factors are, according to 8.2.2.1, $q_x = 3.5$ in longitudinal direction and $q_y = 3.5$ in transverse direction. The design response spectrum that results from all the above is calculated according to EN 1998-1:2004, 3.2.2.5 and is presented in Fig. 8.4.

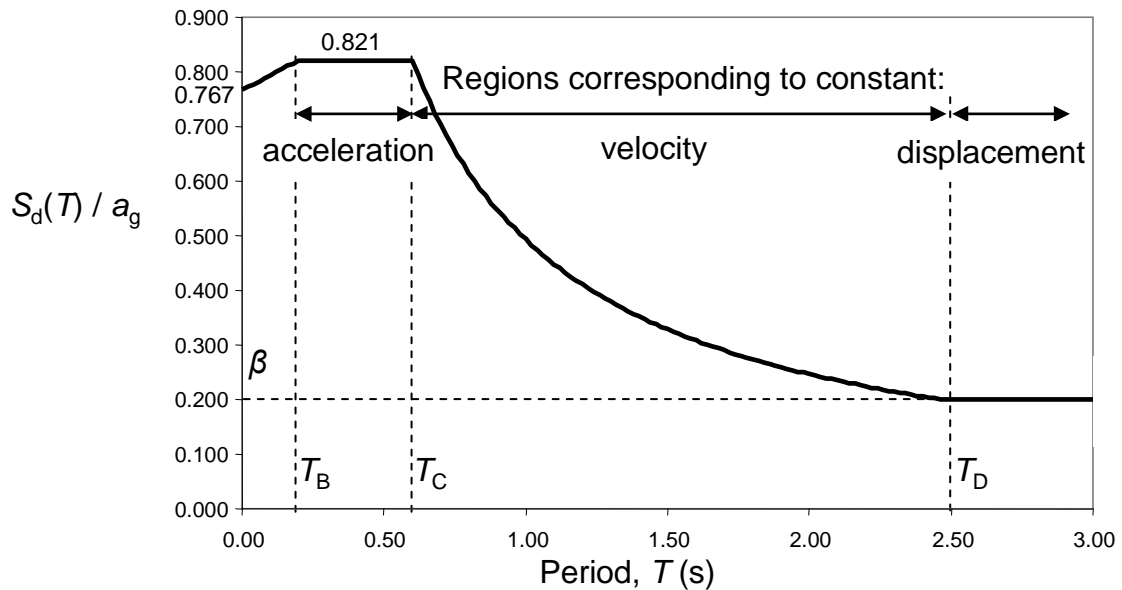


Fig. 8.1 Design response spectrum

8.2.2.4 Permanent load for the design seismic situation

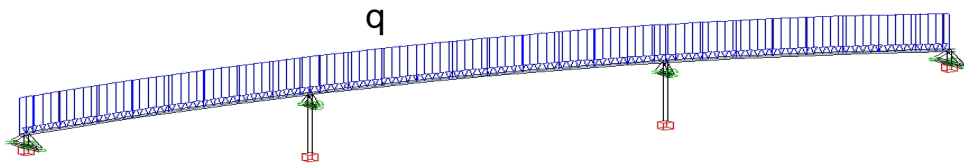


Fig. 8.2 Dead, additional dead and uniform traffic load application

The loads applied in the bridge deck (Fig. 8.5) for the seismic situation are:

1. Self weight (G):

$$q_G = (6.89\text{m}^2 \times 73.5\text{m} + 9.97\text{m}^2 \times 9.0\text{m}) \times 25\text{kN/m}^3 = 14903\text{kN}$$

where the area of the voided section is 6.89m^2 , the area of the solid section is 9.97m^2 , the total length of the voided section is 73.5m and the total length of the solid section is 9.0m .

2. Additional dead (G2):

$$q_{G2} = 2 \times 25\text{kN/m}^3 \times 0.50\text{m}^2 + 2 \times 0.70\text{kN/m} + 7.5\text{m} \times (23\text{kN/m}^3 \times 0.10\text{m}) =$$

(sidewalks) (safety barriers) (road pavement)

$$= 43.65\text{kN/m}$$

Where the area of the sidewalks is $0.50\text{m}^2/\text{m}$, the weight of the safety barriers is 0.70kN/m and the width and thickness of the pavement are 7.5m and 0.10m respectively.

3. Effective seismic live load (L_E). The effective seismic live load is 20% of the uniformly distributed traffic load:

$$q_L = 45.2 \text{ kN/m and}$$

$$q_{LE} = 0.20 \cdot q_L = 0.2 \times 45.2 \text{ kN/m} = 9.04 \text{ kN/m}$$

4. Temperature action (T)*. The temperature action consists of an increase of $+52.5^\circ\text{C}$ and a decrease of -45°C relative to the construction temperature $T_0 = 10^\circ\text{C}$

5. Creep & Shrinkage (CS)*:

A total strain of -32.0×10^{-5} is applied.

* Actions 4, 5 are applicable only for bearing displacements.

The deck total seismic weight is then:

$$W_E = 14903 \text{ kN} + (43.65 + 9.04) \text{ kN/m} \times 82.5 \text{ m} = 19250 \text{ kN}$$

8.2.3 FUNDAMENTAL MODE ANALYSIS IN THE LONGITUDINAL DIRECTION

The fundamental mode period is estimated based on a simplified SDOF cantilever model of the bridge. The mode corresponds to the oscillation of the bridge along its longitudinal axis, assuming both ends of the piers fixed.

For cylindrical column of diameter 1.2m the uncracked moment of inertia is:

$$J_{un} = \pi \times 1.2^4 / 64 = 0.1018 \text{ m}^4$$

The assumed effective moment of inertia of piers is $J_{eff}/J_{un} = 0.40$ (remains to be checked later).

Assuming both ends of the piers fixed and for concrete grade C30/37 with $E_{cm} = 33 \text{ GPa}$, the horizontal stiffness of each pier in longitudinal direction is:

$$K_1 = 12 E J_{eff} / H^3 = 12 \times 33000 \text{ MPa} \times (0.40 \times 0.1018 \text{ m}^4) / (8.0 \text{ m})^3 = 31.5 \text{ MN/m}$$

$$K_2 = 12 E J_{eff} / H^3 = 12 \times 33000 \text{ MPa} \times (0.40 \times 0.1018 \text{ m}^4) / (8.5 \text{ m})^3 = 26.3 \text{ MN/m}$$

The total horizontal stiffness is: $K = 31.5 + 26.3 = 57.8 \text{ MN/m}$

The total seismic weight is: $W_E = 19250 \text{ kN}$

The fundamental period is:

$$T = 2\pi \sqrt{\frac{m}{K}} = 2\pi \sqrt{\frac{19250 \text{ kN} / 9.81 \text{ m/s}^2}{57800 \text{ kN/m}}} = 1.16 \text{ s}$$

The spectral acceleration in longitudinal direction is:

$$S_e = a_g S(\beta_0/q)(T_C/T) = 0.16g \times 1.15 \times (2.5/3.5) \times (0.60/1.16) = 0.068g$$

The total seismic shear force in piers is:

$$V_E = S_e W_E / g = 0.068g \times 19250 \text{ kN} / g = 1309 \text{ kN}$$

The shear force is distributed to piers M1 and M2 proportionally to their stiffness:

$$V_1 = (31.5 / 57.8) \times 1309 \text{ kN} = 713 \text{ kN}$$

$$V_2 = 1309 - 713 = 596 \text{ kN}$$

The seismic moments M_y (assuming full fixity of pier columns at top and bottom) are:

$$M_{y1} \approx V_1 \cdot H_1 / 2 = 713 \text{ kN} \times 8.0 \text{ m} / 2 = 2852 \text{ kNm}$$

$$M_{y2} \approx V_2 \cdot H_2 / 2 = 596 \text{ kN} \times 8.5 \text{ m} / 2 = 2533 \text{ kNm}$$

8.2.4 MULTIMODE RESPONSE ANALYSIS

8.2.4.1 Modal analysis

The characteristics of the first 30 modes of the structure out of total 50 modes considered in the analysis are shown in Table 8.1. The shapes of the first 8 modes are presented in Fig. 8.6 and Fig. 8.7. Modes 1, 4, 5, 6 and 7 have negligible contribution to the total response.

Table 8.1 Modal characteristics for the first 30 modes

Mode No.	Period s	modal mass contribution in %		
		X dir	Y dir	Z dir
1	1.77	0	3.39	0
2	1.43	0	94.8	0
3	1.20	99.19	0	0
4	0.32	0	0	8.92
5	0.32	0	0.34	0
6	0.19	0	0.72	0
7	0.17	0.05	0	0.01
8	0.15	0	0	63.13
9	0.14	0	0	0
10	0.10	0	0	0
11	0.10	0	0	0
12	0.093	0	0.01	0
13	0.069	0	0	0
14	0.058	0	0.01	0
15	0.054	0	0	10.77
16	0.053	0	0	0.16
17	0.052	0	0	1.81
18	0.051	0	0	0.45
19	0.050	0	0.02	0
20	0.047	0	0	0
21	0.040	0	0	0
22	0.036	0	0	0
23	0.035	0	0	0
24	0.032	0	0.07	0
25	0.031	0	0	0
26	0.030	0.19	0	0.23
27	0.029	0	0.09	0
28	0.028	0.02	0	5.39
29	0.028	0	0.07	0
30	0.027	0.14	0	0.06

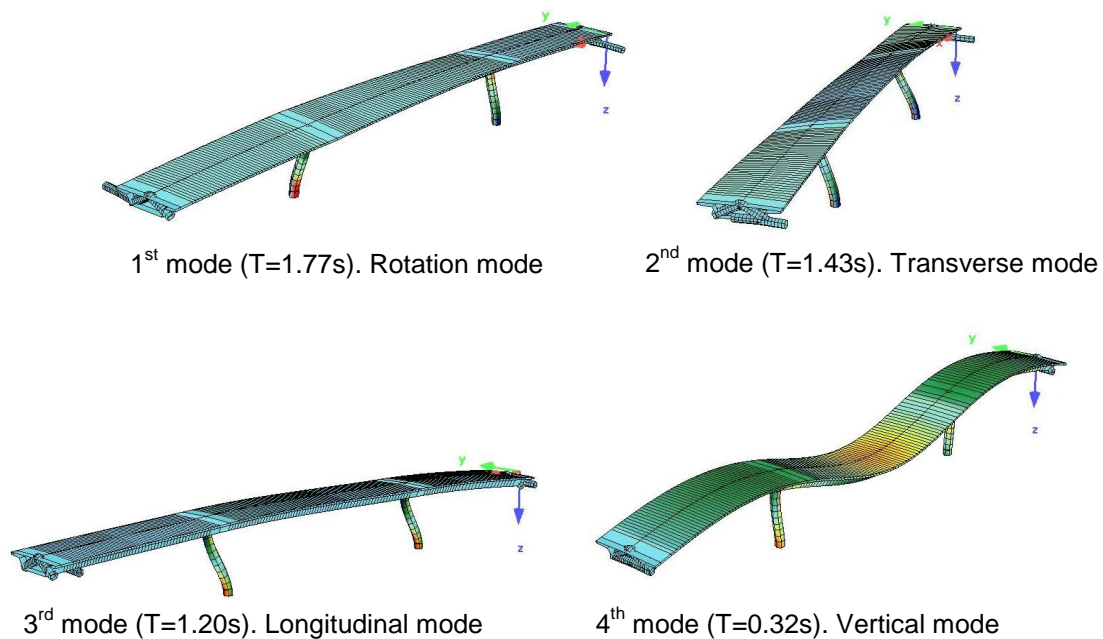


Fig. 8.6 Modes 1, 2, 3 and 4

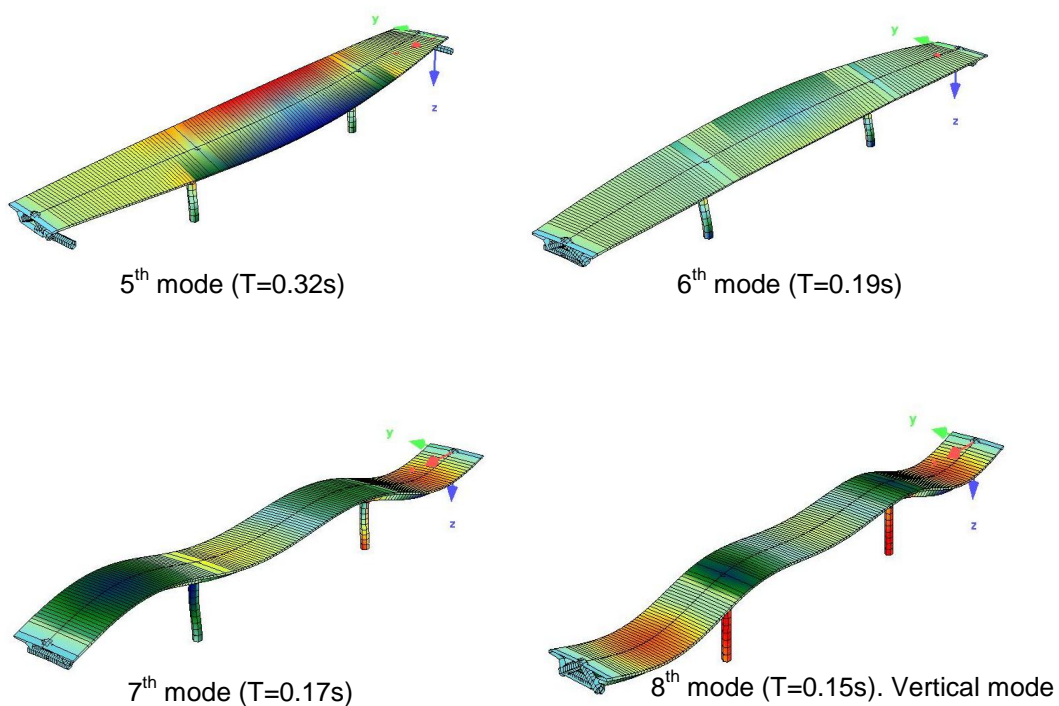


Fig. 8.7 Modes 5, 6, 7 and 8

8.2.4.2 Response spectrum analysis

Response spectrum analysis considering the first 50 modes was carried out. The sum of the modal masses considered amounts to 99.6%, 99.7% and 92% in the X, Y and Z directions respectively. The combination of modal responses was carried out using the CQC rule.

8.2.4.3 Comparison of mode in longitudinal direction

The results in longitudinal direction of the fundamental mode analysis and of the multimode response analysis are presented and compared in Table 8.2.

Table 8.2 Comparison of analyses in longitudinal direction

		Fundamental mode analysis	Multimode response spectrum analysis
Effective Period T_{eff} for longitudinal direction		1.16s	1.20s (3 rd mode)
Seismic shear, V_z	M1	713kN	662kN
	M2	596kN	556kN
Seismic moment, M_y	M1	2852kNm	2605...2672kNm
	M2	2533kNm	2327...2381kNm (values at top and bottom)

8.2.5 DESIGN ACTION EFFECTS AND VERIFICATIONS

8.2.5.1 Design action effects for flexure and axial force verification of plastic hinges

The combination of the components of seismic action is carried out according to 4.2.1.4 (2) of EN 1998-2, by applying expressions (4.20) - (4.22) of 4.3.3.5.2 (4) of EN 1998-1. The pier is of circular section with diameter $D = 1.20\text{m}$ and is made of concrete C30/37 with $f_{\text{ck}}=30\text{MPa}$ and $E_c=33000\text{MPa}$ and reinforcing steel S500 with $f_{\text{yk}}=500\text{MPa}$. The cover to the reinforcement centre is $c=8.2\text{cm}$.

Table 8.3 shows the design action effects (bending moment and axial force) at the bottom section of pier M1 together with the required reinforcement, for each design combination.

Table 8.3 Design action effects & required reinforcement in bottom section of pier M1

Combination	N	M_y	M_z	A_s
	kN	kNm	kNm	cm ²
max $M_y + M_z$	-7159	4576	-1270	198.7
min $M_y + M_z$	-7500	-3720	1296	134.9
max $M_z + M_y$	-7238	713	4355	172.4
min $M_z + M_y$	-7082	456	-4355	170.0

The required reinforcement at the bottom section of Pier M1, which is critical, is 198.7cm^2 . The final reinforcement selected is $25\Phi 32$ (201.0cm^2) as shown in Fig. 8.8. Fig. 8.9 shows the Moment – Axial force interaction diagram for the bottom section of Pier M1 for all design combinations.

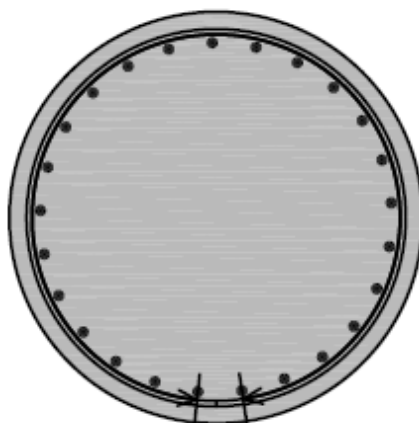


Fig. 8.3 Pier M1 cross section with reinforcement

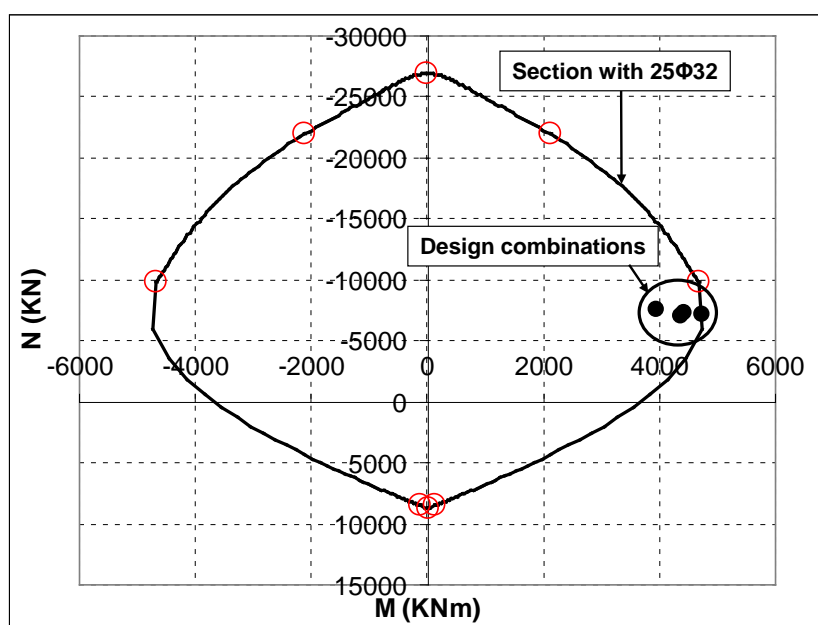


Fig. 8.4 Moment – Axial force interaction diagram for the bottom section of Pier M1

Table 8.4 shows the design action effects of bending moment and axial force at the bottom section of pier M2 together with the required reinforcement, for each design combination.

Table 8.4 Design action effects & required reinforcement in bottom section of pier M2

Combination	N	M_y	M_z	A_s
	kN	kNm	kNm	cm ²
max $M_y + M_z$	-7528	3370	-1072	103.2
min $M_y + M_z$	-7145	-4227	1042	168.0
max $M_z + M_y$	-7317	-465	3324	89.8
min $M_z + M_y$	-7320	-674	-3324	92.5

The required reinforcement in bottom section of Pier M2, which is critical, is 168.0cm^2 . The final reinforcement selected is $21\Phi 32$ (168.8cm^2) as shown in Fig. 8.10. Fig. 8.11 shows the Moment – Axial force interaction diagram for the bottom section of Pier M2 for all design combinations.

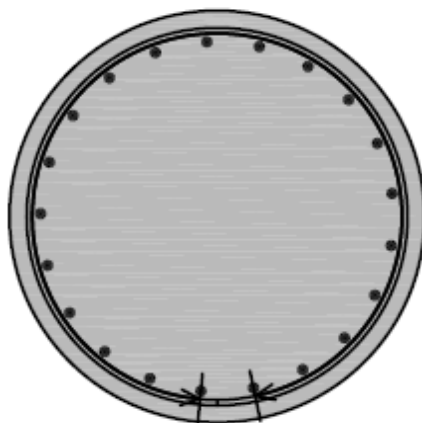


Fig. 8.5 Pier M2 cross section with reinforcement

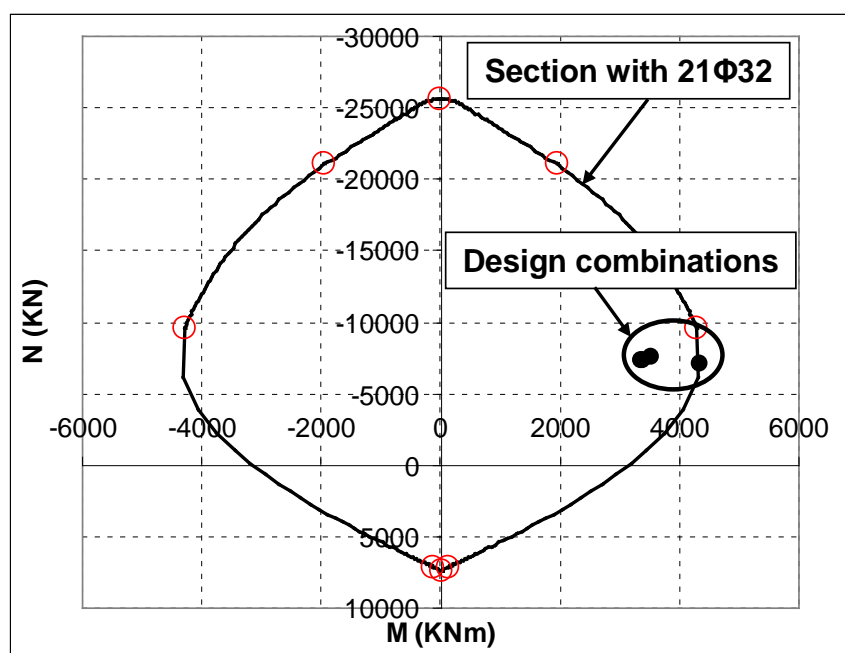


Fig. 8.6 Moment – Axial force interaction diagram for the bottom section of Pier M2

8.2.5.2 Checking of stiffness of ductile elements

The effective stiffness of piers for seismic action is estimated according to EN 1998-2:2005+A1:2009, **Annex C**.

The pier is of circular section with diameter $D = 1.20\text{m}$ and is made of concrete C30/37 with $f_{ck}=30\text{MPa}$ and $E_c=33000\text{MPa}$ and reinforcing steel S500 with $f_{yk}=500\text{MPa}$. The cover to the reinforcement centre is $c=8.2\text{cm}$.

Pier M1

The final reinforcement for pier M1 is 1 layer of 25 Φ 32 (201.0cm²). For axial force $N = -7200\text{kN}$ the yield moment is $M_y = 4407\text{kNm}$ and the corresponding concrete strain is $\epsilon_{cy} = 2.72\text{‰}$. The ultimate moment is $M_{Rd}=4779\text{kNm}$.

The yield curvature is:

$$\Phi_y = (2.17\text{‰} + 2.72\text{‰}) / (1.20\text{m} - 0.082\text{m}) = 4.37 \times 10^{-3} \text{m}^{-1}$$

while the approximation for circular section according to EN 1998-2:2005+A1:2009, **Eq. (C.6)** yields

$$\Phi_y = 2.4\epsilon_{sy}/d = 2.4 \times 2.17\text{‰} / (1.2\text{m} - 0.082\text{m}) = 4.66 \cdot 10^{-3} \text{m}^{-1}$$

Applying method 1 according to EN 1998-2:2005+A1:2009, **C.2** we get:

$$J_{un} = \pi \times 1.20^4 / 64 = 0.1018 \text{m}^4$$

$$J_{cr} = M_y / (E_c \cdot \Phi_y) = 4407\text{kNm} / (33000\text{MPa} \times 4.37 \times 10^{-3} \text{m}^{-1}) = 0.0306 \text{m}^4$$

$$J_{eff} = 0.08J_{un} + J_{cr} = 0.0387 \text{m}^4$$

$$J_{eff}/J_{un} = 0.38$$

Applying method 2 according to EN 1998-2:2005+A1:2009, **C.3** we get:

$$E_c J_{eff} = \nu M_{Rd} / \Phi_y = 1.20 \times 4779\text{kNm} / 4.37 \times 10^{-3} \text{m}^{-1} = 1312000\text{kNm}^2$$

$$J_{eff} = 1312000\text{kNm}^2 / 33000\text{MPa} = 0.0398 \text{m}^4$$

$$J_{eff}/J_{un} = 0.39$$

The assumed value of $J_{eff}/J_{un} = 0.40$ was a good starting value for the analysis.

Pier M2

For pier M2 the final reinforcement is 1 layer of 21 Φ 32 (168.8cm²). For axial force $N = -7200\text{kN}$ the yield moment is $M_y = 4048\text{kNm}$, the corresponding concrete strain is $\epsilon_{cy} = 2.73\text{‰}$ and the ultimate moment is $M_{Rd}=4366\text{kNm}$. Method 1 yields:

$$J_{eff}/J_{un} = 0.35$$

while method 2 yields:

$$J_{eff}/J_{un} = 0.36$$

The assumed value of $J_{eff}/J_{un} = 0.40$ was a good starting value for the analysis.

8.2.5.3 Shear verification of piers**a Over strength moments**

The over strength moment is calculated by $M_o = \gamma_o M_{Rd}$, where γ_o is the over strength factor and M_{Rd} is the ultimate moment provided by the section analysis. Since $\eta_k = 0.22 > 0.1$ the over strength factor is increased according to EN 1998-2:2005+A1:2009, **5.3(4)** by the factor:

$$1 + 2(\eta_k - 0.1)^2 = 1 + 2 \times (0.22 - 0.1)^2 = 1.029,$$

so $\gamma_o = 1.35 \times 1.029 = 1.39$.

The over strength moments for both sections of piers are:

$$M_{o1} = 1.39 \times 4779 = 6643 \text{ kNm and}$$

$$M_{o2} = 1.39 \times 4366 = 6069 \text{ kNm}$$

b Capacity design in longitudinal direction

The capacity shear forces can be calculated directly from the over strength moments:

$$V_{C1} = 2M_{o1}/H_1 = 2 \times 6643 / 8.0 = 1661 \text{ kN and}$$

$$V_{C2} = 2M_{o2}/H_2 = 2 \times 6069 / 8.5 = 1428 \text{ kN}$$

c Capacity design in transverse direction

The base shear on each pier is calculated applying the simplifications of EN 1998-2:2005+A1:2009, **G.2** and Eq. (G.3):

$$V_{Ci} = (M_o/M_{Ei}) V_{Ei}$$

The seismic moment and shear force are:

$$M_{E1} = 3061 \text{ kNm and } V_{E1} = 680.3 \text{ kN}$$

$$M_{E2} = 2184 \text{ kNm and } V_{E2} = 450.2 \text{ kN}$$

The capacity base shear forces are:

$$V_{C1} = (6643 \text{ kNm} / 3061 \text{ kNm}) \times 680.3 \text{ kN} = 1476 \text{ kN}$$

$$V_{C2} = (6069 \text{ kNm} / 2184 \text{ kNm}) \times 450.2 \text{ kN} = 1251 \text{ kN}$$

The capacity effects for the base of the piers are shown for the transverse direction in Fig. 8.12.

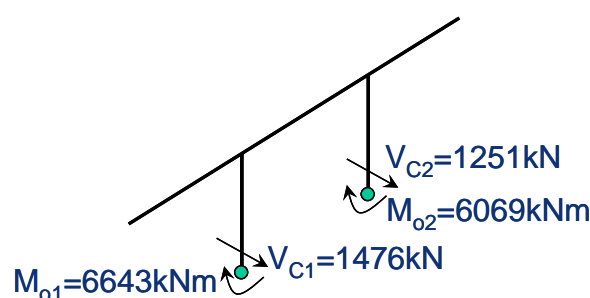


Fig. 8.7 Capacity effects for the transverse direction

d Design for shear

The design is performed according to EN 1998-2:2005+A1:2009, **5.6.3.4**. The design shear force for pier M1 is $V_{C1} = 1661 \text{ kN}$. For circular section according to EN 1998-2:2005+A1:2009, **5.6.3.3(2)** the effective depth is:

$$d_e = r + 2r_s/\pi = 0.60 + 2 \times 0.52 / \pi = 0.93 \text{ m}$$

and the internal lever arm is then:

$$z = 0.9 \cdot d_e = 0.9 \times 0.93\text{m} = 0.84\text{m}.$$

The shear strength of the section is calculated by:

$$V_{Rd,s} = (A_{sw}/s) \cdot z \cdot f_{ywd} \cdot \cot\theta / \gamma_{Bd},$$

where A_{sw} is the total cross section of the shear reinforcement, s is the hoop spacing, f_{ywd} is the design yield strength of the shear reinforcement, $\cot\theta = 1$, according to EN 1998-2:2005+A1:2009, **5.6.3.4(2)P**, θ being the angle between the concrete compression strut and the pier axis and γ_{Bd} is an additional safety factor for which $\gamma_{Bd} = 1.0$ according to EN 1998-2:2005+A1:2009, **5.6.3.3(1)P**.

For pier M1 the required shear reinforcement is:

$$A_{sw}/s = 1.0 \times 1661\text{kN} / (0.84\text{m} \times 50\text{kN/cm}^2 / 1.15 \times 1.0) = 45.5\text{cm}^2/\text{m}$$

Accordingly for pier M2 the shear design force is $V_{C2} = 1428\text{kN}$ and the required shear reinforcement is:

$$A_{sw}/s = 1.0 \times 1428\text{kN} / (0.84\text{m} \times 50\text{kN/cm}^2 / 1.15 \times 1.0) = 39.1\text{cm}^2/\text{m}$$

8.2.5.4 Ductility requirements for piers

a Confinement reinforcement

The confinement reinforcement is calculated according to EN 1998-2:2005+A1:2009, **6.2.1**. The normalized axial force is:

$$\eta_k = N_{Ed}/A_c \cdot f_{ck} = 7600\text{kN} / 1.13\text{m}^2 \times 30\text{MPa} = 0.22 > 0.08, \text{ so confinement of compression zone is required.}$$

For ductile behaviour: $\lambda = 0.37$ and $\omega_{w,min} = 0.18$. The longitudinal reinforcement ratio for pier M1 is:

$$\rho_L = 201.0\text{cm}^2 / 11300\text{cm}^2 = 0.0178,$$

while for pier M2 is:

$$\rho_L = 168.8\text{cm}^2 / 11300\text{cm}^2 = 0.0149.$$

The distance to spiral centreline is $c = 5.8\text{cm}$ ($D_{sp} = 1.084\text{m}$) and the core concrete area is $A_{cc} = 0.923\text{m}^2$.

The required mechanical reinforcement ratio $\omega_{w,req}$ for pier M1 is:

$$\omega_{w,req} = (A_c/A_{cc}) \lambda \eta_k + 0.13 (f_{yd}/f_{cd}) (\rho_L - 0.01) = (1.13/0.923) \times 0.37 \times 0.22 + 0.13 \times (500/1.15) / (0.85 \times 30/1.5) \times (0.0178 - 0.01) = 0.126,$$

while for pier M2 is:

$$\omega_{w,req} = (1.13/0.923) \times 0.37 \times 0.22 + 0.13 \times (500/1.15) / (0.85 \times 30/1.5) \times (0.0149 - 0.01) = 0.116.$$

For circular spirals the mechanical reinforcement ratio (for the worst case of pier M1) is:

$$\omega_{wd,c} = \max(1.4 \cdot \omega_{w,req}; \omega_{w,min}) = \max(1.4 \times 0.126; 0.18) = 0.18.$$

The required volumetric ratio of confining reinforcement is:

$$\rho_w = \omega_{wd,c} (f_{cd}/f_{yd}) = 0.18 \times (0.85 \times 30/1.5) / (500/1.15) = 0.0070,$$

and the required confining reinforcement is:

$$A_{sp}/s_L = \rho_w D_{sp}/4 = 0.0070 \times 1.084\text{m}/4 = 0.00190\text{m}^2/\text{m} = 19.0\text{cm}^2/\text{m}.$$

The required spacing for $\Phi 16$ spirals is $s_{L\text{req}} = 2.01/19.0 = 0.106\text{m}$.

The allowed maximum spacing is:

$$s_L^{\text{allowed}} = \min(6 \times 3.2\text{cm}; 108.4\text{cm}/5) = \min(19.2\text{cm}; 21.7\text{cm}) = 19.2\text{cm} > 10.6\text{cm}$$

b Avoidance of buckling of longitudinal bars

The provisions of EN 1998-2:2005+A1:2009, **6.2.2** are applied for the check of the required transverse reinforcement to avoid buckling of the longitudinal bars.

For S500 steel the ratio $f_{tk}/f_{yk} = 1.15$.

The maximum hoops spacing s_L should not exceed δd_{bL} , where

$$\delta = 2.5 \cdot (f_{tk}/f_{yk}) + 2.25 = 2.5 \times 1.15 + 2.25 = 5.125.$$

Substituting, we get:

$$s_L^{\text{req}} = \delta d_L = 5.125 \times 3.2\text{cm} = 16.4\text{cm}$$

8.2.5.5 Transverse reinforcement of piers – Comparison of requirements

The piers transverse reinforcement requirements for each design check are presented and compared in Table 8.5.

Table 8.5 Comparison of piers transverse reinforcement requirements

Requirement	Confinement	Buckling of bars	Shear design
A_t/s_L (cm^2/m)	$2 \times 19.0 = 38$	-	M1: 45.5 M2: 39.1
$\max s_L$ (cm)	19.2	16.4	-

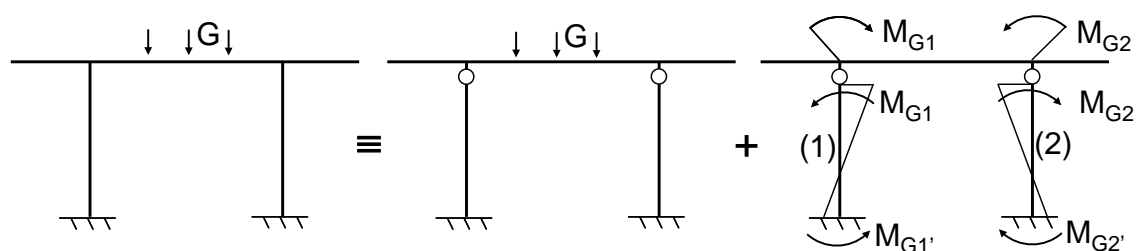
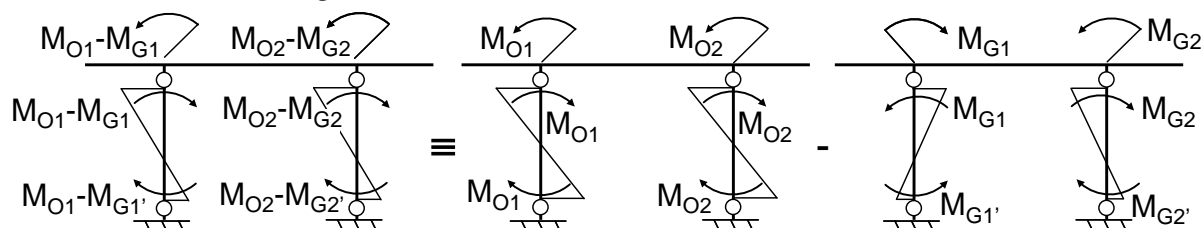
The transverse reinforcement is governed by the shear design. The reinforcement selected for both piers is one spiral of $\Phi 16/8.5$ ($47.3\text{cm}^2/\text{m}$).

8.2.5.6 Capacity verifications of the deck

a Estimation of the capacity design effects – An alternative procedure

The general procedure for calculating the capacity effects, given in EN 1998-2:2005+A1:2009, **G.1**, consists of adding, to the effects of permanent loads “G”, the effects of the loading $\Delta A_C = “M_o - G”$, both acting in the deck-piers frame system of the bridge. An alternative procedure is to work on a continuous beam system of the deck, simply supported on the piers and abutments. On this system the effects of the permanent loads “G” and the effects of the over strength moments “ M_o ” are added. The equivalence of the two procedures is shown in Fig. 8.13.

Permanent Load “G”

 ΔA_c : Over strength – “G”

general procedure \equiv alternative procedure

Fig. 8.8 Equivalence of general and simpler procedures

The effects of the permanent loads “G” are shown in Fig. 8.14.

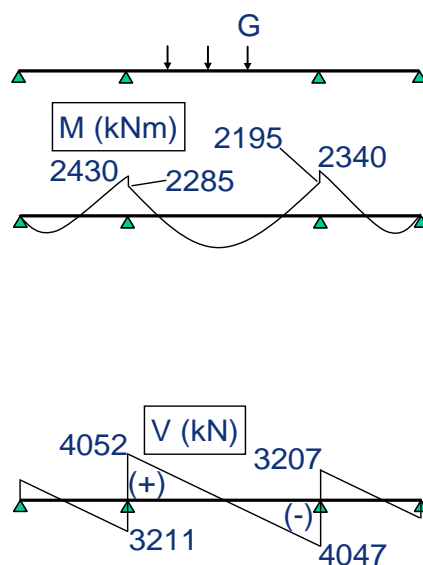


Fig. 8.9 Permanent loads (“G” loading) and resulting moment and shear force diagrams

Fig. 8.15 shows the effects of the over strength loading “ M_o ” for seismic action in +x direction. For the effects due to seismic action in -x direction the signs of the effects are simply reversed. Fig. 8.16 shows the result of adding the previous two loadings to get the capacity effects, again for seismic action in +x direction.

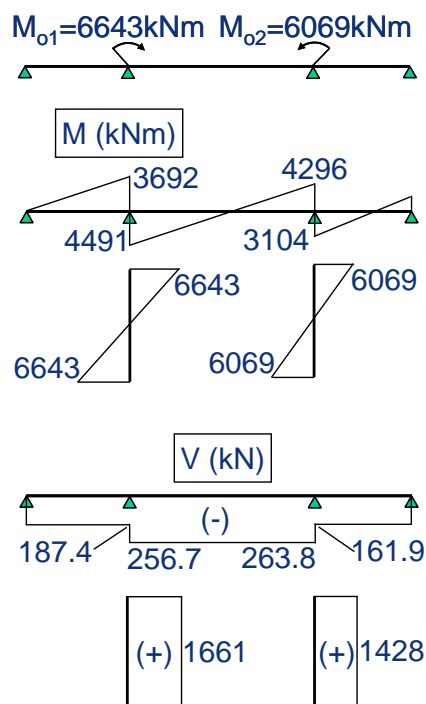


Fig. 8.10 Over strength for seismic action in +x direction (“ M_o ” loading) and resulting moment and shear force diagrams

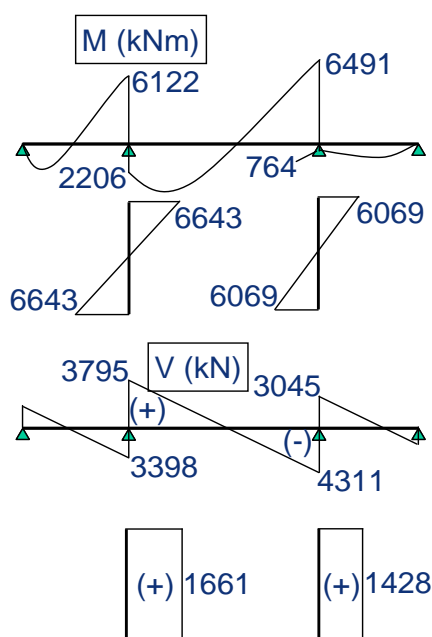


Fig. 8.11 Capacity effects for seismic action in +x direction (“ G ” + “ M_o ”) and resulting moment and shear force diagrams

b Flexural verification of deck

The deck section at each side of the joints connecting the deck with the piers is checked against these capacity effects taking into account the existing reinforcement and tendons as shown in Fig. 8.17.

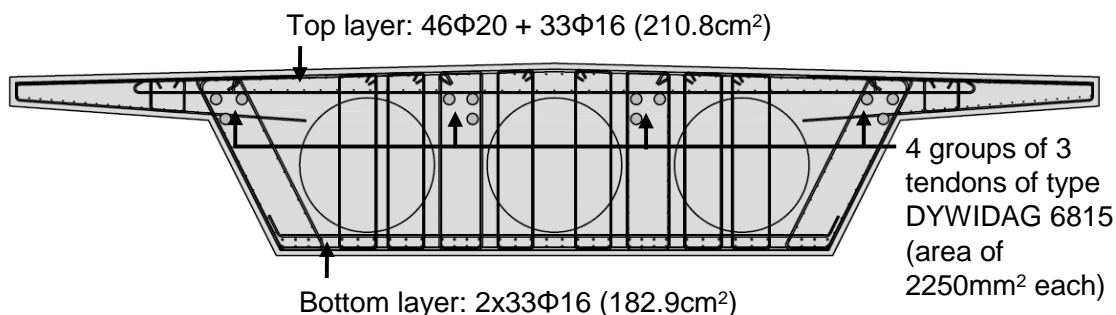


Fig. 8.12 Deck section, reinforcement and tendons

Table 8.6 shows the design combinations (moment and axial force) for which the deck sections are checked, while Fig. 8.18 shows the Moment – Axial force interaction diagram compared with the capacity effects.

Table 8.6 Design combinations for deck section

Combination / location	M_y (kNm)	N (kN)
Pier M1 – left side (+x)	-6122	-29900
Pier M1 – right side (+x)	2206	-28300
Pier M2 – left side (+x)	-6491	-29500
Pier M2 – right side (+x)	764	-28100
Pier M1 – left side (-x)	1262	-28100
Pier M1 – right side (-x)	-6776	-29500
Pier M2 – left side (-x)	2101	-28300
Pier M2 – right side (-x)	-5444	-29900

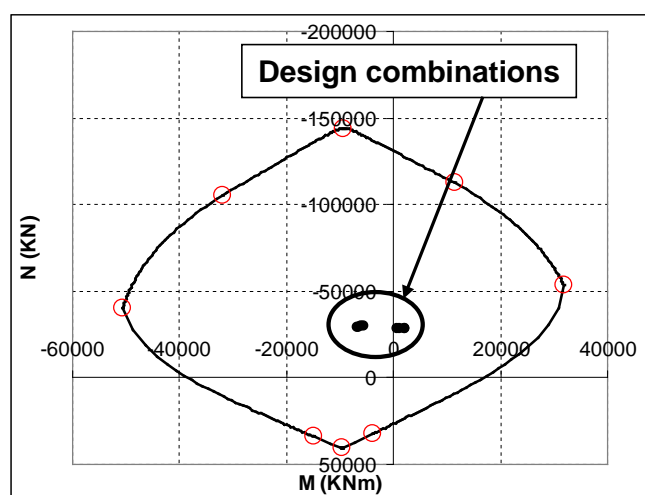


Fig. 8.13 Moment – Axial force interaction diagram for deck section

c Other deck verifications

- Shear verification of deck should be performed according to EN 1998-2:2005+A1:2009, **5.6.3.3**. This verification is not presented here, but is not critical, as a rule.
- The verification of pier – deck joints should be performed according to EN 1998-2:2005+A1:2009, **5.6.3.5**. This verification is not presented here. It is usually critical for the shear reinforcement of joints over slender pier columns monolithically connected to the deck.

8.2.5.7 Design action effects for the foundation design

Fig. 8.19 shows the capacity effects acting on the foundation of pier M1 for the longitudinal direction, for seismic actions in the negative direction $-x$ while Fig. 8.20 shows the capacity effects for the transverse direction. The sign of the effects is reversed for the opposite direction of the seismic action for the transverse direction.

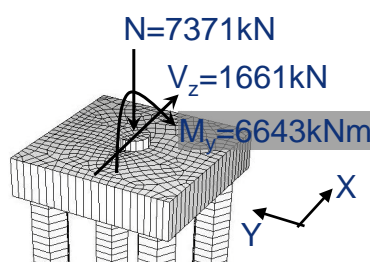


Fig. 8.14 Capacity effects on the foundation of pier M1 for the longitudinal direction (seismic actions in $-x$ direction)

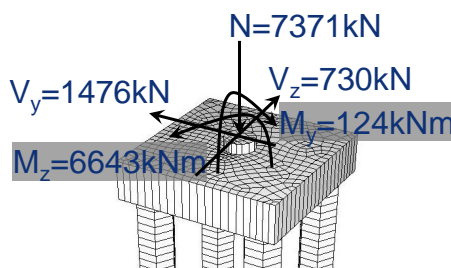


Fig. 8.15 Capacity effects on the foundation of pier M1 for the transverse direction

8.2.6 BEARINGS AND ROADWAY JOINTS

8.2.6.1 Bearings

The design displacement is $d_{Ed} = d_E + d_G + \psi_2 d_T$

The displacements in longitudinal direction are presented in Fig. 8.21. The maximum displacement at bearings is 93.9mm.

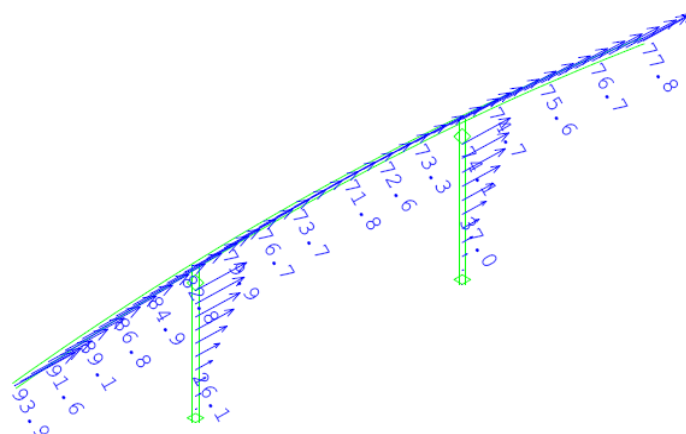


Fig. 8.16 Displacement in longitudinal direction. (mm)

The displacements in transverse direction are presented in Fig. 8.22. The maximum displacement at bearings is 110.0mm.

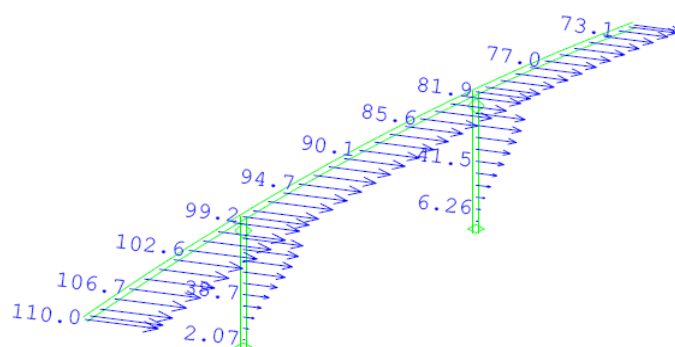


Fig. 8.17 Displacement in transverse direction (mm)

The bridge is simply supported on the abutments through a pair of bearings allowing free sliding and rotation in and about both horizontal axes. The plan view and side view of the bearings are presented in Fig. 8.23.

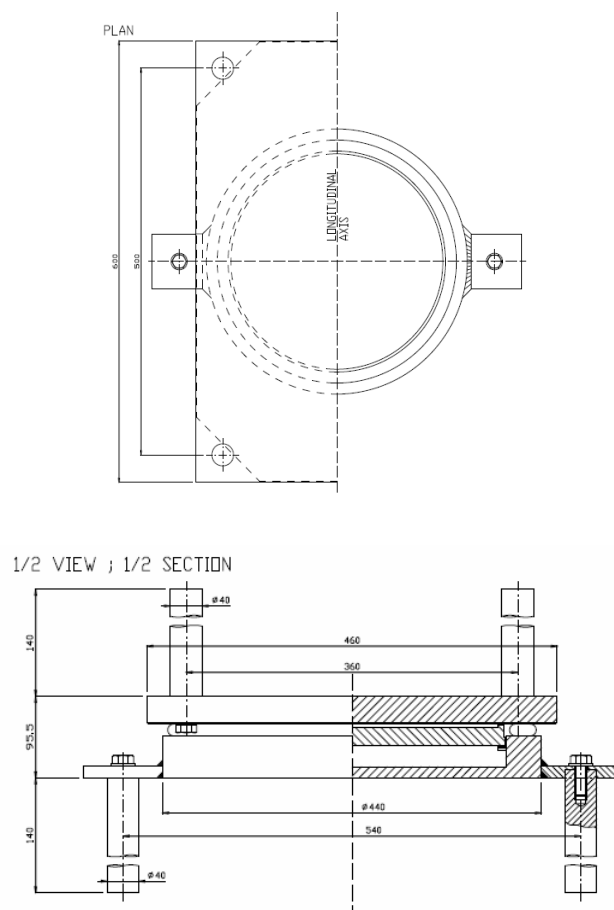


Fig. 8.18 Plan view and side view of sliding bearings

The check for uplifting of bearings is performed according to EN 1998-2:2005+A1:2009, **6.6.3.2(2)** for the design seismic combination. The bearings minimum vertical reaction forces are presented in Fig. 8.24 with total minimum value 17.8kN (compressive value so no uplifting happens).

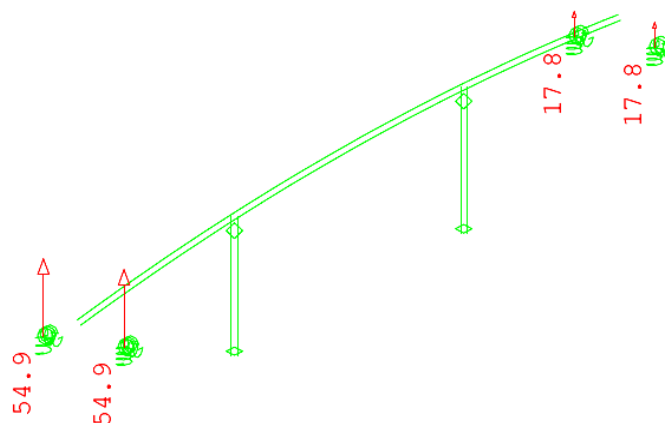


Fig. 8.19 Minimum reaction forces in bearings for seismic combination (kN)

The bearings maximum vertical reaction forces are presented in Fig. 8.25 with total maximum value 2447kN.

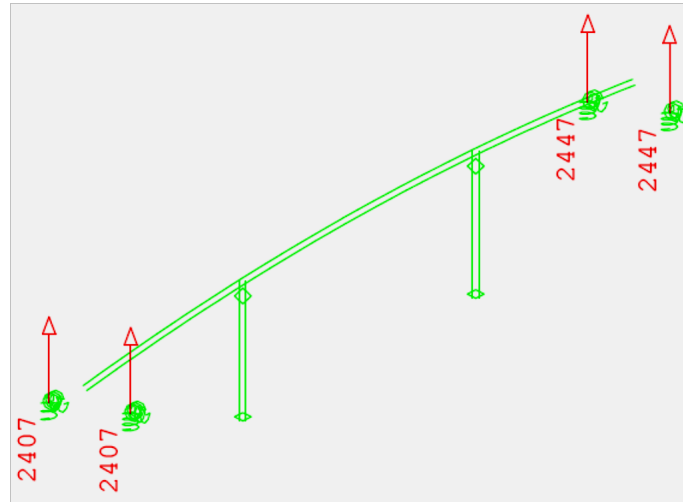


Fig. 8.20 Maximum reaction forces in bearings for seismic combination (kN)

8.2.6.2 Overlapping length

According to EN 1998-2:2005+A1:2009, **6.6.4** the minimum overlapping (seating) length at moveable joints is:

$$l_{ov} = l_m + d_{eg} + d_{es}$$

The support length is $l_m = 0.50\text{m} > 0.40\text{m}$

The design ground displacement is:

$$d_g = 0.025 a_g S T_C T_D = 0.025 \times 0.16 \times 9.81\text{m/s}^2 \times 1.15 \times 0.60\text{s} \times 2.50\text{s} = 0.068\text{m}$$

The distance parameter for ground type C as specified in EN 1998-2:2005+A1:2009, **3.3(6)** is $L_g = 400\text{m}$.

The effective length of the deck is $L_{eff} = 82.50/2 = 41.25\text{m}$

There is no proximity to a known seismically active fault, so the effective displacement is:

$$d_{eg} = (2 d_g / L_g) L_{eff} = (2 \times 0.068 / 400) \times 41.25 = 0.014\text{m} < 2d_g = 0.136\text{m}$$

The effective seismic displacement of the support is $d_{es} = 0.101\text{m}$

Substituting the above to Eq. (2.1) we get:

$$l_{ov} = 0.50 + 0.014 + 0.101 = 0.615\text{m}$$

The available seating length is $1.25\text{m} > l_{ov}$

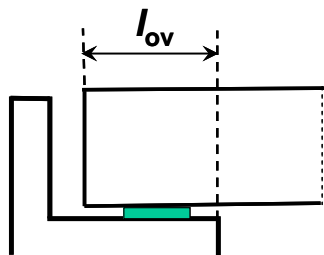


Fig. 8.21 Available seating length

8.2.6.3 Roadway joints

The roadway joint is designed for displacements:

$$d_{Ed,J} = 0.4d_E + d_G + \psi_2 d_T,$$

where d_E is the seismic displacement, d_G is the displacement due to permanent and quasi-permanent actions, d_T is the displacement due to thermal actions and $\psi_2 = 0.5$, is the combination factor.

The clearance of the structure is designed for larger displacements:

$$d_{Ed} = d_E + d_G + \psi_2 d_T$$

Due to the differences between the two clearances the detailing of back-wall should cater for predictable (controlled) damage (EN 1998-2:2005+A1:2009, **2.3.6.3 (5)**). Such a detailing is shown in Fig. 8.27, where impact along the roadway joint is foreseen to occur on the approach slab.

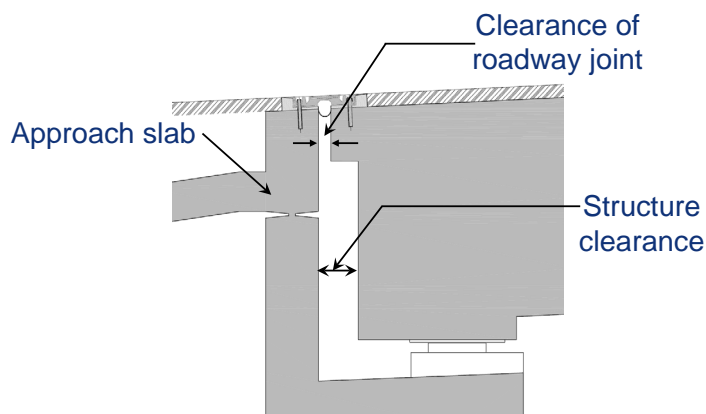


Fig. 8.22 Clearances and detailing of the roadway joint region

Table 8.7 shows the displacements for roadway joint and the displacements for the structure clearance.

Table 8.7 Displacement for roadway joint and clearance at joint region

Displacement (mm)		d_G	d_T	d_E	$d_{Ed,J}$	d_{Ed}
Longitudinal	opening	+18.7	-10.7	+76.0	+54.5	+100.7
	closure	0	-8.5	-76.0	-34.7	-80.3
Transverse		0	0	± 109.9	± 44.0	± 109.9

Fig. 8.28 shows the selected roadway joint type and the displacement capacities for each direction.

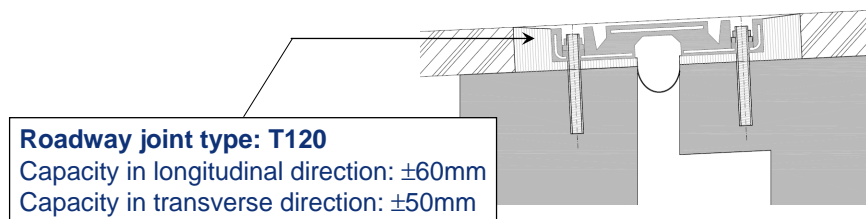


Fig. 8.23 Selected roadway joint type

8.2.7 CONCLUSIONS FOR DESIGN CONCEPT

Optimal cost effectiveness of a ductile bridge system is achieved when all ductile elements (piers) have dimensions that lead to a seismic demand that is critical for the main reinforcement of all critical sections and exceeds the minimum reinforcement requirements.

This is difficult to achieve when the piers resisting the earthquake:

- have substantial height differences, or
- have section larger than seismically required.

In such cases it may be more economical to use:

- limited ductile behaviour for low a_{gR} values, or
- flexible connection to the deck (seismic isolation)

It is noted that EN 1998-2 does not contain a minimum reinforcement requirement (see however 8.4.8.2 9 (b) of the last example).

For the bridge of this example $\rho_{min} = 1\%$ as was required, by the owner. The longitudinal reinforcement of the piers is derived from the seismic demands and is over the minimum requirement ($\rho_L = 1.78\%$ for pier M1 and $\rho_L = 1.49\%$ for pier M2).

8.3 Example of limited ductile piers

8.3.1 BRIDGE CONFIGURATION – DESIGN CONCEPT

Pier dimensions: height 40 m, external diameter 4.0 m, internal diameter 3.2 m, constant for the whole pier height. Pier head 4.0 m width x 1.5 m height. Pier concrete class C35/45.

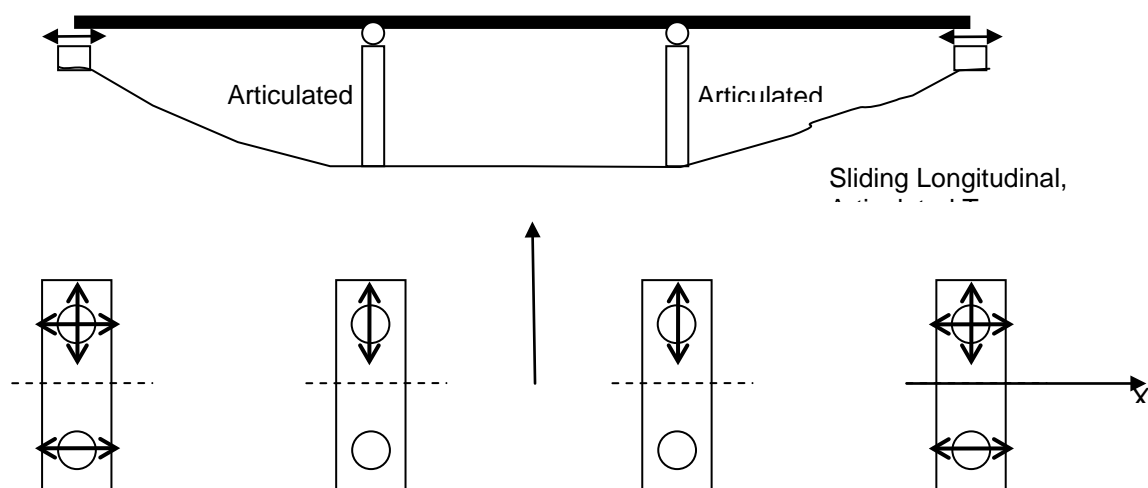


Fig. 8.29 Bridge elevation and arrangement of bearings

The large flexibility of the 40 m high reinforced concrete piers has the following structural consequences:

- The connection of the deck to both pier heads can be articulated (hinge) about the transverse axis, without causing excessive restraints due to imposed deck deformations
- The large flexibility of the seismic forces resisting system corresponds to large values of the fundamental period in both horizontal directions and therefore to quite low seismic response spectral accelerations. For such low seismic response levels it is neither expedient nor cost effective to design the piers for increased ductility. Therefore a limited ductile behavior is selected, corresponding to a value of the behavior factor $q = 1.50$, according to Table 4.1 of EN 1998-2

8.3.2 DESIGN SEISMIC ACTION

Soil type B, Importance factor $\gamma_I = 1.00$

Reference peak ground acceleration: $a_{Gr} = 0.30g$

Soil factor: $S = 1.20$, $a_{Gr}S = 0.36g$

Limited elastic behaviour is selected: $q = 1.50$ $\beta = 0.2$

Following design acceleration response spectrum, for the horizontal seismic components, results from the expressions (3.7) through (3.10) and (3.12) through (3.15) of EN 1998-1

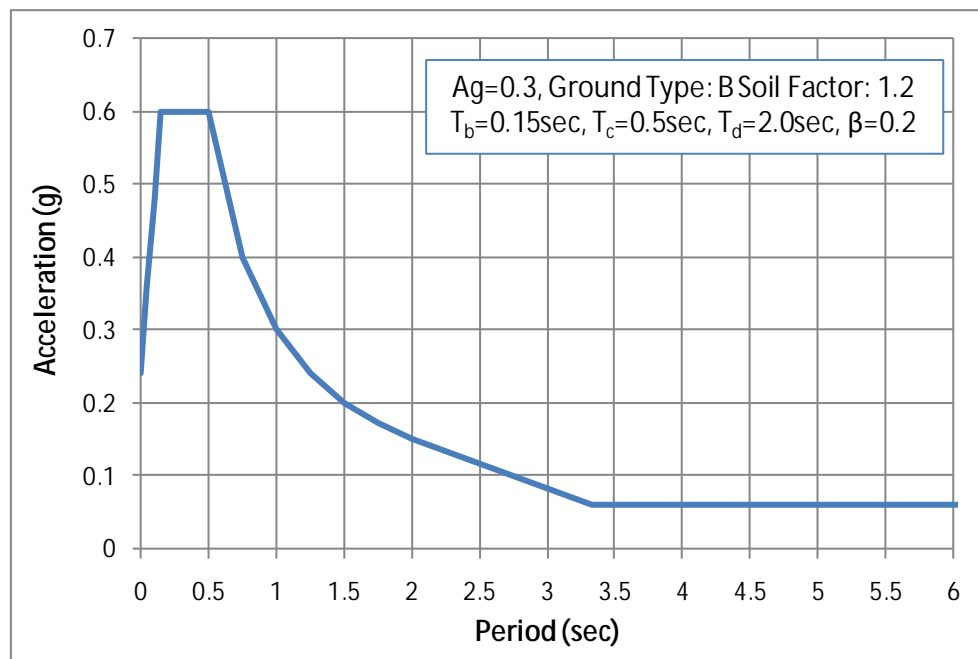


Fig. 8.30 EC8 Design Spectrum for horizontal components for $q = 1.50$

8.3.3 SEISMIC ANALYSIS

8.3.3.1 Quasi permanent traffic Loads:

According to 4.1.2(4)P of EN1998-2 the quasi permanent value $\psi_{2,1} Q_{k,1}$ of the UDL system of Model 1 (LM1) is applied in seismic combination. For bridge with severe traffic (i.e. bridges of motorways and other roads of national importance) the value of $\psi_{2,1}$ is 0.2.

The load of UDL system of Model 1 (LM1) is calculated in accordance with EN1998-2 Table 4.2 (where $\alpha_q = 1.0$ is the adjustment factors of UDL).

Lane Number 1: $\alpha_q q_{1,k} = 3 \text{ m} \times 9 \text{ kN/m}^2 = 27.0 \text{ kN/m}$

Lane Number 2: $\alpha_q q_{2,k} = 3 \text{ m} \times 2.5 \text{ kN/m}^2 = 7.5 \text{ kN/m}$

Lane Number 3: $\alpha_q q_{3,k} = 3 \text{ m} \times 2.5 \text{ kN/m}^2 = 7.5 \text{ kN/m}$

Residual area: $\alpha_q q_{r,k} = 2 \text{ m} \times 2.5 \text{ kN/m}^2 = 5.0 \text{ kN/m}$

Total load = 47.0 kN/m

The traffic load for seismic combination applied per unit of length of the bridge is:

$\psi_{2,1} Q_{k,1} = 0.2 \times 47.0 \text{ kN/m} = 9.4 \text{ kN/m}$

8.3.3.2 Structural Model

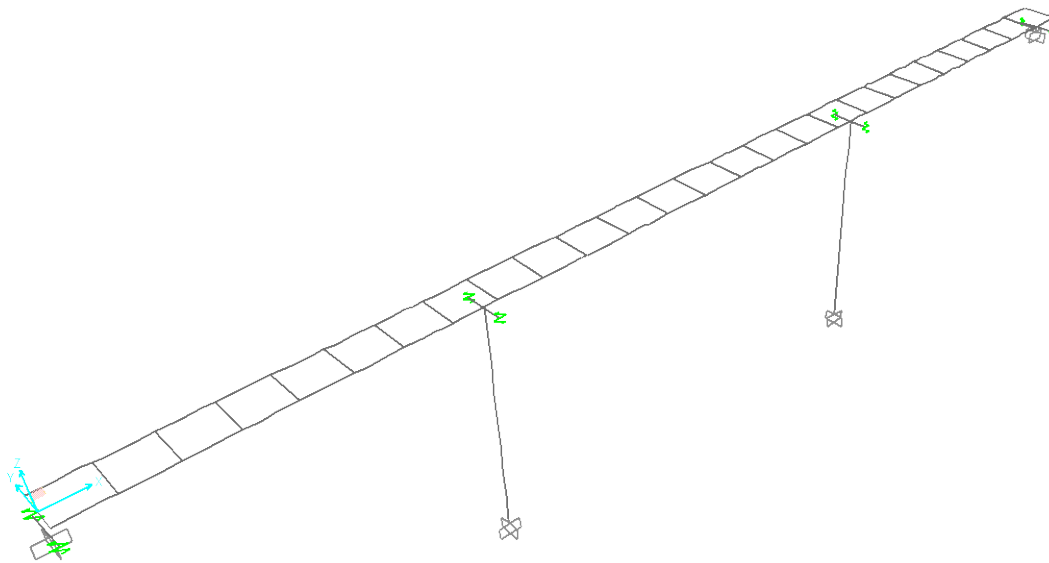


Fig. 8.11 Structural Model

8.3.3.3 Effective pier stiffness

The effective pier stiffness was initially assumed 50% of the uncracked section stiffness. According to modal analysis the first mode (longitudinal direction -x) is 3.88 sec and the second mode (transverse direction -y) is 3.27 sec.

According to EN1998-1 the lower bound of the design spectrum ($\beta = 0.20$) is $S_d/g = 0.20 \times 0.30 = 0.06$, corresponding to $T \geq 3.3$ sec. Consequently the design seismic actions are not significantly affected by the assumption for $(EI)_{eff}$, when $(EI)_{eff} \leq 0.50(EI)$.

For appropriate assessment of the displacements, the final analysis was carried out for $(EI)_{eff} = 0.30(EI)$. This value corresponds well to the required reinforcement ($\rho = 1.5\%$) and the range of the final axial forces and bending moments. This can be seen from the moment- $(EI)_{eff}/(EI)$ ratio diagrams of Fig. 8.35 compared to Fig. 8.33. These diagrams result from the corresponding M- Φ diagrams of Figs. 8.34 and 8.32 using the relation $(EI)_{eff}/(EI) = (M/\Phi)/(EI)$.

According to the final modal analysis the first mode (longitudinal direction -x) is 5.02 sec and the second mode (transverse direction -y) is 3.84 sec.

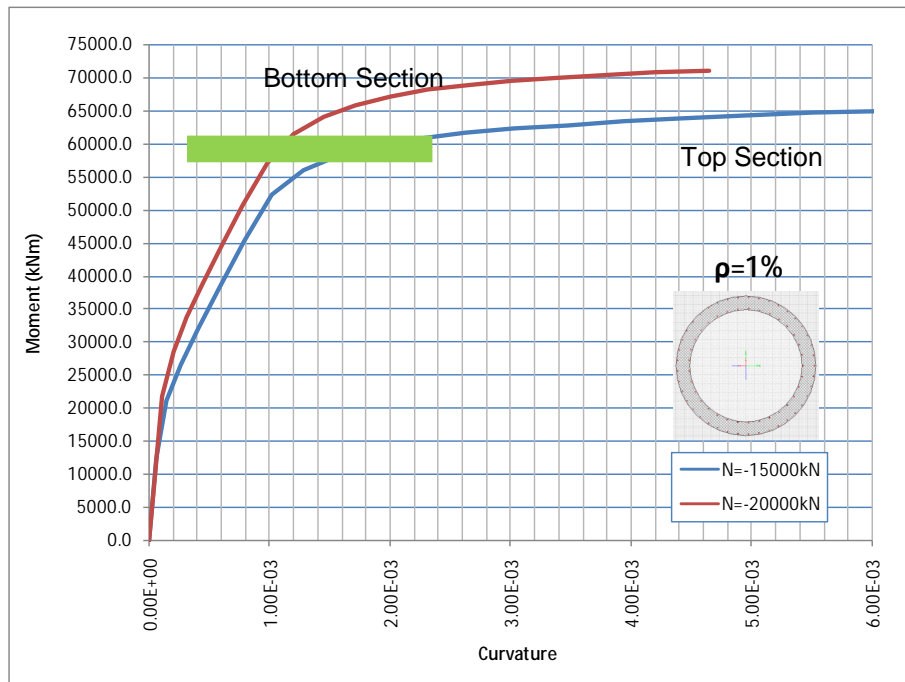


Fig. 8.32 Moment-Curvature curve of Pier Section for $\rho = 1\%$

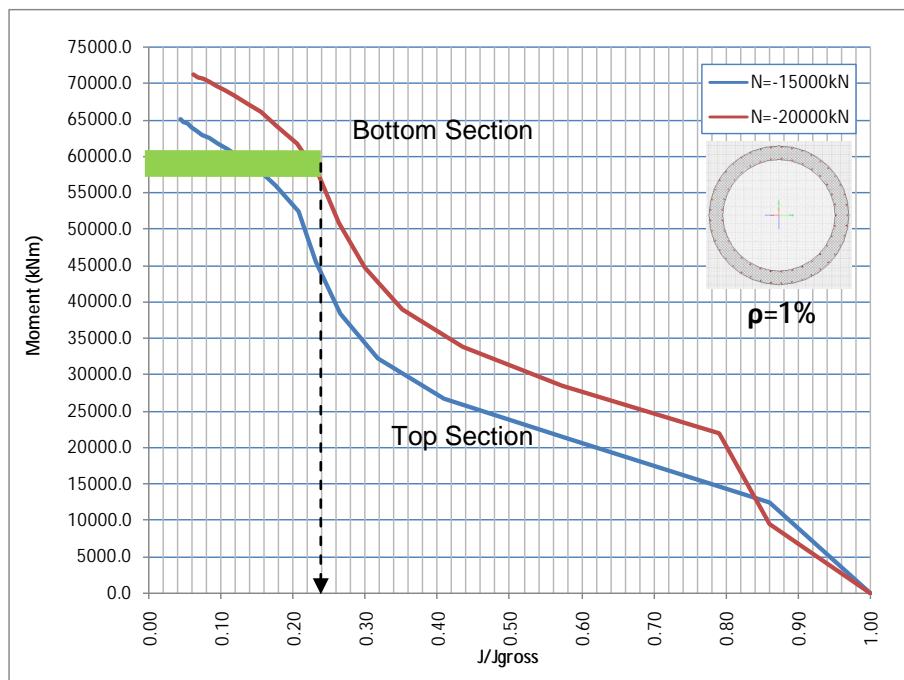


Fig. 8.33 Moment - $(EI)_{\text{eff}} / (EI)$ ratio Curve of Pier Section for $\rho = 1\%$

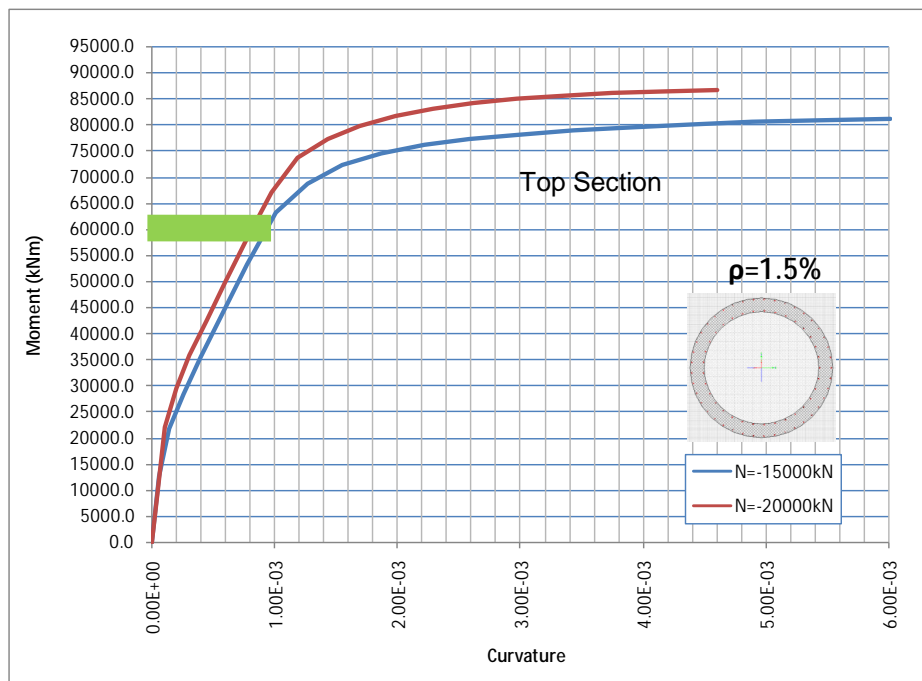


Fig. 8.34 Moment-Curvature curve of Pier Section for $\rho = 1.5\%$

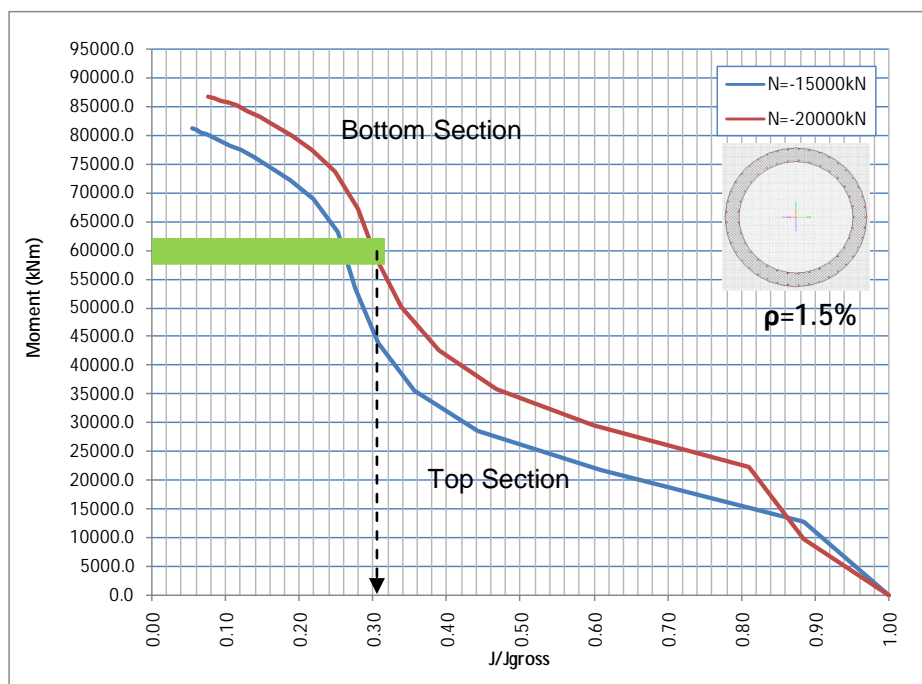


Fig. 8.35 Moment - $(EI)_{\text{eff}} / (EI)$ ratio Curve of Pier Section for $\rho = 1.5\%$

8.3.3.4 Eigenmodes

The characteristics (period and modal mass % in the three principal directions) of the first 30 eigenmodes of the structure are shown Table 8.8. The shapes of modes 1, 2, 3 and 11 are presented in Figures 8.36, 8.37, 8.38 and 8.39 respectively.

Table 8.8 First 30 eigenmodes of the structure

No	Period Sec	Modal Mass %		
		X	Y	Z
1	5.03	92.5%	0.0%	0.0%
2	3.84	0.0%	76.8%	0.0%
3	1.49	0.0%	0.0%	0.0%
4	0.79	0.0%	0.0%	1.2%
5	0.71	0.0%	0.5%	0.0%
6	0.66	0.0%	8.4%	0.0%
7	0.52	0.0%	0.0%	0.0%
8	0.50	0.0%	0.0%	0.0%
9	0.48	0.0%	2.1%	0.0%
10	0.46	0.0%	0.0%	0.0%
11	0.42	0.0%	0.0%	63.2%
12	0.42	0.0%	0.0%	0.0%
13	0.37	0.0%	0.0%	0.0%
14	0.35	0.0%	0.0%	0.0%
15	0.26	0.0%	0.0%	0.0%
16	0.26	0.0%	0.0%	0.0%
17	0.26	0.0%	6.2%	0.0%
18	0.26	4.4%	0.0%	0.0%
19	0.23	0.1%	0.0%	0.0%
20	0.20	0.0%	0.0%	0.0%
21	0.20	0.0%	0.0%	0.0%
22	0.18	0.0%	0.0%	0.0%
23	0.16	0.0%	0.0%	5.0%
24	0.16	0.0%	0.0%	0.0%
25	0.16	0.0%	0.0%	0.0%
26	0.15	0.0%	0.0%	0.0%
27	0.15	0.0%	3.0%	0.0%
28	0.13	0.0%	0.0%	8.8%
29	0.13	0.0%	0.2%	0.0%
30	0.12	0.0%	0.0%	0.0%
		97.1%	97.2%	78.3%

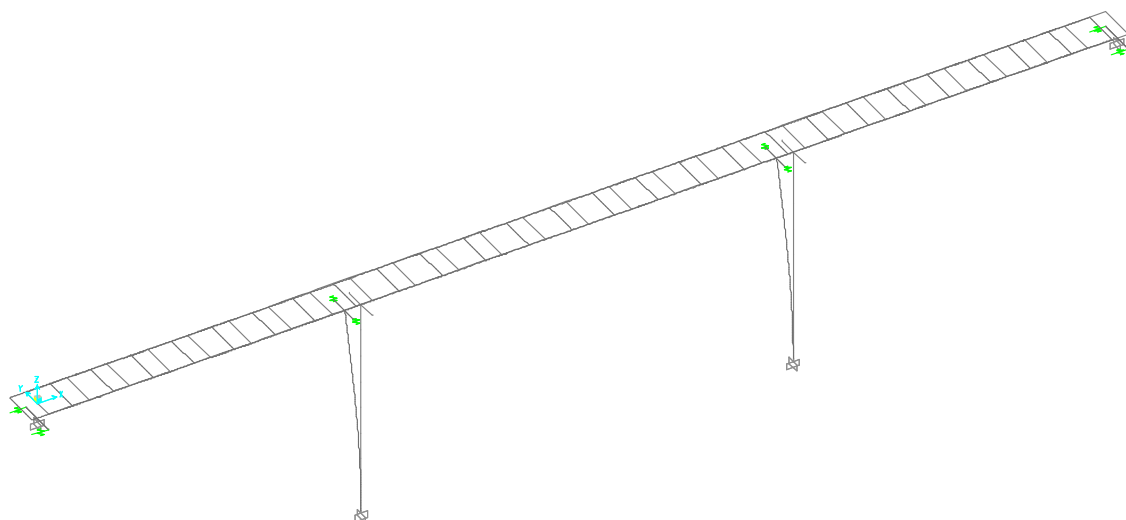


Fig. 8.36 1st Mode - Transverse – Period 5.02 sec c (Mass Participation Factor U_x :93%)

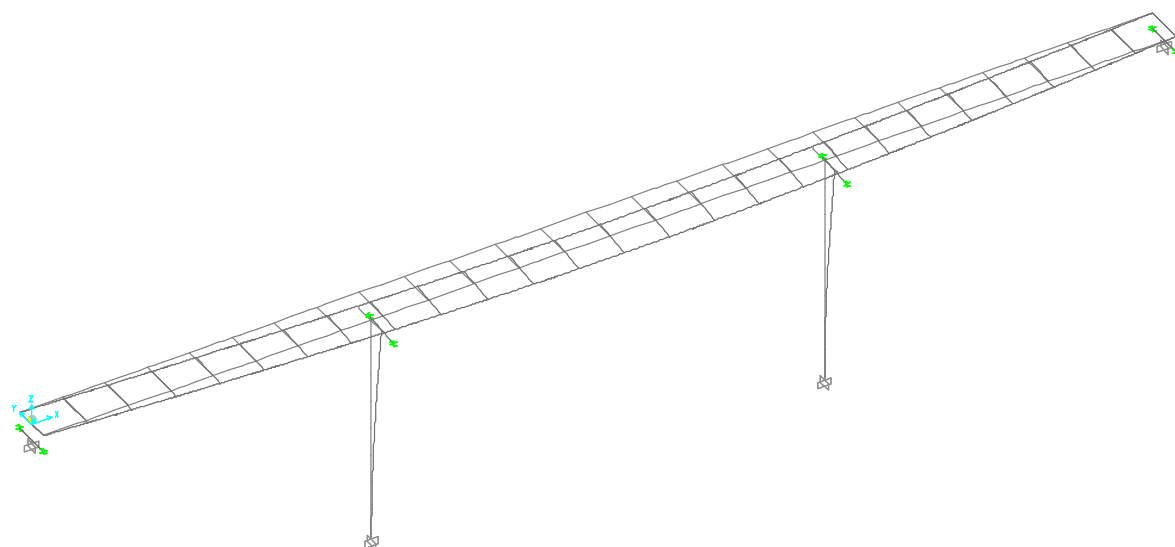


Fig.8.37 2nd Mode - Longitudinal – Period 3.84 sec (Mass Participation Factor U_y :77%)

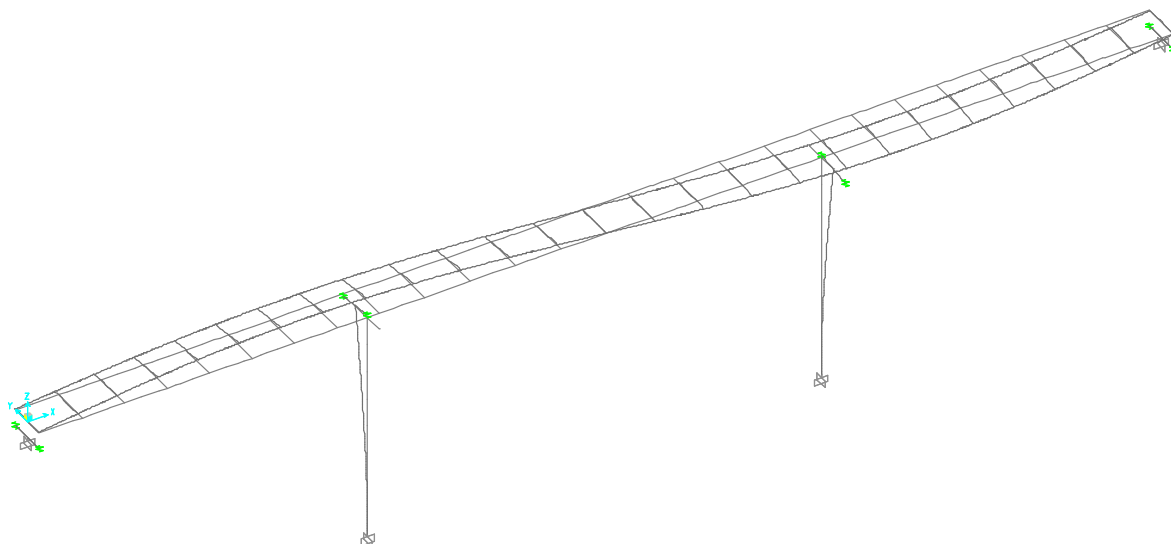


Fig. 8.38 3rd Mode - Rotation– Period 1.49 sec

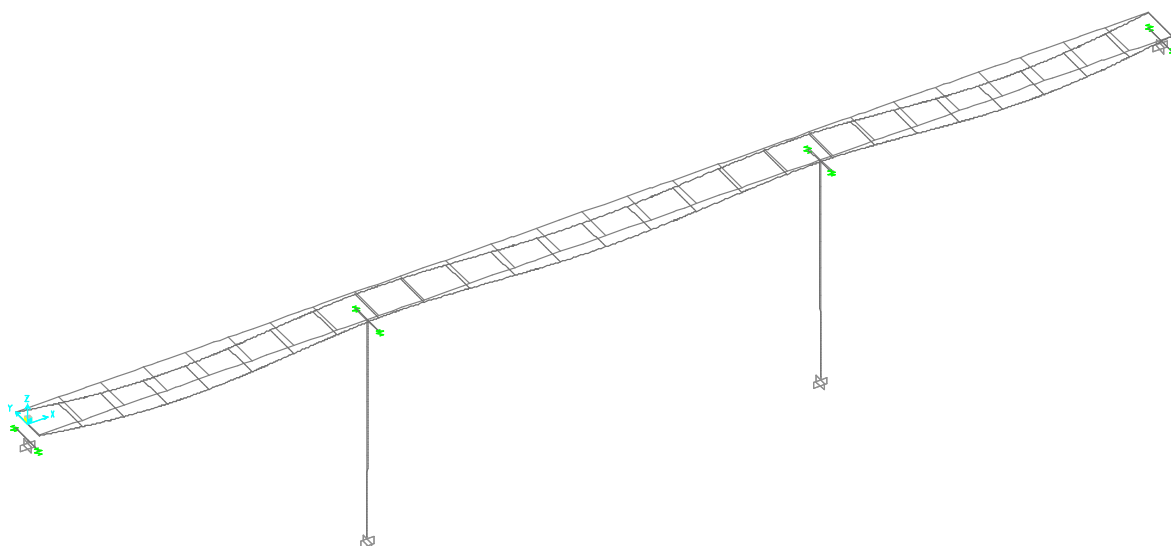


Fig. 3.39 11th Mode - Vertical – Period 0.42sec (Mass Participation Factor Uz:63%)

8.3.3.5 Response spectrum analysis

A response spectrum analysis considering the first 30 modes was carried out, using program SAP 2000. The sum of the modal masses considered amounts to 97.1% and 97.2% in the X and Y directions respectively. The combination of modal responses was carried out using the CQC rule.

Fig. 8.40 shows the max bending moment distribution along pier P1.

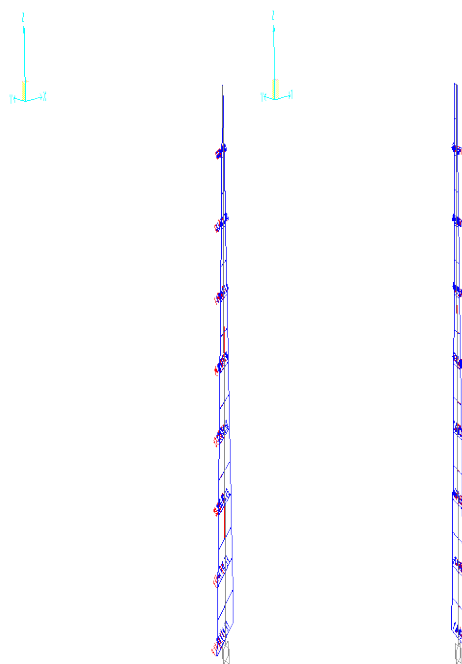


Fig. 8.40 Max bending moment distribution along pier P1

8.3.3.6 Second order effects for the seismic analysis

a Geometric Imperfections of piers

According to 5.2 of EN1992-2:2005:

$$\theta_i = \theta_0 a_h = \frac{1}{200} \frac{2}{\sqrt{l}}$$

Where: l is the length or height ($= 40\text{m}$), therefore $\theta_i = 1.58 \times 10^{-3}$.

The eccentricity according to 5.2(7) of EN1992-1-1:2004, e_i is given by — where l_0 is the effective length:

Longitudinal direction –x: ($l_0 = 80\text{ m}$) is $e_x = 0.063\text{ m}$ (or $V_x' = 2 \times \theta_i \times V_x$)

Transversal direction –y: ($l_0 = 40\text{ m}$) is $e_y = 0.032\text{ m}$ (or $V_y' = \theta_i \times V_y$).

The first and second order effect of these eccentricities under permanent load (G), including the creep effect (for $\varphi = 2.0$), is approximated, using the nominal stiffness method, by the following expression (see b.i. below):

$$e_{\text{imp},\varphi}^{\parallel} = e_{\text{imp}} \left(1 + \frac{1+\varphi}{v-1} \right)$$

Where $v = \frac{N_B}{N_{ED}}$, N_B is the buckling load and N_{ED} is the axial force (see b.i. below, according to 5.8 of EN1992-1-1:2004). The results are shown in Table 8.9.

Table 8.9 Influence of geometric imperfections of piers

Direction	e_i	$v = N_B/N_{ED}$	$e_{i,II}/e_i$	$e_{i,II}$
x	0.063	19.65	1.161	0.073
y	0.032	78.62	1.039	0.033

b Second Order Effects due to seismic first order action effects

These effects are estimated using two approaches:

i) According to 5.8 of EN1992-1-1:2004

The nominal stiffness method (5.8.7) is applied using $(EI)_{eff} = 0.30 (EI)$, compatible with the seismic design situation.

The moment magnification factor is evaluated at the bottom section as:

$$1 + [\beta / ((N_B / N_{Ed}) - 1)]$$

Where: $\beta = 1$, N_{Ed} is the design value of axial load (19538 kN) and N_B is the buckling load based on nominal stiffness $= \pi^2 \times (EI)_{eff} / (\beta_1 \times L_0)^2$, with $\beta_1 = 1$

This results the following moment magnification factor:

- 1.154 in the longitudinal direction –x
- 1.034 in the transversal direction –y

ii) According to 5.4 of EN1998-2:2005

The increase of bending moments at the plastic hinge section (self weight of the pier is also included) is

$$\Delta M = 0.5 (1 + q) d_{Ed} N_{Ed}$$

where, d_{Ed} is the seismic displacement of pier top and N_{Ed} the axial force resulting from the seismic analysis

The second approach results into approximately the same moments in the longitudinal direction but substantially higher in the transverse and is used in the further design combinations in Table 8.11 and Table 8.12.

Table 8.10 shows the displacements d_{Ed} of the pier top which are used in the above expression.

8.3.3.7 Action effects for the design of piers and abutments

Table 8.11 gives the action effects of the loadings and of the loading combinations relevant to the seismic design situations. The effects are given:

- for the piers P1 and P2 at the base of the biers, and
- for abutments C0 and C3 at the midpoint between the bearings at their level

The designation of the individual loadings is as follows:

G Permanent + seismic traffic load

E_x Earthquake in x direction

E_y Earthquake in y direction

2nd Ord.(EC2) Additional second order effects according to 5.8 of EN1992-1-1

2nd Ord.(EC8) Additional second order effects according to 5.4 of EN1998-2

Imperf First and second order effects (including creep) of geometric pier imperfections

The action effects of earthquake actions correspond to the response spectrum analysis under the design spectrum (i.e. the elastic spectrum divided by $q = 1.50$).

According to 5.5(2) of EN 1998-2, force effects due to imposed deformations need not be included in the seismic design combinations.

Table 8.10 Pier Top Displacements d_{Ed}

Pier Top Displacements for:	dx (m)	dy (m)
Ex+0.3Ey	0.373	0.065
Ey+0.3Ex	0.110	0.197

Table 8.11 Action effects for the design of piers and abutments: $q = 1.50$ (Eff. Stiffness = 30%)

Pier	Loading	Fx kN	Fy kN	Fz kN	Mx kN-m	My kN-m	Mz kN-m
P1	G	5.4	-0.2	19539.3	6.8	216.9	-0.2
P2	G	-5.4	-0.2	19539.3	6.8	-216.9	0.2
C0	G	0.0	0.2	3505.2	-0.4	0.0	0.0
C3	G	0.0	0.2	3505.2	-0.4	0.0	0.0
P1	Ex+0.3Ey	1254.4	187.4	28.8	7885.5	50803.5	342.8
P2	Ex+0.3Ey	1254.4	187.4	28.8	7885.5	50803.5	342.8
C0	Ex+0.3Ey	0.0	322.2	21.5	1134.3	0.0	0.0
C3	Ex+0.3Ey	0.0	322.2	21.5	1134.3	0.0	0.0
	Sum:	2508.8	1019.1				
P1	Ey+0.3Ex	376.3	624.6	8.6	26285.1	15241.0	1142.5
P2	Ey+0.3Ex	376.3	624.6	8.6	26285.1	15241.0	1142.5
C0	Ey+0.3Ex	0.0	1073.9	6.4	3781.1	0.0	0.0
C3	Ey+0.3Ex	0.0	1073.9	6.4	3781.1	0.0	0.0
	Sum:	752.6	3397.1				
P1	Ex+0.3Ey+2nd Ord. (EC2)	1254.4	187.4	28.8	8153.6	58576.4	342.8
P2	Ex+0.3Ey+2nd Ord.(EC2)	1254.4	187.4	28.8	8153.6	58576.4	342.8
P1	Ey+0.3Ex+2nd Ord.(EC2)	376.3	624.6	8.6	27178.8	17572.9	1142.5
P2	Ey+0.3Ex+2nd Ord.(EC2)	376.3	624.6	8.6	27178.8	17572.9	1142.5

Continuation of Table 8.11

Pier	Loading	F _x kN	F _y kN	F _z kN	M _x kN-m	M _y kN-m	M _z kN-m
P1	Ex+0.3Ey+2nd Ord.(EC8)	1254.4	187.4	28.8	9279.0	58298.5	342.8
P2	Ex+0.3Ey+2nd Ord.(EC8)	1254.4	187.4	28.8	9279.0	58298.5	342.8
P1	Ey+0.3Ex+2nd Ord.(EC8)	376.3	624.6	8.6	30508.3	17451.4	1142.5
P2	Ey+0.3Ex+2nd Ord.(EC8)	376.3	624.6	8.6	30508.3	17451.4	1142.5
	θ :	0.067	0.017				
P1	Ex+0.3Ey+2nd Ord. (EC8)+Imperf	1254.4	187.4	28.8	9826.3	59393.1	342.8
P2	Ex+0.3Ey+2nd Ord.(EC8)+imperf	1254.4	187.4	28.8	9826.3	59393.1	342.8
P1	Ey+0.3Ex+2nd Ord.(EC8)+Imperf	376.3	624.6	8.6	31055.6	18546.0	1142.5
P2	Ey+0.3Ex+2nd Ord.(EC8)+Imperf	376.3	624.6	8.6	31055.6	18546.0	1142.5
P1	G+Ex+0.3Ey+2nd Ord.(EC8)+Imperf	1259.8	187.2	19568.0	9833.1	59610.0	342.5
P2	G+Ex+0.3Ey+2nd Ord.(EC8)+imperf	1249.1	187.2	19568.0	9833.1	59176.2	343.0
C0	G+Ex+0.3Ey	0.0	322.3	3526.6	1134.0	0.0	0.0
C3	G+Ex+0.3Ey	0.0	322.3	3526.6	1134.0	0.0	0.0
P1	G+Ey+0.3Ex+2nd Ord.(EC8)+Imperf	381.7	624.4	19547.9	31062.4	18762.9	1142.3
P2	G+Ey+0.3Ex+2nd Ord.(EC8)+Imperf	371.0	624.4	19547.9	31062.4	18329.1	1142.7
C0	G+Ey+0.3Ex	0.0	1074.1	3511.6	3780.8	0.0	0.0
C3	G+Ey+0.3Ex	0.0	1074.1	3511.6	3780.8	0.0	0.0

8.3.3.8 Action effects for the design of foundation

Table 8.12 gives the action effects corresponding to the loading combinations of the seismic design situation, which are required, according to 5.8.2 (2) of EN 1998-2 for the design of the foundations. The seismic effects correspond to $q = 1.00$.

The action effects are given:

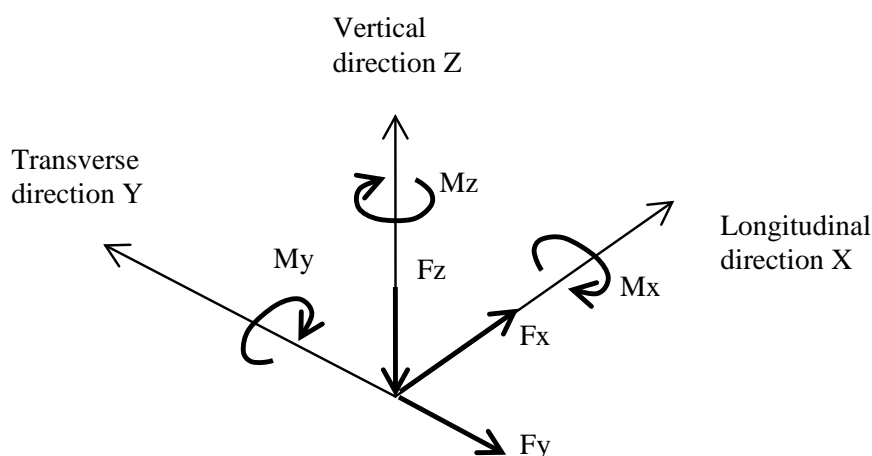
- for piers P1 and P2 at the top of the footing
- for abutments at the midpoint between the bearings at their level

with the designation shown in the sketches.

The signs of shear forces and bending moments given are mutually compatible. However, as these effects (with the exception of the vertical axial force F_z) are due predominantly to earthquake action, their signs and senses may be reversed.

Table 8.12 Action effects for the design of the foundation: $q = 1.00$ (Eff. Stiffness = 30%)

Pier	Loading	F _x kN	F _y kN	F _z kN	M _x kN-m	M _y kN-m	M _z kN-m
P1,P2	G+Ex+0.3Ey+2nd Ord.(EC8)+Imperf	1887.0	280.9	19582.4	13775.8	85011.7	513.9
	G+Ey+0.3Ex+2nd Ord.(EC8)+Imperf	569.8	936.7	19552.2	44204.9	26383.4	1713.5
C0,C3	G+Ex+0.3Ey	0.0	483.4	3537.4	1701.1	0.0	0.0
	G+Ey+0.3Ex	0.0	1611.1	3514.8	5671.3	0.0	0.0

**Fig. 8.41 Direction of forces F_x , F_y , F_z and moments M_x , M_y , M_z with positive sign for foundation design**

8.3.4 VERIFICATIONS OF PIERS

8.3.4.1 Flexure and axial force

Reinforcement requirement at the base section:

Design Action effects: $N_{Ed} = 19568$ kN, $M_y = 59610$ kNm, $M_x = 9833$ kNm $\rightarrow A_{s,req} = 678$ cm².
 Longitudinal Reinforcement: External perimeter: 62Φ28 (= 381 cm²), Internal perimeter: 49Φ28 (= 301 cm²). Fig. 8.42 shows the design interaction diagram of base section.

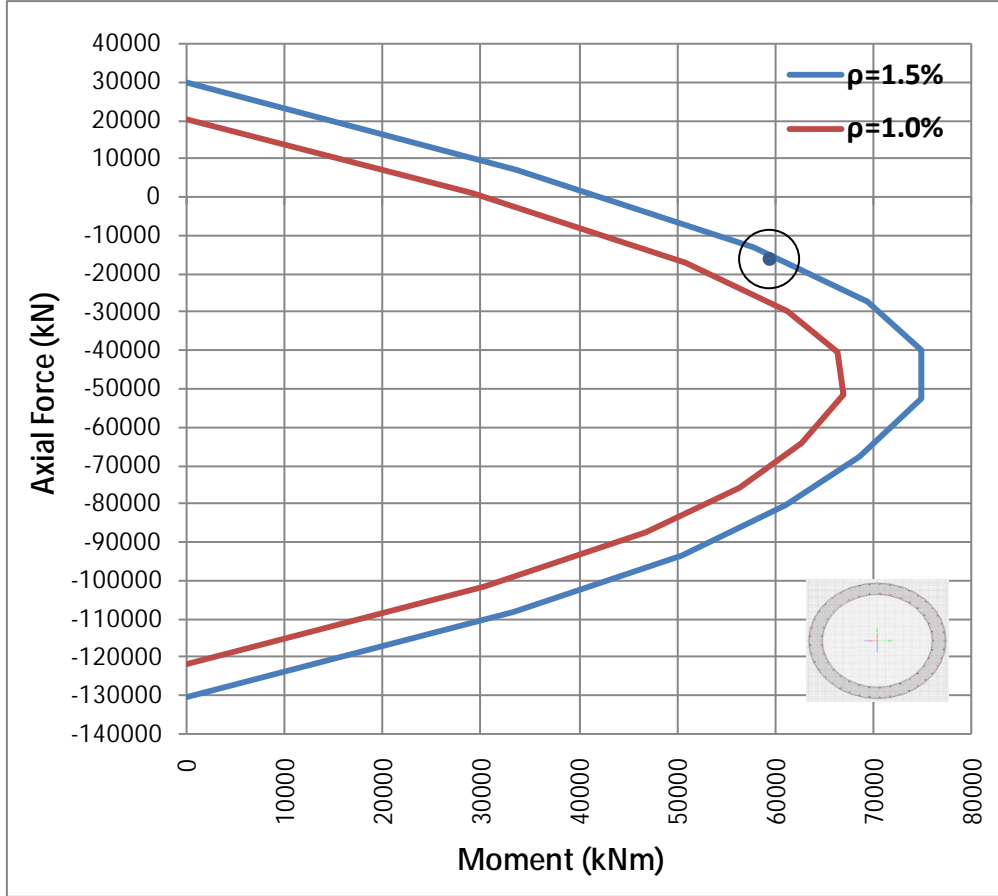


Fig. 8.42 Design Interaction Diagram of Pier Base Section

8.3.4.2 Shear

According to 5.6.2 of EN1998-2:2005, the design action effect shall be multiplied by $q (= 1.5)$ and the resistance values $V_{Rd,c}$, $V_{Rd,s}$, $V_{Rd,max}$ derived by 6.2 of EN1992-1-1:2004 shall be divided by $\gamma_{Bd1} (= 1.25)$. Therefore:

$$V_{Rd,c} = [C_{Rd,c} k (100 \rho_l f_{ck})^{1/3} + k_1 \sigma_{cp}] b_w d$$

where:

$$C_{Rd,c} = \frac{0.18}{\gamma_c} = \frac{0.18}{1.5} = 0.12$$

$$d_e = r + \frac{2 \times r_s}{\pi} = 2.0 + \frac{2 \times 1.8}{\pi} = 3.15 \quad (\text{EN1998-2:2005, 5.6.3.3.(2)})$$

$$k = 1 + \sqrt{\frac{200}{d}} = 1 + \sqrt{\frac{200}{3150}} = 1.25$$

$$k_1 = 0.15$$

$$\sigma_{cp} = \frac{N_{Ed}}{A_c} = \frac{15}{4.52} = 3.32$$

$$V_{Rd,c} = [0.12 \times 1.25 \times (100 \times 0.015 \times 35)^{1/3} + 0.15 \times 3.32] \times 0.80 \times 3.15 \times 1000 = 2670 \text{ kN}$$

$$\frac{V_{Rd,c}}{\gamma_{Bd1}} = \frac{2670}{1.25} = 2136 \text{ kN} > \sqrt{1887^2 + 281^2} = 1908 \text{ kN} \text{ (no shear reinforcement required)}$$

8.3.4.3 Ductility requirements

a Confining Reinforcement

According to 6.2.1.4 of EN1998-2:2005 the minimum amount of confining reinforcement shall be for limited ductile:

$$\omega_{wd,c} \geq \max(1.4\omega_{w,req}; 0.12) = \max(1.4 \times 0.058; 0.12) = 0.12$$

where:

$$\begin{aligned} \omega_{w,req} &= \frac{A_c}{A_{cc}} \times 0.28 \times \eta_k + 0.13 \times \frac{f_{yd}}{f_{cd}} \times (\rho_l - 0.01) = \\ &= \frac{4.52}{3.39} \times 0.28 \times \frac{19580}{35000 \times 4.52} + 0.13 \times \frac{500000 \times 1.5}{35000 \times 1.15} \times (0.015 - 0.01) = 0.058 \\ \rho_w &= \omega_w \frac{f_{cd}}{f_{yd}} = 0.12 \times \frac{35000 \times 1.15}{500000 \times 1.5} = 0.0064 \text{ and } \rho_w = \frac{\pi D_{sp} A_{sp}}{A_{cc} s_l} \rightarrow \Phi 16 / 11 \end{aligned}$$

b Avoiding of buckling of compressed reinforcement

In order to avoid buckling of longitudinal compression reinforcement the longitudinal bars along the external pier face should be restrained, according to 6.2.2(2) of EN 1998-2, by transverse reinforcement consisting of circular hoops at a spacing $s_L < 5d_{bL} = 14 \text{ cm}$ (satisfied).

It is however noted that along the inside face of the hollow pier the provision of circular transverse bars is not in general sufficient to prevent buckling of compressed longitudinal reinforcement; as such bars do not offer tensile hoop action. In case that compressive yield of this reinforcement is reached under the seismic action (which is not the case in this example), the provision of the minimum amount of transverse ties, as specified by 6.2.2(3) and (4) for straight boundaries, is necessary..

8.3.5 BEARINGS AND JOINTS

Table 8.13 and Table 8.14 show the deformation and force seismic demands of the bearings respectively.

Example for the design for overlapping length at the movable supports and for roadway joints is given in sections 8.2.6.2 and 8.2.6.3 respectively.

Table 8.13. Element Deformations – Bearings

Bearing	Combination		U1 m	U2 m	U3 m	R1 Radians	R2 Radians	R3 Radians
M1a	X	Max	-0.007	0.001	0.003	0.001	0.000	0.015
M1a	X	Min	-0.007	-0.001	-0.003	-0.001	-0.001	-0.014
M1a	Y	Max	-0.006	0.000	0.009	0.003	0.000	0.005
M1a	Y	Min	-0.008	0.000	-0.010	-0.003	-0.001	-0.004
M1b	X	Max	-0.007	0.001	0.000	0.001	0.001	0.015
M1b	X	Min	-0.007	-0.001	0.000	-0.001	0.000	-0.014
M1b	Y	Max	-0.006	0.000	0.001	0.003	0.003	0.005
M1b	Y	Min	-0.008	0.000	-0.001	-0.003	-0.002	-0.004
A1a	X	Max	-0.002	0.396	0.000	0.001	0.001	0.003
A1a	X	Min	-0.002	-0.380	0.000	-0.001	-0.001	0.002
A1a	Y	Max	-0.001	0.126	0.001	0.005	0.002	0.003
A1a	Y	Min	-0.002	-0.111	-0.001	-0.005	-0.002	0.002
A1b	X	Max	-0.002	0.396	0.000	0.001	0.001	0.003
A1b	X	Min	-0.002	-0.380	0.000	-0.001	-0.001	0.002
A1b	Y	Max	-0.001	0.126	0.001	0.005	0.002	0.003
A1b	Y	Min	-0.002	-0.111	-0.001	-0.005	-0.002	0.002

Table 8.14 Element Forces – Bearings

Bearing	Combination		P KN	V2 KN	V3 KN
M1a	X	Max	-6658.87	674.191	0
M1a	X	Min	-7271.258	-668.901	0
M1a	Y	Max	-6273.436	374.961	0
M1a	Y	Min	-7656.692	-369.671	0
M1b	X	Max	-6658.976	674.256	159.055
M1b	X	Min	-7271.362	-668.836	-158.737
M1b	Y	Max	-6273.543	375.025	529.812
M1b	Y	Min	-7656.795	-369.606	-529.494
A1a	X	Max	-1531.503	0	173.98
A1a	X	Min	-1973.792	0	-187.313
A1a	Y	Max	-1095.842	0	595.489
A1a	Y	Min	-2409.453	0	-608.821
A1b	X	Max	-1531.398	0	187.129
A1b	X	Min	-1973.687	0	-174.115
A1b	Y	Max	-1095.739	0	608.582
A1b	Y	Min	-2409.347	0	-595.567

8.4 Example of seismic isolation

This section covers the design of the bridge of the general example with a special seismic isolation system capable of resisting high seismic loads. The design of bridges with seismic isolation is covered in Section 7 of EN 1998-2:2005+A1:2009.

Seismic isolation aims to reduce the response due to horizontal seismic action. The isolating units are arranged over the isolation interface, usually located under the deck and over the top of the piers/abutments. The reduction of the response may be achieved by:

- a) Lengthening of the fundamental period of the structure (effect of period shift in the response spectrum), which reduces the forces but increases displacements,
- b) Increasing the damping, which reduces displacements and may reduce forces,
- c) Preferably by a combination of the two effects.

The selected seismic isolation system consists of triple friction pendulum bearings. The friction pendulum system achieves both period lengthening and increased damping by sliding motion of special low friction material on a concave steel surface. Period lengthening is achieved by the low friction of the sliding interface and the large radius of curvature of the concave surface. Increased damping is achieved by energy dissipation due to friction.

The analysis of the seismic isolation system is carried out with both fundamental mode method and non-linear time-history method. The results of the two analysis methods are compared.

8.4.1 BRIDGE CONFIGURATION – DESIGN CONCEPT

8.4.1 1 Bridge Configuration

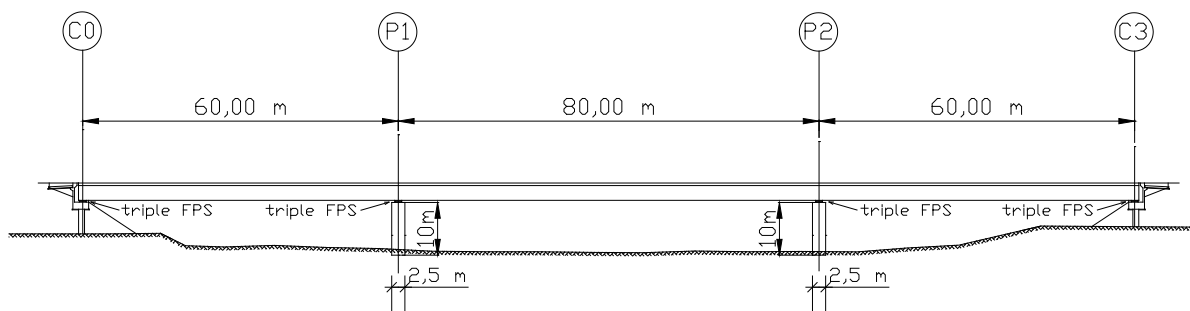
The bridge consists of a composite steel and concrete continuous deck, with spans of 60 + 80 + 60 m and two solid rectangular 10.0 m high piers. The lower part of the pier with 8.0m height has rectangular cross-section 5.0m x 2.5m. The seismic isolation bearings are supported on a widened pier head with rectangular plan 9.0 m x 2.5 m and 2.0 m height. The pier concrete class is C35/45. In Fig. 8.43 the elevation and the typical deck cross-section of the example bridge is presented. In Fig. 8.44 the layout of the piers is presented.

The large stiffness of the squat piers, in combination with the high seismicity (design ground acceleration $a_{gR} = 0.40g$) leads to the selection of a seismic isolation solution. This selection offers following advantages:

- Large reduction of constraints due to imposed deck deformation
- Practically equal and therefore minimized action effects on the two piers. This would be achieved even if the piers had unequal heights.
- Drastic reduction of the seismic forces

The additional damping offered by the isolators keeps the displacements to a cost effective level.

Bridge elevation:



Typical deck cross-section:

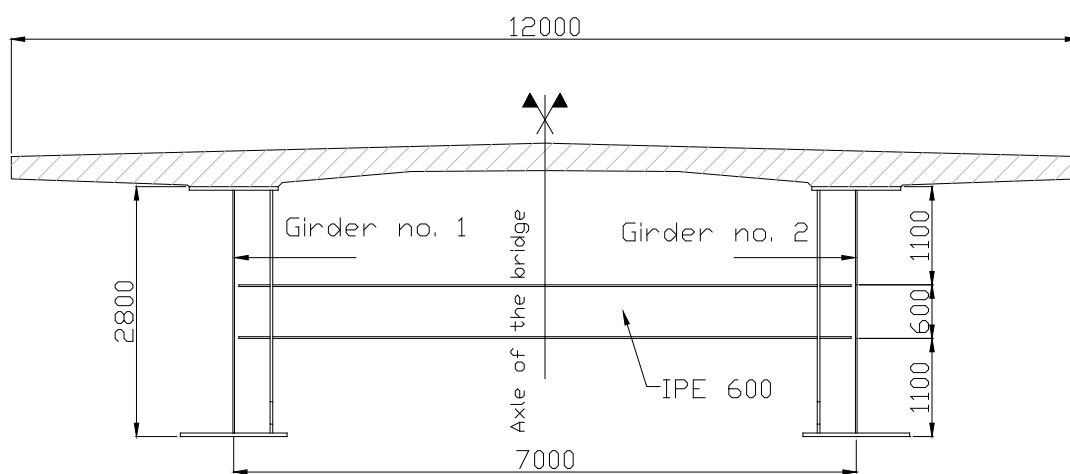


Fig. 8.43 Bridge configuration

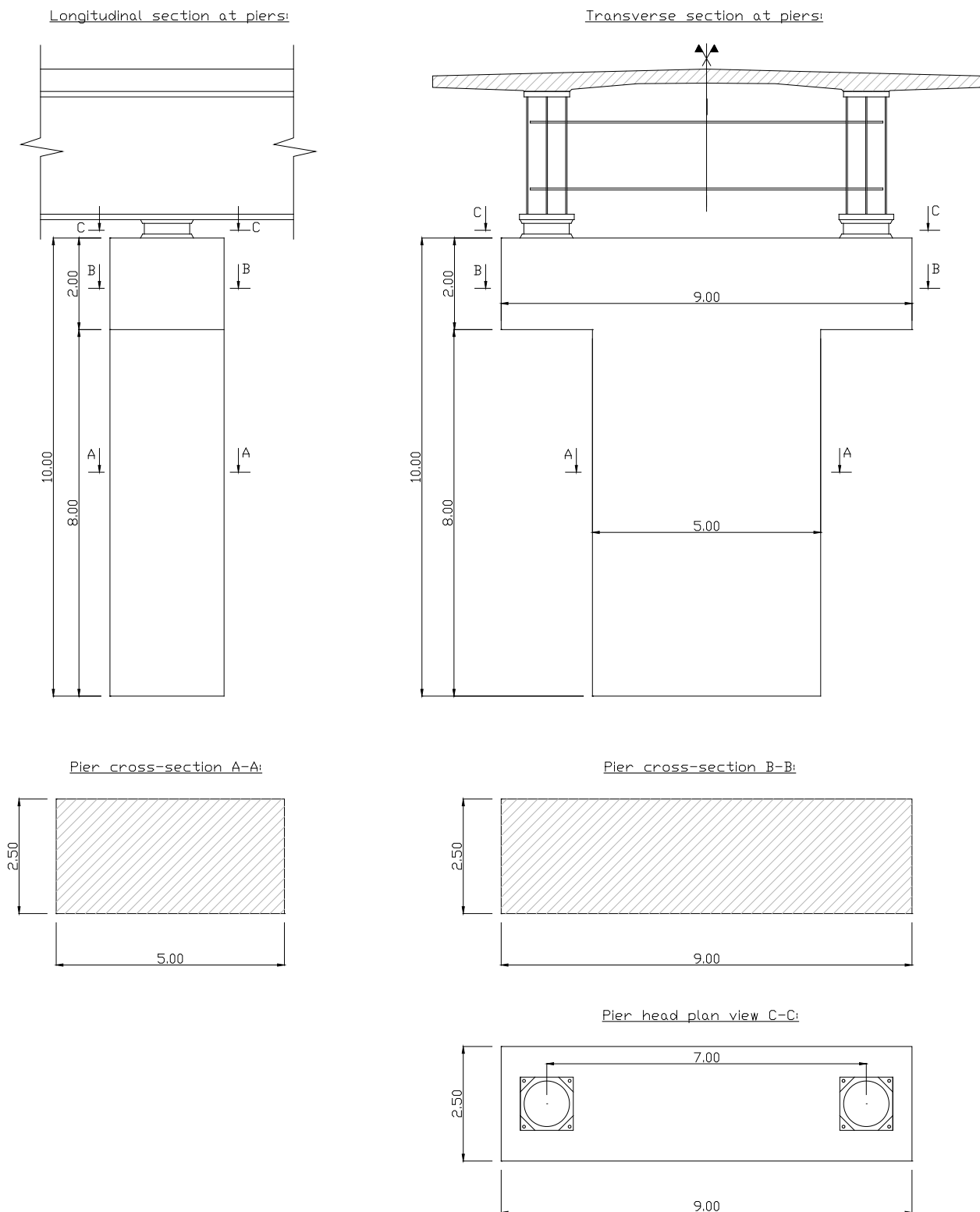


Fig. 8.44 Layout of piers

8.4.1.2 Seismic isolation system

The seismic isolation system consists of eight bearings of type Triple Friction Pendulum System (Triple FPS). Two Triple FPS bearings support the deck at the location of each of the abutments C0, C3 and piers P1, P2. The Triple FPS bearings allow displacements in both longitudinal and transverse

direction with non-linear frictional force displacement relation. The approximate bearing dimensions are: at piers 1.20 m x 1.20 m plan, 0.40 m height, and at abutments 0.90 m x 0.90 m plan, 0.40 m height. The layout of the seismic isolation bearings is presented in Fig. 8.45, where X is the longitudinal direction of the bridge and Y is the transverse direction. The label of each bearing is also shown.

Plan:

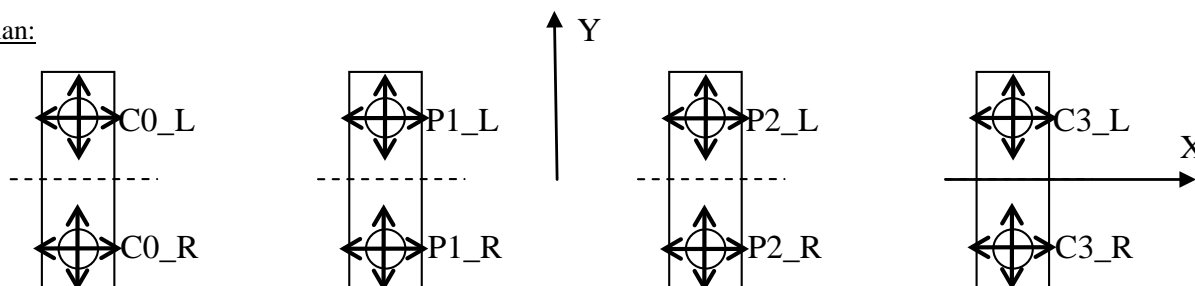
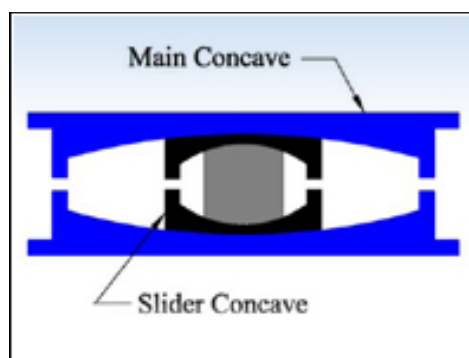


Fig. 8.45 Layout of seismic isolation bearings

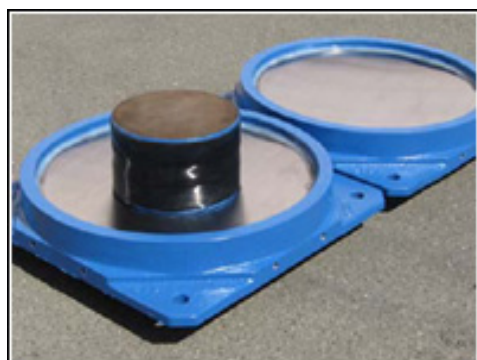
The layout of a typical Triple FPS bearing is shown in Fig. 8.46.



Photo of Triple Pendulum™ Bearing



Schematic Cross Section



Concaves and Slider Assembly



Concaves and Slider Components

Fig. 8.46 Layout of Triple Pendulum™ bearing (data from Earthquake Protection Systems web site)

Friction Pendulum bearings are sliding devices with a spherical sliding surface. They consist of an articulated slider coated with a controlled low friction special PTFE material. Sliding occurs on a concave stainless steel surface with radius of curvature in the order of 2 m. The coefficient of friction at the sliding interface is very low, in the order of 0.05 ~ 0.10 and can be reduced even more with

application of lubrication. The combination of low friction and restoring force due to the concave surface provides the bearing with bilinear hysteretic behaviour.

The behaviour of sliding devices with a spherical sliding surface is presented in EN 1998-2:2005+A1:2009, **7.5.2.3.5(2)**. In Fig. 8.47 the force-displacement relation is shown. The behaviour consists of the combined effect of:

- A linear elastic component which provides restoring force corresponding to stiffness $K_p = N_{sd} / R_b$ due to the spherical sliding surface with radius R_b , where N_{sd} is the normal force thought the device,
- A hysteretic frictional component which provides force at zero displacement $F_0 = \mu_d N_{sd}$ and dissipated energy per cycle $E_D = 4\mu_d N_{sd} d_{bd}$ at cyclic displacement d_{bd} , where μ_d is the dynamic coefficient of friction of the sliding interface.

The maximum force F_{max} and the effective stiffness K_{eff} at displacement d_{bd} are:

$$F_{max} = \frac{N_{sd}}{R_b} d_{bd} + \mu_d N_{sd} \text{sign}(d_{bd}), \quad K_{eff} = \frac{N_{sd}}{R_b} + \frac{\mu_d N_{sd}}{d_{bd}}$$

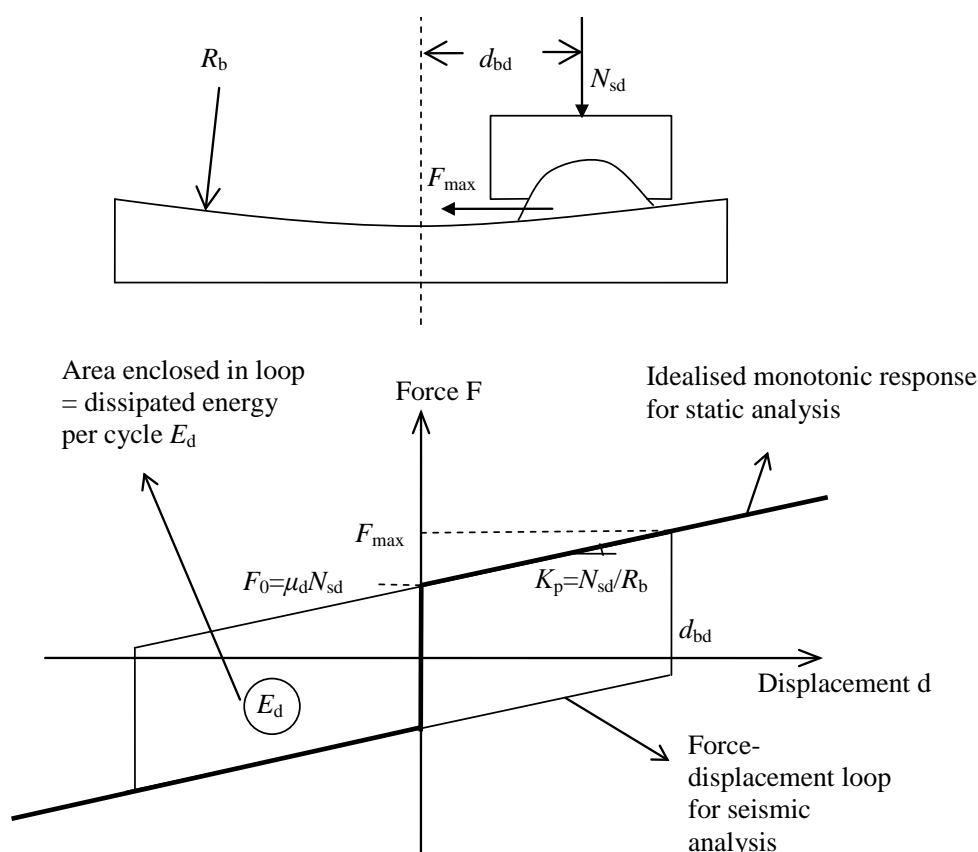


Fig. 8.47 Friction force-displacement behaviour of a sliding device with a spherical sliding surface

Certain special features of sliding devices with a spherical sliding surface are worth mentioning:

- The horizontal reaction is proportional to the vertical force of the isolator. This means that the resultant horizontal reaction passes approximately through the centre of mass. No eccentricities appear.

- As both the horizontal reactions and the inertia forces are proportional to the mass the period and the seismic motion characteristics are independent of the mass.

The Triple FPS bearing has a more complex sliding behaviour which offers an “adaptive” seismic performance and smaller bearing dimensions. The inner isolator consists of an inner slider that slides along two inner concave spherical surfaces. The two slider concaves, sliding along the two main concave surfaces, comprise two more independent spherical sliding isolators. Depending on the friction coefficient of the sliding interfaces and the radii of the spherical surfaces sliding occurs at different interfaces as the magnitude of displacement increases. Properties of the second sliding response are typically chosen to minimize the structure shear forces that occur during the design basis earthquake. Properties of the third sliding response are typically chosen to minimize bearing displacements that might occur at extreme events. This is characterized as the “adaptive” behaviour. The force-displacement relationship is presented in Fig. 8.48.

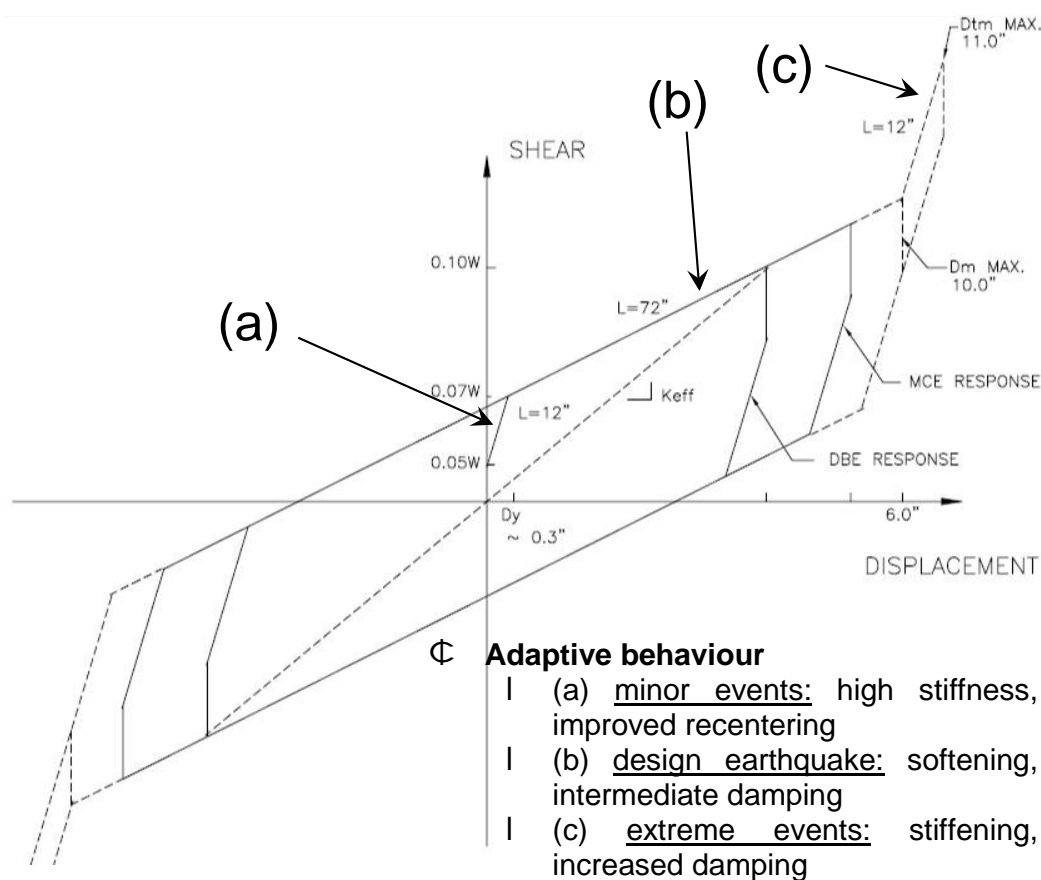


Fig. 8.48 Adaptive friction force-displacement behaviour of a Triple FPS bearing

The nominal properties of the selected Triple FPS bearings for seismic analysis are:

- Effective dynamic friction coefficient: $\mu_d = 0.061$ (+/- 16% variability of nominal value)
- Effective radius of sliding surface: $R_b = 1.83\text{m}$
- Effective yield displacement: $D_y = 0.005\text{m}$

8.4.2 DESIGN FOR HORIZONTAL NON-SEISMIC ACTIONS

8.4.2.1 Imposed horizontal loads – Braking force

Table 4.2 gives the distribution of the permanent reactions on the supports according to the gravity load analysis of the bridge. As time variation of loads is very small, it is ignored.

The minimum longitudinal load that can cause sliding of the whole deck on the bearings is calculated from the minimum deck weight and the minimum bearing friction: $F_{y,min} = 25500 \times 0.051 \approx 1300$ kN. This load is not exceeded by braking load of $F_{br} = 900$ kN, therefore the pier bearings do not slide for this load. As the horizontal stiffness of the abutments is very high sliding shall occur at the abutments, associated with development of friction reactions μW_a , where W_a is the corresponding permanent load. The appropriate static system for this loading has therefore articulated connection between pier tops and deck and sliding over the abutments with the above friction reactions (see Fig. 8.49). The total forces at the abutments may be calculated from the corresponding displacement of the deck and the force-displacement relation of the bearings (additional elastic reaction W_a/R (see also Fig. 8.50). A similar situation appears for the transverse wind loading.

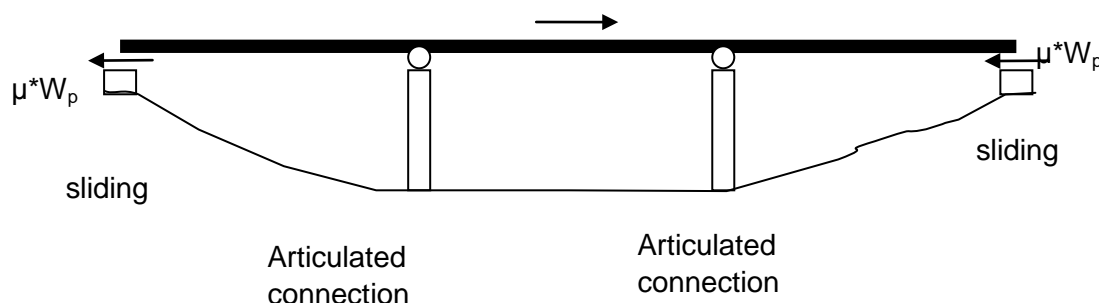


Fig. 8.49 Structural system for imposed horizontal load

8.4.2.2 Imposed deformations that can cause sliding of the pier bearings

Assuming the structural system in the longitudinal direction to be the same as above, the imposed deformation that can cause sliding in the pier bearings is calculated from the minimum sliding load of the bearings, and the stiffness of the piers:

Minimum sliding load $F_{y,min} = 0.051 \times 12699 = 648$ kN

Pier stiffness $K_{pier} = 3EI / h^3 = 3 \times 34000000 \times (9 \times (2.5m)^3 / 12) / (10)^3 = 1195313$ kN/m

Minimum displacement of deck at pier top to cause sliding $d_{min} = F_{y,min} / K = 648 / 1195313 = 0.5$ mm

This displacement is very small and is practically exceeded even by small temperature imposed deformations. Consequently sliding occurs in the bearings of at least one of the piers, under temperature induced imposed deformations.

8.4.2.3 Imposed deformation due to temperature variation

A conservative approach for estimating forces and displacements for this case, is the following: Due an inevitable difference of the sliding friction coefficient of the bearings of the two piers, even if this difference is small, one of the two pier supports is assumed not to slide, under non-seismic conditions. Calculation of horizontal support reactions and displacements should therefore be based on two systems with deck articulated on one of the two piers alternatively. On the other moving supports an elastic connection between deck and support equal to $K_{pb} = W_p / R$ value (see Fig. 4.5, $R = R_b = 1.83$ m) calculated on the basis of W_p equal to the corresponding permanent load should be used. At these

supports, friction forces equal to $\mu \cdot W_p$, should also be introduced, where μ is either the minimum or the maximum value of friction, with opposite signs on the deck and the supporting element, and directions compatible to the corresponding sliding deformation at the support, as shown in the following Fig. 8.50. Both displacements and forces can be derived from these systems.

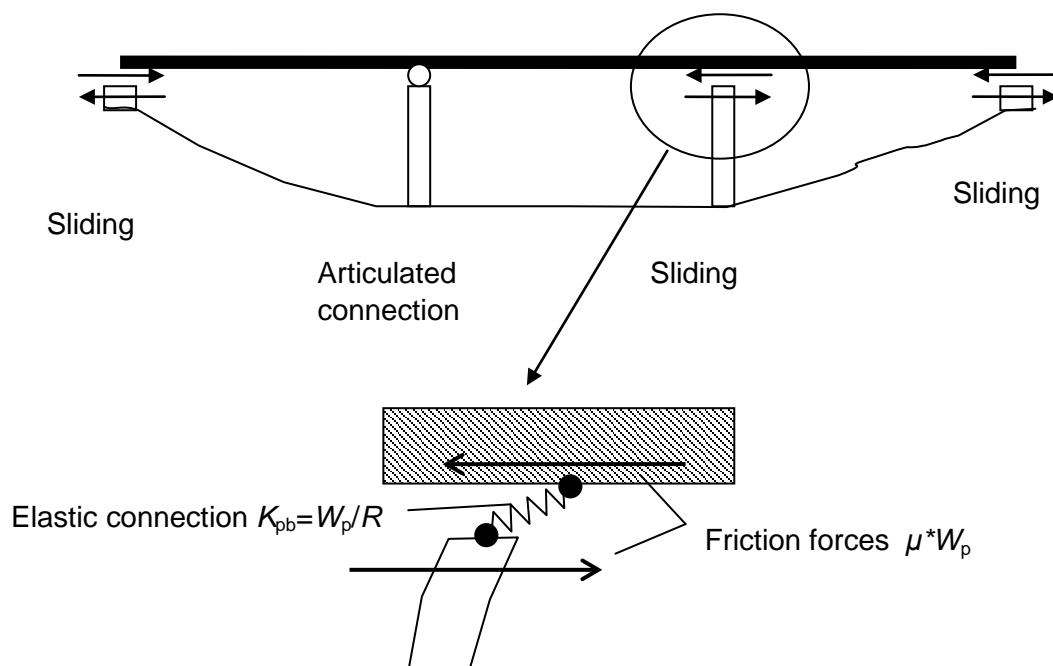


Fig. 8.50 Structural system for imposed deformations

8.4.2.4 Superposition of effects of braking load and imposed deck deformations

The superposition of the effects of braking load and imposed deformations needs care, as the two cases correspond in fact to nonlinear response of the system, due to the involvement of the friction forces. The application of braking force on the system on which imposed deformations are already acting, causes in general a redistribution of the friction forces estimated according to 8.4.2.3.

Namely, those of the original friction forces, acting on one of the piers and the corresponding abutment, which had the same direction with the braking force, shall be reversed, starting from the abutment, where full reversal, amounting to a force of $2\mu W_a$, will take place. The remaining part of the braking force $F_{br} - 2\mu W_a = 900 - 2 \times 0.051 \times 2993 = 595$ kN shall be equilibrated mainly by a decrease of the reaction of the relevant pier. This decrease is associated with a displacement of the deck, in the direction of the braking force, an upper bound of which can be estimated as: $\Delta d = (F_{br} - 2\mu W_a) / K_{pier} = 595 / 1195313 = 0.0005$ m = 0.5 mm. The corresponding upper bound of the force increase on the reactions of the opposite pier and abutment amounts to $\Delta_d W_p / R = 0.0005 \times 12699 / 1.83 = 3.5$ kN and $\Delta_d W_a / R = 0.0005 \times 2993 / 1.83 = 0.8$ kN respectively. Consequently, for this example, both the displacement Δd and the force increases can be neglected.

A comparison with the forces and displacements resulting from the seismic design situation (see 8.4.7), shows the evident, i.e. that the later are always governing, for a bridge with seismic isolation.

8.4.3 DESIGN SEISMIC ACTION

8.4.3.1 Design seismic spectra

The design spectra that are applicable for the analysis of bridges with seismic isolation is specified in EN 1998-2:2005+A1:2009, **7.4.1**. More specifically for the horizontal directions the horizontal elastic response spectrum specified in EN 1998-1:2004, **3.2.2.2** is used. The project dependent parameters that define the horizontal response spectrum for this particular example are as follows:

- Type 1 horizontal elastic response spectrum
- No near source effects
- Importance factor $\gamma_I = 1.00$
- Reference peak ground acceleration for type A ground: $a_{gR} = 0.40g$
- Design ground acceleration for type A ground: $a_g = \gamma_I \cdot a_{gR} = 0.40g$
- Ground type B (soil factor $S = 1.20$, periods $T_B = 0.15$ s, $T_C = 0.5$ s)
- Period $T_D = 2.5$ s

According to the note in EN 1998-2:2005+A1:2009, **7.4.1** the value of the period T_D is particularly important for the safety of bridges with seismic isolation because it affects proportionally the estimated displacement demands. For this reason the National Annex to this part of Eurocode 8 may specify a value of T_D specifically for the design of bridges with seismic isolation that is more conservative (longer) than the value ascribed to T_D in the National Annex to EN 1998-1:2004. For this particular example the selected value is $T_D = 2.5$ s, which is longer than the value $T_D = 2.0$ s which is recommended in EN 1998-1:2004, **3.2.2.2(2)P**.

For the vertical direction the vertical elastic response spectrum specified in EN 1998-1:2004, **3.2.2.3** is used. The project dependent parameters that define the vertical response spectrum are selected for this particular example as follows:

- Type 1 vertical elastic response spectrum
- Ratio of design ground acceleration in the vertical direction to the design ground acceleration in the horizontal direction: $a_{vg} / a_g = 0.90$
- Periods $T_B = 0.05$ s, $T_C = 0.15$ s, $T_D = 1.0$ s

The design spectra for horizontal and vertical directions are illustrated in Fig. 8.51 and Fig. 8.52 respectively.

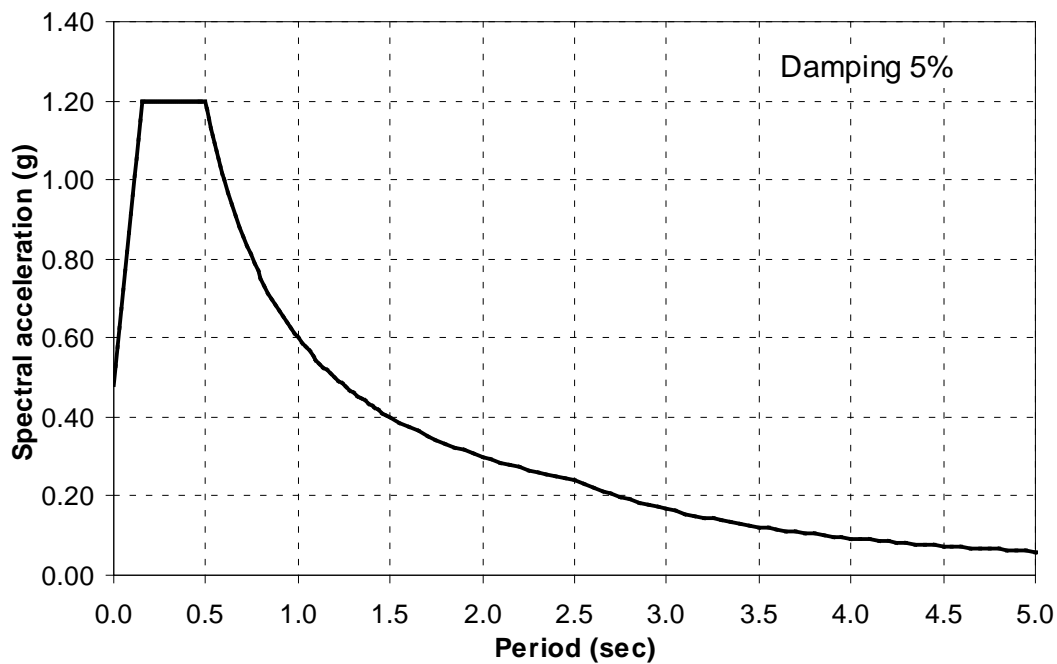


Fig. 8.51 Horizontal elastic response spectrum

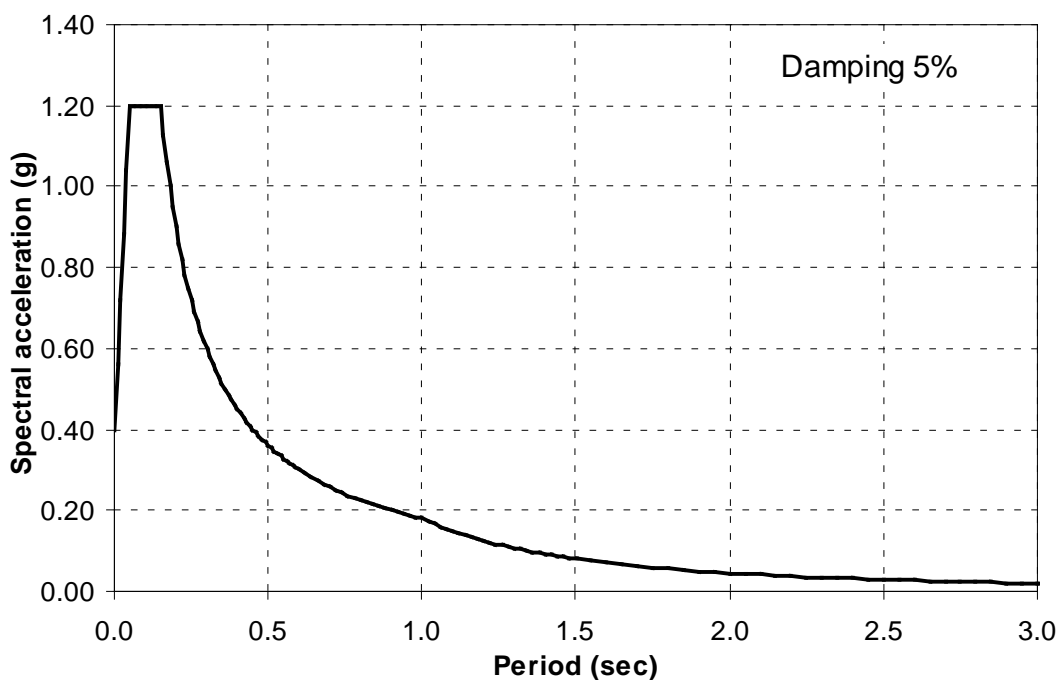


Fig. 8.52 Vertical elastic response spectrum

8.4.3.2 Accelerograms for non linear time-history analysis

In accordance with EN 1998-2:2005+A1:2009, **7.4.2** the provisions of EN 1998-2:2005+A1:2009, **3.2.3** apply concerning the time-history representation of the seismic action.

Seven (7) ground motion time-histories are used (EQ1 to EQ7), each one consisting of a pair of horizontal ground motion time-history components and a vertical ground motion time-history

component, as presented in Table 8.15. Each component ACC01 to ACC14 and ACV01 to ACV07 is selected from simulated accelerograms that are produced by modifying natural recorded events so as to match the Eurocode 8 design spectrum (semi-artificial accelerograms). The modification procedure consists of applying unit impulse functions that iteratively correct the accelerogram in order to better match the target spectrum. Analytical description of selected initial records, the modification procedure and the produced semi-artificial accelerograms is presented in Appendix D.

Table 8.15 Components of ground motions

Ground Motion	Horizontal component in longitudinal direction	Horizontal component in transverse direction	Vertical component
EQ1	ACC01	ACC02	ACV01
EQ2	ACC03	ACC04	ACV02
EQ3	ACC05	ACC06	ACV03
EQ4	ACC07	ACC08	ACV04
EQ5	ACC09	ACC10	ACV05
EQ6	ACC11	ACC12	ACV06
EQ7	ACC13	ACC14	ACV07

8.4.3.3 Verification of ground motion compatibility with the design response spectrum

The compatibility of the ground motions EQ1 to EQ7 with the design response spectra is verified in accordance with EN 1998-2:2005+A1:2009, **3.2.3**. For the produced semi-artificial accelerograms that are used in this work no scaling of the individual components is required to ensure compatibility because each component is already compatible with the corresponding design spectrum due to the applied modification procedure presented in Appendix D.

The consistency of the ensemble of ground motions is verified for the horizontal components in accordance with EN 1998-2:2005+A1:2009, **3.2.3(3)P**:

- For each earthquake consisting of a pair of horizontal motions, the SRSS spectrum is established by taking the square root of the sum of squares of the 5%-damped spectra of each component.
- The spectrum of the ensemble of earthquakes is formed by taking the average value of the SRSS spectra of the individual earthquakes of the previous step.
- The ensemble spectrum shall be not lower than 1.3 times the 5%-damped elastic response spectrum of the design seismic action, in the period range between $0.2T_1$ and $1.5T_1$, where T_1 is the effective period (T_{eff}) of the isolation system.

The consistency of the ensemble of ground motions is verified for the vertical components in accordance with EN 1998-2:2005+A1:2009, **3.2.3(6)**:

- The spectrum of the ensemble of earthquakes is formed by taking the average value of the vertical response spectra of the individual earthquakes.
- The ensemble spectrum shall be not lower than 1.1 times the 5%-damped elastic response spectrum of the design seismic action, in the period range between $0.2T_v$ and $1.5T_v$, where T_v is the period of the lowest mode where the response to the vertical component prevails over the response to the horizontal components (e.g. in terms of participating mass).

The aforementioned consistency criteria are presented graphically in Fig. 8.53 and Fig. 8.54 for horizontal and vertical components respectively. It is verified that the selected accelerograms are consistent with the design spectrum of EN 1998-2 for all periods between 0 and 5 s for horizontal components and for all periods between 0 and 3 s for vertical components. Therefore consistency is

established for all isolation systems with effective period $T_{\text{eff}} < 5\text{ s} / 1.5 = 3.33\text{ s}$ and prevailing vertical period $T_V < 3\text{ s} / 1.5 = 2\text{ s}$, which are fulfilled for the isolation system of the presented example.

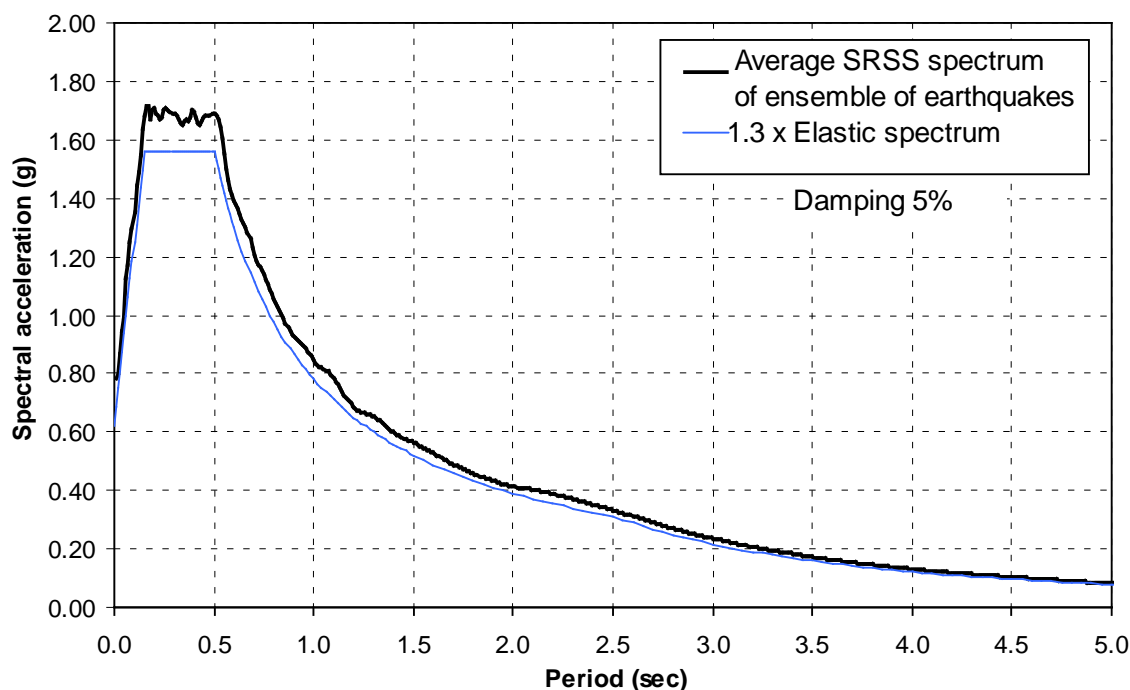


Fig. 8.53 Verification of consistency between design spectrum and spectrum of selected accelerograms for horizontal components.

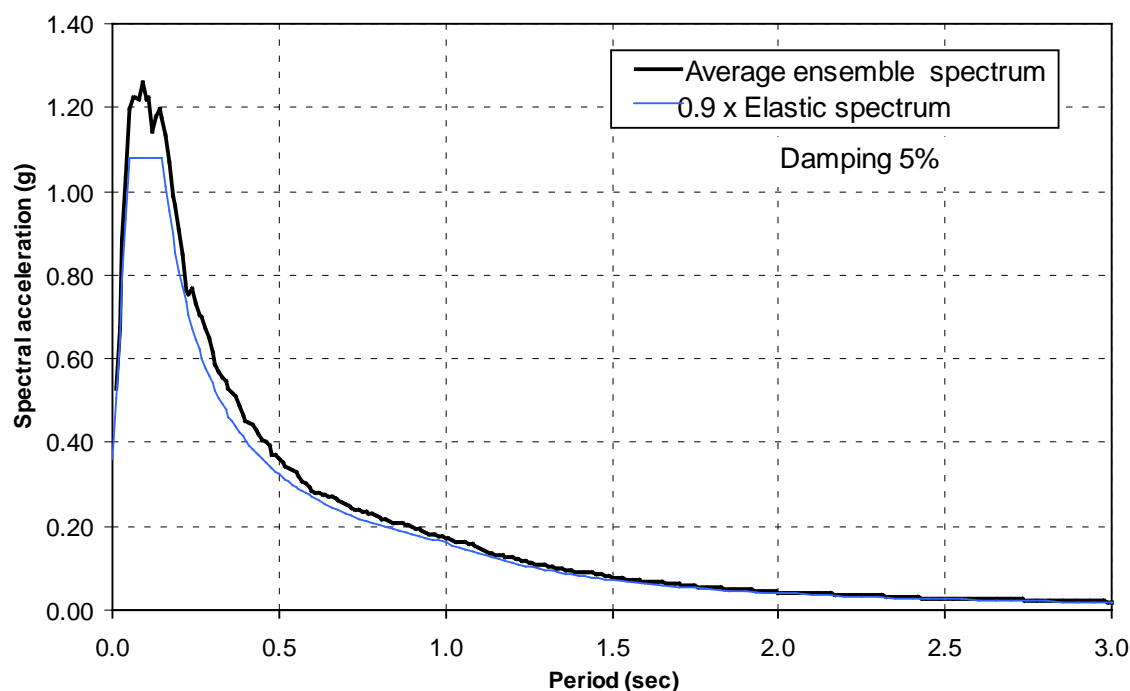


Fig. 8.54 Verification of consistency between design spectrum and spectrum of selected accelerograms for vertical components.

8.4.4 SEISMIC STRUCTURAL SYSTEM

8.4.4.1 Structural system – Effective stiffness of elements

a Bridge Model

For the purpose of non-linear time-history analysis the bridge is modelled by a 3D model that accurately accounts for the spatial distribution of stiffness and mass of the bridge. The geometry of the bridge is accurately modelled. The superstructure and the substructure of the bridge are modelled with linear beam finite elements with properties in accordance with the actual cross-section of the elements. The mass of the elements is considered lumped on the nodes of the model. The discretization of the finite elements is adequate to account for the actual distribution of the bridge mass. Where necessary kinematic constraints were applied to establish proper connection of the elements. Non-linear time-history analysis was carried out in computer program SAP2000. In Fig. 8.55 the model of the bridge for time-history analysis is shown.

b Isolator model

The Triple FPS bearings are modelled with non-linear hysteretic friction elements. The isolator elements connect the deck and pier nodes at the locations of the corresponding bearing. In the SAP 2000 model the behaviour of the isolator elements in the horizontal direction follows a coupled frictional law based on the Bouc-Wen model. In the vertical direction the behaviour of the isolators corresponds to stiff support that acts only in compression. The actual vertical load of the bearings at each time instant is taken into account to establish the force-displacement relation of the bearing. The effects of bridge deformation and vertical seismic action are taken into account in the estimation of vertical bearing loads.

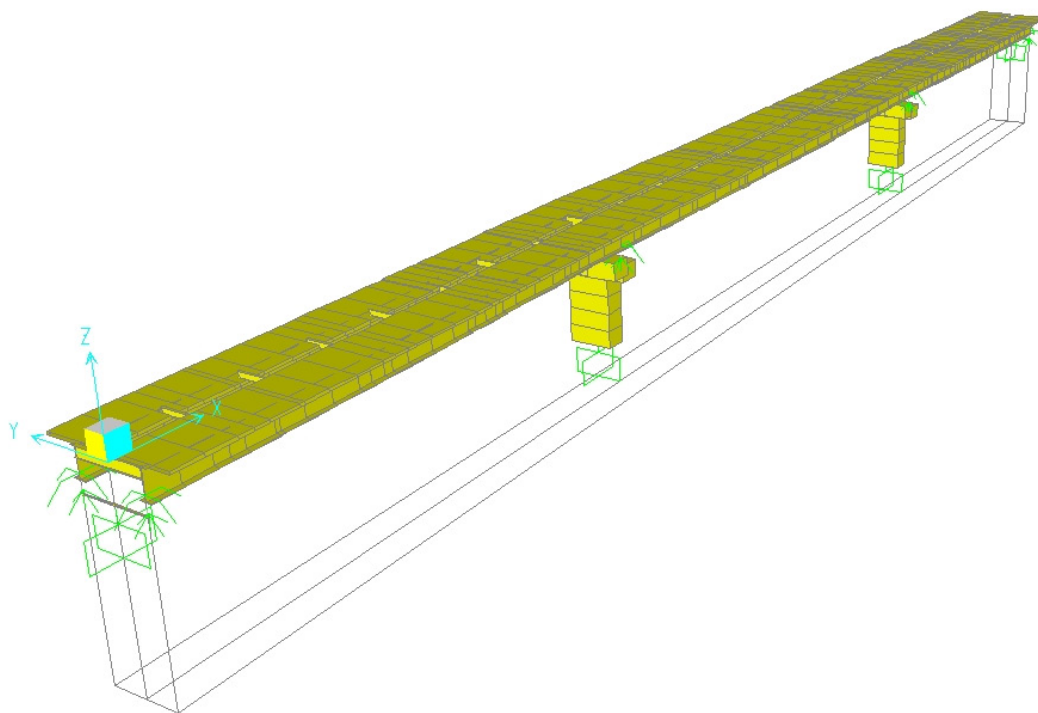


Fig. 8.55 Bridge model for time-history analysis

c Foundation flexibility

For the purpose of this example the effect of the foundation flexibility is ignored. The piers are assumed fixed at their base.

d Effective pier stiffness

The effective pier stiffness is derived from the uncracked section stiffness of the gross concrete cross-section and the secant modulus of elasticity $E_{cm} = 34$ GPa for C35/45 concrete. Because the stiffness of the piers is much larger than the effective stiffness of the isolation system its contribution to the total effective stiffness of the structure may be ignored without significant loss of accuracy. This approach is followed in the fundamental mode analysis which is presented with analytical hand calculations. In the non-linear time-history analysis which is carried out with computer calculation the effect of pier stiffness is included.

8.4.4.2 Bridge loads applicable for seismic design

a Permanent loads

In Table 8.16 the distribution of the permanent reactions of the deck supports is provided, according to the provided data of the general example. The time variation of the permanent reactions due to creep & shrinkage is very small. Because of this small variation only one distribution of permanent reactions is considered in this example, which is selected as the distribution after creep & shrinkage become fully developed.

Table 8.16 Permanent loads

Total support loads in MN (both beams)	Self weight after construction	Minimum equipment load	Maximum equipment load	Total with minimum equipment	Total with maximum equipment	Time variation due to creep & shrinkage
C0	2.328	0.664	1.020	2.993	3.348	-0.172
P1	10.380	2.440	3.744	12.819	14.123	0.206
P2	10.258	2.441	3.745	12.699	14.003	0.091
C3	2.377	0.664	1.019	3.041	3.396	-0.126
Sum of reactions	25.343	6.209	9.528	31.552	34.871	0.000

According to the provided data of the general example, the longitudinal displacements due to permanent actions are approximately 8mm for abutments and 3mm for piers, both towards the center of the bridge.

b Quasi-permanent traffic loads

According to EN 1998-2:2005+A1:2009, **4.1.2** for the case of road bridges with severe traffic the quasi permanent value $\psi_{2,1}Q_{k,1}$ of the traffic action to be considered in the seismic combination is calculated from the UDL system of traffic Load Model 1 (LM1). For bridges with severe traffic (i.e. bridges of motorways and other roads of national importance) the value of the combination factor $\psi_{2,1}$ is 0.2.

The division of the carriageway in 3 notional lanes in accordance with EN1991-2, **4.2.3** is shown in Fig. 8.56.

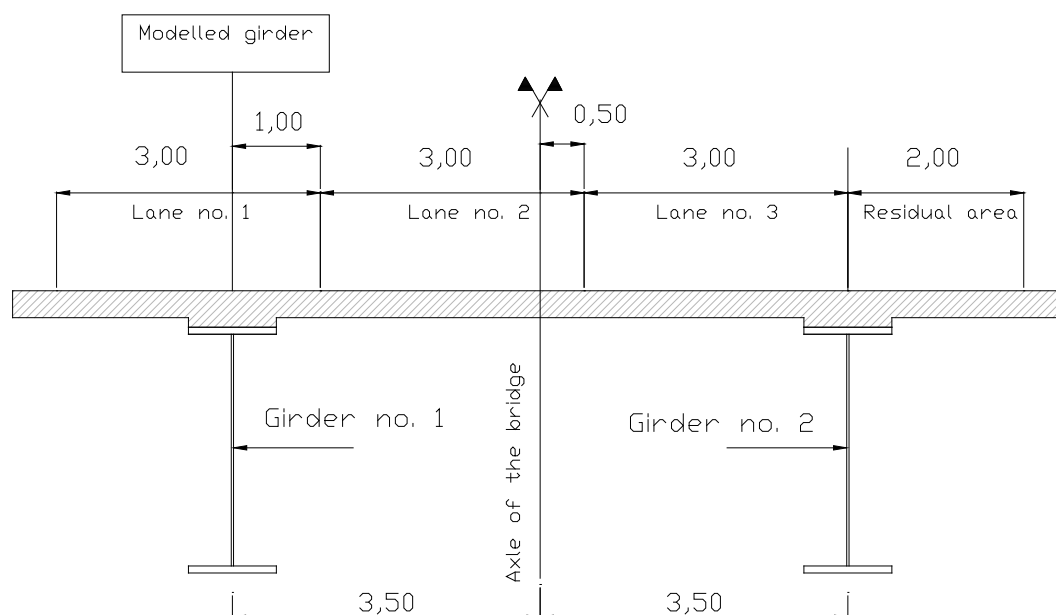


Fig. 8.56 Division of carriageway into notional lanes

The values of UDL system of Model 1 (LM1) is calculated in accordance with EN1998-2, Table 4.2 (where $\alpha_q=1.0$ is the adjustment factor of UDL).

Lane Number 1: $\alpha_q q_{1,k} = 3 \text{ m} \times 9 \text{ kN/m}^2 = 27.0 \text{ kN/m}$

Lane Number 2: $\alpha_q q_{2,k} = 3 \text{ m} \times 2.5 \text{ kN/m}^2 = 7.5 \text{ kN/m}$

Lane Number 3: $\alpha_q q_{3,k} = 3 \text{ m} \times 2.5 \text{ kN/m}^2 = 7.5 \text{ kN/m}$

Residual area: $\alpha_q q_{r,k} = 2 \text{ m} \times 2.5 \text{ kN/m}^2 = 5.0 \text{ kN/m}$

Total load = 47.0 kN/m

The quasi-permanent traffic load in the seismic combination applied per unit of length of the bridge is:

$$\psi_{2,1} Q_{k,1} = 0.2 \times 47.0 \text{ kN/m} = 9.4 \text{ kN/m}$$

The reactions of the deck supports for the quasi-permanent traffic load are presented in Table 8.17, according to the provided data of the general example:

Table 8.17 Traffic load in seismic combination

Total support loads in MN (both beams)	Traffic load in seismic combination ($\psi_{2,1} Q_{k,1}$)
C0	0.201
P1	0.739
P2	0.739
C3	0.201
Sum of reactions	1.880

c Deck seismic weight

The weight W_d of the deck in seismic combinations includes the permanent loads and the quasi-permanent value of the traffic loads:

$$W_d = \text{Dead load} + \text{quasi-permanent traffic load} = 34871 \text{ kN} + 1880 \text{ kN} = 36751 \text{ kN}$$

d Thermal action

The minimum ambient air temperature (mean return period of 50 years) to which the structure is subjected is assumed to be equal to $T_{\min} = -20^\circ\text{C}$. The maximum ambient air temperature (mean return period of 50 years) to which the structure is subjected is assumed to be equal to $T_{\max} = +40^\circ\text{C}$. The initial temperature is assumed equal to $T_0 = +10^\circ\text{C}$.

The uniform bridge temperature components $T_{e,\min}$ and $T_{e,\max}$ are calculated from T_{\min} and T_{\max} using EN1991-1-5, Figure 6.1 for Type 2 deck type (i.e. composite deck).

The ranges of the uniform bridge temperature component are calculated as:

- maximum contraction range: $\Delta T_{N,\text{con}} = T_0 - T_{e,\min} = 10^\circ\text{C} - (-20^\circ\text{C} + 5^\circ\text{C}) = 25^\circ\text{C}$
- maximum expansion range: $\Delta T_{N,\text{exp}} = T_{e,\max} - T_0 = (+40^\circ\text{C} + 5^\circ\text{C}) - 10^\circ\text{C} = 35^\circ\text{C}$

In accordance with EN 1991-1-5, 6.1.3.3(3) Note 2 for the design of bearings and expansion joints the temperature ranges are increased as follows:

- maximum contraction range for bearings = $\Delta T_{N,\text{con}} + 20^\circ\text{C} = 25^\circ\text{C} + 20^\circ\text{C} = 45^\circ\text{C}$
- maximum expansion range for bearings = $\Delta T_{N,\text{exp}} + 20^\circ\text{C} = 35^\circ\text{C} + 20^\circ\text{C} = 55^\circ\text{C}$

8.4.4.3 Design properties of isolators

a General

The nominal values of the design properties (DP) of the isolators as presented in 4.1 are:

- Effective dynamic friction coefficient: $\mu_d = 0.061$ (+/- 16% variability of nominal value)
- Effective radius of sliding surface: $R_b = 1.83\text{m}$
- Effective yield displacement: $D_y = 0.005\text{m}$

The nominal properties of the isolator units, and hence those of the isolating system, may be affected by ageing, temperature, loading history (scragging), contamination, and cumulative travel (wear). This variability is accounted for in accordance with EN 1998-2:2005+A1:2009, **7.5.2.4(2)P**, by using two sets of design properties of the isolating system:

- Upper bound design properties (UBDP), which typically lead to larger forces governing the design of the structural elements of the bridge, and
- Lower bound design properties (LBDP), which typically lead to larger displacements governing the design of the isolators.

In general two analyses are performed, one using the UBDP and another using LBDP.

For the selected isolation system only the effective dynamic friction coefficient μ_d is subject to variability of its design value. The effective radius of the sliding surface R_b is a geometric property not subject to any variability. The UBDP and the LBDP for μ_d are calculated in accordance with EN 1998-2:2005+A1:2009, Annexes **J** and **JJ**.

$$\text{Nominal value: } \mu_d = 0.061 \pm 16\% = 0.051 \div 0.071$$

$$\text{LBDP: } \mu_{d,\min} = \text{minDP}_{\text{nom}} = 0.051$$

UBDP: According to EN 1998-2 Annexes J and JJ

b Minimum isolator temperature for seismic design

$$T_{\min,b} = \psi_2 T_{\min} + \Delta T_1 = 0.5 \times (-20^\circ\text{C}) + 5.0^\circ\text{C} = -5.0^\circ\text{C}$$

where:

$\psi_2 = 0.5$ is the combination factor for thermal actions for seismic design situation, in accordance with EN 1990:2002 – Annex A2,

$T_{\min} = -20^\circ\text{C}$ is the minimum shade air temperature at the bridge location having an annual probability of negative exceedance of 0.02, in accordance with EN 1990-1-5:2004, 6.1.3.2.

$\Delta T_1 = +5.0^\circ\text{C}$ is the correction temperature for composite bridge deck in accordance with EN 1998-2:2005+A1:2009, Table J.1N.

c λ_{\max} factors in accordance with EN 1998-2:2005+A1:2009, Annex JJ

f1 - ageing: $\lambda_{\max,f1} = 1.1$ (Table JJ.1, for normal environment, unlubricated PTFE, protective seal)

f2 - temperature: $\lambda_{\max,f2} = 1.15$ (Table JJ.2 for $T_{\min,b} = -5.0^\circ\text{C}$, unlubricated PTFE)

f3 - contamination $\lambda_{\max,f3} = 1.1$ (Table JJ.3 for unlubricated PTFE and sliding surface facing both upwards and downwards)

f4 – cumulative travel $\lambda_{\max,f4} = 1.0$ (Table JJ.4 for unlubricated PTFE and cumulative travel ≤ 1.0 km)

Combination factor $\psi_{fi} = 0.70$ for Importance class II, i.e. average importance (Table J.2)

Combination value of λ_{\max} factors: $\lambda_{U,fi} = 1 + (\lambda_{\max,fi} - 1)\psi_{fi}$ (eq. J.5)

f1 - ageing: $\lambda_{U,f1} = 1 + (1.1 - 1) \times 0.7 = 1.07$

f2 - temperature: $\lambda_{U,f2} = 1 + (1.15 - 1) \times 0.7 = 1.105$

f3 - contamination $\lambda_{U,f3} = 1 + (1.1 - 1) \times 0.7 = 1.07$

f4 – cumulative travel $\lambda_{U,f4} = 1 + (1.0 - 1) \times 0.7 = 1.0$

d Effective UBDP:

$$\text{UBDP} = \text{maxDP}_{\text{nom}} \cdot \lambda_{U,f1} \cdot \lambda_{U,f2} \cdot \lambda_{U,f3} \cdot \lambda_{U,f4} \quad (\text{equation J.4})$$

$$\mu_{d,\max} = 0.071 \times 1.07 \times 1.105 \times 1.07 \times 1.0 = 0.071 \times 1.265 = 0.09$$

Therefore the variability of the effective friction coefficient is: $\mu_d = 0.051 \div 0.09$

8.4.5 FUNDAMENTAL MODE METHOD

8.4.5.1 General

The fundamental mode method of analysis is described in EN 1998-2:2005+A1:2009, 7.5.4. In each of the principal horizontal directions the response of the isolated bridge is determined considering the superstructure as a linear single-degree-of-freedom system using:

- the effective stiffness of the isolation system K_{eff} ,
- the effective damping of the isolation system ξ_{eff} ,

- the mass of the superstructure M_d ,
- the spectral acceleration $S_e(T_{eff}, \xi_{eff})$ corresponding to the effective period T_{eff} and the effective damping ξ_{eff} .

The effective stiffness at each support location consists of the composite stiffness of the isolator unit and the corresponding substructure. In this particular example the stiffness of the piers is much smaller than the stiffness of the isolators therefore the contribution of pier stiffness may be ignored without significant loss of accuracy. The effective damping is derived using the following equation, where $\Sigma E_{D,i}$ is the sum of dissipated energies of all isolators i in a full cycle at the design displacement d_{cd} .

$$\xi_{eff} = \frac{1}{2\pi} \left[\frac{\Sigma E_{D,i}}{K_{eff} d_{cd}^2} \right]$$

The design displacement d_{cd} is calculated from effective period T_{eff} and effective damping ξ_{eff} , both of which depend on the value of the unknown design displacement d_{cd} . Therefore the fundamental mode method is in general an iterative procedure, where a value for the design displacement is assumed in order to calculate T_{eff} , ξ_{eff} and then a better approximation of d_{cd} is calculated from the design spectrum using T_{eff} , ξ_{eff} . The new value of d_{cd} is used as the initial value for the new iteration. The procedure converges rapidly and a few iterations are adequate to achieve the desired accuracy. In this example hand calculations are presented for the Fundamental Mode analysis for both LBDP and UBDP. Only the first and the last iteration are presented.

8.4.5.2 Fundamental Mode analysis for Lower Bound Design Properties (LBDP)

The presented analysis corresponds to Lower Bound Design Properties (LBDP) of isolators i.e. $\mu_d=0.051$. The iteration steps are presented analytically

Seismic weight: $W_d = 36751 \text{ kN}$ (see loads)

Iteration 1

Assume value for design displacement d_{cd} :

$$\text{Assume } d_{cd} = 0.15 \text{ m}$$

Effective Stiffness of Isolation System K_{eff} : (ignore piers):

$$\begin{aligned} K_{eff} &= F / d_{cd} = W_d \times [\mu_d + d_{cd} / R_b] / d_{cd} = \\ &36751 \text{ kN} \times [0.051 + 0.15 \text{ m} / 1.83 \text{ m}] / 0.15 \text{ m} \\ \Rightarrow K_{eff} &= 32578 \text{ kN/m} \end{aligned}$$

Effective period of Isolation System T_{eff} : (EN1998-2 eq. 7.6)

$$T_{eff} = 2\pi \sqrt{\frac{m}{K_{eff}}} = 2\pi \sqrt{\frac{(36751 \text{ kN} / 9.81 \text{ m/s}^2)}{32578 \text{ kN/m}}} = 2.13 \text{ s}$$

Dissipated energy per cycle E_D : (EN1998-2, 7.5.2.3.5(4))

$$\begin{aligned} E_D &= 4 \times W_d \times \mu_d \times (d_{cd} - D_y) = \\ &4 \times 36751 \text{ kN} \times (0.051) \times (0.15 \text{ m} - 0.005 \text{ m}) \\ \Rightarrow E_D &= 1087.09 \text{ kNm} \end{aligned}$$

Effective damping ξ_{eff} : (EN1998-2 eq. 7.5, 7.9)

$$\xi_{eff} = \Sigma E_{D,i} / [2 \times \pi \times K_{eff} \times d_{cd}^2] =$$

$$1087.09 \text{ kNm} / [2 \times \pi \times 32578 \text{ kN/m} \times (0.15 \text{ m})^2] = 0.236$$

$$\eta_{\text{eff}} = [0.10 / (0.05 + \xi_{\text{eff}})]^{0.5} = 0.591$$

Calculate design displacement d_{cd} : (EN 1998-2 Table 7.1)

$$d_{\text{cd}} = (0.625/\pi^2) \times a_g \times S \times \eta_{\text{eff}} \times T_{\text{eff}} \times T_C =$$

$$(0.625/\pi^2) \times (0.40 \times 9.81 \text{ m/s}^2) \times 1.20 \times 0.591 \times 2.13 \text{ s} \times 0.50 \text{ s} = 0.188 \text{ m}$$

Check assumed displacement

Assumed displacement 0.15 m

Calculated displacement 0.188 m

⇒ **Do another iteration**

Iteration 2

Assume new value for design displacement d_{cd} :

Assume $d_{\text{cd}} = 0.22 \text{ m}$

Effective Stiffness of Isolation System K_{eff} : (ignore piers):

$$K_{\text{eff}} = F / d_{\text{cd}} = W_d \times [\mu_d + d_{\text{cd}} / R_b] / d_{\text{cd}} =$$

$$36751 \text{ kN} \times [0.051 + 0.22 \text{ m} / 1.83 \text{ m}] / 0.22 \text{ m} =$$

$$\Rightarrow K_{\text{eff}} = 28602 \text{ kN/m}$$

Effective period of Isolation System T_{eff} : (EN1998-2 eq. 7.6)

$$T_{\text{eff}} = 2\pi \sqrt{\frac{m}{K_{\text{eff}}}} = 2\pi \sqrt{\frac{(36751 \text{ kN} / 9.81 \text{ m/s}^2)}{28602 \text{ kN/m}}} = 2.27 \text{ s}$$

Dissipated energy per cycle E_D : (EN1998-2, 7.5.2.3.5(4))

$$E_D = 4 \times W_d \times \mu_d \times (d_{\text{cd}} - D_y) =$$

$$4 \times 36751 \text{ kN} \times (0.051) \times (0.22 \text{ m} - 0.005 \text{ m})$$

$$\Rightarrow E_D = 1611.90 \text{ kNm}$$

Effective damping ξ_{eff} : (EN1998-2 eq. 7.5, 7.9)

$$\xi_{\text{eff}} = \Sigma E_{D,i} / [2 \times \pi \times K_{\text{eff}} \times d_{\text{cd}}^2] =$$

$$1611.90 \text{ kNm} / [2 \times \pi \times 28602 \text{ kN/m} \times (0.22 \text{ m})^2] = 0.1853$$

$$\eta_{\text{eff}} = [0.10 / (0.05 + \xi_{\text{eff}})]^{0.5} = 0.652$$

Calculate design displacement d_{cd} : (EN 1998-2 Table 7.1)

$$d_{\text{cd}} = (0.625/\pi^2) \times a_g \times S \times \eta_{\text{eff}} \times T_{\text{eff}} \times T_C =$$

$$(0.625/\pi^2) \times (0.40 \times 9.81 \text{ m/s}^2) \times 1.20 \times 0.652 \times 2.27 \text{ s} \times 0.5 \text{ s} = 0.22 \text{ m}$$

Check assumed displacement:

Assumed displacement 0.22 m

Calculated displacement 0.22 m

⇒ **Convergence achieved**

Spectral acceleration S_e : (EN 1998-2 Table 7.1)

$$S_e = 2.5 \times (T_C / T_{\text{eff}}) \times \eta_{\text{eff}} \times a_g \times S =$$

$$2.5 \times (0.5\text{s}/2.27\text{s}) \times 0.652 \times 0.40\text{g} \times 1.20 = 0.172 \text{ g}$$

Isolation system shear force V_d : (EN 1998-2 eq. 7.10)

$$V_d = K_{\text{eff}} \times d_{\text{cd}} = 28602 \text{ kN/m} \times 0.22\text{m} = 6292 \text{ kN}$$

8.4.5.3 Fundamental Mode analysis for Upper Bound Design Properties (UBDP)

The presented analysis corresponds to Upper Bound Design Properties (UBDP) of isolators i.e. $\mu_d=0.09$.

Seismic weight: $W_d = 36751\text{kN}$ (see loads)

Iteration 1

Assume value for design displacement d_{cd} :

$$\text{Assume } d_{\text{cd}} = 0.15\text{m}$$

Effective Stiffness of Isolation System K_{eff} : (ignore piers):

$$\begin{aligned} K_{\text{eff}} &= F / d_{\text{cd}} = W_d \times [\mu_d + d_{\text{cd}} / R_b] / d_{\text{cd}} = \\ &36751\text{kN} \times [0.09 + 0.15\text{m}/1.83\text{m}] / 0.15\text{m} \\ \Rightarrow K_{\text{eff}} &= 42133 \text{ kN/m} \end{aligned}$$

Effective period of Isolation System T_{eff} : (EN1998-2 eq. 7.6)

$$T_{\text{eff}} = 2\pi \sqrt{\frac{m}{K_{\text{eff}}}} = 2\pi \sqrt{\frac{(36751 \text{ kN}/9.81 \text{ m/s}^2)}{42133 \text{ kN/m}}} = 1.87 \text{ s}$$

Dissipated energy per cycle E_D : (EN1998-2, 7.5.2.3.5(4))

$$\begin{aligned} E_D &= 4 \times W_d \times \mu_d \times (d_{\text{cd}} - D_y) = \\ &4 \times 36751\text{kN} \times (0.09) \times (0.15\text{m} - 0.005\text{m}) \\ \Rightarrow E_D &= 1984.55 \text{ kNm} \end{aligned}$$

Effective damping ξ_{eff} : (EN1998-2 eq. 7.5, 7.9)

$$\begin{aligned} \xi_{\text{eff}} &= \Sigma E_{D,i} / [2 \times \pi \times K_{\text{eff}} \times d_{\text{cd}}^2] = \\ &1984.5\text{kNm} / [2 \times \pi \times 42133\text{kN/m} \times (0.15\text{m})^2] = 0.333 \\ \eta_{\text{eff}} &= [0.10 / (0.05 + \xi_{\text{eff}})]^{0.5} = 0.511 \end{aligned}$$

Calculate design displacement d_{cd} : (EN 1998-2 Table 7.1)

$$\begin{aligned} d_{\text{cd}} &= (0.625/\pi^2) \times a_g \times S \times \eta_{\text{eff}} \times T_{\text{eff}} \times T_C = \\ &(0.625/\pi^2) \times (0.40 \times 9.81\text{m/s}^2) \times 1.20 \times 0.511 \times 1.87\text{s} \times 0.50\text{s} = 0.142 \text{ m} \end{aligned}$$

Check assumed displacement

Assumed displacement 0.15 m

Calculated displacement 0.142 m

\Rightarrow Do another iteration

Iteration 2

Assume new value for design displacement d_{cd} :

$$\text{Assume } d_{\text{cd}} = 0.14\text{m}$$

Effective Stiffness of Isolation System K_{eff} : (ignore piers):

$$K_{eff} = F / d_{cd} = W_d \times [\mu_d + d_{cd} / R_b] / d_{cd} =$$

$$36751 \text{ kN} \times [0.09 + 0.14 \text{ m} / 1.83 \text{ m}] / 0.14 \text{ m}$$

$$\Rightarrow K_{eff} = 43541 \text{ kN/m}$$

Effective period of Isolation System T_{eff} : (EN1998-2 eq. 7.6)

$$T_{eff} = 2\pi \sqrt{\frac{m}{K_{eff}}} = 2\pi \sqrt{\frac{(36751 \text{ kN} / 9.81 \text{ m/s}^2)}{43541 \text{ kN/m}}} = 1.84 \text{ s}$$

Dissipated energy per cycle E_D : (EN1998-2, 7.5.2.3.5(4))

$$E_D = 4 \times W_d \times \mu_d \times (d_{cd} - D_y) =$$

$$4 \times 36751 \text{ kN} \times (0.09) \times (0.14 \text{ m} - 0.005 \text{ m})$$

$$\Rightarrow E_D = 1799.32 \text{ kNm}$$

Effective damping ξ_{eff} : (EN1998-2 eq. 7.5, 7.9)

$$\xi_{eff} = \Sigma E_{D,i} / [2 \times \pi \times K_{eff} \times d_{cd}^2] =$$

$$1799.32 \text{ kNm} / [2 \times \pi \times 43541 \text{ kN/m} \times (0.14 \text{ m})^2] = 0.331$$

$$\eta_{eff} = [0.10 / (0.05 + \xi_{eff})]^{0.5} = 0.512$$

Calculate design displacement d_{cd} : (EN 1998-2 Table 7.1)

$$d_{cd} = (0.625/\pi^2) \times a_g \times S \times \eta_{eff} \times T_{eff} \times T_C =$$

$$(0.625/\pi^2) \times (0.40 \times 9.81 \text{ m/s}^2) \times 1.20 \times 0.512 \times 1.84 \text{ s} \times 0.5 \text{ s} = 0.14 \text{ m}$$

Check assumed displacement

Assumed displacement 0.14 m

Calculated displacement 0.14 m

 \Rightarrow Convergence achieved**Spectral acceleration S_e : (EN 1998-2 Table 7.1)**

$$S_e = 2.5 \times (T_C/T_{eff}) \times \eta_{eff} \times a_g \times S =$$

$$2.5 \times (0.5 \text{ s} / 1.84 \text{ s}) \times 0.512 \times 0.40 \text{ g} \times 1.20 = 0.166 \text{ g}$$

Isolation system shear force V_d : (EN 1998-2 eq. 7.10)

$$V_d = K_{eff} \times d_{cd} = 43541 \text{ kN/m} \times 0.14 \text{ m} = 6096 \text{ kN}$$

Typically LBDP analysis leads to maximum displacements of the isolating system and UBDP analysis leads to maximum forces in the substructure and the deck. However the latter is not always true as it is demonstrated by this example. In this particular example the LBDP analysis leads to larger shear force ($V_d=6292 \text{ kN}$) in the substructure than the corresponding shear force from UBDP analysis ($V_d=6096 \text{ kN}$). This is attributed to the fact that the increase of forces due to the effect of reduced effective damping in the LBDP analysis ($\xi_{eff}=0.1853$ for LBDP vs $\xi_{eff}=0.331$ for UBDP) is more dominant than the reduction of forces due to the effect of increased effective period in the LBDP analysis ($T_{eff}=2.27 \text{ s}$ in LBDP vs $T_{eff}=1.84 \text{ s}$ in UBDP).

8.4.6 NON-LINEAR TIME-HISTORY ANALYSIS

8.4.6.1 General

The non-linear time-history analysis for the ground motions of the design seismic action is performed with direct time integration of the equation of motion using the Newmark constant acceleration integration method with parameters $\gamma=0.5$, $\beta=0.25$. The integration time step is generally constant and equal to 0.01s, which is subdivided in its half value if convergence is not achieved. At each iteration convergence is achieved when the non-balanced non-linear force is less than 10^{-4} of the total force.

The equation of motion that describes the response of the system is:

$$M\ddot{U} + C\dot{U} + KU + F_{NL}(U, \dot{U}) = -M\ddot{U}_g$$

where:

M is the mass matrix of the structure

C is the damping matrix of the structure

K is the stiffness matrix for the linear part of the structure

F_{NL} is the force of the non-linear part of the structure (i.e. the isolators) which depends on the displacements U , the velocities \dot{U} , and the loading history.

The stiffness matrix K and the mass matrix M are determined from geometry, cross-section properties and element connectivity of the structure. The damping matrix C is determined as a linear combination of mass matrix and stiffness matrix according to the following equation (Rayleigh damping):

$$C = aK + bM$$

For the examined structure the damping ratio of the system is $\xi=5\%$ for all modes except for the modes where seismic isolation dominates for which the damping of the rest of structure is ignored $\xi=0$. This behaviour is established by setting $b=0$. The coefficient a is determined as $a = T_n \xi_n / \pi$ in order to achieve damping ξ_n at period T_n . Assuming damping 5% at period 0.10s the coefficient is $a=0.00159$ s. In Fig. 8.57 the damping ratio as a function of mode period is shown corresponding to the applied damping matrix C . The damping for periods $T > 1.5$ s where seismic isolation dominates is very small ($\xi < 0.3\%$). For these periods energy dissipation occurs primarily from the non-linear response of the isolators. For very small periods $T < 0.05$ s the damping increases significantly ($\xi > 10\%$). This is desirable because modes with periods in the same order of magnitude as the time step cannot be integrated with accuracy and it is preferable to filter them with increased damping.

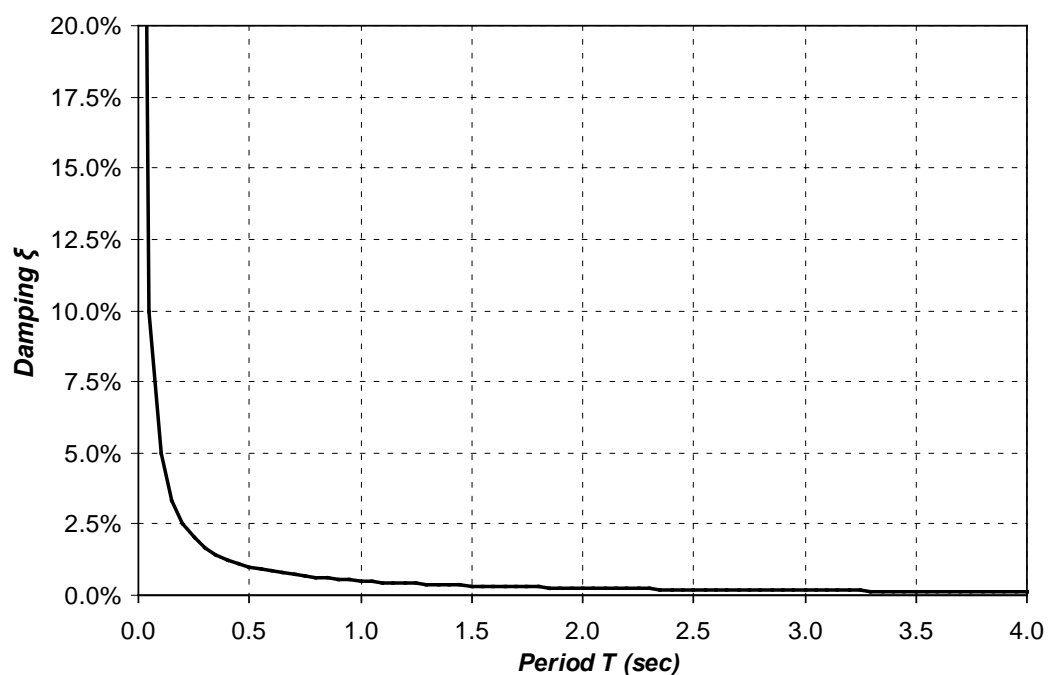


Fig. 8.57 Damping as a function of the period of the modes

8.4.6.2 Action effects on the seismic isolation system

In the following figures the hysteresis loops are shown for an abutment bearing (C0_L) and a pier bearing (P1_L) for both LBDP and UBDP analyses.

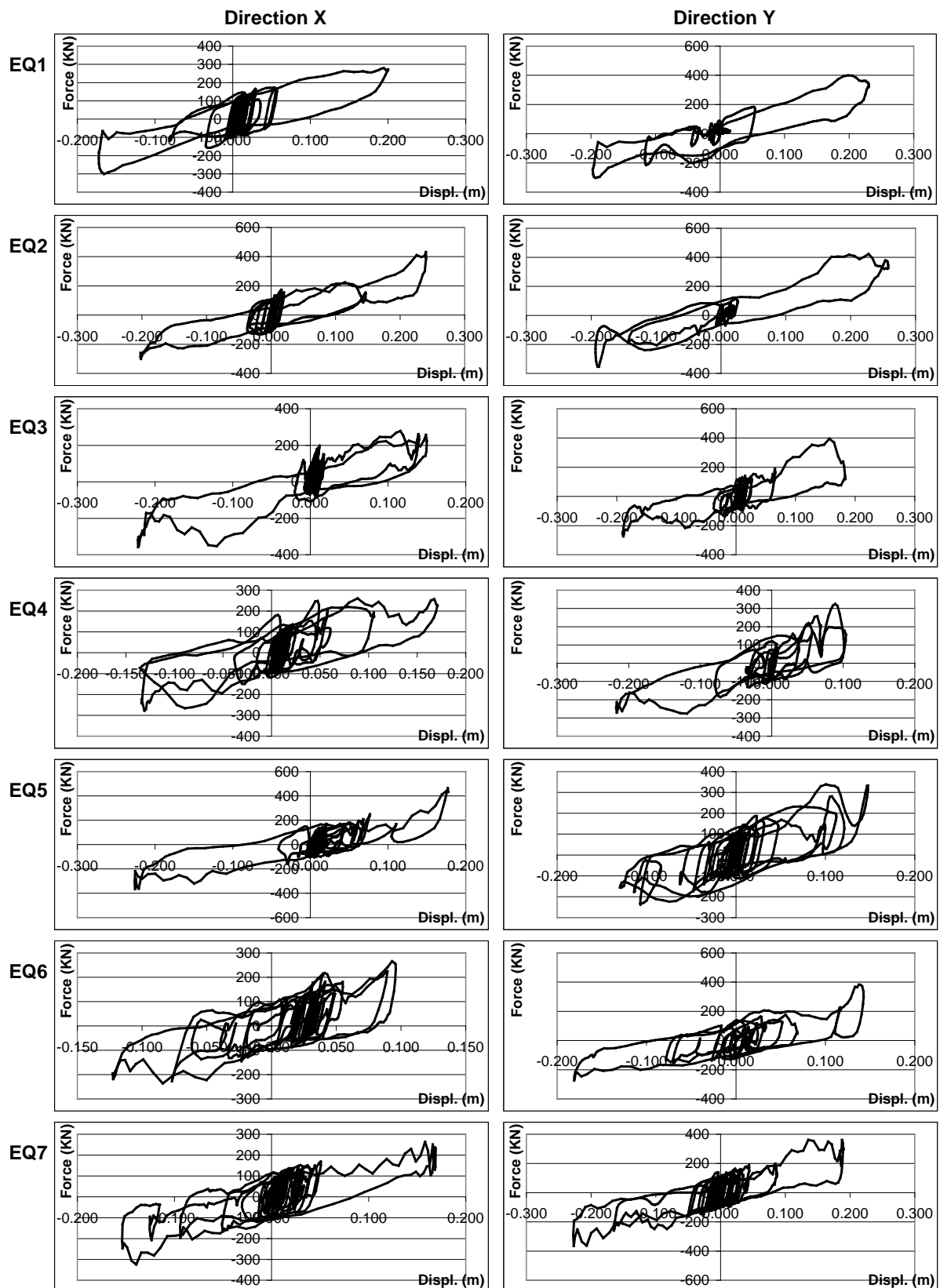


Fig.8.58 Hysteresis loops for abutment bearing C0_L for the analysis with LBDP.

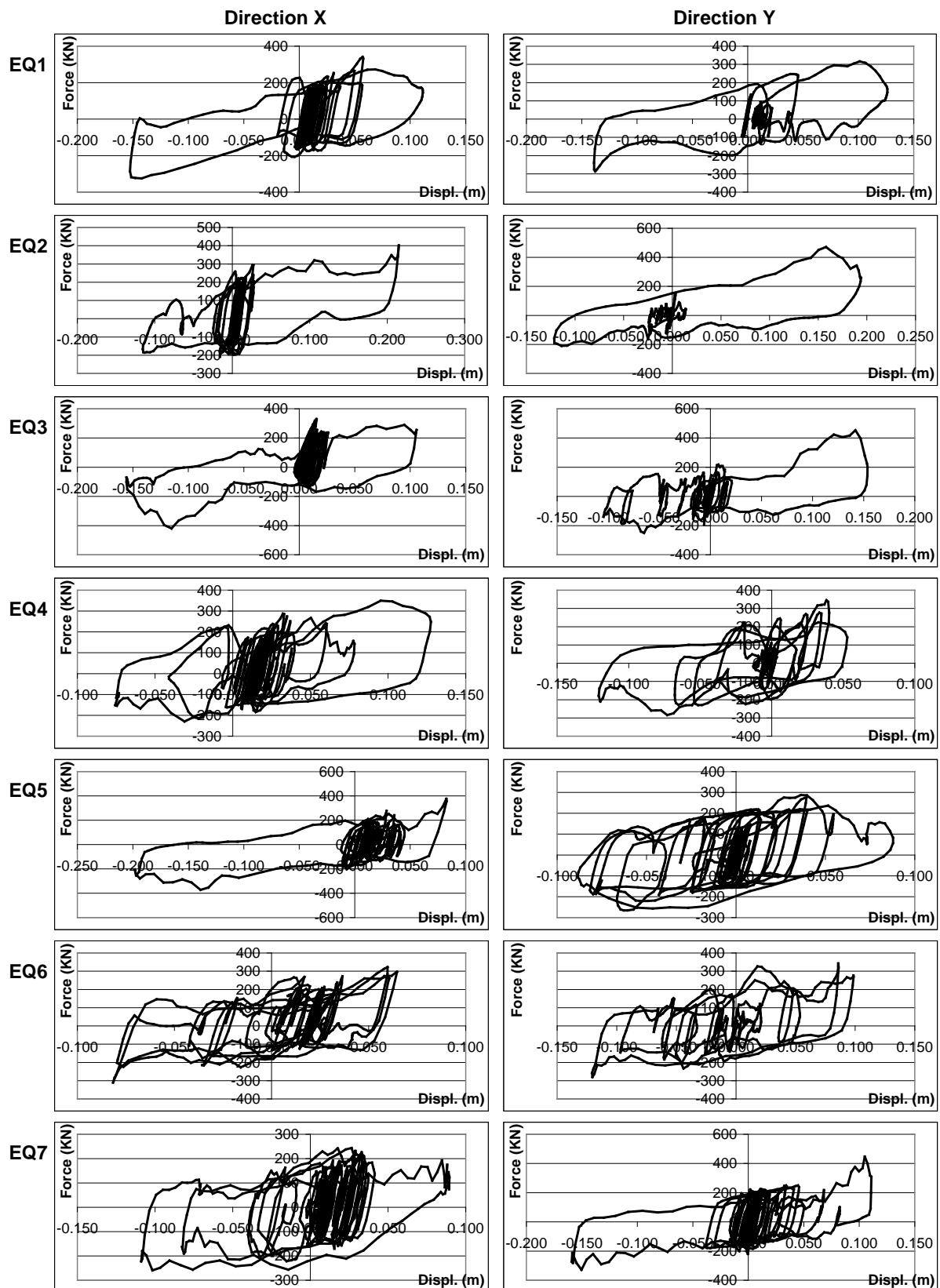


Fig. 8.59 Hysteresis loops for abutment bearing C0_L for the analysis with UBDP.

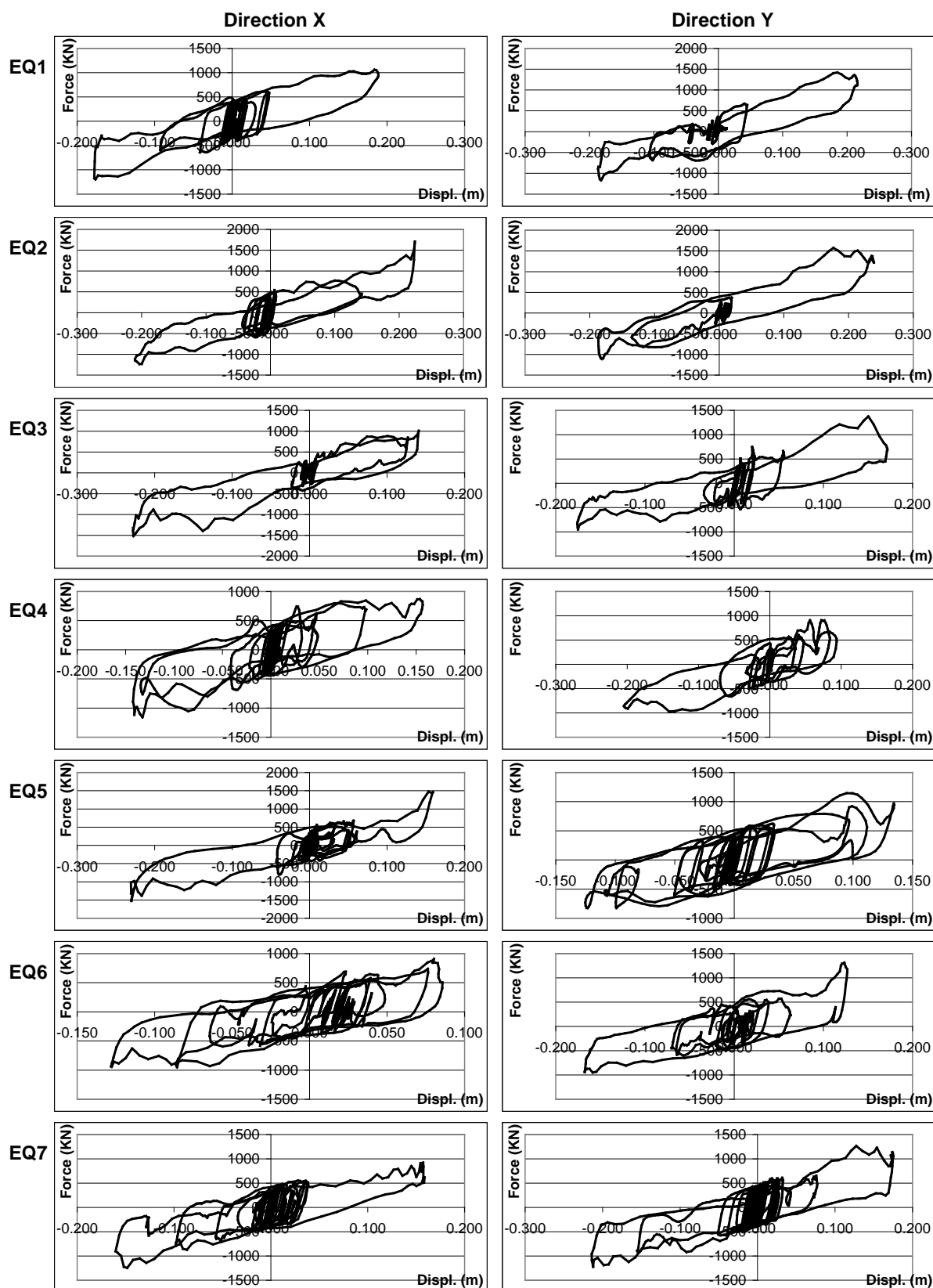


Fig. 8.60 Hysteresis loops for pier bearing P1_L for the analysis with LBDP.

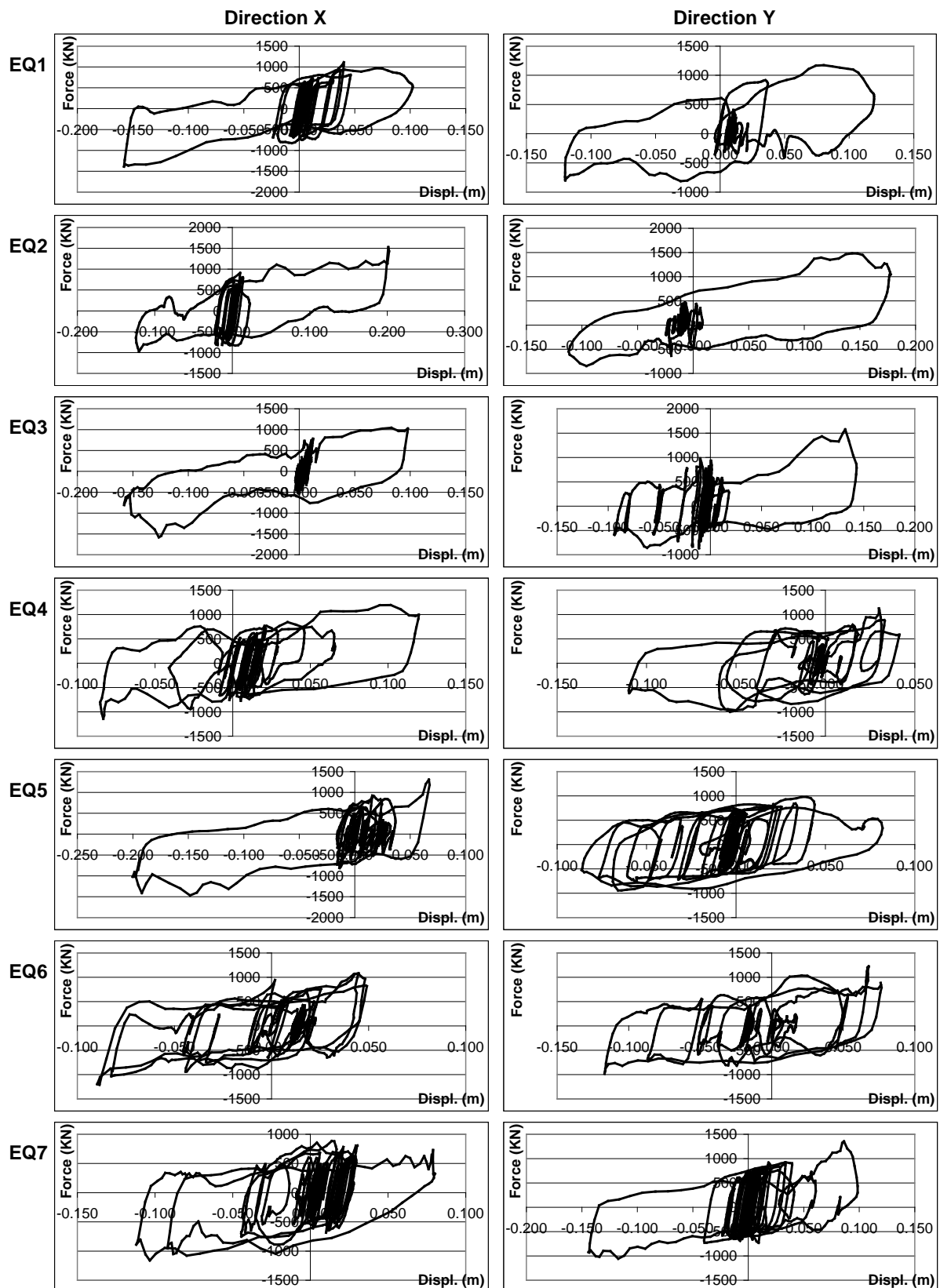


Fig. 8.61 Hysteresis loops for pier bearing P1_L for the analysis with UBDP.

In Table 8.18 and Table 8.19 the time-history analysis results are presented for the left and right bearing at each pier (P1_L, P1_R, P2_L, P2_R) and abutment location (C0_L, C0_R, C3_L, C3_R). According to EN 1998-2:2005+A1:2009, 4.2.4.3 when the analysis is carried out for at least 7 seismic motions, the average of the individual responses may be assumed as design value. The analysis results correspond to the average of seven earthquake ground motions EQ1 to EQ7. The results include the action effects of seismic action and permanent loads. They do not include the effects of temperature and creep/shrinkage in the seismic design combination.

$d_{Ed,x}$ is the displacement along longitudinal direction, $d_{Ed,y}$ is the displacement in transverse direction, d_{Ed} is the magnitude of the displacement vector in horizontal plane, a_{Ed} is the magnitude of the rotation vector in horizontal plane, N_{Ed} is the vertical force on the bearing (positive when compressive), $V_{Ed,x}$ is the horizontal force of the bearing in longitudinal direction, $V_{Ed,y}$ is the horizontal force of the bearing in transverse direction, V_{Ed} is the magnitude of horizontal force vector.

Table 8.18 Bearings - Results of Analysis for Lower Bound Design Properties (LBDP)

Bearing	$ d_{Ed,x} $ (m)	$ d_{Ed,y} $ (m)	d_{Ed} (m)	a_{Ed} (rad)	$N_{Ed,min}$ (kN)	$N_{Ed,max}$ (kN)	$ V_{Ed,x} $ (kN)	$ V_{Ed,y} $ (kN)	V_{Ed} (kN)
C0_L	0.193	0.207	0.255	0.00498	848.7	3310.3	346.0	375.7	469.0
C0_R	0.193	0.207	0.254	0.00509	860.4	3359.4	363.2	389.8	482.4
C3_L	0.199	0.207	0.258	0.00486	855.3	3323.9	402.5	372.0	501.4
C3_R	0.199	0.207	0.257	0.00494	858.5	3309.3	418.4	368.4	496.0
P1_L	0.188	0.193	0.244	0.00367	4541.1	12086.0	1328.5	1295.0	1654.2
P1_R	0.188	0.192	0.243	0.00381	4435.4	11994.8	1369.8	1284.5	1690.0
P2_L	0.189	0.193	0.245	0.00369	4560.3	12084.6	1336.1	1283.5	1654.3
P2_R	0.189	0.192	0.243	0.00380	4498.0	11912.9	1365.0	1283.2	1688.5
Total							6929.3	6652.1	

Table 8.19 Bearings - Results of Analysis for Upper Bound Design Properties (UBDP)

Bearing	$ d_{Ed,x} $ (m)	$ d_{Ed,y} $ (m)	d_{Ed} (m)	a_{Ed} (rad)	$N_{Ed,min}$ (kN)	$N_{Ed,max}$ (kN)	$ V_{Ed,x} $ (kN)	$ V_{Ed,y} $ (kN)	V_{Ed} (kN)
C0_L	0.149	0.139	0.182	0.00469	655.0	3157.9	352.6	380.4	449.8
C0_R	0.149	0.139	0.181	0.00475	624.1	3110.3	363.4	366.8	452.3
C3_L	0.157	0.139	0.185	0.00466	677.2	3112.5	400.6	368.6	489.6
C3_R	0.157	0.138	0.185	0.00461	684.8	3096.8	390.6	360.1	473.0
P1_L	0.149	0.128	0.173	0.00361	3912.7	11246.7	1361.8	1273.8	1630.8
P1_R	0.149	0.128	0.172	0.00355	3781.8	11408.5	1352.6	1185.7	1587.1
P2_L	0.150	0.128	0.173	0.00359	3793.6	11246.2	1379.7	1255.4	1605.7
P2_R	0.149	0.127	0.173	0.00354	3886.4	11378.4	1370.1	1187.1	1603.4
Total							6971.3	6377.8	

8.4.6.3 Check of lower bound on action effects

According to EN 1998-2:2005+A1:2009, 7.5.6(1) and 7.5.5(6) the resulting displacement of the stiffness centre of the isolating system (d_{cd}) and the resulting total shear force transferred through the isolation interface (V_d) in each of the two-horizontal directions, are subject to lower bounds which correspond to 80% of the corresponding quantities d_{cf} , V_f which are respectively the design displacement and the shear force transferred through the isolation interface, calculated in accordance

with the Fundamental mode spectrum analysis. These lower bounds are applicable for both multi-mode spectrum analysis and time-history analysis. The verification of the displacement and shear lower bounds is presented below:

- Displacement in X direction: $\rho_d = d_{cd} / d_f = 0.193\text{m} / 0.22\text{m} = 0.88 > 0.80 \Rightarrow \text{ok}$
- Displacement in Y direction: $\rho_d = d_{cd} / d_f = 0.207\text{m} / 0.22\text{m} = 0.94 > 0.80 \Rightarrow \text{ok}$
- Total shear in X direction: $\rho_v = V_d / V_f = 6929.3\text{kN} / 6292\text{kN} = 1.10 > 0.80 \Rightarrow \text{ok}$
- Total shear in Y direction: $\rho_v = V_d / V_f = 6652.1\text{kN} / 6292\text{kN} = 1.06 > 0.80 \Rightarrow \text{ok}$

From the above ratios it is concluded that the time-history analysis results compared to those of the fundamental mode analysis are 12% smaller for displacements and 10% larger for total shear force. This discrepancy between the comparison of displacements and forces is attributed to the effect of vertical earthquake component on bearing forces, which is not taken into account in the Fundamental Mode method of analysis. For spherical sliding bearings the horizontal bearing shear forces are always proportional to the vertical bearing loads. The variation of the vertical bearing loads due to the vertical ground motion component affects also the horizontal shear forces. This effect is evident in the wavy nature of the force-displacement hysteresis loops of the isolators that were presented in the previous paragraph.

8.4.7 VERIFICATION OF THE ISOLATION SYSTEM

8.4.7.1 Displacement demand of the isolation system

The displacement demand of the isolators is determined in accordance with EN 1998-2:2005+A1:2009, **7.6.2(1)P** and **7.6.2(2)P**. In each direction the displacement demand $d_{m,i}$ is determined by adding the seismic design displacement $d_{bi,d}$ increased by the amplification factor γ_{IS} with recommended value $\gamma_{IS} = 1.50$ and the offset displacement $d_{G,i}$ due to permanent actions, long-term deformations, and 50% of the thermal action.

The offset displacement due to 50% of the thermal action is determined as follows. The design values of the uniform component of the thermal action in the range -25°C to $+35^\circ\text{C}$. Assuming that the fixed point of thermal expansion/contraction is located at one of the two piers this leads to an effective expansion/contraction length L_T of 140m for abutment bearings and 80m for pier bearings. Therefore the offset displacement due to 50% of thermal action is:

Abutments: $0.5 \times \Delta T \times L_T \times \alpha = 0.5 \times (-45^\circ\text{C}) \times 140000\text{mm} \times 1.0 \times 10^{-5} = -31.5\text{mm}$

$$0.5 \times \Delta T \times L_T \times \alpha = 0.5 \times (+55^\circ\text{C}) \times 140000\text{mm} \times 1.0 \times 10^{-5} = +38.5\text{mm}$$

Piers: $0.5 \times \Delta T \times L_T \times \alpha = 0.5 \times (-45^\circ\text{C}) \times 80000\text{mm} \times 1.0 \times 10^{-5} = -18.0\text{mm}$

$$0.5 \times \Delta T \times L_T \times \alpha = 0.5 \times (+55^\circ\text{C}) \times 80000\text{mm} \times 1.0 \times 10^{-5} = +22.0\text{mm}$$

Where sign “+” corresponds to deck movement towards abutments and sign “-” corresponds to deck movement towards bridge center.

The total offset displacement including the effects of permanent actions, long term deformations and 50% of the thermal action is calculated as follows:

Abutments: Towards bridge center: $-8\text{mm} - 31,5\text{mm} = -39,5\text{mm}$

Towards abutments: $+38.5\text{mm}$

Piers: Towards bridge center: $-3\text{mm} - 18,0\text{mm} = -21,0\text{mm}$

Towards abutments: $+22.0\text{mm}$

A particular aspect of FPS isolators is the fact that the displacement capacity of the bearing is the same in all horizontal directions. The maximum displacement of the isolator occurs in a direction that does not coincide in general with one of the two principal directions. The maximum required displacement demand in the most critical direction may be estimated by examining the time history of the magnitude of the resultant displacement vector in horizontal plane XY, including the effect of offset displacements due to permanent actions, long term displacements, and 50% of the thermal action. According to EN 1998-2:2005+A1:2009, **7.6.2(1)P** and **7.6.2(2)P** the displacement demand is required to be estimated in the principal directions and not in the most critical direction. However this is not adequate for bearings with the same displacement capacity in all horizontal directions such as the FPS bearings.

In Table 8.20 the displacement demand of the abutment and pier bearings is estimated in both principal directions. Moreover the critical displacement demand in the horizontal XY plane is estimated. It is concluded that for the examined case the displacement demand in the horizontal XY plane is approximately 25% larger than the estimated displacement demand in the principal directions.

Table 8.20 Required displacement demand of isolators

Bearing	Abutment bearings C0_L, C0_R, C3_L, C3_R	Pier bearings P1_L, P1_R, P2_L, P2_R
Required displacement demand in longitudinal direction X	329	305
Required displacement demand in transverse direction Y	311	290
Required displacement demand in horizontal plane XY	407	382
Maximum	407	382

Therefore the required displacement demand of the isolators is 407mm for abutment bearings and 382mm for pier bearings.

8.4.7.2 Restoring capability of the isolation system

The lateral restoring capability of the isolation system is verified in accordance with EN 1998-2:2005+A1:2009 **7.7.1**. The equivalent bilinear model of the isolation system is shown in Fig. 8.62, where:

$F_0 = \mu_d N_{Ed}$ is the force at zero displacement

$K_p = N_{Ed} / R_b$ is the post-elastic stiffness

d_p is the maximum residual displacement for which the isolation system can be in static equilibrium in the considered direction.

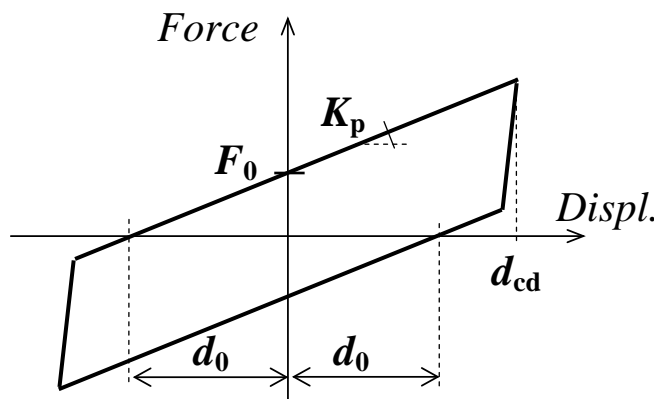


Fig. 8.62 Properties of bilinear model for restoring capability verification.

The displacement d_0 is given for an isolation system consisting of spherical sliding isolators as:

$$d_0 = F_0 / K_p = \mu_d \times N_{Ed} / (N_{Ed} / R_b) = \mu_d \times R_b$$

According to EN 1998-2:2005+A1:2009, **7.7.1(2)** isolation system has adequate self-restoring capability if $d_{cd} / d_0 > \delta$ is true in both principal directions, where δ is a numerical coefficient with recommended value $\delta = 0.5$. This criterion is verified for both UBDP and LBDP of the isolators. Lower values of design displacement d_{cd} give more conservative results:

- Longitudinal direction, LBDP: $d_{cd} / d_0 = 0.193\text{m} / (0.051 \times 1.83\text{m}) = 2.07 > 0.50$
- Transverse direction, LBDP: $d_{cd} / d_0 = 0.207\text{m} / (0.051 \times 1.83\text{m}) = 2.22 > 0.50$
- Longitudinal direction, UBDP: $d_{cd} / d_0 = 0.149\text{m} / (0.09 \times 1.83\text{m}) = 0.90 > 0.50$
- Transverse direction, UBDP: $d_{cd} / d_0 = 0.138\text{m} / (0.09 \times 1.83\text{m}) = 0.84 > 0.50$

Therefore in accordance with EN 1998-2:2005+A1:2009, **7.7.1(2)** the restoring capability of the isolation system is adequate without additional increase of the displacement capacity d_m . It is noted that UBDP give more unfavourable results because d_{cd} is larger and d_0 is smaller as compared to LBDP.

8.4.8 VERIFICATION OF SUBSTRUCTURE

8.4.8.1 Action effect envelopes for piers

In Table 8.21 and Table 8.22 action effect envelopes are provided for the substructure based on the results of time-history analysis. The results are given for the piers P1, P2 at their base and for abutments C0, C3 at the midpoint between the bearings (i.e. at the bearing level). According to EN 1998-2:2005+A1:2009, **4.2.4.3** when time history analysis is carried out for at least 7 seismic motions, the average of the individual responses may be assumed as the design seismic action. Therefore the design value of the seismic action is calculated as the average of the seven earthquake ground motions EQ1 to EQ7.

The action effects envelopes correspond to the seismic combination of EN 1998-2:2005+A1:2009, **5.5(1)P**, which includes the permanent actions, the combination value of traffic load, and the design seismic action. In accordance with EN 1998-2:2005+A1:2009, **5.5(2)P** the action effects due to imposed deformations need not be combined with seismic action effects. Therefore the presented action effects do not include the effects of temperature and shrinkage. In accordance with EN 1998-2:2005+A1:2009 **7.6.3(2)** the design seismic forces due to the design seismic action alone, may be derived from time history analysis forces after division by the q-factor corresponding to limited

ductile/essentially elastic behaviour, i.e. $q \leq 1.50$. The effect of q-factor is not included in the presented results, and it will be included at the design stage of the pier cross-sections.

The following notation is used:

- P is the vertical force i.e. axial force (positive when acting upwards),
- $V_2 = V_X$ is the shear force along X axis, $V_3 = V_Y$ is the shear along Y axis,
- T is the torsional moment,
- $M_2 = M_X$ is the moment about X axis (i.e. moment produced by earthquake acting in the transverse direction), and $M_3 = M_Y$ is the moment about Y axis (i.e. moment produced by earthquake acting in the longitudinal direction).
- The signs of V_2 / M_3 are the same when their directions are compatible with earthquake forces acting in the longitudinal direction. The signs of V_3 / M_2 are the same when their directions are compatible with earthquake forces acting in the transverse direction.

Envelopes of maximum/minimum and concurrent internal forces are presented for each pier/abutment location. For instance envelope max P corresponds to the design situation where the value of the vertical force P is algebraically maximum. The values of other forces V_2 , V_3 , T, M_2 , M_3 at max P envelope are the “concurrent” forces when P becomes maximum.

The maximum/minimum and the “concurrent forces” for each envelope are derived as follows:

1. The maxima/minima of each force (say $\max M_2$, $j=1 \div 7$) over all time steps of the history of each motion $j=1 \div 7$ are assessed. The design value of the maximum/minimum of the examined force (say $M_{2,d}$) is assumed equal to the average of these maxima/minima ($\max M_2$, $j=1 \div 7$) for the 7 motions, i.e

$$M_{2,d} = \Sigma (\max M_2, j=1 \div 7) / 7$$

2. The results of the seismic motion producing the extreme value (say $\max \max M_2$) of these maxima/minima for all motions, and the corresponding time step, are used as basis for the assessment of the “concurrent” values of the other forces. At the aforementioned results a scaling factor is applied which is equal to the ratio of the design value of the examined force ($M_{2,d}$) divided by the extreme value ($\max \max M_2$), i.e. $= M_{2,d} / \max \max M_2$.

Table 8.21 Substructure - Envelopes of Analysis for Lower Bound Design Properties

Location	Envelope	Fz (kN)	V2 (kN)	V3 (kN)	T (kNm)	M2 (kNm)	M3 (kNm)
C0	max P	-1754.3	-18.3	158.3	-14.6	824.8	-1.8
C0	min P	-6535.1	-347.5	123.9	23.1	380.1	-34.7
C0	max V2	-4930.5	616.5	-163.2	85.1	-475.4	61.6
C0	min V2	-3688.2	-660.5	-115.7	-82.2	-482.2	-66.0
C0	max V3	-5623.1	617.2	684.1	-192.6	1933.0	61.7
C0	min V3	-4124.3	-469.5	-694.6	-190.5	-2002.9	-47.0
C0	max T	-2759.9	358.3	-393.2	183.1	-1388.7	35.8
C0	min T	-2989.8	-341.2	-505.2	-216.0	-1867.7	-34.1
C0	max M2	-3789.3	-383.9	608.9	272.1	2575.8	-38.4
C0	min M2	-4324.0	-493.4	-730.7	-312.4	-2701.2	-49.3
C0	max M3	-4930.5	616.5	-163.2	85.1	-475.4	61.6
C0	min M3	-3688.2	-660.5	-115.7	-82.2	-482.2	-66.0
C3	max P	-1787.9	-105.4	113.9	31.5	654.5	-10.5
C3	min P	-6439.8	379.4	134.5	-32.2	446.2	37.9
C3	max V2	-4241.8	783.1	-110.8	56.9	-328.9	78.3
C3	min V2	-3389.9	-562.1	-106.0	-66.8	-429.4	-56.2
C3	max V3	-5460.4	666.9	680.5	-238.2	2046.7	66.7
C3	min V3	-4149.3	-401.9	-660.4	-172.9	-1867.8	-40.2
C3	max T	-1975.2	257.9	-301.0	172.4	-1131.7	25.8
C3	min T	-2760.7	312.5	435.8	-215.7	1809.1	31.2
C3	max M2	-4001.7	453.0	631.7	-312.7	2622.4	45.3
C3	min M2	-4533.2	591.8	-690.8	395.7	-2597.2	59.2
C3	max M3	-4241.8	783.1	-110.8	56.9	-328.9	78.3
C3	min M3	-3389.9	-562.1	-106.0	-66.8	-429.4	-56.2
P1	max P	-12756.8	50.1	-236.8	60.2	-3971.0	254.0
P1	min P	-27232.5	228.2	640.6	451.2	7982.2	2143.8
P1	max V2	-16241.5	3339.4	-500.1	105.8	-4786.2	29347.6
P1	min V2	-17636.3	-2906.9	86.6	-77.7	-1838.1	-22629.6
P1	max V3	-16658.7	1112.7	2666.1	-758.9	33869.5	11127.1
P1	min V3	-15829.2	-909.9	-2698.2	-450.8	-27964.5	-9661.0
P1	max T	-8022.6	961.5	-813.0	575.0	-12731.0	9403.4
P1	min T	-13056.5	2514.3	919.9	-768.1	17367.8	22613.0
P1	max M2	-16393.7	1095.0	2623.7	-746.9	33330.7	10950.1
P1	min M2	-18669.2	-1073.1	-3182.3	-531.7	-32981.8	-11394.4
P1	max M3	-16142.4	3319.0	-497.1	105.2	-4756.9	29168.5
P1	min M3	-18598.0	-2499.2	-1830.2	-240.9	-15284.0	-26831.4

Continuation of Table 8.21

Location	Envelope	Fz (kN)	V2 (kN)	V3 (kN)	T (kNm)	M2 (kNm)	M3 (kNm)
P2	max P	-12560.1	-792.5	-174.2	161.5	4432.2	-6724.3
P2	min P	-27066.2	-230.7	715.6	-339.1	8957.0	-2180.8
P2	max V2	-16266.7	3383.2	-506.5	156.6	-4842.4	29890.9
P2	min V2	-17867.1	-2879.8	84.6	-83.3	-1807.9	-22406.6
P2	max V3	-16650.4	1099.1	2678.2	-777.1	34062.3	11054.4
P2	min V3	-15988.2	-956.8	-2711.5	-429.9	-28164.0	-10018.0
P2	max T	-7732.6	960.9	-781.8	575.5	-12189.7	9395.1
P2	min T	-12784.1	2478.8	860.4	-766.8	16575.8	22343.7
P2	max M2	-16276.3	1074.4	2618.0	-759.6	33297.0	10806.1
P2	min M2	-18798.5	-1125.0	-3188.1	-505.5	-33114.5	-11778.9
P2	max M3	-16195.0	3368.3	-504.3	155.9	-4821.0	29759.0
P2	min M3	-18734.3	-2470.9	-1809.2	-255.8	-15186.2	-26514.7

Table 8.22 Substructure - Envelopes of Analysis for Upper Bound Design Properties

Location	Envelope	Fz (kN)	V2 (kN)	V3 (kN)	T (kNm)	M2 (kNm)	M3 (kNm)
C0	max P	-1326.0	116.0	-80.6	-12.6	62.0	11.6
C0	min P	-6076.0	-594.2	-94.3	-38.4	-365.0	-59.4
C0	max V2	-3620.5	627.6	-93.9	53.1	-347.0	62.8
C0	min V2	-3503.1	-693.8	-158.1	-133.9	-687.2	-69.4
C0	max V3	-3737.8	149.9	686.9	-105.3	2696.7	15.0
C0	min V3	-3996.2	-375.4	-640.2	-176.4	-2085.3	-37.5
C0	max T	-2699.6	-22.2	-197.0	300.3	149.2	-2.2
C0	min T	-3260.5	479.0	471.3	-241.3	1937.6	47.9
C0	max M2	-3222.0	97.5	597.8	-89.8	2655.5	9.7
C0	min M2	-4111.4	-219.5	-555.6	-199.5	-2575.7	-21.9
C0	max M3	-3620.5	627.6	-93.9	53.1	-347.0	62.8
C0	min M3	-3503.1	-693.8	-158.1	-133.9	-687.2	-69.4
C3	max P	-1417.6	-76.4	45.9	61.4	384.7	-7.6
C3	min P	-6053.3	614.1	-86.6	37.5	-339.1	61.4
C3	max V2	-4215.2	768.4	-147.3	39.3	-381.3	76.8
C3	min V2	-3079.4	-586.3	-151.7	-96.5	-525.6	-58.6
C3	max V3	-4496.6	636.9	669.0	-347.4	2340.9	63.7
C3	min V3	-3930.0	-296.3	-635.4	-149.4	-2069.0	-29.6
C3	max T	-2417.7	325.0	-359.0	233.9	-1283.0	32.5
C3	min T	-2709.4	390.4	425.5	-285.9	1840.4	39.0

Continuation of Table 8.22

Location	Envelope	Fz (kN)	V2 (kN)	V3 (kN)	T (kNm)	M2 (kNm)	M3 (kNm)
C3	max M2	-3961.3	570.8	622.0	-418.1	2690.9	57.1
C3	min M2	-4233.5	-117.5	-558.0	-8.8	-2615.1	-11.8
C3	max M3	-4215.2	768.4	-147.3	39.3	-381.3	76.8
C3	min M3	-3079.4	-586.3	-151.7	-96.5	-525.6	-58.6
P1	max P	-11444.7	-125.6	566.0	7.6	7410.2	-1131.0
P1	min P	-25719.8	320.3	1735.7	382.5	22258.8	3219.5
P1	max V2	-15188.6	3632.5	-168.5	83.2	-2160.6	32565.5
P1	min V2	-17329.4	-3190.1	-282.4	-106.6	-3773.0	-27647.3
P1	max V3	-16196.9	1183.0	2666.2	-949.5	33694.2	12871.0
P1	min V3	-14597.6	1.4	-2828.3	-175.7	-29913.1	-580.6
P1	max T	-12907.1	1473.0	-804.9	693.2	-13503.0	14798.4
P1	min T	-11198.9	2406.9	983.3	-1016.0	18338.9	21664.8
P1	max M2	-15952.1	1165.1	2626.0	-935.1	33185.2	12676.5
P1	min M2	-15337.1	1.4	-2971.5	-184.6	-31428.6	-610.0
P1	max M3	-14829.4	3546.6	-164.5	81.2	-2109.5	31795.4
P1	min M3	-15090.4	-3183.3	127.2	-99.0	-246.6	-28584.3
P2	max P	-11479.8	216.1	583.7	-1.8	7643.4	2007.6
P2	min P	-25746.2	-28.7	1764.3	-409.5	22556.9	-372.2
P2	max V2	-15433.8	3702.6	-165.4	75.4	-2114.8	33190.2
P2	min V2	-15216.5	-3197.1	106.6	-115.6	-609.4	-28697.8
P2	max V3	-20549.5	280.4	2618.8	-304.4	29039.5	3324.9
P2	min V3	-14855.2	-49.9	-2856.8	-190.7	-30281.5	-930.3
P2	max T	-12267.8	1464.3	-764.4	741.6	-12727.1	14684.7
P2	min T	-11612.0	2520.1	953.8	-1006.9	17940.3	22796.5
P2	max M2	-16623.8	-340.0	2495.7	-120.7	32509.5	-2377.2
P2	min M2	-15508.7	-52.1	-2982.5	-199.1	-31613.6	-971.2
P2	max M3	-15110.2	3625.0	-161.9	73.8	-2070.5	32494.1
P2	min M3	-15128.2	-3178.6	106.0	-114.9	-605.9	-28531.2

8.4.8.2 Section verification of piers

a General

The maximum normalized axial force of the piers is calculated in accordance with EN1998-2 §5.3(4) as:

$$\eta_k = N_{Ed} / (A_c \times f_{ck}) = 27.2325 \text{ MN} / (5 \text{ m} \times 2.5 \text{ m} \times 35 \text{ MPa}) = 0.062 < 0.08$$

Therefore in accordance with EN1998-2 §6.2.1.1(2)P no confinement reinforcement is necessary. However due to the small axial force the pier should be designed by taking into account the minimum reinforcement requirements for both beams and columns.

b Verification for flexure and axial force

In accordance with EN 1998-2:2005+A1:2009 **7.6.3(2)** for the substructure the design seismic forces F_E due to the design seismic action alone, may be derived from the analysis forces after division by the q -factor corresponding to limited ductile/essentially elastic behaviour, i.e. $F_E = F_{E,A} / q$ with $q \leq 1.50$.

EN 1998-2:2005+A1:2009 6.5.1 contains certain reduced ductility measures (confinement reinforcement and buckling restraint reinforcement). However, it also offers the option to avoid these measures if the piers are designed so that $M_{Rd} / M_{Ed} < 1.30$. This option is selected in this example for reasons which will become transparent. Therefore for the design of longitudinal reinforcement the design seismic forces F_E are derived from the time-history analysis forces $F_{E,A}$ as follows. $F_E = F_{E,A} \times 1.30 / 1.50$.

The required reinforcement for the aforementioned design forces is calculated for flexural resistance in accordance with EN 1998-2:2005+A1:2009 **5.6.2(1)P**, for the most adverse design seismic actions, N_{Ed} , $M_{2,ed}$, $M_{3,ed}$ amounts to $A_s = 213.7 \text{ cm}^2$, uniformly distributed over the section perimeter

c Minimum longitudinal reinforcement

No specific requirement for a minimum value of the longitudinal reinforcement is specified in EN 1998-2.

The minimum reinforcement for columns as specified in EN1992-1-1:2004, **9.5.2(2)** is equal to:

$$A_{s,min} = \max(0.1 \times N_{Ed} / f_{yd}, 0.002A_c) = \max(0.1 \times 27232.5 \text{ kN} / (500000 \text{ kPa} / 1.15), 0.002 \times 5 \text{ m} \times 2.5 \text{ m}) = 0.025 \text{ m}^2 = 250 \text{ cm}^2$$

$$\text{i.e. } \min \rho = 0.2\%$$

EN1992-1-1:2004, **9.2.1.1(1)** specifies (for beams) a minimum tensile reinforcement for avoiding brittle failure following exceeding of the tensile concrete strength. This minimum is also applicable for any member for which flexural ductility is required. For uni-axial bending the minimum reinforcement of the tensioned face amounts

$$\rho_{1,min} = \max(0.26 \times f_{ctm} / f_{yk}, 0.0013)$$

For the total minimum reinforcement ρ_{min} of a rectangular section this leads to:

$$\rho_{min} \approx 3 \rho_{1,min} = 3 \max(0.26 \times f_{ctm} / f_{yk}, 0.0013) \approx \max(0.8 \times f_{ctm} / f_{yk}, 0.004)$$

For concrete C35/45 with $f_{ctm} = 3.2 \text{ MPa}$ and for reinforcement class C $f_{yk} = 500 \text{ MPa}$

$$\rho_{min} = 0.00512 = 0.51 \%$$

For the examined pier cross-section

$$A_{s,min} = 0.00512 \times 500 \text{ cm} \times 250 \text{ cm} = 640 \text{ cm}^2$$

In summary:

Required longitudinal reinforcement from section analysis: 213.73 cm^2 ($\rho=0.17\%$)

Required minimum longitudinal reinforcement: 640 cm^2 ($\rho_{min}=0.51\%$)

Provided longitudinal reinforcement: 1 layer $\Phi 28/13.5 = 45.61 \text{ cm}^2/\text{m}$ or 640 cm^2 in total ($\rho=0.51\%$)

Comment: The cross section of the piers could be substantially reduced

d Shear

For the design of shear reinforcement in accordance with EN 1998-2:2005+A1:2009 **5.6.2(2)P** verifications of shear resistance of concrete members shall be carried out in accordance with EN 1992-1-1:2004, **6.2**, with the following additional rules.

- a) The design action effects shall be calculated in accordance with EN1998-2 5.5(1)P, where the seismic action effect A_{Ed} shall be multiplied by the behaviour factor q used in the linear analysis.
- b) The resistance values, $V_{Rd,c}$, $V_{Rd,s}$ and $V_{Rd,max}$ derived in accordance with EN 1992-1-1:2004, **6.2** shall be divided by an additional safety factor γ_{Bd1} against brittle failure, with recommended value $\gamma_{Bd1} = 1.25$. Therefore for the design of shear reinforcement the design seismic forces F_E are derived from the time-history analysis forces F_{EA} as follows. $F_E = F_{EA} \times 1.25$.

The required reinforcement for the aforementioned design forces is calculated for flexural resistance in accordance with EN 1998-2:2005+A1:2009 **5.6.2(2)P**. The results are presented below:

Required shear reinforcement in longitudinal direction: $59.03 \text{ cm}^2/\text{m}$

Required shear reinforcement in transverse direction: $23.66 \text{ cm}^2/\text{m}$

Provided shear reinforcement in longitudinal direction: $4 \times 2 \times 7.54 \text{ cm}^2/\text{m} + 2 \times 13.40 \text{ cm}^2/\text{m} = 87.1 \text{ cm}^2/\text{m}$ ($\rho_w = 0.174\%$)

Provided shear reinforcement in transverse direction: $2 \times 13.40 \text{ cm}^2/\text{m} = 26.8 \text{ cm}^2/\text{m}$ ($\rho_w = 0.107\%$)

The provided shear reinforcement satisfies the minimum requirements of EN1992-1-1:2004, **9.5.3** for columns:

- max. spacing = $0.6 \times \min(20 \times 28\text{mm}, 2500\text{mm}, 400\text{mm}) = 240\text{mm}$, Provided longitudinal spacing = $150\text{mm} < 240\text{mm} \Rightarrow \text{ok}$
- min. diameter = $(6\text{mm}, 28\text{mm} / 4) = 7\text{mm}$, Provided bar diameter = $12\text{mm} > 7\text{mm} \Rightarrow \text{ok}$

The provided shear reinforcement also satisfies the minimum requirements of EN1992-1-1:2004, **9.2.2** for beams:

- max. longitudinal spacing $s_{l,max} = 0.75 \times d \times (1 + \cot \alpha) = 0.75 \times 2400\text{mm} \times (1 + 0) = 1800\text{mm}$, Provided longitudinal spacing = $150\text{mm} < s_{l,max} = 1800\text{mm} \Rightarrow \text{ok}$
- max. transverse spacing $s_{t,max} = \min(0.75 \times d, 600\text{mm}) = \min(0.75 \times 2400\text{mm}, 600\text{mm}) = 600\text{mm}$, Provided transverse spacing = $530\text{mm} < s_{t,max} = 600\text{mm} \Rightarrow \text{ok}$
- min. shear reinforcement ratio $\rho_{w,min} = 0.08 \times (f_{ck})^{0.5} / f_{yk} = 0.08 \times (35)^{0.5} / 500 = 0.095\%$, Provided shear reinforcement ratio: $\rho_w = 0.174\%$ in longitudinal direction and $\rho_w = 0.107\%$ in transverse direction $> \rho_{w,min} = 0.095\% \Rightarrow \text{ok}$

The reinforcement of the pier base cross-section is shown in Fig. 8.63.

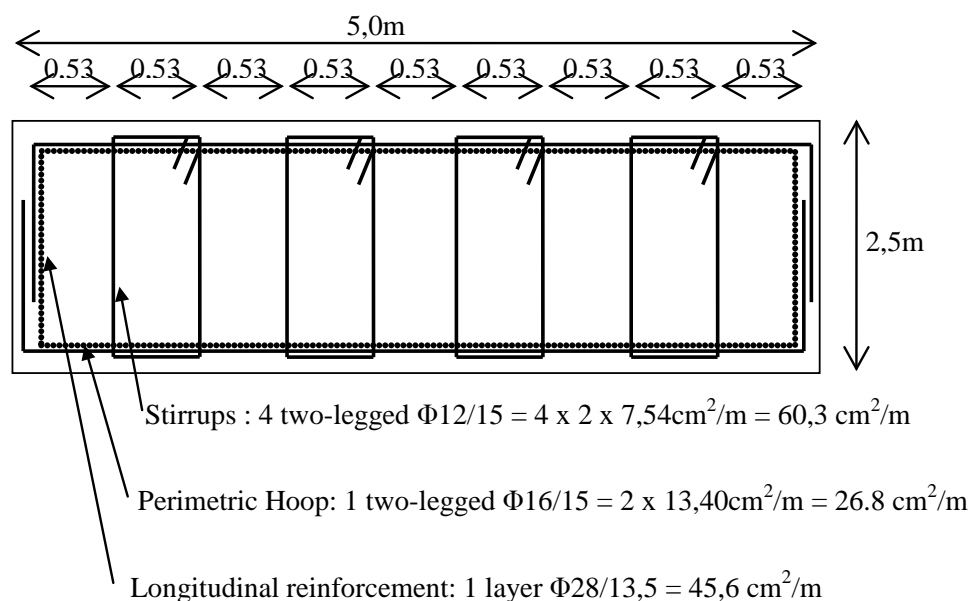


Fig. 8.63 Provided pier reinforcement.

8.4.9 DESIGN ACTION EFFECTS FOR THE FOUNDATION

8.4.9.1 Design actions effects from time-history analysis

In Table 8.23 action effect envelopes are provided for the design of the foundation based on the results of time-history analysis. The action effects for foundation design are derived in accordance with EN 1998-2:2005+A1:2009, **7.6.3(4)P** and **5.8.2(2)P** for bridges with seismic isolation. The seismic action for foundation design corresponds to the analysis results multiplied by the q -value (1.5) used for the design of the substructure (i.e. effectively corresponding to $q = 1$). The set of forces that are critical for the foundation design are the maximum/minimum shear force envelopes for the design of abutment foundation and the maximum/minimum bending moment at the base of the pier for the design of pier foundation. The analysis results for seismic combination are given for the piers P1, P2 at their base and for abutments C0, C3 at the midpoint between the bearings (i.e. at the bearing level). As mentioned before the presented action effects include permanent actions, combination value of traffic action, and seismic action. The signs of the forces for foundation design are presented in Fig. 8.64 below.

Table 8.23 Seismic combination action effects for foundation design

Location	Envelope	F _x (kN)	F _y (kN)	F _z (kN)	M _x (kNm)	M _y (kNm)	M _z (kNm)
C0, C3	Max F _x envelope	783	111	4242	329	78	57
	Max F _y envelope	470	695	4124	2003	47	191
P1, P2	Max M _y envelope	3625	162	15110	2070	32494	74
	Max M _x envelope	1095	2624	16394	33331	10950	747

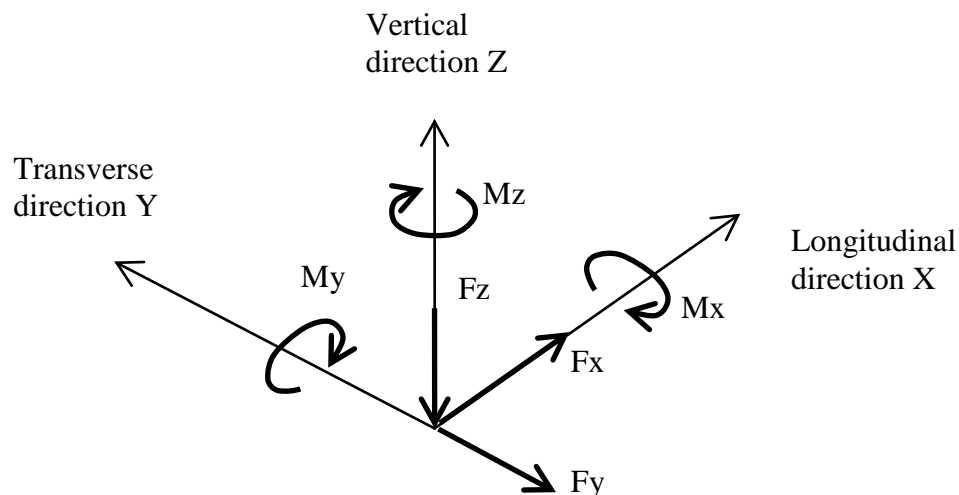


Fig. 8.64 Direction of forces F_x , F_y , F_z and moments M_x , M_y , M_z with positive sign for foundation design.

8.4.10 COMPARISON WITH FUNDAMENTAL MODE METHOD

The force and displacement results at the abutments and the base of piers derived from the time-history analysis are compared to the corresponding results of the fundamental mode method. Lower Bound Design Properties give the most unfavorable results with respect to substructure forces.

Before attempting this comparison, some practical considerations are necessary in the present case. These considerations refer to certain special features of the friction pendulum type of isolators and to their influence on the proper application of the fundamental mode method (FMM), as a stand-alone analysis:

- It is evident that the displacement of the FPS isolator in one direction only, as is considered by the FMM, is by necessity coupled to a simultaneous displacement in the transverse direction. This is of course valid also for the max displacement d_{cd} that is estimated by the FMM. For estimating an appropriate value for the transverse displacement occurring simultaneously with the max value d_{cd} , one should take account of the following two facts. The behavior of this isolator type is the same in all directions and the two seismic motion components, are considered to be statistically independent, but having similar frequency content. It is evident that the targeted value depends heavily on the characteristics of the two horizontal components of the seismic motion. However, a reasonable assumption for the probable value of the simultaneous transverse displacement appears to be $\frac{1}{2}$ of the max displacement i.e. $0.5d_{cd}$. Consequently, the effective value $d_{cd,e}$ of the max displacement, i.e. the length of the vector sum of the simultaneous displacements, may be assumed equal to $d_{cd,e} \approx 1.15d_{cd}$.
- The increased value $d_{cd,e}$ should be used also for the estimation of the max forces transferred through the isolator in any direction, as the isolator has no preferred directions.
- The vertical seismic motion component on the other hand, has also an effect on the variation of the friction forces of the isolator. The effect oscillates, with equal positive and negative values, about a zero mean value. This effect can be observed in the hysteresis loops of Fig.8.58, Fig. 8.59, Fig. 8.60, Fig. 8.61, for some of the seismic motions used (e.g. EQ7, and EQ3). The oscillations occur at much shorter periods than those of the horizontal motion, corresponding to the much higher frequency content of the vertical seismic component (see Fig. 8.51 and Fig. 8.52). Consequently this influence may be ignored at least regarding the

max displacements. Regarding the forces, the application also on the friction forces of the 1.15 multiplier estimated above, is a convenient approximation.

In Table 8.24 the displacement demand of abutment bearings and the total abutment shear are presented. In this table the following results are compared: a) the results of the time-history analysis as presented in the previous paragraphs and b) the results of the Fundamental Mode Method (FMM) using the 1.15 multiplier estimated above. The estimated displacement demand using the FMM is 3% larger than the corresponding displacement demand from time-history analysis. The estimated total shear using the FMM is 13% less in longitudinal direction and 3% less in transverse direction than the corresponding shear from time-history analysis.

Table 8.24 Comparison of displacement demand and total shear for abutment bearings in longitudinal direction

Method of analysis	Displacement demand (mm)	Total shear in longitudinal direction (kN)	Total shear in transverse direction (kN)
Time-history analysis	407	783	695
Fundamental Mode Method (FMM)	419	683	683

References

- Boore, D. M. and J. J. Bommer. 2005. Processing of Strong-Motion Accelerograms: Options and Consequences. *Soil Dynamics and Earthquake Engineering* 25: 93–115.
- Choi, D. H., and S. H. Lee. 2003. Multi-Damping Earthquake Design Spectra-Compatible Motion Histories. *Nuclear Engineering and Design* 226: 221–30.

APPENDICES

APPENDIX A

Design of steel bridges. Overview of key content of EN 1993.

Gerhard HANSWILLE

Bergische Universität

Wolfgang HENSEN

PSP - Consulting Engineers

Markus FELDMANN

RWTH Aachen University

Gerhard SEDLACEK

RWTH Aachen University

1. Introduction

- (1) Sustainability is a key-issue for the design of bridges including steel bridges. The most important sustainability indicator for bridges is durability with its effect on life cycle costs for an intended service life of about 100 years.
- (2) Durability is produced by various elements including
 - a sustainable definition of the service-condition including the bridge loading,
 - choice of the bridge system, its structural and non-structural components and products and appropriate detailing also considering fatigue,
 - design and execution for a quality of structure that effects durability.
- (3) Therefore this report does not focus only on design rules in Eurocode 3, but also comprises the other elements of the European Standard Family affecting durability, amongst which Eurocode 3 plays an important role.
- (4) According to the general concept of the Eurocodes these codes consist of a European part (the EN-codes) and National Annexes to the EN-codes, that complement the “harmonized” European EN-codes by “National choices”.
- (5) In conclusion the practical design of a bridge on a certain territory is not possible without the use of the National Annex valid for that territory.
- (6) The choices that are contained in the Eurocodes comprise the following:
 1. National responses to opening notes to Eurocode rules that include technical classes or factors related to safety, climatic, cultural and other aspects (see Guidance Paper L “Use and application of Eurocodes”).
 2. Response to “informative annexes” with technical rules and sets of alternative technical rules in the main code-text for which no agreement could be achieved during the code-writing phase and from which CEN/TC250 expects either National acceptance or better founded National Alternatives that could be used by CEN/TC250 for further harmonisation of the rules and the reduction of complexity and volume.
 3. “Non conflicting complementary informations”, (NCCI’s) that comprise National choices of additional technical rules necessary for filling gaps in the Eurocodes and to make them fully operable. From these NCCI’s CEN/TC250 expects important impulses for the further development of the Eurocodes.
- (7) Therefore in this report reference is made to the “Nationally Determined Parameters”, which are recommended in the Eurocodes for the design of Steel bridges and in some cases to the draft German National Annex, that may be considered as an example for the variations that may be induced by the many National Annexes in the EU.

2. Contents of the report

- (1) Figure 1 gives the structure of the report with a short introduction to the European Standard Family, the aspect of durable load assumption in particular from traffic on road bridges, an

example how to overcome shortcomings in the Eurocode-rules for the technical specifications for the delivery of bearings, the background and use of EN 1993-1-10 for the choice of steel to avoid brittle fracture and the core of the design of steel elements in bridges, that encompasses the stability rules, the fatigue rules and rules for tension elements, e.g. for stayed cable bridge.

LIST OF CONTENTS	
Dissemination of information for training – Vienna, 4-6 October 2010	2
1. The European Standard Family and Steel bridges	
2. Load assumptions for steel bridges	
3. Modelling of steel bridges	
4. Specification of bearings	
5. Choice of steel	
6. Design of bridge elements	
6.1. Stability rules	
6.2. Fatigue rules	
6.3. Rope structures	

Figure 1

3. General remarks to the European Standard Family for the design of steel bridges

- (1) Steel bridges for roads comprise full steel bridges with steel decks (orthotropic plates) and steel-concrete-composite bridges with a concrete deck, see [Figure 2](#) and [Figure 3](#).

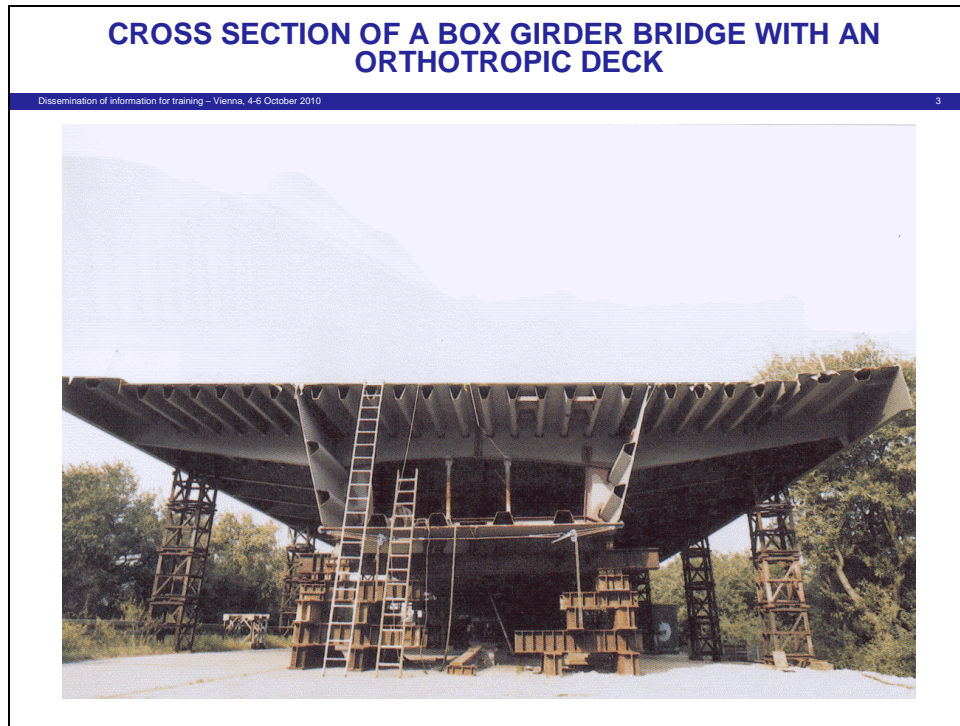


Figure 2



Figure 3

- (2) In both examples the main structure is a stiffened box-girder with cantilevering plates with the assembly of sections prefabricated in the workshop on one shore on site and erection by launching.
- (3) There is a criticism that the design of bridges would become more and more complicated because of the large amount and large volumes of the standards making the users life difficult.

As the detailing of rules that produces the volumes is however required by the users there are two possibilities to create a better survey:

1. to develop appropriate “navigation systems” through the standards (as practiced e.g. for the EN-standards for energy-efficiency),
2. to develop “consolidated handbooks” from the standards for particular application fields as e.g. bridges, in which the technical rules and references from the Eurocodes are assembled in a way suitable for “water-tight” contracting and security of use. Examples for such “handbooks” in bridge design are
 - No. 1: Basis and design of actions for bridges
 - No. 2: Design of concrete bridges
 - No. 3: Design of steel bridges
 - No. 4: Design of composite bridges
 as practiced in Austria and Germany.

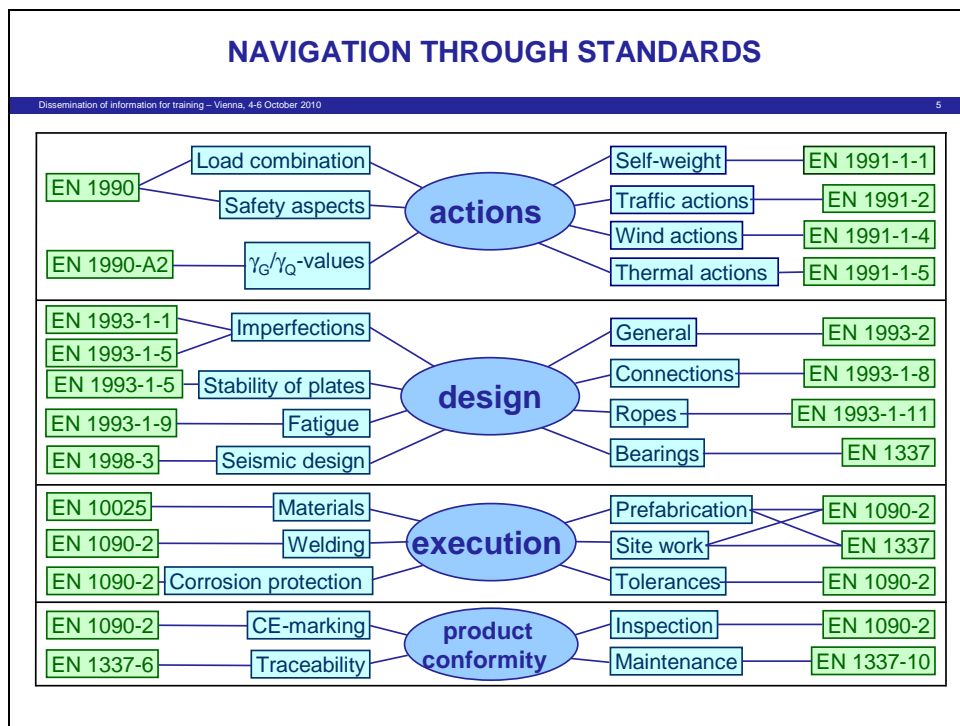


Figure 4

- (4) Figure 4 shows a shortened example for a navigation system related to actions, design, execution and product conformity that allows the user to “google” the rule he needs.

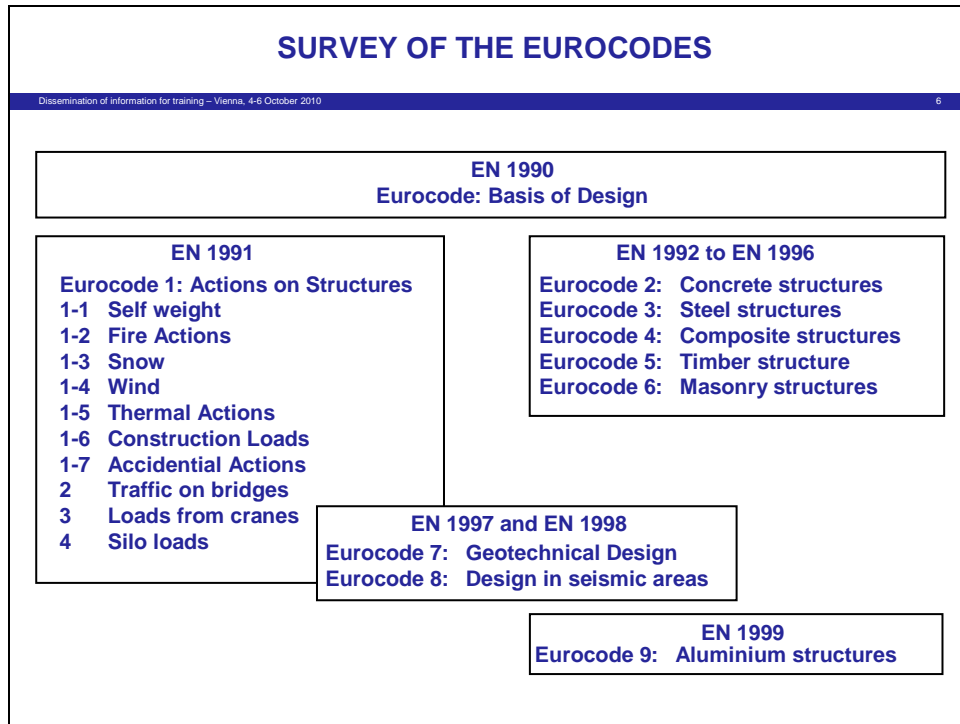


Figure 5

- (5) Figure 5 gives a survey on all Eurocodes from which the user should select those rules relevant to his design works:

Under the general principles in EN 1990 - Basis of Design - there are on one side the various generic rules for actions (as snow and wind) and the specific action rules as e.g. traffic loads on bridges and on the other side the material-dependant rules for various materials and types of structures. EN 1997 - Geotechnical Design - and EN 1998 - Design in seismic areas - comprise both generic rules for actions and specific rules for resistances and materials.

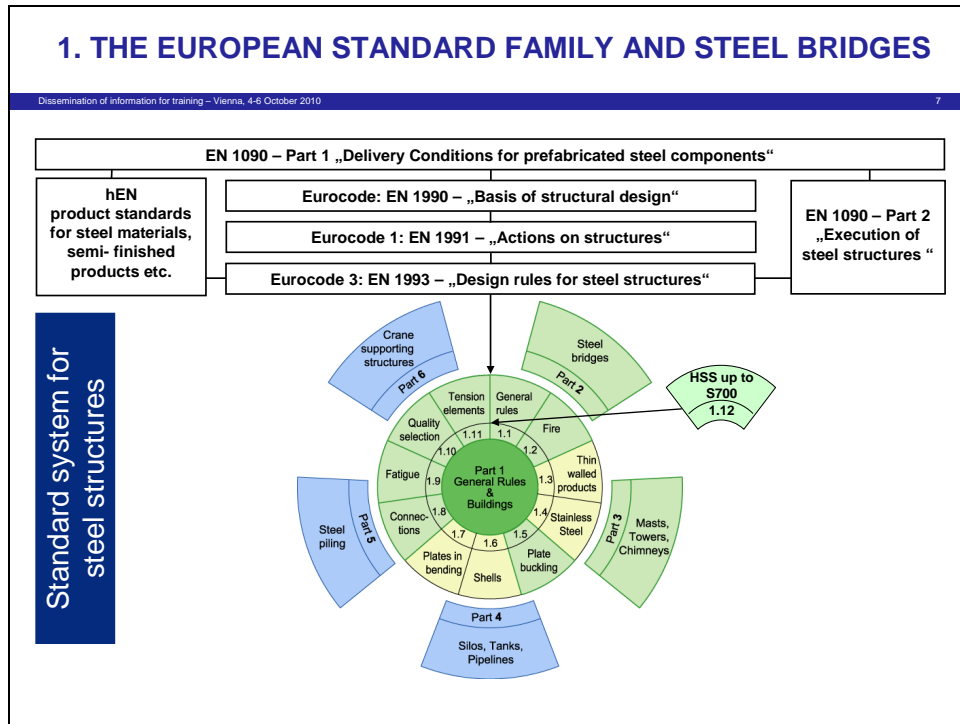


Figure 6:

- (6) Figure 6 shows the organisation of the family of standards for the design of steel bridges.

The umbrella standard for “Delivery Conditions for prefabricated steel components” on the global market with a part for the conformity assessment is EN 1090-Part 1.

This part takes reference to

- hEN product standards that give product properties from testing methods defined by statistical characteristics that are suitable for a reliable design,
 - the Eurocodes that give design rules both for prefabricated components and for structural works,
 - EN 1090-2 that contains the rules for execution in the workshop and on site with rules for good workmanship, tolerances etc.
- (7) Eurocode 3 comprises in a similar way as the action-code generic design rules in its central part 1 addressing e.g. plate buckling and fatigue, and specific additional rules in peripheric application parts as for bridges (Eurocode 3 - Part 2), that take reference to the generic rules in Part 1.

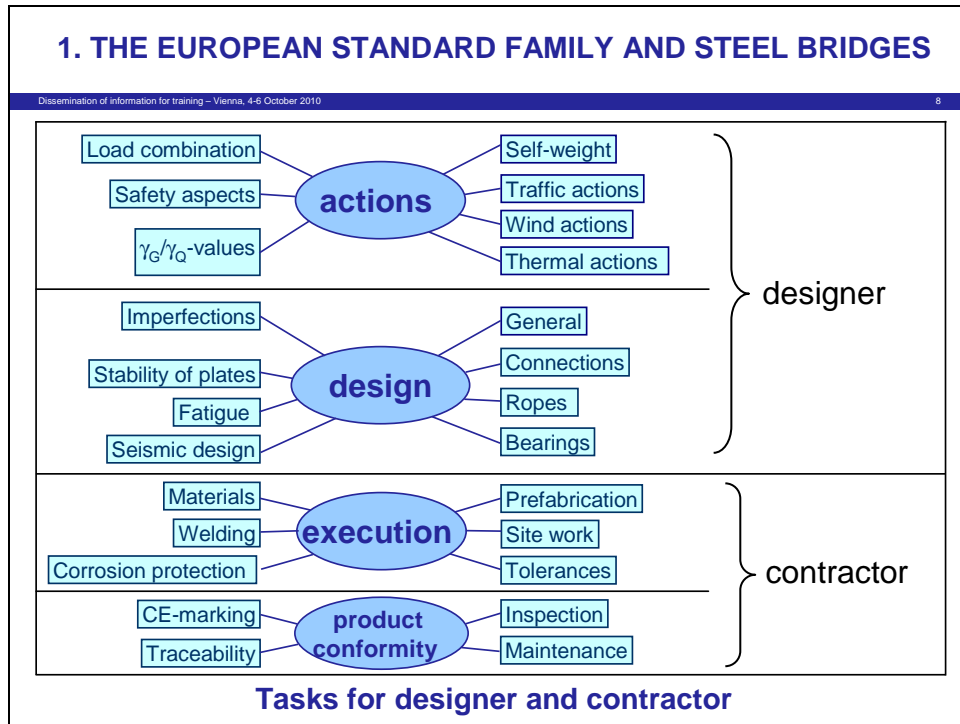


Figure 7

- (8) In this report only rules for actions and for design are addressed as demonstrated in Figure 7, whereas rules for execution and product conformity that are mainly used by the contractors are not dealt with.

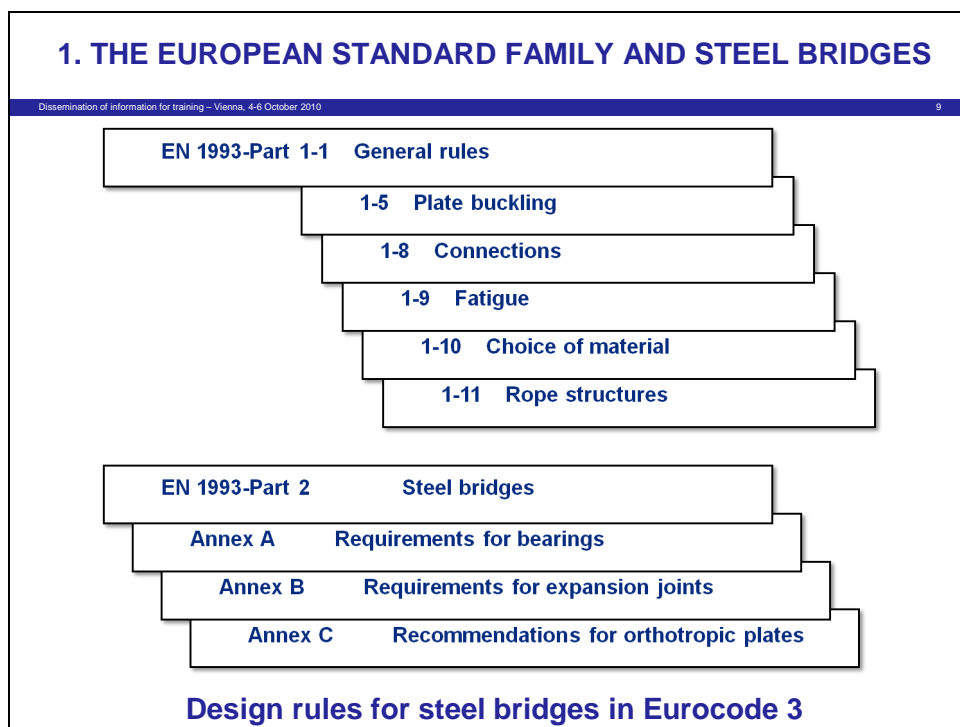


Figure 8

- (9) Figure 8 gives the design rules in Eurocode 3 which are relevant for the design of steel bridges.

The controlling part for design is Eurocode 3 - Part 2, with reference to Eurocode 3 - Part 1-1, in particular to general rules for structural analysis, cross-sectional verifications, use of imperfections for stability checks e.g. flexural buckling, and lateral torsional buckling, to Part 1-5 for plate buckling, to Part 1-8 covering connections, to Part 1-9 for fatigue, to Part 1-10 for choice of material and to Part 1-11 for rope structures.

- (10) EN 1993-2 has an Annex C with recommendations for the design and the execution of orthotropic steel bridge decks covering now 50 years of experience with durable deck plates, that may make specific numerical fatigue checks unnecessary.
- (11) EN 1993-2 contains also the annexes A and B for the preparation of specifications for the delivery of bearings and transition joints, for which EN 1990 – Annex A 2 did not give specific rules. These annexes are material independent so that they are applicable to concrete-, steel- and composite-bridges. Therefore in the future they will be transferred to EN 1990, and the tentative titles Annex E₁ and E₂ have been agreed.
- (12) These new Annexes should in particular contain appropriate rules for the representative values of actions and their combinations to give design values of forces and movements that are in compliance with the evaluations of measurements as obtained from many decades of use; the values now recommended in the Eurocodes would produce movements that are in the range of 1.5 ÷ 2.0 of the values experienced in the past and also would not be suitable for the specification of bearing characteristics from an integral analysis of the total system of superstructure, bearings, piers and foundations.
- (13) Therefore the draft of German National Annex related to Requirements for bearings and transition joints is related to the future Annexes E₁ and E₂ and contains a proposal that prevents the problems as described above.

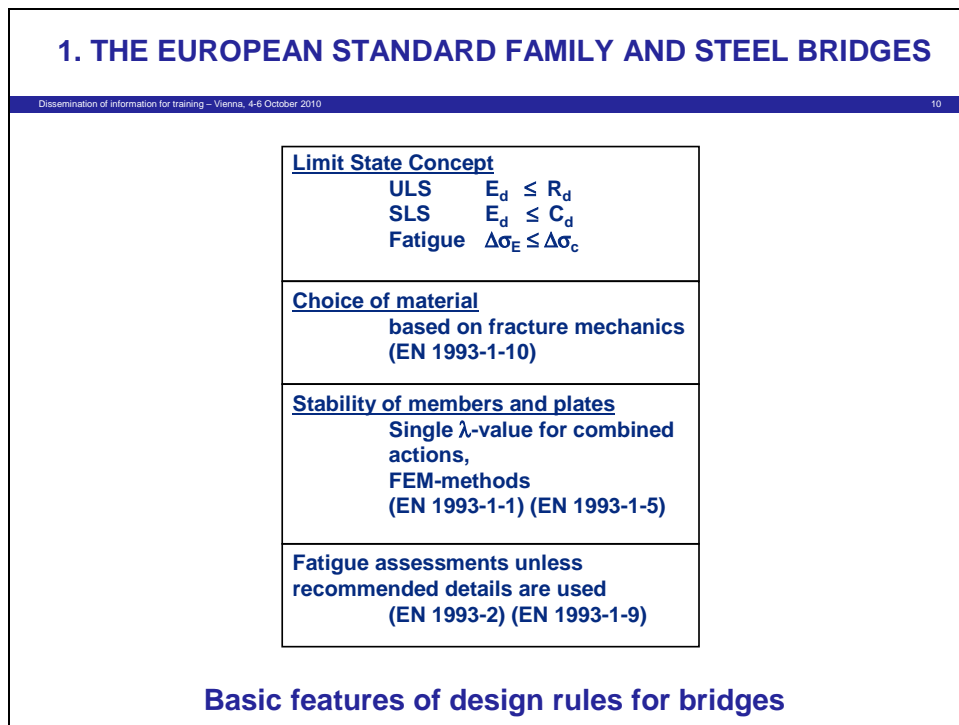


Figure 9

(14) The basic assessments that a bridge designer has to accomplish are listed in [Figure 9](#):

- Checks comprise the Limit States ULS, SLS and Fatigue.
- A particularity of steel structures exposed to external climate actions and fatigue from traffic, wind and rain is the choice of steel to avoid brittle failure.
- Another particularity is the use of thin-walled slender components, which need stability checks for out-of-plane stability as lateral torsional buckling and plate buckling, suitable for computer-aided design.
- Fatigue assessments are necessary because of the fatigue effects of traffic actions, unless structural details successfully time-tested are used that need no further numerical fatigue check.

4. How to get a sustainable loading model

4.1 Loading model and 100 years of service life

- (1) The loading model LM1 as specified in EN 1991-Part 2 gives a European uniform geometric pattern of concentrated loads and uniformly distributed loads the magnitudes of which have been decided to leave them to the choice of each Member State to obtain a sustainable loading model, see [Figure 10](#).

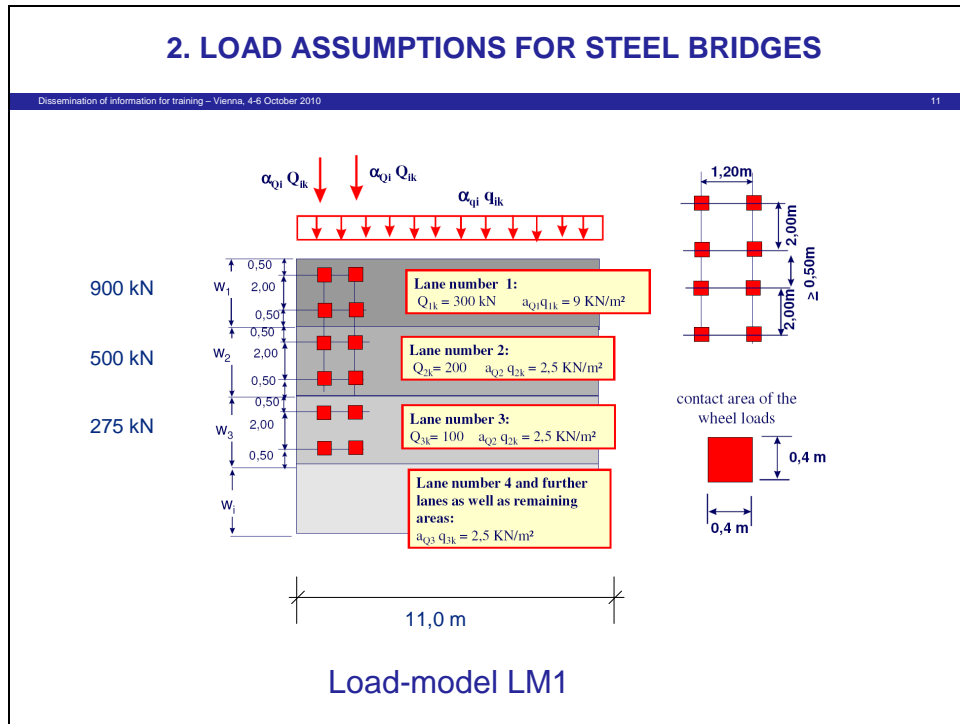


Figure 10

- (2) The loading pattern as well as the recommended values for the loads originate from a common European study made under the chairmanship of H. Mathieu in the 1st phase and Prof. J.A. Calgaro in the final phase, that was carried out by specialists of various EU-members on the basis of measurements in the various countries undertaken in the late 1980ths.
- (3) The composition of the road traffic in the Highway Paris-Lyon at Auxerre has been decided to be the statistical basis for defining recommendations for characteristic values, as this composition seemed to be representative for future developments in all Europe.
- (4) The characteristic values were defined with a return period of 1000 years instead of the usual values of 50 years because of the prevailing requirement of serviceability on this level and sustainability of decision.

Whereas a 50 years-return period would have meant a 98%-fractile of the annual distribution of extreme values in the mean (i.e. for 50% of the bridge population), the 1000 years-return period means a 98%-fractile of the annual distribution of extreme values for 95% of the bridge population.

- (5) The responses of Member States in their NA's are expected not to be homogeneous, because
 - traffic conditions are very regional,
 - some countries use extraordinary loads in addition to the standard load model,
 - some countries use load classes for their road-network.

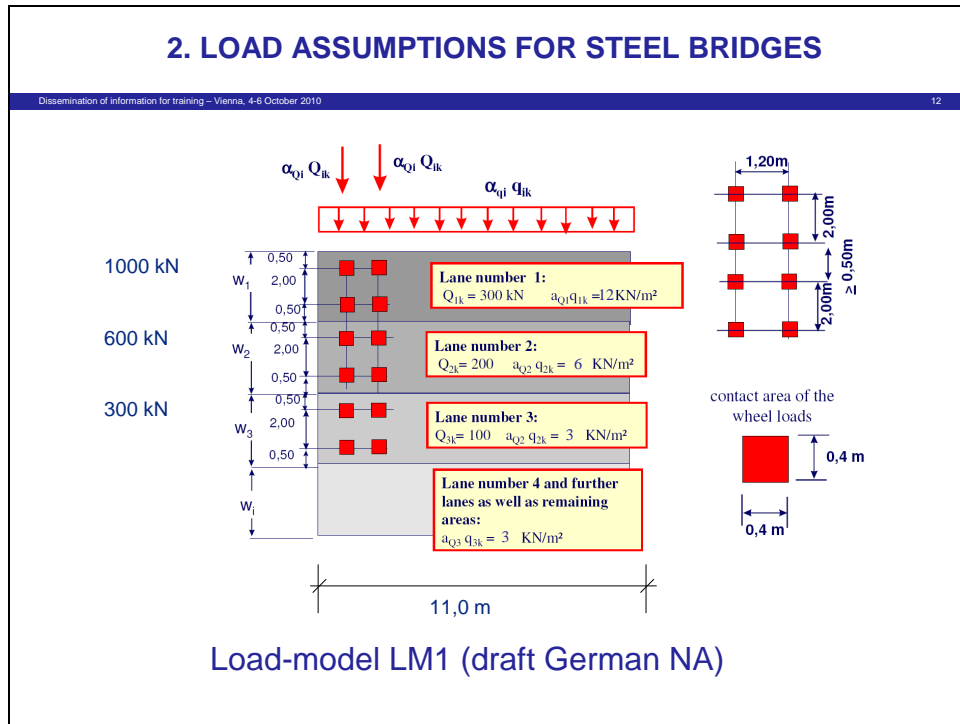


Figure 11

- (6) An example for a response is the draft loading model in the German NA as given in [Figure 11](#). It reflects the following conditions:
1. All α -values are equal or above 1.0 because the future trends in traffic developments must be taken into account. In comparing the characteristic vehicle weights for a length of 11m the increase is about 10%.
 2. The values of the uniformly distributed loads are increased by $\alpha = 1.30$ except for the second heavy lane where the increase is by 2.40. This is due to the results of evaluations of traffic measurements performed during the drafting works and explained hereafter.
 3. The increase of about 1.30 is justified by simulations of future traffic compositions (including 60 t modular heavy vehicles) taking account of “rubber trains” with a freight volume substantially larger than used today and with a smarter freight management.
- (7) This example is specific for Germany being the largest transit country at the crossing point of North-South- and East-West-traffic and with limited controls on the roads.

4.2. Background of the load model LM1 and of the recommended characteristic load values

- (1) The statistical background of traffic measurements on the highway in Auxerre has been documented as given in [Figure 12](#).
- (2) It has been used with other statistical data to perform dynamic numerical simulations with bridges of various influence surfaces to obtain a realistic view on the statistics of action effects in the bridges. To this end the dynamic behaviour of vehicles has been modelled by rigid bodies with non linear springs, dampers and friction elements and the surface roughness

of the asphalt was artificially generated with Power Spectral Density classifications according to ISO-TC 108, see Figure 13.

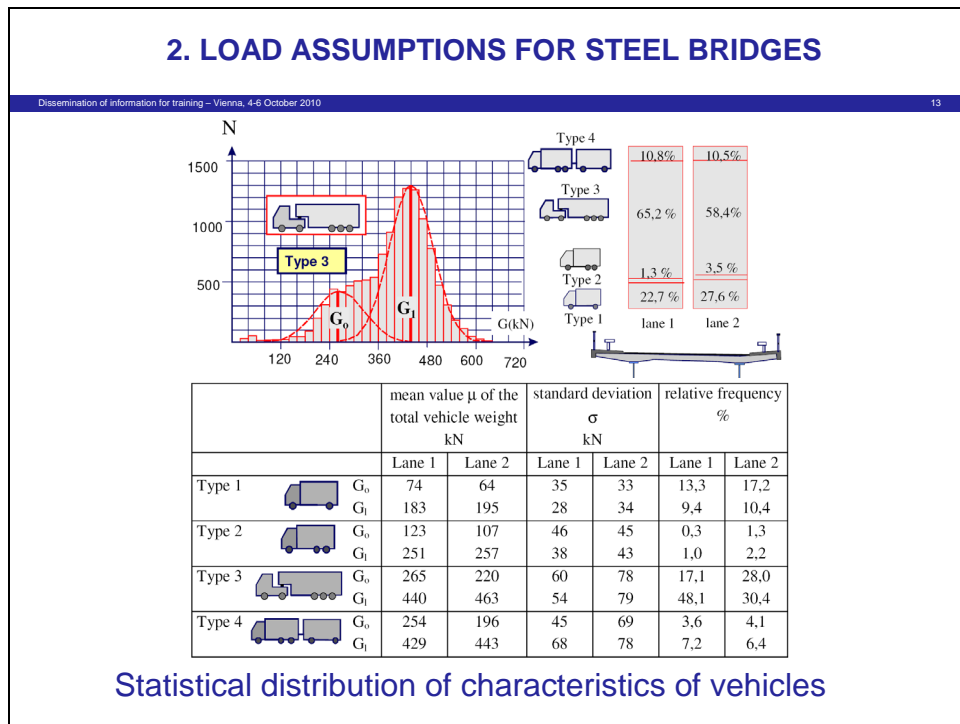


Figure 12

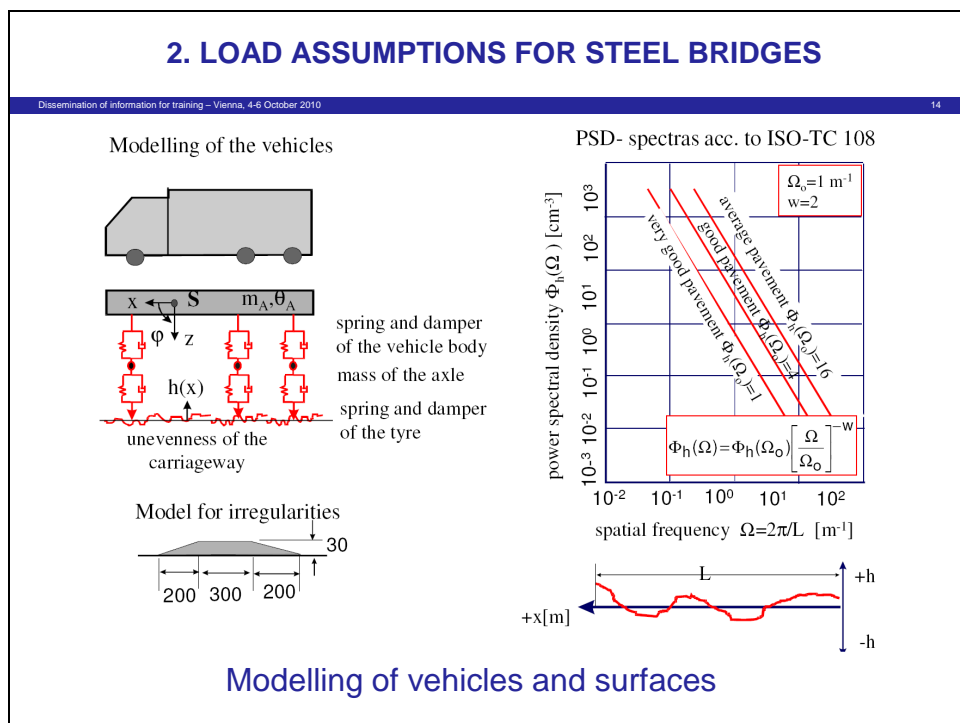


Figure 13

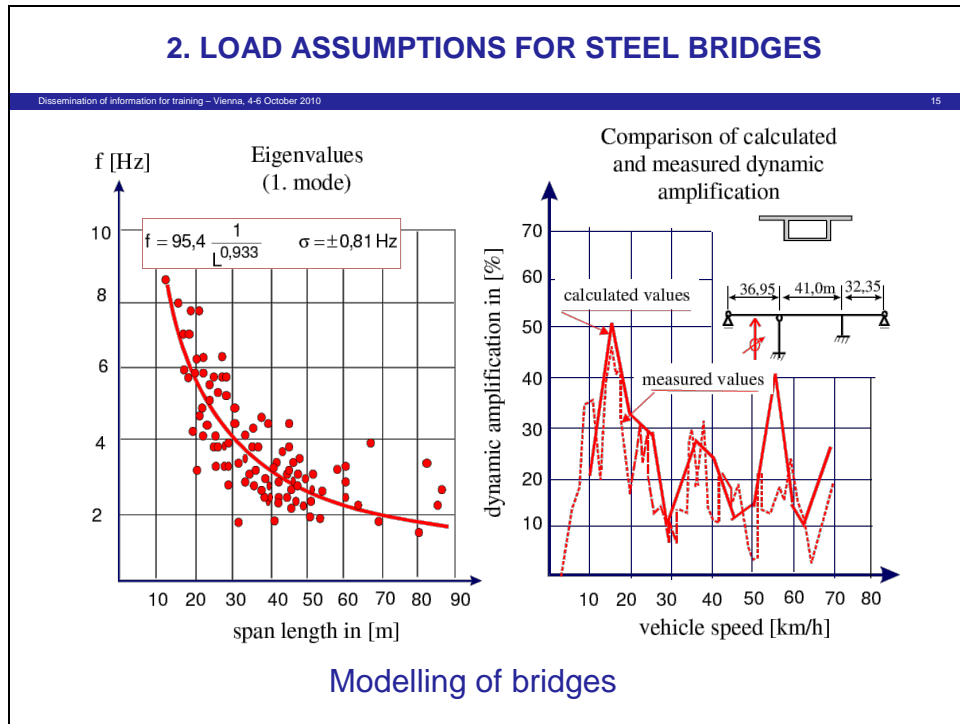


Figure 14

- (3) Bridges were modelled as elastic-mass-systems with an eigenfrequency-span characteristic given in [Figure 14](#). This Figure also gives the results of model calibration with tests carried out at EMPA-Zürich.
- (4) The results of the simulations are given in [Figure 15](#) for the case of mid-span moments of a three span continuous bridge. Apparently the effects of load model LM1 are safesided in this case to cope for other requirements from other influence lines.

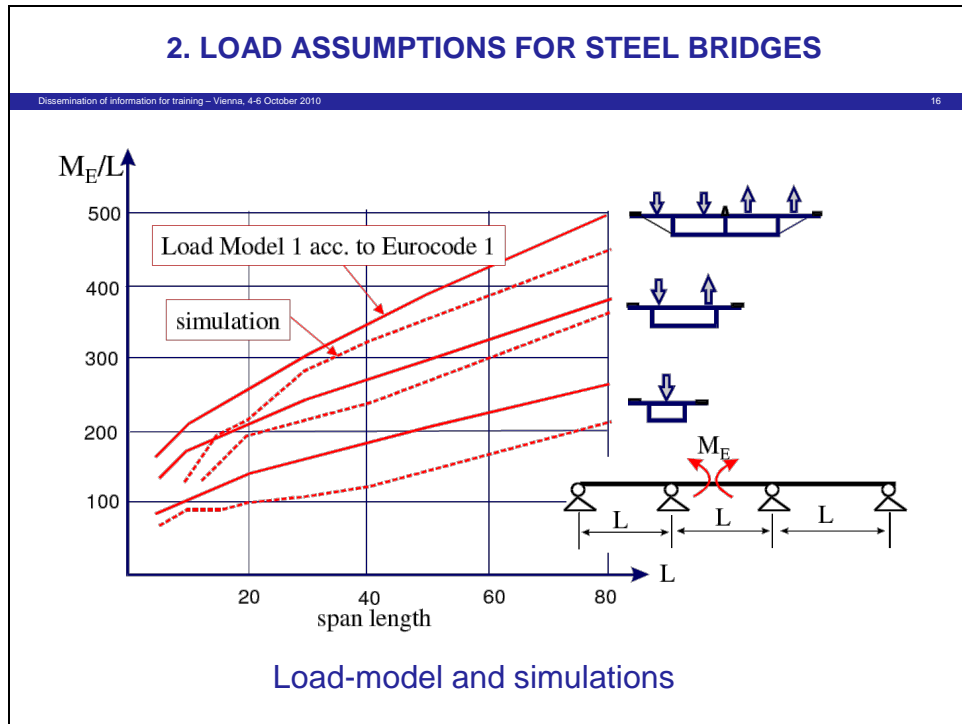


Figure 15

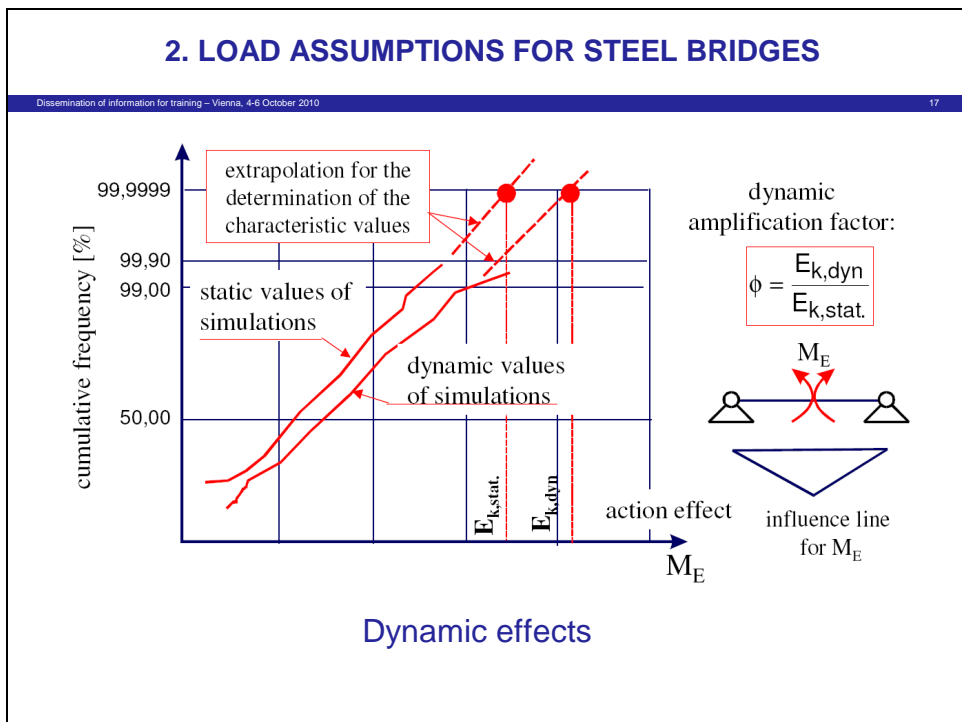


Figure 16

- (5) A by-product of the simulations is a comparison of “static” and “dynamic” action effects as given in Figure 16. The distribution lines show that dynamic effects cause an additional ΔM - value (constant shift) rather than an amplification by a dynamic factor. That is the reason why “dynamic factors” are included in load-model LM1.

4.3 Reliability analysis and partial factors

- (1) Reliability analysis of load model LM1 was performed with two medium spanned steel bridges with orthotropic decks that were built in Germany with the National Loading Code DIN 1072, see Figure 17.

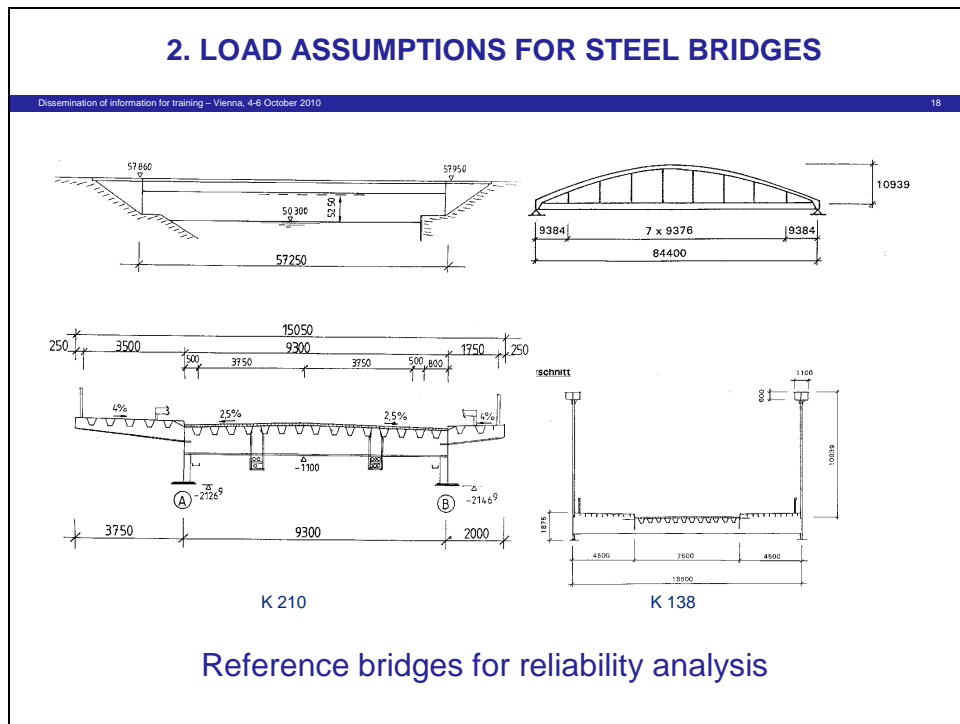


Figure 17

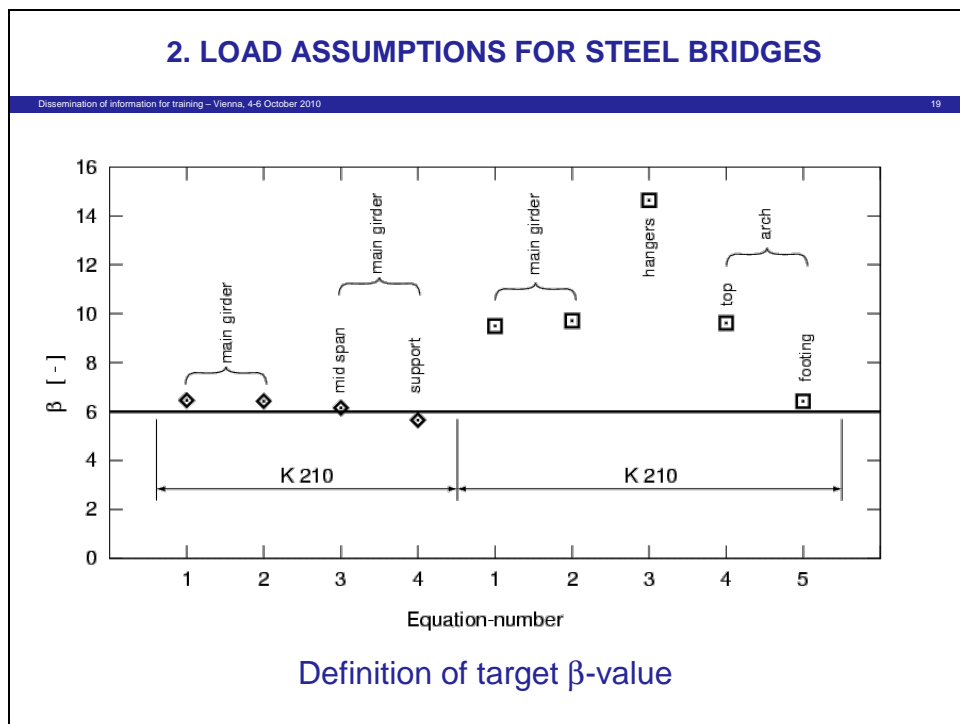


Figure 18

- (2) A reliability analysis on the basis of the statistics of the traffic in Auxerre and the statistics of large-scale tests used to define characteristic values of resistances in Eurocode 3 gives the β -values (reliability indices) as plotted in Figure 18.
- (3) The Figure shows that the minimum β -value found is $\beta = 6.00$. This was then used as the target value for a probabilistic design of bridges with various influence lines to identify a partial factor γ_G for the load-model LM1.

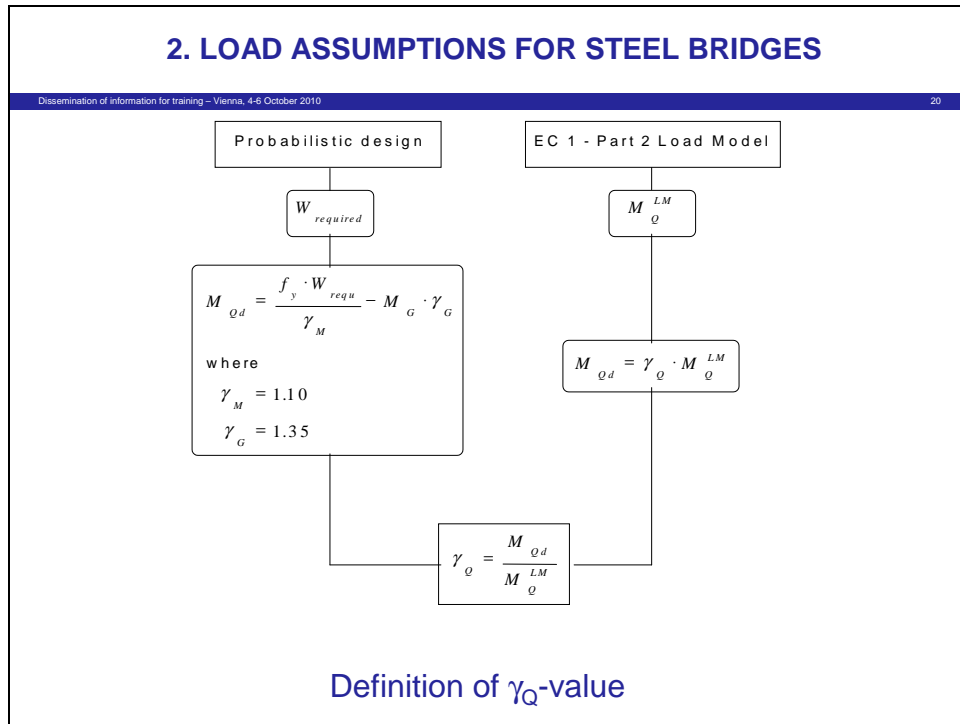


Figure 19

- (4) Figure 19 gives the method for identifying γ_Q [Bez]:
- The probabilistic design gives for various shapes of influence lines and spans the resistances $W_{required}$ of the main girders that comply with $\beta = 6.00$.
 - In using the definitions:

$$f_y = \text{yield strength}$$

$$M_G = \text{moment for permanent weights as defined in the Eurocodes}$$

$$\gamma_G = 1.35$$

$$\gamma_M = 1.10$$
 a design value M_{Qd} can be defined from the probabilistic design on one hand.
 - In using on the other hand load model LM1 the moment caused by traffic loads M_Q^{LM} can be determined and the design value is defined by $M_{Qd} = \gamma_Q \cdot M_Q^{LM}$.
 - From a comparison of M_{Qd} from the two routes the value γ_Q is obtained.

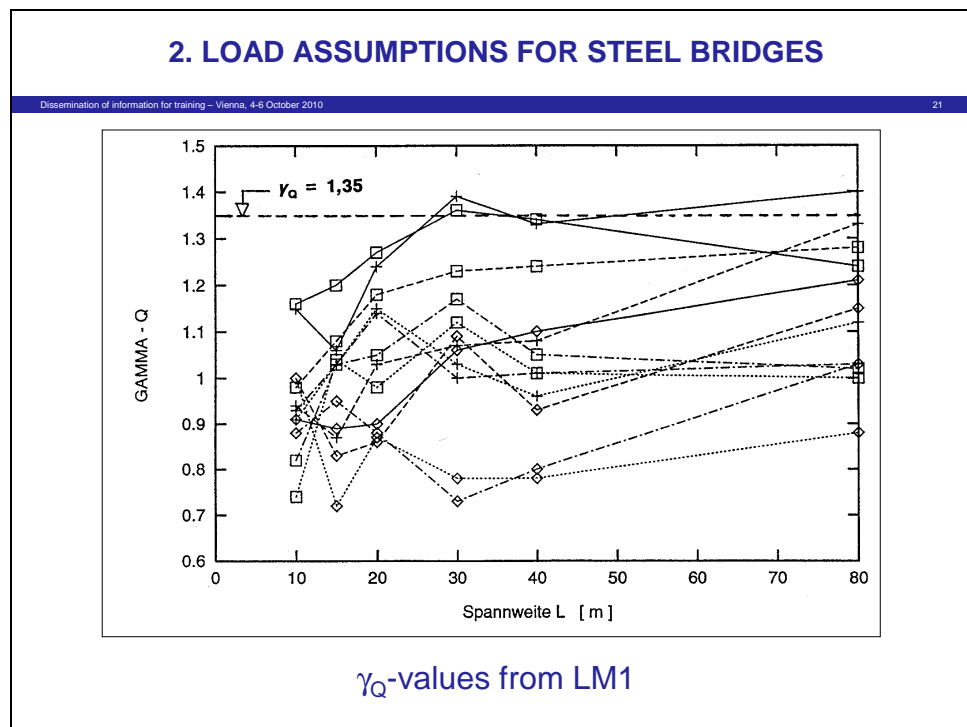


Figure 20

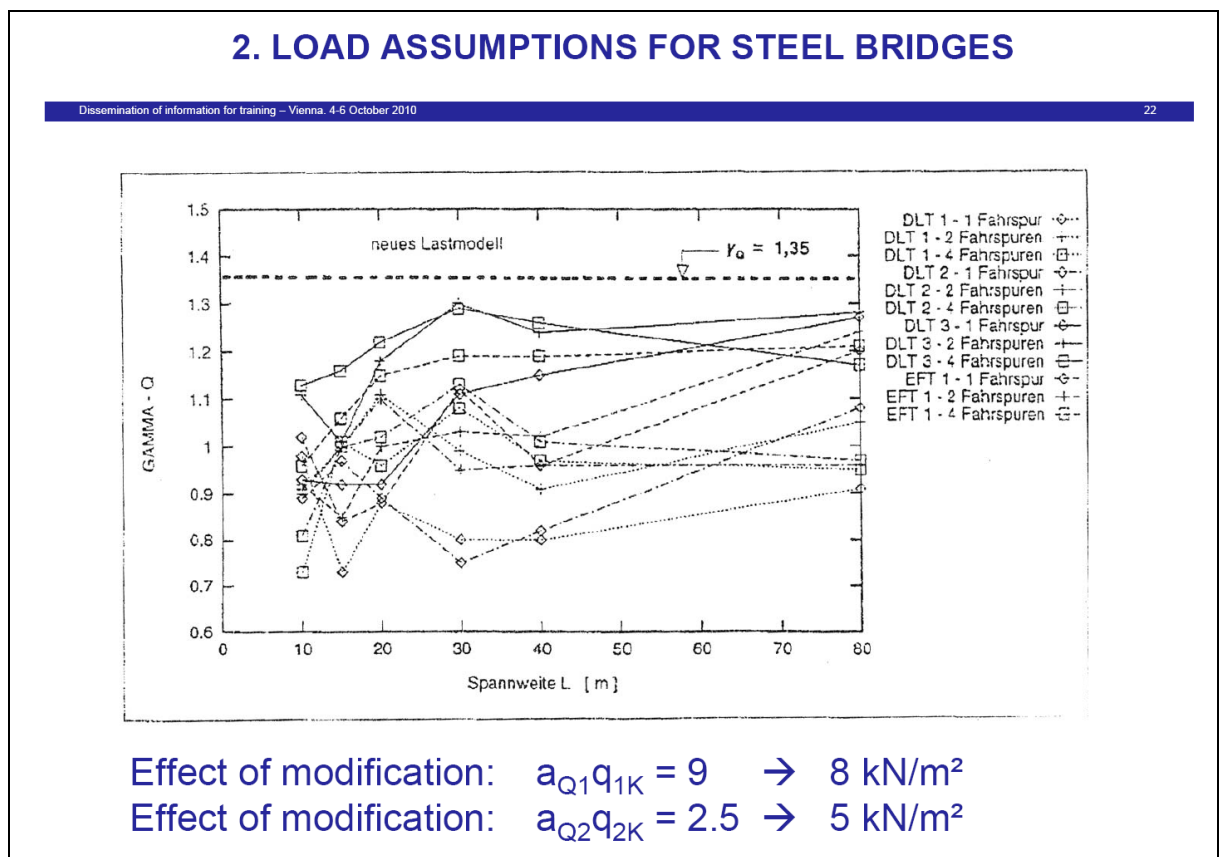


Figure 21

- (5) Figure 20 gives the distributions of γ_Q -values obtained in this way for various influence lines, spans and road widths. It shows the large scatter of values and also that $\gamma_Q=1.35$ is the maximum.

- (6) Figure 21 demonstrates what happens if in the load model LM1 the uniformly distributed load in lane 1 is slightly reduced and in lane 2 enhanced by a factor of 2:

The scatter of γ_Q is smaller and the maximum values are in the range of 1.25, so that γ_M could be reduced to $\gamma_M=1.00$.

- (7) This effect was one of the reasons for the choice of α -values in the draft German NA.

4.4 Tendency of traffic development

- (1) Figure 22 gives a forecast of the year 2000 for the future development of freight volume of terrestrial traffic that has been exceeded in 2010 by far.
- (2) Figure 23 gives the development of requests for permanent travelling permissions for heavy vehicles exceeding the legal weight limits, resulting in about 100 requests per day.

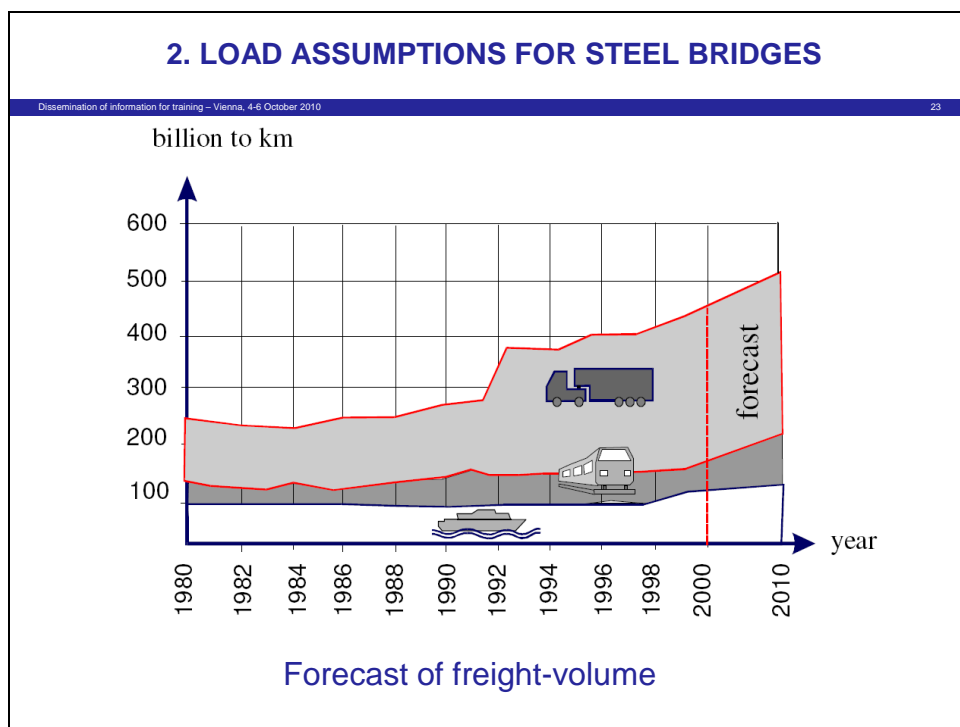


Figure 22

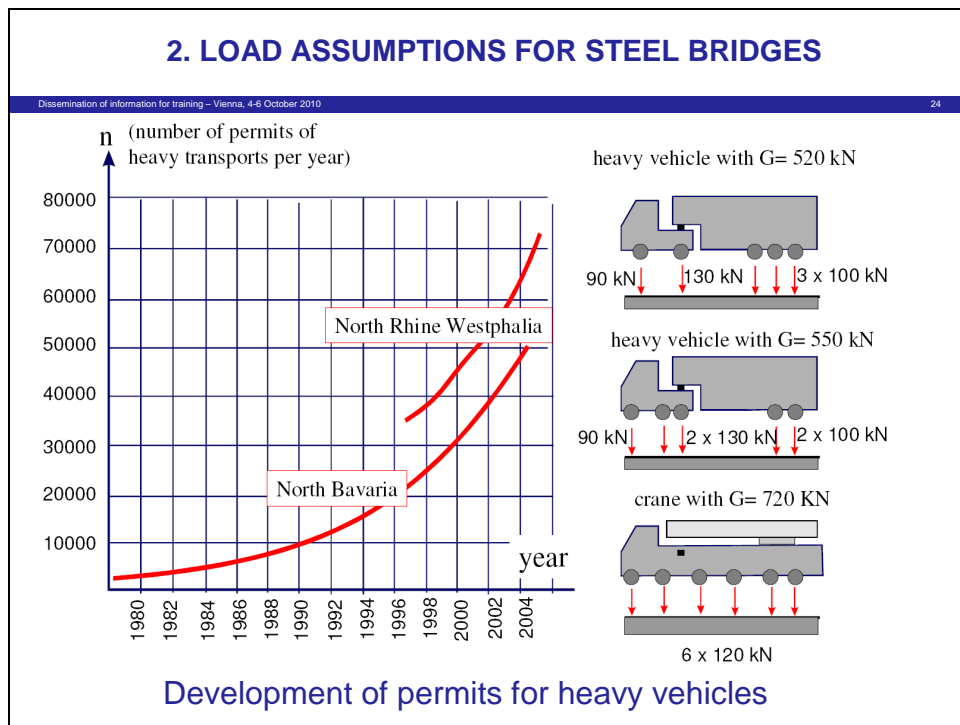


Figure 23

- (3) Figure 24 gives the vehicle and axle loads and accumulated number of vehicles as measured by weigh-in-motion (WIM) methods in an access highway to Rotterdam in the Netherlands for 1 year.

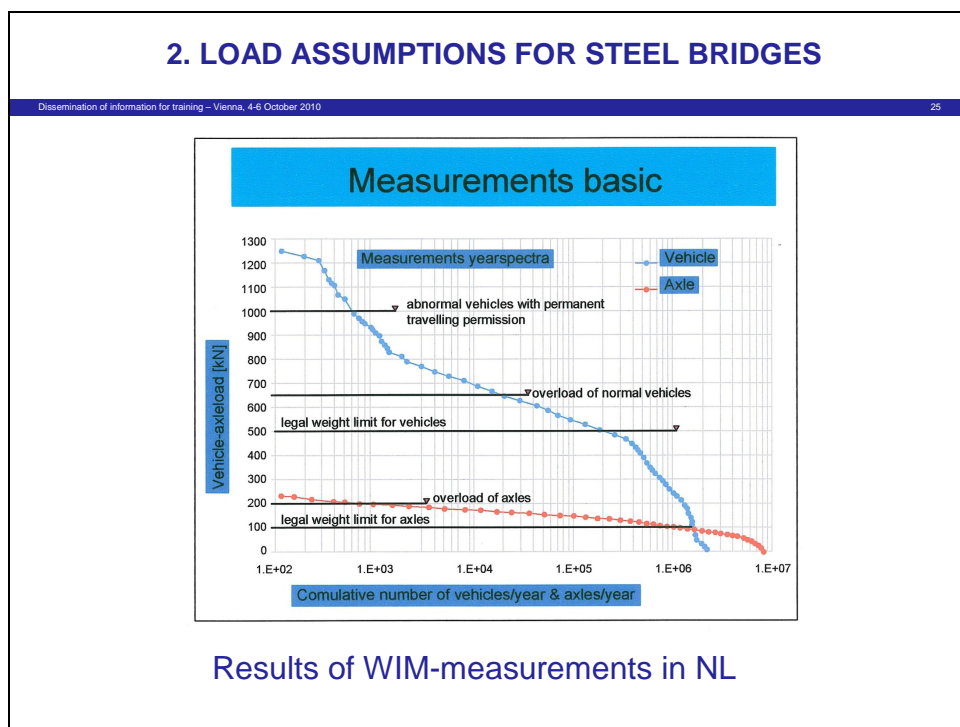


Figure 24

- (4) All these measurements show that

1. the recommendations for LM1 are not overcautious,
2. there are tendencies to increase the traffic loads by developing larger vehicles to reduce CO₂-emissions,
3. a clear picture of a future load-model can only be obtained where clear decisions from transport-politics are made. Such decisions should not ignore the large impact of such decisions on the sustainability of the loading model for the existing infrastructure.

4.5 The load model FLM3 for fatigue verifications

4.5.1 General

- (1) A numerical means to assess durability is the fatigue assessment, that requires the definition of the two-dimensional fatigue actions in terms of a pair of values:
 - the fatigue load, in general given with a frequency distribution or as a constant “damage-equivalent” load,
 - the number of load reversals in the required service time.
- (2) EN 1991-2 specifies a damage-equivalent vehicle FLM3 with a symmetric geometric loading pattern, that contains two tandem axle loads with an axle load of 120 kN and a vehicle load of 480 kN.

EN 1991-2 also gives the annual number of heavy vehicles depending on the category of highway, [Figure 25](#).

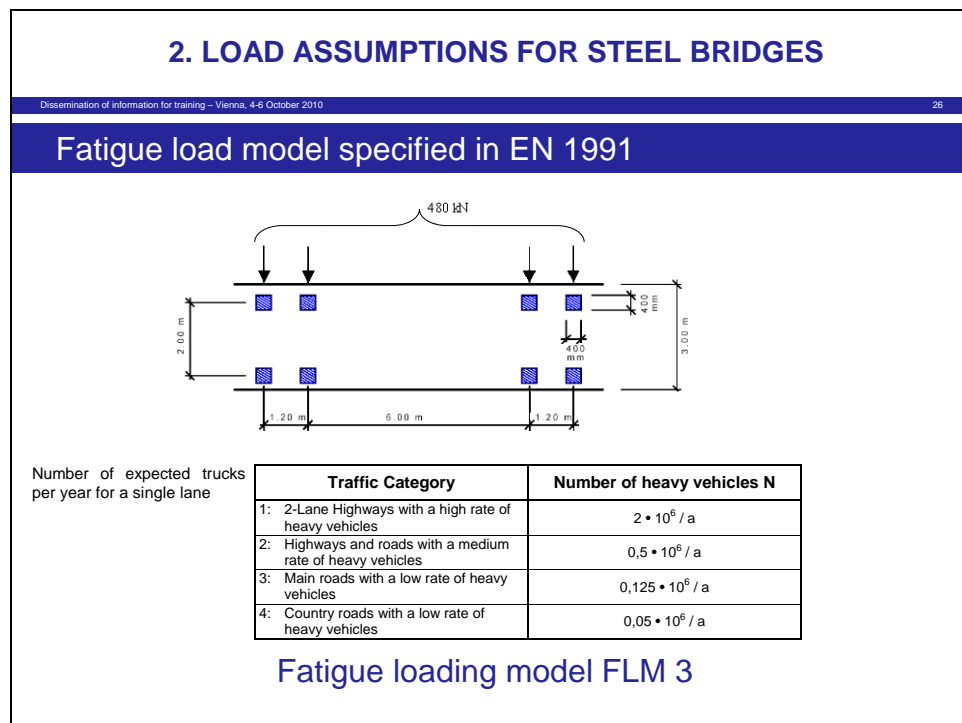


Figure 25

- (3) This damage equivalent vehicle represents a certain frequency distribution of various heavy vehicles in the traffic spectrum, evaluated with the slope $m=5$ of the fatigue resistance lines.

For application in numerical fatigue assessments, which are not based on fatigue damage (two dimensional), but on stress-ranges $\Delta\sigma$ only (one dimensional), the model is used in the following way:

- The stress range $\Delta\sigma_{max} = \sigma_{max} - \sigma_{min}$ is determined from the extreme positions of the vehicles on the static influence surface,
- the values $\Delta\sigma_{max}$ are modified with equivalent factors ϕ_{fat} and λ to take account of dynamic effects and the specific characteristics of the spectrum considered in the project.

- (4) Figure 26 gives the concept for this fatigue assessment, that usually works with partial factors γ_{Ff} and γ_{Mf} , depending on the safety concept applied. Usually the concept of “Damage tolerance” is used, which requires, that any fatigue damage, i.e. the formation and growth of cracks, can be detected in regular inspections of the structure, before the damage attains a size critical for the ultimate resistance of the structure.

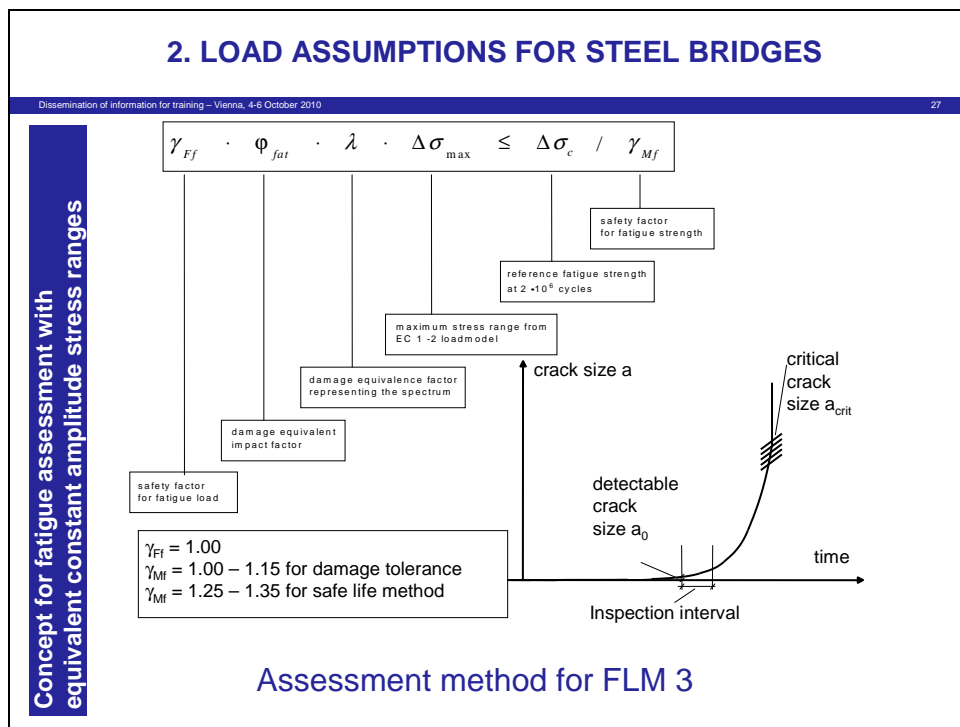


Figure 26

- (5) The fatigue resistances $\Delta\sigma_c$ are based on constant amplitude tests with large scale specimens, that contain all features of welded structures (discontinuities and residual stresses). Figure 27 gives an example for detail categories $\Delta\sigma_c$ as specified in EN 1993-1-9 and evaluations of test results that support the choice of $\Delta\sigma_c$ made in EN 1993-1-9.

The comparison shows that for some details there may be a large scatter of tests, from which the choices have been made and that for other details the basis of tests is rather small.

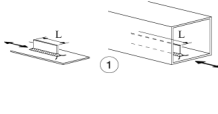



There may be also the problem, that for details chosen in a project either the fatigue loading or the fatigue resistance may only be roughly estimated, so that ways of fatigue assessment other than by the numerical way are preferred, e.g. prescriptive rules for fatigue or substitutive rules for serviceability.

2. LOAD ASSUMPTIONS FOR STEEL BRIDGES

Dissemination of information for training – Vienna, 4-6 October 2010

28

Fatigue details – welded attachments and stiffeners

Detail category	Constructional detail	Detail	New Evaluation for prEN 1993-1-9 (2002)	$\Delta\sigma$				
			# of data	m	$m=var$	$m=const$		
				variable	constant			
80	$L \leq 50\text{mm}$		17	3,26	3	89,10	87,00	
71	$50 < L \leq 80\text{mm}$							
63	$80 < L \leq 100\text{mm}$		109	2,45	3	67,04	77,14	
56	$L > 100\text{mm}$		62	3,24	3	58,06	55,96	
			18	3,32	3	76,08	72,31	
			15	3,05	3	94,57	94,73	
			17	3,27	3	79,37	76,49	
			6	3,81	3	80,59	59,53	
			8	3,48	3	84,22	76,73	
			12	3,54	3	69,12	60,14	
			4	4,59	3	78,39	50,12	
			9	2,43	3	53,43	74,94	
71	$L > 100\text{mm}$ $\alpha < 45^\circ$		53	2,92	3	69,24	70,58	
			27	2,99	3	58,97	59,85	
			39	2,73	3	78,95	83,41	
80	$r > 150\text{mm}$		6	3,06	3	100,94	105,20	
			4	3,29	3	97,27	96,41	
			4	3,31	3	36,16	62,94	
			10	3,12	3	59,00	63,76	
90	$\frac{r}{L} \geq \frac{1}{3}$ or $r > 150\text{mm}$							
71	$\frac{1}{6} \leq \frac{r}{L} \leq \frac{1}{3}$		13	1,26	3	18,43	72,84	
50	$\frac{r}{L} < \frac{1}{6}$							

EN 1993-1-9 - Fatigue resistance

EN 1993-1-9 - Fatigue resistance

Figure 27

4.5.2. Example for descriptive rules for sufficient fatigue resistance

- An example for the derivation of a descriptive rule for achieving sufficient fatigue resistance is given in Figure 28. In comparing the moment resistances of main girders resulting from ULS-verifications with Load-model LM1 and from fatigue assessments with Load-model FLM3 all for a certain minimum fatigue resistance, e.g. $\Delta\sigma_c = 71 \text{ MPa}$, a certain maximum span length can be determined where fatigue is no more relevant.

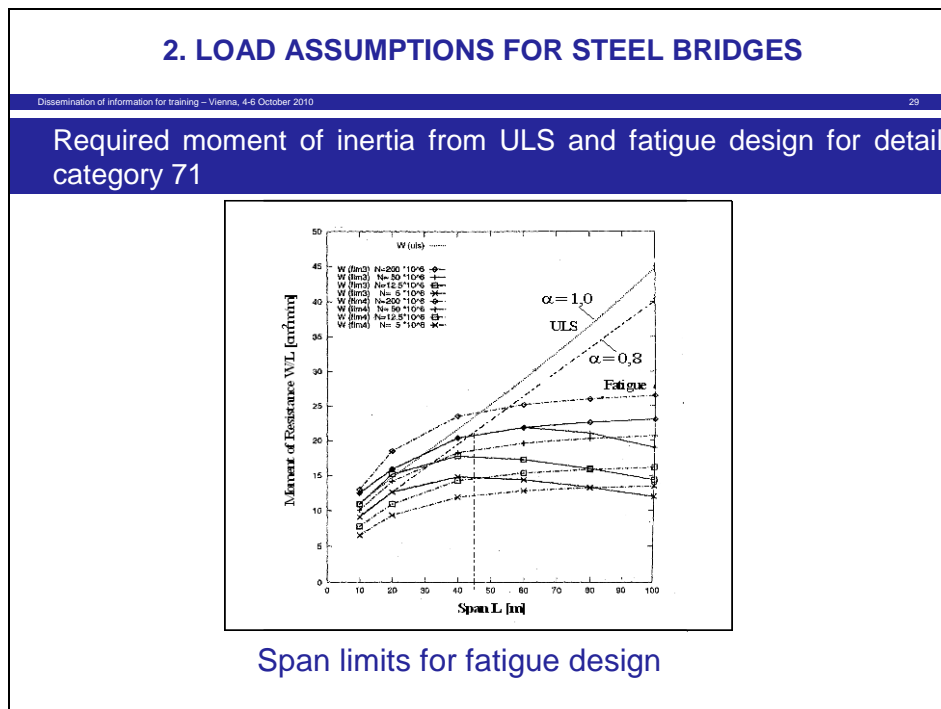


Figure 28

- (2) So a descriptive rule could be
- to specify a minimum requirement for the fatigue resistance of all details, e.g. $\Delta\sigma_c = 71 \text{ MPa}$,
 - to define a minimum span length from which on numerical assessments are necessary.
- (3) Figure 29 gives another example for descriptive rules for certain details. In this case the connection of hangers of tied arch bridges, for which various details are common could be standardised in such a way, that fatigue from:
- vortex induced vibrations
 - rain-wind-induced vibrations
 - fatigue from imposed deformations from the passing of fatigue vehicle on the bridge
- are taken into account.

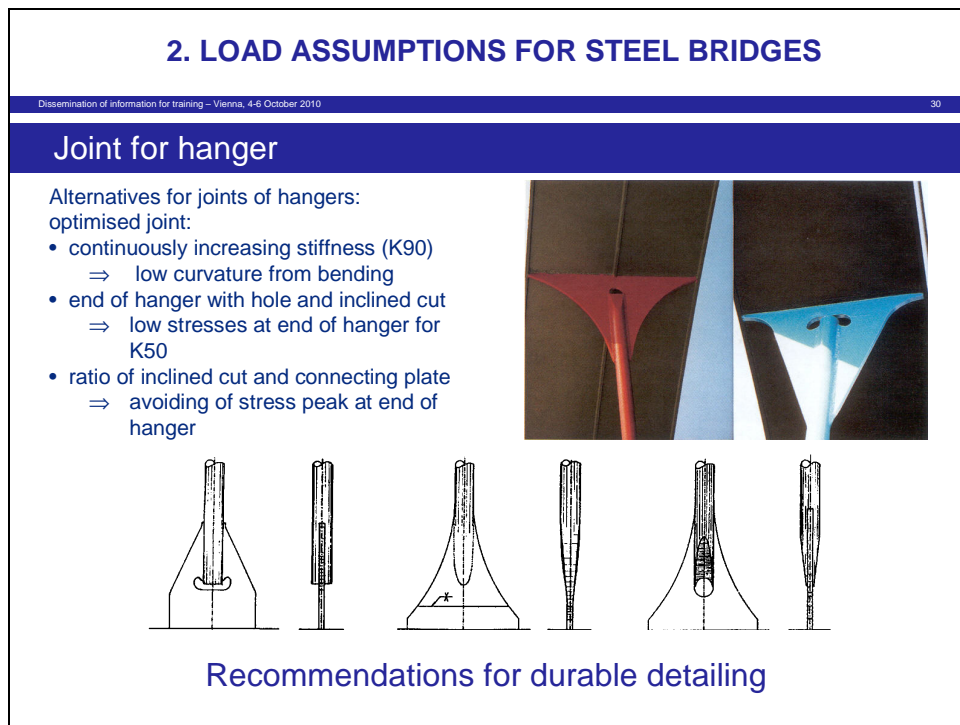


Figure 29

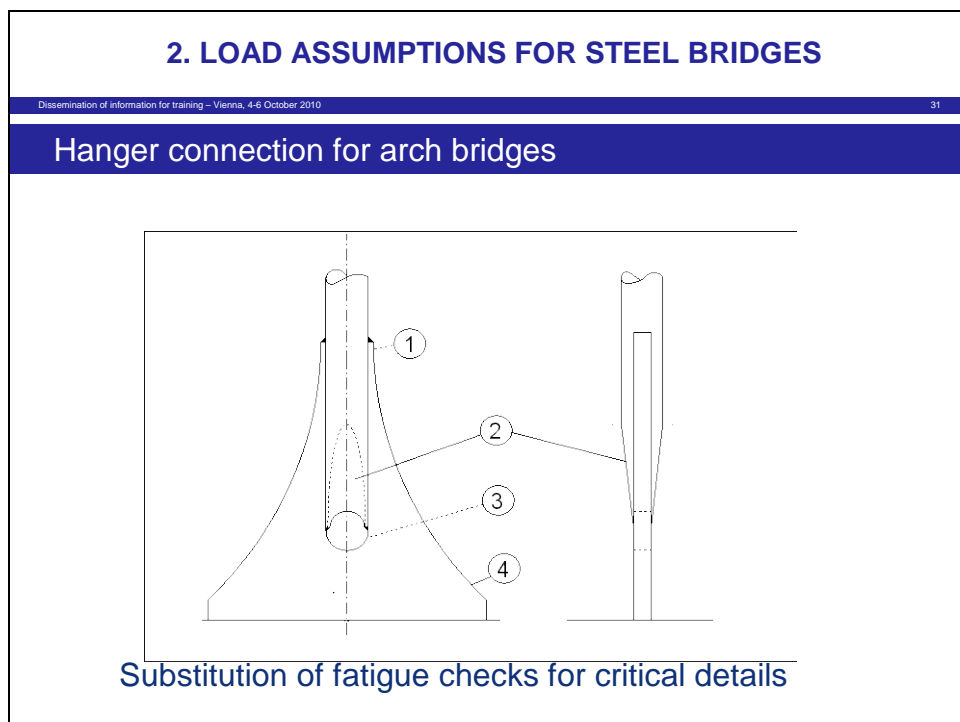


Figure 30

- (4) Figure 30 gives such an example for a standardized solution that may be defined by geometric descriptions only. The background of these geometric descriptions are fatigue assessments for the critical “hot spots” • , , , f , „ that have been undertaken for a large variety of bridges to prove their safety.

- (5) A particular case for descriptive rules is the “orthotropic” steel deck of bridges, see [Figure 31](#). The most critical hot spot for such plates is the welded connection of the deck-plate to the troughs or to the webs of the cross-beams.

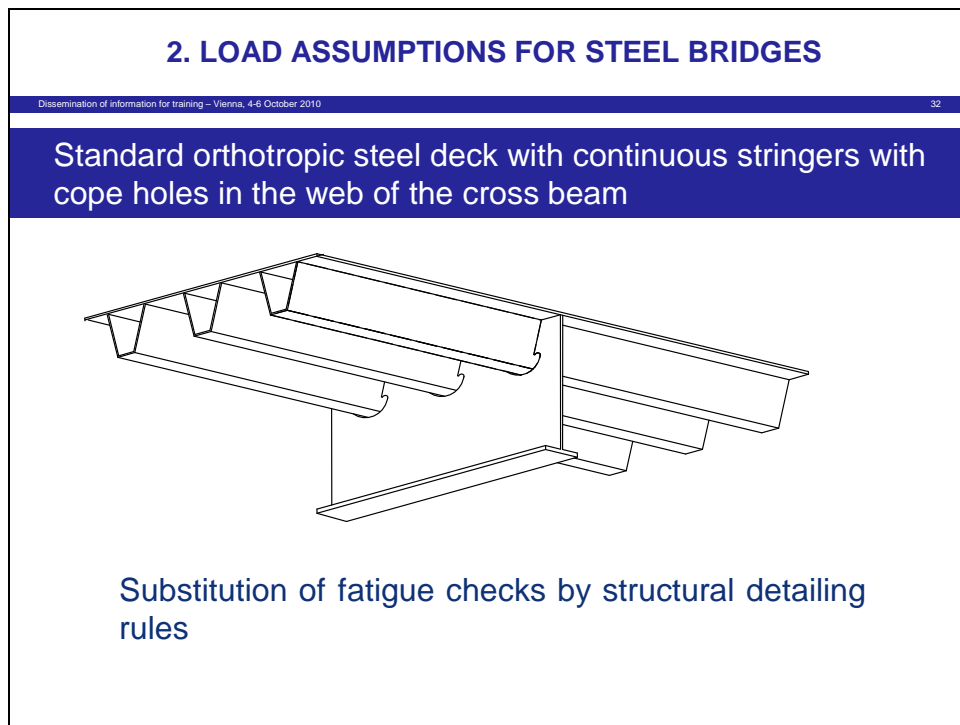


Figure 31

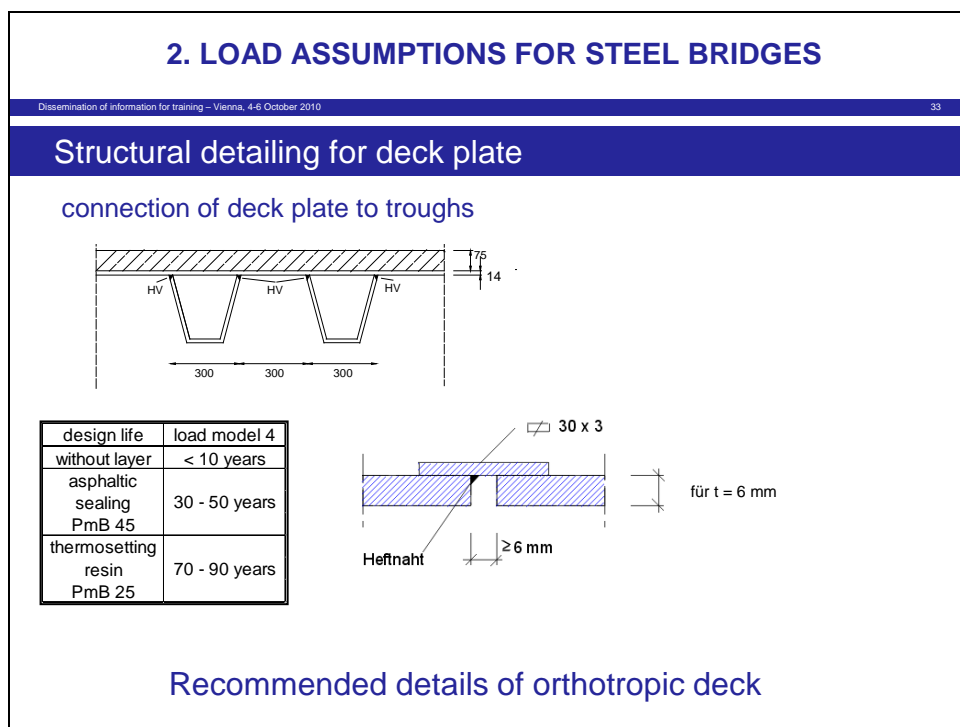


Figure 32

- (6) The fatigue loading model FLM3 is not applicable for verifying these hot spots, because it does not sufficiently model the effects of the tyre-pressure of the wheels. Also the analysis model for fatigue is not sufficient, if it is restricted to modelling the steel structure only.
- (7) Figure 32 demonstrates in what way the steel-deck adhesively connected with the asphalt layer is affected by the stiffness of the layer and its sensitivity to temperature and loading frequency.

Taking Polymer modified Bitumen PmB45 into account produces an enhancement of service life by a factor of 3 to 5 and PmB25 generates an enhancement by a factor of 7 to 9.

- (8) Therefore Annex C to EN 1993-2 gives prescriptive rules for the most critical details of orthotropic plates, e.g. deck-plate thickness, distance of troughs, weld preparations for welded joints of stiffeners etc. to secure a sufficient fatigue life.

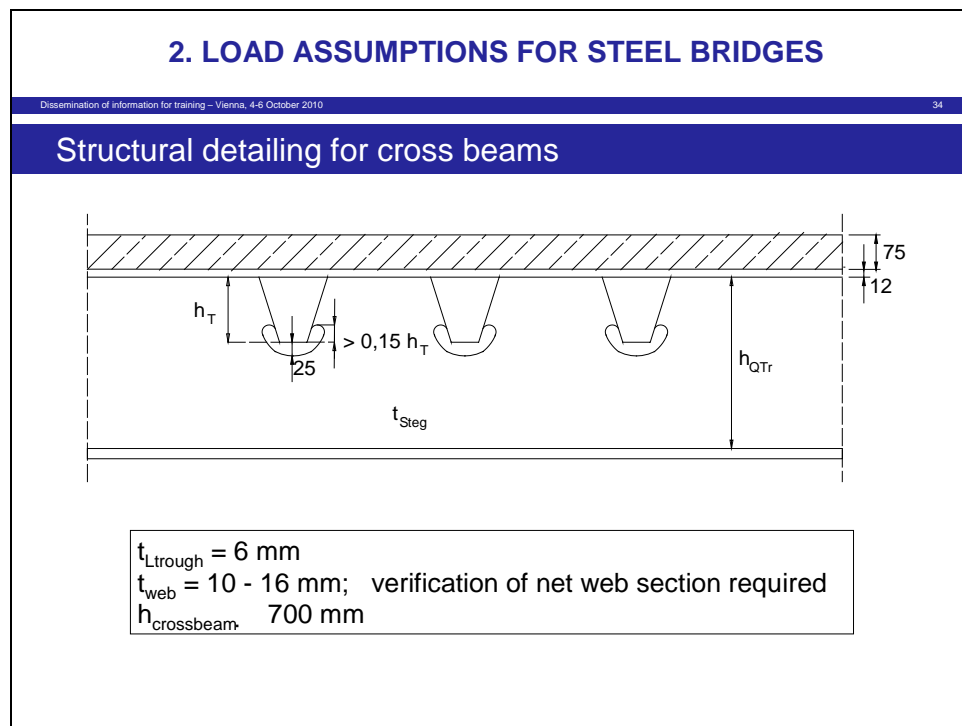


Figure 33

- (9) An example for the structural details dealt with in Annex C is the interconnection of troughs and webs of cross-beams according to Figure 33 and the definition of a minimum depth of cross-beams and minimum thickness of web-plate to avoid the formation of cracks at the cut-out for which a “tooth-assessment” in the critical horizontal section between the cut-outs is necessary.

4.5.3 Examples for indirect fatigue assessments

- (1) A particular protection aim for orthotropic steel decks is to avoid cracks in the asphalt-layer that could lead to corrosion of the deck-plate and in case of disintegration of the layer to security problems of the road users.
- (2) The causes of such cracks are
 - insufficient strainability of the asphalt in particular during winter,
 - excessive flexibility of the deck-plate in particular due to differential deflections of the troughs, see [Figure 34](#).

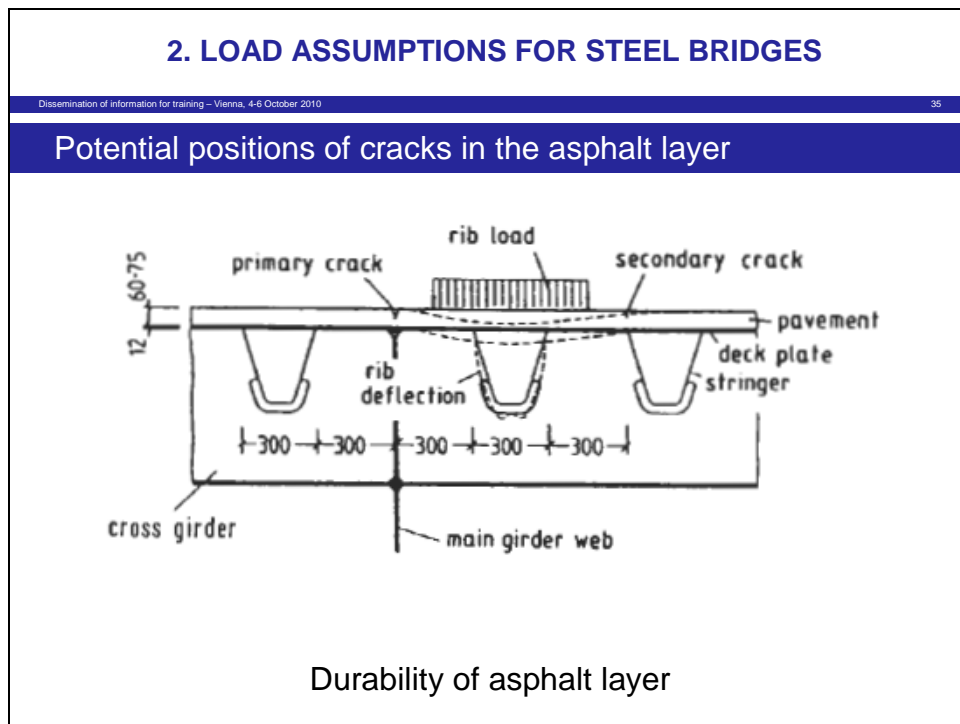


Figure 34

- (3) From an evaluation of the ratio of the frequency of occurrence of cracks in the asphalt versus the maximum strain exerted from differential deflections of the ribs a minimum requirement of the stiffness of troughs has been derived that is given in [Figure 35](#).

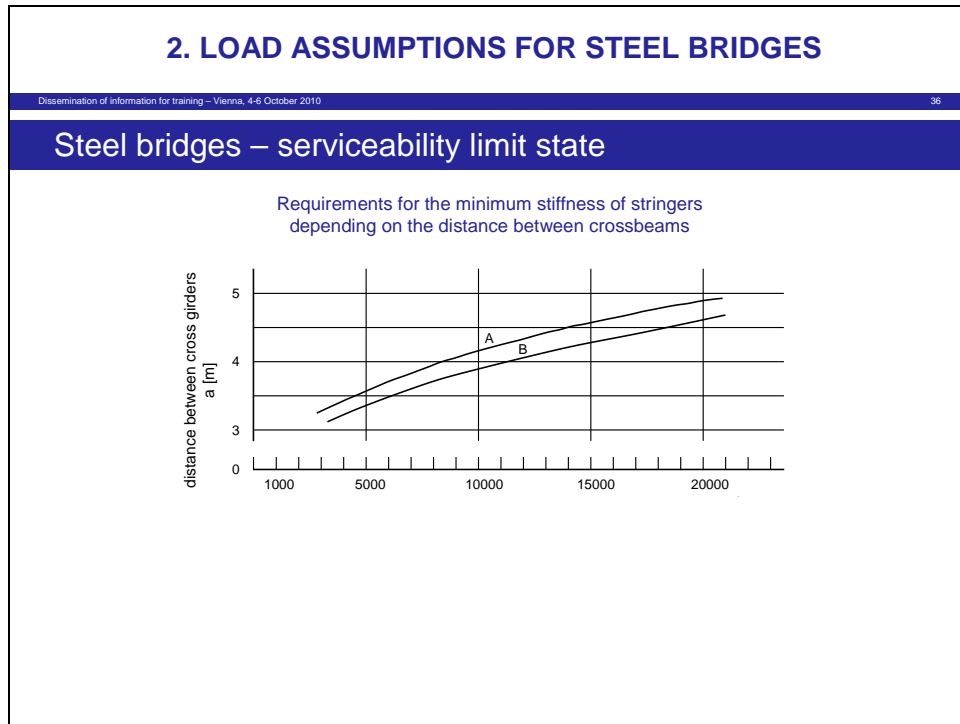


Figure 35

- (4) This minimum stiffness requirement, specified in EN 1993-2, also protects the deck-plate from excessive fatigue stresses.
- (5) Another indirect fatigue assessment given in EN 1993-2 is the verification to excessive web-breathing, that may lead to cracking at the welded edges of the web-plate and also avoids the “hungry horse”-appearance.
- (6) Figure 36 shows the relevant “plate-buckling”-formula applied for stresses on the service level.

2. LOAD ASSUMPTIONS FOR STEEL BRIDGES

Dissemination of information for training – Vienna, 4-6 October 2010 37

Plate buckling

Verification to web breathing

Definition of a plated element

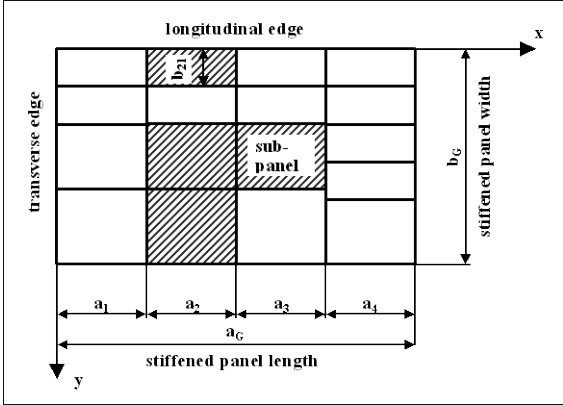
$$\sqrt{\left(\frac{\sigma_{x,Ed,ser}}{k_{\sigma}\sigma_E}\right)^2} + \left(1.1\frac{\tau_{Ed,ser}}{k_{\tau}\sigma_E}\right) \leq 1.15$$


Figure 36

2. LOAD ASSUMPTIONS FOR STEEL BRIDGES

Dissemination of information for training – Vienna, 4-6 October 2010 38

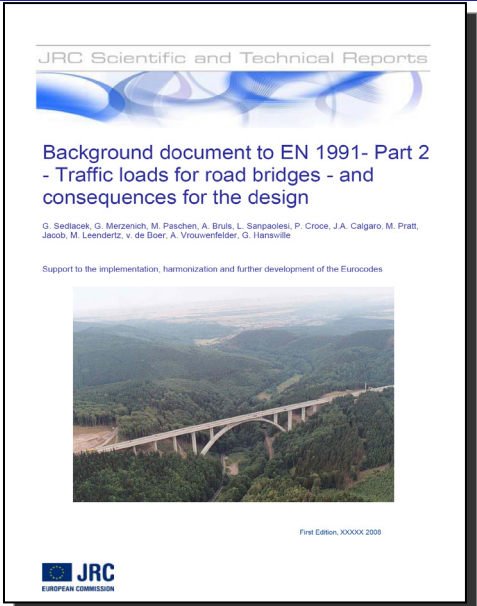


Figure 37

4.5.4 Background information to the Eurocode-specifications for traffic loads

- (1) The JRC has prepared a background document to EN 1991-Part 2 – Traffic loads for road bridges and consequences for the design -, see [Figure 37](#), that is currently being extended to include also the background of the traffic loads for railway bridges.

- (2) That background document gives the origine of the load specifications and could be used as a source for determining tendencies from more recent traffic measurements or from studies that include further developments of heavy vehicles.

5. Modelling of steel bridges for the analysis

5.1 General

- (1) Two examples for models used for the design of steel bridges are presented in this report, that are connected with durability checks:
- Model for shear lag for wide flanges e.g. the bridge-deck cooperating with the main girders as top flange,
 - Model for fatigue design.

5.2 Model for shear lag

- (1) The basis for the model of shear lag in EN 1993-1-5, to which EN 1993-2 makes reference, is the “beam theory extended to cover shear deformations”.

- (2) Figure 38 shows the principle:

- the bending theory of beams with loads P_z and bending moments M_z apply to the full cross-section with the full geometric flange width b . It gives the warping distribution z ,
- an additional warping distribution w for longitudinal stresses σ_x is found, the distribution of which complies with a linear shear distribution $\frac{\partial w}{\partial s}$ in the wide flange

and has the following properties:

- it is orthogonal to the warping distributions $w_1 = I$ for normal forces and for bending $w_2 = z$, in that the equations:

$$\int w dA = \int w_0 dA + k_{Iw} \cdot A = 0$$

$$\int w \cdot z dA = \int w_0 \cdot z dA + k_{zw} \cdot A_{zz} = 0$$

apply,

- it gives a vertical deformation v that can be determined from the second order analysis model of a beam with the bending stiffness $E \cdot A_{ww}$ where

$$A_{ww} = \int w^2 dA$$

and the “tension force” $G \cdot S$, representing the shear stiffness of the wide flange.

- this analysis model also gives “warping moments” M_w that may be used to determine the self-equilibrating stress pattern

$$\sigma_w = \frac{M_w}{A_{ww}} \cdot w$$

- the sum of

$$\sigma_z = \frac{M_z}{A_{zz}} \cdot z$$

and

$$\sigma_w = \frac{M_w}{A_{ww}} \cdot w$$

gives the final stress distribution in equilibrium with external forces taking account of the non-linear stress distribution in the wide flange,

- the equivalence to this non-linear stress distribution is a constant stress distribution in the wide flange however reduced to the effective

width

$$b_{eff} = \beta \cdot b$$

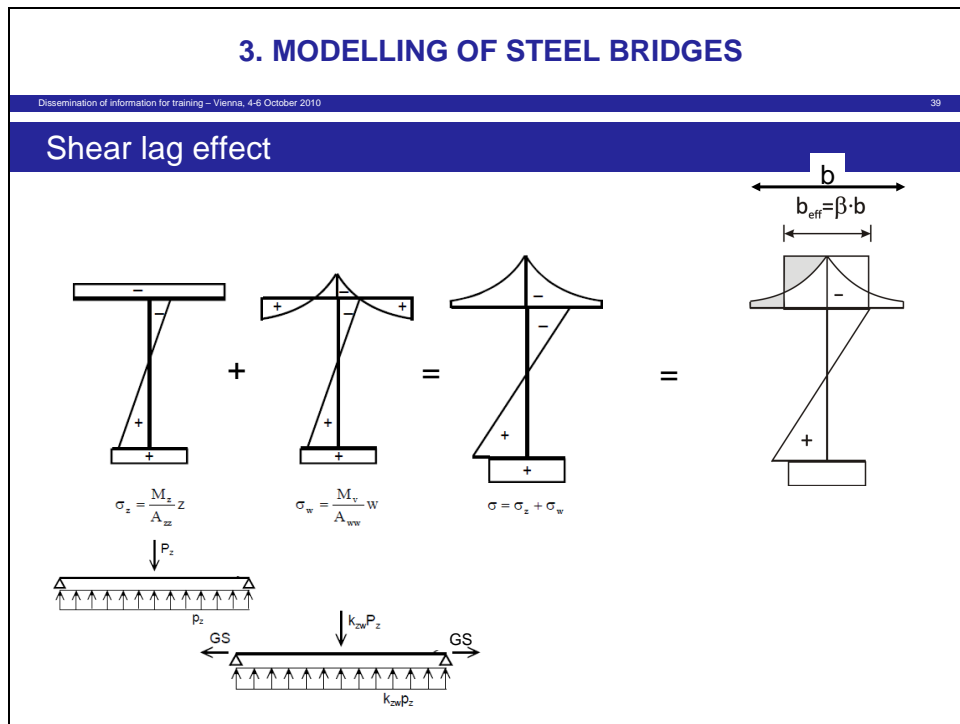


Figure 38

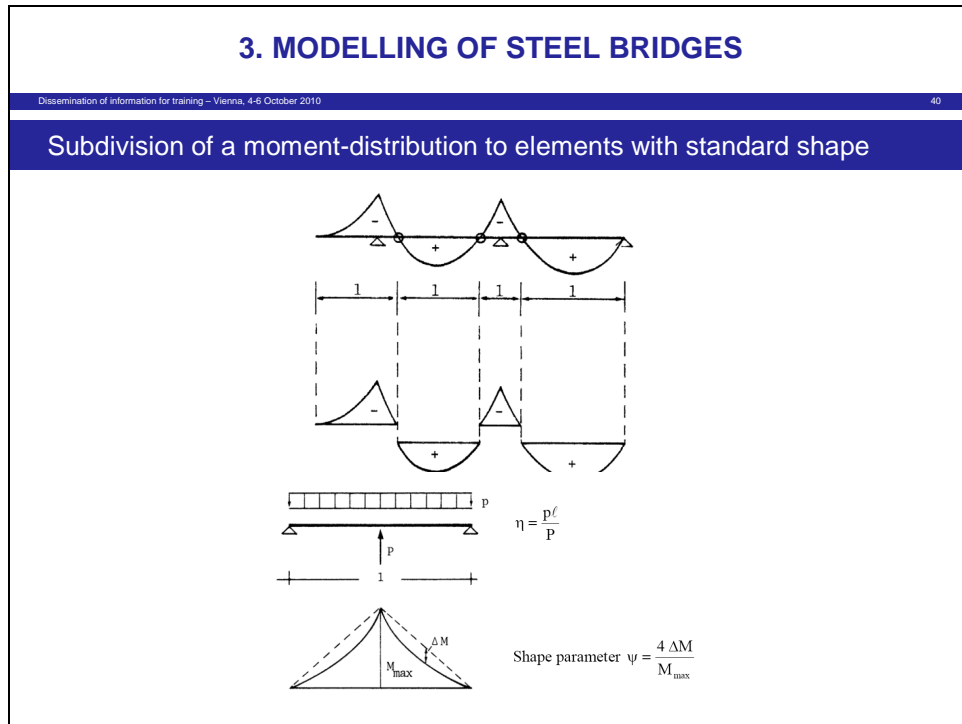


Figure 39

- (3) Figure 39 shows a moment distribution for a continuous beam where this model could be applied:
- σ_z is calculated on the basis of M_z from a beam analysis
 - σ_w is calculated from M_w determined from 2nd order theory for a continuous beam with the tension force $G \cdot S$.
- (4) For the ease for use however the moment distribution of the continuous beam is divided into various unit distributions, each of which can be modelled by a simply supported beam with a combination of uniformly distributed load and concentrated load, where ψ is the relevant shape parameter for the moment shape.

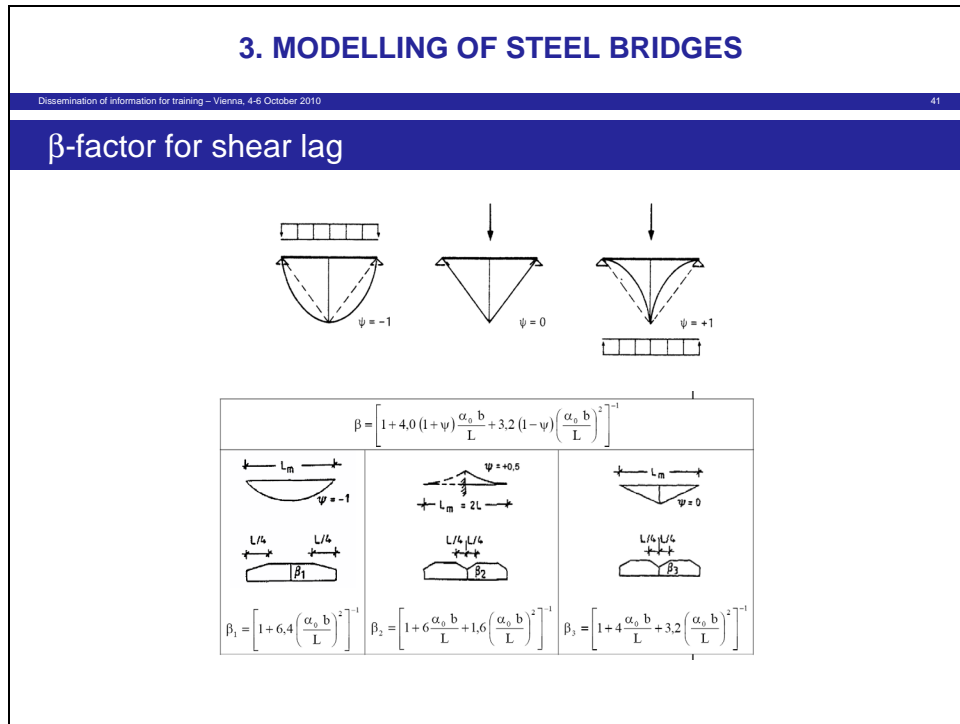


Figure 40

- (5) Figure 40 gives the algebraic solution for β for various shapes ψ taking account of the possible orthotropy of the wide flange by $\alpha_0 \cdot b$, where

- $\alpha_0 = 1$ for isotropic flange plates
- $\alpha_0 > 1$ for orthotropic flange plates, where the longitudinal stiffness is larger than the shear stiffness
- $\alpha_0 < 1$ for cracked concrete slabs, where the longitudinal stiffness for tension is smaller than the shear stiffness

- (6) Figure 40 also shows the formulae for β specified in EN 1993-1-5 for the extreme value envelopes of bending moments, for which a reference length of beam and a ψ -value has been chosen.

5.3 Modelling for ultimate limit state verifications and for fatigue assessments

- (1) Whereas the modelling of the structures for ultimate limit state verifications may be simplified, e.g. by hinged connections at the junction of deck-plate and vertical stiffeners of cross-frame, fatigue assessments need a modelling of the monocoque structure taking into account the continuity of deformations of the deck-plate and of the transverse frame to take the restraining moments into account, see Figure 41.

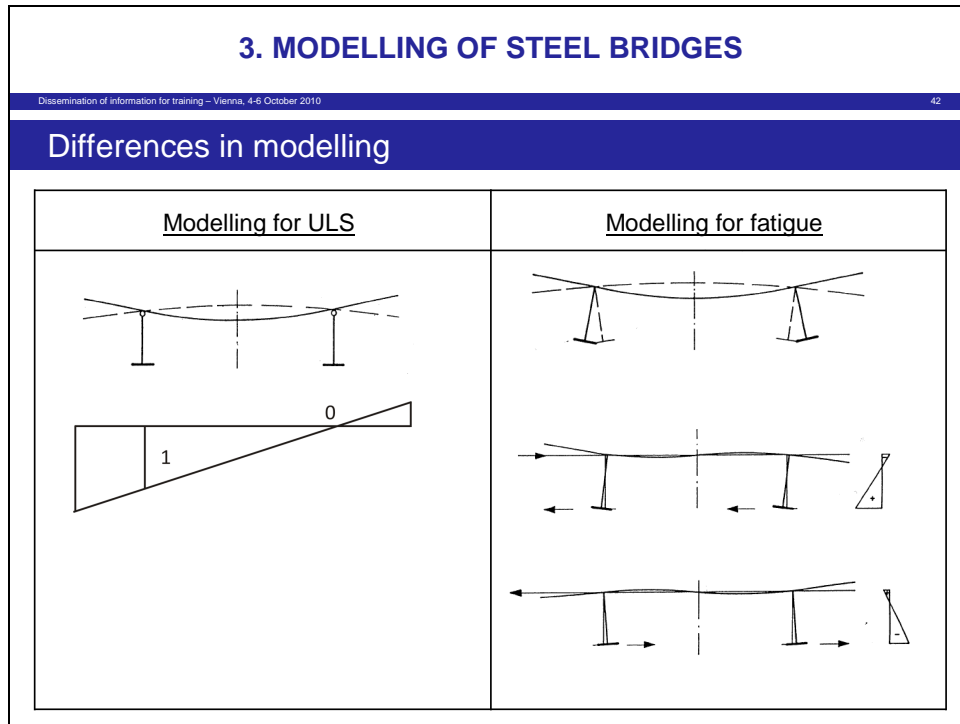


Figure 41

- (2) Also small curvatures of a bridge in plan view normally neglected in the analysis for ULS may induce lateral forces in the hogging and sagging moment regions of the main-girders that may enhance the restraining moments in the transverse frame.
- (3) Fatigue damages have also been observed at the connections of longitudinal stiffeners in webs of main-girders, that normally are designed for plate buckling under perfect-loading conditions for ULS, however in case of flexible deck-plates may receive lateral imposed deformations from deflections of the cross-beams under traffic loads, see [Figure 42](#).

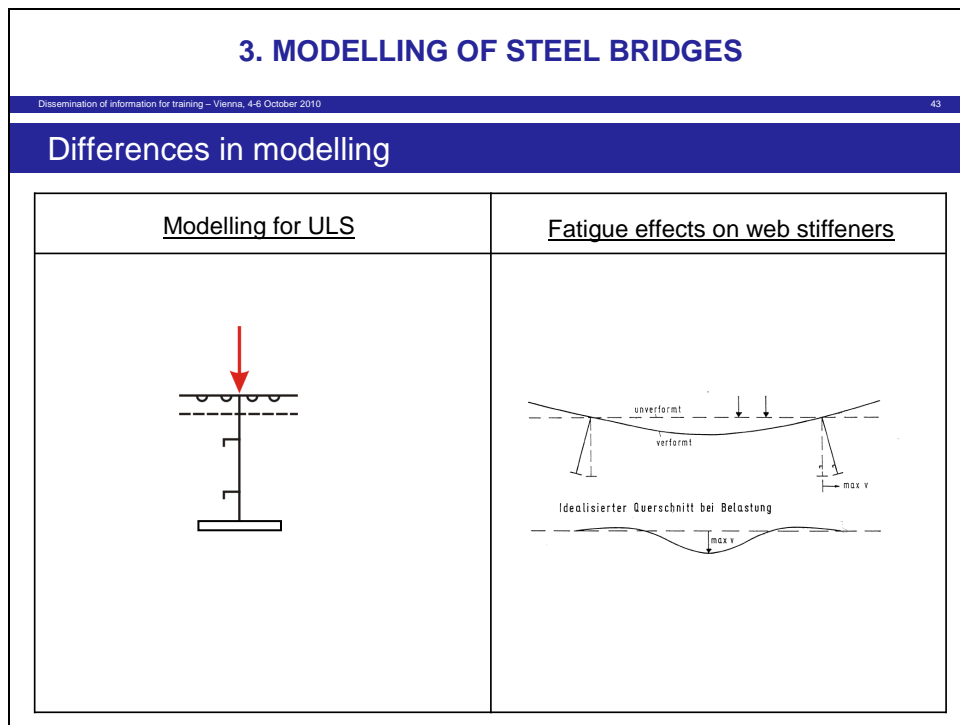


Figure 42

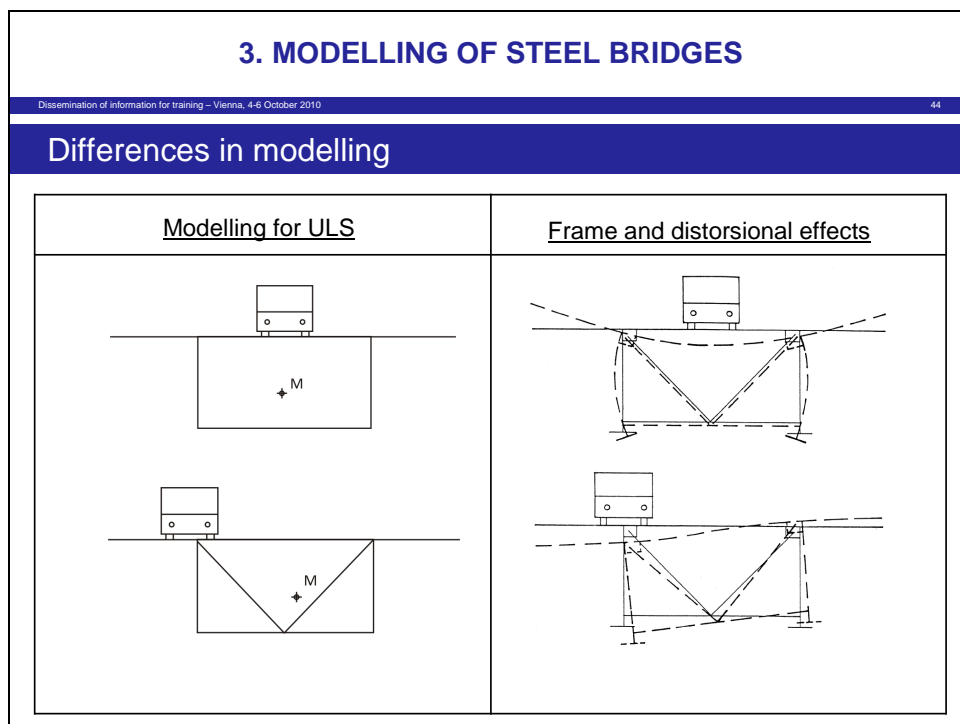


Figure 43

- (4) A typical difference in modelling for ULS and fatigue is given in [Figure 43](#) for box-girder-bridges, where transverse frames are usually designed for load distributing forces calculated on the basis of rigid cross-section shapes, whereas for fatigue the distortion of the cross-section and secondary moments induced by the continuity of deformations of the deck-plate and the transverse frame may be relevant.

6. Specifications for bearings

6.1 General

- (1) EN 1990 – Annex A2 does not give rules for the determination of action effects as forces, moments and movements for specifying the performance conditions for the delivery of bearings.
- (2) Therefore the preparation of such rules is a first priority task for “Non-conflicting complementary information” to EN 1990 A2 to make the Eurocodes fully operable for the design of bridges.
- (3) EN 1993 – Part 2 gives in its Annex A “Requirements for bearings” that are meant to be independent on different materials and ways of construction.
- (4) This Annex needs however further development to achieve the following goals:
 - the rules should give realistic results in that they comply with measurements of forces and movements from many decades,
 - the rules should be applicable for all types of fixed, sliding, rolling and deforming bearings,
 - the rules should allow to derive the specifications for bearings from a global analysis of the bridge for ULS comprising the interaction of superstructure, bearings, piers, foundation and the soil. This specification should be consistent with the design of the support area of the superstructure (e.g. for eccentricities), the design of the piers (e.g. loading and excentricities) and of the foundations.
- (5) The rules should also be consistent with the properties of bearings, as specified in the product standard for bearings, i.e. EN 1337.
- (6) In the following the main contents of such a future Annex E to EN 1990, that would substitute the now Annex A to EN 1993-2 is presented.

6.2 Design principles for the preparation of construction documents

- (1) Figure 44 gives the design principles for the preparation of construction documents needed to order the delivery of bearings according to EN 1337.

4. SPECIFICATION FOR BEARINGS

Dissemination of information for training – Vienna, 4-6 October 2010 45

Design principles for individual bearings

- Permission of movements minimizing the reaction forces
- No tensile forces
- No significant redistribution of forces to other bearings from accommodation to installation tolerances
- Specification of installation conditions with details of construction sequence and time variable conditions
- Measure to avoid unforeseen deformation of the bearings (non uniform contact)

Figure 44

4. SPECIFICATION FOR BEARINGS

Dissemination of information for training – Vienna, 4-6 October 2010 46

Construction documents

- Bearing plan (drawing of the bearing system)
- Bearing installation drawing (structural details)
- Bearing schedule (characteristic values from each action, design values from combination of action)

Figure 45

(2) The construction documents, see [Figure 45](#), are

- the bearing plan, that shows the bearing system,
- the bearing installation drawing,
- the bearing schedule.

6.3 Preparation of bearing schedules

- (1) After the choice of the bearing plan with selection of the types of bearing, see [Figure 46](#), bearing schedules need to be prepared, for which [Figure 47](#) and [Figure 48](#) give models.

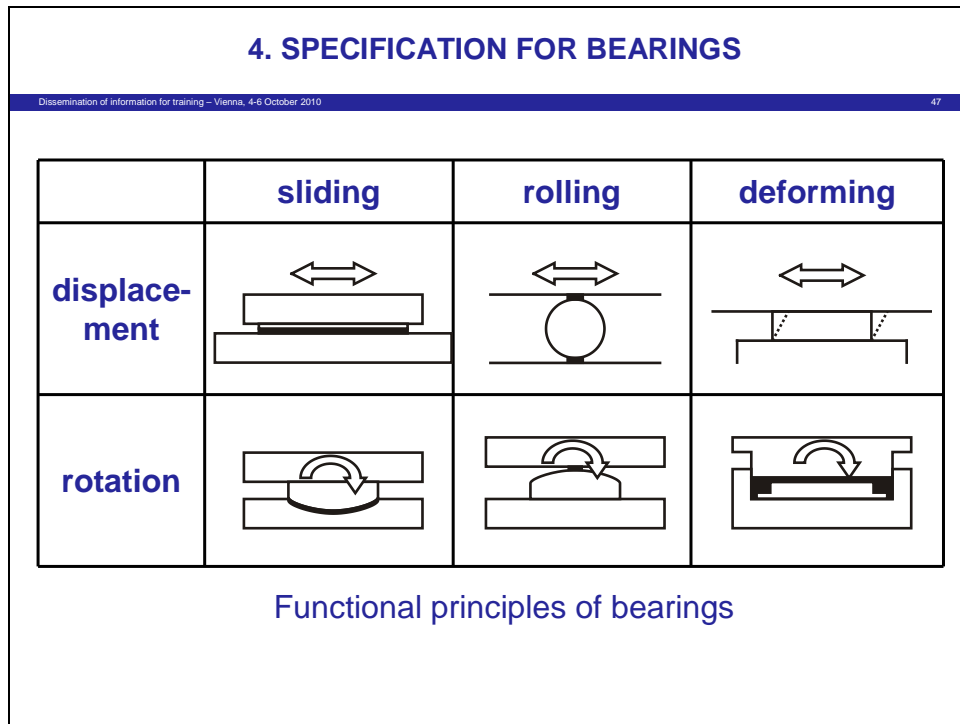


Figure 46

- (2) In [Figure 47](#) the characteristic values of action-effects (forces, moments and movements) are given for each individual action, so that load combinations can be performed that allow to define either extreme values together with simultaneous accompanying actions or conservative combinations of extreme values only.

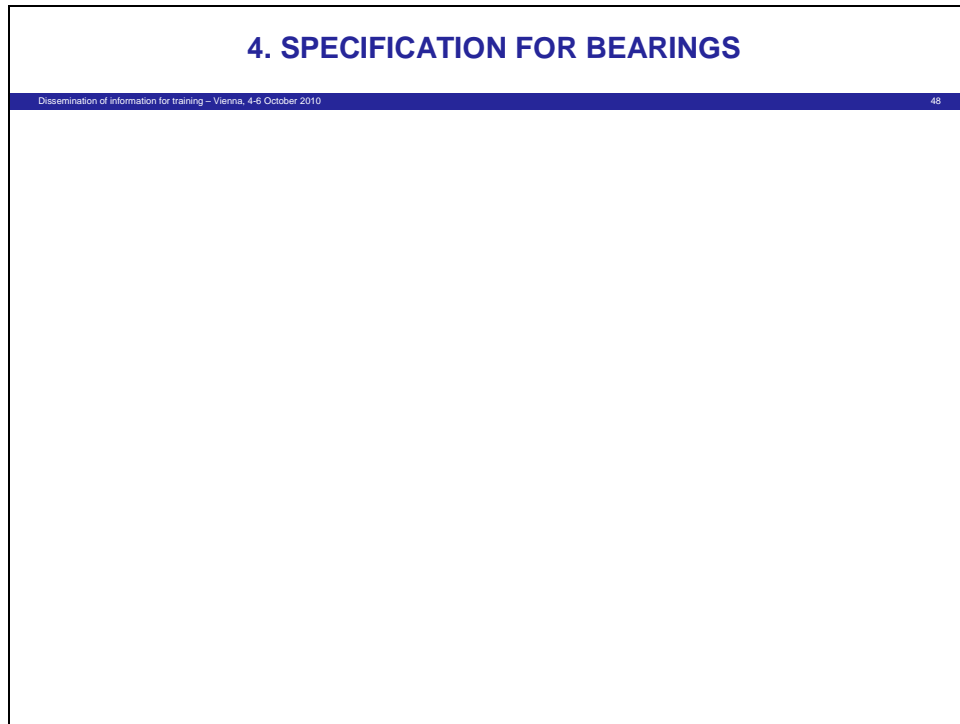


Figure 47

4. SPECIFICATION FOR BEARINGS

Dissemination of information for training – Vienna, 4-6 October 2010 49

Project:

Bearing No.:

This bearing list gives the characteristic values of bearing forces and movements for the final stage of the bridge. Where bearings are installed during construction of the bridge and where the forces and movements in this stage exceed the values in the final stage the relevant forces and movements under construction should be given in a separate bearing list.

Related design values of bearing forces and movements acc. to the combination in clause E.5

N	V _x	V _y	M _x	v _x	v _y	φ _x	φ _y
[kN]	[kN]	[kN]	[kNm]	[mm]	[mm]	[mrad]	[mrad]
Design values of bearing forces and movements at ultimate limit states							
Bearing forces of the fundamental combination acc. to clause E.5							
1.1	max N _{Ed}						
1.2	min N _{Ed}						
1.3	max V _{x,Ed}						
1.4	min V _{x,Ed}						
1.5	max V _{y,Ed}						
1.6	min V _{y,Ed}						
1.7	max M _{x,Ed}						
1.8	min M _{x,Ed}						
Bearing movements of the fundamental combination acc. to clause E.5							
2.1	max v _{x,d}						
2.2	min v _{x,d}						
2.3	max v _{y,d}						
2.4	min v _{y,d}						
2.5	max φ _{x,d}						
2.6	min φ _{x,d}						
2.7	max φ _{y,d}						
2.8	min φ _{y,d}						

Figure 48

- (3) Figure 48 gives an example for the indication of design values from the combination of extreme characteristic values.
- (4) The bearing schedules are then used by the bearing producers to design the bearings according to the rules in EN 1337.

- (5) The reference standards for the preparation of the bearing schedules are given in [Figure 49](#) and [Figure 50](#). For accidental design situations also EN 1991-2 should be taken into account with particular rules for the impact scenarios for bridges to be considered. The National Annex may give descriptive rules (e.g. limitation of bridge movements by structural measures) that apply instead of numerical assessments.

4. SPECIFICATION FOR BEARINGS		
Dissemination of information for training – Vienna, 4-6 October 2010		
50		
Actions for permanent and transient design situations		
No.	Action	Eurocode
	Reference to temperature T_0	DIN EN 1991-1-5:2004-07
1.1	Self-weight	DIN EN 1991-1-7:2007-02
1.2	Dead loads	DIN EN 1991-1-7:2007-02
1.3	Prestressing	DIN EN 1992-1:2005-10 and DIN EN 1994-2:2006-07
1.4	Creep concrete	DIN EN 1992-1:2005-10
1.5	Shrinkage of concrete	DIN EN 1992-1:2005-10
2.1	Traffic loads	DIN EN 1991-2:2004-05
2.2	Special vehicles	DIN EN 1991-2:2004-05
2.3	Centrifugal forces	DIN EN 1991-2:2004-05
2.4	Nosing forces	DIN EN 1991-2:2004-05
2.5	Brake and acceleration forces	DIN EN 1991-2:2004-05
2.6	Footpath loading	DIN EN 1991-2:2004-05
2.7	Wind on structure without traffic	DIN EN 1991-4:2005-07
2.8	Wind on structure with traffic	DIN EN 1991-4:2005-07
2.9	Range uniform temperature	DIN EN 1991-1-5:2004-07, 6.1.3 and 6.1.5
2.10	Vertical temperature difference	DIN EN 1991-1-5:2004-07, 6.1.4 and 6.1.5
2.11	Horizontal temperature difference	DIN EN 1991-1-5:2004-07, 6.1.4 and 6.2
2.12	Soil Settlements	DIN EN 1997-1:2009-09
2.13	Bearing resistance/friction forces	DIN EN 1337, Part 2 to 8
2.14	Replacement of bearing	DIN EN 1991-2:2004-05
2.15	Pressure and suction from traffic	DIN EN 1991-2:2004-05
2.16	Wind during erection	DIN EN 1991-4:2005-07 and DIN EN 1991-1-6:2005-09
2.17	Construction loads	DIN EN 1991-1-6:2005-09
2.18	Accidental actions	DIN EN 1991-1-7:2007-02

• For transient design situations reduction of variable actions due to limited duration → EN 1991-2, 4.5.3. For steel bridges also actions from installation of hot asphalt according to technical project specifications.

Figure 49

4. SPECIFICATION FOR BEARINGS	
Dissemination of information for training – Vienna, 4-6 October 2010	
51	
<u>Actions in accidental design situations</u>	
<ul style="list-style-type: none"> • Specifications according to EN 1991-2 • Limitation of bridge movements by structural measures, e.g. stop devices at abutments 	
<u>Actions in seismic design situations</u>	
Specifications according to EN 1998-1 and EN 1998-2	

Figure 50

6.4 Particularities of combination rules

- (1) Figure 51 gives the principles for the determination of design values of movements and bearing forces when using the combination rules.

4. SPECIFICATION FOR BEARINGS

Dissemination of information for training – Vienna, 4-6 October 2010
52

Determination of design values of movements and bearing forces
Principles

- Combination according to EN 1990, 6.5.3.2 (2) with partial factors according to EN 1990, A.2 and particular rules for climatic temperature effects
- Movements due to creep and shrinkage by multiplying mean values in EN 1992-2 and EN 1994-2 by a factor of 1.35
- Verification of static equilibrium (uplift of bearings) and anchoring devices by applying $\pm 0.05 G_K$ spanwise
- Consideration of deformations of foundation, piers and bearings in the modelling of the structure, see EN 1991-2, 6.5.4.2
- Use of 2nd order theory for accounting for deformations of piers after installation of bearings if required by EN 1992-1-1, 5.8.2 (6).
 For calculation of pier deformations $k_y = 0,5$ may be applied to geometric member imperfections in EN 1992-1-1, 5.2.

Figure 51

- (2) In order to comply with the requirement of realistic behaviour the following particularities should be taken into account:

- the γ_F -value for climatic temperature effects cannot exceed the value $\gamma_F = 1.35$, so that this value should be chosen instead of the recommended value $\gamma_F = 1.5$.
- Creep and shrinkage should be taken into account by using mean values multiplied with a factor of 1.35.
- Non uniform distribution of permanent loads should be considered by applying $\pm 0.05 G_k$ on the influence line for uplift and for anchoring.
- Equivalent geometric imperfections with only 50 % of the geometric member imperfections specified in EN 1992-1-1, 5.2 should be applied.

- (3) For determining the design values of movements from the design values of extreme temperatures $T_{Ed,min}$ and $T_{Ed,max}$ the safety system in Figure 52 should be used. It comprises two elements

- the design values $\pm \gamma_F \cdot \Delta T_N$ with $\gamma_F = 1.35$
- the reference temperature $T_0 \pm \Delta T$ with ΔT from uncertainties of the temperature of the structure during installation, where ΔT_N depends on type of construction and the

typical hour of measurement (e.g. early morning for steel-structures, afternoon for composite structures).

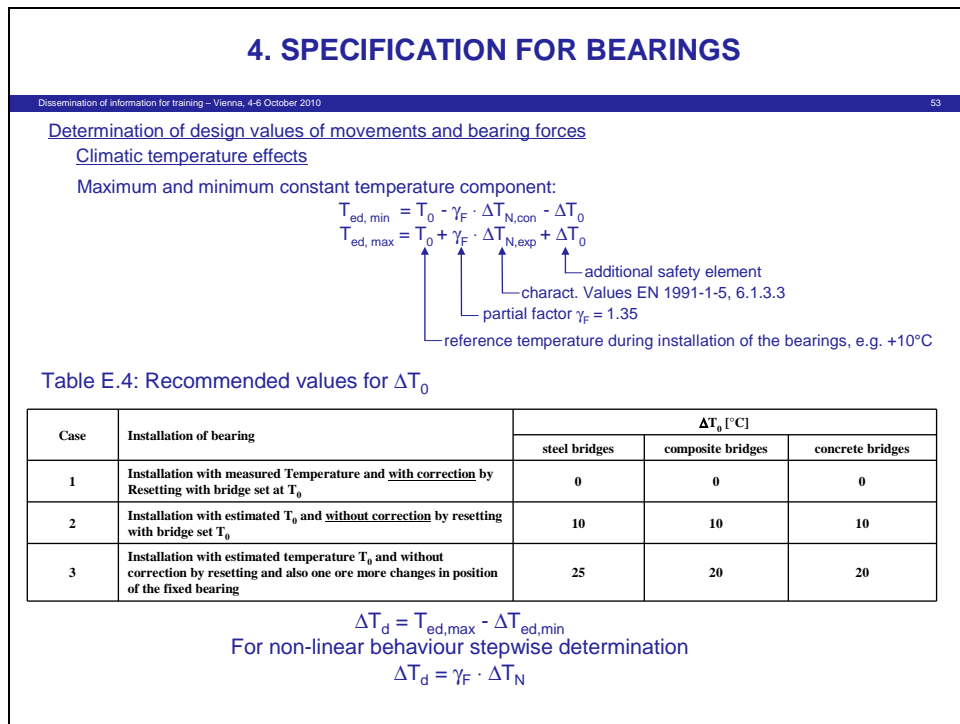


Figure 52

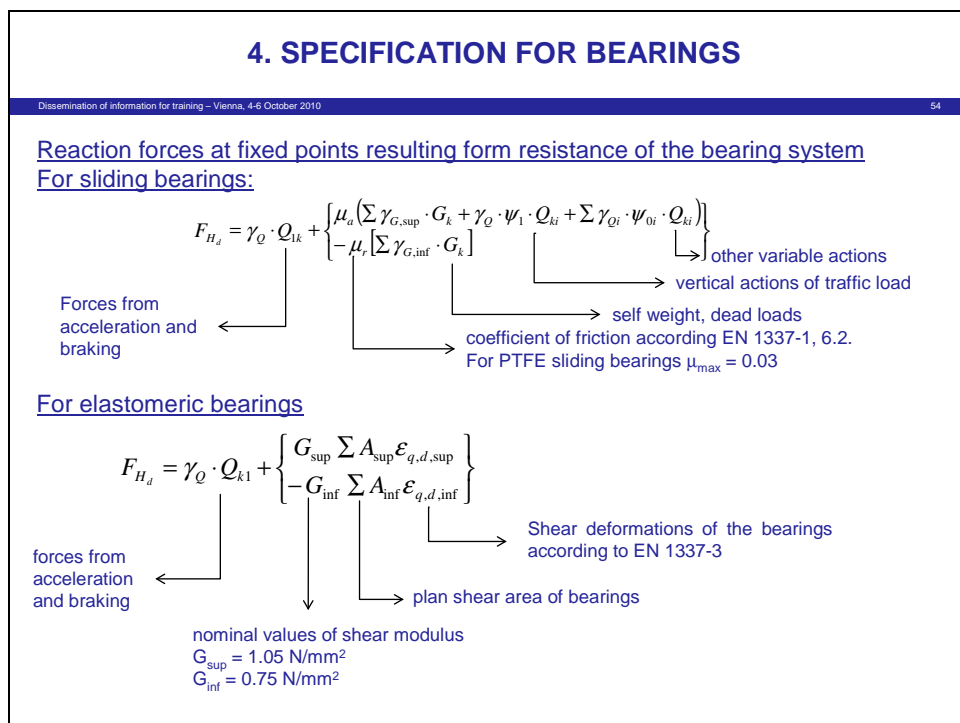


Figure 53

- (4) For continuous bridges over deep valleys with tall piers the fixed bearings may be installed on one or two of the tall piers in the middle of the bridge.

- (5) In this case the horizontal forces from braking and friction in the bearings to be applied to these fixed bearings may be taken from [Figure 53](#).
- (6) This Figure also gives the horizontal forces for the case that bearing may not be caused by friction but by elastic restraints (elastomeric bearings).

7. Choice of material to avoid brittle fracture

7.1 General

- (1) All design rules for steel-structures are based on the evaluation of large scale tests that have been performed at room temperature.
- (2) At this temperature (~20°C) steel normally exhibits a ductile plastic behaviour, so that large plastic strains occur at the ultimate limit state, that cause stress-redistributions in the cross-section and make the use of “nominal stresses” without geometric and metallurgic notch effects and without consideration of secondary moments possible and hence make the design rules simple.
- (3) Not so in the low temperature region where ferritic steels may show in dependancy of their toughness properties a fracture mechanism under tension loads that macroscopically may be classified as brittle, because plastic deformations are small and failure occurs without significant plastic deformations.
- (4) The choice of material to avoid brittle fracture therefore mainly aims at choosing the toughness properties of steel such, that only ULS-verifications in the ductile domain are necessary and other failure mechanisms in the low temperature region can be ignored.
- (5) To meet this goal the toughness of steel that is required, needs to be determined by a fracture mechanics assessment of the component, taking account of
 - the geometric shape and dimensions of the component,
 - the stresses in the component,
 - the hypothetical presence of a crack at the “hot spot” where the geometrical metallurgical and stress situation gives the highest probability for the formation of a crack,
 - a shape and size of the crack that complies with observations in testing and with the accuracy of the testing method as it should be at the limit of detectability,
 - the fatigue loading and inspection management to account for possible crack-growth in service until the crack is detected,
 - the lowest temperature in the component.
- (6) This fracture mechanics assessment is not a “fitness for purpose” check, as the assumptions e.g. the presence of cracks are only hypothetical. It has the character of a check for an “accidental design situation” and hence produces “robustness” for the improbable case that one or more of the hypothetical assumptions would hold true.

- (7) Whereas the requirement of “robustness” is often described in qualitative terms, e.g. by the requirement to avoid progressive collapse, the robustness from the choice of material to avoid brittle fracture is expressed quantitatively.

7.2 Input for the choice of material for steel bridges

- (1) A particularity of the choice of material for steel-bridges is that the design value of crack a_d assumed at the hot spot of a structural component is very much affected by fatigue, see [Figure 54](#).
- (2) Hence the initial crack size a_0 overlooked in testing after fabrication is assumed to be enhanced by crack growth due to fatigue actions. The fatigue action taken into account is one quarter of the full fatigue damage

$$D = \Delta\sigma_c^3 \cdot 2 \cdot 10^3$$

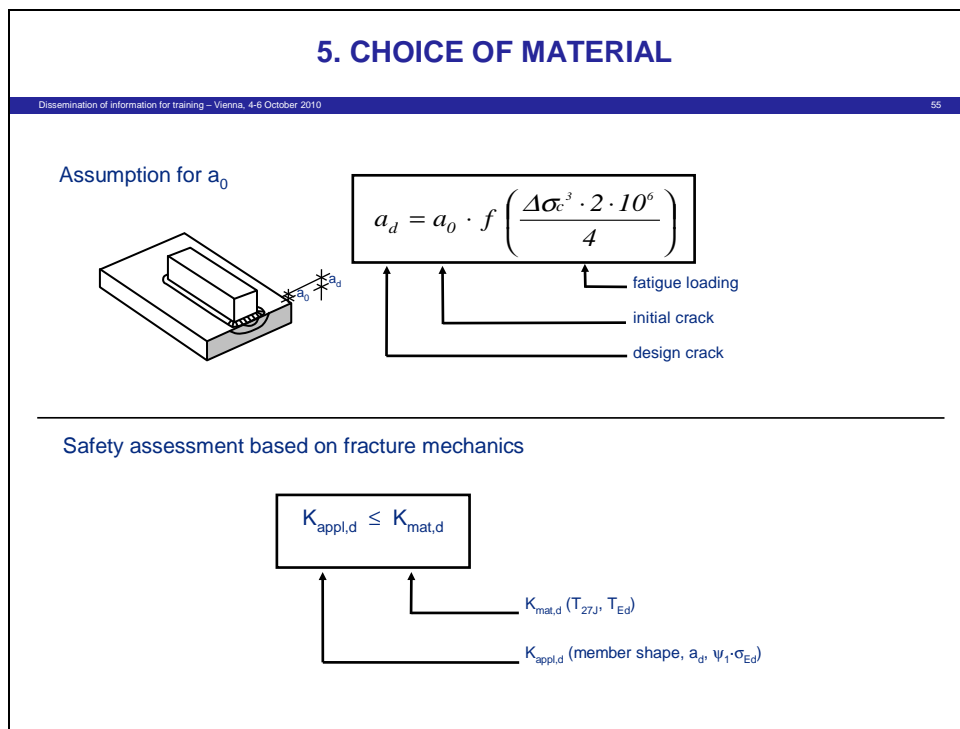


Figure 54

- (3) The fracture mechanics assessment is performed with stress intensity factors K , one for the action side

$$K_{appl,d}$$

which is influenced by the member shape, the crack size and the “frequent” stresses

$$\sigma_{Ed} = \psi_1 \cdot \sigma_{E,ULS}$$

according to the combination rules for accidental design situations, and on the resistance side

$$K_{mat,d}$$

which includes the temperature T_{27J} from Charpy-V-notch impact tests that produce an impact energy of 27 Joule.

This assumption makes it possible to establish a link between the fracture mechanics assessment and the necessary number of inspections during the service life of the structure.

- (5) It also produces structures that are “damage tolerant”, because the crack growth from hypothetical cracks is sufficiently slow, to provide long inspection intervals, and the inspections create a “prewarning system”, so that in case unforeseen damages are detected, there is sufficient time to intervene before damages attain a critical size.

7.3 Basic fracture mechanics procedure

- (1) The safety approach that links the fracture mechanics assessment for ductile material behaviour in the various temperature domains may be taken from [Figure 55](#).
- (2) This Figure shows the toughness-temperature curve with the upper shelf domain B_I and the transition temperature domain A_I with low toughness values. It also shows the load-deformation characteristic from large scale tests to determine design resistances in the ductile domain B_3 and in the elastic domain A_2 .
- (3) The third graph in Figure 55 gives the lines of equal probability of action effects from combinations of actions for bridges:
- For persistent and transient design situations the load level B_2 applies for normal temperatures resulting in upper shelf behaviour and ductile structural responses in tests.
 - For the accidental design situation at extremely low temperatures the load level is at “frequent loads”, A_2 , with toughness properties in the lower part of the toughness-temperature-transition domain, A_I , and elastic structural response in tests, A_3 , compatible with the use of stress-intensity factors K .

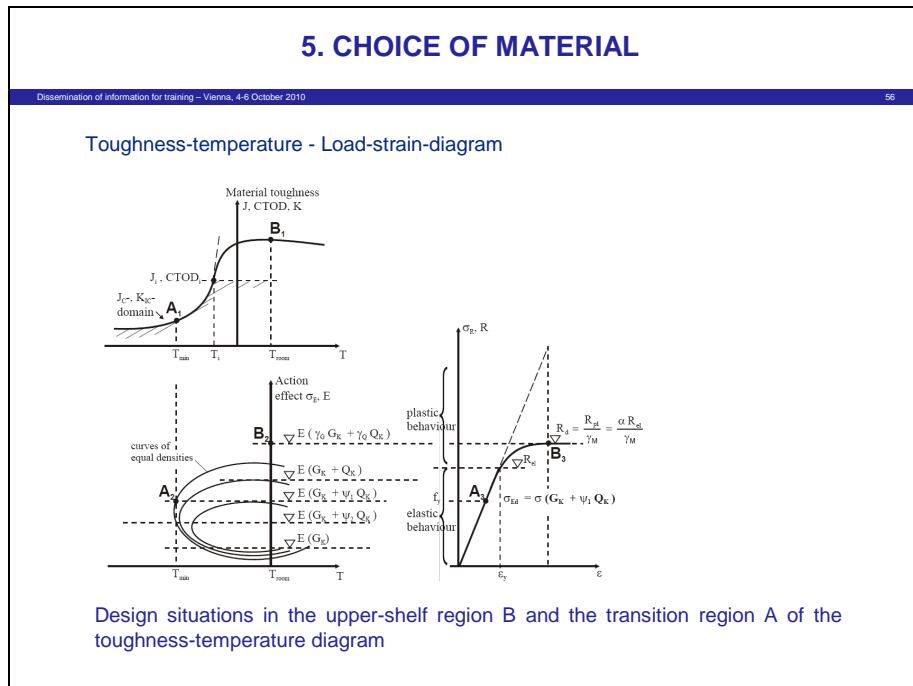


Figure 55

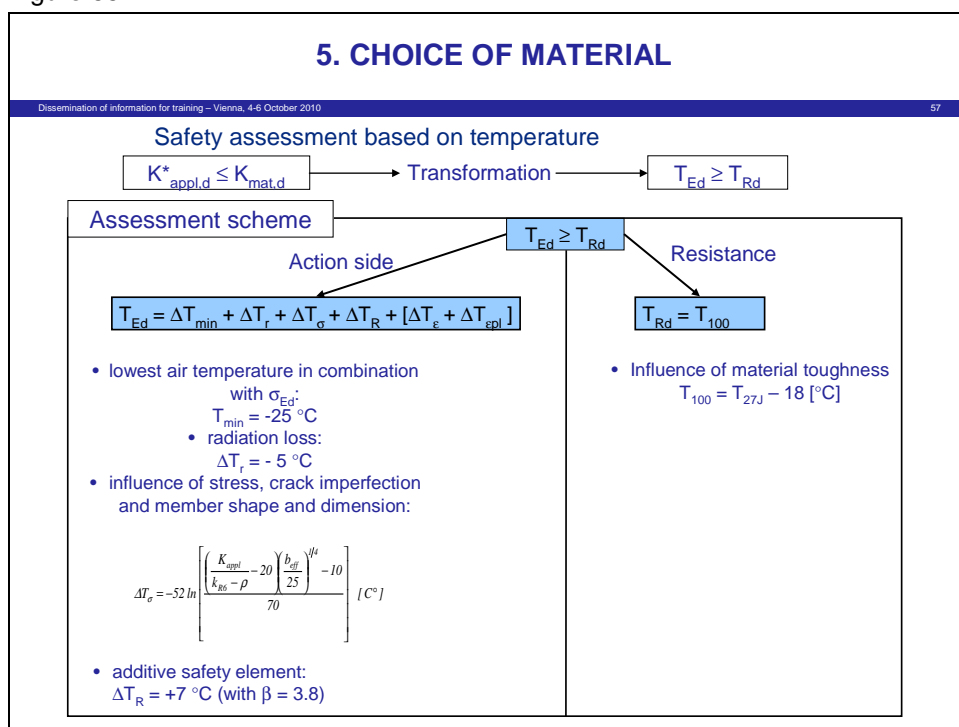


Figure 56

- (4) Figure 56 shows the basic formula for the determination of the minimum toughness properties in EN 1993-1-10 which results from the transformation of the equation with stress intensity factors K to temperatures T .

This temperature oriented equation allows to take additional strain rate effects and cold-forming effects into account by simple temperature-shifts ΔT .

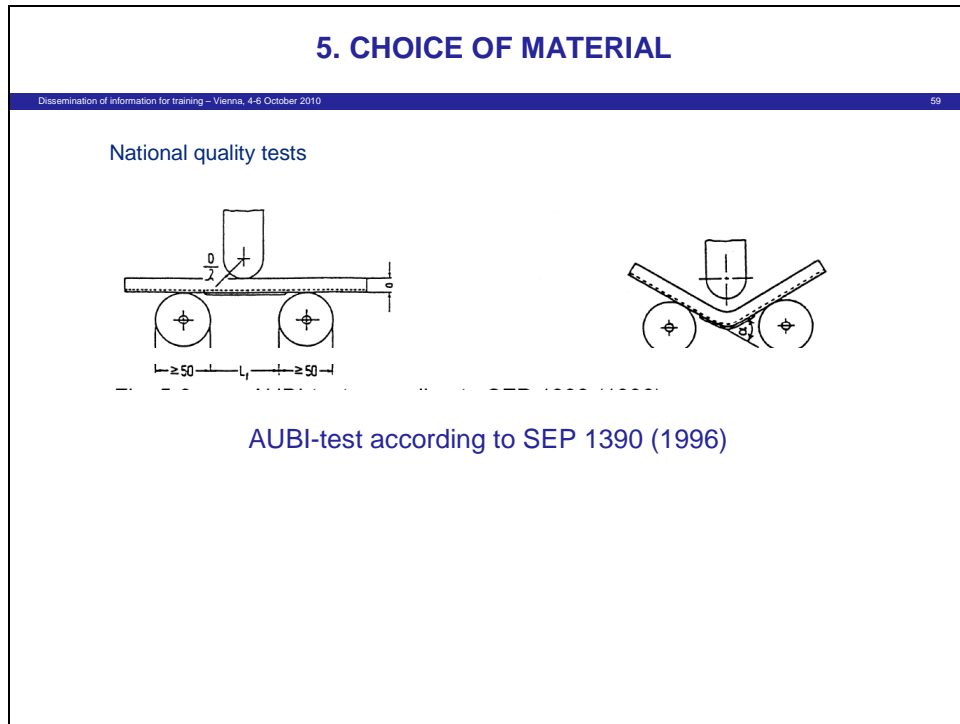


Figure 58

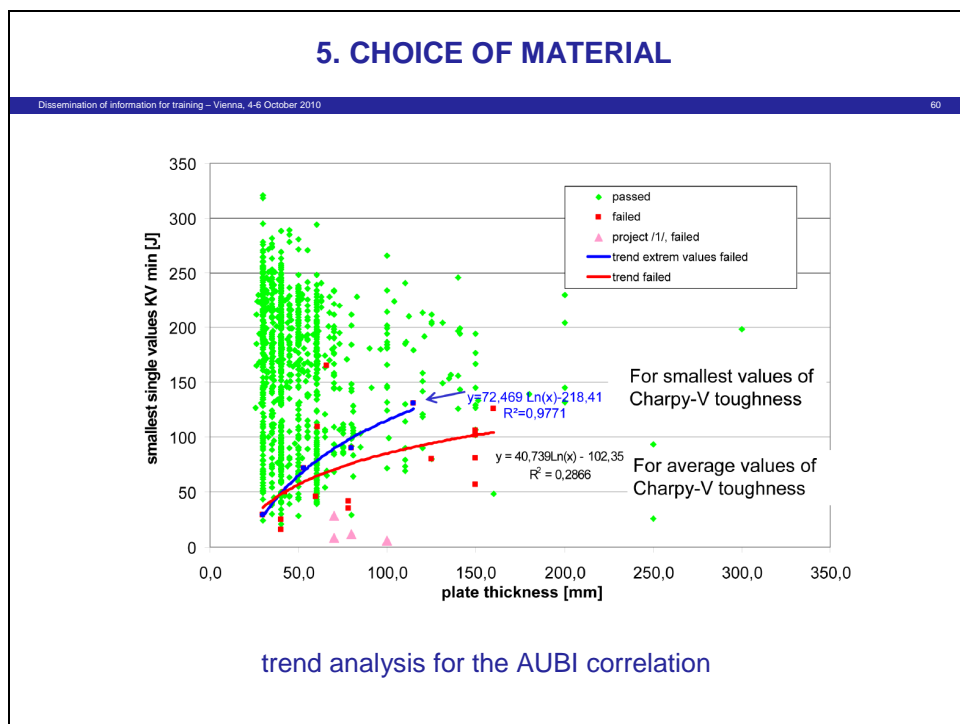


Figure 59

- (5) Figure 59 gives the results of such tests from quality tests of steel producers related to the Charpy-V-notch impact energy and the thickness of the product from which the samples were taken.

- (6) The conclusion from [Figure 59](#) is the recommendation in [Figure 60](#), according to which the choice of fine grain steels is necessary for product thicknesses greater than 30 mm.
- (7) This choice supersedes the choice according to the table in [Figure 57](#).

5. CHOICE OF MATERIAL		
Dissemination of information for training – Vienna, 4-6 October 2010		
61		
Example	Nominal plate thickness	Additional requirement
1	$t \leq 30 \text{ mm}$	$T_{27J} = -20 \text{ °C}$ acc. to EN 10025
	$30 < t \leq 80 \text{ mm}$	Fine grained steel acc. to EN 10025, e.g. S355N/M
	$t > 80 \text{ mm}$	Fine grained steel acc. to EN 10025, e.g. S355NL/ML

Choice of material given in Table 3.1 of EN 1993-2

Figure 60

7.5 Examples for use of EN 1993-1-10 for choice of material in steel bridges

- (1) A conventional steel bridge, with composite box-girder section is given in [Figure 61](#).

The plate thickness of the upper flange and the bottom plate of the box girder that attain values up to 135 mm have been chosen to EN 1993-1-10.

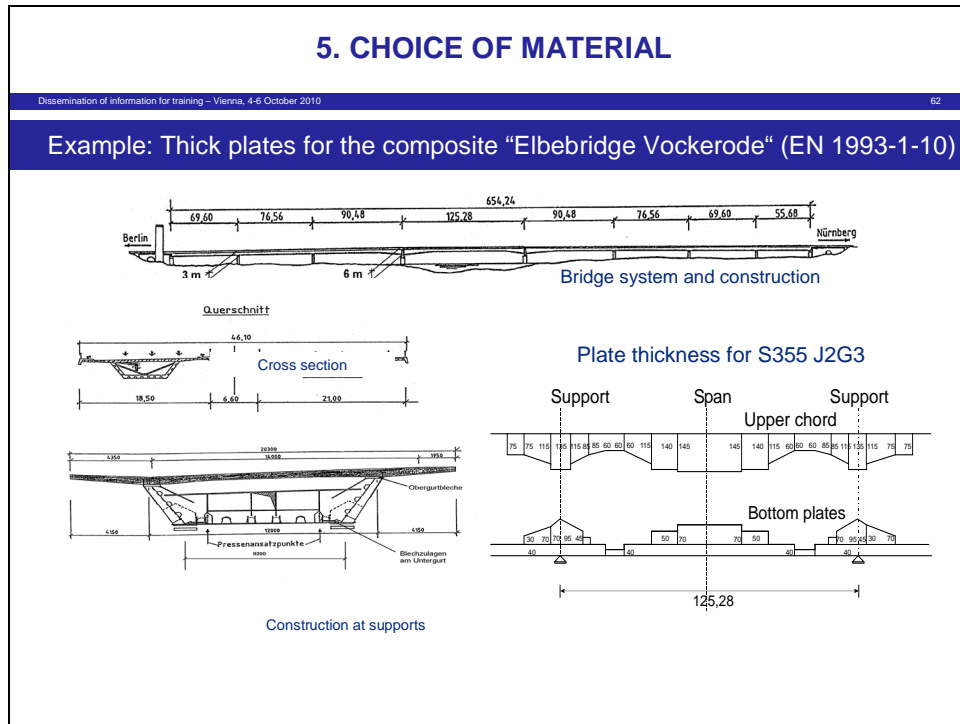


Figure 61

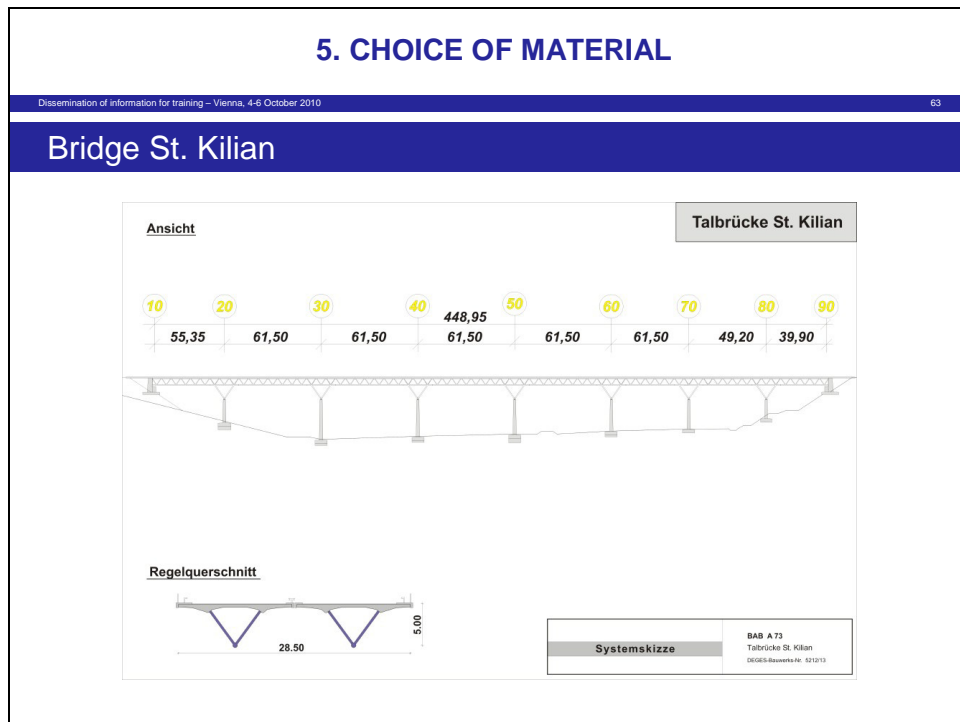


Figure 62

- (2) A non-conventional composite bridge consisting of two separate bridge parts with a triangle cross-section (and an open joint between the decks in the middle) is the St. Kilian bridge in [Figure 62](#).
- (3) The bottom chord of this truss bridge with circular hollow sections is a single tube with nodes made of cast steel.

- (4) The robustness of this structural concept is assured by the choice of material according to EN 1993-1-10 that produces “damage tolerance” together with the usual inspection regime for bridges.

In conclusion the cross-section with a single bottom chord made of steel with sufficient toughness is robustness-equivalent with other cross-sections with more than 1 bottom chord or bottom chords made of steel lamellas (because of redundancies) that have low toughness values (as experienced for existing riveted bridges).

- (5) A particular feature of this robustness concept is the appropriate choice of the fatigue class, which is mainly influenced by the execution quality.
- (6) Figure 63 gives an impression of the erection work, Figure 64 shows the weld preparation between the cast steel nodes and the tubes (with small tolerances) and Figure 65 gives an impression of the cast nodes.

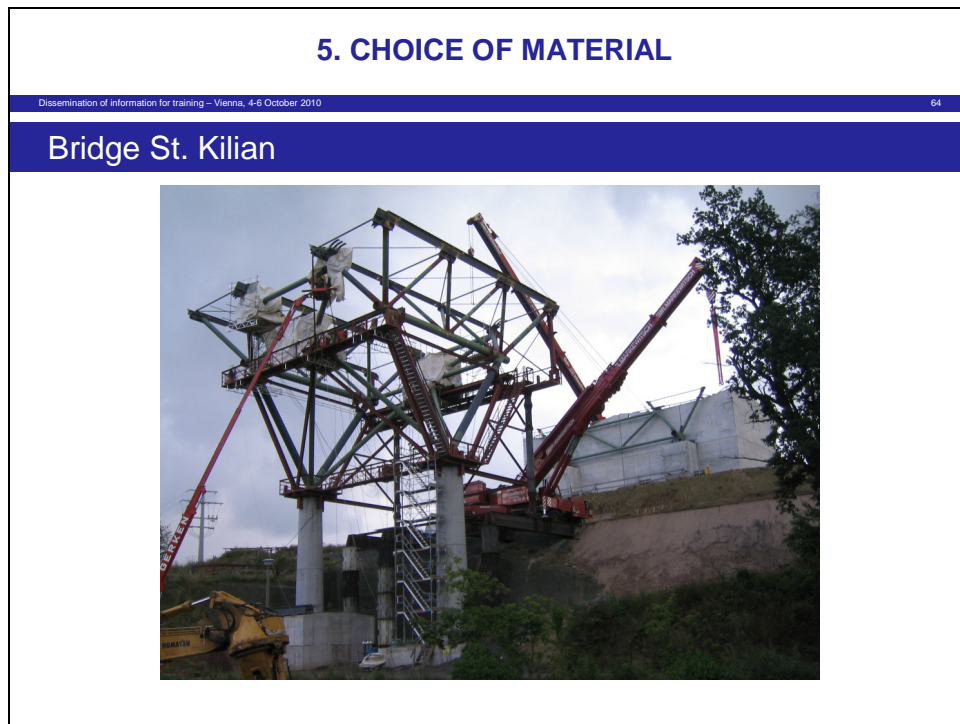


Figure 63

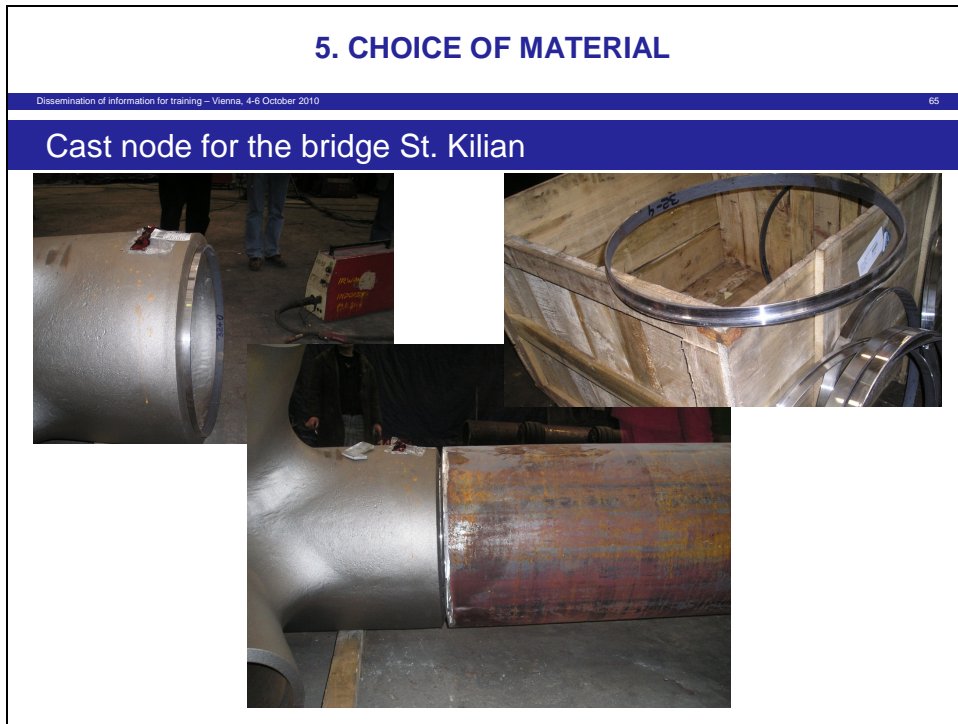


Figure 64

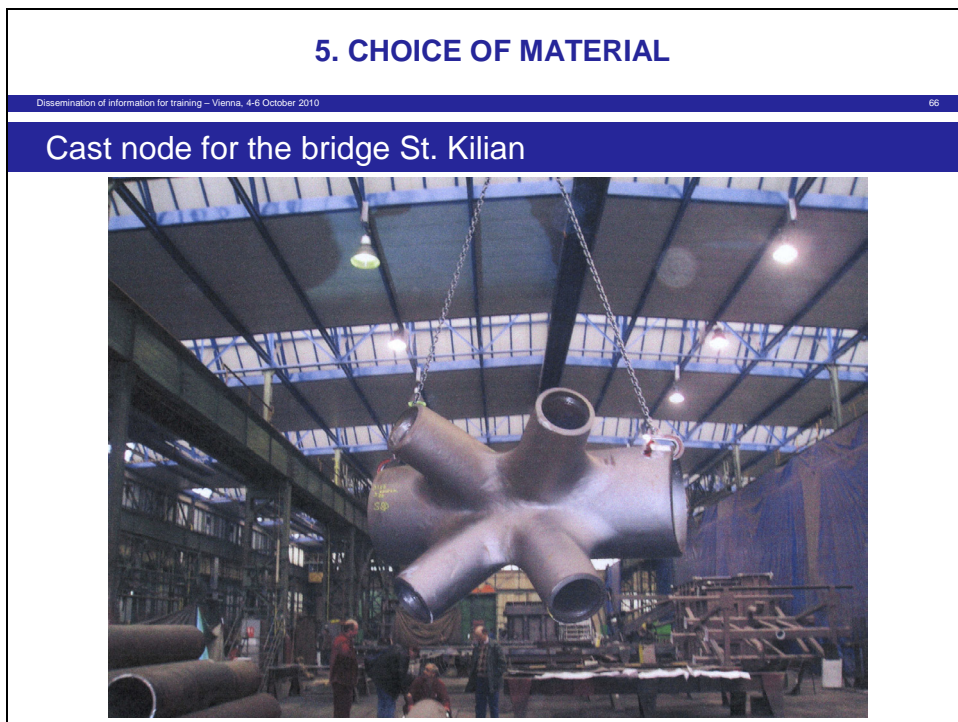


Figure 65

7.6 Further information

- (1) More details of the background of the choice of material for bridges may be taken from the JRC report “Commentary and Worked examples to EN 1993-1-10 “Material toughness and through thickness properties” and other toughness oriented rules in EN 1993”, see [Figure 66](#).

5. CHOICE OF MATERIAL

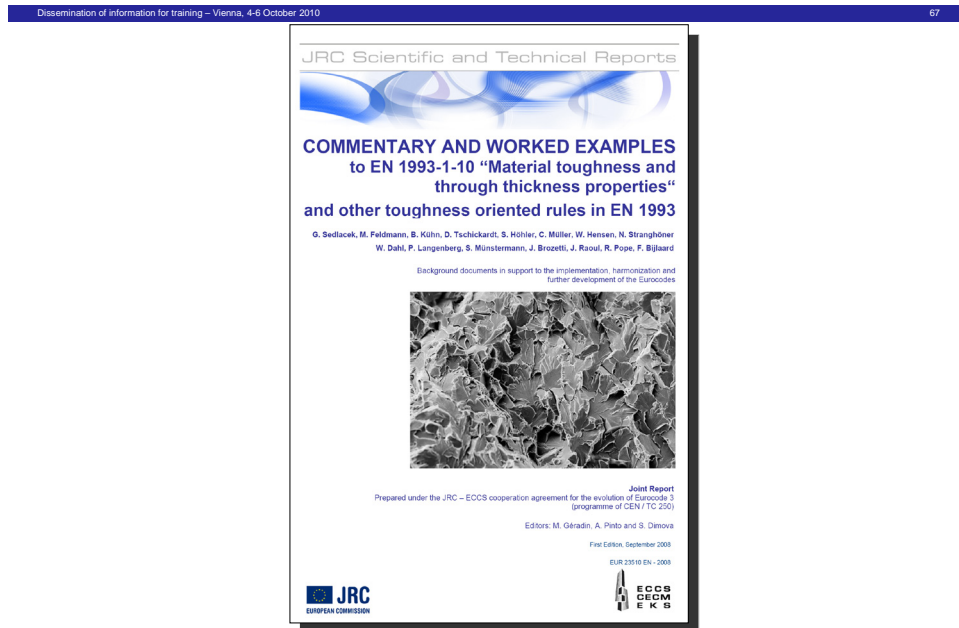


Figure 66

8. Stability rules

8.1 General

- (1) The stability rules dealt with in Eurocode 3 relate to
 - column buckling, see EN 1993-1-1
 - lateral torsional buckling, see EN 1993-1-1
 - plate buckling, see EN 1993-1-5
 - shell buckling, see En 1993-1-6.
- (2) For these buckling phenomena in general two assessment approaches are applicable:
 1. 2nd order assessment with initial equivalent imperfections, that cover the various structural and geometric imperfections a structural member may have,
 2. use of buckling formulas for uniform structural member with defined loading and boundary conditions which should have been derived from 1.
- (3) For practical use buckling formulas for standard cases are very important. Figure 67 gives the common verification concept applicable to the various buckling phenomena, where the definitions are:

$\alpha_{ult,k}$ = magnification factor to design action effects to obtain the characteristic resistance R_k without considering out-of-plane imperfections and out-of-plane buckling.

- α_{crit} = magnification factor to design action effects to obtain elastic critical resistances R_{crit}
- $\bar{\lambda}$ = global slenderness
- χ = reduction coefficient for buckling, depending on the buckling phenomenon, the imperfection factor α and the slenderness $\bar{\lambda}$.

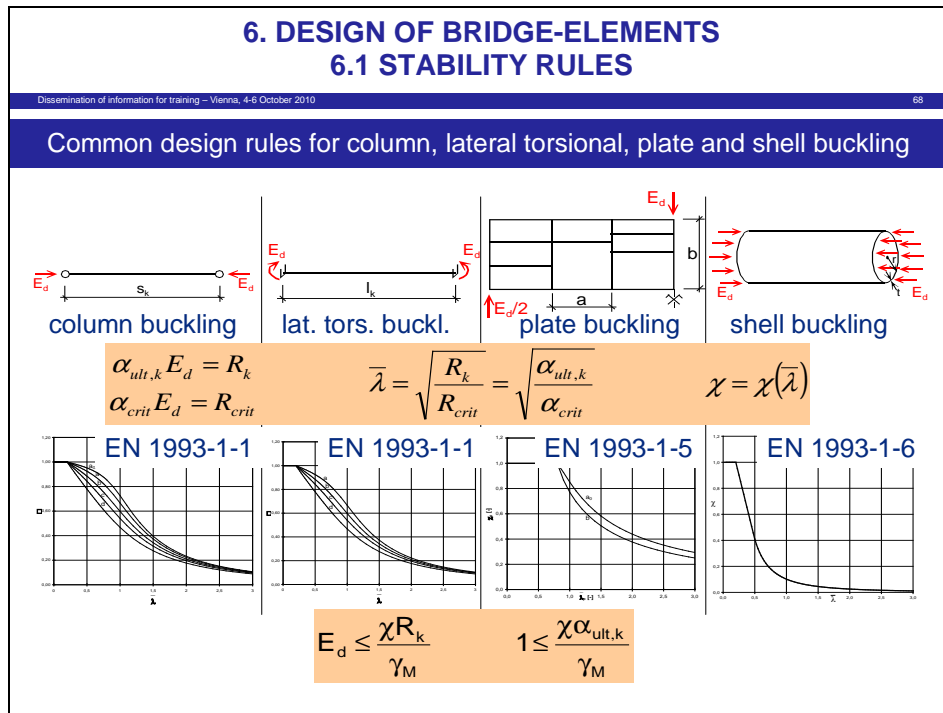


Figure 67

- (4) For steel bridges the conditions for the application of standard formulas are rare, so that a 2nd order assessment or a simplified 2nd order assessments are preferred.
- (5) For steel bridges also
- column buckling and lateral torsional buckling on one side and
 - plate buckling on the other side
- are the relevant phenomena, and shell buckling does in general not occur.
- (6) Therefore this report gives the background of the imperfections to be used in 2nd order analysis and a simplified 2nd order analysis which includes the application of such imperfections in the so-called “General method” that allows to use reduction coefficients for buckling also in cases where loading and boundary conditions are not standardized.

8.2 The uniform column with hinged ends

- (1) The uniform column with hinged ends loaded in compression is the reference component for the definition of equivalent geometric imperfections and simplified procedures with reduction

formula as it is also used for resistance tests to column buckling to which the methods are calibrated.

(2) Figure 68 gives the principles for the derivation of the European flexural buckling curve:

1. It is assumed that the buckling resistance of the column can be expressed in terms of the cross-sectional resistance to compression and to bending that results from equivalent geometric imperfections and second order effects.
The critical cross section is in the middle of the column.

2. The shape of the equivalent geometric imperfection is taken equal to the elastic critical buckling mode, that corresponds to the elastic critical eigenvalue (Euler-critical load), to establish a link to boundary and loading conditions other than those of the reference component.

3. The amplitude of the imperfection factor e^* is composed of three factors

- the imperfection factor α
- the slenderness $\bar{\lambda}$
- the cross sectional value $\frac{M_{Rk}}{N_{Rk}}$

4. The imperfection factor α is the open parameter determined from test evaluation; this parameter is associated with a linear resistance model

$$\frac{N_{Ed}}{N_{Rk}} + \frac{M_{Ed}}{M_{Rk}} = 1$$

in which N_{Rk} and M_{Rk} are the characteristic values of resistances, that may be either elastic or plastic.

5. The verification format allows a two step assessment:

1. A unified European characteristic resistance:

$$R_k = \chi \cdot N_{pl,k}$$

2. A „national“ design value:

$$R_d = \frac{R_k}{\gamma_M}$$

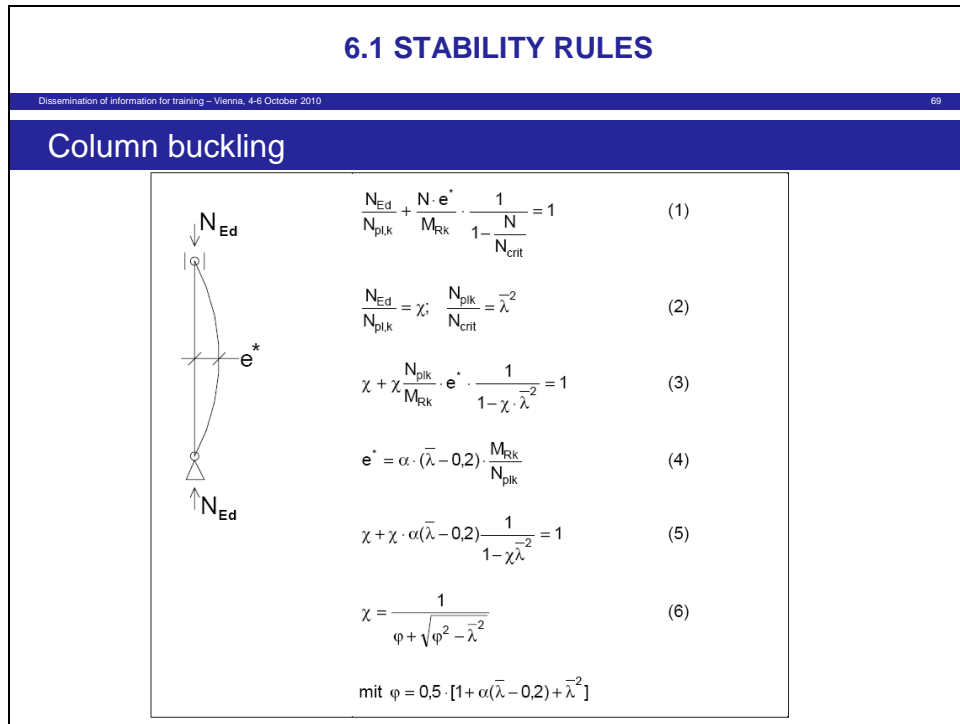


Figure 68

- (3) As a result of the derivation in [Figure 68](#), [Figure 69](#) gives the shapes of the reduction factors χ for various cross sectional shapes, to which various α -values belong, see [Figure 70](#).

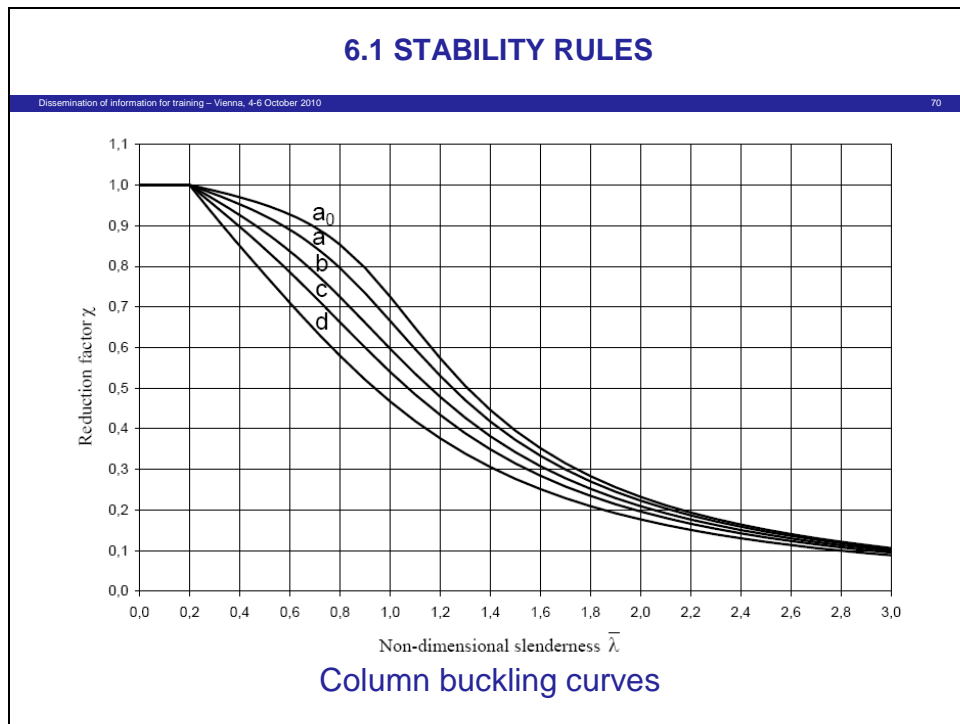


Figure 69

6.1 STABILITY RULES

Dissemination of information for training – Vienna, 4-6 October 2010 71

Cross section		Limits	Buckling about axis	Buckling curve
Rolled sections		$t_f \leq 40 \text{ mm}$	y-y z-z	a a ₀
		$40 \text{ mm} < t_f \leq 100$	y-y	b
			z-z	c
		$t_f \leq 100 \text{ mm}$	y-y z-z	b e
Welded I-sections		$t_f \leq 40 \text{ mm}$	y-y z-z	b c
		$t_f > 40 \text{ mm}$	y-y z-z	c d
Hollow sections		hot finished	any	a
		cold formed	any	c
Welded box sections		generally (except as below)	any	b
		thick welds: $a > 0.5t_f$ $b/t_f < 30$ $h/t_w < 30$	any	c
U-, T- and solid sections		any	any	c
L-sections		any	any	b

Selection of buckling curves

Figure 70

- (4) The ratios of experimental results r_e and results calculated with the formula for the reduction coefficient χ are given in [Figure 71](#) for weak axis buckling. [Figure 72](#) shows the partial factors γ_M that result from test-evaluation according to EN 1990 – Annex D, to obtain the design values ($\alpha_R \beta = 0.8 \cdot 3.8 = 3.03$).

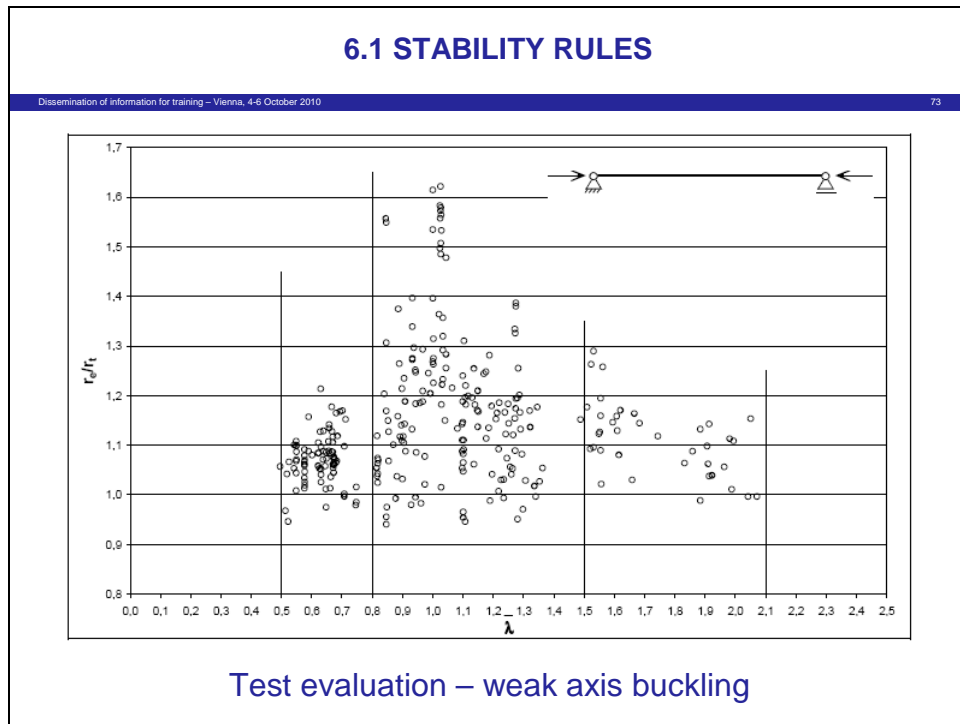


Figure 71

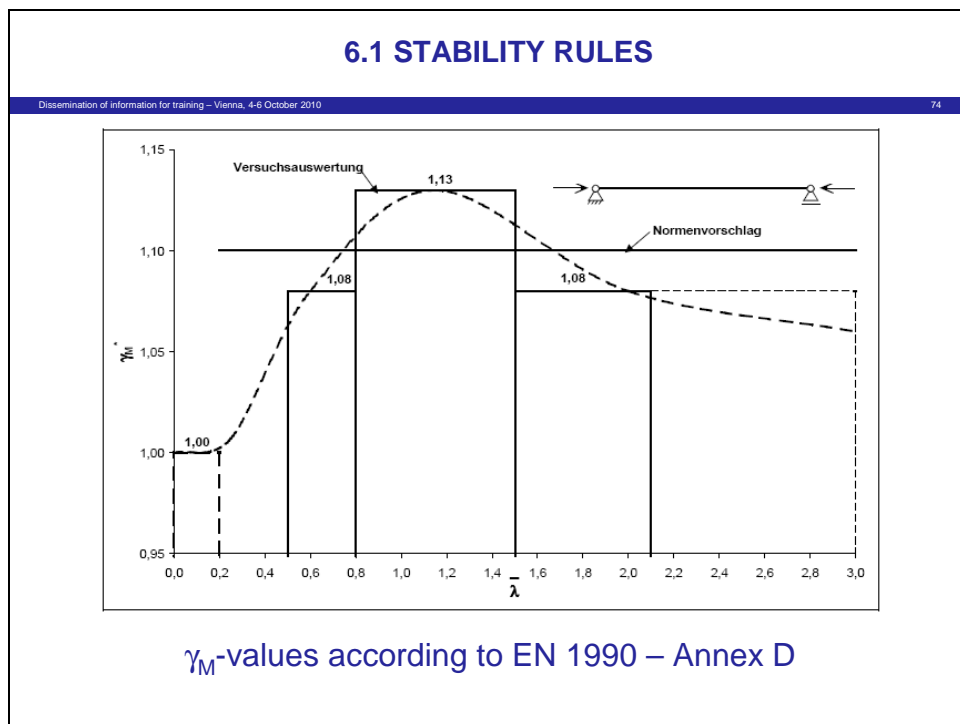


Figure 72

8.3 Conclusions for second order analysis

- (1) The derivation of the characteristic value R_k of column resistance to compression via a reduction value χ includes a 2nd order approach for the balance

$$E_d \leq R_k$$

see [Figure 73](#). The usual 2nd order approach with imperfections is based on the balance

$$E_d \leq R_d \cdot$$

- (2) In conclusion the results for the two different balances can be only made consistent, if for the normal 2nd order approach with imperfections one of the following options is applied:

1. the partial factor on the action side is $\gamma_F \cdot \gamma_M$
2. a γ_M -factor is applied to the modulus of elasticity
3. γ_M is taken as equal 1.0
4. the amplitude of imperfection e_0 is factored by a function of γ_M to obtain e_d
5. for normal 2nd order theory the partial factor γ_M^* is larger than γ_M for the buckling curve.

6.1 STABILITY RULES	
Dissemination of information for training – Vienna, 4-6 October 2010	
75	
European buckling curve	2nd order theory with imperfection
$E_d = R_k$ $\bar{\lambda} = \sqrt{\frac{N_{pl}}{N_{crit}}}$ $\chi = (\alpha, \bar{\lambda})$ $R_k = \chi \cdot N_{pl}$ $R_d = \frac{R_k}{\gamma_M}$	$E_d = R_d$ $\bar{\lambda}_d = \sqrt{\frac{N_{pl,d}}{N_{crit}}}$ $\chi_d = (\alpha, \bar{\lambda}_d)$ $R_d = \frac{\chi_d \cdot N_{pl}}{\gamma_M}$
	<p><u>Consequences:</u></p> <p>Option 1: $\bar{E}_d = \gamma_M \cdot E_d$</p> <p>Option 2: $\bar{N}_{crit,d} = \frac{N_{crit}}{\gamma_M}$</p> <p>Option 3: $\gamma_M = 1.0$</p> <p>Option 4: $e_d = e_0 \frac{1 - \chi^2}{1 - \chi_d^2}$</p> <p>Option 5: $\gamma_M^* = \frac{\chi_d}{\chi} \cdot \gamma_M$</p>
Equivalence of buckling curves and 2 nd order theory	

Figure 73

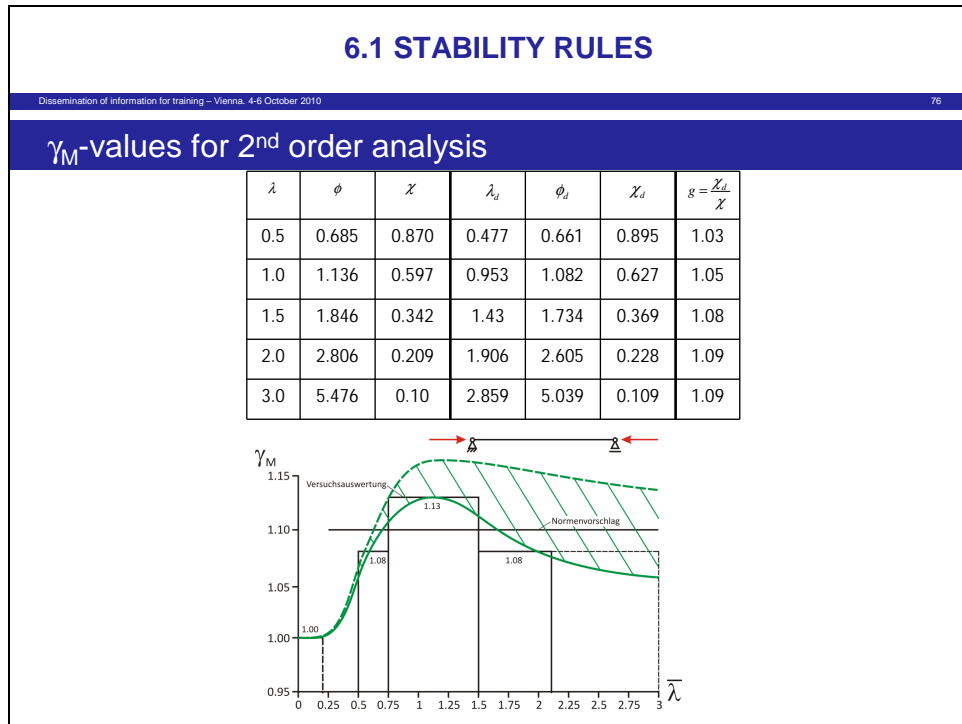


Figure 74

- (3) Figure 74 gives the modification of the partial factor to obtain

$$\gamma_M^* = g \cdot \gamma_M.$$

- (4) In conclusion there are two possibilities depending on National Choice:

1. γ_M is chosen equal to 1,00 and consistency is automatically achieved,
2. in case of $\gamma_M > 1.00$, e.g. $\gamma_M = 1.10$, the difference between the functions γ_M and γ_M^* to the constant value γ_M is so small that both for the use of buckling curves χ and for 2nd order analysis with imperfections e_0 the same γ_M -factor can be used (with a slight advantages for 2nd order analysis in relation to the use of χ -values).

8.4 Extension to other boundary conditions

- (1) The use of the elastic critical buckling mode η_{crit} allows to extend the applicability of the cross-sectional check in Figure 68 and hence the reduction factor χ to any other boundary conditions as given in Figure 75, e.g. by modifying the “buckling length”.

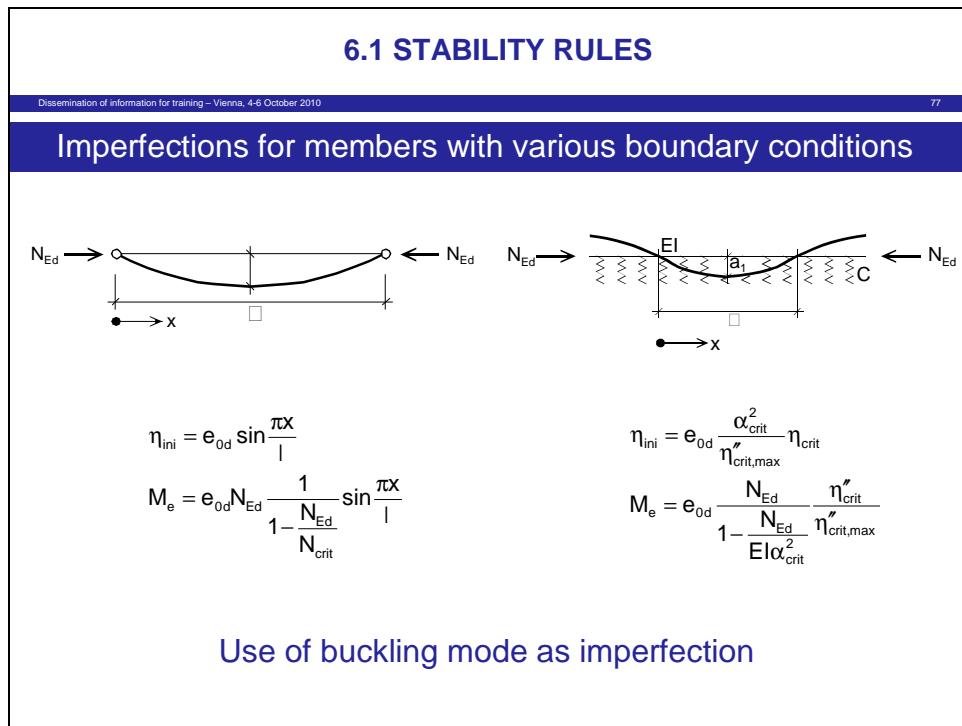


Figure 75

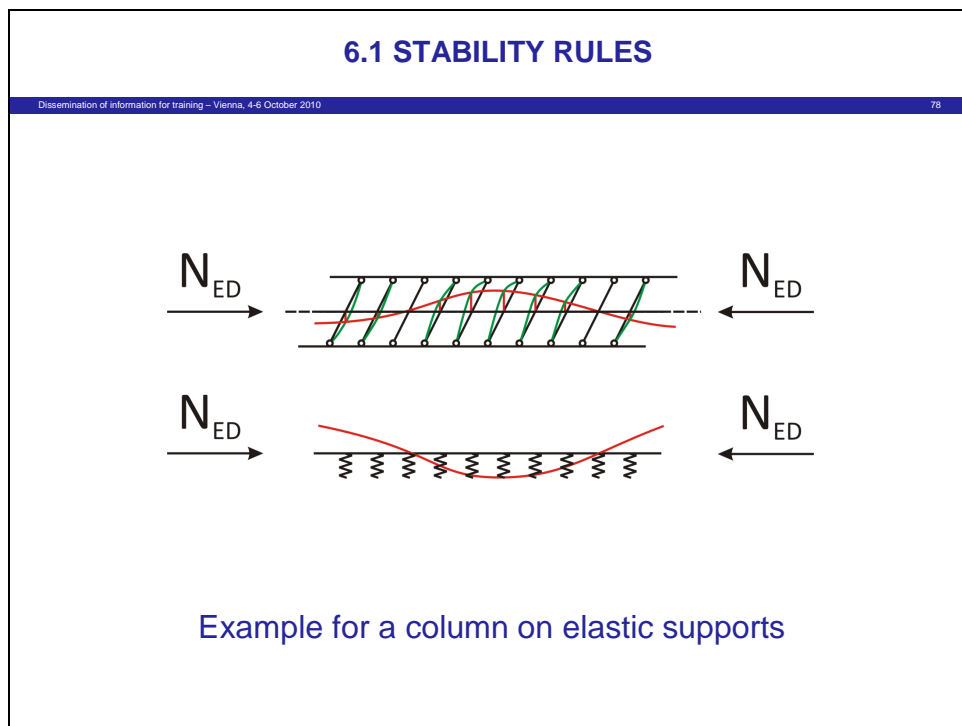


Figure 76

- (2) The comparison in Figure 75 shows that
- the initial equivalent geometric imperfection is not referred to max. η_{crit} , but to max. η_{crit}'' , and the shape of η_{crit}'' is the shape of bending moment from imperfections.

Therefore the equivalent geometric imperfection is not an out-of straightness imperfection in terms of displacement but a curvature imperfection.

- The advantage of taking the buckling mode η_{crit} as shape of imperfection is that with η_{crit} also the bending moment M_e according to 2nd order theory can be easily determined.
- The extension of the application of the flexural buckling curve is not limited to one-dimensional structures as columns, bars etc., but also to two dimensional structures as grids, see [Figure 76](#), for which the condition applies that external forces do not change their value in dependance of buckling deformations (conservative loading).

8.5 Lateral torsional buckling

- (1) A beam with equal end-moments, which effects compression in one flange can be assessed in a similar way as a column, if the assessment is performed for the flange in compression for out-of-plane buckling, see [Figure 77](#).

6.1 STABILITY RULES	
Dissemination of information for training – Vienna, 4-6 October 2010 79	
Column buckling	Lateral torsional buckling
$\frac{N_{Ed}}{N_{pl,Rk}} + \frac{M_{Ed}}{M_{y,Rk}} = 1$	$\frac{N_{Ed}^{FI}}{N_{pl,Rk}^{FI}} + \frac{M_{Ed}^{FI}}{M_{y,Rk}^{FI}} = 1$
$\frac{N_{Ed}}{N_{pl,Rk}} + \frac{N_{Ed} e^*}{M_{y,Rk} \left(1 - \frac{N_{Ed}}{N_{crit}}\right)} = 1$	$\frac{M_{z,Ed}}{M_{z,Rk}} + \frac{M_{z,Ed}}{M_{z,crit}} \frac{N_{crit}^{FI}}{M_{y,Rk}^{FI}} e^* \frac{1}{1 - \frac{M_{z,Ed}}{M_{z,crit}}} = 1$
$e^* = \alpha \left(\bar{\lambda}_N - 0.2 \right) \frac{M_{y,Rk}}{N_{pl,Rk}}$ $\chi_N + \chi_N \alpha \left(\bar{\lambda}_N - 0.2 \right) \frac{I}{I - \chi_N \bar{\lambda}_N^2} = 1$	$e^* = \alpha \left(\bar{\lambda}_M - 0.2 \right) \frac{M_{y,Rk}^{FI}}{N_{pl,Rk}^{FI}}$ $\chi_M + \chi_M \alpha \frac{\bar{\lambda}_M^2}{\bar{\lambda}_{FI}^2} \left(\bar{\lambda}_M - 0.2 \right) \frac{I}{I - \chi_M \bar{\lambda}_M^2} = 1$
$\chi = \frac{1}{\varphi + \sqrt{\varphi^2 - \bar{\lambda}^2}}$ $\varphi = 0.5 \left(1 + \alpha \left(\bar{\lambda} - 0.2 \right) + \bar{\lambda}^2 \right)$	
Equivalence of flexural and lateral torsional buckling	

Figure 77

- (2) The hypothesis used in the derivation in Figure 77 is that the equivalent geometric imperfection e^* for the flange is the same as for a column with flexural out-of-plane buckling.
- (3) The derivation shows that for lateral torsional buckling the same expression as for flexural buckling is obtained, however with the difference, that the imperfection factor α is reduced to α^* by the effect of the St. Venant-torsional rigidity, which is determined by the ratio

$$\frac{\bar{\lambda}_M^2}{\bar{\lambda}_{FI}^2} = \frac{\alpha_{crit}^*}{\alpha_{crit}}$$

where

$\bar{\lambda}_M^2$ is the slenderness for the lateral torsional buckling problem based on α_{crit}

$\bar{\lambda}_{Fl}^2$ is the slenderness of the isolated flange in compression; that can also be expressed by α_{crit}^* calculated without St. Venant-torsional rigidity.

- (4) Figure 78 gives the difference between the flexural buckling curve b and the lateral torsional buckling curve with reduced imperfection factor α^* for a HEB 200 beam.
- (5) Test evaluations with all available test reports for lateral torsional buckling tests have proven that the lateral torsional buckling curve as given in Figure 77 gives the best fit with γ_M -values in the range of 1.05.

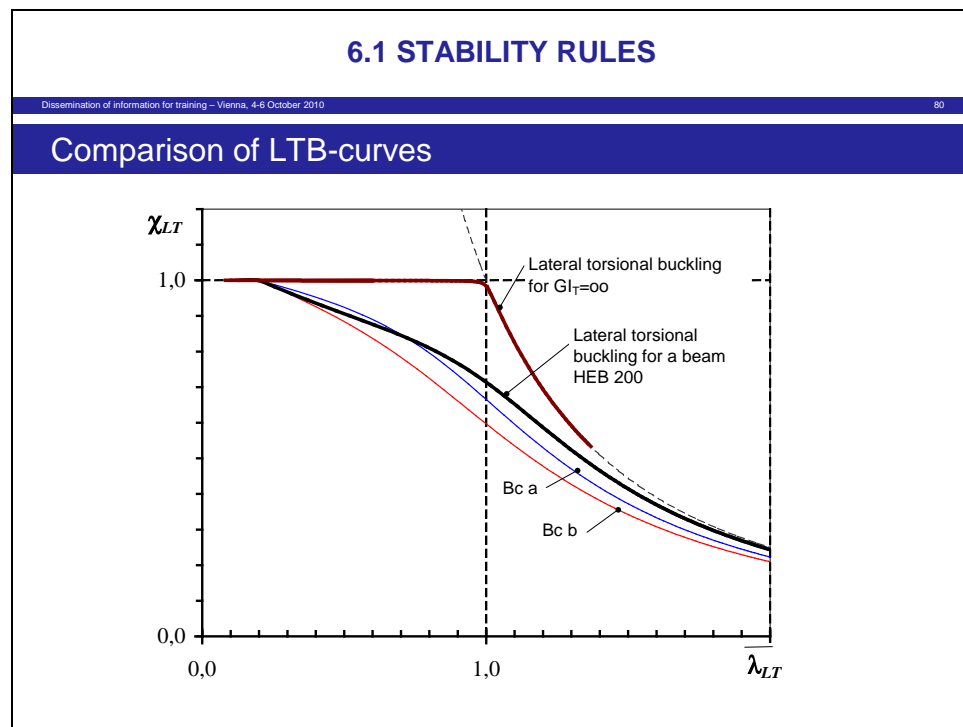


Figure 78

- (6) A generalisation of the procedure in Figure 77 leads to the rule for determining the reduction factor χ for any out-of-plane stability problem, that may be composed of mixed flexural and lateral torsional buckling and includes any out-of-plane boundary condition, see Figure 79.

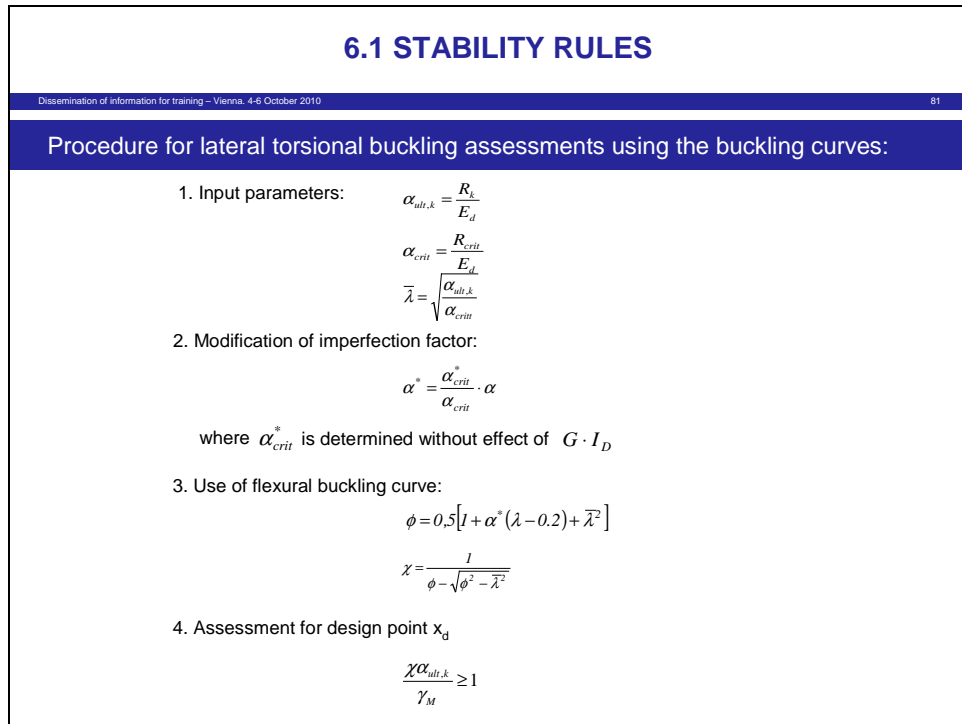


Figure 79

- (7) If the design point x_d is known, where the sum of in-plane stresses and out-of-plane stresses from imperfections give the relevant maximum value, the input parameters can be calculated.

In this case $\alpha_{ult,k}$ is determined at the point x_d .

If the design point x_d is not known, $\alpha_{ult,k}$ can be conservatively estimated as $\alpha_{ult,k,min}$.

- (8) If the two elastic critical values α_{crit} with torsional rigidity and α_{crit}^* without torsional rigidity are available the modified α^* -value can be determined.

A conservative approach is

$$\alpha^* = \alpha$$

- (9) Figure 80 shows an example for a beam with unequal end-moments, where the design point is at a distance $x_d = 0,155 l$ from the maximum loaded end.

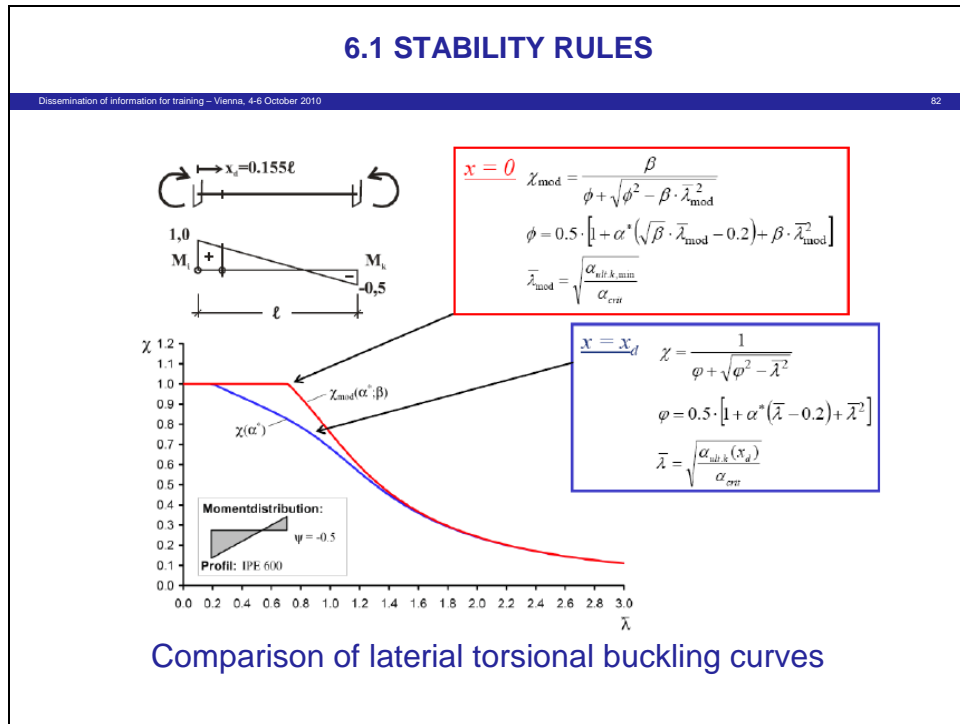


Figure 80

- (10) If for convenience the assessment is carried out with $\alpha_{ult,k}$ at the maximum loaded end $x=0$, the results are either conservative or a modified buckling curve χ_{mod} is used, that includes a correction with β on the basis of knowledge where the design point x_d is.

8.6 Determination of the design point x_d for lateral torsional buckling

- (1) The location of the design point x_d for lateral torsional buckling where in-plane- and out-of-plane effects sum up to a maximum can be determined with the knowledge of the distribution of in-plane effects and out-of-plane effects.
- (2) Figure 81 shows for a two span beam, the loaded top flange of which is to be checked, the distribution of in-plane moments and in-plane stresses in the flange and the modal out-of-plane displacements η_{crit} and modal out-of-plane flange moments $E I(x) \eta_{crit}''$, that are produced together with the elastic critical eigenvalue α_{crit} .
- (3) There are two possibilities for the lateral torsional buckling check:
- either to determine the out-of-plane 2nd order moments from the modal out-of-plane flange moments $E I(x) \eta_{crit}''$ and to perform a cross-sectional check, at x_d ,
 - or to apply a χ -check, where the distributions of the in-plane- and out-of-plane stresses suggest to be the critical points x_d .

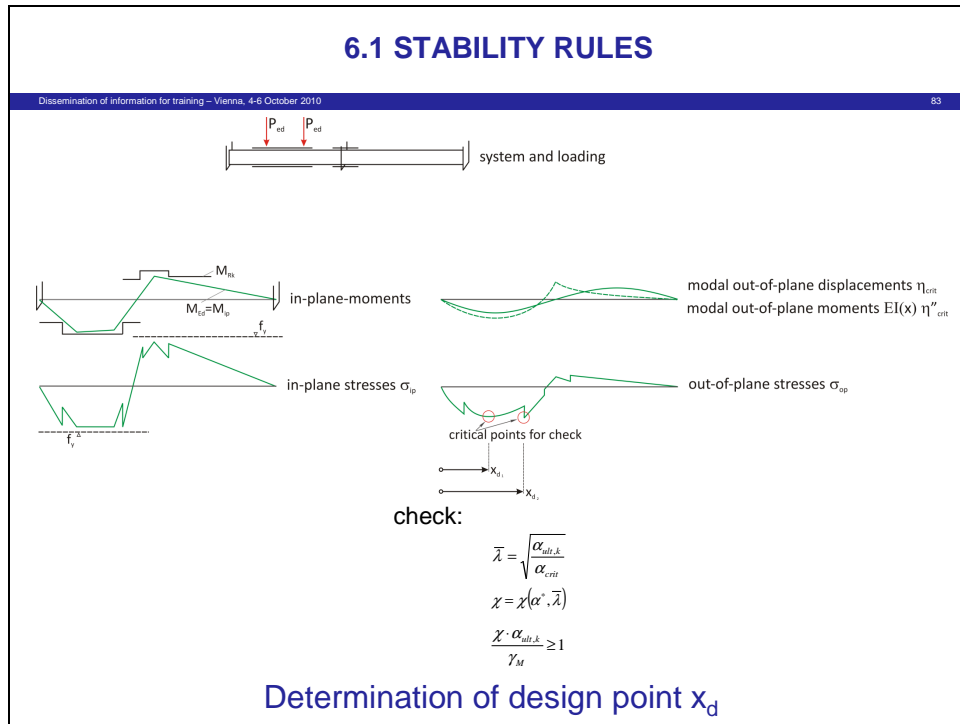


Figure 81

8.7 Examples for lateral torsional buckling verification at the design point x_d

- (1) For a welded portal frame of an industrial hall with the dimensions and support conditions for out-of-plane movements as given in [Figure 82](#) the distribution of in-plane-action effects according to [Figure 83](#) apply.

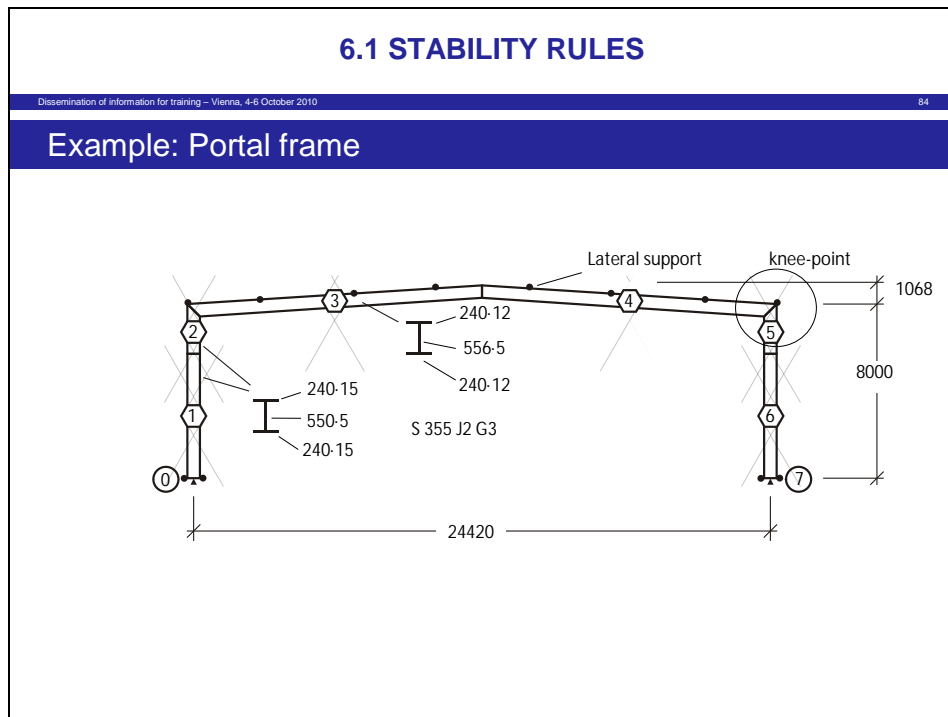


Figure 82

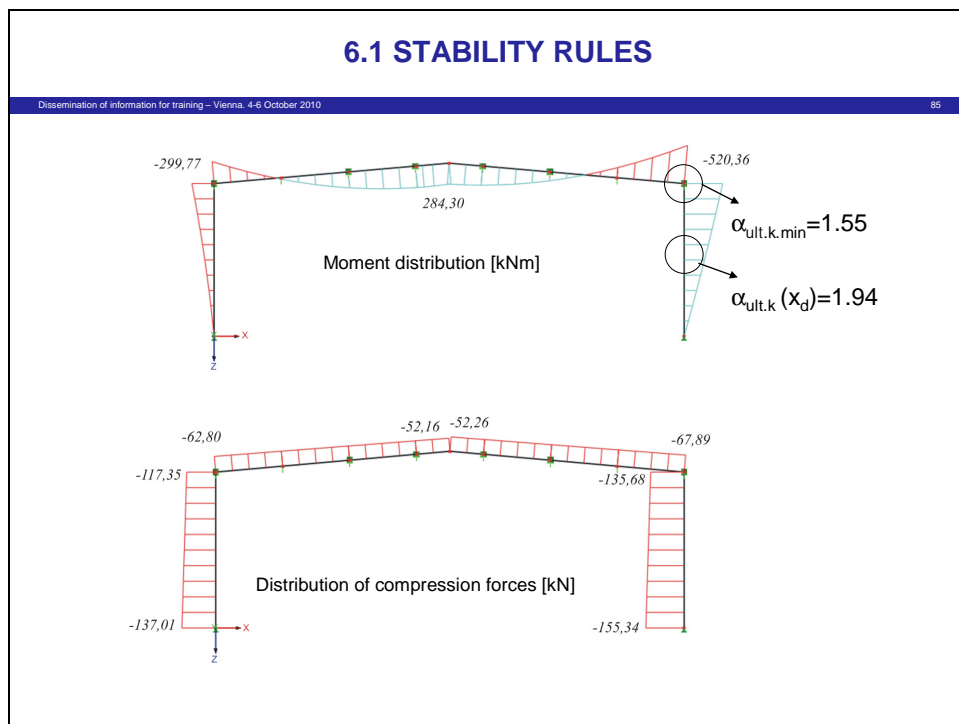


Figure 83

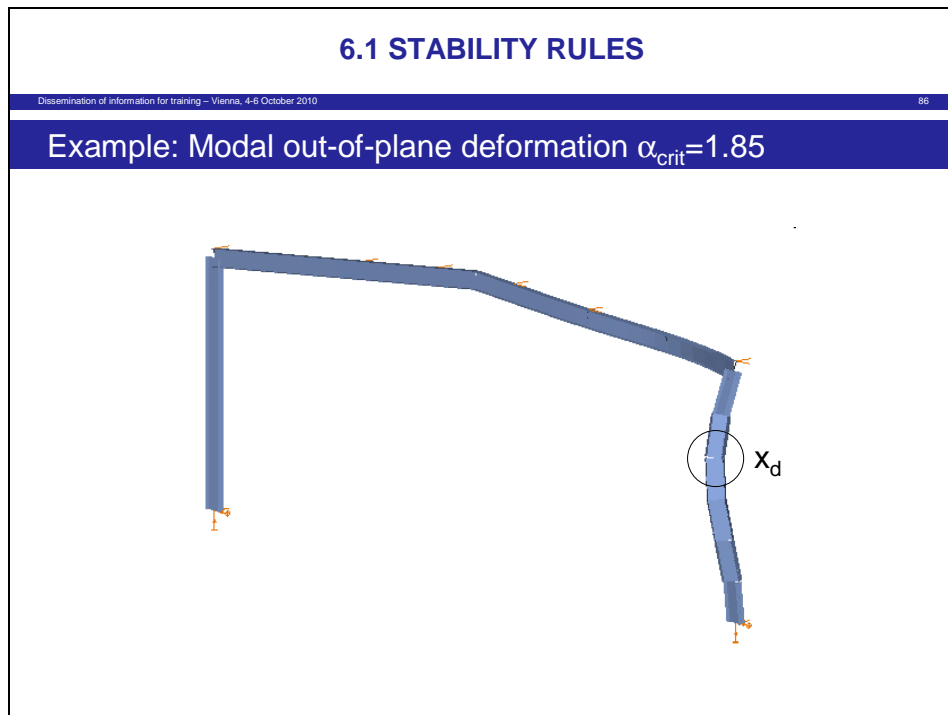


Figure 84

- (2) The distribution of bending moments in [Figure 83](#) gives the location for $\alpha_{ult,k,min} = 1.55$ and the maximum curvature in [Figure 84](#) gives the design point x_d , for which $\alpha_{ult,k}(x_d) = 1.94$ applies.

6.1 STABILITY RULES	
Dissemination of information for training – Vienna, 4-6 October 2010 87	
1. Calculation with extreme value $\alpha_{ult,k,min}$	2. Calculation design point x_d
$\alpha_{ult,k} = 1.55$ $\alpha_{crit} = 1.85$ $\alpha_{crit}^* = 1.84$ $\bar{\lambda} = \sqrt{\frac{1.55}{1.85}} = 0.915$ $\alpha^* = \frac{\alpha_{crit}^*}{\alpha_{crit}} \alpha = \frac{1.84}{1.85} \cdot 1.55 = 1.54$ $\alpha = \frac{1.54}{1.85} = 0.49$ $\phi_{LT} = 0.5[1 + \alpha^*(\bar{\lambda} - 0.2) + \bar{\lambda}^2] = 1.064$ $\chi = \frac{1}{\phi + \phi^2 - \frac{\lambda^2}{2}} = 0.622 > 0.50$ <p style="text-align: center;">contact splice sufficient</p> $\frac{\chi \cdot \alpha_{ult,k}}{\gamma_M} = \frac{0.622 \cdot 1.55}{1.10} = 0.88 < 1.00$	$\alpha_{ult,k} = 1.94$ $\bar{\lambda} = \sqrt{\frac{1.94}{1.85}} = 1.05$ $\phi_{LT} = 1.225$ $\chi = 0.59 > 0.50$ <p style="text-align: center;">contact splice sufficient</p> $\frac{\chi \cdot \alpha_{ult,k}}{\gamma_M} = \frac{0.59 \cdot 1.94}{1.10} = 1.04 > 1.00$
Check of out-of-plane stability	

Figure 85

- (3) In [Figure 85](#) two calculations are carried out:

1. a conservative calculation for the point with $\alpha_{ult,k,min}$,
 2. a calculation at the design point x_d .
- (4) A by-effect of the calculation is that χ takes values $\chi \geq 0.5$, so that in the bolted end-plate connection at the knee points of the frame out-of-plane bending moments can be resisted by full contact and no additional loads to bolts have to be considered.
- (5) Figure 86 and Figure 87 give the example of a composite bridge with an open cross section, for which the out-of-plane stability of the bottom chord in compression in the hogging moment region of the continuous beam is of concern.

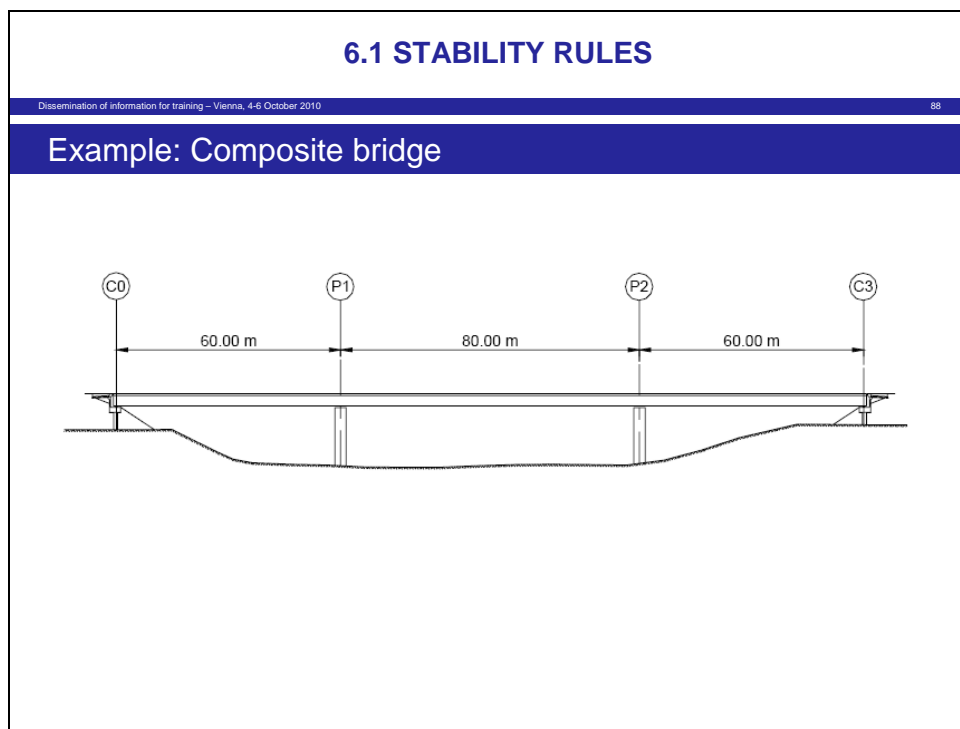


Figure 86

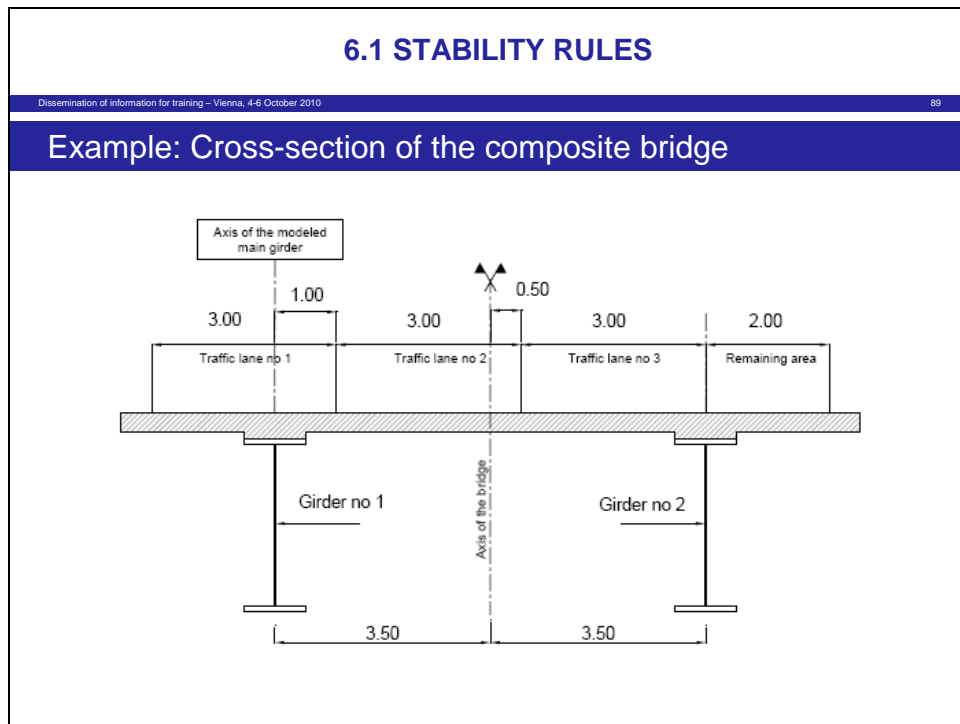


Figure 87

- (6) The moment distribution for girder no. 1 for which the out-of-plane stability check has to be carried out is given in [Figure 88](#).

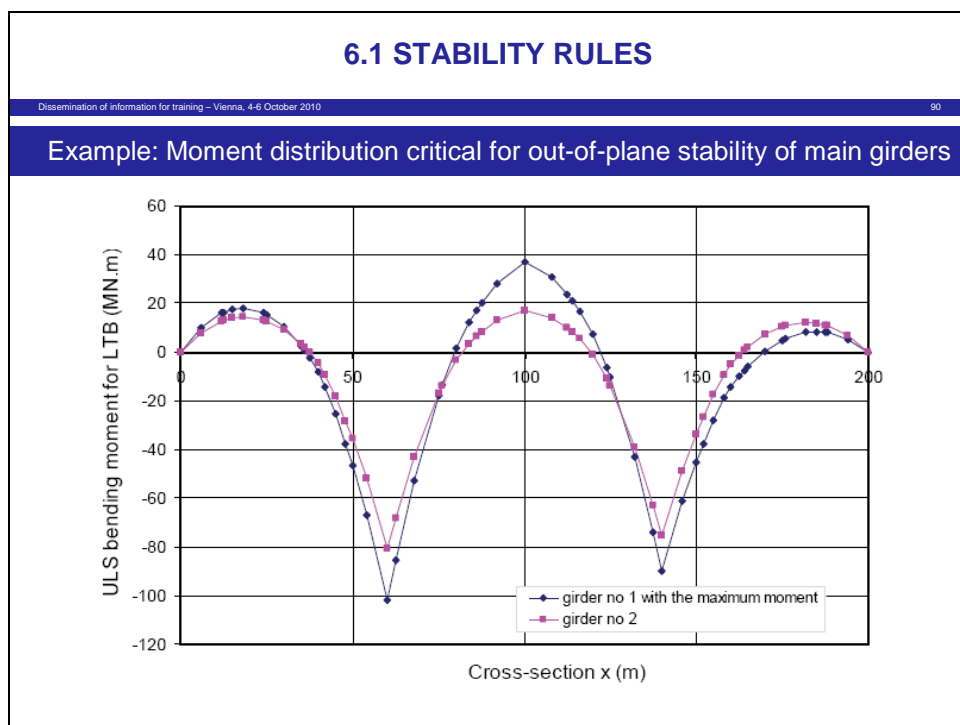


Figure 88

- (7) For the lateral torsional buckling check the bottom chord can be either regarded as a continuous column, laterally supported by the elastic transverse frames at the support, see [Figure 89](#), and all 7.50 m, see [Figure 90](#).

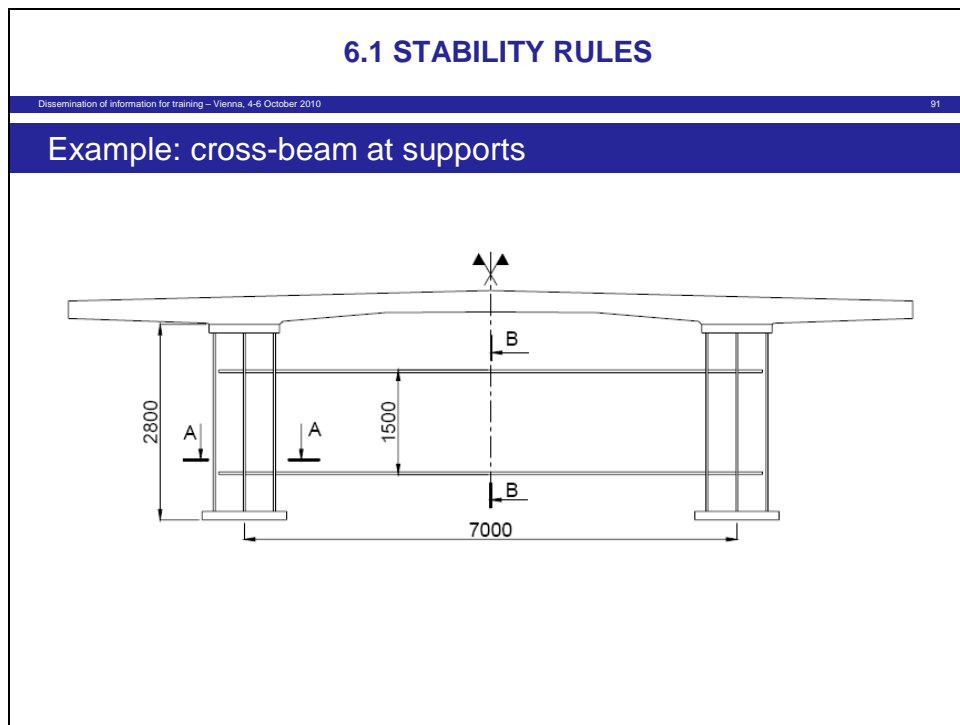


Figure 89

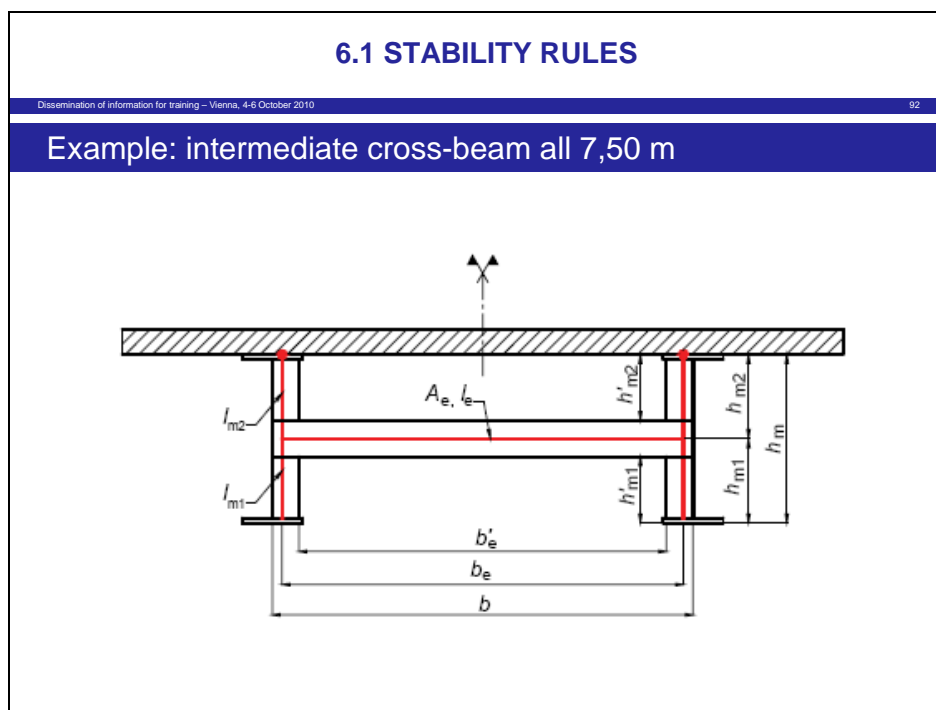


Figure 90

- (8) In this case 1/3 of the web should be taken into account.

- (9) The other possibility is to model the cross section fully or partly with FEM, to consider the effects of torsion and distortion of the steel cross section.
- (10) In Figure 91 modal transverse displacements of the bottom flange of the critical girder are given for the first 3 eigenvalues. The area where the modal transverse moments attain their maximum values are marked.

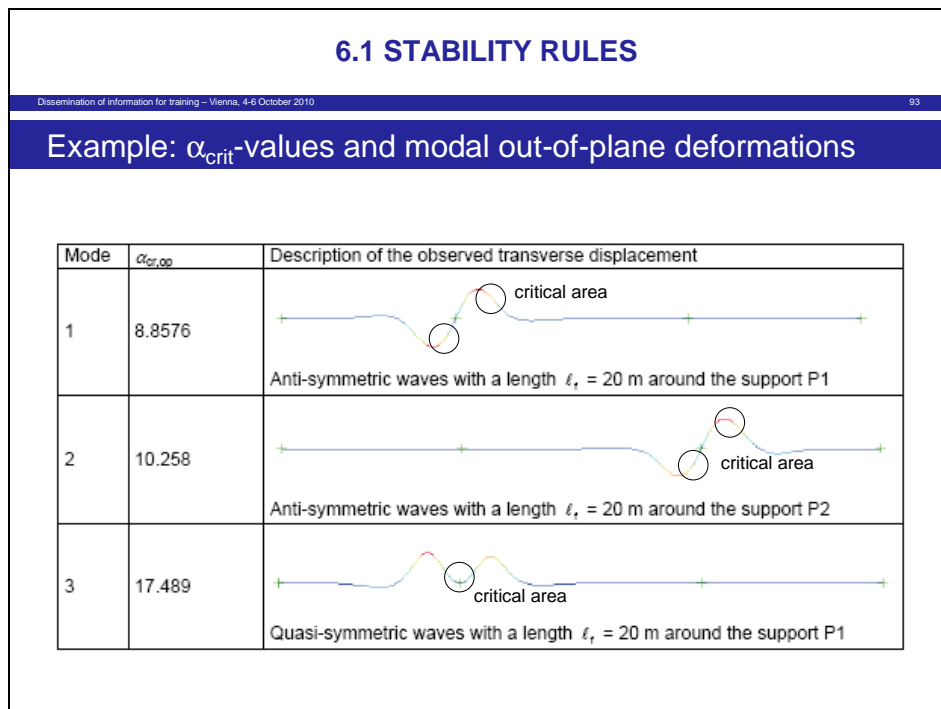


Figure 91

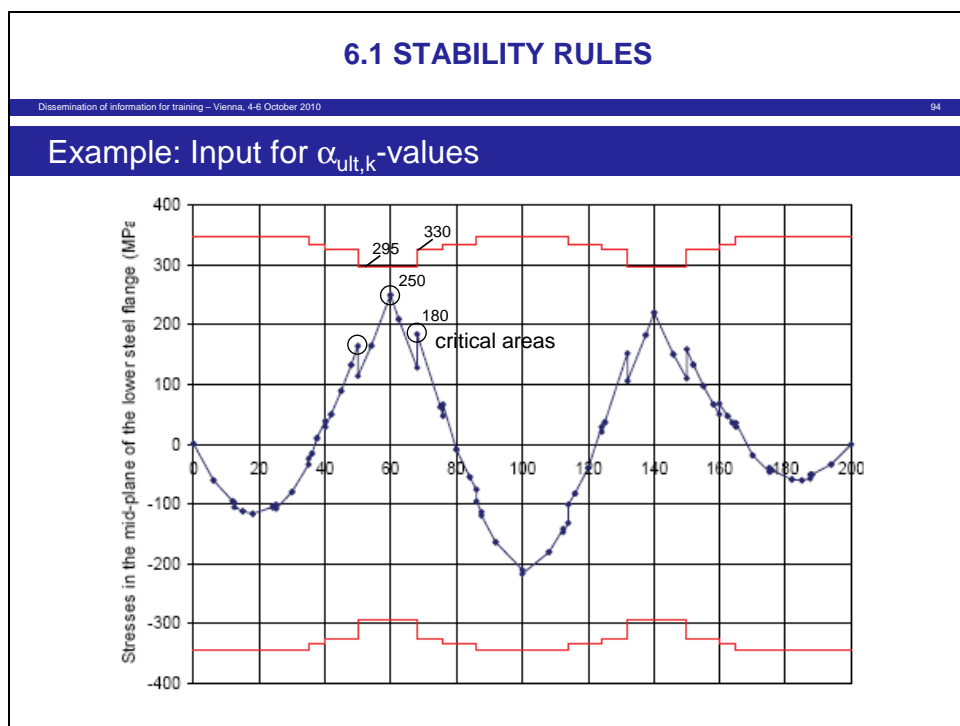


Figure 92

- (11) Figure 92 gives the inplane stresses in the centre line of the bottom flange as well as the yield stresses from which $\alpha_{ult,k}$ -values can be determined, that are possible choices for the design point x_d .
- (12) In Figure 93 two calculations are carried out
1. at the design point x_d for the first modal displacement (in field)
 2. at the design point x_d for the third modal displacement (at the support).

In these calculations also the modification of the imperfection factor α by torsion has been taken into account.

6.1 STABILITY RULES	
Dissemination of information for training – Vienna, 4-6 October 2010	
Checks for lateral-torsional buckling	
in field at point P1	at support (point P1)
$\alpha_{ult,k} = \frac{330}{180} = 1.83$ $\alpha_{crit} = 8.8576$ $\bar{\lambda} = \sqrt{\frac{1.83}{8.8576}} = 0.45$ $\alpha_{crit}^* = 8.37$ $\alpha^* = \frac{8.37}{8.86} \cdot 0.76 = 0.72$ $\phi = 0.69$ $\chi = 0.82$ $\frac{\chi \cdot \alpha_{ult,k}}{\gamma_M} = \frac{0.82 \cdot 1.89}{1.10} = 1.37 > 1.00$	$\alpha_{ult,k} = \frac{295}{250} = 1.184$ $\alpha_{crit} = 17.489$ $\bar{\lambda} = \sqrt{\frac{1.184}{17.489}} = 0.26$ $\alpha_{crit}^* = 15.20$ $\alpha^* = \frac{15.20}{17.49} \cdot 0.76 = 0.66$ $\phi = 0.554$ $\chi = 0.96$ $\frac{\chi \cdot \alpha_{ult,k}}{\gamma_M} = \frac{0.96 \cdot 1.184}{1.10} = 1.03 > 1.00$

Figure 93

9. Plate buckling effects

9.1 General

- (1) It is a common feature of column buckling and lateral torsional buckling, that in-plane stresses that initiate out-of plane buckling are not affected by out-of plane deformations; i.e. the normal compression force in a column does not vary with imperfections or buckling displacements and the in-plane stress situations in a beam-column does not vary if lateral deformations in terms of lateral displacements and torsion take place.
- (2) The only differences between flexural buckling and lateral torsional buckling is the effect of torsional rigidity that is expressed by the modification of the imperfection factor α in the formula for the reduction factor χ .

(3) For plate structures as given in [Figure 94](#) an additional phenomenon may occur:

- “column-like behaviour” without any “overcritical resistance” however with the effect of torsional rigidity occurs if the edge loads are imposed and do not vary with the displacements under these loads. In consequence the displacements of the loaded edges are non-linear.
- “plate-like” behaviour with “overcritical resistance” and also with the effect of torsional rigidity occurs if under the effect of imperfections the edge loads are applied as a group of loads, that cause a linear displacement of the loaded edge. In this case the individual loads of the group may vary with the displacement and cause a non-linear distribution with a load shedding from the centre to the edges.

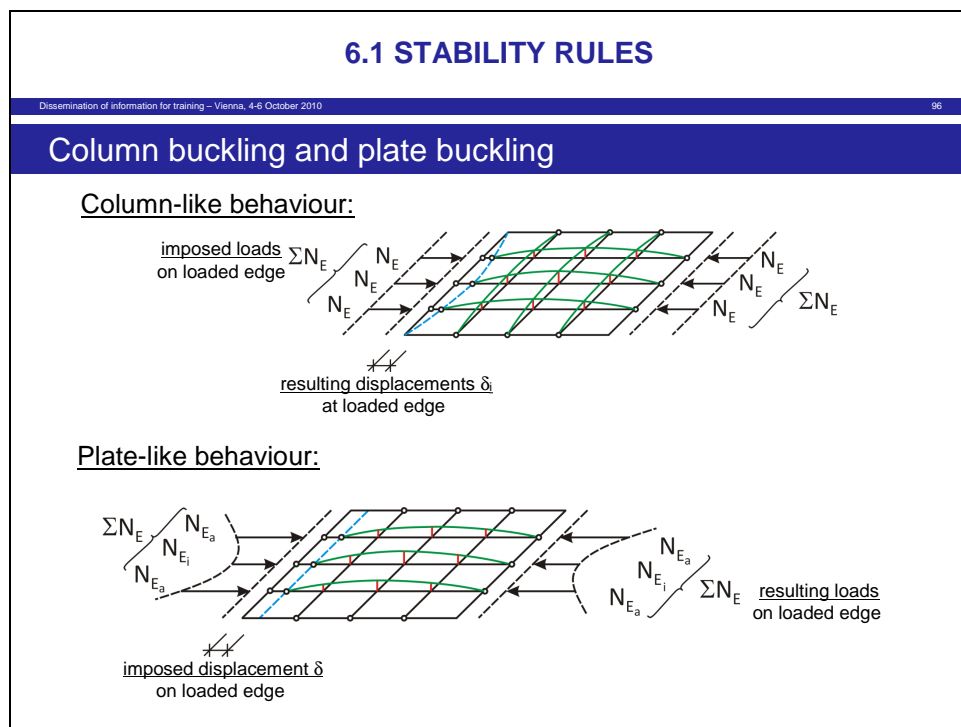


Figure 94

- (4) In general plate-buckling verifications are made for plated elements of girders, beams and columns under action effects as bending moments, normal forces and shear forces. For these structures the axiom of Navier applies, i.e. linear distributions of strains and not of stresses may be assumed.
- (5) At points of local load introductions as patch loads on the flanges of girders, beams and columns however the loads are normally controlled by mechanisms that limit their variation with displacements (e.g. by introduction by rollers on springs). In this case the behaviour is more column-like or in between column-like and plate-like behaviour.

9.2 Effects of column-like and plate-like behaviour

- (1) [Figure 95](#) gives the example of a column with a cross-section in the form of a cross, for which according to EN 1993-1-1 a torsional buckling check may be performed.

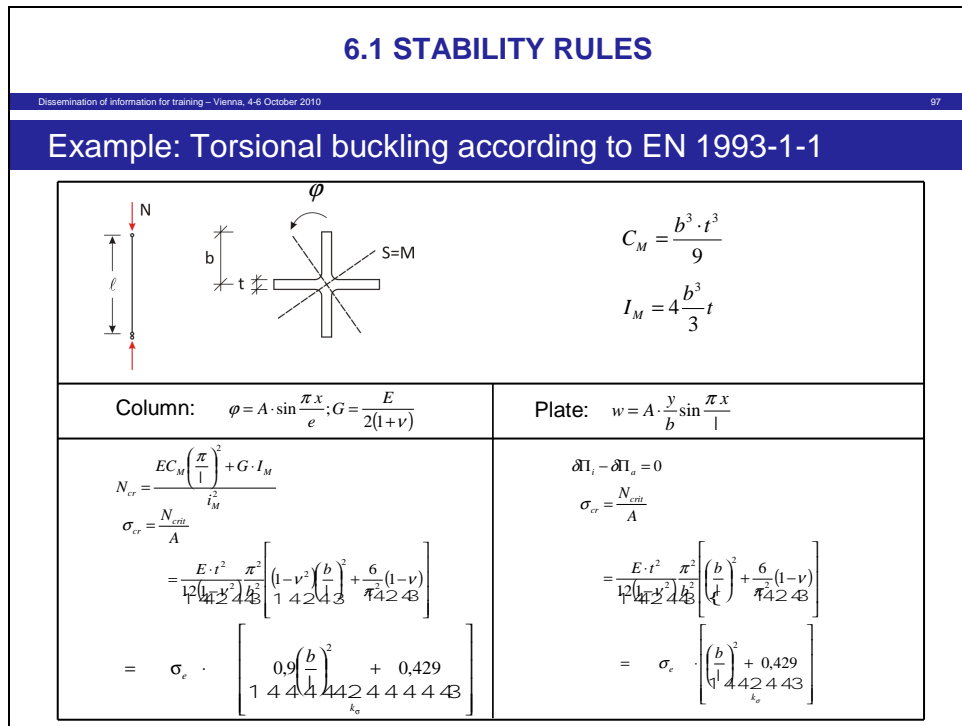


Figure 95

- (2) Using the column approach for torsional buckling a critical stress σ_{cr} may be determined with the cross-sectional data C_M and I_M , from which a buckling coefficient k_σ may be derived.
- (3) Using the plate theory a buckling coefficient k_σ may also be determined using the energy-method with a modal buckling deformation that corresponds to the assumptions mode for torsion in the column check.
- (4) Apparently the two results are almost identical.
- (5) The differences result from the type of loading as given in [Figure 96](#).

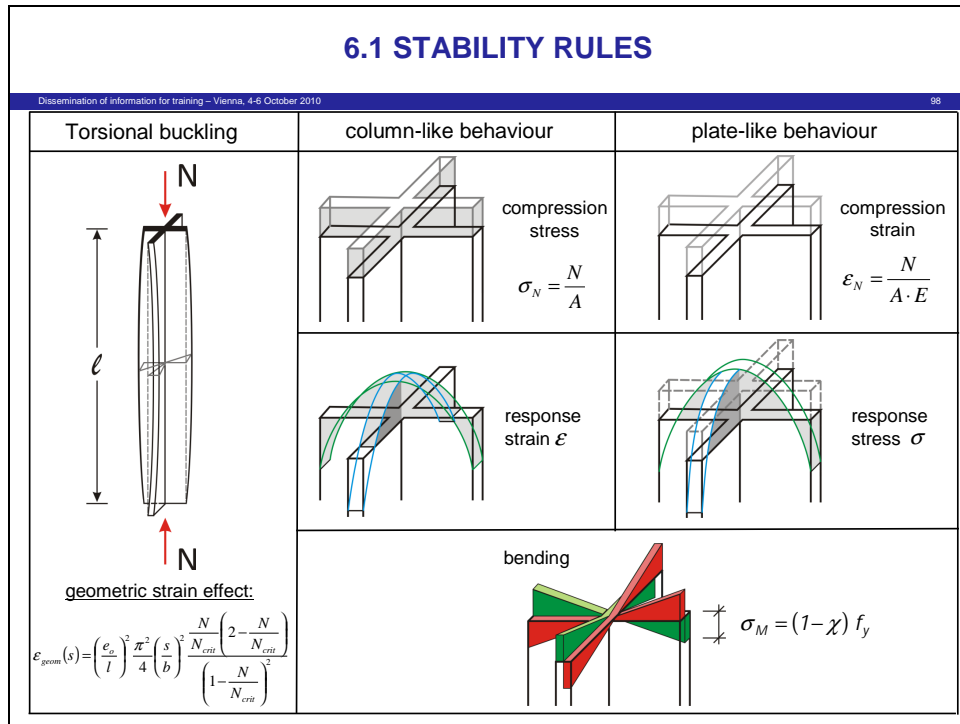


Figure 96

- (6) In torsional buckling a geometric strain effect occurs due to the torsional deformations, that
- in case of loading by uniformly distributed compression stress would cause a parabolic distribution of strains over the cross-section and
 - in case of loading by a uniformly distributed compression strain would cause a parabolic distribution of stress over the cross-section.
- (7) These different distributions of stress σ_N from compression, either constant or parabolic, are superimposed with linear distribution of stresses σ_M in the plated elements from plate bending.

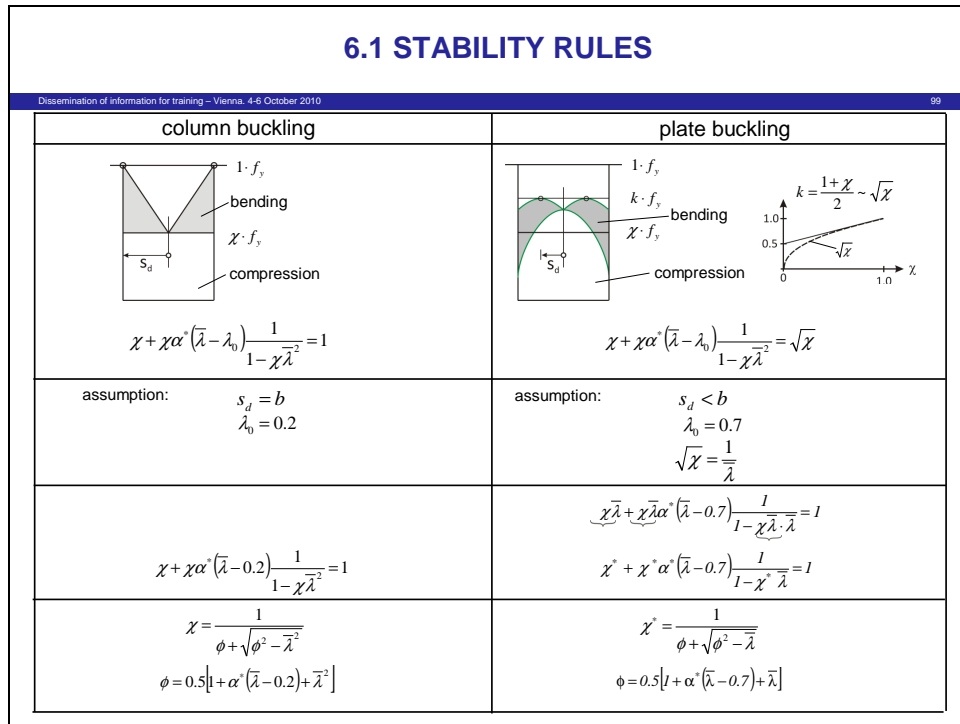


Figure 97

(8) Figure 97 shows the effects of the assumptions of a constant or parabolic distributions of the compression stress:

- The conclusion of a constant stress distribution is the column buckling formula with the modified imperfection value α^*
- the conclusion of the constant strain distribution is the modified imperfection value α^* and that
 - the basic equation of the column buckling formula does not attain the value 1.0 (for the yield stress) but only a mean value between χ and 1.0, best represented by $\sqrt{\chi}$,
 - the design point in the cross-section s_d moves from the edges to the centre of the cross-section which causes a “ β -effect” as for lateral torsional buckling.

(9) As a result λ_0 moves from 0.2 to 0.7 and $\sqrt{\chi}$ on the right side of the formula may be approximately expressed by $\frac{1}{\bar{\lambda}}$, so that

- for constant stress distributions the lateral torsional buckling formula is obtained with the use of $\bar{\lambda}^2$, whereas

- for constant strain distribution a new plate-buckling formula is obtained, that differs from the lateral torsional buckling formula by the use of $\bar{\lambda}$ instead of $\bar{\lambda}^2$ and the value $\bar{\lambda}_0 = 0.7$ instead of $\bar{\lambda}_0 = 0.2$.

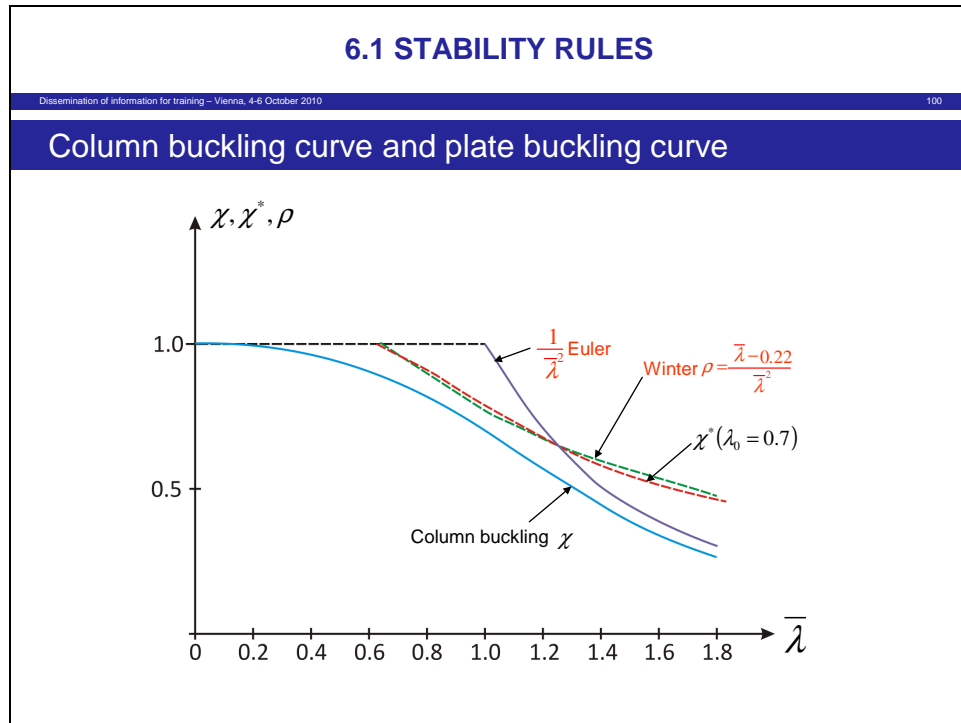


Figure 98

- (10) Figure 98 gives a comparison between the column buckling curve χ and the plate buckling curve χ^* from Figure 97 and also the Winter formula, which is quite close to the new plate buckling formula. Both the new plate buckling formula and the winter formula are specified in EN 1993-1-5.

9.3 Interpolation between column-like and plate-like behaviour

- (1) Figure 99 shows the differences between the effects of constant stress distribution and constant strain distribution resulting from imperfections for a plate without stiffeners and with constant stress loading in case no imperfections would occur:
- a sinusoidal displacement of edges in case of imposed constant stresses,
 - a sinusoidal stress distribution at the edges in case of imposed constant strains.

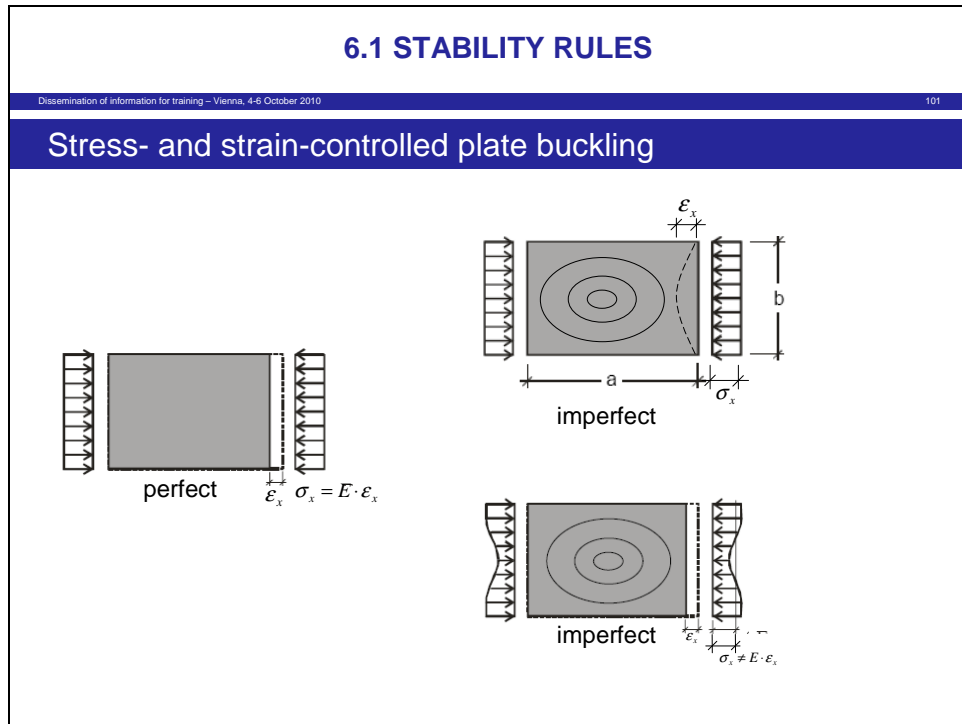


Figure 99

- (2) The different effects of constant imposed stresses and constant imposed strains depend on the aspect ratio $\alpha = \frac{a}{b}$ of the plate and can be correlated with the torsion effect

$$\frac{\alpha_{crit}^*}{\alpha_{crit}}$$

where α_{crit}^* is determined without torsional rigidity,

α_{crit} is determined with torsional rigidity,

see [Figure 100](#).

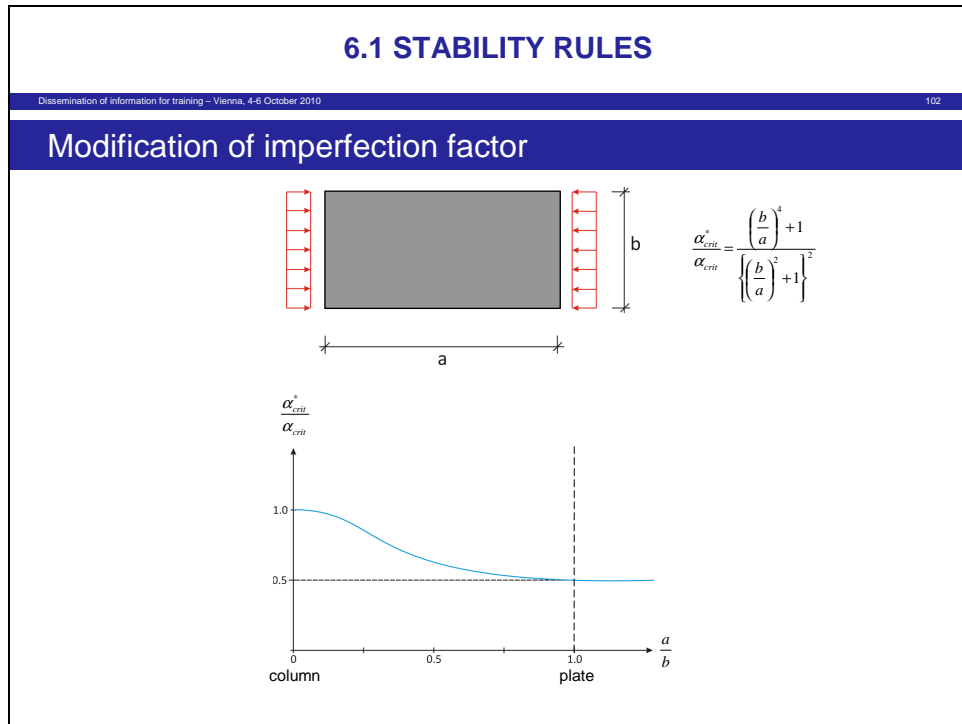


Figure 100

- (3) Hence the torsional effect could be used as parameter for the distinction of “column-like”-behaviour and “plate-like”-behaviour for plates in a similar way as it is used for “flexural buckling” and “lateral-torsional” buckling for girders, beams and columns.
- (4) Figure 101 shows the column curve and the Winter curve for plates in monoaxial compression versus the aspect ratio α .

It also shows the interpolation according to FEM-calculations and to the procedure given in EN 1993-1-5.

- (5) A general approach could be the use of the formula:

$$\Phi = 0.5 \left[1 + \alpha^* \left(\bar{\lambda} - 1.2 + \frac{\alpha_{crit}^*}{\alpha_{crit}} \right) + \bar{\lambda}^2 \frac{\alpha_{crit}^*}{\alpha_{crit}} \right]$$

$$\chi = \frac{1}{\Phi + \sqrt{\Phi^2 - \bar{\lambda}^2 \frac{\alpha_{crit}^*}{\alpha_{crit}}}}$$

which gives for

$$\frac{\alpha_{crit}^*}{\alpha_{crit}} = 1 \quad \text{the column formula and for}$$

$$\frac{\alpha_{crit}^*}{\alpha_{crit}} = 0.5 \quad \text{the plate formula.}$$

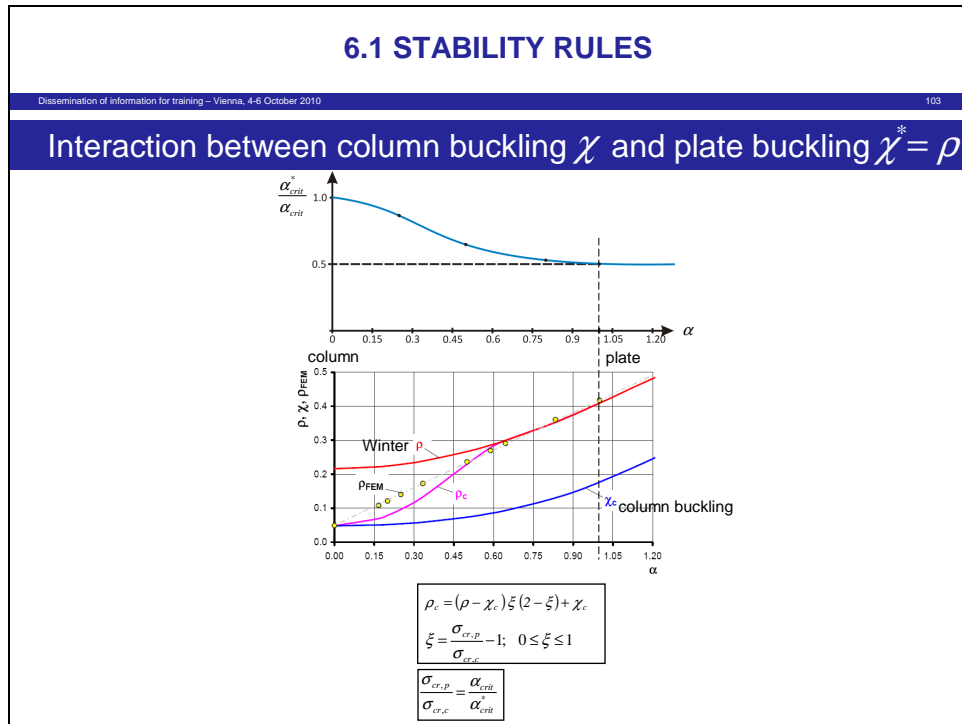


Figure 101

- (6) This buckling curve is applicable to all types of plate field (un-stiffened and stiffened) and all fields of stresses (combined σ_x , σ_z and τ).

9.4 Resistances of “hybrid” cross-sections

- (1) Cross-sections as given in Figure 102 may consist of plates, which under compression exhibit different ultimate buckling strengths, expressed by different limit stresses $\sigma_{Limit,h}$ and $\sigma_{Limit,b}$.
- (2) In assuming a “yield-plateau” at the various levels of σ_{Limit} the cross-section reacts to an increasing compression force like a cross-section with plates with different yield strengths and therefore can be classified as “hybrid”.

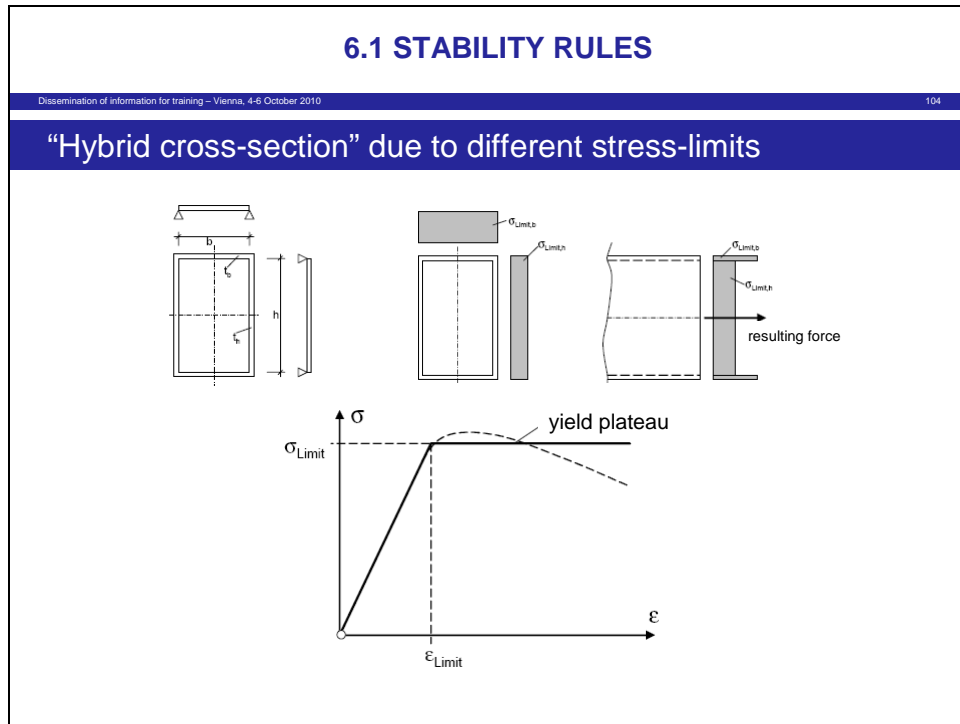


Figure 102

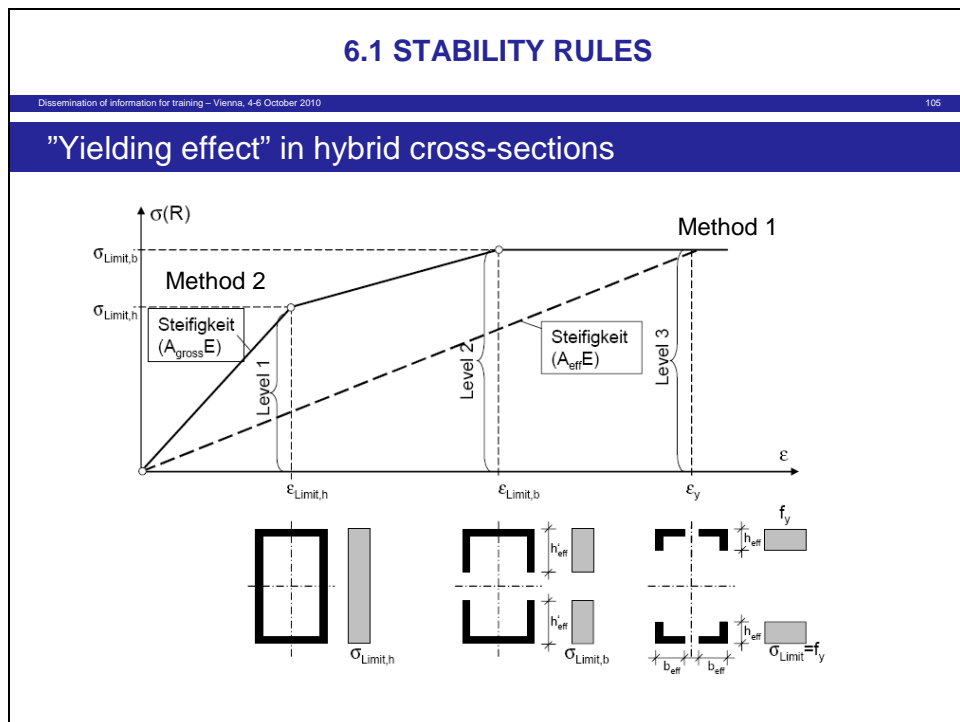


Figure 103

- (3) The ultimate resistance of such a “hybrid” cross-section can be determined by summing up the resistances of the individual plates.

(4) Figure 103 shows the strength-strain line for such a hybrid cross section:

1. In the first phase (until the weakest plate has reached its buckling resistance $\sigma_{Limit,h}$) the full elastic gross cross-section applies.

This is the field, where the elastic critical buckling load coefficient α_{crit} can be calculated from the stress fields of the individual plates or the full cross-section with gross cross-sectional properties.

The method in EN 1993-1-5 that usually limits the resistances of the cross-section to the limit of the weakest plate field is Method 2 (section 10 in EN 1993-1-5).

2. In the second phase further straining actions give further elastic reactions of the stronger plate field only, until $\sigma_{Limit,b}$ is reached in this field, whilst the weakest plate yields with the resistance $\sigma_{Limit,h}$ being constant.

When reaching $\sigma_{Limit,h}$ the resistance of the full cross section can be determined in three equivalent ways:

1. The resistances $A_h \cdot \sigma_{Limit,h}$ and $A_b \cdot \sigma_{Limit,b}$ are summed up.
2. An effective thickness of the weakest plate

$$t_{eff} = t \cdot \frac{\sigma_{Limit,h}}{\sigma_{Limit,b}}$$

is chosen and the resistance is determined with the unique strength $\sigma_{Limit,b}$ and an effective cross-section with t_{eff} for the weakest plate.

3. An effective width of the weakest plate

$$b_{eff} = b \cdot \frac{\sigma_{Limit,h}}{\sigma_{Limit,b}}$$

is chosen and the resistance is determined with the unique strength $\sigma_{Limit,b}$ and on effective cross-section with b_{eff} for the weakest plate.

3. In a third phase further straining actions can be applied to reach the yield strain ε_y corresponding to f_y .

This third phase does not rouse any further resistances because the two plates yield on their resistance levels $\sigma_{Limit,h}$ and $\sigma_{Limit,b}$.

However, the calculation for the resistances on the basis of effective thickness or effective width can be referred to the yield strength f_y :

$$t_{eff_h} = t \cdot \frac{\sigma_{Limit,h}}{f_y}$$

$$t_{eff_b} = t \cdot \frac{\sigma_{Limit,b}}{f_y}$$

or

$$b_{eff_h} = b \cdot \frac{\sigma_{Limit,h}}{f_y}$$

$$b_{eff_b} = b \cdot \frac{\sigma_{Limit,b}}{f_y}$$

and the cross-sectional resistance be determined with

$$R = A_{eff} \cdot f_y$$

This method in EN 1993-1-5 is called Method 1.

- (5) Figure 104 demonstrates the differences between the phase 1-procedure (Method 2) and a multiphase-procedure (Method 1) for the case of bending.

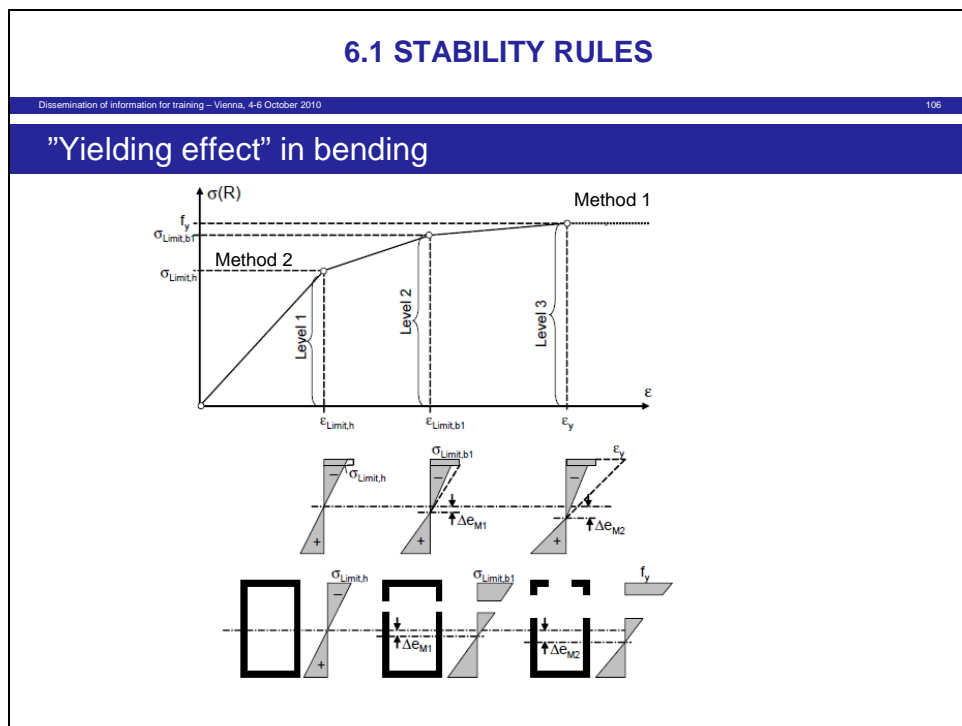


Figure 104

- (6) It is evident, that the bending resistance may be also determined for different levels of curvature (straining ϵ_{Limit}) either by integration of the distribution of limiting stresses σ_{Limit} or from effective cross-sections using either effective thicknesses or effective widths.
- (7) The use of effective cross-section is preferred because of the iterative calculation of the neutral axis (Δe_M) which can be carried out more easily with effective cross-sectional data.
- (8) In general Method 2 gives more conservative resistances than Method 1 due to the "plastic reserves" of the hybrid-cross-section. There is however a possibility to take plastic reserves from "Load-shedding" also into account in Method 2, as illustrated in Figure 105.

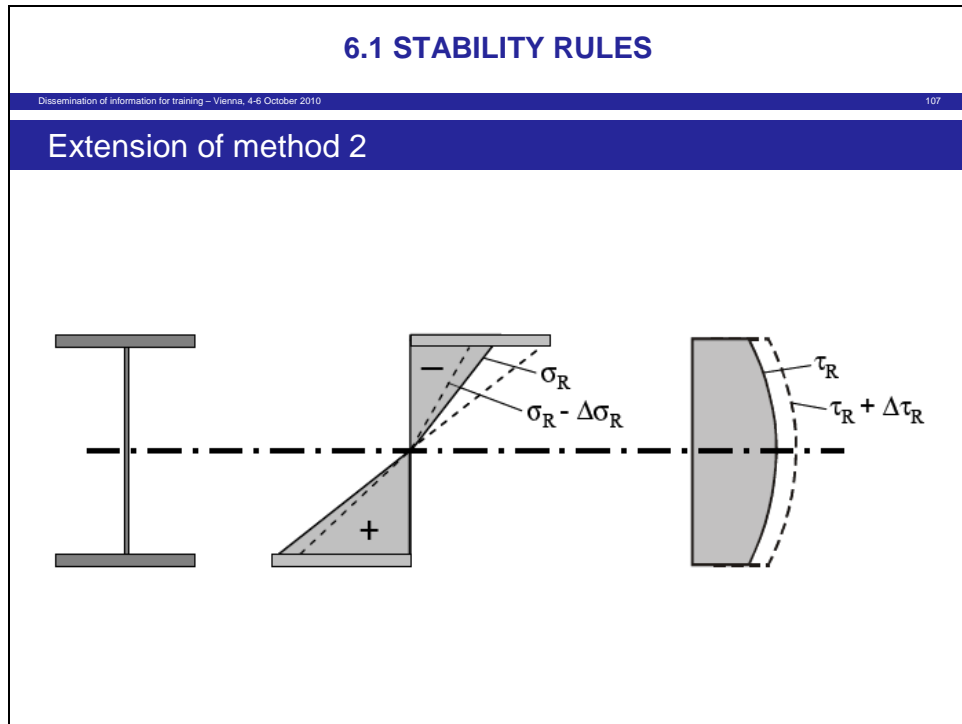


Figure 105

- (9) This requires a further step in method 2, where the increase of the moment resistances $M_R + \Delta M_R$ by exploiting the yield strength of the stronger flange is accompanied by an increase of the shear resistance of the web $\tau_R + \Delta\tau_R$ by reducing the limit stress of the web $\sigma_R - \Delta\sigma_R$. This increase $\Delta\tau_R$ and reduction $\Delta\sigma_R$ in the web causes a non-linear interaction.

9.5 Method 1 and Method 2 in EN 1993-1-5

- (1) Figure 106 shows the principles of Method 1 (use of effective cross-section) and Method 2 (use of stress-limit) as specified in EN 1993-1-5 and used in design of steel bridges.

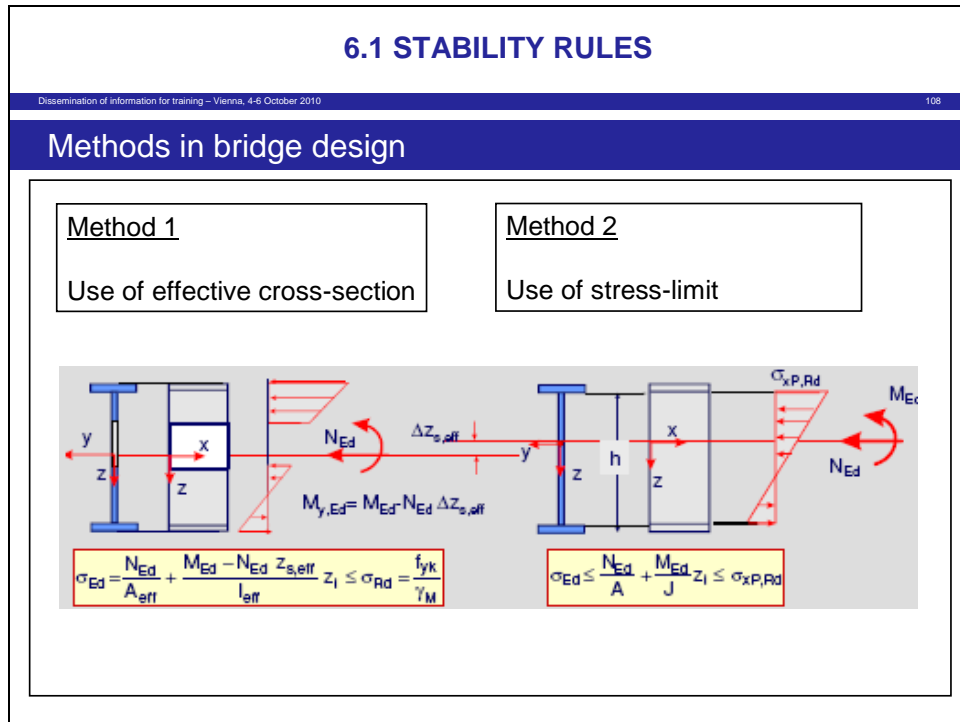


Figure 106

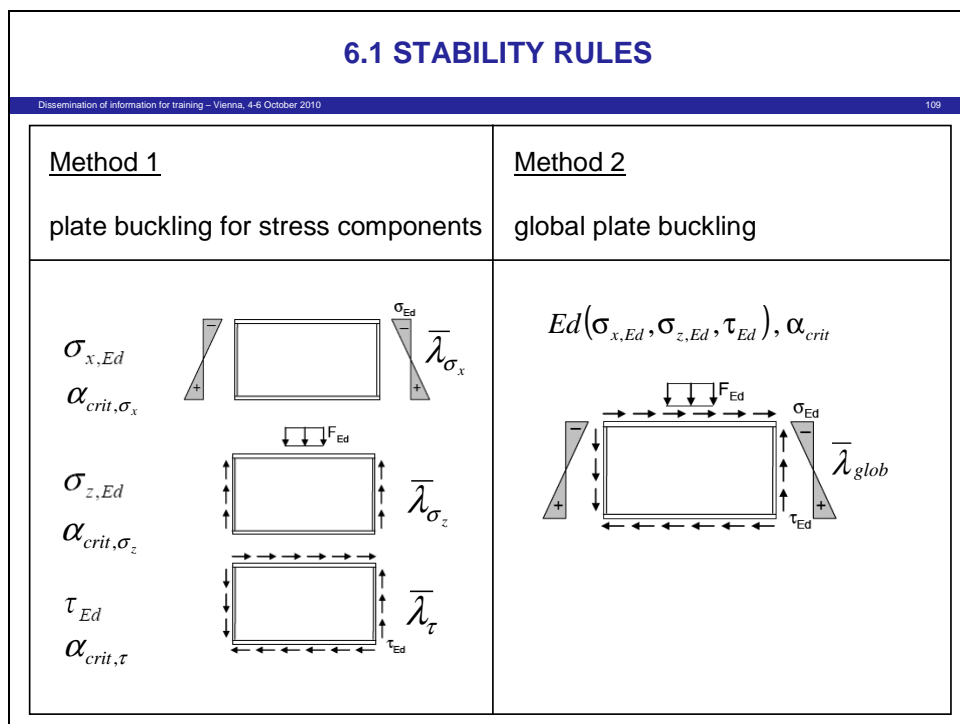


Figure 107

(2) The procedures for the use of these methods are different as demonstrated in [Figure 107](#):

- In [Method 1](#) the stress field of a plate is subdivided into 3 simplified standard fields, for which design aids are available:
 - for longitudinal stress σ_x

- for transverse stresses (patch loading) σ_z
 - for shear stresses σ_z .
 - A verification is undertaken for each standard stress field component and the verification for the combined stress field is carried out by an interaction formula.
 - In Method 2 the combined stress field is used to determine a global stress-field amplification factor α_{crit} , to perform the stress field verification in a single step.
- This method is applicable to FEM-calculations.

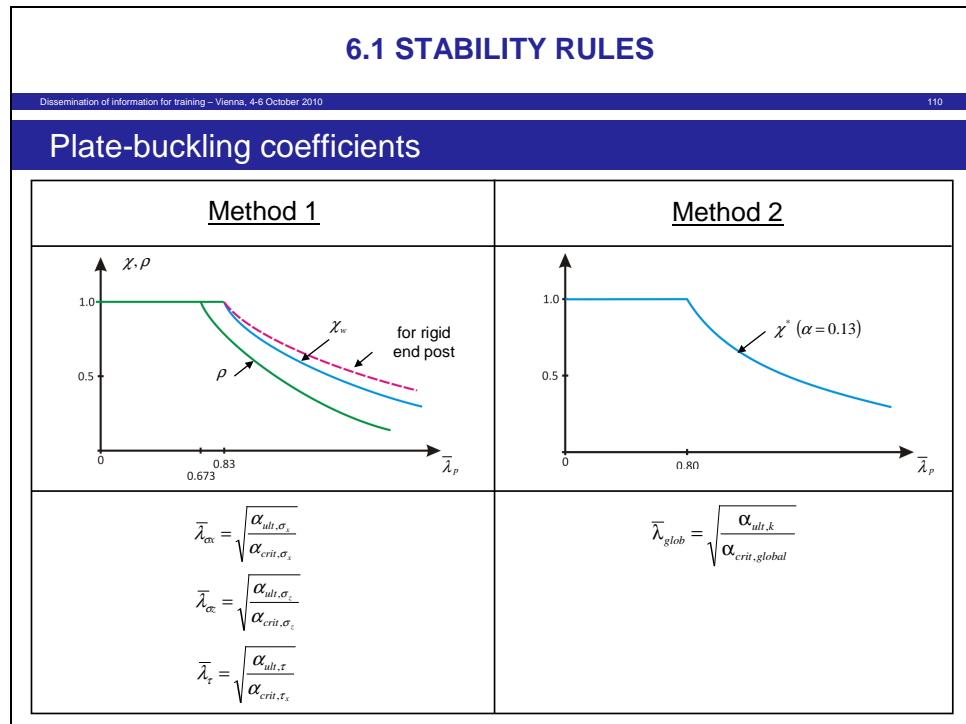


Figure 108

- (3) Figure 108 gives the plate-buckling reduction factors for Method 1 and Method 2: Whereas in Method 1 each standard stress field component yields a particular slenderness and a particular buckling curve, Method 2 only uses a single global slenderness value and a single global buckling curve χ^* .

9.6 Application of Method 1 to composite cross-sections

- (1) Figure 109 shows the various steps for the verification of an effective composite cross-section for the standard σ_x -field component.

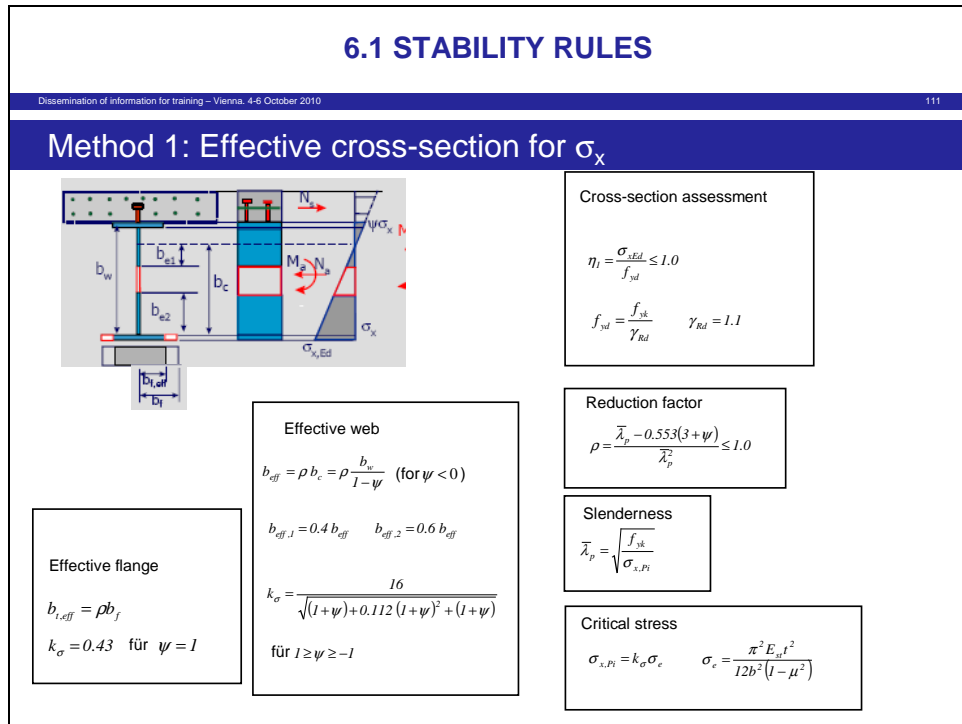


Figure 109

- (2) The steps are the following:
1. From the stress-distribution of the gross cross section the critical stresses are determined, that give
 2. the slenderness of the web and of the bottom flange.
 3. With the reduction factor ρ using the Winter-curve the effective web and the effective flange using effective widths are calculated.
 4. Using the effective cross-sectional data the cross-section check is performed resulting in the utilisation rate η_I for the σ_x -component.

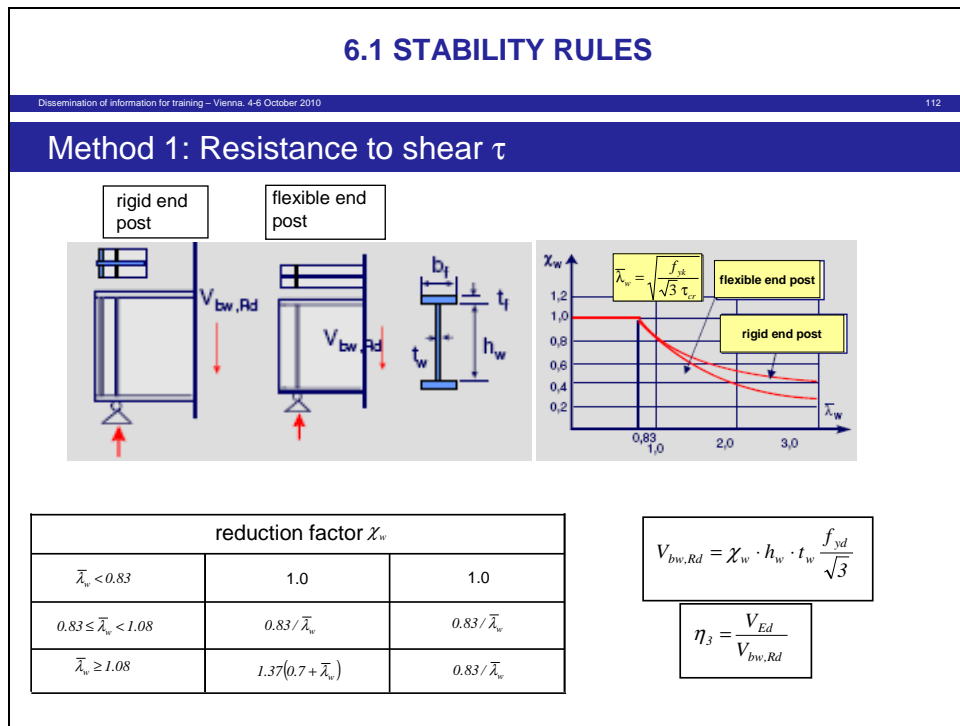


Figure 110

- (3) Figure 110 demonstrates the check for the standard shear stress field component with the following steps:
1. From the critical stresses τ_{cr} for the web the slenderness is determined, for which the structural detailing of the end-post gives different shear buckling curves χ_w .
 2. With χ_w the shear-resistance V_{Rd} of the web can be calculated that permits to determine the utilisation rate η_3 for the τ -component.
- (4) The interaction formula to verify the combined stress field is based on the utilisation rates η_1 and η_3 and also uses parameters of the steel cross-section that describe fictitious extreme situations of exploitation of web, see Figure 111.

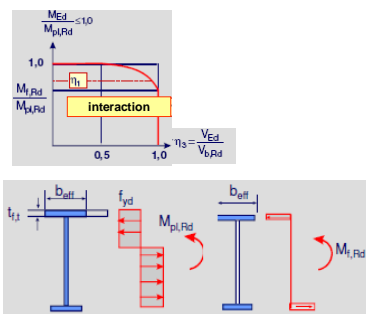
6.1 STABILITY RULES	
Dissemination of information for training – Vienna, 4-6 October 2010	
113	
Assessment for plate buckling	
Method 1	Method 2
<p>Interaction</p>  $\left. \begin{aligned} \eta_1 = \frac{\sigma_{Ed}}{f_y} \leq 1 \\ \eta_3 = \frac{V_{Ed}}{V_{Rd}} \leq 1 \end{aligned} \right\} \eta_1 + \left[1 - \frac{M_{f,Rd}}{M_{pl,Rd}} \right] [2\eta_3 - 1]^2 \leq 1$	$\frac{\chi_{glob} \cdot \alpha_{ult,k}}{\gamma_M} \geq 1$

Figure 111

Method 2 uses a global check instead of the interaction formula.

(5) An example for the National Choice of Method 1 and Method 2 is given in [Figure 112](#):

- Method 1 is preferred for bridges with webs without any stiffeners or with vertical stiffeners only, whereas Method 2 applies to multi-stiffened webs and bottom plates of box-sections.
- Method 1 is clearly related to ULS-verifications, which has an advantage where the Limit stresses for webs and flanges differ significantly. Method 2 also limits straining to the elastic range and can therefore also be used for serviceability limit checks.
- In particular in cases, where the elastic stress distributions at the characteristic load level and the “stress-bloc-distribution” assumed at the Ultimate Limit State, give significant differences of compression stress in the web, a serviceability limit check with Method 2 should be applied.

6.1 STABILITY RULES

Dissemination of information for training – Vienna, 4-6 October 2010 114

German National Annex

- Method 1 only applicable to girders without longitudinal stiffeners
- The use of Method 1 should be supplemented by checking global buckling with Method 2 for characteristic load level E_k and $\gamma_M = 1.10$

Figure 112

9.7 Design example

- (1) Figure 113 gives for the design example of a composite bridge the ultimate limit state assessments of the cross-sections at the support P1 and at midspan, using Method 1.

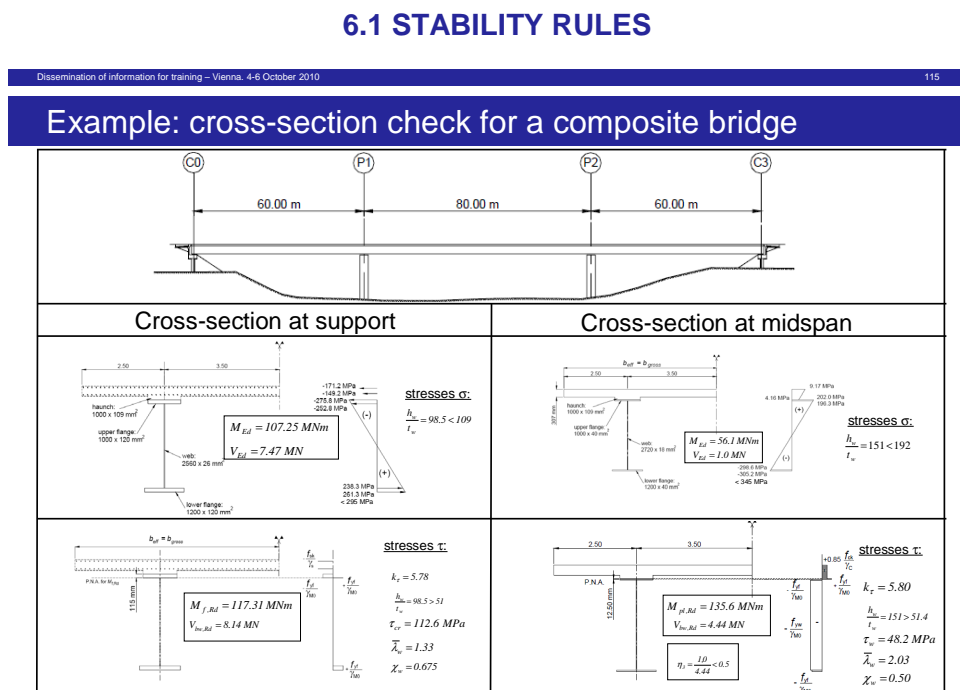


Figure 113

- (2) For the σ_x -stress field component the cross-sections comply with Class 3 limits $\frac{h_w}{t_w}$, so that the elastic stress distribution for M_{Ed} satisfies the yield strength.
- (3) For the τ -stress field-component the Class 3 – limits are exceeded, so that a shear plate buckling assessment using χ_w is necessary, that gives resistances satisfying V_{Ed} .
- (4) Interaction checks are no more needed, as for the cross-section at support the web could be fully used for shear, because the extreme resistance-value $M_{f,Rd}$ satisfies M_{Ed} , and as for the cross-section at midspan the shear utilisation rate is below $\eta_3 = 0,5$, so that the interaction is anyway satisfied.

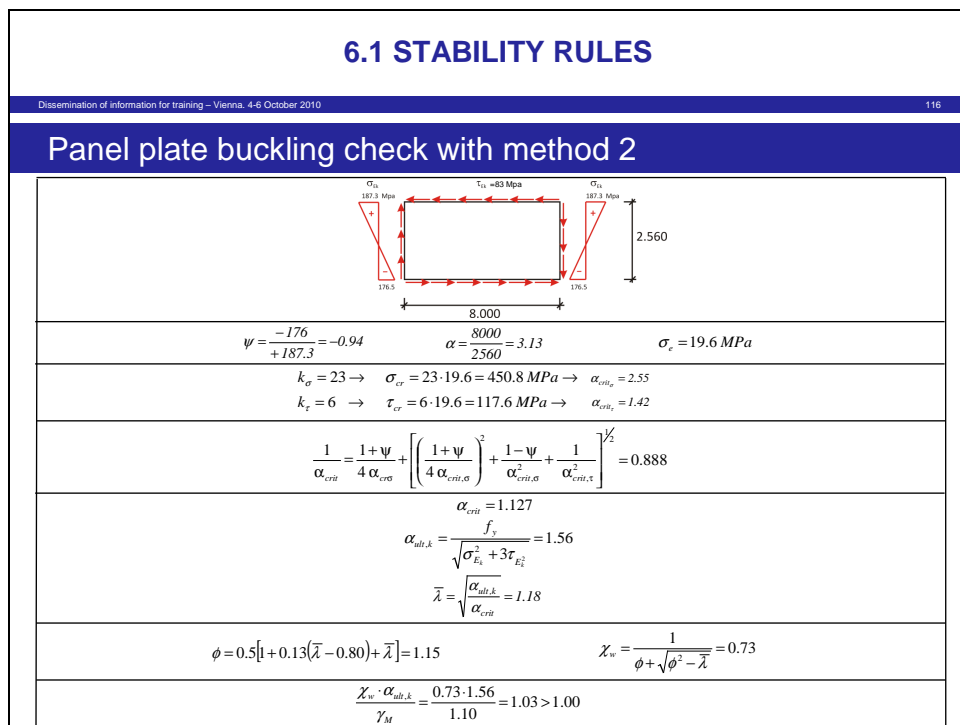


Figure 114

- (5) Figure 114 gives an example for the serviceability check with Method 2 at the support P1 using extreme values of action effects at one edge. For a more accurate check the design location x_d could be used.
- (6) The critical value α_{crit} for the combined values σ_x and τ could be calculated directly with the Programme EB-Plate (CTICM); however a conservative approach is used in Figure 114.

9.8 Web plate assessment for launching the bridge

- (1) Figure 115 shows an example of a composite bridge erected by launching with a launching nose.

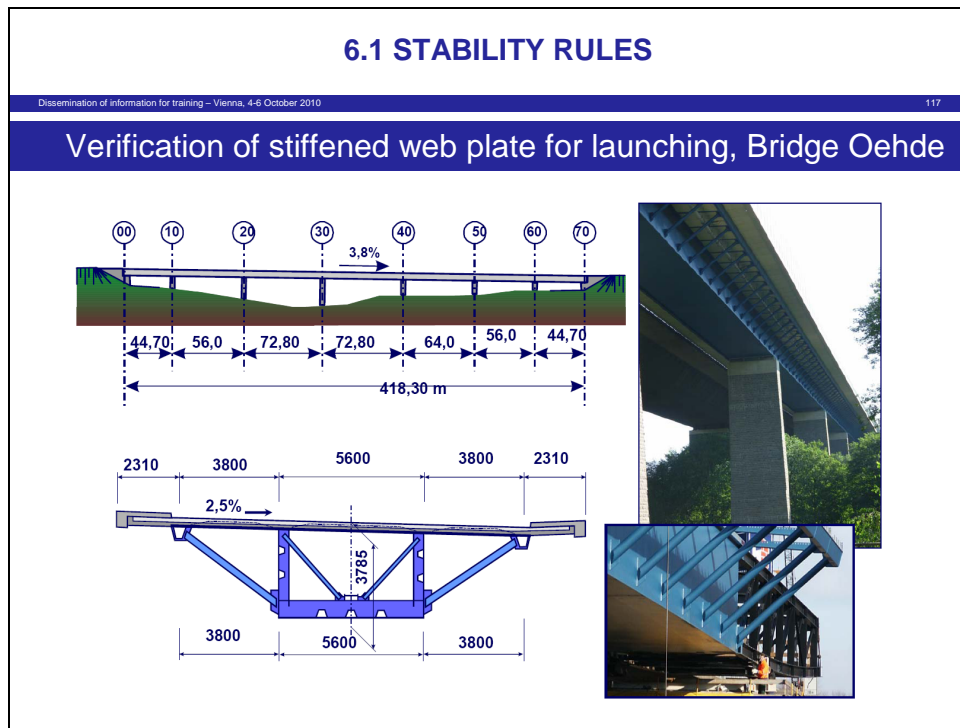


Figure 115

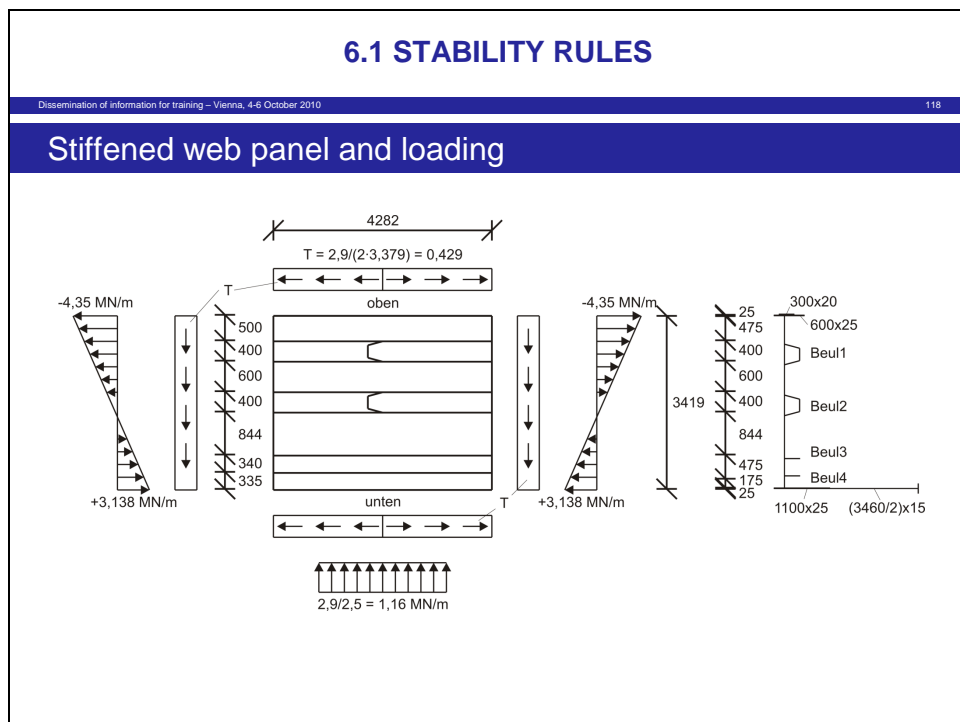


Figure 116

- (2) Figure 116 gives the dimensions and edge loading of the stiffened web, that was verified on the basis of a 2nd order analysis of a grid of longitudinal stiffeners and transverse strips of the plate.
- (3) This model produces $\frac{\alpha_{crit}^*}{\alpha_{crit}} \approx 1$ and gives the moment distributions of the stiffeners as given in Figure 117.

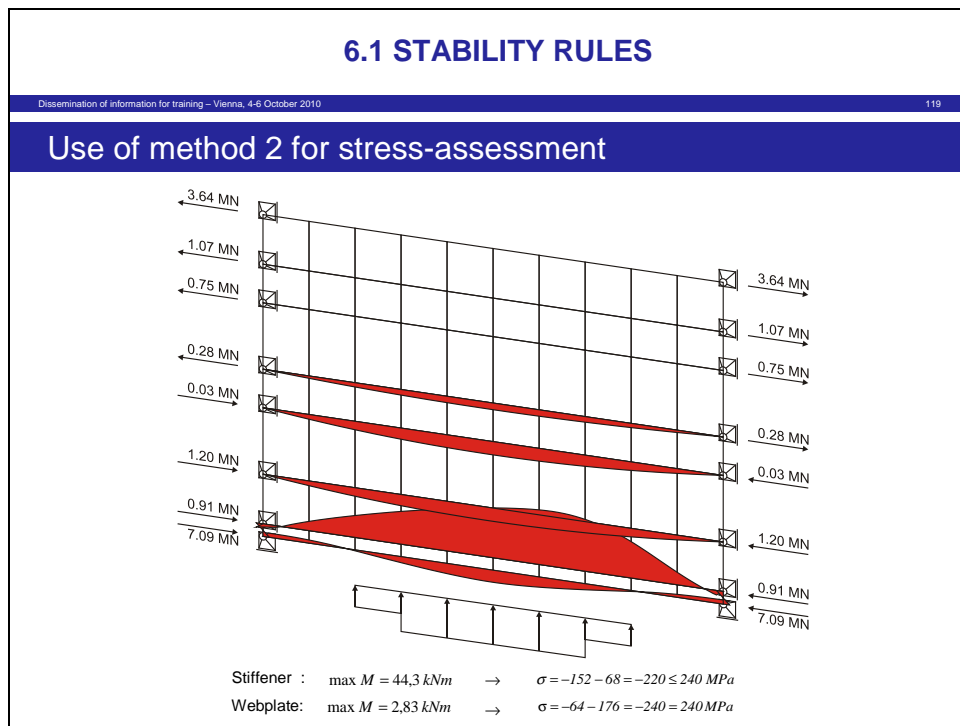


Figure 117

- (4) The addition of the effects of normal forces and bending moments for the stiffeners and the plate strips satisfies the yield strength.

9.9 Further informations to plate buckling

- (1) Further informations to the background and the application of the plate-buckling rules in EN 1993-1-5 may be taken from the JRC report “Commentary and worked examples to EN 1993-1-5” Plated structural elements”, see Figure 118, as well as from the DAST-Report “Entwicklung und Aufbereitung wirtschaftlicher Bemessungsregeln für Stahl- und Verbundträger mit schlanken Stegblechen im Hoch- und Brückenbau” (Development and preparation of economic design rules for steel- and composite girders with slender web-plate in buildings and bridges).



Figure 118

10. Fatigue rules

10.1 General

- (1) Fatigue is a typical technical area, where the large number of test results and the variety of test interpretations requires the use of agreed technical classes and agreed verification procedures for the standardization of the numerical fatigue assessment, so that in particular cases discrepancies between the standard model and individual tests for a certain product may occur.
- (2) EN 1993-1-9 gives such a classification model which is based on the following agreements:

1. The basis of fatigue assessments is a fatigue resistance function applicable to a large variety of welded structural details as given in [Figure 119](#).

This resistance function

$$\Delta\sigma_R^3 \cdot N_R = \Delta\sigma_c^3 \cdot 2 \cdot 10^6$$

is bilinear in double-logarithmic scale and represents the characteristic values (~95%-fractiles) of large scale fatigue tests with constant amplitude stress ranges $\Delta\sigma$ that include all features of design and execution (scale effect, notches, imperfections and discontinuities in the frame of tolerances, residual stresses) relevant for fatigue behaviour.

The reference point $\Delta\sigma_c$ is the classification number of a detail. The classification system includes steps of $\Delta\sigma_c$ with a factor $R_{20} = \sqrt[20]{10} = 1.122$.

The value $\Delta\sigma_c$ at $2 \cdot 10^6$ cycles has been chosen in appreciation of Wöhler. The constant amplitude endurance limit $\Delta\sigma_D$ at $5 \cdot 10^6$ cycles has been chosen as a constant value for ease of use.

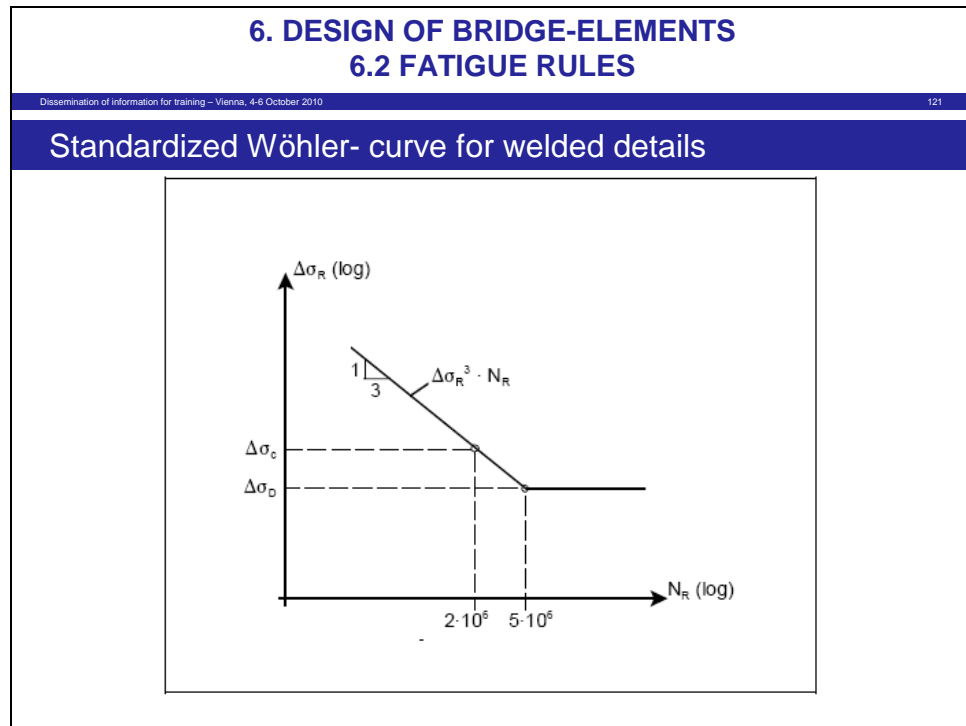


Figure 119

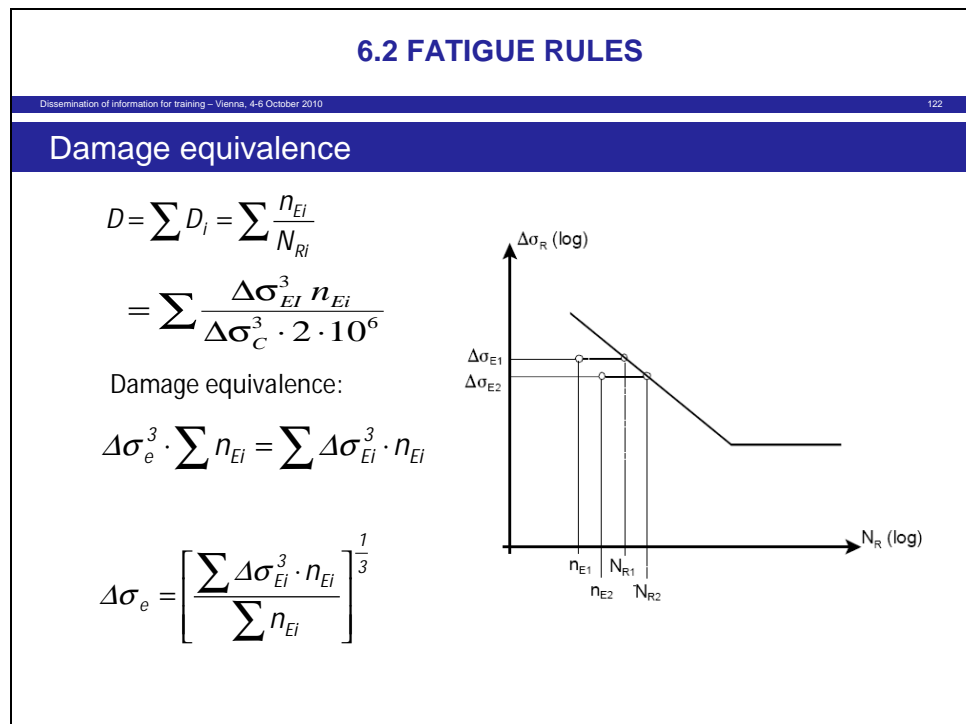


Figure 120

2. The fatigue resistance curve

$$\Delta\sigma_R^3 \cdot N_R = \Delta\sigma_c^3 \cdot 2 \cdot 10^6$$

represents the damage $D = 1$.

Fatigue loads represented by a spectrum of various pairs of data

$$\Delta\sigma_{Ei}^3 \cdot n_{Ei}$$

give a partial damage

$$D = \sum \frac{n_{Ei}}{N_{Ri}} = \sum \frac{\Delta\sigma_{Ei}^3 \cdot n_{Ei}}{\Delta\sigma_c^3 \cdot 2 \cdot 10^6}$$

from a linear damage accumulation and allow to calculate for the spectrum of stress-ranges a damage equivalent constant stress range

$$\Delta\sigma_e = \sqrt[3]{\frac{\Delta\sigma_{Ei}^3 \cdot n_{Ei}}{\sum n_{Ei}}}$$

3. A stress-time history can be evaluated by an agreed counting method as the “rainflow method” or the “reservoir-method”, see [Figure 121](#), which gives an array of $\Delta\sigma$ -ranges that can be ordered in a spectrum or a frequency distribution.

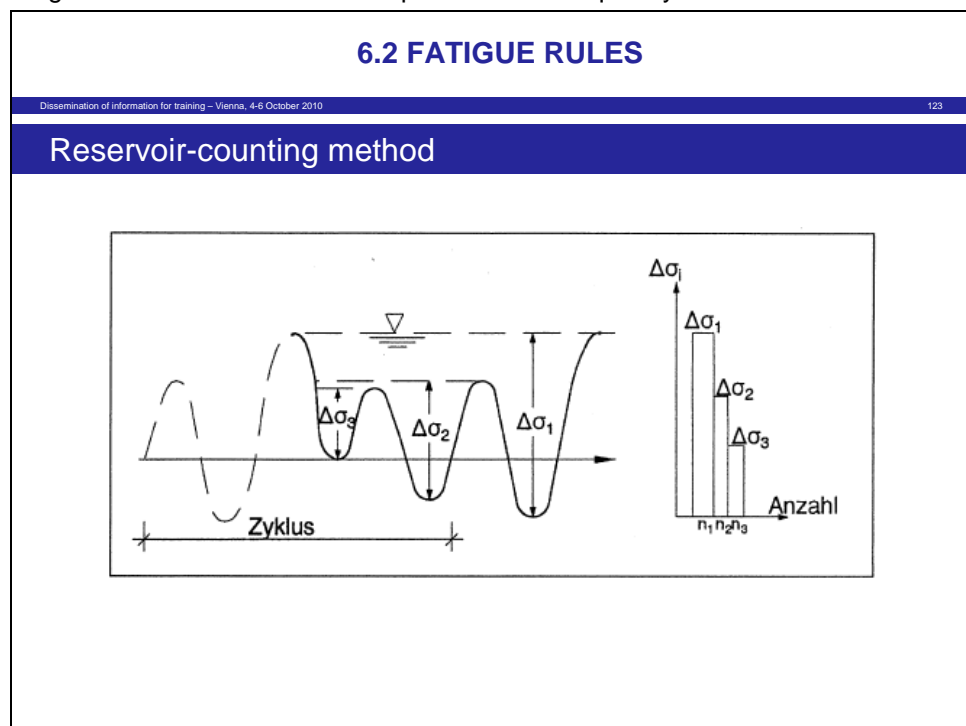


Figure 121

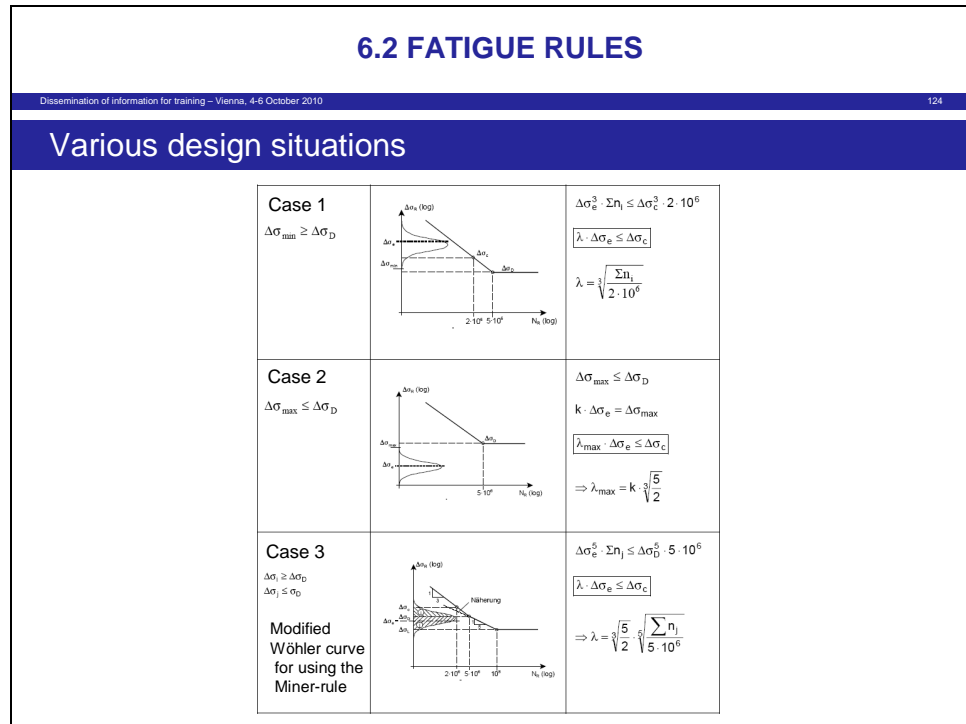


Figure 122

4. For the fatigue assessment using damage equivalent stress ranges $\Delta\sigma_e$ the position of the frequency distributions in relation to the endurance limit $\Delta\sigma_D$ for constant amplitude stress-ranges is relevant, see [Figure 122](#).

- Case 1 applies where all stress ranges of the distribution are larger than the endurance limit $\Delta\sigma_D$ from constant amplitude tests.

In this case a damage-equivalent factor $\bar{\lambda}$ can be applied to $\Delta\sigma_e$ to compare it directly with $\Delta\sigma_c$.

- Case 2 applies where all stress ranges of the distribution are smaller than the endurance limit $\Delta\sigma_D$ from constant amplitude tests.

In this case the comparison of $\Delta\sigma_e$ determined with the slope m requires the use of a damage equivalent factor $\bar{\lambda}_{\max}$.

- Case 3 applies where a part of the distribution of stress ranges is larger and a part is smaller than the endurance limit $\Delta\sigma_D$ from constant amplitude tests.

In this case it must be considered that any damage from stress ranges above $\Delta\sigma_D$ reduces the value of $\Delta\sigma_D$.

This can be approximatively taken into account by using the Haibach-line with a slope $m = 5$ below $\Delta\sigma_D$ and a cut off limit $\Delta\sigma_L$ at 10^8 cycles.

The damage equivalent factor $\bar{\lambda}$ is then influenced by the domain with $m = 3$ and the domain with $m = 5$.

In general frequency distributions for bridges are located in the area of $m = 5$, so that a fictitious Wöhler-line with $m = 5$ covering the full range of $\Delta\sigma_{Ei}$, n_{Ei} has been applied for the evaluation of fatigue equivalent traffic loads. By this

- procedure any complication by the relationship between the λ -value and the level of $\Delta\sigma_c$ could be avoided.
5. The spectrum of stress ranges used for the fatigue assessment can either be expressed by the damage equivalent load model from standards or from numerical simulations of traffic effects or measurements of traffic effects. Such spectra in general have peaks from rare heavy loads and from a large number of small “after”-vibrations. Whereas the cut-off-limit at 10^8 cycles cares for ignoring the after-vibrations, the peak effects from heavy vehicles are normally cut-off by a limit of 1% damage, that corresponds approximately to the definition of frequent loads or ~100 load cycles.

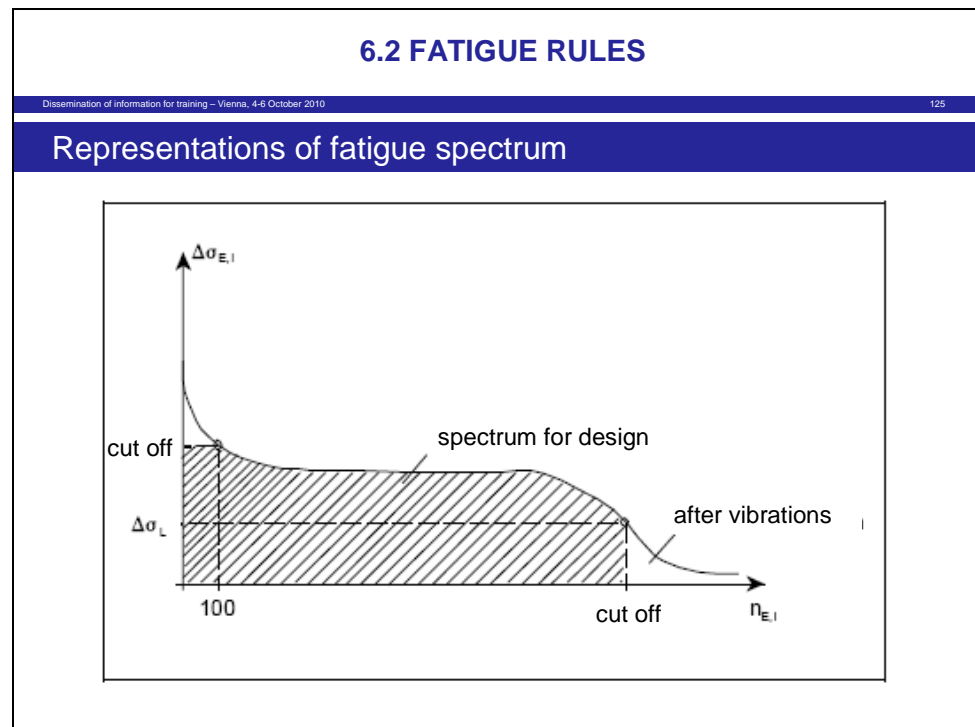


Figure 123

10.2 Fatigue loading models for bridges in EN 1991-2

- (1) The frequency-distributions for heavy vehicles and axle distances according to [Figure 124](#) are suitable to develop a singular loading pattern for a damage-equivalent vehicle and to determine the damage-equivalent values of axle load and vehicle loads as given by the fatigue loading model FLM 3 in [Figure 125](#).

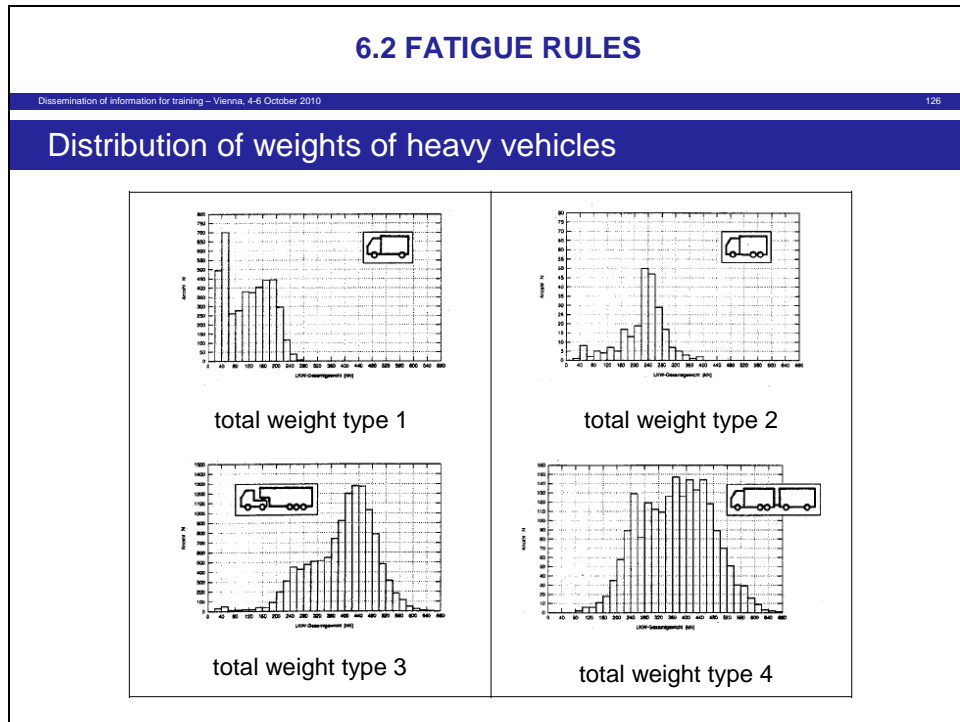


Figure 124

6.2 FATIGUE RULES

Dissemination of information for training – Vienna, 4-6 October 2010 127

Load-models for fatigue checks of road bridges

FLM 3 Main structure	Detailed FLM 4		
	LKW-Typen	Achslasten	Anteil Fernverkehr
<p>4x120 kN = 480 kN</p>		70-130	20%
		70-120-120	5%
		70-150-90-90-90	40%
		70-140-90-90	25%
		70-130-90-80-80-80	10%

Figure 125

- (2) EN 1991-2 also gives a set of silhouettes of damage-equivalent vehicles defined as Fatigue loading model FLM 4, that may be used to estimate the fatigue loading of an existing bridge from counting the types of silhouettes. It is however rarely used for fatigue design, because for the design of bridge structures in combination with descriptive rules for details the model FLM 3 is normally sufficient.

- (3) FLM 3 is in general used together with damage-equivalent factors λ describing the effects of various parameters of the bridge and composition of traffic, which control the relevant fatigue assessment.

10.3 Safety system for fatigue assessment

- (1) The partial factors γ_{Ff} and γ_{Mf} for the fatigue assessment as recommended in EN 1993-1-9 depend on the fatigue-safety-concept, see [Figure 126](#).

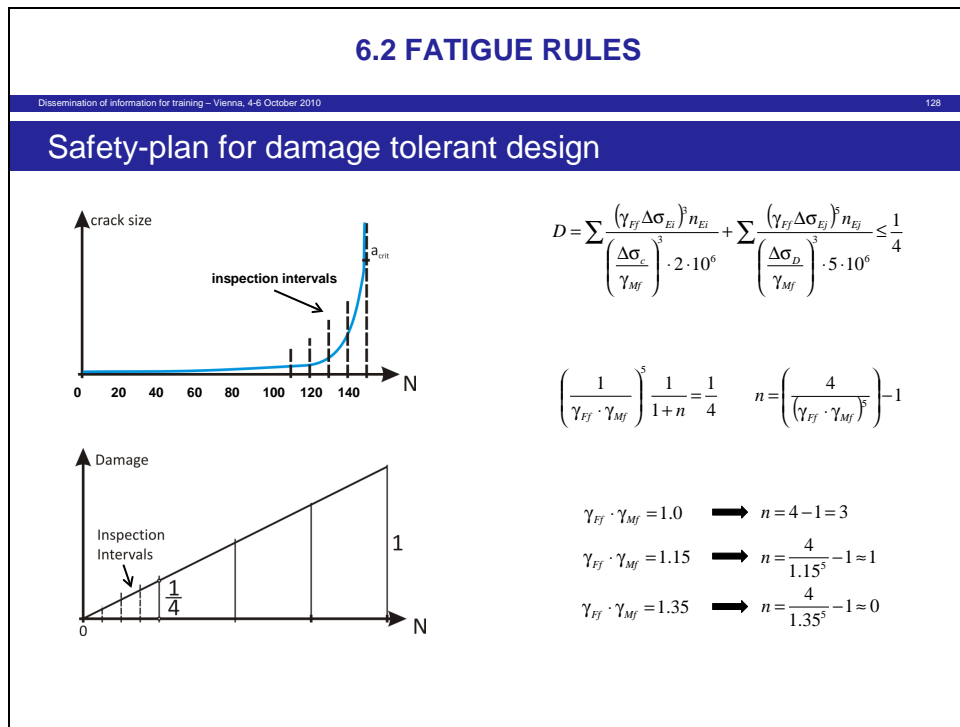


Figure 126

- (2) There are two fatigue safety concepts, that may be applied:
1. The “damage tolerance” concept, which is the standard concept aimed at in design, where failure by fatigue is excluded by sufficiently early pre-warning by visible damages like cracks so that the serviceability of the structure is infringed before critical situations that could lead to failure may occur.
This concept requires regular inspections in service; it has the advantage, that partial factors may be low and the service life of an existing bridge can be extended from its target design life as long as the inspections do not produce critical adverse signals.
[Figure 126](#) shows a way how the partial factors $\gamma_{Ff} \cdot \gamma_{Mf}$ chosen for fatigue can be associated with a safe service period $\frac{T}{n+1}$, defined by the total service life T and the number n of inspections in this total service life.
Using the steel material according to EN 1993-1-10 where a quarter of the full damage $\Delta \sigma_c^3 \cdot 2 \cdot 10^6$ has been used as safe service period, the choice of

$\gamma_{Mf} \cdot \gamma_{Ff} = 1,00$ would lead to a number of inspection of 3 (corresponding to $\frac{T}{n+1} = \frac{T}{4}$). Other choices of $\gamma_{Mf} \cdot \gamma_{Ff}$ would lead to a smaller number of inspections, and $\gamma_{Mf} \cdot \gamma_{Ff} = 1,35$ would result in a safe service period equal to the full service life T .

2. The “safe-life” concept, which requires that fatigue is treated as an ultimate limit state, as pre-warning signals may not be detected sufficiently early (e.g. because of disproportionate quick crack growth as for bolts or because access for inspection is not possible as for tension ties buried in the soil or underwater structures).

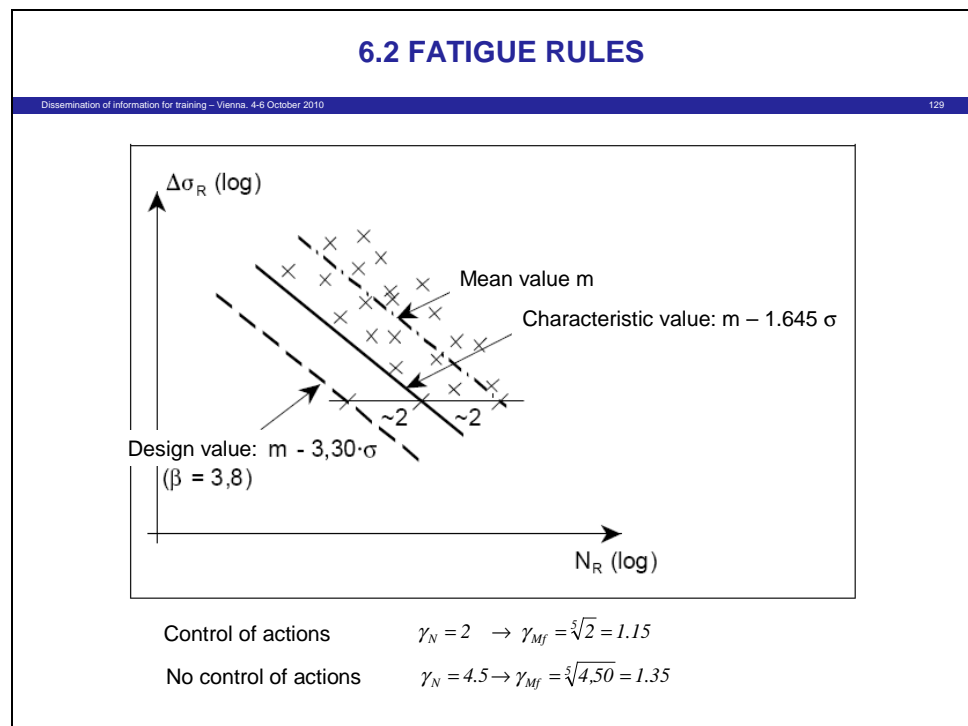


Figure 127

Figure 127 shows the characteristic fatigue strength function $(m - 1.645 \cdot \sigma)$ which for attaining the design function $(m - 3.30 \cdot \sigma)$ needs about a partial factor $\gamma_N = 2$ in design life, which gives a partial factor $\gamma_{Mf} = 1.15$ for $m = 5$.

According to the “Tri-lateral Design and Analysis Code” for temporary bridges the requirements for safe-life design is also $\gamma_N = 2$ in case the traffic loads are regularly controlled in view of the fatigue load assumed, but it is $\gamma_N = 4.5$ in case traffic loads may develop with the time without control. In that case the partial factor would be $\gamma_{Mf} = 1.35$.

In case the safe-life-concept is chosen, the structure has to be taken out of service independently on whether inspections reveal damages or not, when the target design life has been reached.

10.4 The use of Fatigue loading model FLM 3

(1) The fatigue loading model FLM 3 may be used in two ways, see [Figure 128](#).

1. Use as a damage equivalent vehicle together with influence surfaces for the various lanes to determine the stress-history from the crossing over the bridge and to calculate $\Delta\sigma_{E2}$ by using the counting method, the Miner rule and informations on traffic distributions on lanes and design life.

In this case a single FLM 3 underestimates the fatigue effects for influence lines for hogging moments of continuous bridges so that it should be supplemented by a second vehicle.

2. Use of the damage equivalent vehicle to determine $\Delta\sigma_{E2}$ from the differences of σ_{max} and σ_{min} from extreme positions of FLM 3 on the influence line for a single lane, that is multiplied with the damage equivalent factor

$$\lambda = \lambda_1 \cdot \lambda_2 \cdot \lambda_3 \cdot \lambda_4$$

which include all necessary informations. λ_1 is the span length factor that has been determined from numerical simulations with the Auxerre-traffic and constitutes an enveloping function versus the span length, see [Figure 129](#).

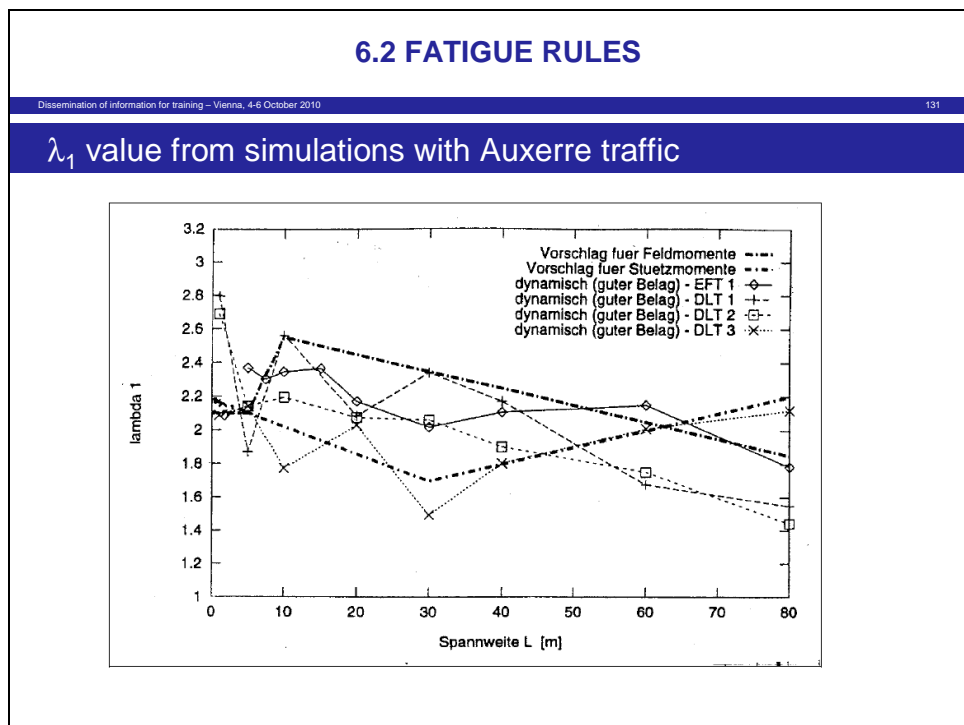


Figure 129

10.5 Design example

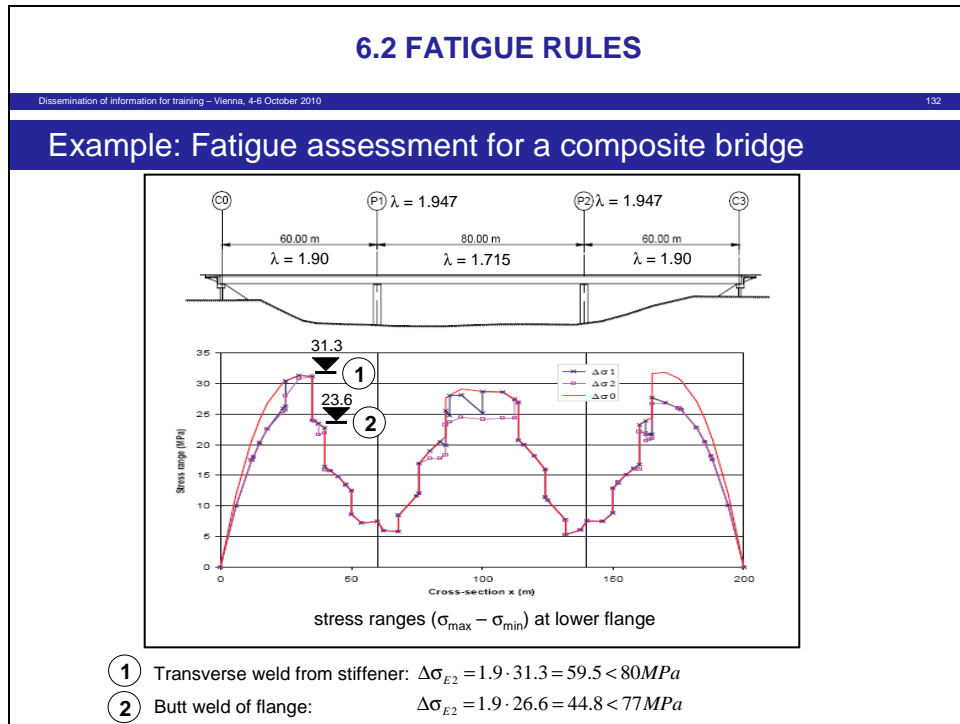


Figure 130

- (1) For the design example in [Figure 130](#) the stress ranges $\Delta\sigma = (\sigma_{\max} - \sigma_{\min})$ caused by FLM3 on extreme positions of the influence line are given.
- (2) The distribution of these stress ranges shows that at the midspans the stress ranges from traffic action attain the largest values, whereas at the support, the stress ranges are low.
- (3) This indicates that at the supports, where thick flanges are needed, the use of high strength steels could be appropriate, that gives small plate thicknesses and therefore economic advantages in weld-volume.
- (4) The λ -values for midspan and at the supports differ a bit and vary between 1,715 and 1,947.
- (5) The fatigue assessment is carried out at two locations of the bottom flange in the field of the side-span:
 1. Transverse weld from stiffener
 2. Butt weld of flange.

It satisfies the requirement even for safe-life-design.

10.6 Further informations

- (1) Further informations on the background of the fatigue rules in EN 1993-1-9 and on design examples is given in the JRC-Report "Commentary to Eurocode 3 – EN 1993 – Part 1.9 – Fatigue), see [Figure 131](#).



Figure 131

11. Use of preloading in bridges

11.1 General

- (1) There is no common definition of Preloading or Prestress " P " in EN 1990; it leaves such definitions and also the choice of partial factors to be applied to " P " to the Eurocodes for different materials and ways of construction.
- (2) It is therefore a purpose of this report to give this definition for steel bridges, in particular for bridges with ropes, as stayed cable bridges.
- (3) This report also explains how the permanent action G and preloading P are treated in combinations of actions and how 2nd order theory shall be applied, so that the design of e.g. ropes and pylons in a cable stayed bridge is consistent.

11.2 Definitions

- (1) The definition of prestress and preloading may be taken from [Figure 132](#).

Preloading is systematically used in cable-stayed bridges to optimize the distribution of action effects for serviceability and ultimate criteria.

6. DESIGN OF BRIDGE-ELEMENTS

6.3 ROPE STRUCTURES

134

Rope-structures - Stayed cable bridges

Definition

- Any prestress is generated by preloading
- Preloading is a process to impose
 - forces or
 - deformations
- The effects of preloading may be
 - variations of stresses (prestress)
 - variations of deformations
 - other variations of permanent stage

Figure 132

11.3 Examples for preloading processes

- (1) Figure 133, Figure 134 and Figure 135 give examples for different preloading processes in different application fields

6.3 ROPE STRUCTURES

135

Examples for preloading processes

1a) Prestressing by internal tendons

1b) Prestressing of trusses by cables in hollow sections

1c) Prestressing by external tendons

1d) Prestressing of joints subjected to tension or friction

Figure 133

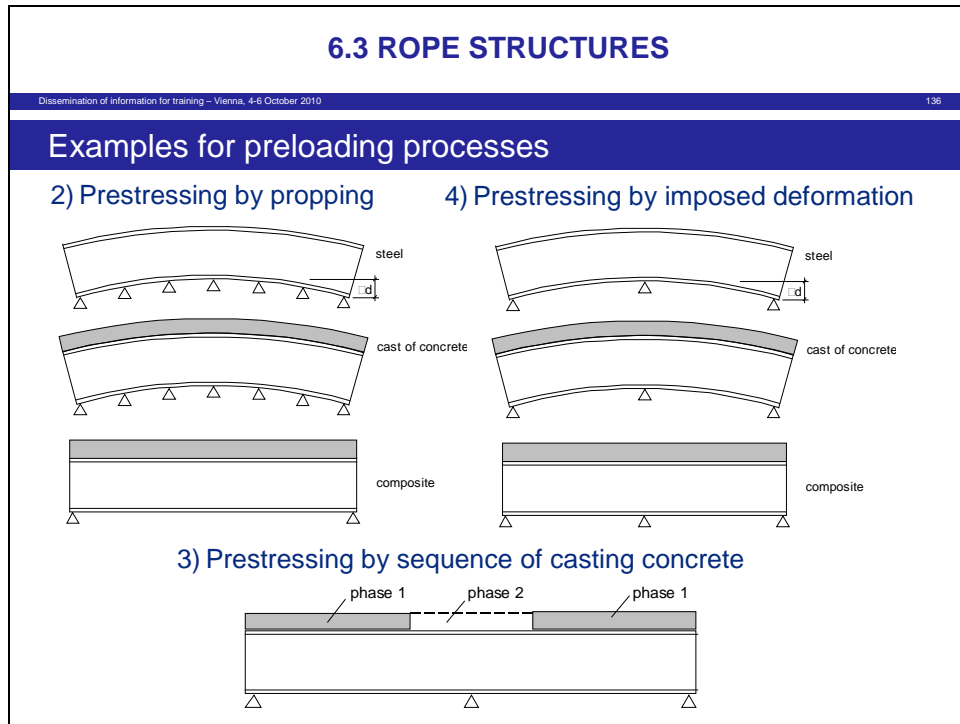


Figure 134

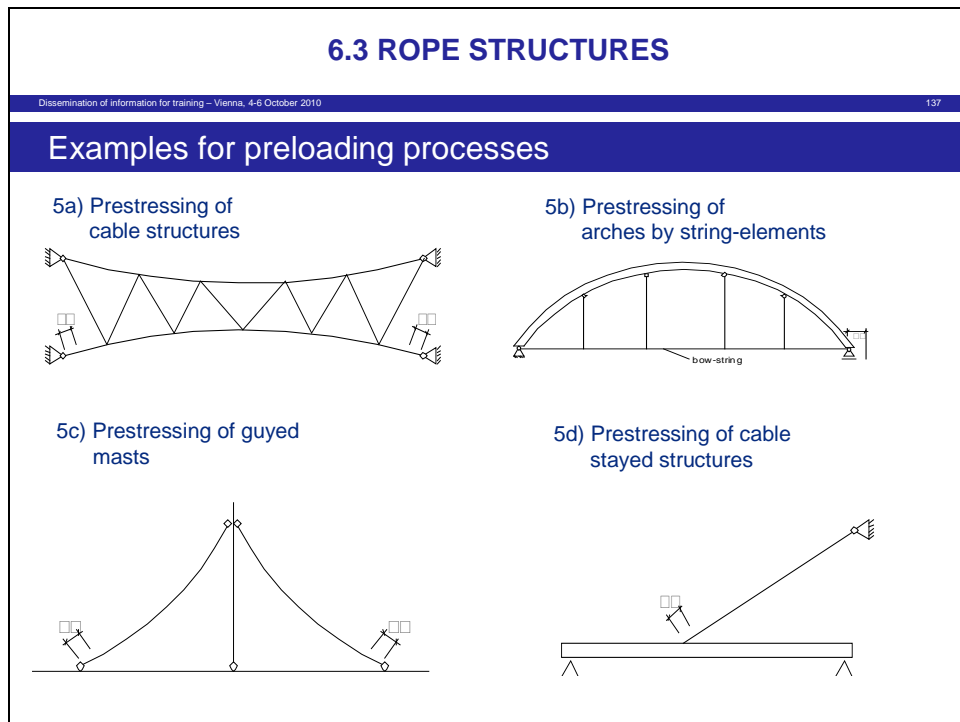


Figure 135

6.3 ROPE STRUCTURES

Dissemination of information for training – Vienna, 4-6 October 2010 138

Principles

- It is possible to define the preloading or prestressing process by all necessary steps including controls
- It is not possible to define “prestress” as an effect of prestressing or preloading in a general way, that covers all cases

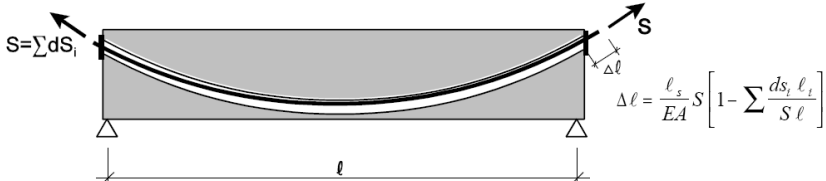
Figure 136

- (2) Due to the different aims of preloading or prestress in the various application fields it is not possible to define preloading or prestressing in a common way.
- (3) Figure 137 and Figure 138 give examples for such different ways, prestress and preloading are treated:

6.3 ROPE STRUCTURES

Dissemination of information for training – Vienna, 4-6 October 2010 139

Example for the applicability of “prestress”



$$\Delta \ell = \frac{\ell_s}{EA} S \left[1 - \sum \frac{ds_i \ell_i}{S \ell} \right]$$

stress before prestresses: $\sigma_{q0, \Delta l=0}$

stress immediately after prestressing: $\sigma_{q0, \Delta l}$

prestress: $\sigma_{q0, \Delta l=0, \Delta l} = \sigma_{q0, \Delta l} - \sigma_{q0, \Delta l=0}$

Figure 137

- (4) Figure 137 shows the effect of prestressing of a concrete beam by applying imposed displacements Δl to a tendon. Prestress is defined by the difference between the stress before the imposed displacement and after.
- (5) Figure 138 shows the effect of the same displacement to a catenarian rope. The effects are non-linear and do not permit to define the effects as a difference of stress in the rope only.

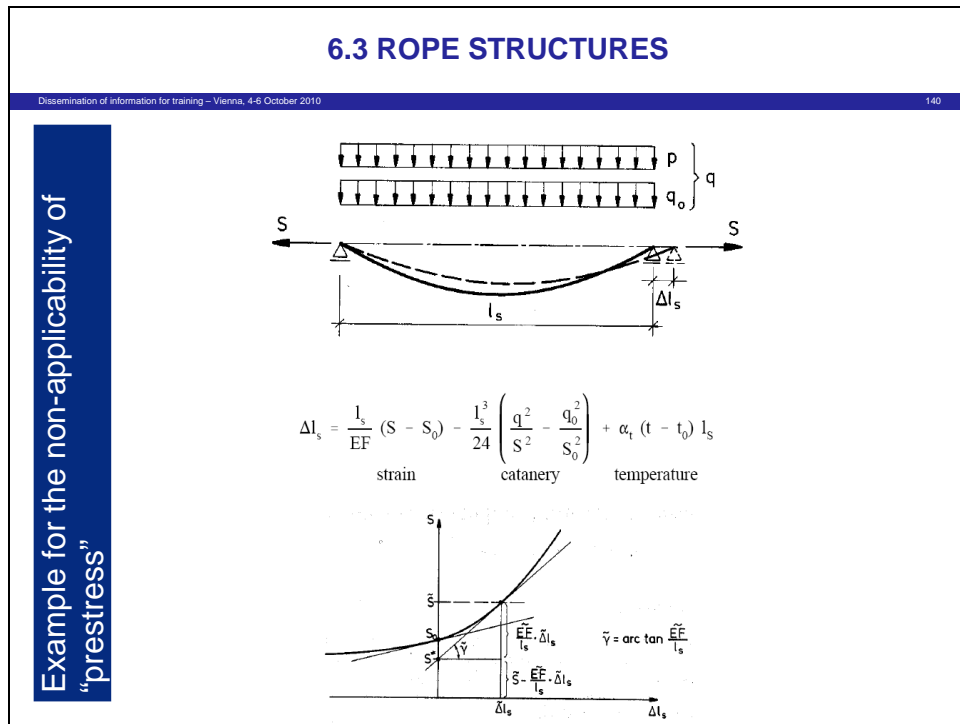


Figure 138

- (6) Therefore the action "*P*" in EN 1990 is defined as a process aiming at a particular structural shape or behaviour, see Figure 139.

6.3 ROPE STRUCTURES	
<small>Dissemination of information for training – Vienna, 4-6 October 2010</small>	<small>141</small>
Conclusion	
<p style="text-align: center;">“P” in EN 1990</p> <ul style="list-style-type: none"> a) preloading or prestressing process leading to a structural shape or behaviour as required b) prestress in specific cases where defined 	

Figure 139

11.4 Treatment of preloading and prestressing processes in the construction phase

- (1) The target of the preloading and prestressing process in the construction phase is to attain the required structural form and distribution of effects of permanent actions and preloading process ($G + P$), see Figure 140.

6.3 ROPE STRUCTURES	
<small>Dissemination of information for training – Vienna, 4-6 October 2010</small>	<small>142</small>
Treatment of preloading and prestressing processes in the construction phase	
<p>Target: attainment of the required structural form and distribution of permanent effects of ($G+P$)</p> <p>Conclusion: calculation with characteristic values, linear material law: stress limitations and prestressing of cables.</p>	

Figure 140

- (2) Therefore calculations are carried out with characteristic values (mean values), linear material law and stress-limitations in the cables.

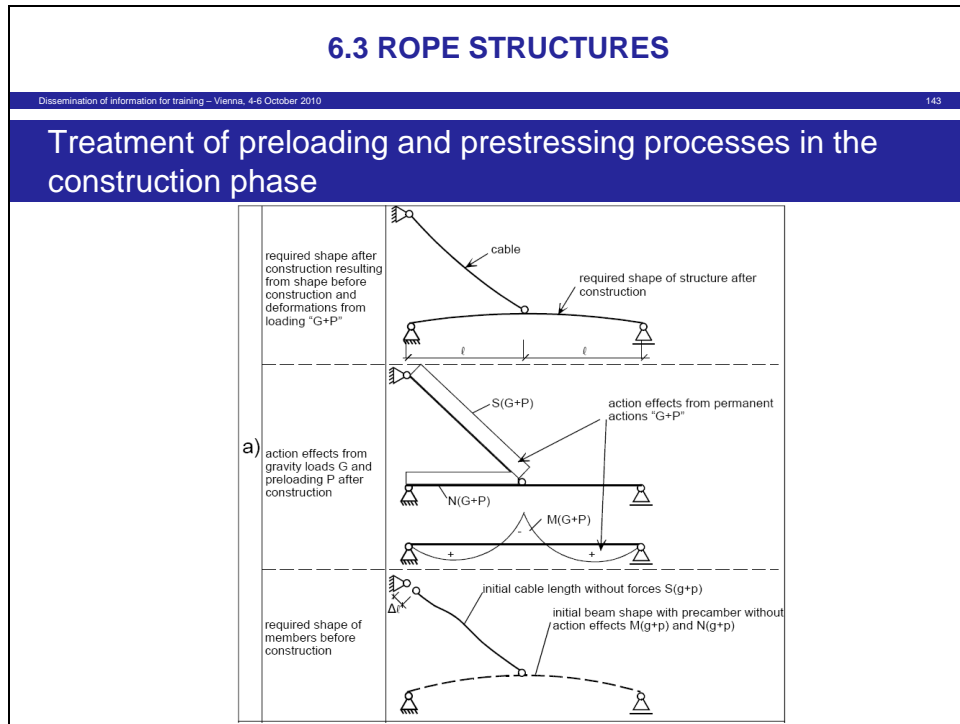


Figure 141

- (3) Figure 141 shows:

- in the first line the shape of a stayed structure after execution under the actions $(G + P)$
- in the second line the action effects in the various components of the structure with a shape as indicated in the first line under the gravity loads G and the preloading P
- in the third line the “stress-free” shape of the structural components (rope and beam) when they are released from all actions and give their length’s and curved form as geometrical requirements for fabrication

11.5 Treatment of preloading and prestressing in the service phase

- (1) The taking in service of the structure starts with the initial geometry and initial distribution of action effect from the actions $(G + P)$ achieved after execution, that may have certain imperfections, see figure 142.

6.3 ROPE STRUCTURES

Dissemination of information for training – Vienna, 4-6 October 2010
144

Treatment of preloading and prestressing processes in the service phase

Target: ULS verification on the basis of:

- permanent actions $\gamma_G(G+P)$
- permanent form resulting from $(G+P)$
- imperfections of the form
- variable actions $\gamma_Q\{Q_{k1} + \psi_0 Q_{k2}\}$

Conclusion: Calculation with the permanent form associated with the effect from $\gamma_G(G+P)$

Figure 142

- (2) For the ultimate limit state verification the various components of the structure all with a structural shape after execution resulting from $(G + P)$ should be assumed to be loaded by the design values of action effects

$$\gamma_G(G + P)$$

- (3) Design values of variable actions

$$\gamma_Q(Q_{k1} + \psi_0 \cdot Q_{k2})$$

are assumed to act on the structure with the shape resulting from $(G + P)$ and with an initial load $\gamma(G + P)$.

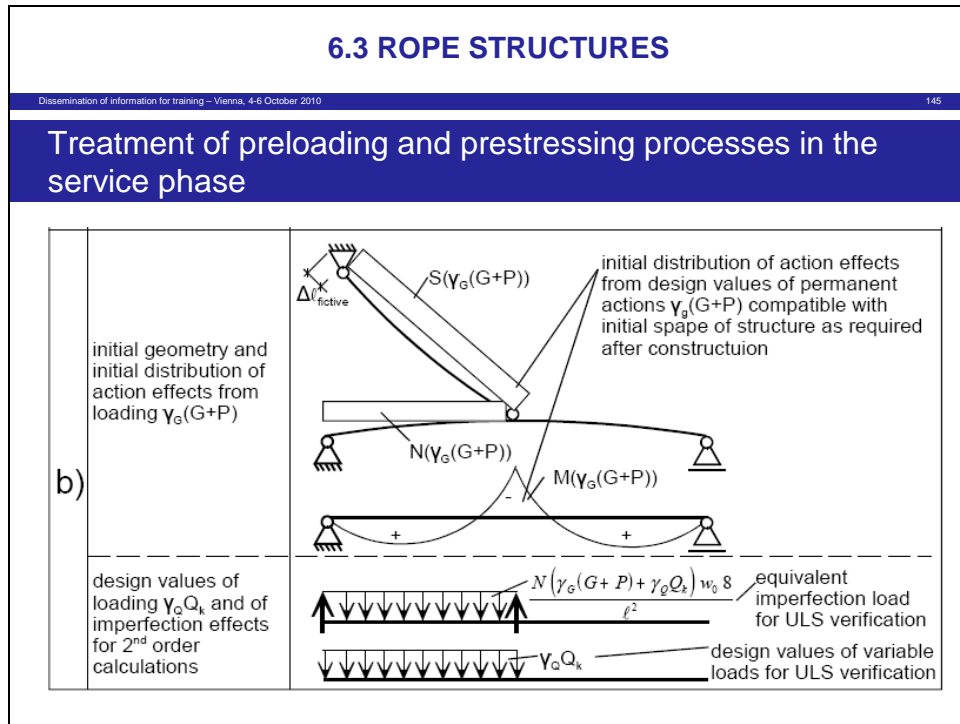


Figure 143

(4) Figure 143 illustrates the procedure:

- the first line gives the structural shape resulting from $(G + P)$ with an initial loading of components from $\gamma(G + P)$
- the second line gives the design values of the additional imperfections w_0 that give a fictitious loading from $\gamma_G(G + P) + \gamma_Q(Q_{k1} + \psi_0 + Q_{k2})$.

(5) This procedure explains why

$$(G + P)$$

should represent an action from a “single process” and therefore have common partial factors

$$\gamma_{(G+P)} = 1,35 \text{ or}$$

$$\gamma_{(G+P)} = 1,00$$

depending on unfavourable or favourable effects in combination with external loads Q_k .

(6) Where however effects of G from P are counteracting so that $(G + P)$ is small, e.g. at the limit state of decompression, either G and P should be modified by $\Delta G = \alpha \cdot G$ and $\Delta P = \alpha \cdot P$ where α takes values ≤ 0.05 , see Figure 144.

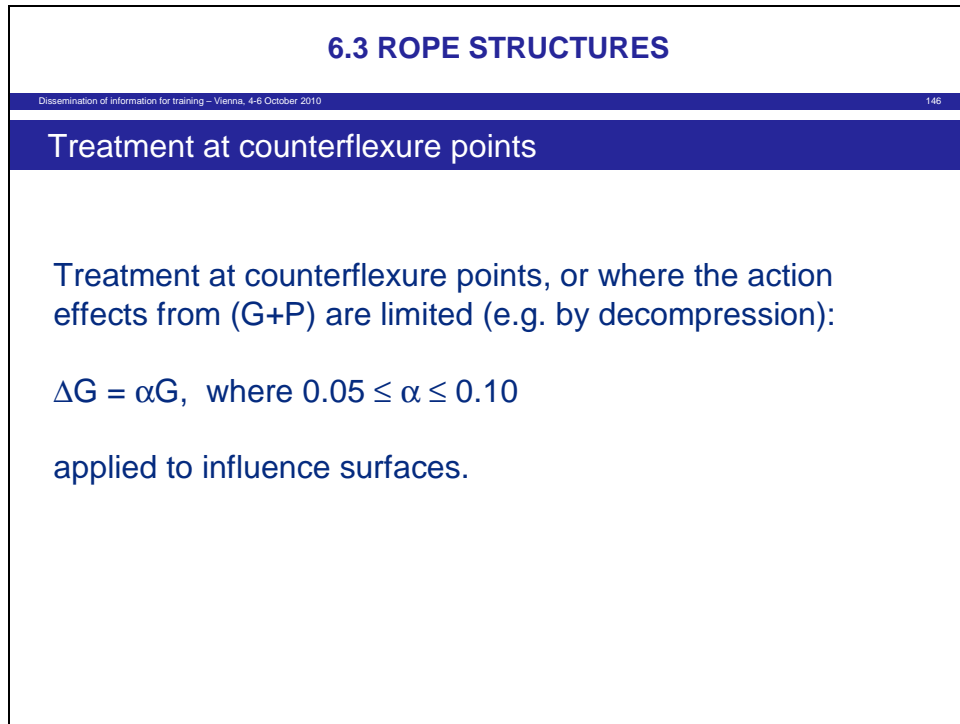


Figure 144

12. Further informations to design rules for steel bridges

- (1) Gaps in the Eurocodes identified during use are being subject of the development of “Non conflicting complementary informations (NCCI)”.
- (2) Apart from the items mentioned in this report as
 - rules for actions on bridges, e.g. treatment of combined wind-, rain- and traffic-induced vibrations
 - extension of rules for choice of material
 - stability rules for lateral torsional and plate buckling
 - fatigue rulesthere are further items, for some of which JRC-report have already been published.
- (3) The JRC-reports “Design of light-weight footbridges for human induced vibrations”, see [Figure 145](#) and “Assessment of existing steel structures: Recommendations for Estimation of Remaining Fatigue life”, see [Figure 146](#), are examples of such publications.

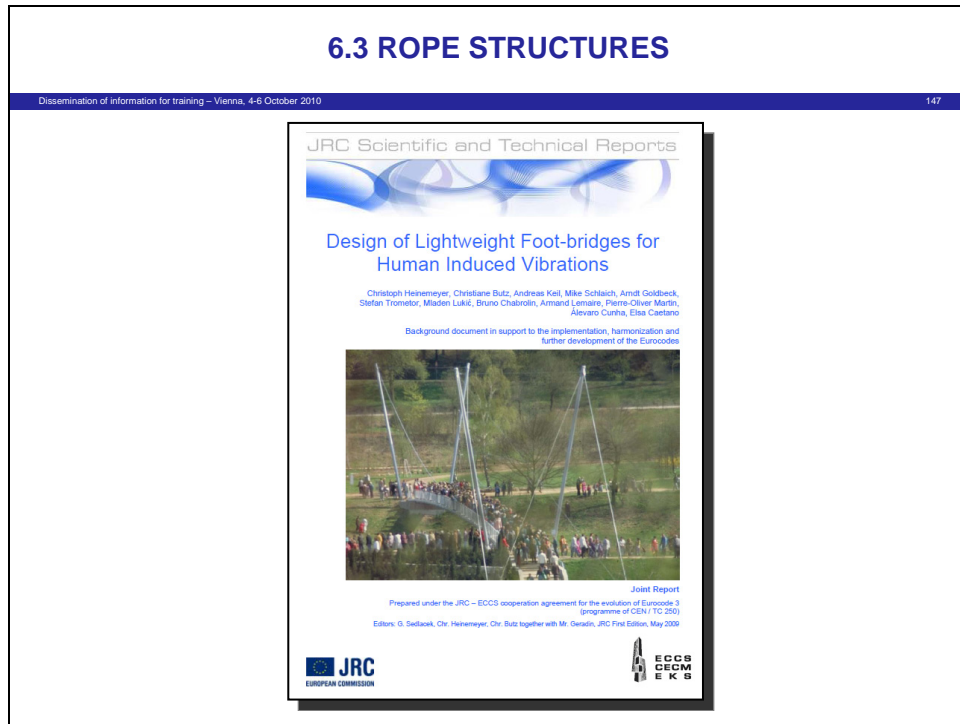


Figure 145

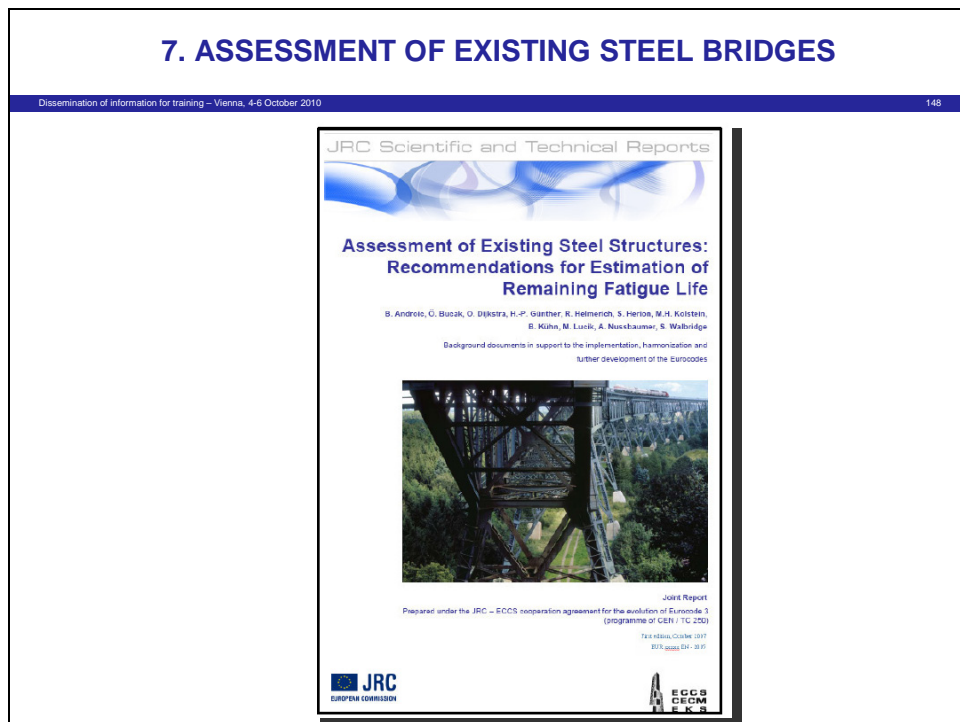


Figure 146

Appendix B

A sample analytical method for bearing resistance calculation - From EN 1997-2 (CEN, 2004): Annex D (informative)

D.4 Drained conditions

(1) The design bearing resistance may be calculated from:

$$R/A' = c' N_c b_c s_c i_c + q' N_q b_q s_q i_q + 0,5 \gamma' B' N_\gamma b_\gamma s_\gamma i_\gamma \quad (D.2)$$

with the design values of dimensionless factors for:

— the bearing resistance:

$$N_q = e^{\pi \tan \varphi'} \tan^2 (45^\circ + \varphi'/2)$$

$$N_c = (N_q - 1) \cot \varphi'$$

$$N_\gamma = 2 (N_q - 1) \tan \varphi', \text{ where } \delta \geq \varphi'/2 \text{ (rough base)}$$

— the inclination of the foundation base:

$$b_c = b_q - (1 - b_q) / (N_c \tan \varphi')$$

$$b_q = b_\gamma = (1 - \alpha \cdot \tan \varphi')^2$$

— the shape of foundation:

$$s_q = 1 + (B' / L') \sin \varphi', \text{ for a rectangular shape;}$$

$$s_q = 1 + \sin \varphi', \text{ for a square or circular shape;}$$

— $s_\gamma = 1 - 0,3 (B'/L')$, for a rectangular shape;

$$s_\gamma = 0,7, \text{ for a square or circular shape}$$

— $s_c = (s_q \cdot N_q - 1) / (N_q - 1)$ for rectangular, square or circular shape;

— the inclination of the load, caused by a horizontal load H :

$$i_c = i_q - (1 - i_q) / (N_c \tan \varphi');$$

$$i_q = [1 - H / (V + A' c' \cot \varphi')]^m;$$

$$i_\gamma = [1 - H / (V + A' c' \cot \varphi')]^{m+1}.$$

where:

$$m = m_B = [2 + (B' / L')] / [1 + (B' / L')] \text{ when } H \text{ acts in the direction of } B';$$

$$m = m_L = [2 + (L' / B')] / [1 + (L' / B')] \text{ when } H \text{ acts in the direction of } L'.$$

In cases where the horizontal load component acts in a direction forming an angle θ with the direction of L' , m may be calculated by:

$$m = m_\theta = m_L \cos^2 \theta + m_B \sin^2 \theta.$$

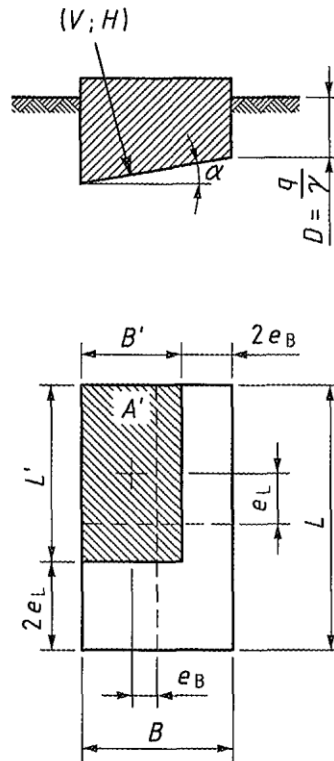


Figure D.1 — Notations

Appendix C

Example of a method to calculate the settlements for spread foundations - From EN 1997-2 (CEN, 2004): E.2

(1) The following is an example of a method to calculate the settlement, (s), of spread foundations using a semi-empirical method developed for MPM tests.

$$s = q - \sigma_{v0} \times \left[\frac{2B_0}{9E_d} \times \left(\frac{\lambda_d B}{B_0} \right)^a + \frac{\alpha \lambda_c B}{9E_c} \right]$$

where

B_0 is a reference width of 0.6 m;

B is the width of the foundation;

λ_d, λ_c are shape factors given in Table E.2;

α is a rheological factor given in Table E.3;

E_c is the weighted value of E_M immediately below the foundation;

E_d is the harmonic mean of E_M in all layers up to $8 \times B$ below the foundation;

σ_{v0} is the total (initial) vertical stress at the level of the foundation base;

q is the design normal pressure applied on the foundation.

Table E.2 — The shape coefficients, λ_c, λ_d , for settlement of spread foundations

L/B	Circle	Square	2	3	5	20
λ_d	1	1.12	1.53	1.78	2.14	2.65
λ_c	1	1.1	1.2	1.3	1.4	1.5

Table E.3 — Correlations for deriving the coefficient α for spread foundations

Type of ground	Description	E_M/p_{LM}	α
Peat			1
Clay	Over-consolidated	<16	1
	Normally consolidated	9–16	0,67
	Remoulded	7–9	0,5
Silt	Over-consolidated	>14	0,67
	Normally consolidated	5–14	0,5
Sand		>12	0,5
		5–12	0,33
Sand and gravel		>10	0,33
		6–10	0,25
Rock	Extensively fractured		0,33
	Unaltered		0,5
	Weathered		0,67

NOTE This example was published by the French Ministère de l'Équipement du Logement et des Transport (1993).

Appendix D

Generation of semi-artificial accelerograms for time-history analysis through modification of natural records

D.1 NATURAL EARTHQUAKE RECORDS

The components of the ground motions used for time-history analysis are produced by modifying natural earthquake records in order to match the design spectrum of Eurocode 8. The natural records are from earthquakes with magnitude, distance to fault, generation mechanism, and ground conditions compatible as much as possible with the design seismic action for the project. In this example records from the following earthquakes are used: Loma Prieta, USA 17/10/1989, Athens, Greece 07/09/1999, Kalamata, Greece 10/10/1986, Pyrgos, Greece 23/4/1993, Morgan Hill, USA 24/04/1984, Gazli, USSR 17/05/1976, Loma Prieta, USA 17/10/1989, Kobe, Japan 16/01/1995, Kocaeli, Turkey 17/08/1999, Leukada, Greece.

D.2 MODIFICATION PROCEDURE OF NATURAL RECORDS TO MATCH DESIGN SPECTRUM

The modification procedure of the recorded accelerograms is performed by application of the single impulse method (Choi and Lee, 2003). This method consists of a simple iterative procedure in the time domain for matching multiple damping design spectra, in which the adjustment of the time history is calculated for one frequency and one damping at a time using the unit impulse function. In this work several modifications are introduced in the original method that estimate in a better manner the parameters of the impulse function and improve the convergence for big periods and damping values that are typically present in seismically isolated structures. After several iterations the method converges and the response spectrum of the modified accelerogram does not deviate significantly from the target spectrum in the examined period and damping range of values.

The modification procedure is applied in accordance to the following algorithm:

1. Calculation of the response spectrum of the accelerogram for various period and damping values.
2. Check of the acceptance criteria. If the response spectrum of the accelerogram is acceptable with respect to the design spectrum then terminate the algorithm.
3. Find the period and the damping value for which the deviation of the accelerogram response spectrum and the design spectrum becomes maximum.
4. Correction of the acceleration time history by addition of a suitable impulse function so that the deviation of the new accelerogram response spectrum and the design spectrum is almost zero for the particular period and damping that was found in step 3.
5. Return to step 2.

The impulse function is defined as follows:

$$0 \leq t \leq t_m \quad f(t) = -\alpha_0 \frac{1}{\omega_0} \exp(-\xi_0 \omega_0 (t_0 - t)) \sin(\omega_0 (t_0 - t)) \quad (D.1)$$

$$\text{otherwise } f(t) = 0$$

where:

- a_0 is a scaling coefficient calculated so as to fulfil the condition of step 4 of the algorithm
- ω_0 is a circular frequency calculated so that the response spectrum of the impulse function becomes maximum for the circular frequency calculated in step 3 of the algorithm
- ξ_0 is the damping value calculated in step 3 of the algorithm
- t_m is the time value for which the maximum response occurs in accordance with step 3 of the algorithm
- t_0 is a time parameter so that the response of the impulse function becomes maximum for time equal to t_m

The coefficients a_0 , ω_0 , t_0 are analytically calculated from lengthy functions that fulfill the requirements presented in their definition.

After convergence of the algorithm is achieved baseline correction is applied to the produced accelerograms in order to remove baseline trends (Boore and Bommer, 2005). These trends are well noticeable in the displacement time-histories which may deviate significantly from the zero value for the uncorrected accelerograms.

Baseline correction is applied as follows:

1. Determination, through regression analysis (least-squares-fit method), of the quadratic polynomial curve that best fits the time-acceleration pairs of values.
2. Subtraction from the actual acceleration values of their corresponding counterparts as obtained with the regression-derived equation.

In this work the modification procedure is applied to achieve compatibility with the 5%-damped design spectra, although it is possible to apply it for a set of other damping values.

D.3 PRODUCED SEMI-ARTIFICIAL ACCELEROGRAMS

In the following pages the various ground motion parameters defined in Fig. D-1.1 are presented for ground motion EQ1, longitudinal component ACC01. The modified accelerogram is created using the original record from Loma Prieta earthquake, Corralitos 000 record (Magnitude $M_s=7.1$, distance to fault 5.1km, USGS ground type B). For the produced accelerogram the acceleration, velocity and displacement time-histories are also presented. By comparison of the initial recorded accelerogram and the final semi-artificial accelerogram it is concluded that the modification method does not alter significantly the naturally recorded waveform. The 5%-damped pseudo-acceleration and displacement response spectra of the semi-artificial accelerogram is also presented and compared with the corresponding Eurocode 8 design spectra. It is verified that the produced accelerogram adequately matches the design spectra for the whole range of examined periods shown. Similar results are obtained for the rest of the semi-artificial accelerograms.

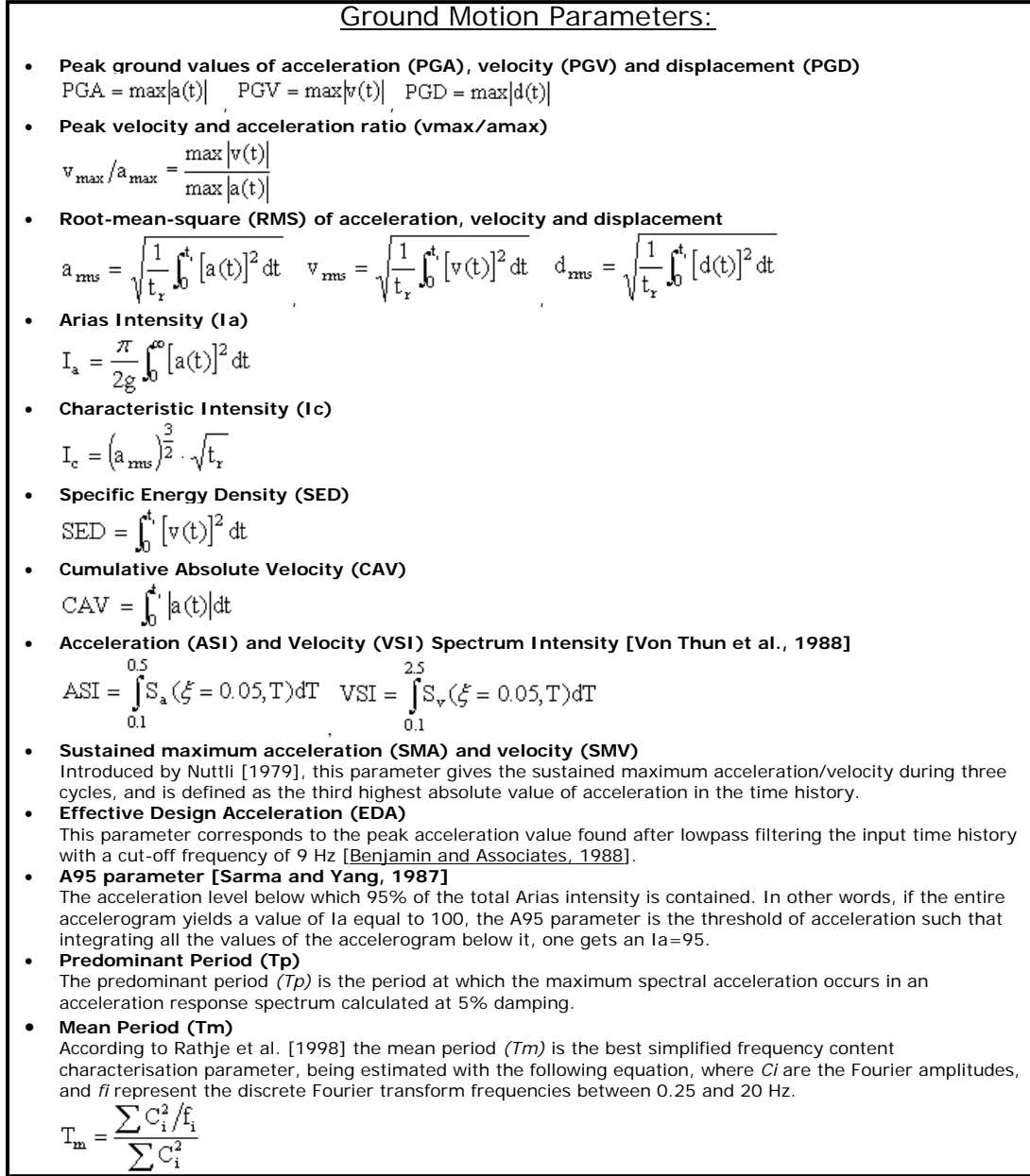


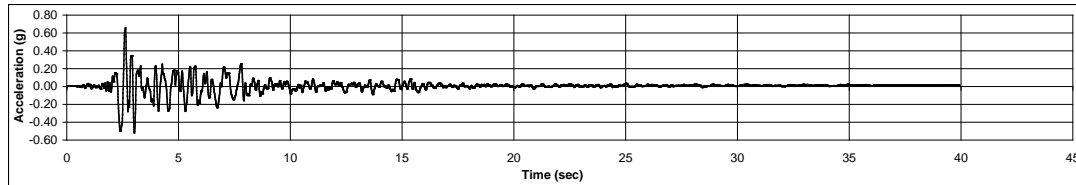
Fig. D-1.1 Definition of accelerogram properties

Appendix D: Generation of semi-artificial accelerograms for time-history analysis through modification of natural records

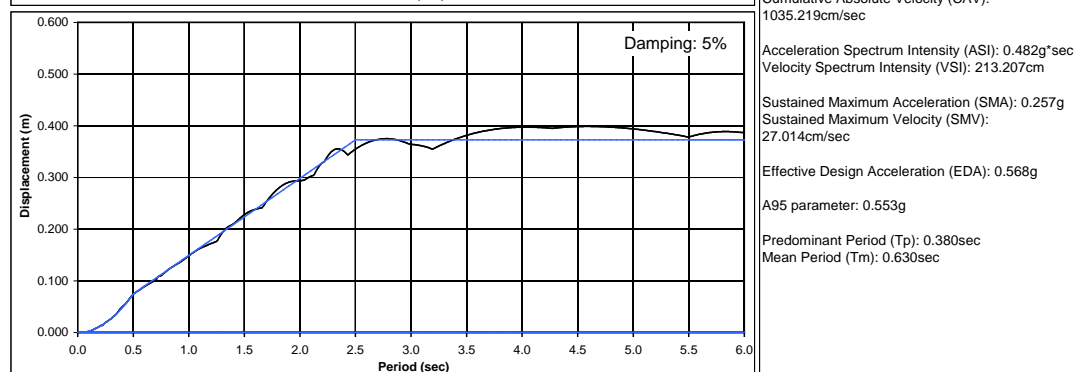
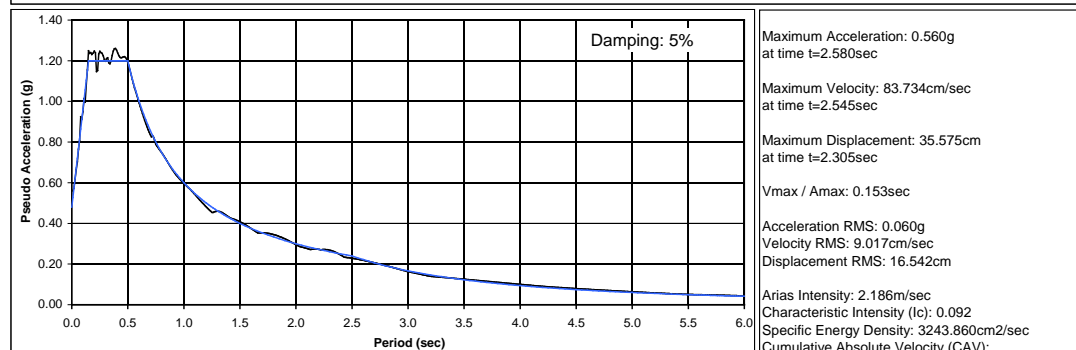
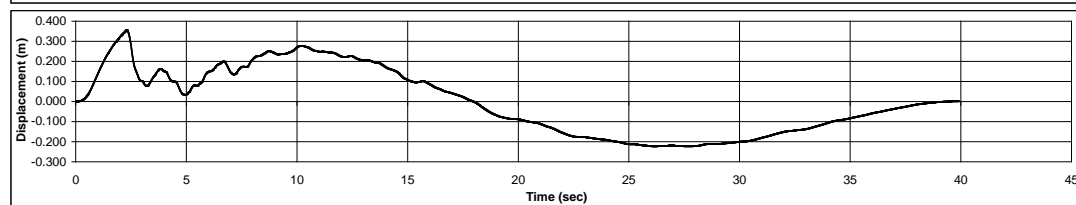
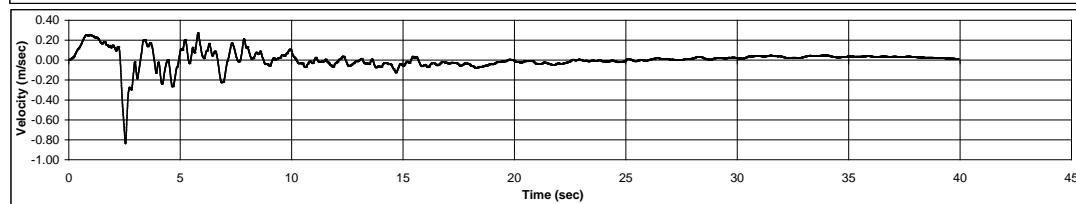
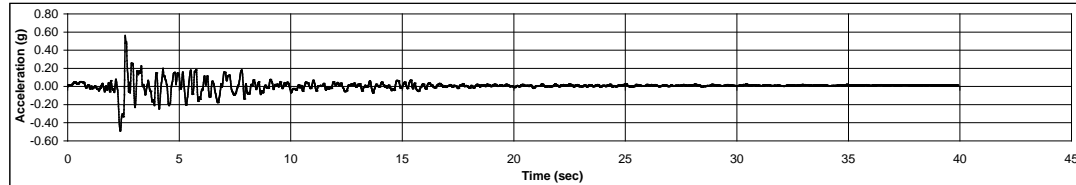
Ground Motion EQ1 – Long Direction:

ACC01

Original Record:



Modified Record:



References

- Boore, D. M. and J. J. Bommer. 2005. Processing of Strong-Motion Accelerograms: Options and Consequences. *Soil Dynamics and Earthquake Engineering* 25: 93–115.
- Choi, D. H., and S. H. Lee. 2003. Multi-Damping Earthquake Design Spectra-Compatible Motion Histories. *Nuclear Engineering and Design* 226: 221–30.

Authors: Yosra Bouassida, Emmanuel Bouchon, Pilar Crespo, Pietro Croce, Laurence Davaine, Steve Denton, Markus Feldmann, Roger Frank, Gerhard Hanswille, Wolfgang Hensen, Basil Kolias, Nikolaos Malakatas, Giuseppe Mancini, Miguel Ortega Cornejo, Joel Raoul, Gerhard Sedlacek, Georgios Tsionis
(Editors: Adamantia Athanasopoulou, Martin Poljansek, Artur Pinto, Georgios Tsionis, Steve Denton)

Luxembourg: Publications Office of the European Union
2012 – 438 pp. – 21 x 29.7 cm
EUR – Scientific and Technical Research series – ISSN 1831-9424
ISBN 978-92-79-22823-0
doi: 10.2788/82360

Abstract

This document is a Technical Report with worked examples for a bridge structure designed following the Eurocodes. It summarizes important points of the Eurocodes for the design of concrete, steel and composite road bridges, including foundations and seismic design, utilizing a common bridge project as a basis.

The geometry and materials of the example bridge as well as the main assumptions and the detailed structural calculations are presented in the first chapter of the report. Each of the subsequent chapters presents the main principles and rules of a specific Eurocode and their application on the example bridge, namely:

- The key concepts of basis of design, i.e. design situations, limit states, the single source principle and the combinations of actions (EN 1990);
- Permanent, wind, thermal, traffic and fatigue actions on the bridge deck and piers and their combinations (EN 1991);
- Bridge deck modeling and structural analysis;
- The design of the bridge deck and the piers for the ULS and the SLS, including the second-order effects (EN 1992-2);
- The classification of the composite cross-sections, the ULS, SLS and fatigue verifications and the detailed design for creep and shrinkage (EN 1994-2);
- The settlement and resistance calculations for the pier, three design approaches for the abutment and the verification of the foundation for the seismic design situation (EN 1997);
- The conceptual design for earthquake resistance considering the alternative solutions of slender or squat piers; the latter case involves seismic isolation and design for ductile behavior (EN 1998-1, EN 1998-2).

The bridge worked example analyzed in this report was prepared and presented at the workshop “Bridge Design to the Eurocodes” that was held on 4-6 October 2010 in Vienna, Austria. The workshop was organized by JRC with the support of DG ENTR and in collaboration with CEN/TC250/Horizontal Group Bridges, the Austrian Federal Ministry for Transport, Innovation and Technology and the Austrian Standards Institute.

The document is part of the Report Series “Support to the implementation, harmonization and further development of the Eurocodes”, prepared by JRC in collaboration with DG ENTR and CEN/TC250 “Structural Eurocodes”.

How to obtain EU publications

Our priced publications are available from EU Bookshop (<http://bookshop.europa.eu>), where you can place an order with the sales agent of your choice.

The Publications Office has a worldwide network of sales agents. You can obtain their contact details by sending a fax to (352) 29 29-42758.

The mission of the JRC is to provide customer-driven scientific and technical support for the conception, development, implementation and monitoring of EU policies. As a service of the European Commission, the JRC functions as a reference centre of science and technology for the Union. Close to the policy-making process, it serves the common interest of the Member States, while being independent of special interests, whether private or national.

